JPL PUBLICATION 82-23

Proceedings of the NASA Workshop on Registration and Rectification

Nevin A. Bryant
Editor

(NASA-CR-169133) PROCEEDINGS OF THE NASA WORKSHOP ON REGISTRATION AND RECTIFICATION (Jet Propulsion Lab.) 335 p HC A23/MF A01 CSCL 08B

N82-28699
THRU
N82-28739
Unclas
G3/43 28449

June 1, 1982

National Aeronautics and
Space Administration

Jet Propulsion Laboratory
California Institute of Technology
Pasadena, California

JPL PUBLICATION 82-23

Proceedings of the NASA Workshop on Registration and Rectification

Nevin A. Bryant
Editor

June 1, 1982

National Aeronautics and
Space Administration

Jet Propulsion Laboratory
California Institute of Technology
Pasadena, California

This publication was prepared by the Jet Propulsion Laboratory, California Institute of Technology, under contract with the National Aeronautics and Space Administration.

ABSTRACT

A workshop on issues associated with registration and rectification of NASA sensor data for earth applications was held on November 17-19, 1981. Attendees from NASA centers, other federal agencies and departments, industry, and educational institutions discussed the issues in a broad context ranging from NASA earth observations systems to user applications.

The points and recommendations presented at the workshop can be divided into three categories: a) concerns about the present situation and suggestions for improvement, b) well defined near- and long-range applications research tasks having low manpower and funding requirements, c) some medium-range technology augmentation research areas, elements of which were brought up by several panels, which would require significant manpower and budget resources Most of the concerns raised can be forwarded to the NASA branches and program offices for the appropriate disciplines, or incorporated as justification for Information Systems Office funded SRT. Similarly, the suggestions for small applications research tasks can be incorporated within the Information Systems SRT program or other programs.

The medium-range (3-5 year) technology augmentation research areas provide an opportunity for the Information Systems Office to propose significant new starts in FY83. Three proposed areas are: 1) Advanced Image Registration System, 2) Master Ground Control Point/Pattern Library System, 3) Error Budget Modelling and Sensor Verification Testing System.

A longer-range goal should be the development of sensor platform stability and associated attitude control to provide 5-10 meter multi-temporal registration accuracy with minimal or no ground control.

TABLE OF CONTENTS

1.0 EXECUTIVE SUMMARY

1.1 HIGHLIGHTS

A workshop on issues associated with registration and rectification of NASA sensor data for earth applications was held on November 17-19, 1981. Attendees from NASA centers, other federal agencies and departments, industry, and educational institutions discussed the issues in a broad context ranging from NASA earth observations systems to user applications. The results of the presentations and deliberations showed that some promising technologies and procedures can and should be implemented within the next few years to advance the current technology and improve future ground segment processing. A goal for 1990 should be the development of sensor platform stability and associated attitude control to provide 5-10 meter multitemporal registration accuracy with minimal or no ground control.

A long range goal of the Information Systems Office is to provide the set of techniques needed to digitally register and rectify remotely sensed data, integrate remotely sensed data with conventional data, reduce image geometric and mapping errors while maintaining image quality, and reduce system and product costs through improving processing efficiency and adopting more automated techniques. The workshop sought to provide a solid basis for NASA planning in this area by identifying current needs, determining current technology, and recommending programmatic elements. The agenda was structured to achieve the stated objectives by having presentations on user needs, space segment errors and ground segment errors during the first day. For half of the second day, presentations were given on salient aspects of the registration and rectification process as well as error analysis procedures. The remainder of the workshop was devoted to working group discussions. Each of the seven working groups was charged to assess the state of the art, and identify research tasks suitable for their subject area. The results of the working group recommendations and general discussions are summarized below.

The essential elements with registration were apportioned to three working groups: image sharpness, feature extraction, and inter-image matching. All three working groups noted the large amount of non-NASA work that has been performed and recommended that state-of-the-art surveys be quickly undertaken to prepare for key technology augmentation research projects of significant scope and provide justification for initiating low-budget SRT tasks. The image sharpness group proposed near-term SRT tasks on the relationship between sensor IFOV and effective IFOV on sharpening images for matching and ground control point identification. They also noted the need for improved SAR image formation SRT. Longer-range studies proposed were concerned with the potential of techniques to avoid aliasing errors and diffraction-related blurring on MLA sensor systems. The feature extraction group noted that recent research results have revealed the potential to use subpixel estimation of local features to improve ground control point selection and inter-image matching. Focused funding should provide significant near-term results here. A longer-range project of much greater scope would be the development of ground control pattern (as opposed to control point) libraries to provide improved accuracy, greater generality, and world-wide capability for the registration process. As similar suggestions were brought up by other working groups, they were treated in greater detail later. The inter-image matching group recommended

that several low-level SRT tasks be slated for early funding to assess the accuracy of matching by different techniques under different conditions to guide individual users and project-oriented image registration/rectification systems. This group also suggested that multitemporal and multisensor registration systems with their associated libraries be a major endeavor over the next 3-5 years.

The essential elements associated with rectification were apportioned to one group concerned with remapping and another associated with resampling procedures. Both groups pointed out the need for state-of-the-art technology assessments prior to initiation of major programs, and the high potential return from well formulated testing of algorithms on selected data sets of actual and synthetic imagery. In addition, the remapping group pointed out the need for SRT tasks that incorporate standard photogrammetric methodology and formulas and more fully utilize platform and calibration data from current and proposed sensors to reproject digital imagery. The impact of improved platform stability and integration of GPS measurements on reduced ground segment processing needs to be critically assessed. The group also highlighted the need for a substantial effort in the development of remapping software and systems that are modular and transportable. This need stems from the fact that previous and current ground segment image data rectification tasks are faced with external forces difficult to resolve, namely users wanting a wide variety of map projections and data processing capabilities which private industry has not yet cost-effectively developed nor has an individual government facility efficiently supplied. The resampling group also raised the need for transportable software and systems that could be integrated with remapping systems. They pointed out the need for an SRT effort in algorithms to compensate and provide valid estimates for missing data occurrences in upcoming TM and MLA sensor systems. As a general point, it was noted that future sensor design should take into account the fact that resampling/reprojection will be undertaken and as a result sensor system designs should optimize for resampling rather than IFOV concerns.

The error analysis procedures were subdivided into an error characterization and an error budget group and methods of verification group. Both groups pointed out that this area has little prior history within NASA but is experiencing considerable attention now that sensor systems data are being integrated with other information whose only common attribute is a latitude and longitude position identified to a given level of accuracy. The error characterization and error budget group recommended several SRT tasks, both short and long term but at a modest level of effort, to evaluate existing error models (i.e., for Landsat D/TM) and develop error models for future systems definition and trade-off studies. A major effort was proposed to help break down the impasse that frequently occurs between user requirements and system development decisions. It was proposed that a system that iterates user requirements and space imaging system error budget characteristics be developed to achieve a satisfactory balance of alternatives that are most cost-effective. The verification methods group proposed a similar, large-scale program which could mesh the error budget predictive modeling with end-to-end image verification testing systems.

In summary, the points and recommendations presented at the workshop can be divided into three categories: a) concerns about the present situation and suggestions for improvement, b) well defined near- and long-range applications

research tasks having low manpower and funding requirements, c) some medium-range technology augmentation research areas, elements of which were brought up by several panels, which would require significant manpower and budget resources. Most of the concerns raised can be forwarded to the appropriate NASA discipline branches and project program offices or incorporated as justification for Information Systems Office funded SRT. Similarly, the suggestions for small applications research tasks can be incorporated within the Information Systems SRT program or other programs.

The medium-range (3-5 year) technology augmentation research areas, however, provide an opportunity for the Information Systems Office to propose significant new starts in FY83. Each of the technology augmentations should improve upon the registration and rectification elements of ground segment data handling to a degree which would permit major as opposed to incremental improvement of the situation as it exists today. The three proposed programs are:

1. Advanced Image Registration System: Expanded user needs in registration of multiple sensor data and more precise local registration can best be met for the next decade by improving the analyst capability to discern matching ground control patterns/points. The system would include smart imaging terminals augmented with image enhancement algorithms and procedures designed to improve an individual analyst's throughput and success/accuracy probability for registering multitemporal and multisensor ground control pattern/points. The system would also include automated registration procedures and selected projections for remapping imagery as transportable software modules.

2. Master Ground Control Point/Pattern Library System: Expanded requirements for automated ground control point/pattern integration with imaging sensor data will best be met by the orderly development of a library that accepts and verifies data from a variety of sources and is upwardly expandable to future sensor systems. The library would include the variety of algorithms required for testing and updating ground control point location in images of different sensors under different conditions. It would also include the data archive and data base management required to provide world-wide coverage for NASA satellite sensor systems.

3. Error Budget Modelling and Sensor Verification Testing System: NASA project management needs an iterative capability to evaluate user requirements and potential engineering design trade-offs prior to launch. It also needs a general purpose end-to-end verification of performance postlaunch. The testing system would provide a dynamic environment to test and verify alternative registration and rectification strategies (e.g., use of GPS for Landsat D) for ongoing and future sensors which can be readily understood by potential users, and minimize ambiguity associated with specifications and performance.

1.2 RECOMMENDED RESEARCH TASKS BY PANEL

1.2.1 Image Sharpness Panel

Near-Term Tasks

1. Study relationships between effective IFOV and "optimal" image structures for sharpening images (4 manyears, $20k computer, 2 year duration).

2. Study relationships of IOFV on performance of matching algorithms (1 manyear, $10k computer, 1 year duration).

   Undertake a state-of-the-art survey of published and unclassified research in image sharpening funded by DOD in recent years. (1 manyear, 1 year duration).

Long-Range Tasks

3. Study the potential of using optical prefiltering on MLA systems to reduce the potential for aliasing errors. (3 manyears, $20k computer, 3 years duration).

4. Determine appropriate compensation/sharpening techniques needed to reduce defractor limited image blurring associated with thermal IR MLA sensors and passive microwave sensors (5 manyears, $40k computer, 5 years duration).

   Investigate optical and digital correlator techniques to sharpen SAR images. (3 manyears, $40k computer, 3 years duration).

1.2.2 Feature Extraction Panel

Near-Term Tasks

1. Inventory of current capabilities and concepts of image/feature models for estimating the positions of image features to less than a pixel. (1 manyears, 1 year duration).

2. Accuracy assessment of models used to estimate the positions of image features to less than a pixel. (3 manyears, $20K computer, 2 manyears duration).

Long-Range Tasks

3. Development of subpixel feature estimation models for ground control point identification and selection. (6 manyears, $40k computer, 4 years duration).

4. Ground control pattern library design development and testing including single or multiple sensor feasibility and DBMS capabilities. (10 manyears, $50k computer, 5 years duration).

1.2.3 Inter-Image Matching Panel

Near-Term Tasks

1. Investigate the potential utility of commercially available special purpose hardware to determine whether it is economical to speed up commonly used algorithms for inter-image matching. (1 manyear, 1 year duration).

2. Study to determine interaction of inter-image matching procedures and selection of GCPs for a given sensor, thereby providing guidance on selection criteria for future libraries (3 manyears, $50k computer, 2 years duration) (multiple task).

3. Determine the feasibility of developing a centralized system to perform registration and rectification for various sensors (i.e., SAR, MLA, MSS, etc.) (2 manyears, 2 years duration).

Long-Range Tasks

1. Investigate the effect of number and distribution of control points required for rectification of a given image (sensor) and its characteristics using: a priori model, selection of degree model, or development of a model with an adaptive warping function capability; and determining the adequacy of fit. (5 manyears, $40k computer, 4 years duration).

2. Study to determine the feasibility of a highly automated, global, multisensor control point library. (Similar to Feature Extraction and Remapping Panel Recommendations).

1.2.4 Remapping Panel

Near-Term Tasks

1. • Development of a transportable software and general hardware design specification for image warping and rotation for remapping. (4 manyears, $20k computer, 2 years duration).

2. Generate simulated and standard data sets for aircraft and spacecraft images and design simulation study algorithms for remapping. (4 manyears, $20k computer, 2 years duration).

3. Develop suitable techniques for image mosaicking and multitemporal overlays (3 manyears, $20k computer, 2 years duration).

4. Develop and implement photogrammetric rectification and block adjustment techniques for overlapping digital imagery (3 manyears, $20k computer, 2 years duration).

5. Establish optimized aircraft mission design alternatives (1 manyear, 1 year duration).

Long-Range Tasks

1. Investigate, model, and implement rectification to sensors (scanner, MLA, SAR). (10 manyears, $50k computing, 5 years duration).

2. Develop correspondence (similarity) measures for finding control points between images from different sensors. (4 manyears, $20k computing, 4 years duration).

3. Investigate and develop models for compensation/correction of attitude. Design advanced attitude sensors and develop capability for on-board compensation (aircraft and spacecraft). (7 manyears, $20k computing, 5 years duration).

4. Develop Ground Control Point Files (similar to feature extraction and inter-image Mapping Panel recommendations).

1.2.5 Resampling Panel

Near-Term Tasks

1. Define the point spread function (PSF) that will yield the "best" result following resampling. Parameters would include noise, shape of the desired output PSF, and instrumental constraints. (3 manyears, $10k computing, 3 years duration).

2. Develop standard data sets of both real and synthetic data, test and compare resampling algorithms under varying conditions, and publish results. (5 manyears, $40k computing, 2 years duration).

3. Develop methods of filling data gap regions on scanner and MLA type systems associated with dead detectors or scan gaps. (6 manyears, $20k computing, 3 years duration).

4. Document and test and last squares resampling approach. Cost benefit analyses must also be done and clear definitions of applicability and limitations ascertained. (1 manyear, $5k computing, 1 year duration).

5. Investigate the benefits of going beyond the linear restriction on resampling algorithms. (2 manyear, $5k computing, 1 year duration).

Long-Range Tasks

1. Discover a "benign" resampling method for archiving data (5 manyears, $20k computing, 5 years duration, 2+ groups).

2. Investigate, from the end use perspective, optimal resampling functions. Determine optimal resamples based upon: radiometric accuracy, geometric fidelity, or spatial feature extraction (5 manyears $20k computing, 5 years duration, 2+ group).

1.2.6 Error Characterization and Error Budget Panel

Near-Term Tasks

1. Obtain and evaluate the existing Thematic Mapper error models (5 manyears, $50k computing, 3 years duration).

2. Develop error models for future system definition and tradeoff studies on advanced sensors, spacecraft/shuttle, processing, and information. (5 manyears, $50k computing, 3 years duration).

Long-Range Tasks

1. Develop the system and procedures required to provide iterative user involvement in system error budgeting and error model development, with verification on real and synthetic data sets. (20 manyears, $100k computing, 5 years duration).

2. Create a Positioning Error Budget Study Group (2 manyears, $100k travel, 5 years duration).

1.2.7 Verification Methods Panel

Near-Term Tasks

1. Identify verification performance measures and review current verification approaches. (3 manyears, $20k computer, 1 year duration).

2. Undertake an image verification end-to-end test using a selected system as a test bed. (3 manyears, $20k computer, 1 year duration).

Long-Range Tasks

1. Compile synthetic and real data sets displaying the range of distortion characteristics for advanced sensors (MLA, SAR, stereo) and identify recommended verification techniques (10 manyears, $100k computing, 5 years duration).

2. Undertake image verification end-to-end tests on advanced sensors (i.e., MLA, SAR, stereo). (10 manyears, $100k computing, 5 years duration).

1.3 PROPOSED TECHNOLOGY AUGMENTATION PROGRAM

Three major systems developments or Technology Augmentations were determined from several of the panel's recommendations to provide significant improvement in the registration and rectification process for terrestrial (or planetary) imaging systems planned for launch in this decade. All would involve a significant commitment of manpower and budget resources over a 3- to 5-year development phase. They represent significant engineering, systems, and scientific modeling design challenges for NASA which, if accomplished, would serve a wide community of research and applications users. The recommended systems include:

I. Advanced Image Registration System: Expanded user needs in registration of multiple sensor data and more precise local registration can best be met for the next decade by improving the analyst's capability to discern matching ground control patterns/points. The system would include smart imaging terminals augmented with image enhancement algorithms and procedures designed to improve an individual analyst's throughput and success/accuracy probability for registering multitemporal and multisensor ground control pattern/points. The system would also include automated registration procedures and selected projections for remapping imagery as transportable software modules. (20 manyears, $500k procurements, 5 years duration).

II. Master Ground Control Point/Pattern Library System: Expanded requirements for automated ground control point/pattern integration with imaging sensor data will best be met by the orderly development of a library that accepts and verifies data from a variety of sources and is upwardly expandable to future sensor systems. The library would include the variety of algorithms required for testing and updating ground control point location in images of different sensors under different conditions. It would also include the data archive and data base management required to provide world-wide coverage for NASA satellite sensor systems. (10 manyears, $500k procurements, 4 years duration).

III. Error Budget Modeling and Sensor Verification Testing System: NASA project management needs an iterative capability to evaluate user requirements and potential engineering design tradeoffs prior to launch. It also needs a general purpose end-to-end verification of performance postlaunch. The testing system would provide a dynamic environment to test and verify alternative registration and rectification strategies (e.g., use of GPS for Landsat D) for ongoing and future sensors which can be readily understood by potential users and minimizing ambiguity associated with specifications and performance. (40 manyears, $500k procurements, 5 years duration).

2.0 INTRODUCTION

2.1 BACKGROUND

The range of useful applications for processed data have met initial expectations since the launch of the first satellites two decades ago. However, there have been some areas of concern regarding data delivery, the need for improved spatial and spectral resolution, and the desire for registered and map rectified data. Improved ground systems throughput and sensor and spacecraft related technology have shown continuous progress over the years; however, the rapid generation of accurately registered and/or map rectified data has not progressed as quickly. There are several reasons that have contributed to this state of affairs, and they are the principal concern of this workshop.

Remotely sensed data, particularly the Landsat series, present several challenges to digital data acquisition. First, the files are very large, requiring special purpose algorithms and hardware for efficient processing. Second, continuous along- and across-track distortions in the imagery -- attributable to sensor geometry and orbit ephemeris changes both systematic and nonsystematic -- make precise data capture a difficult and sometimes costly procedure. Third, NASA experimenters have been most interested in the spectral range, spatial resolution, wide-area coverage, and rapid repeat cycle of earth observational systems. Only with time has an appreciation of the need for geocoding to accomplish an easy interface with other data sets become a task of significant proportions to warrant a concerted effort.

There have been several developments in Landsat data capture in recent years. The mission ground segment processing has moved from the initial photo product orientation to a greater concentration on preparing computer compatable tapes. Improvements have occurred in both expanding the number of frames processed per day and provision for precision correction. Much work still is ahead, however, handling the data rates and geometric distortions associated with the upcoming Landsat-D/Thematic Mapper and proposed MLA systems. In parallel with the mission ground segment processing has been the development at local facilities of precision processing of selected areas to meet national map accuracy standards. These products characteristically overlap other maps or are digitally interfaced with geographic information systems.

The workshop was convened in an effort to review Techniques used for efficient and accurate registration/rectification and identify key research areas which need to be addressed.

2.2 THE DATA SYSTEMS PROGRAM

A. Villasenor, NASA Headquarters*

The data systems program in OSTA has fairly specific goals that try to improve user access to space derived data (see Appendix 9.6). In the process of doing that, we have to develop data management activities, put together catalogs and provide data networks to move data from the space producers to the space data users. At the same time we expect to reduce the cost and risk of flight missions. After all, the primary reason for flying missions is to gather data and, historically, there has been considerable cost in processing space data. Also, we expect to provide a base whereby providing new tools and making data more available will enable more questions to be asked of the data and therefore enable new information capabilities. Our philosophy is to specifically try to work with the users. We really don't have a program without requirements and that's one of the reasons why the first block of speakers represents the user community. Once we know what the needs are, we can encourage and apply advanced technology to meet their need. I say "encourage" because the OSTA role is not to develop technology, it is to apply technology. There is another office at Headquarters which is chartered to develop new components, new hardware technologies. What we want to do is serve as a focal point to encapsule the common requirements throughout NASA programs and have systems which can be transported from one application to another. Our role is in the data system arena and not in data interpretation. We stop at the point of extracting specific information, image classification for example, and try to develop in-house expertise.

A Data Systems Branch role is to coordinate the data system needs which are common; the Branch has the charter from NASA's applications office to develop a data system plan. That means for the applications projects, common data registration activities, common catalogs, and also pilot system developments. We provide technical support to the program offices with respect to data system activities. We try to apply advanced data systems technology such as pipeline or parallel processors technology where needed to improve processing speeds and efficiencies. We also need to establish and develop a skill base for the data system managers in the various NASA flight projects and establish a focal point for NASA interfaces with other agencies or private industry.

We have several programs actively involved in applying technology to support current and proposed flight missions. The Application Developmental Data System is to provide a near-real-time processing capability for Thematic Mapper on Landsat-D. We are working on a synthetic apperture radar data system to process Seasat/SAR-type images in preparation for future SAR flights. We're trying to transfer some of the software-intensive image processing activities into the VLSI technology (specifically image rotation). We are going to be looking at digital disk applications in the '82-'83 time frame. Our second thrust is in networking capabilities and what we are doing here is linking together a number of data management systems and data analysis facilities which support the atmosphere and climate program. This specifically is done at the Goddard Space Flight Center. A similar activity is planned for the Earth Resources Program strongly based on Landsat imagery at the JSC facility. We

* Edited oral presentation.

just began this year to develop a system for oceanographic research at Jet Propulsion Laboratory.

In the information extraction area we are trying to build a program; hence, today's workshop on image registration/rectification. We will also be looking at data integration and at developing executive level software which can be carried from one host system to another. Smart user terminals are being developed at NSTL's laboratory. The intention there is to develop low-cost user terminals for the market for the small user. In the data management area we have evaluated several commercial data base management systems with an application to on-line catalog activities plus on-line image data bases. That is an activity which we have begun and will continue into the '83 time frame. We also intend to look at data base hardware to make data access of image data sets more efficient. There is a new activity in '82 if we receive full funding to look at data compression techniques and some elements of information science. I know for example there are some questions as to why we should acquire all of the possible data that a sensor generates. Perhaps we can apply some intelligence in either on-board or ground-based systems to be more selective in acquiring the data we need. We also look at modeling elements, modeling for the CYBER 205.

Let me just run through the accomplishments to date. In the distributed data systems area we did initiate activities in the ocean pilot at JPL. We've got the full network operation at Goddard and developed an on-line catalog for some of the Nimbus CZCS data. At JSC, we developed the requirements for a network of the earth resources users. Within the Atmosphere Pilot we did put together medium-speed networks to exchange image data and to develop a software for exchanging data files, building upon the manufacturers supplied software. We also had an active program in standards for applications data sets and data formats and protocols. In the advanced processing systems I did mention the pipeline system which is built around a VAX minicomputer with a goal to produce 500 MSS and 100 TM scenes a day six months after launch. In the SAR processor we can now process a complete SAR digital image in 2-1/2 hours and this year we expect to achieve approximately one hour.

In data management we evaluated several systems for some of the Pilots and took advantage of the user requirements for on-line catalogs to install on-line interactive inquiries for the climate and the ocean pilot systems. In the information extraction area we started developing some improved registration techniques at JSC. The AgRISTARS related work accomplished the capability to look at and register three multitemporal scenes to one pixel accuracy. JPL did extensive work on automosaicing in support of the renewable resources program. The Transportable Applications Executive which Goddard developed is being installed in several computers at Goddard and JPL. We are developing information extraction software libraries for meteorology, geology, and the oceans pilot is working on a similar package of algorithms for oceanographic work.

The element in the program on image registration and rectification requires attention We have a very limited budget and have to make some choices as to which center performed what kind of activity or in fact what made sense to do. Our commitment to support the user environment raised a number of questions, and I felt it was time for us to stop and to sit down with experts in registration and rectification and try to develop a program for a 5- to 10-year

period. There are needs for data compatibility so that we can exchange data not only among NASA centers and between NASA and industry and universities. We need to look at data integrity, data quality, and the kind of algorithms to use. Perhaps we need tc look at transportable geocoded information systems. The use of the VLSI technology to solve high-compute algorithm problems. We'd like to look at improved ways to order and receive data, and, of course, we are always interested in low-cost user terminal systems. I wanted to assemble experts in industry and government and universities to help identify what the user requirements are and learn what the state of the art is. Knowing where we are today we can identify what the "tall poles" are and develop a programmatic schedule through the next few years. I will be looking for specific issues that we can pursue in the data systems program. I expect several results out of the workshop. I expect we are going to publish proceedings and they will be distributed by April and I will follow that up shortly with a data system program plan.

N82 28700

2.3 WORKSHOP RATIONALE

F. C. Billingsley, JPL*

For the future, we've got to worry about how we can actually do data processing in a manner that produces data which is of greater accuracy by the time we use it. Very likely we are going to be dealing with a set of sensors which may not be on a given spacecraft. This says that the data may or may not be optimized for the type of processing which we are going to apply. This in turn gives us some implications on the processing needed prior to analysis, i e.. geographic registration and the whole question of how to get data geocoded and in condition to register one set of data to the other. There are also questions of on-board processing, data compression, and various special pipeline parallel processor elements which are going to be required to get the data through the system in the reasonable time.

As illustrated by Figure 1, we're dealing with a set of processing in one piece of this total system starting with a sensor, a set that goes through a preprocessing step, becomes archived, and is extracted from the archive; the data is processed and finally applied to user models. We're trying to put the data in a condition so that when the users request through the system they can get the set of data they want in the condition they require.

In the general area of preprocessing we are going to be dealing with a number of potential topics, among which is geometric rectification (which, of course, is our main interest here). The question of radiometric preprocessing in terms of this conference comes into play regarding whether or not the radiometric properties of the data have any effect on our ability to do any of the geometric operations required. For instance in the earlier Landsats, until the data were properly destriped, the correlations which were done for registration of ground control points tended to lock in on a striping rather than on the data. For spatial resolution, we are concerned about frequency responses for interpolation kernels and what effect they may have on applications. For georeferencing and cataloging, if one can't find the data, it doesn't do one much good. Georeferencing simply says that if we can register any given set of data to a reference (I'll call it a grid), then, implicitly, various data sets are "more or less" registered to each other and part of that more or less is what we want to talk about in this workshop and panel sessions. What we're trying to do is make the data correct, make data sets compatible so they can be used together, and eventually make them available, which means put them in such a condition that when we call for them from the archives, we get can get the data back fairly expediciously.

Now the net result: the net use of the data in the long run is extraction of information. Most of the models which are now being developed required data from numerous data sets. One example of the potential interplay of sets of data from various sources is illustratd in Figure 2, which indicates some of the interplays between data for a particular problem having to do with weather questions. I don't expect to go through this illustration in detail except to indicate that there are a lot of crossing arrows and many particular processes that have to be modeled in solving the users information extraction problem.

*Edited oral presentation.

This calls for data from various sources in order to allow multiple users to expeditiously do their problem solving.

Use of various data sets together is one thing, using data sets together with data from other sources such as maps, or producing data in which the required output information is map-related is another. What's involved basically, is to produce a data set in which the indiviual data items in one form of geographic coding are implicitly related to a given position on the ground, because we have defined where the entire image matrix lies on the ground. Thus we can convert latitude and longitude into a line and pixel in the data set. In addition to the question of using data sets from various sources there is a general question of being able to put it into the archives and get it out of the archives in a geographically coded sense, so that we can begin to produce data in a form that will make that whole process fairly expeditious.

The requirements involved the removal of distortions and then placing of that rectified data in an archive where we can retrieve it; placing rectified data on the ground in a given location is reviewed in Table 1. This is not supposed to be a definative list, but a little table of some of the sources of geometric distortion. Many of the items which are included in the table and and figures are going to be subjects of the panel discussions. What I want you to think about is the fact that there are a number of causes of distortion: some of them in the sensor itself, some of them in the spacecraft in terms of its pointing, and some of them which are implicit in a remote sensing system (such as the fact that the earth is round). And it may well be useful in your panel discussions to consider the sequence of causes of distortions and decide whether or not that sequence of causes of distortions gives you any clues as to the sequence to remove the distortions and what might be done in that process. Depending on which types of distortions you are faced with you may treat them differently. Again these types of items and their specifics are the kinds of things that you will be discussing in the panel meetings.

There are a series of problems involved in attempting to match one interest to the other; I won't try to go through those because you have a set of questions which has been outlined for the various panels as a guide to thinking. I do have Figure 3, which will indicate the type of problem we are involved with in doing the correlation of images to maps. Some of you may be familiar with this process, and some of you may not, so I'll indicate it briefly. We are trying to find a piece of an image and it's location with respect to a map. We take each piece of an image control point area, taking a series of those that are scattered around the face of a total frame, then that series of ties between line and pixel and the location on the ground (latitude and longitude) gives you the data you need to do a geometrical warping of the image, so that when you complete the dewarping process, you now have an image which can lay on the ground -- hopefully with all pixels registered. The essence of the process simply is that maps and images do not cross-correlate very neatly in a computer, as maps and features in images look different. We've got a real problem in trying to define a way to do that correlation. The way it is currently being done is to optically correlate, that is optically mix and overlay, and shuffle around until they match, a digital display of a small piece of image and a piece of a map. When those two are optically mixed, then a surveyed point on the map can be located in the small piece of visual image by running a digital cursor around on the display until it overlays the particular ground control surveyed point. The computer would know where the cursor

is in line and pixel coordinates, and you'll tell it in latitude and longitude where it is on the map. That gives you a tie between this little piece of image, which in the NASA parlance is a ground control point chip, and the ground. We know from the geometry of the general situation approximately where that is in the incoming frame, so we pull out a large piece of the incoming frame digitally, and we know from whence we got it. Now we have two images. Those can be cross-correlated in a computer more or less accurately, and since we know the position of the surveyed benchmark in the little piece of image, we can determine through cross-correlation the position of each little piece within the large incoming image to tie the large incoming image's line and pixel with latitude and longitude. We have the transfer data now to take that into the total frame domain, tie individual ground control points to the ground, and develop the equations needed for the entire image. That's the kind of process we currently go through. It requires building a library of ground control points ahead of time, so when the incoming frames come we can do this cross-correlation expeditiously on the way through the system, two-hundred frames a day. Anything that people can think of during the workshop to improve the process will be appreciated.

The process that I described for ground control points requires that that particular control point be known in x, y, and z altitude, and the basic dewarping is normally a process of fitting a best-fit plane through that set of ground control points. That's fine, but, as you know, in hilly country there are intermediate points in the image, which may or may not be on that same plane. If you have hills or valleys in between, they are going to be displaced by a distance which is a function of the angle from which you are viewing those particular points, i.e., the relief displacement question. I worked up a little graph (Figure 4) which shows that relief displacement is larger than you like to believe when you are dealing with pixels of the Thematic Mapper size. In particular, although a repeat visit over a given area on the ground is intended to be a new image from precisely the same point, in practice that would not be true. It will be from some other point nearby. And the question is how bad does that slight displacement displace pieces of the image which are not on the same best fit plane. Well, here is the net result when you scale the Thematic Mapper pixels. It says, that with a surprisingly small difference in elevation between a given local point and the best fit plane, with a surprisingly small separation of the two vantage points (and remembering that the scatter of repeat visits on a given point is in the neighborhood of 5-10 km), there is a fairly large displacement potentially of pixels which are not on that original plane. Even though you have a good fit to normal control points, you may or may not have some other problems in areas of high relief. In particular with Landsat, the overlap area from side to side is a 170-km line of displacement between the wings of paraoverlap images from adjacent tracks. We are going to get a fair amount of displacement distortion due to elevation alone.

While there are a number of other items which we could talk about, I think that is enough to give you the flavor of the kinds of problems that we see coming up: potential areas of distortion, potential areas of lack of registration of the images to the ground. There are a number of specific questions which have been outlined for the various individual panels and you will get your crack at thinking about these and some of the other topics as you get into the panel discussion.

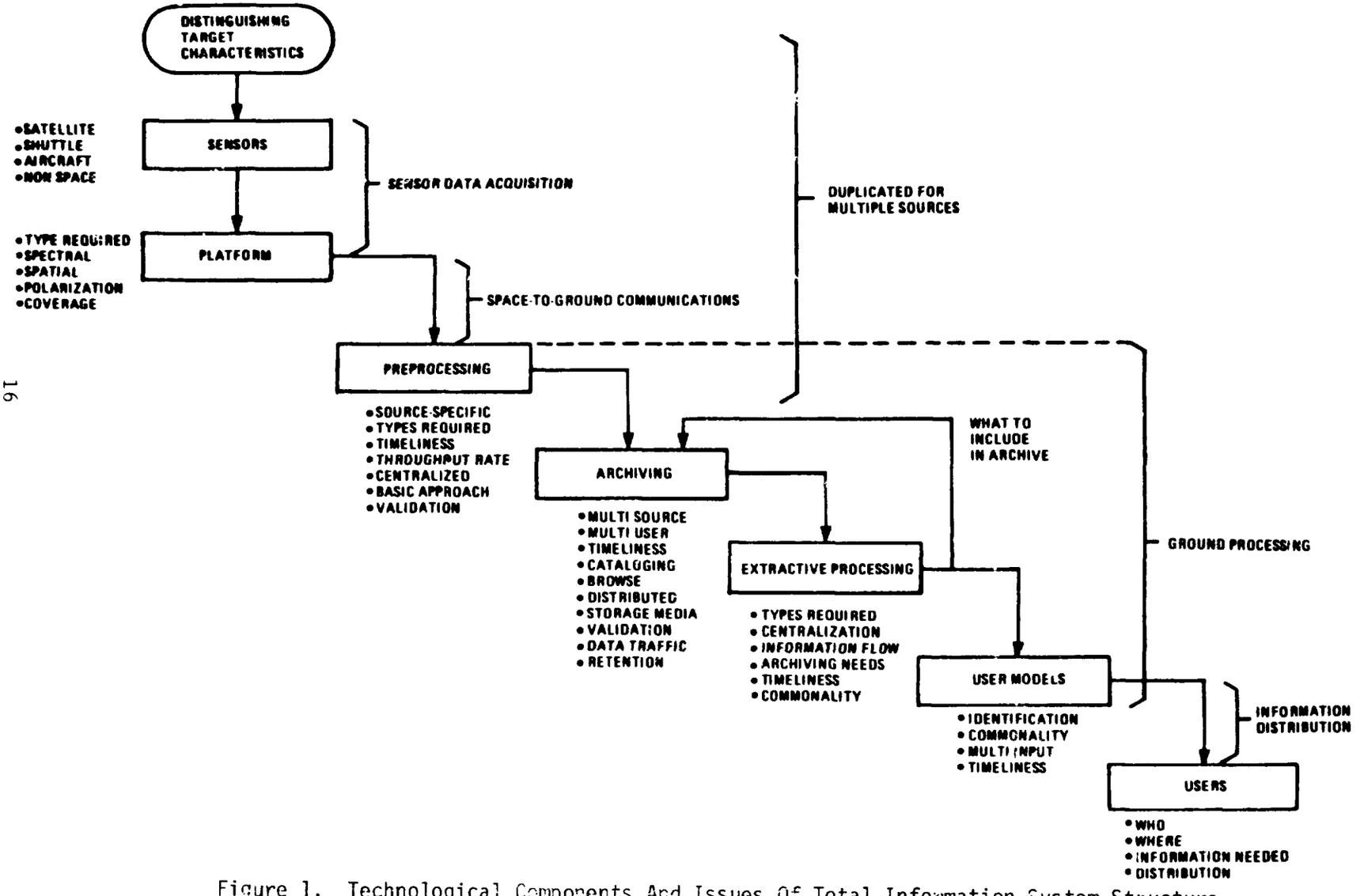

Figure 1. Technological Components And Issues Of Total Information System Structure

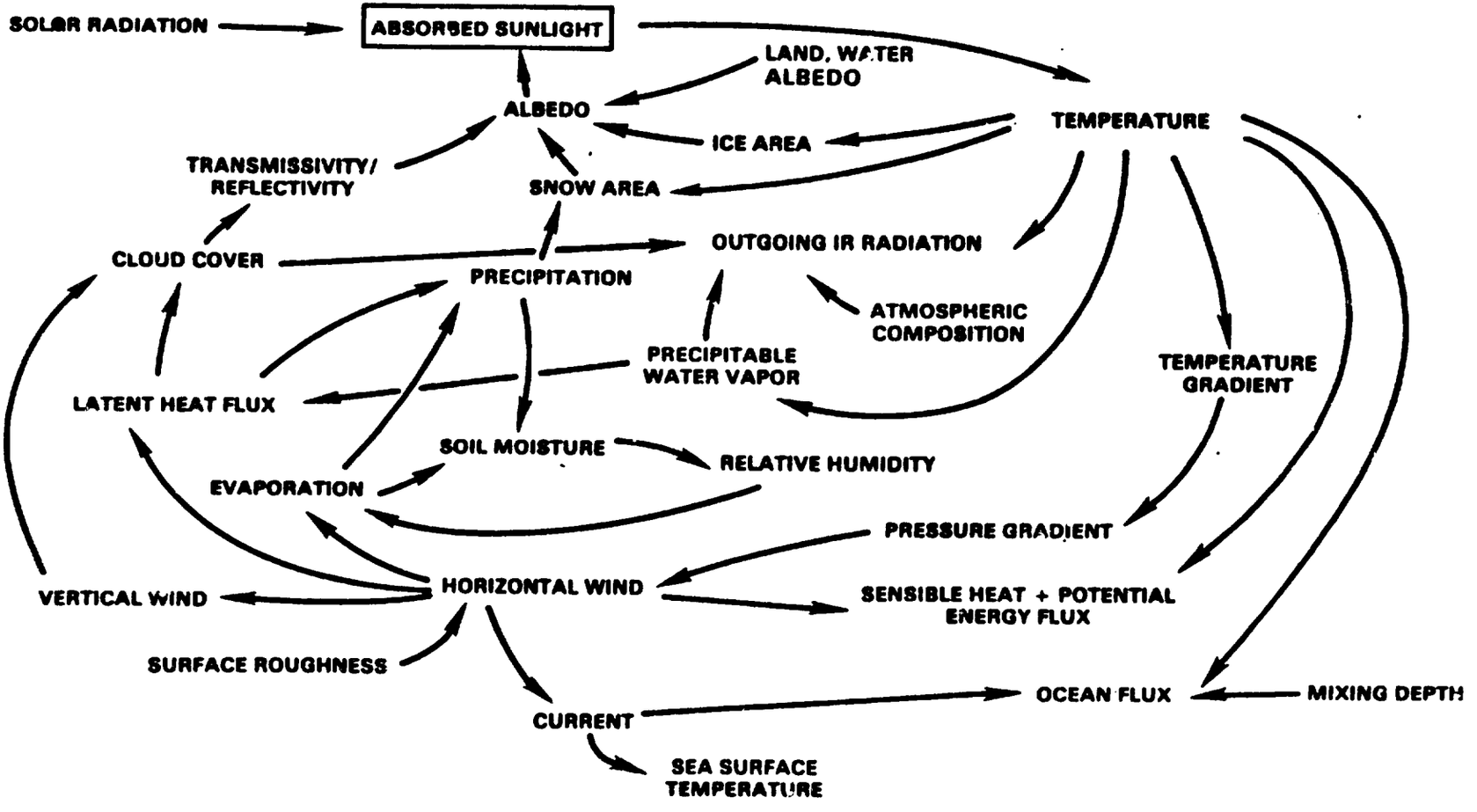

Figure 2. Complex Problems Require Many Data Sources and Models
Climate Cause-and-Effect Linkages

Table 1.

GEOMETRIC ERROR TABLE

CAUSES	MODEL	EXPECTED ERRORS
	SENSOR/SPACECRAFT DIST'S	NYQUIST IS SMALL
ANTENNA, SOLAR PANEL MOTION	JITTER	SINUSOIDAL - ≈10 PIXELS/CYCLE
ATTITUDE CONTROL SYSTEM	ATTITUDE DRIFT	SLOW, SYSTEMATIC - ≈SEVERAL CYCLE/FRAME POTENTIAL JITTER DURING CONTROL - SEVERAL PIXELS
SCAN LINE CORRECTOR	SCAN CORR (TM)	SEVERAL CYCLES/LINE
SPRING MOUNT	MIRROR SCAN	≈1 CYCLE/LINE
	EXTERNAL DIST'S	NYQUIST IS LARGE
ATTITUDE CONTROL ACCURACY	ATTITUDE PROJECTION	MANY FRAMES/CYCLE, UNLESS ATTITUDE JITTER
Δ ALTITUDE, GEOID	ROUND EARTH	MANY FRAMES/CYCLE
EARTH ROTATION	SKEW	CALCULATABLE TO FRACTIONAL PIXEL
EPHEM CONTROL, TIMING	S/C POSITION (EPHEM)	SEVERAL KM
EPHEM CONTROL	ALTITUDE	GLOBAL
	SCENE DIST'S	
TOPOGRAPHY, LACK OF S/C COINCIDENCE	RELIEF DISPLACEMENT	COULD BE PER PIXEL
BASIC SURVEY. GEOID	GCP INACCURACY MAP LOCATION	FEW TO MANY PIXELS TO NO MAP
SEASONAL, LACK OF GOOD POINTS IN REQ'D LOCATION, CORRELATION TECHNIQUE	ABILITY TO CORRELATE RCP INACCURACY	PARTIAL TO MANY PIXELS
SEASONAL, LACK OF REQ'D POINTS, CORRELATION TECHNIQUE	ABILITY TO CORRELATE	PARTIAL TO MANY PIXELS
DIFFERENCE BETWEEN WARPING MODEL AND REALITY	SCENE WARPING MODEL	PARTIAL TO MANY PIXELS
ALGORITHM SELECTION	NEAREST-NEIGHBOR WARPING	PARTIAL PIXEL

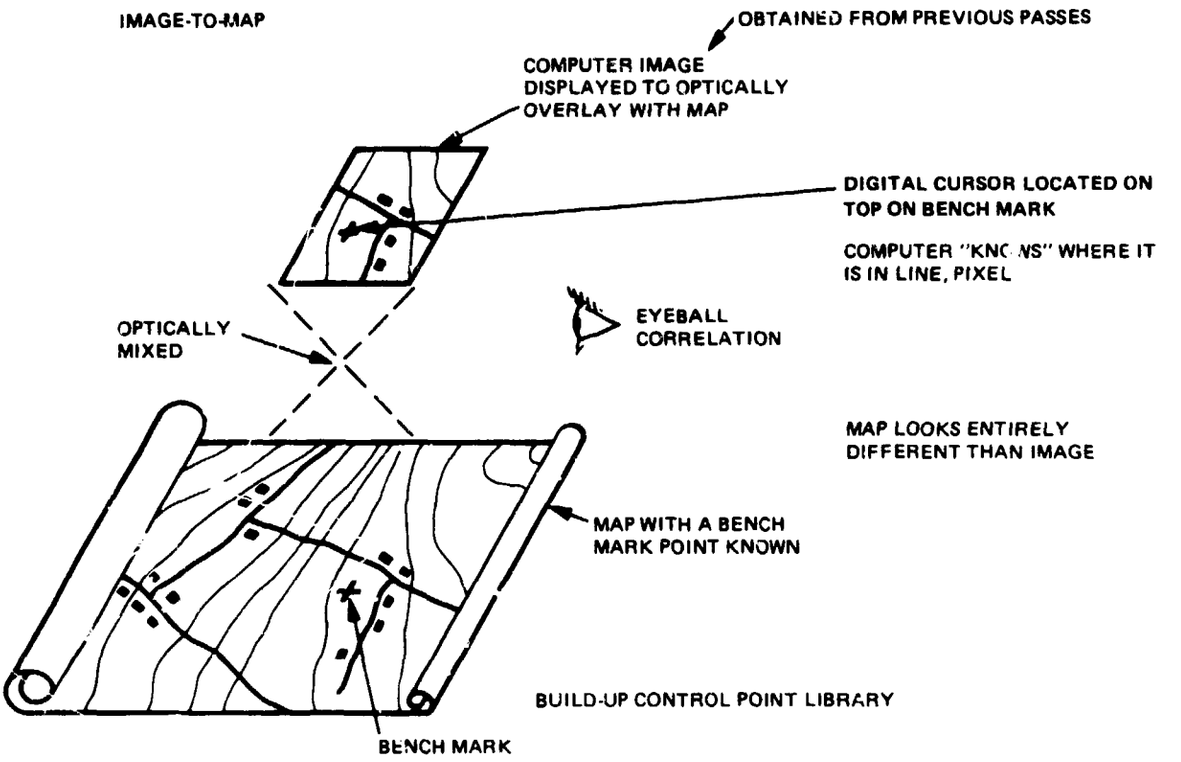

CORRELATION FOR CONTROL POINT LOCATION BY CONVOLUTION

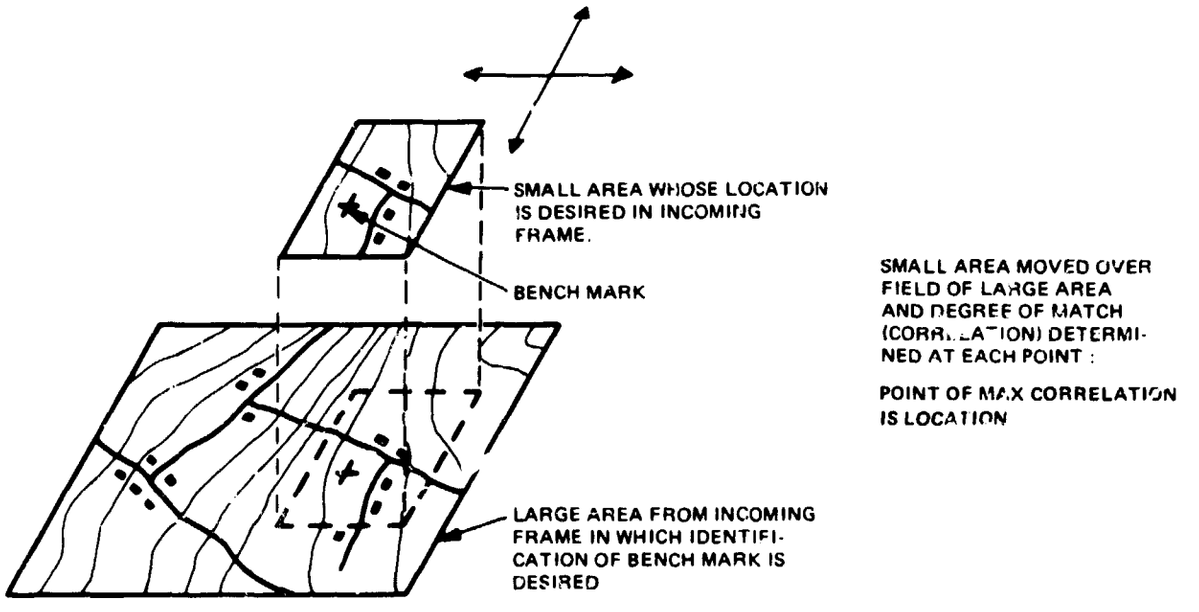

Figure 3. Ground Control Point Operations

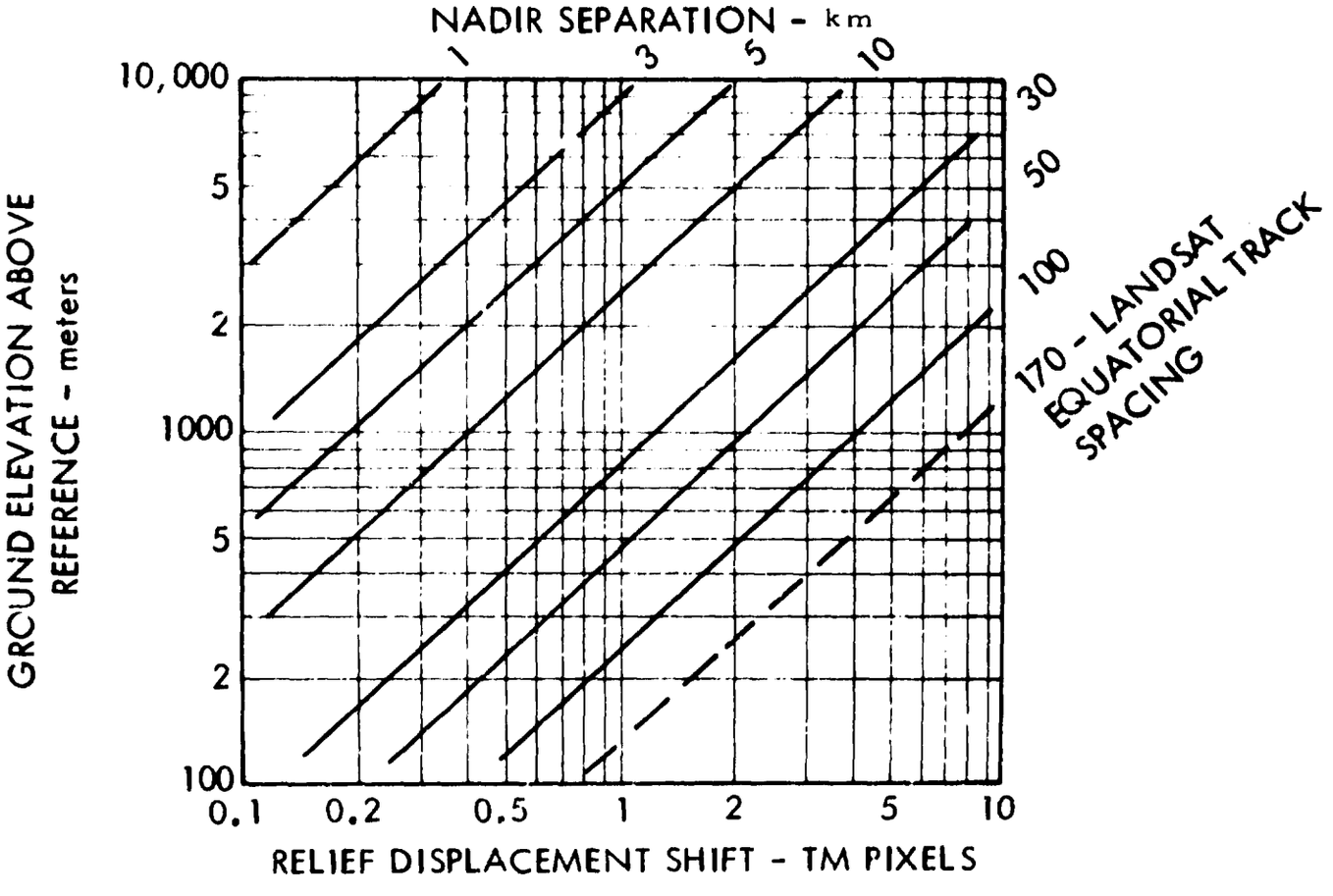

Figure 4. Relief Displacement Effects

3.0 PANEL RECOMMENDATIONS AND SUPPORTING DISCUSSION

3.1 CHARGE TO THE PANELS

For each panel, the six following items were requested. Appendix 9.4 provides a complete listing of materials provided to initiate panel discussions. Each panel was able to respond to most, if not all, of the requests.

a. Develop a position statement on the state of the art for those elements in applications' techniques of concern to this subpanel for the registration/rectification of imaging sensor data. Use the paper presented as a point of departure, adding new elements neglected and deleting elements of little concern to NASA and the user community.

b. Develop a position statement on anticipated requirements for those elements in applications' techniques of concern to this subpanel for the registration/rectification of imaging sensor data. Use the paper presented as a point of departure, adding new elements neglected and deleting elements of little concern to NASA and the user community.

c. Outline the current status of the technology within NASA. List the centers of expertise (field center groups and university/industry support groups).

d. Propose experiments that should be conducted to test document areas of concern to this panel in technique applications. This should include synthetic and standardized data sets.

e. Discuss the feasibility of providing tested software systems packages to implement standard procedures presently developed. Recommend candidate systems for the "registration processors" survey.

f. Identify research tasks that the subpanel feels should be pursued to enhance near- and medium-range capabilities. Recommend levels of effort (manyears, dollars) and task duration. Prioritize the research tasks.

3.2 REPORT OF SUBPANEL ON IMAGE SHARPNESS

The image sharpness subpanel met for a four-hour period on November 18 and again for four hours on November 19 to define research needs in this subject area for earth resource observation systems. The panel consisted of:

Bob Barker	St. Regis Paper Co.
Bill Shelley	St. Regis Paper Co.
Bill Alford	NASA/Goddard
Orback Zvi	Honeywell E.O.O.
Marvin Maxwell	NASA/GSFC, Code 920
Arch Park	G.E. Lanham, Md.
Jack Engel	Santa Barbara Resch. Ctr.
Demetrios Poros	G.E. Lanham, Md.
Joseph Kundholm	NASA/GSFC
Peter Hyde	Un. of Md. Cmptr.Sci.Ctr.

The format for the subpanel given as a starting point was followed in the initial discussions, but as time was short, it was decided to focus on the task descriptions and the expected costs. The required items are included here to the extent they were discussed and further information is to be added later.

3.2.1 Definitions

Initial discussion considered the definitions of the various functions and parameters defining the sensor scene viewing process. Conflicts with existing definitions occurred throughout and no consensus could be reached in the short time without adequate references. The panel adopted the conventions that are described and used in NASA SP-335, Advanced Scanners and Imaging Systems For Earth Observations. Special reference is made to the section entitled "Resolution Improvement Considerations" on pages 89 through 103 and on the section entitled "Definitions Pertaining to Resolution and Sample Data" on pages 105 through 109.

PSF - Point Spread Function: blur due to optical elements in system

IFOV - Instantaneous Field of View: aperture width in scanner sensor system

EIFOV - Effective Instantaneous Field of View: composite blur function after filter effects, PSF, and IFOV have been combined.

These are really working definitions to allow panel members to separate the blur components of the sensor. They are not to be widely applied. Figure 1 depicts these steps. It was natural to have the thinking focus on multispectral scanners and not on all the sensors which are of interest. These other sensors include: Imaging Synthetic Aperture Radar (SAR), Separate Thermal IR Images (HCMM), Multispectral Linear Array (MLA). The MLA contains unique characteristics which set it apart from the scanning optics of TM and MSS, so it is called out separately.

3.2.2 State of Knowledge

The parameters defining the state of the art in sharpness were discussed but not quantified. It was generally assumed that TM was the state of the art in

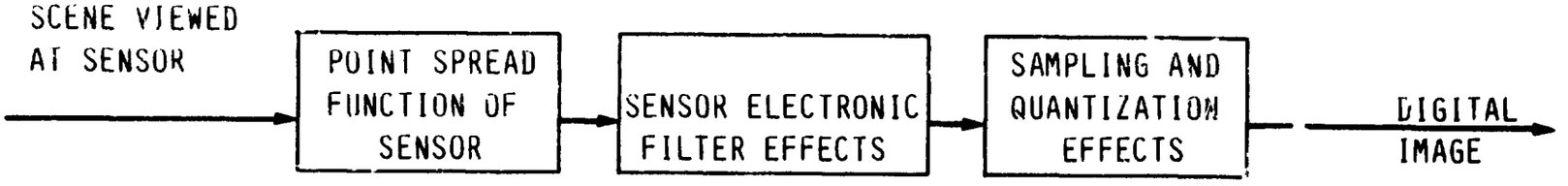

OTHER FACTORS

POINT SPREAD FUNCTION OF ATMOSPHERE
ATMOSPHERIC SCATTERING

FIGURE 1 FACTORS RELATED TO SHARPNESS

multispectral scanners and the digitally processed SAR was state of the art in radar. Order of magnitude numbers are included in some cases.

Sensor:	Atmospheric Blur/Scatter Function	
	Optical PSF	
	Scanner Aperture	30 m
	Filter Characteristics	
	Sample Rate	30 m
	Quantization	8 bits
Ground Processing:		
	Effects of Resampling on Sharpness	cubic convolution
	Sharpening Filters	Much work done but not used
	Sharpness Effects on Classification	a few studies
	Atmospheric Connection	A few users doing

3.2.3 Requirements

Discussion initially focused on whether sharpness was to be considered from the standpoint only of registration or of impacts on classification as well as registration. It was decided that unusual sampling rates would be needed in the future to enable improved sharpening of images through deconvolution. Present sampling rates are too low to allow much improvement. Severe noise effects arise even when moderate improvement is attempted. Requirements were cited for sharpening in the context of forestry applications: a) resolution of mixed (edge) pixel problem (improved classification precision, reliable change detection results, more precise areal estimates); b) improved rectification (improved definition of manually located GCP locations, verification of cartographics).

3.2.4 Recommended Research Tasks

Several key research tasks were proposed and are listed here:

I. Study of Relationships of IOVF or Performance of Matching: Unenhanced, raw data is being used for template matching in major image geocorrection systems (e.g., MDP). Sharpening processes appear to produce more visual detail. This apparent sharpness could reduce position errors in template matching. Various sharpening techniques should be applied to images before matching. Since nonlinear processes are used for matching, usual linear analysis cannot be used. Performance should be measured by experiments with real data.

II. Conduct a study to determine the "optimum" shape for the Effective Instantaneous Field of View (EIFOV) and the sampling lattice to allow the generation of an Output EIFOV (OEIFOV) in the sharpening or resampling operation which is "optimized" for various applications such as photomap generator, multitemporal multispectral classification, etc. In the study the variations in EIFOV shape, size, and sample spacing in x and y will be construed to keep the system cost approximately constant by keeping the number of detectors or the data rate constant.

III. Optical Prefilterting: We proposed to research the advantage of an optical filter, to filter the image data before it reaches the "detector array." It seems that for a system like MLA, where the image data is sampled by a distinct detector array, an antialiasing optical low-pass filter can be very

helpful. In fact, an antialiasing filter for such a system can only be an optical filter. It also seems that such an optical low-pass filter may be more easily achieved than time-domain electronic low-pass filters. Therefore we recommend that a research be established to evaluate the needs and the practical feasibility of an optical low-pass filter for an image-sampling-type camera in order to avoid aliasing.

The sampling theory states that in a sampling-type system, a prefilter is required to avoid aliasing.

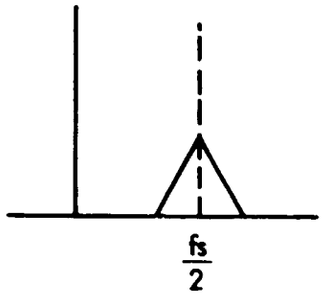

1.a. Original signal

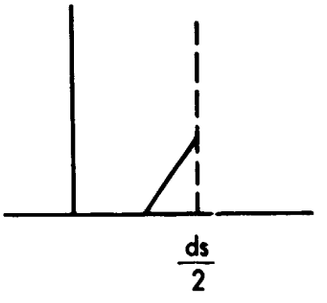

1.b. The signal after ideal low-pass filter of fs/2

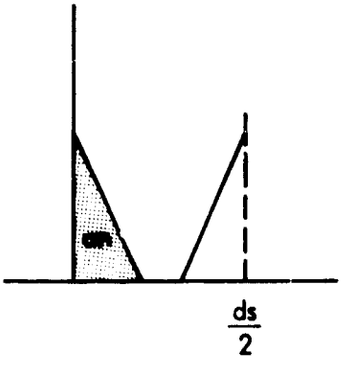

2.a. Original signal after sampling and reconstruction
(an = aliasing noise)

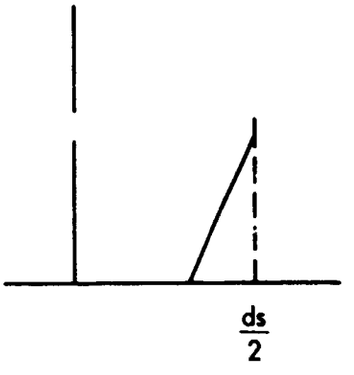

2.b. Filtered signal after sampling and reconstruction

As it is described by Figures 1a, 1b, 2a, and 2b, the sampling theory states that if the sampling rate is fs, the output has no frequency content above fs/2, or the input will appear as aliasing noise at the output. Sampling systems in the time domain are very common today. In practice, a project time-type low-pass filter cannot be achieved, and so a lot of systems use oversampling to avoid aliasing noise. The new generation of ground observation

imaging devices like MLA use a detector array approach. Such a system is image sampling and obeys the sampling theory. As such, any spatial frequencies greater than the half-sampling frequency will appear at the detector output as an alaising noise. At that point the removing of the noise from the real image is hardly possible. It then seems that the image data should be filtered before it is sampled by the detector array. Such a filter could only be optical. It also seems that a spatial optical low-pass filter can better achieve the ideal performance since the whole data exists instantaneously as opposed to time type of filtering. When the signal from $t = -\infty$ to $t = +\infty$ cannot be available to the filter, the optical filter then should be part of the optical subsystem used to bring the image data to the detector array. A research should be established to evaluate what kind of benefit would come out of an optical filter in front of the detector array imaging devices. The performance of a low-pass optical filter should be studied. The problem of different optical bands should also be considered. The final result of such research should be the requirements for a low-pass optical filter for a specific detector array, and whether or not such filter is cost effective at all.

IV. Utilization of DOD Capabilities by NASA

An effort should be made to establish the state of the art on the capability of the Department of Defense and the intelligence community to produce image processors for sharpening (also resampling and feature extraction), to establish if their techniques could be useful to civilian applications. Efforts could then be made to have this information declassifed and made available through publication in the open literature.

V. Investigation of Effects of Diffraction

Appropriate compensation (sharpening) techniques need to be developed for use on data in which the dominant cause of the image blur is defraction. Advanced Thermal IR MLA sensors and passive microwave sensors will be "Defractor Limited." Study should be conducted to establish the technique that would be used and the performance improvement to be expected as a function of the scene characteristics.

VI. SAR Image Sharpening

Research activity in support of synthetic aperture radar (SAR) must be identified, but there was no member of the panel with real experience in SAR processes or interpretation. These tasks should be addressed later with appropriate people providing the needed inputs.

3.3 REPORT OF SUBPANEL ON FEATURE EXTRACTION*

The feature extraction panel met during two sessions to define research needs in this subject area for earth resource observation systems. The panel consisted of:

Mr. Doug Carter
USGS

Mr. R. Kent Lennington
Lockheed

Mr. Michael Rassbach
Elogic, Inc.

Mr. John T. Dalton
NASA/GSFC

Dr. Thomas Lynch
NASA/GSFC

Dr. Ray Wall
JPL

Ms. Ruth Whitman
ORI

Dr. Robert Haralick
Virginia Polytechnic Institute

3.3.1 State of Knowledge

There are three issues in the subpixel feature estimation problem: 1) the identification of image models which adequately describe the data and the sensor it is using, 2) the construction of local feature models based on those image models, and 3) the important problem of trying to understand these effects of preprocesing on the entire process. We identified two classes of image models for subpixel feature estimation which we thought were worthwhile pursuing. We don't want to give the impression we thought that those were the only two, but in terms of both what we heard from Bob Haralick and the experience of the people on the panel, we first distinguished techniques based on surface fitting which have underlying assumptions about continuity and deferentiability of the intensity surface; these people tend to do their analysis on a pixel-by-pixel basis, without any direct concern for the overall organization of features of edges and lines to form long straight lines with smooth curves in the picture. This was opposed to what might be called structural models, which essentially accommodate geometrical models which describe the shape, size, and arrangement of pieces in a picture, and statistical models, which tell you about the ways in which they are colored. These second types have been distinguished from surface fitting models in terms of computations by the fact that the feature detection is done more on the basis of analyzing local neighborhoods to take advantage of the information in the geometric model. For example, assume that a picture is piecewise constant upon the edges between piecewise constant regions to better than a pixel. That doesn't preclude combinations of these approaches or others, but we certainly think it's important that people pay serious attention to this problem of being very specific about exactly what models they are using to describe the images and exactly what the local feature models are that they are using to estimate the location of these local features.

Another topic which we felt deserves some attention here, is integration of these features into high-level descriptions of content in the image. Some examples, in case people aren't sure what we were talking about, include line, curve, and intersection detection, shape detection for specific classes of

*Edited oral presentation.

shape that might be important, deriving information about the topology of areas in the picture, and more generally, segmentation techniques based upon construction of local features. It is important to note that the analysis of the effect of preprocessing on these local feature estimation techniques is going to vary from sensor to sensor.

The development of ground control point libraries for automated selection presents two concerns. One is the organization of these GCP libraries for rectification problems, i.e. the problems of automatically selecting by computer the specific GCP's for particular registration tasks. Of concern are the types of things that have to be contained in the description of any one of these patterns, because we were looking for more general representations that you can find in pictures besides just a range of spectral information say derived from a particular sensor in a particular time to represent that pattern for matching for all other times. Second is the importance of integrating ground control patterns in a data base management system, so that you can interface to a large number of sensor image types with an automatic selection system.

In terms of problems of operational and experimental validation, the issues include choosing appropriate simulated and real-image and ancillary data, and being able to establish validation criteria, to compare different techniques.

3.3.2 Recommended Research Tasks

We spent much of our time trying to establish a set of priorities in each one of these areas. Figures 1 and 2 summarize our conclusions. In the local feature detection area we felt that priorities should lie with the construction, design, and development of image and feature models. A second priority ought to be the actual data-set selection and the design of operational validation techniques. A third should be investigation of these feature integration mechanisms again; that is, compute more structural description of image patterns and put together the results of these local analyses. Then fourth, the effects of preprocessing on feature detection should be considered.

The other major topic was ground control point library priorities. Here, we felt that the first thing that needs to be looked at is what the content would be of such a library. Would it be an extended version of what's planned to be made available now, in terms of including standard types of chips you have now, or things like chain codes of shapes, information about texture and spectral content? A second effort should be creating an automatic selection system for a single sensor (based around a data base management system, feasibility study in that area). A third possibility is dynamic ground control pattern libraries; the idea here being that as you use chips over and over again, you begin to collect information about not only the reliability of particular points for rectification, but also information on the what patterns would be derived from map information only. Thus, when you start looking at different types of sensors, and try to use these patterns to rectify, you can collect information about the actual spectral properties on the ground for that type of sensor. Furthermore, you can integrate that into the definition of that chip and use it for subsequent selections. Then a fourth priority, a much longer range task, is to look at the feasibility of multisensor systems that have a much larger data base. Here we have to really face up to the problem

of whether or not you really can effectively construct patterns which can be used across sensors.

In Figure 3 we tried to show course approximations to times that should be allocated to these tasks and their ordering in time; i.e., which one can overlap, and which necessarily proceed others for logical or cost reasons.

1. IMAGE AND FEATURE MODELS

2. DATA-SET SELECTION AND OPERATIONAL VALIDATION

3. FEATURE INTEGRATION MECHANISMS TO COMPUTE MORE STRUCTURAL DESCRIPTION OF IMAGE PATTERNS

4. EFFECT OF PREPROCESSING ON FEATURE DETECTION

FIGURE 1. LOCAL FEATURE DETECTION - PRIORITIES

GCP LIBRARY DESIGN AND DEVELOPMENT/TESTING

1. INITIAL PATTERN CONTENT

   - STANDARD CHIPS

   - CHAIN CODES OF SHAPES

   - TEXTURE

   - SPECTRAL CONTENT

2. SINGLE-SENSOR OBMS FEASIBILITY

3. DYNAMIC GCP LIBRARIES

4. FEASIBILITY OF MULTISENSOR SYSTEMS

FIGURE 2. GCP LIBRARIES - PRIORITIES

FIGURE 3. TIME FRAME

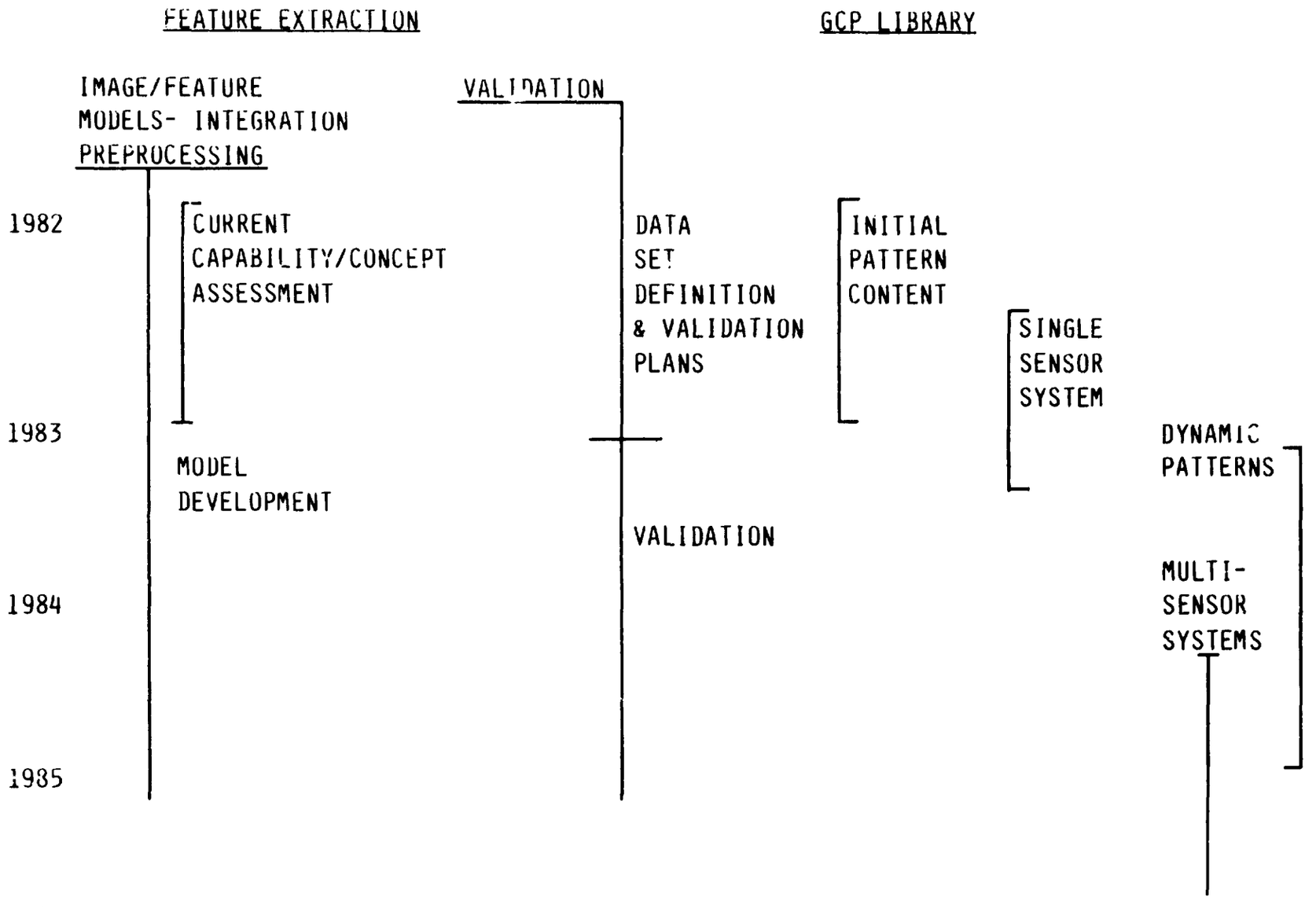

N82 28703

3.4 REPORT OF THE SUBPANEL ON INTER-IMA MATCHING

The inter-image matching panel met for two sessions to define research needs in this subject area for earth resource observation systems. The panel consisted of:

Mr. H. K. Ramapriyan
NASA/GSFC

Mr. R. Bryan Erb
JSC

Ms. June Thormodsgard
USGS

Mr. Jerry M. Cantril
Computer Sciences-Technicolor Associates

Mr. Frederick W. McCaleb
NASA/GSFC

Mr. George Austin
Lockheed

Mr. Donald Brandshaft
Santa Barbara Research Center

Mr. Paul F. Maynard
Earth Satellite Corporation

Mr. Terry Silverberg
U of MD

Mr. Richard Sigman
Department of Agriculture

Professor Laveen Kanal
U of MD

The survey paper prepared by R. Wolfe and R. Juday provided a good overview of the state of the art and requirements. The panel concentrated upon developing the design of and rationale for research efforts in this area.

3.4.1 Recommended Research

Six research areas were identified by the panel and are described below:

I. Correlation Considerations

The issues to be addressed under this topic are those relating to matching small sections of images (or information derived from images) to other images (or map-derived information). We recommend considering the following topics: a) types of correlation algorithms, b) preprocessing techniques, c) limits on subpixed accuracy, d) relief and atmospheric refraction effects, e) evaluation of success rate, f) evaluation of accuracy.

We are aware of various matching and preprocessing techniques as indicated in the survey paper. However, a study is still needed to compare these from the points of view of interactions among them and their effects on accuracy of matches. A study should be made of the theoretical limits on the subpixed accuracy that can be achieved given that the images are sampled data. The validity of techniques used for estimating "subpixel offsets" (e.g., surface fitting) for matching maps should be examined. The effects of relief and atmospheric refraction on the image-matching process should be quantified, especially in relation to higher resolution sensors. Techniques should be developed for estimating probabilities of image matching success, false-alarm and miss rates.

The correlation techniques to be considered should include "nonraster" data types. Extraction of image features to match with "digital map" representations should be considered due to its potential for a common data base for multiple sensors. Different data types may require different algorithms. Both sensor data correlation and the required preprocessing should be studied. A tradeoff study should be made to find the optimum combination of preprocessing correlation and surface fitting for offset estimation in relation to various sensor types (resolution, spectral characteristics, geometrics), ground characteristics, and imaging seasons.

If correlation techniques guaranteeing successful image matching are not available and verified, the specifications such as the Thematic Mapper equipment of .3 (relative) and .5 (absolute) accuracy cannot be met. It has been shown that hard specifications such as these imply high ground system costs. Therefore it is necessary to establish realizability of such accuracies so that we either not be as stringent with the specifications and let users "live with" the errors, or come up with techniques for achieving and verifying the accuracies. Multisensor image matching and image to nonimage data matching techniques have the potential of saving the effort needed in building multiple control point libraries.

Items a through d listed below constitute a coherent group. The prioritization should be in terms of theoretical work and the experiments to be performed on various sensor types, data types, etc The sequence of events should be as follows: a) create a common software brary to be shared among researchers; b) perform theoretical studies of : pixed accuracies, relief distortions and atmospheric refraction effects; c) identify sensor types and experimental data sets (synthetic and real) to be used; d) conduct tests of technicians and trade off studies.

II. Study to determine interaction of inter-image matching procedures and selection of GCPs for a given sensor.

The types of GCPs which should be selected for future libraries will most likely depend not only on the characteristics of the GCP, but also on the matching procedures in which the GCPs will be used. For remote sensing data from a given sensor, an experimental design with the following analysis elements is proposed: a) preprocessing procedure analysis, b) inter-image matching factors analysis (correlation measure, correlation peak determination, match reject/accept criteria), c) GCP factors analysis (type of GCP, season and scene characteristics of base chip, season and scene characteristics of test chip).

Within each factor combination, chip pairs with known image-to-image matches (determined manually) will be subjected to the processing factors. Measured response data for the experimental design will be matches and summary statistics (average, dispersion, percentiles) of the difference between true offset and automatically determined offset for nonrejected matches, and measures of the temporal stability of matching performance. The benefits of the above described study are that the study conclusions will provide guidance in selection of GCPs for future libraries. The penalties for not performing the study is that future GCP libraries will be built but will have low success rate in automatically registering data.

III. Global multisensor control point library feasibility study.

If ground control points are to be used to rectify and/or register future remotely sensed image data, the feasibility of a highly automated, global, multisensor control point library should be determined. Such a system should incorporate improved methods of loading control points, improved user access (including the capability for users to interactively load their own control points from remote terminals), standard control point formats, and a multisensor data base.

A global multisensor control point library would reduce the operational costs associated with precision rectification and registration of future sensor systems. In addition, the capability for users to load special sets of GCPs and access the GCP library allows the user to guarantee the rectification and/or registration accuracy of specific data sets of interest to him.

The initial capital outlay to implement such a system would probably be in excess of $10 million. In addition, multisensor registration may well not be easy to achieve.

IV. Multiple Control Point Considerations

Elevation of observed control point mismatches to an image-level mismatch characterization is effected by fitting a distortion function to the GCP offsets. This distortion function could arise from (1) inadequacy in a priori definition of the geometrical model (e.g., not including scan anomalies, terrain effects, atmospheric differential refraction, etc.), (2) from an incomplete characterization of its form (e.g., role is modeled as third-order in time but the data is first order), or (3) the case that the a priori model is properly characterized but with imprecise parameters (e.g., polynominal coefficients are refined with GCP data). Characterization of the model dictates the optimal sizing and placement of control points. The possibility of undetected GCP outliers (i.e., erroneous matches) dictates the need for estimation techniques beyond conventional least squares.

The proposed research would investigate the effect of number and distribution of control points required as an effect of image (sensor) characteristics adequacy of fit to an a priori model or selection of degree or model for warping function in an adaptive sense. The adaptive capability will reduce the number of correlations required for mapping well ordered data sets and consequently the processing time or equipment complexity while extending the capability to handle diverse data sets at limited throughput rates.

The following specific areas are recommended: a) Investigate spatial distortion filtering; derive new techniques or expand existing techniques, e.g. Kahlman filtering; b) Test polynomial rubber sheeting in terms of compromise between order selection and reducing RMS error; c) Investigate application of robust estimation techniques to rubber-sheeting and to fitting a pricri forms; d) Investigate adaptive placement of control points, e.g., to effect minimum RMS fit errors; e) Investigate magnitude of high-frequency geometrical distortions (atmospheric distortion, sensor anomalies) and control point sizing; f) Investigate methods to overcome geometrical distortions with a GCP patch.

Candidate methods include iterative registration (correlate, remap, recorrelate, remap, etc.) and application of the affine/Fourier technique of Emmert and McGillam to determining the offset in an affinely distorted GCP.

V. Centralized System Study

A trade-off study needs to be undertaken that considers the optimal hardware configuration for image production of data derived from different sensor types with emphasis on software/hardware tradeoff for balanced computation and I/O. Of particular interest is the need to determine feasibility of developing a centralized system to perform registration and rectification for various sensors (i.e., SAR, MLA, MSS, etc.). Development of a centralized system could be the most economical and efficient approach to meet future image processing requirements.

VI. User System Studies

By using a combination of systems analysts, a survey of user experience, and experimental tests, it should be possible to determine the speedup factors a user can expect by using commercially available special purpose hardware such as array processors and bulk core memory. It should also be possible to determine whether it is economical to speed up commonly used algorithms by using simple custom electronics. This study would assist users in hardware systems design.

3.4.2 Research Priorities

Priorities for the proposed research are subdivided in Figures 1 and 2 into near- or long-term tasks. The elements listed are subsets of the six recommended research areas.

NEAR TERM

TYPES OF CORRELATION ALGORITHMS

PREPROCESSING TECHNIQUES

STUDY W.R.T. SENSOR/GEOMETRY/SPECTRAL CHARACTERISTICS/
RESOLUTION/SEASON/GROUND CHARACTERISTICS

EVALUATE SUCCESS RATE AND ACCURACY

MULTISENSOR REGISTRATION

ADAPTABILITY OF GCP'S FOR DIFFERENT SENSORS

STUDY OF SUBPIXEL ACCURACY QUESTION

STUDY OF HARDWARE ARCHITECTURE

ROBUST ESTIMATION TECHNIQUES

EVALUATION OF RELIEF DISTORTION

Figure 1. Near term recommendations for Research

LONG TERM

INVESTIGATE FEASIBILITY OF NON-
OR MINIMUM-GCP REGISTRATION
(IMPROVED SYSTEMATIC ACCURACIES)

MULTISENSOR REGISTRATION
SAR, MSS, TM, MLA
PASSIVE MICROWAVE RADIOMETER

CORRECTION OF RELIEF DISTORTION

Figure 2. Long Term Recommendations
For Research

N82 28704

3.5 REPORT OF THE SUBPANEL ON REMAPPING PROCEDURES

The remapping procedures subpanel met for two sessions to define research needs in remapping for earth resources observational systems. The panel consisted of:

Howard S. Heuberger
NASA/GSFC

Dave Nichols
JPL

Stephen G. Ungar
Goddard Institute for Space Studies

Bert Guindon
Canada

Victor Conocchioli
EROS Data Center

M. Naraghi
JPL

Christine Hlavka
NASA/ARC

Phil Cressy
NASA/GSFC

Edward Mikhail
Purdue University

Al Zobrist
JPL

3.5.1 State of Knowledge

Remapping is done by government data centers, private industry, and users. Systems developed by government data centers (e.g., MDP) deliver a few types of products which do not meet the range of needs of users. The need for subsets and mosaics of frames, map quadrangles, various map projections, etc. were documented at the 1977 Santa Maria Conference on Geobase Information System Impacts on Space Image Formats. A value-added private industry service has not developed because there is little available software and it is not profitable for a company to fund remapping software efforts. Users typically develop bits and pieces of remapping software as needed. All three types of organizations would benefit from a fundamental research effort on remapping software and systems which achieve a range of products and are modular and transportable. Related research is needed in areas of platform modeling and calibration and photogrammetric methodology for current and proposed sensors including spaceborne and airborne. Table I summarizes key problems facing the space image data user community today.

It was noted by the panel that the remapping/rectification process could be significantly aided through engineering systems improvements in attitude control, with subsequent improvement in spacecraft ephemeris modeling accuracy. Attitude/alignment error is the largest source of image rectificator error. Thermally induced relative alignment error between the image instrument and the spacecraft must be measured or actively compensated for. An alternative is to place the attitude sensors in close proximity to the image instrument to minimize misalignment effects. It was noted that attitude error can be controlled to 36 seconds with current generation star trackers and hydro. A star tracker/hydro package capable of 3 seconds accuracy could be developed. Furthermore, an ephemeris accuracy of 10 meters is possible with the NAVSTAR/GPS system. With the GPS system it would appear we will achieve 150-400 meter accuracy in the absence of ground control points. This can be contrasted with

TABLE I. Problems in Remapping

o MANY USERS DESIRE PRODUCTS IN MAP PROJECTED FORM AND USUALLY IN QUADRANGLES ORIENTED NORTH
o REMAPPING SOFTWARE IS NOT TRANSPORTABLE/EFFICIENT
o GCP LIBRARY NOT DISTRIBUTED
o QUALITY CONTROL ON STANDARD PRODUCTS (E.G., MDP) NOT SUFFICIENT
o SENSOR/PLATFORM MODELS ARE NOT COMPLETELY UNDERSTOOD OR UTILIZED
o PHOTOGRAMMETRIC RECTIFICATION MODELS FOR SINGLE AND MULTIPLE IMAGES NOT WELL DEVELOPED
o MODEL CALIBRATION DATA ARE INADEQUATE
o RECTIFICATION ACCURACY LIMITED BY INADEQUATE KNOWLEDGE/AVAILABILITY OF TERRAIN RELIEF DATA

the 10-15 meter accuracy possible without GCPs but using advanced attitude sensors and misalighment compensation and measurement on the next generation spacecraft.

3.5.2 Recommended Research

The research tasks recommended are summarized in Table II.

There is a need for state-of-the-art technology assessments prior to initiation of major programs, and the high potential return from well formulated testing of algorithms on selected data sets of actual and synthetic imagery. In addition, there is a need for SRT tasks that incorporate standard photogrammetric methodology and formulas and that more fully utilize platform and calibration data from current and proposed sensors to reproject digital imagery. The impact of improved platform stability and integration of GPS measurements on reduced ground segment processing needs to be critically assessed. The group also highlighted the need for a substantial effort in the development of remapping software and systems that are modular and transportable. This need stems from the fact that previous and current ground segment image data rectification tasks are faced with external forces difficult to resolve, namely users wanting a wide variety of map projections and data processing capabilities which private industry has not yet cost-effectively developed nor has an individual government facility efficiently supplied.

TABLE II.
RECOMMENDED RESEARCH TASKS

- o IMAGE WARPING AND ROTATION SOFTWARE AND HARDWARE SYSTEM DESIGN
- o GROUND CONTROL POINT FILES
  - MULTISENSOR APPLICABILITY
  - ALTERNATIVE CONTROL DATA SETS
  - UPDATE AND REVIEW POLICY
  - PACKAGING, FORMATS, AND ANCILLARY DATA/DISTRIBUTION METHODS
  - SPATIAL DISTRIBUTION NEEDED
- o TRANSPORTABLE SOFTWARE STANDARDS AND TOOLS
- o GENERATE SIMULATED AND STANDARD DATA SETS FOR AIRCRAFT AND SPACECRAFT IMAGERIES
- o DESIGN SIMULATION STUDY ALGORITHMS FOR RECTIFICATION OF SINGLE AND MULTIPLE IMAGES

TABLE II (CONTINUED)

o MODEL INFLUENCE OF SENSOR/PLATFORM PARAMETERS AND TERRAIN RELIEF ON RECTIFICATION ACCURACY
o DEVELOP AND IMPLEMENT PHOTOGRAMMETRIC RECTIFICATION AND BLOCK ADJUSTMENT FOR OVERLAPPING IMAGES
o DEVELOP SUITABLE TECHNIQUES FOR MOSAICKING
o RESOLVE THE REGISTRATION/RECTIFICATION SEQUENCE PROBLEMS FOR MULTITEMPORAL OVERLAYS
o DEVELOP ADVANCED ATTITUDE SENSORS
o DEVELOP TECHNIQUES FOR COMPENSATION OF RELATIVE MISALIGNMENT OF IMAGE SENSOR WITH PLATFORM SENSOR
o DEVELOP CAPABILITY TO SYSTEMATICALLY CORRECT AIRCRAFT SCANNER DATA FROM ON-BOARD ATTITUDE SENSORS

TABLE II (CONTINUED)

- USE OF MULTIPASS IMAGERY TO PRODUCE ELEVATION MODELS
- DEVELOP PLATFORM MODEL AND DTM-DRIVEN RECTIFICATION MODELS
- DEVELOP CORRESPONDENCE MEASURES FOR FINDING CONTROL POINTS BETWEEN IMAGES FROM DIFFERENT SENSORS
- ESTABLISH OPTIMIZED AIRCRAFT MISSION DESIGN ALTERNATIVES.

N82 28705

3.6 REPORT OF THE SUBPANEL ON RESAMPLING FUNCTIONS

The resampling functions subpanel met in two four-hour sessions on November 18 and 19 to define research needs in this area for earth resource observation systems. The panel consisted of:

Richard Juday
NASA/JSC

Lee Bender
USGS

Arun Prakash
General Electric

Scott Cox
NASA/GSFC

Allan Mord
Ball Aerospace

Robert H. Dye
ERIM

Henry Muse
E-Systems Inc.

Roger A. Holmes
General Motors Institute

Paul Heffner
NASA/GSFC

David Dow
NASA/NSTL

Carter Glass
Goodyear Aerospace

3.6.1 State of the Art

The state of current practice in resampling appears limited to the use of linear filters, usually cubic convolution on nearest neighbor. Less frequently used alternatives are bilinear and least squares filters. Nearest neighbor is usually the choice when low cost is important or when it is believed that other methods degrade the data. Resampling functions are established on incomplete theory. Cubic convolutions, for example, is based on a sine function but does not employ statistical noise characteristics. There are several different bases for determining the cubic convolution parameters. It is unsettled as to the "optimum" set of parameters.

Several important points related to resampling were brought up. The term "resampling" is not clearly defined. A universally agreed upon "figure of merit" does not exist. Communications between disciplines which enter the resampling problem from different directions and with different terminology is confused. Cubic convolution can not be used to fill image pixel gaps. The TM uses spine weights for this purpose. Nonlinear filter techniques are reported in the literature but do not appear to be used extensively in the civilian remote sensing community.

3.6.2 Anticipated Requirements

Improvements in the use of resampling in applications of remote sensing will require development of a sound theoretical and philosophical basis predicated on argueable cost, error, or benefit criteria. Two reasonably distinct areas of resampling usage are identifiable, with different levels of difficulty in theoretical development. Spatially periodic and complete input lattices of

sampled points to be resampled to periodic output lattices of point values describes the more tidy area of resampling. Input lattices which are irregular, including such phenomena as missing points, missing lines, skew from one line subset to another (TM extended line problem or MLA sudden yaw or pitch problem), attitude warp, and bow-tie or other mapping distortions pose a more difficult area with significant overlap with registration and rectification techniques. When such sound bases are established, the applications field will require a portable set of standard resampling codes featuring various known levels of affordability in time and money and well-designed linkages with archival data annotation blocks.

The wide range of potential applications and expanded needs for resampling versatility in new imaging sensors leads to a concern for creating standardized test data sets and ground training sites. The following steps need to be taken: a) We need to develop synthetic data sets related to specific disciplines. b) Data sets based on actual measurements should be tightly controlled both geometrically and radiometrically. Information concerning the creation of the data set should be made universally obtainable. For aircraft acquired scanner data, extensive pre- and postflight performance evaluations should be undertaken. c) Ground training sites used for evaluation of various sensor types and processing functions should be extensively mapped and photographed. Updates at reasonable intervals are mandatory. d) Experiments involving registration and rectification require precise geometric and geodetic control, sites should be surveyed to present cadastral standards. Ancillary recorded data such as DTM, soil type, etc. should be made available at a grid size smaller than the expected IFOV or spaceborne sensors. One order of magnitude smaller is desirable.

With respect to resampling algorithms, the possibility exists to construct a library of tested algorithms available from NASA/Cosmic or an alternate source. In pursuit of this goal, standards need to be developed with respect to: a) transportability, b) documentation (should include the mathematical basis of the algorithm as well as a thorough description of the algorithm itself), c) test data sets, and d) standardized performance specifications.

3.6.3 Recommended Research

Seven research areas were identified by the panel and are described below.

I. Perform a study research task to develop a theory for defining an input psf of an instrument such that upon resampling of the processed data into the desired output grid the radiometric and geometric properties are a best estimate of the true upwelling radiances. Such a theory would include noise, desired output psf, and application specific best estimate parameter.

II. Develop algorithms for estimating missing data or for ignoring missing data. Such missing data sources to be considered are: a) dead detectors in multiscanners (including MLSs), b) scanner sweep gaps, c) transmission dropouts. Such algorithms should be characterized by their effect on the output image such that the choice of procedure can be made by the user for the application being considered.

III. Perform a study on optimal resampling functions. These optimal functions may be application specific or determined for: a) radiometric accuracy,

b) geometric fidelity, c) spatial feature enhancement and extraction. Questions to be addressed include the nature of data characteristics which permit such optimality and what kind of trade-offs are made between the different kinds of optimal filter and under what conditions can an optimal filter be designed to be optimal for both radiometric accuracy and geometric fidelity.

IV. Standard Data Sets. The choice of a resampling function is problem dependent. For a complex problem, the specific effects of a given resampling function cannot be predicted by pencil-and-paper methods. As a result, a two-stage simulation with standard data sets is recommended. Both real and synthetic data sets are required because there are really two functions to be performed. The synthetic data set can be used to study the behavior of various resamplers on controlled data. We can derive various figures of merit for comparing filter performance and add controlled amounts of noise to study noise-rejection performance. Synthetic data exhibits the following properties: (a) ability to control dimensionality, (b) power spectral density, (c) type and magnitude of noise, and (d) features, etc. An authentic data set is needed to give the final level of credibility to the resampler performance. Real data is essential to uncover phenomena which cannot be anticipated by artifically contrived data. Real data should represent the problem ("Typical" scene or even "worst-cast" scene). The synthetic data set lends itself well to determining quantitative, controlled performance measures. The real-data set lends itself to qualitative (visual) comparison and discovery of gross processing artifacts.

V. The least squares resampler developed by Dye should be further developed and tested. Cost benefit analyses must also be done and clear definitions of of applicability and limitations.

VI. There is a need for merit functions for assessing resampling techniques. Various numbers and/or functions have been proposed as measures of goodness of resampling operations. Confusion exists regarding the relationships between them and what they measure. People expect that different end users will need to optimize different figures of merit, but aren't quite sure which. The research approach would: a) List and define all candidate merit functions. Perform theoretical analysis to find the relationship between them and what information they convey. b) Survey users in various disciplines to see which merit functions look most useful to each. c) Compute all promising merit functions for one or two examples of resampling. Focus on exploring the merit functions, not the resampling.

VII. Develop a benign resampling algorithm. Present "A to P" conversion for Landsat D imagery introduces problems in the "P" data that makes some users undertake the conversion themselves, or wish they could. Modern pipeline processors may make some sort of A to P conversion strongly attractive, provided that a kernal can be found which does not damage the data unacceptably. Research should be undertaken to analyze resampling althorithms to find ones which retain nearly all of the quality of the data originally collected while doing rubber sheet resampling plus filling small fixed gaps. Characterize it in terms of suitable merit functions. Design algorithms to be implemented in fast hardwired processor. Demonstrate feasibility on real data.

N82 28706

3.7 REPORT OF THE SUBPANEL ON ERROR CHARACTERIZATION AND ERROR BUDGETS

The subpanel on error characterization and error budgets met in two sessions during November 18 and 19, 1982. The panel consisted of:

Dr. John L. Barker
NASA/GSFC

Mr. Charles J. Finley
NASA Headquarters

Dr. Joseph L. Bishop
NASA Headquarters

Dr. William R. Case
NASA/GSFC

Mr. John M. Driver
JPL

Col. Alden P. Colvocoress
USGS

Mr. Arthur J. Fuchs
NASA/GSFC

Mr. Eric Beyer
General Electric

Mr. William Pictrowski
NASA Headquarters

Mr. Ken Ando
NASA Headquarters

Dr. Roy Welch
University of Georgia

Mr. Fred Billingsley
JPL

Mr. Frank Wong
MacDonald-Detweiler Associates

The ultimate objective of this end-to-end error analysis program is to maximize the utility of the data to the user by minimizing the overall positioning error in a cost effective manner. For existing land remote sensing systems, such as Landsat-D, this implies measuring and isolating the key components of error in order to predict errors in inferred output variables, and to modify, if necessary, mission operations and ground processing procedures. For future systems, such as possible multisensor multiresource missions, error analysis starts by modeling and predicting the key error sources and sensitivity in systems performance for specific products in order to assist in the design, fabrication and trade-off phases. The methodology for this error analysis must be in place during the study phase of future systems in order to fully examine both hardware and software approaches to meeting requirements.

The report is organized into two sections. The first reviews our current state of knowledge of both user positioning requirements and error models of current and proposed satellite systems. The second section gives a broad outline of the subpanel recommendations. In addition, there are two appendices. Appendix A details the implications of an assumption that a strawman 1:24,000 scale mapping requirement might be the critical driver for an operational land observing system. Appendix B is a listing of subpanel members.

3.7.1 State of Knowledge

3.7.1.1 User Requirements

Analysis of extensive user surveys on spatial and spectral requirements for an operational land observing system have recently been completed (Barker et al.

1980). There is little if any information in these surveys to quantitatively justify any specific positioning requirement. This is an indication of the need to provide for iterative interaction with informed technical and professional users since a significant mapping requirement was not anticipated. Furthermore, the majority of potential users of map quality digital imagery would not have been surveyed because neither they nor the surveyers recognized the applicability of satellite data to mapping. There were consistent requirements for 2-m data for foresters and others in the USDA. These requirements are about the same size as those needed to meet the most important mapping requirement of 1:24,000 (Barker, 1980) which was identified in a separate initial study of mapping requirements. Informal queries on foreign maps indicate that a scale of 1:50,000 is probably the one most generally used. Actual requirements for mapping from future sensors are part of an ongoing study under the ELOS activities at Goddard Space Flight Center (ERIM, 1981). Appendix 3.7.A details the implied requirements for a strawman 1:24,000 scale map.

3.7.1.2 Generic Error Source Modeling

Spacecraft systems need accurate characterization for error budget development to accuracies commensurate with cartography to NMA standards at 1:24,000 scale. Analytic orbit propagators are not yet adequate to meet the need. Assuming a minimal use of ground control points in the image registration process, the accuracy standards delineated in the following paragraphs must be met.

Ephemeris measurement capability commensurate with GPS capability (10-m position) is essential for geodetic positioning adequate to satisfy the stated user need. The operational processing of GSTDN (Goddard Space Tracking and Data Network) data and the projected processing of TDRSS data do not provide these accuracies.

Knowledge and/or control of platform dynamics to better than 0.001 deg pointing accuracy and 10^{-6} deg/s pointing stability is needed for adequate geodetic position accuracy. Landsat-D pointing control with 0.01 deg pointing control and 10^{-4} deg/s stability represents the present state of the art for nadir oriented platforms.

Sensor dynamics have been modeled to a significant extent for the scanning type instruments as discussed below under "Existing Geometric Error Analysis Models for Landsat-D".

HLA and SAR do not present any obvious dynamics problems and no significant analyses have been done to date. However, the need for continuous alignments to a few arc seconds do not allow ruling out the need for such analyses. Also, pointable imagers such as may characterize an OLOS will certainly necessitate analyses with regard to pointing dynamics and view angle aberrations. Preliminary effects of view angle are indicated by Driver (1982).

Error sources not subject to control such as earth rotation, curvature, and topographic variability have significant impact on potential geodetic position accuracy and must be modeled and compensated for error minimization.

Surface velocity and image configuration on a rotating triaxial ellipsoid must be modeled and analyzed and methods sought for error minimization.

Ground control pattern utilization is common for obtaining high-accuracy geodetic position. However, this is a costly and slow method for image registration and rapidly becomes untenable for rapid repeat coverage on a global scale, particularly for inadequate a priori estimate of geodetic position. Furthermore, adequate ground control does not exist in many parts of the world. Tentative error-compensation options have been advanced for the major sources (Driver, 1982). Significant work is needed to determine the feasibility of such compensation options or others which will enable acquisition of images with inherently accurate geodetic position on a global scale. The projected 5-10 year time scale for the development of a TM GCP (Ground Control Point) library indicates that future sensor systems of high spatial resolution must place a greatly reduced reliance on GCPs.

3.7.1.3 Existing Geometric Error Analysis Models for Landsat-D

A number of error analysis models and simulations currently exist for the Landsat-D TM image processing. These techniques can be categorized into TM sensor, attitude measurement, attitude control, spacecraft structural dynamics, Systematic Correction Data Generation, and control point error dynamics.

The TM sensor models include a dynamic simulation of the TM scan mirror assembly (including open loop and closed loop structural interaction effects), a scan line corrector dynamic simulation, and a TM optical model which categorizes off-axis pointing of each detector as a function of detector location and optical misalignments.

The attitude measurement models include jitter response (above 0.01 Hz) and models of the Attitude Control DRIRU (gyro) and the angular Displacement Sensors (ADS). These models are incorporated into a simulation which imparts attitude motion into the sensors, processes the data through prototype Attitude Data Processing software and evaluates the accuracies of the processing system. This simulation is used to determine the effects of DRIRU or ADS calibration error on overall system performance.

The attitude control model is a detailed simulation of the Attitude Control System and low-frequency (less than 7-Hz) structural dynamics. Included in this simulation are effects of the solar array drive and TDRSS antenna drive. This model has been used to estimate the attitude control pointing accuracy and the low-frequency spacecraft jitter.

The structural dynamics model is a detailed NASTRAN model of the Landsat-D spacecraft from which modal analysis is performed. This model has been verified by performing component modal tests of the TDRSS Antenna and boom, the solar array, the Instrument Module Center body (including TM and MSS Mass Simulators), and Multimission Spacecraft. This model is used to predict on orbit high-frequency (greater than or equal to 7-Hz) jitter caused by the TM and MSS mirror impacts.

The accuracy of Systematic Correction Data Generation is tested by comparing the outputs of prototype software to those of a high precision earth look point and map projection models.

The control point error dynamics analysis includes an 18-state covariance analysis and a detailed simulation of control point location errors (this simulation is currently in development). The covariance analysis and simulation include dynamic error models for ephemeris, alignment, and low-frequency attitude. The covariance analysis has been used for system studies to determine processing feasibility and the simulation will be used to test the operational control point processing software.

In addition to the above error analysis, the effects of gap resampling have been studied using simulated TM edge responses and small sections of analytically generated TM imagery. The entire resampling processing has been developed in a prototype software simulation which includes a bit-by-bit emulation of the resampling hardware.

It must be noted that these analysis models and simulations are not currently deliverable software packages. They are analysis tools used by General Electric to design and analyze the TM processing system.

3.7.2 Recommendations For Position Error Modeling Research

Four specific recommendations were made by the panel in the limited time they had to collectively discuss the issues. These are summarized below and are discussed in more detail in Sections 2.1 thru 2.4. In addition, a very preliminary assessment was made by several of the panel members of the resources that may be required to carry out the recommended research. Due to lack of time at the workshop, the full panel was not able to be consulted onto the required resources.

The recommendations are:

1. Obtain and evaluate the existing error models for Landsat-D/TM (see Section 2.1 for discussion). Expected resources required: $0.5M over 3 years with 5 MY civil service.

2. Provide iterative user involvement in system error budgeting and error model development and verification on real and synthetic data sets (see Section 2.2 for discussion). Expected resources required: $2.0M over 5 years with 20 MY civil service.

3. Develop error models for future system definition and trade-off studies on: a) sensors (MLA Advanced scanner SAR) b) spacecraft/shuttle c) processing/information (see Section 2.3 for discussion). Expected resources required: $0.5M over 3 years with 5 MY civil service.

4. Create a Positioning Error Budget Study Group (see Section 2.4 for discussion) Expected resources required: $0.1M over 5 years with 2 MY civil service.

3.7.2.1 Needed Geometric Error Analysis Model for TM

A number of potential error models may be needed to more fully characterize TM sensor and processing errors. These include:

- o A TM dynamic structural model to evaluate the critical rigid body assumption between the ADS mounting location and the TM optical axis.

- o Effects of topological variation resulting from the orbit and attitude control on the Landsat-D geodetic and temporal registration accuracies. Examination of the feasibility and desirability of developing and appending a quantitative measure of topographic variability within a TM scene as a direct or surrogate estimate of misplacement of pixels within the scene due to topography.

- o Analyses of the correlation location accuracy which can be expected from TM resolution imagery.

RECOMMENDATION - Obtain and evaluate the existing TM processing error models. This may require upgrades of the software documentation to deliverable status.

3.7.2.2 Create Interactive User Involvement In System Error Budgeting and Modeling and Verification on Real Data Sets

User "requirements" have been solicited from a variety of users, generally without consideration of costs of obtaining them, without verbalized consideration of any losses in utility if they are not met, and without verbalized consideration of parameter tradeoffs. This prevents the system engineer or scientist from being able to iterate potential system designs with the users.

To solve this problem, it is recommended that specific efforts be planned to involve the users iteratively in the generic development of error budget methodology prior to and during the mission designs.

One possible mechanism for facilitating cooperative involvement of the user and system engineer in the translation of user requirements into system performance specification, subsystem allocations, error budgets, and error models would be the use of mission system analytical models which are capable of producing an output which simulates the actual data that the user would get from the mission. A capability could be generated for processing undistorted input scenes (real and synthetic) and creating distorted output scenes in the users data format. The analytical processing would be done using system models for the mission and would include distorting estimates due to all sources of error that the platform, instrument, and ground and flight data processing systems would introduce. In the early stages of mission definition and instrument conceptual design, these analytical studies could be based on simple models of the mission and the distortions. As the instrument and mission design forms up, the models and analysis could be updated and take on more complexity if required. If the models also contained representatives of the other electro-optical imaging characteristics of the instrument, the analysis would produce an output image containing representations of all radiometric, spatial, and geodetic instrument data degradations. A byproduct of this capability would be that analytically produced data products would be obtained which could be used to aid in the design and testing of ground data processing systems. The expected result of an effort to produce this overall mission analytical simulation would be to provide a systematic, highly visible, interactive approach for establishing optimum instrument performance specifications

and error budgets which could also be used to assess expected instrument system performance including ground data processing algorithms.

Before embarking on extensive data collection schemes, however, a study should be conducted to see if synthetic scenes can contribute to the understanding of positioning errors for future systems.

3.7.2.3 Identify Strawman Mission For Modeling Key Error Sources And Identify Hardware and Software Methods For Minimizing Errors

In order to identify the hardware and software technology needed to obtain the registration and rectification requirements expected of advanced spaceborne imaging systems, complete end-to-end system trade-off studies need to be performed. These can be accomplished by identifying several strawman missions which are expected to drive image registration/rectification technology and by performing system studies on these missions. The system studies would identify the error budgets for the missions which would include errors due to the orbit, platform, sensor dynamics, scene variability, as well as errors introduced due to any processing of data on-board or on the ground. Trade-off studies could then be performed using system registration/rectification models for the missions with all sources of error modeled. Trade-offs involving hardware and software improvements for positioning error minimization could be made in the areas of:

1. Platform attitude and ephemeris measurements/estimation/control
2. Instrument pointing and alignment measurement/estimation/control
3. On-board or ground processing of the data, including GCPs. To register and rectify the images both within one mission data set as well as with other data sets.

3.7.2.4 Develop Error Models for Future System Definition and Trade-off Studies

3.7.2.4.1 Sensors

a) MLA: The MLA sensor operates in an integrating mode where the cross-track scene is simultaneously imaged with fixed geometry and perspective. Unlike a scanner, any spacecraft or sensor induced jitter or other disturbance will affect all detectors equally. No pixel-to-pixel high-frequency jitter correction will be necessary.

The fixed nature of the detectors and the simultaneous imaging in the cross-track direction should substantially reduce the processing required to produce geometrically correct images.

Studies should be conducted to investigate the geometric effects which are unique to an MLA-type sensor and its impact on rectification. One-dimensional dewarping algorithms to simplify geometric rectification and the residual errors resulting from attitude and ephemeris uncertainties should be investigated. In order to realize the advantage of the smaller pixels and higher resolving capability provided by an MLA sensor, concurrent improvements in the capabilities of the spacecraft attitude and ephemeris system will be required.

Models and sensor simulations need to be developed to investigate and identify the trade-offs between sensor ACS and ephemeris determination improvements and sensor performance for various pixel size. Semiempirical models of the sensor/spacecraft interface including dynamic effects should be developed to determine whether some form of active jitter or image motion compensation will be needed to realize the 10-m baseline resolution of MLA.

A potential pushbroom sensor containing a central segment(s) of higher resolution end segments could provide the possibility of obtaining high-resolution data for mapping and ground control point location concurrently with acquisition of the "normal" multispectral data.

The added high-precision data allows the possibility of minimizing geometric errors related to ground point locations (as well as providing the possibility for subpixel texture information). This also provides data which can be used to iterate spacecraft attitude models, at higher precision than would the normal lower resolution data.

b) Advanced Scanner: Scanning instruments such as MSS and TM create unique problems with error budgeting and modeling. There is a suggestion that TM could be modified to more than double its IFOV by increasing the number of detectors in the focal plane and putting on more scan mirror monitors (to better identify the scan profile).

Due to the torques involved in the scanning process, especially for highly efficient scanning techniques, high-frequency positioning errors (jitter) can result from flexible body effects in the instrument as well as in the platform to which it is attached. Techniques need to be developed, beyond those which exist in the Landsat-D/TM, for budgeting and modeling these errors. This would include the possibility of having to measure the instrument boresight including effects of individual optical element motions.

In addition, techniques need to be developed to reduce the magnitude of the positioning errors through the use of actively controlled optical elements and the isolation of instrument dynamics from those of the platform.

c) SAR: Unlike the scanning and MLA sensors, a significant amount of geometric distortion can result in the signal processing segment. The purpose of such segments is to convert from a raw image into a slant range/azimuth image.

Processing errors include: a) estimation of FM rate, b) azimuth compression technique (time domain, frequency domain), c) range cell migration correction and associated interpolation, d) block processing techniques, e) doppler centered tracking accuracy, and f) terrain variation effect on point target locations.

To map the slant range/azimuth image to a certain map projection, remapping and resampling errors are introduced. Remapping does not require attitude information. Remapping errors include: a) ephemeris, b) earth curvature, c) GCP accuracy, d) terrain variation, and e) atmospheric refraction (very severe for VOIR).

A focus of the study on the following is recommended: a) Study various signal processing algorithms on the raw image and their tradeoffs. Develop error

models. Investigate how error propagates from one processing stage to the another. b) Develop remapping/resampling error model. c) Develop an error model for using DTM for rectification/registration. In SAR imagery, terrain distortion is more severe than it is in the scanner imagery. d) Study the effect of terrain variation on processing algorithms, since terrain affects the target trajectory in the raw image. e) For planetary missions, no GCPs will be available. Study whether automatic focusing on strip-to-strip registration can be used to replace ephemeris parameters. Develop an error model.

3.7.2.4.2 Spacecraft/Shuttle

Spacecraft and Shuttle models for future systems should include advanced sensor and system models which would provide increased knowledge of spacecraft induced error sources which are commensurate with increased resolution expected from advanced sensors. Spacecraft subsystems which must be modeled include: a) attitude measurement systems, b) attitude control systems, c) orbit determination systems, d) orbit control systems, e) sensor alignment measurement systems, f) time and frequency standards.

Examples of future spacecraft systems which must be modeled are: advanced star trackers, advanced horizon sensors, fine pointing sun sensors, and ultrastable gyro systems. The above system models are components of the attitude measurements and control systems.

An instrument could be provided which, through repeated overlapping images of the ground, can provide the data to allow generation of attitude history without reference to maps or other surveyed ground points. This will be of particular use in shuttle or aircraft systems. This data, in turn, allows image line-by-line data to be positioned properly in the rectified image. This will allow modifications of the error budget by providing images with greater geometric accuracy.

For orbit measurement and control systems, on-board orbit determination using Global Positioning System (GPS) data or utilizing Tracking and Data Relay Satellite System (TDRSS) data must be modeled. Accelerometer packages to measure nonconservative accelerations could be modeled along with on-board actuators for orbit control. Ephemeris data resulting from precision ground based orbit determination must also be modeled.

Time maintenance and time transfer systems to be modeled include GPS and TDRSS time transfer and/or flying with stable oscillators.

Studies resulting from the development of the above models would be the generation of error budgets for varying system configuration and performing end-to-end trade-off studies such as cost impacts and enabling technology impacts of improving spacecraft system knowledge such that GCP processing can be either eliminated or substantially reduced.

3.7.2.4.3 Processing/Information

Often in the design and development of processing systems there are not strong and specific identifications as to what function must be performed to insure that the end product is most beneficial to the user needs. The functions may

be isolated to hardware or software components but must include/reflect algorithms that eliminate/reduce errors from the data source, sensor/spacecraft.

The development of supporting processing system should begin concurrent with the development of the sensor/spacecraft at or during the phase A/B studies. If the processing system was designed with the understanding of possible error enhancement to this data source, then data recovery, correction, and error removal procedures should be considered in the design.

Some factors that must be considered in this processing system to eliminate/minimize errors are: a) ephemeris accuracy/variations, b) sensor alignment, c) data translation, d) geometric errors and systematic correction (orbit/attitude), e) scanning sensor's rates, gaps, and profile, f) lessons learned from historical sensors, g) image corrlation/matching techniques, h) temporal processing/data translation, i) pixel errors, j) cartographic and mosaic errors, k) integration of multisensor data, l) ground control point/pointing tolerances, m) edge detection/image sharpness/filtering, and n) image warping.

The processing system should also give the users some information about what corrections, algorithms, filters, etc., were used in correlating the product. This data will facilitate the user understanding and use of the final product.

3.7.2.4.4 Study Group

It is recommended that a permanent Ad Hoc Earth Observing System Error Analysis Working Group be established at the NASA Headquarters level. The purpose of this working group is to advise the NASA Program Manager on technical requirements and limitations relating to error characterization, error budgets, and system verification.

Establishment of this working group is imperative to preserve continuity in the Earth Observing Systems Techniques and Data Processing Development Program. The working group members should be comprised of system designers and system users and be representative of the government, industry, and university communities.

3.7.3 References

Barker, J. L., P. J. Cressy, C. C. Schnetzler and V. V. Salomonson, Characterizing User Requirements for Future Land Observing Satellites, GSFC TM 83-867, Dec. 1980. Goddard Space Flight Center, Greenbelt, MD.

ERIM, Cartographic Mapping Study, Contract No. NAS 5C26820 with GSFC under FLOS/MLA study, 1981.

Barker, J., ECOsystems International, Inc., Summary Report in Support of Benefit/Value Assessment from Improved Sensor Performance, July 30, 1980. P.O. Box 225 Gambrills, MD, Contract with GSFC on Mapping Requirements for Operational Land Observing Systems, 1980.

Driver, J. M., "A Case for Inherent Geometric and Geodetic Accuracy in Remotely Sensed UNIR and SWIR Imaging Products", Proc. of NASA Workshop on Registration and Rectification, (to be published in March 1982).

3.7.4 Appendices to Error Characterization and Error Budgets Subpanel

APPENDIX A

POSITIONING REQUIREMENTS COMPATIBLE WITH NMAS FOR 1:24,000 TOPOGRAPHIC MAPS

The basic assumption in this exercise is to set-up a "straw-man" mission designed to provide data suitable for meeting National Map Accuracy Standards NMAS for 1:24,000 scale topographic and planimetric map products. This is a geometric requirement rather than a nonmetric informational requirement. In addition, the change is to produce these x, y, z earth system coordinate data with minimal reference to ground control. The geometric requirements will, in turn, define the IFOV of the system. As will be noted, an IFOV of about 3-4 m will be required to meet the accuracy standards. The following statements are not meant to advocate this system, but rather to consider its feasibility in terms of error budgets and error budget modeling methodology.

I. National map accuracy standards (NMAS) for 1:24,000 scale map products require:

a. 90% of horizontal positions (for well defined points) be established to $\pm$12 m of their correct location. The acceptable $RMSE_{X,Y}$ (68%) is approximately $\pm$7 m.

b. 90% of elevations interpolated from contour lines will be correct to within 1/2 the contour interval (CI). The acceptable RMSE will therefore be equal to the C.I./3.3. As most 1:24,000 scale maps have C.I. of 5, 10, 20, or 40 feet (depending on the terrain), the RMSE requirements are approximately $\pm$0.5, 1, 2, and 4 m respectively. Because elevation standards are the most stringent requirement, they will control system design.

II. System Design Assumptions

a. The assumed imaging system consists of three line-array cameras operating in the pushbroom mode. Two of the cameras will be oriented approximately 24 degrees from the vertical in a convergent arrangement in order to provide fore and aft coverage while the third camera is aligned vertically so as to produce near orthographic coverage of the terrain. This configuration results in potential base-height (B/H) ratios of 1.0 for fore and aft stereopairs and 0.49 when the vertical is employed with either fore or aft coverage.

b. Altitude - set between 500 and 1000 km, e.g., 713 km or 919 km

c. IFOV $\leq$ 5 m: to be determined by NMAS, geometric and correlation requirements, rather than by nonmetric information requirements

d. Swath - TBD in the range 60-185 km

e. The feasibility of a mission designed to most of the above NMAS requirements remains to be demonstrated.

III. Error Considerations and Sources

a. Maximum RMSEs
   1. Horizontal (X,Y) = ± 7 m
   2. Vertical (Z) = ± 3 m (for 10 m C.I.)

b. Error Considerations

   1. General

      The mission must provide essentially error-free geometric and radiometric data if accurate map products are to be developed. In theory, the spacecraft and sensor systems can be controlled so as to preclude any special ground based computer processing (to correct the errors), which is both expensive and subject to delay.

      The parameters which influence the geometric fidelity of the image data include pointing control rate motion stability and jitter. The satellite line-array sensor system (which is recording the terrain as a series of cross-track strips) must be pointed correctly and held stable for approximately 100 seconds to produce error-free stereo imagery. Any perturbation of the sensor system during the recording period will cause displacements/errors in the data which, in turn, may require geometric correction and resampling at a ground receiving station. Rotation of the spacecraft about the X, Y, and Z axes (roll, pitch, and yaw, respectively), although constrained, will cause deformations of the nominal image format as will changes in spacecraft altitude and oblateness of the Earth.

   2. Earth Rotation

      The basic imaging concept is straightforward, however, because of Earth rotation, the satellite ground track is no longer a simple great-circle route, and the vertical, fore, and aft cameras will not automatically image the same ground area, even with a perfectly stable satellite. In order to obtain ground coverage common to any two cameras, a yaw motion must be introduced into the camera/spacecraft. This motion is not constant, but must vary with latitude to maintain image registration.

   3. Oblate Earth

      The basic imaging concept assumes a spherical Earth and a circular satellite orbit so that a constant satellite altitude is maintained. In practice, however, we must consider an oblate spheroid and an orbit which only approximates to a circle due to variations in the gravitational effect of the Earth. These deviations from the ideal situation create increases in slant range and altitude which in turn cause scale variations as the satellite increases its distance from the equator.

4. Resampling Considerations

Any image deformations which are not maintained within specified limits must be removed in the ground data processing. The pixels may be resized, reshaped, realigned, and new grey level values determined to provide the necessary image quality. An objective of the mission is to acquire error-free data which will eliminate the need for resampling (and minimize geometric corrections).

5. Spacecraft Performance

In order to reach some conclusions regarding the geometric accuracy, it is necessary to consider the pointing, stability, and jitter of the spacecraft and its sensors. Pointing accuracy is the factor most often quoted as a measure of geometric performance. For example, the Multimission Modular Spacecraft (MMS) which will be employed for Landsat-D has a pointing accuracy specification of ± 0.01 degree (one sigma). Thus, by design, the summation of all factors that include the attitude control subsystem should have a root-mean-square value of less than the design specification. In addition, other factors such as orbit determination, timing, sensor alignment with the attitude control system (including the effects of thermal instabilities), and the torquing motions of a tape recorder (if used) influence the pointing geometry. Satellite stability is an important consideration. Extremely tight tolerance will be required (e.g., 10^{-6} deg/sec at the 3T level or better).

The third problem is jitter. The satellite will respond to dynamic disturbances caused by antenna or solar panel motions as would a tuning fork. Response is frequency dependent because of structural qualities. No moving parts are desired.

IV. Error Sources Influencing the Mapping Potential

From a cartographic viewpoint, the most significant problems are likely to be of a geometric nature. Consequently, it is desirable to determine the accuracy to which X, Y, Z terrain coordiantes can be recovered from image data recorded by the proposed line-array system.

Major factors which appear to determine the accuracy to which X, Y, and Z terrain coordiantes can be recovered are listed below: An attempt is made to estimate quantitatively the magnitudes of the starred error sources in terms of root-mean-square error (RMSE).

1. Position of S/C Error Sources
2. Pointing of sensors and attitude control
3. Satellite velocity
4. Precision of measurement
5. Reliability of ground control
6. Earth curvature, atmospheric refraction, etc.
7. Processing equipment and procedures
8. Adjustment Procedures

a) Position of S/C

The positional determination of the S/C must be within 10 m for all three axes.

b) Sensor Pointing and Attitude Control

Nominal correction values for a constant bias can be determined with the aid of ground control. In many areas of the world, however, ground control is inadequate for mapping tasks, and alternative methods of establishing corrections for pointing errors must be made available.

Attitude stability and maintenance of controlled yaw are critical parameters. In order to achieve acceptable coordinate values with reasonable consistency, a worst-case correction rate value of 10^{-6} deg/sec at the 3-sigma level of confidence is required. This equates to ± 4 m (approximately 1 pixel) over the 10-minute time interval and should provide an epipolar condition.

The overall requirement for pointing determination accuracy is better than one arc sec (~4 m from 800 km). This will be a major source of error.

c) Satellite Velocity

Variation in satellite velocity can be accounted for if accurate timing marks can be incorporated in the data. GPS is a source for time data.

d) Measurement Error

Measurement or correlation error must be limited to well within one-half the $RMSE_{X,Y}$ value in order to meet vertical accuracy requirements. Thus, RMSEs in horizontal measurement must be on the order of 1-2 m.

e) Reliability of Ground Control

It is anticipated that a minimum number of ground control points will be required. However, they will have to be accurate to 1-2 m. Possibilities for autotriangulation exist, but error figures cannot be determined at this time.

f) Earth Curvature and Refraction

Errors due to Earth curvature and refraction are systematic and can be corrected during processing. The influence of variations in refraction is negligible for a narrow (5^{o}) field-of-view.

There are other error sources which will need to be considered. However, the magnitude of the above errors in relation to NMAS can be estimated.

3.8 REPORT OF THE SUBPANEL ON METHODS OF VERIFICATION*

The methods of verification subpanel met for two 4-hour sessions on November 18 and 19, 1981, to define research needs in this area for Earth resource observational systems. The panel consisted of:

John C. Lyon
GSFC

Maria Kalcic
NASA/NSTL

B.R. Seyfarth
NASA/NSTL

John Sos
NASA/GSFC

Gerald Grebowsky
NASA/GSFC

John Snyde
USGS

Ai Chun Fang
NASA Headquarters

R.B. MacDonald
NASA/JSC

William P. Clark
NASA/GSFC

Len Gaydos
USGS

3.8.1 State of Knowledge

We refer to verification as a production oriented question because we are not really doing verification for the uses of research activities. We're trying to verify output data products from a production system for production oriented users. Included in that class of production oriented users is the production system itself, i.e., quality control of output. Verification is not a well defined problem. We're just beginning to focus on understanding what we're talking about. Therefore we recommend a program to improve the state of understanding and of the meaning of verification and the application of verification procedures to a variety of sensor systems.

3.8.2 Recommended Research

The topics of interest that were identified are very strongly interrelated. To show this we have developed a task flow in Figures 1, 2, and 3. Other than having done that, it was found that there is no real priority scheme that could be assigned, as this is an integrated activity designed to provide more understanding into what needs to be done in image rectification. Task one (Figure 1) is to develop verification procedures. Task two (Figure 2) involves an experimental hands-on data demonstration and evaluation of those procedures in a controlled test-bed experiment. For task one, the flow is as follows: you first need to identify what performance measures you're really concerned about. We've suggested a handful of starters such as the number of control points, residual correlation mapped across an image, and the distribution of errors within the image plane for individual and coincident sets of images. Using that information, it is possible to go directly to existing data and compile real and synthetic data sets that can address that problem. In parallel, one can review the current verification procedures that are used.

*Edited oral presentation.

This is not a trivial undertaking in spite of the fact that the current verification procedures are very casual and unsystematic. There are some activties going on in other fields, in mapping especially, that have orderly procedures that are not exactly remote sensing oriented procedures but can be training grounds for a subsequent task. From the existing procedures, identify and recommend the ones on hand that are usable in an operational system, develop additional techniques necessary with some synthetic data sets, and perform specific tests on individual package procedures to analyse the results. The end result then is a set of verfication procedures and software, or at least algorithms, that can be useable. The output of that then goes to task two, which is the verification experiment.

Task two is the end-to-end test experiment. The very first step in task two is to identify the test bed. There are several possible options and it's a matter of timing and some other subtle details that relate to exactly what procedures and requirements you want to develop. The output of the first part of task one delineates what verification you really want to do that will help to choose a test-bed. The obvious choices on-hand are Landsat MSS data or, in the near future, the Landsat-D data processing capabilities. The next step is to design the experiment to test verification procedures. This procedure in development and selection activity is from task one, as it is essentially task one that feeds into that knowledge of the sensor system itself, including error budgets, as a part of establishing the design. Then it's a matter of implementing the experiment. The output of doing software oriented measurements on standardized data sets allows one to perform some accuracy measurements. You want to pay very close attention to the feedback loop so that when you get part way there you start looking at the users on the other side of the information system that need to see the results to help better understand what they really wanted to have asked you for in verification. That finally leads you to moving one step beyond to the internal problem and you start deriving the error sources observed and finally report and assess the results of this experiment.

Tables I and II outline in summary form the required elements for each task described.

TABLE I

TASK 1
DEVELOP VERIFICATION PROCEDURES

1. IDENTIFY PERFORMANCE MEASURES

   - O DETERMINE CHARACTERISTICS OF GEOMETRIC DISTORTIONS
   - O ANALYZE DISTORTIONS RELATIVE TO USER PERFORMANCE NEEDS
   - O IDENTIFY REQUIRED VERIFICATION PARAMETERS AND THEIR EXPECTED VALUE RANGES
   - C OTHER

2. REVIEW CURRENT VERIFICATION APPROACHES

   - O REVIEW EVALUATION PROCEDURES CURRENTLY USED IN REMOTE SENSING COMMUNITY AND RELATED FIELDS (E.G., PROGRAMMETRY)

3. COMPILE SYNTHETIC AND REAL DATA SETS

   - O SYNTHETIC DATA SETS SIMULATING DIFFERENT KINDS AND RANGES OF DISTORTIONS
   - O REAL DATA SETS WITH KNOWN DISTORTION CHARACTERISTICS

4. IDENTIFY RECOMMENDED VERIFICATION TECHNIQUES

   - O ANALYZE DERIVED VERIFICATION REQUIREMENTS VS CURRENT APPROACHES
   - O IDENTIFY VERIFICATION APPROACHES

TABLE I (CONTINUED)

5. DEVELOP ADDITIONAL TECHNIQUES

   - MSS, FM, MLA, MICROWAVE, STEREO, ETC.

6. UNIT-TEST TECHNIQUES

TABLE II

IMAGE VERIFICATION END-TO-END TEST

SELECT REMOTE SENSING SYSTEM(S) AS TEST-BED

DESIGN EXPERIMENT

- SELECT IDENTIFIED PROCEDURES (TASK 1)
- ESTABLISH SUCCESS CRITERIA

IMPLEMENTATION

- MEASURE ACHIEVED ACCURACIES OF PRODUCTS
  - SYSTEMATIC ERRORS
  - RANDOM ERRORS
  - COMPUTATIONAL SYSTEM IMPRECISIONS
- DERIVE ERROR SOURCE ESTIMATES
  - SPACE SEGMENT (S/C/, INSTRUMENT)
  - GROUND SEGMENT
- RECOMMEND PROCESS CHANGES TO IMPROVE PRODUCT QUALITY

EVALUATION

- USER CHECK OF ACCURACY REPORT
- SENSOR SYSTEM DEVELOPER OPINION OF RECOMMENDED CHANGES

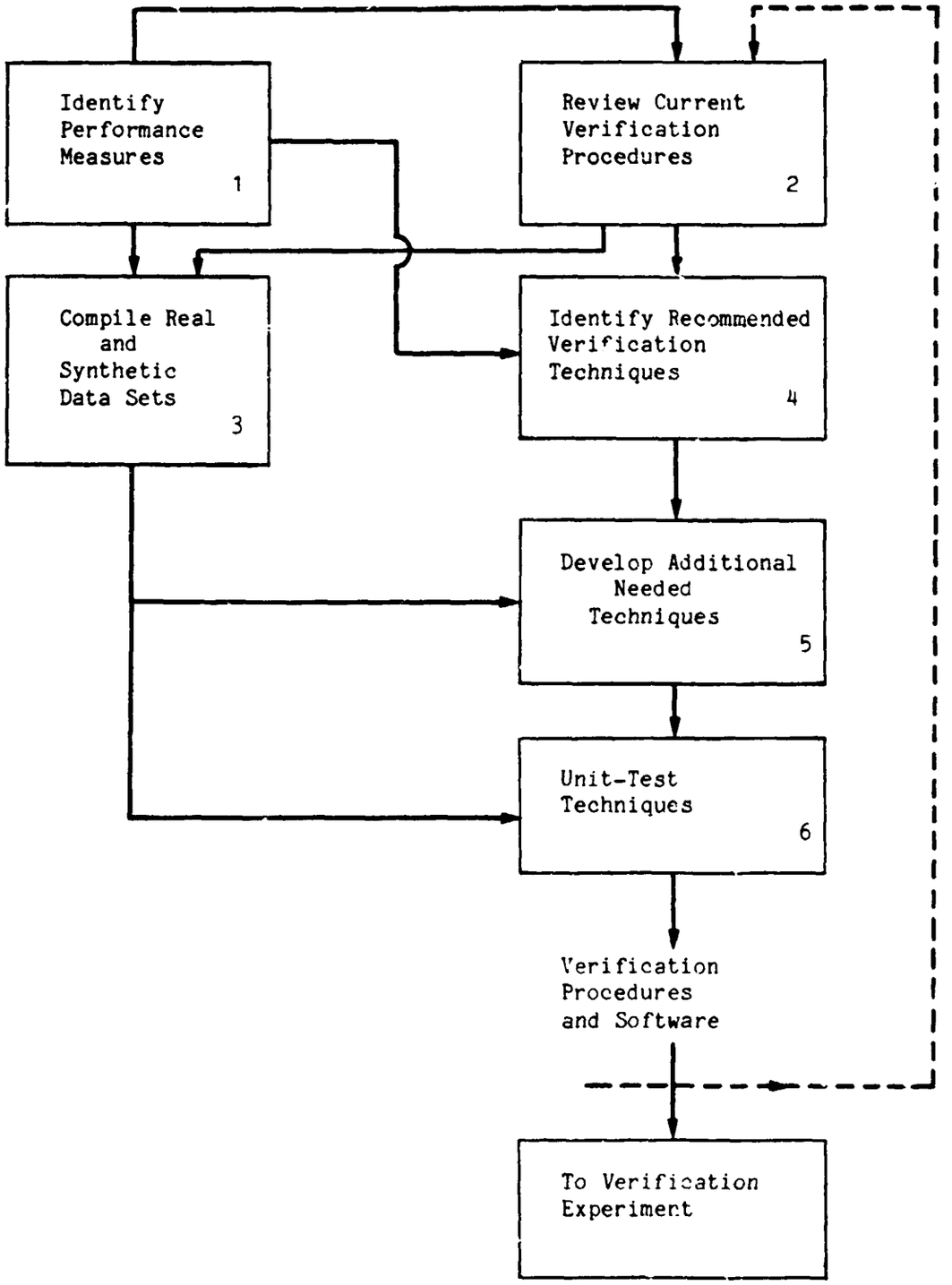

FIGURE 1. TASK ONE: ACTIVITY FLOW

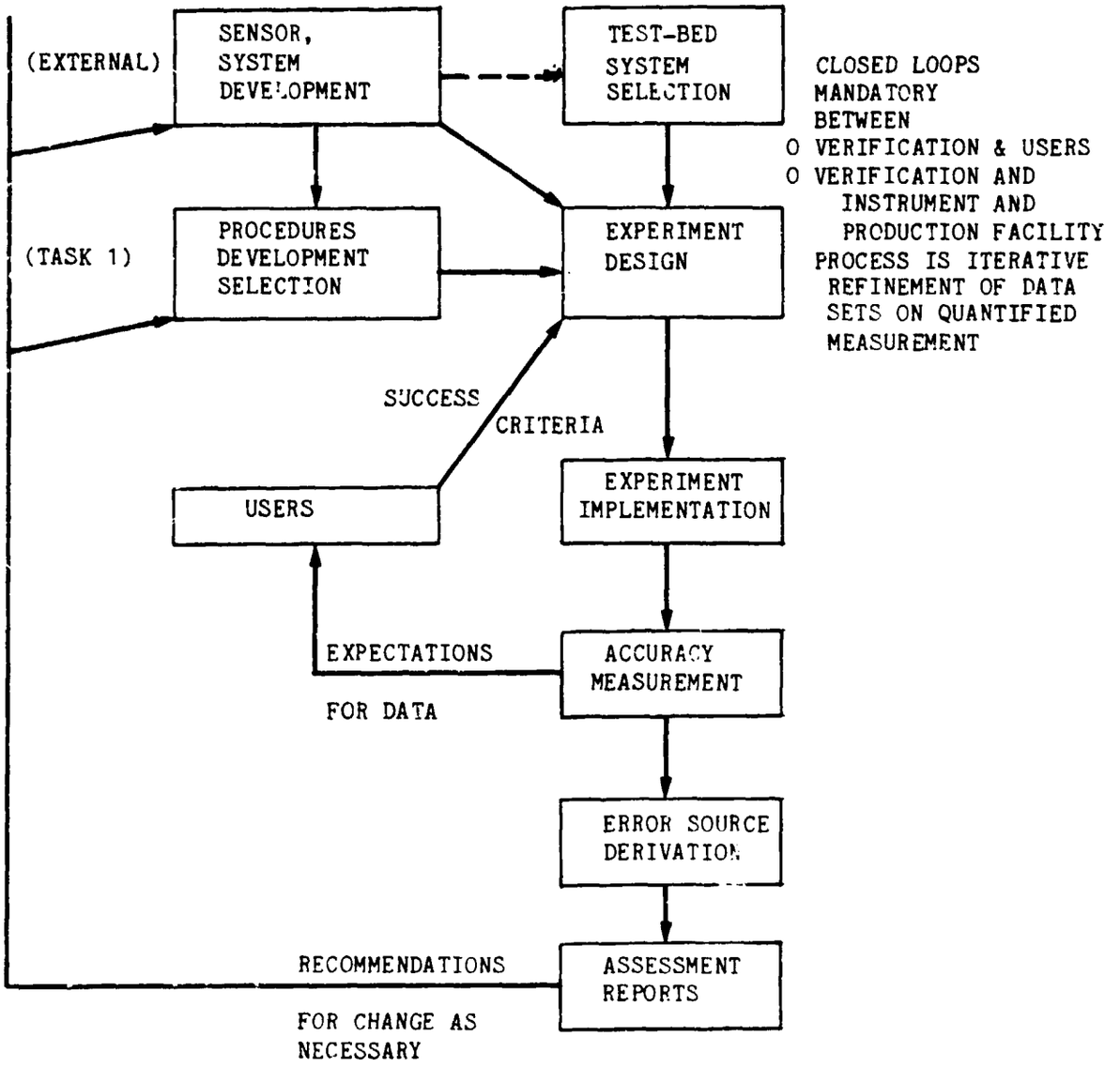

FIGURE 2. IMAGE VERIFICATION END-TO-END TESTING

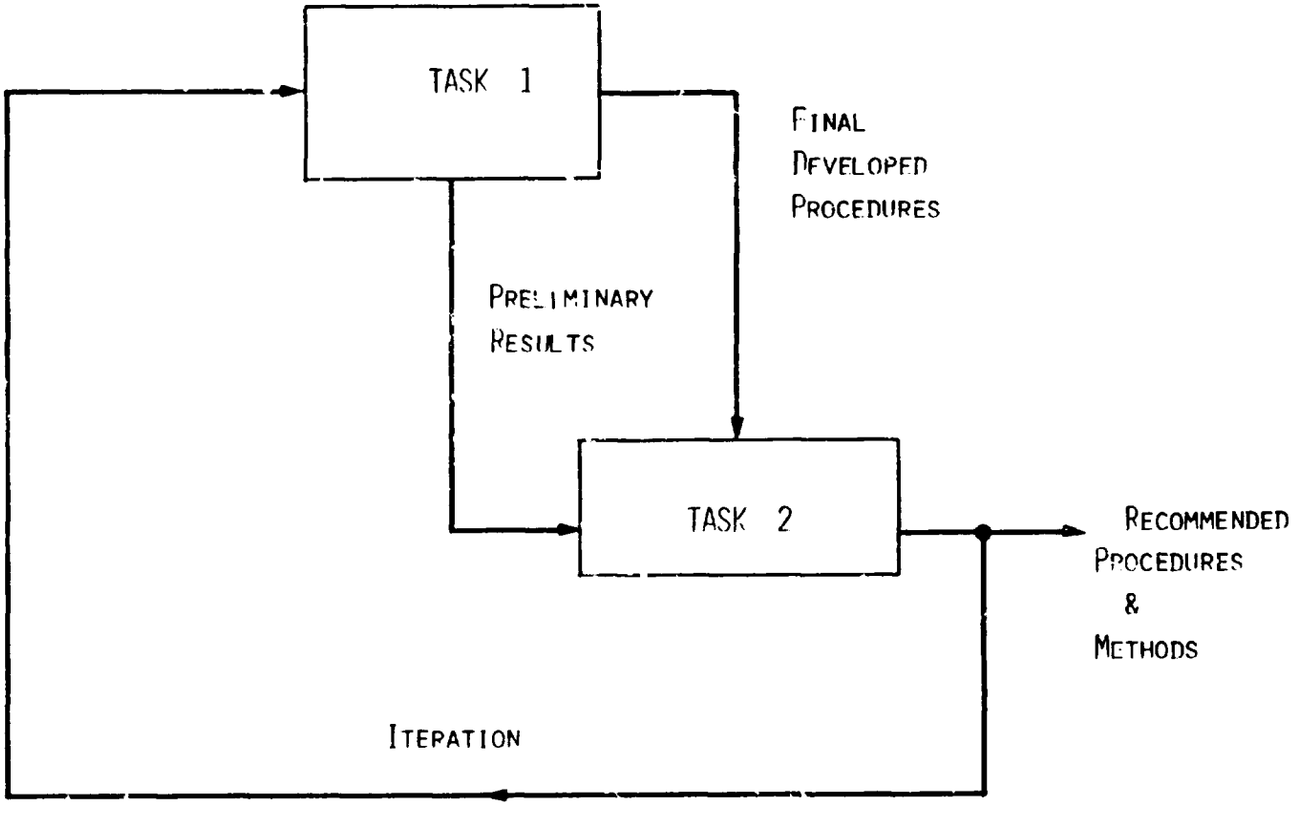

FIGURE 3. PROGRAM TASK FLOW

4.0 PRESENTATIONS ON USER NEEDS

4.1 INTRODUCTION

It was the purpose of the User Needs presentations to discuss the implications of satellite image positional accuracy capabilities upon their discipline's use of the data. Discipline experts discussed the manner in which data are incorporated into their inventory, decision, or analysis models and operations. For each discipline area, monitoring and data base integration strategies were discussed; in particular, implications for registration and rectification requirements. In addition, the discussants pointed out the potential benefit that might accrue from improved registration/rectification accuracy. Where applicable, the discipline experts discussed their desire to implement multitemporal, multistage, and multisensor data sources for addressing a problem, as these imply constraints on registration and rectification accuracies. Users also described the experimental design (e.g., sample segments or full-image area coverage) used to analyze a problem.

4.2 USDA REGISTRATION AND RECTIFICATION REQUIREMENTS

Rich Allen
Statistical Reporting Service
U.S. Department of Agriculture

I am glad to have this opportunity to discuss some of the requirements of the United States Department of Agriculture (USDA) for accuracy of aerospace acquired data, and specifically, requirements for registration and rectification of remotely-sensed data acquired by space vehicles, such as Landsat, the Shuttle, and so on. The views presented are for the most part my observations and opinions from work completed to date or underway in the Department of Agriculture since only limited documentation exists on the accuracy required for registration and rectification as such.

Definition of Terms

It is perhaps wise to first explain the terms to be used in the presentation. One of the organizers of this conference indicated that registration refers to the accuracy of location of identical points on repeated acquisitions of data while rectification refers to accuracy of matching remotely-sensed data with corresponding points on the ground. Many people in the USDA use the expression "registration" for matching both scene-to-scene and scene-to-map and use the term "rectification" for indicating accuracy of maps or aerial photographs. I will try to utilize the announced definitions of this conference, although I may often use the broader term of positional accuracy to refer to the USDA requirements.

Remotely-Sensed Data: An Important Source of Information

In order to carry out its assigned missions, the Department of Agriculture must have information relating to observations of soils, crops, and other physical features. For example, we identify and map soil types, monitor conservation practices and conservation structures (construction of new conservation measures), and verify farmers' compliance with planting restrictions under various farm programs. All of these types of information programs have intense, detailed data needs. Aerial photography has been utilized to provide much of the needed data for these programs. An aerospace sensor is not now foreseen as being capable of providing comparable data required in such domestic programs. I emphasize the term "domestic". However, we can characterize the positional accuracy needs of these information programs, and, in so doing, may provide general guidance for aerospace sensor development programs.

If an aerospace sensor could be developed, budgets permitting, to satisfy some of the needs above, the sensor would have to have spatial resolution similar to that of aerial photography to be judged useful to USDA or, better put, to be competitive with aerial photography. By the same analogy, the USDA would need the same rectification as with aerial photography to utilize that spatial resolution.

Satellite Data Uniquely Suited for Specific Programs

However, in this paper I want to concentrate on four other types of information programs, ones for which satellite data are being routinely used or at least currently investigated for possible use later. In these, because of the unique features of the requirements, satellite data are "competitive" with other information sources. These four information programs are:

Foreign crop forecasting
Domestic crop acreage estimation
Forestry information applications
Rangeland condition evaluations

I believe there are similarities and contrasts among these four programs which will illustrate the range of USDA requirements for positional accuracy. These examples are not considered an exhaustive list of USDA's present interests for satellite data.

Landsat and Metsat Data Used for Foreign Crop Condition Assessment

The foreign crop assessment approach that I wish to discuss is that of the Foreign Agriculture Service's Foreign Commodity Condition Assessment Division (FCCAD). FCCAD is processing large numbers of satellite scenes from both Landsat and meterological satellites in its current efforts to monitor areal extent of anomolies and production of major crops in selected foreign areas. For the most part, FCCAD does not have access to ground collected data. Thus, it depends on sequential reviews of satellite data as a procedure for monitoring and evaluating change.

Presently FCCAD does not perform any registration on the data received from Landsat in the form of High Density Computer Compatible Tapes. Each scene is reduced to subsets or samples of full resolution data by subsampling rows and pixels to obtain a data set better suited to FCCAD's processing capabilities. This reduced data set can then be displayed on image processing equipment as raw data or by transformation to vegetative indexes, which measure the "greenness" of plants, and are indicators of plant vigor and stress. The Vegetative Index approach is an effort to standardize responses and allow meaningful comparisons within seasons and across seasons.

Much of the present analysis of FCCAD involves calculation of average values for a 25-mile square grid. Without registration procedures there may be some shifting of points included in a particular grid cell from acquisition to acquisition but the shifting should be minor compared to the size of the grid cells.

The approach of not performing any additional registration of satellite acquired data is not an optimum one in FCCAD's point of view but, in light of equipment and personnel resources and the volume of data being handled, it is not feasible to devote time to registration activities at this time. If each satellite scene obtained had consistently "high" positional accuracy to the ground and thus to corresponding scenes of other data, FCCAD would be interested in a major refinement of its multitemporal analysis procedure. A much better measure of changes in conditions or crop area could be obtained if the data for specific sampling segments could be matched throughout a season and across seasons. Based on the spatial resolution of the current Landsat Multispectral Scanner (MSS) this might mean use of a segment of approximately 15-20 square miles in size. All data, including vegetative indices or other transformations, would be calculated and stored for these segments.

Based on the size of the segment visualized it would be reasonable to employ this sampling approach if satellite data were rectified or registered to a mean accuracy of plus or minus one pixel. This error in location from acquisition to acquisition would be small enough compared to the size of the segment to be effective.

If a sensor with finer spatial resolution was available, the FCCAD's accuracy requirement would likely remain at one pixel. Its approach might become one of utilizing somewhat smaller segment sizes but with data registered within one pixel to maintain the same relative accuracy.

Use of Landsat Data for Domestic Crop Acreage Assessment

Research into the use of Landsat MSS data by the Statistical Reporting Service (SRS) for the improvement of acreage estimates of major domestic crops provides a marked contrast to the procedures for foreign areas. Unlike the Foreign Agricultural Service which often has no ground data, SRS has available a sample of ground observation data which by itself provides an accurate estimate of acreage.

One of the major inputs to crop acreage estimates in the United States is the June Enumerative Survey (JES) conducted each year by SRS in the 48 coterminous states. The JES is a probability area frame survey in which each state has been divided into land use strata

based on percentage of cultivation and type of land use. Each stratum is divided into sampling units, with size depending on the stratum. In the Midwest, intensive agricultural sampling units or segments are typically one square mile in size. Segment sizes in rangeland strata are much larger and sizes in residential or commercial strata are much smaller.

The JES survey provides estimates of major crop acreages with coefficients of variation ranging from 2.5 percent to 6.0 percent in major states. At the U.S. level these coefficients of variation are as small as 1.0 - 2.0 percent.

Thus, the SRS research effort is an attempt to improve the precision for relatively "good" acreage estimates. This is in direct contrast to the foreign crop forecasting problem. Therefore, the demands for positional accuracy are much higher.

SRS uses the JES data for training of classification algorithms, for testing of classification results, and for estimation of acreage through a regression estimator. The JES data is closely edited on a field-by-field basis. Random fields of each cover of interest are selected for training. The SRS approach extracts interior pixels of training fields for labelling so it is important to ensure accuracy of field locations. The training fields for a scene are selected from JES segments located throughout the scene. Typically, about 30 segments are available in a Landsat scene.

Once an analyst is satisfied with the clustering relationships for a scene, each segment in the scene and the entire scene (within boundaries of geographic counties and excluding cloud covered areas) is classified. The classification of segments provides the correlation results and regression parameters. The classification of the entire scene provides an adjustment for any differences in crop acreage relationship between the sample of segments and the entire population of possible segments within the scene.

The measure of effectiveness of using the satellite data which is most meaningful to SRS is relative efficiency. Relative efficiency is defined as the variance of the direct expansion (ground) estimate divided by the variance of the regression estimator. This number indicates what amount of additional ground data would be needed to give an estimate with the same precision as the regression estimator. Relative efficiencies in practice have ranged from 2.0 to 4.0 or higher in most situations.

The research approach that SRS uses for full state estimates (having a revised acreage estimate by the end of the estimation season) was first utilized in 1978 for the State of Iowa and has been utilized in 1980 for Iowa and Kansas and in 1981 for those two States plus Missouri and Oklahoma. Based on those experiences and other research SRS is projecting an approach of utilizing unitemporal satellite data for estimates rather than a multitemporal approach. While multitemporal data have been used and would give better discrimination for some classification problems, it is rare to obtain cloud free images during the growing season in the Midwest or the Great Plains. Some counties in a scene are usually lost due to clouds in the growing season acquisition date and if other counties are lost in a spring scene, the resultant multitemporal data set might not have enough segments remaining for proper training and estimation. SRS does have multitemporal procedures on line and will use them for land cover estimates and for crop research in areas such as California.

Two Stages of Registration Insure Positional Accuracy of Landsat MSS Data

Since the SRS approach depends on the use of very specific data sets of fields for training it is important to match as exactly as possible the satellite and ground locations. Presently SRS uses two stages of "registration" to insure adequate positional accuracy of Landsat MSS data. The first effort is called "global registration". A sample of points is selected across the scene from transparency data products. The corresponding points on U.S. Geological Survey base maps are located and digitized. A mathematical transformation is calculated to adjust all pixels to predicted longitude/latitude locations. This process usually ends up with rectification within $\pm$ 1 to 2 pixels across the scene. This operation is now performed by the Remote Sensing Branch Support Staff and most scenes can be "registered" in about 3 hours, even with editing of outlier points.

The second stage of "registration" is called "local segment shifting" by SRS. This step is necessary because of scanner anomalies. A gray scale of a window enclosing the predicted segment is created. An overlay of the digitized segment and field boundaries (printed on transparent paper at satellite data scale and with boundaries adjusted for the path of the satellite) is then placed over the gray scale. The overlay is shifted as needed to properly line up segment and field boundaries. This row and column shift from predicted location is then utilized to correctly identify the most accurate location of each field in the segment.

This segment shifting processing results in rectification of data to the nearest one half pixel for each segment. No adjustment is made in the remainder of the scene from the first stage of rectification. Experience has shown that the segment shifting adjustments will normally vary across the scene in direction and size of shifts so the segment shifting results are not imposed on the global rectification stage. This indicates that although SRS needs ½ pixel accuracy for small scale classification of segments the accuracy of 1 pixel or so across the rest of the scene is sufficient. There are large numbers of pixels associated with each stratum within a scene and the 1 pixel potential error is not a critical percentage. SRS would replace either or both of these "registration" procedures if data received always were rectified to the appropriate accuracy.

The "40 meter Accuracy Requirement" Better Stated as "One-Half Pixel"

This might be the best point to discuss the USDA's "40 meter accuracy requirement". In the Domestic Crops and Land Cover project of the AgRISTARS research program SRS has specified 40 meters as the desired precision for both scene-to-scene and scene-to-map applications which utilize LANDSAT MSS data. Some members of the remote sensing community have interpreted this to be an absolute (ground distance) requirement. The 40 meters originated because the resolution of the MSS data as acquired was assumed to be 80 meters. Accuracy to a half pixel would be 40 meters. Regardless of effective pixel size due to processing techniques the 40 meters was regarded as the feasible positional accuracy for Landsat MSS. The 40 meters is not the important measure; the half pixel is the key.

SRS regards one half pixel to be the accuracy goal for any advanced resolution sensor. This is due to the emphasis on providing the most accurate data set for training on a field to field basis. A sensor with improved resolution such as the thematic mapper should result in improved classification results but only if a pure training and testing set can be insured.

Rectification and Registration in Forestry Applications

The U.S. Forest Service (USFS) has utilized aerial photography as a tool in providing a number of inventory and management needs. The USFS approach is similar to that of SRS in that ground observation data is or can be available. The USFS objectives are more demanding than those of SRS because a variety of types of information are desired. Instead of just estimating area of forest land there is a need for determination of forest types, measures of change, and some detailed estimates such as the annual increment of production. USFS is often interested in production estimates for land with considerable slope and varied terrain in contrast to the relatively level terrain for crop acreage estimates.

The USFS has a major research effort referred to as the Multiresource Inventory Methods Pilot Test (MIMPT) which is an advanced demonstration of the use of Landsat satellite technology to supplement current methods of conducting recurrent inventories over large land areas. The base program has established a large sample of sites which can be periodically monitored for change and new resource assessment data. Much of the necessary data can be obtained from aerial photography and thousands of aerial photos are utilized when new photography acquisitions become available. The basic reference link is provided by 7-1/2 minute USGS quadrangle maps.

Results from the first phases of the MIMPT indicated that computer interpreted Landsat data combined with data from a relatively few aerial photos can replace human interpretation of thousands of photos to estimate land use acreages. When the Landsat data are included in a geographic information system with other data sources such as topographic and soils data, it is possible to derive variables needed in multiresource surveys such as sedimentation, disturbances and other spatial dependencies such as public use, utilities, or transportation infrastructures.

Because of the combination of Landsat data with other data in a geographic information system and the necessity to extract specific features from ground sites for training and evaluation, very precise rectification of imagery is needed. The desired accuracy of the USFS would be rectification of 95 percent of all pixels within ground sites to within $\pm$ 20 meters of true ground location. This very precise goal is because of the irregular shape of many features being observed and of other variables such as topographic information. In this specific application, the agency requirement is stated in terms of a physical measurement irrespective of pixel size, in contrast to FAS and SRS requirements.

Rangeland Applications: One Pixel Accuracy May be Sufficient

The last aerospace remote sensing application of the USDA that I would like to discuss is that of assessing rangeland condition. I will not attempt to discuss any programs of the Bureau of Land Management related to rangeland carrying capacity or other measures. Instead I want to focus on research interests of USDA, notably of the Soil Conservation Service (SCS). Although some initial work has been done, research is basically just getting underway, and conclusions on accuracy are tentative at best.

SCS is interested in such factors as conservation needs of rangeland as well as range condition and biomass production. There is a great need for additional research into methods for using satellite data in proper estimation of range condition. Rangeland typically is quite variable across an area of any size. That is, there is not usually the homogeneity that would be expected in a field of a planted crop. Sampling procedures tend to obtain kinds and amounts of biomass for relatively small areas, often for points selected by the range conservationist on the ground which are "representative" of conditions observed.

One approach which might be helpful in the evaluation of range condition would be to utilize an image as a stratification device and to collect biomass data for each stratum present in the image. However, while range condition changes with longer term use or abuse, range biomass changes quickly with rapid response to rainfall and drought. By the time an image is available, interpreted, and in the hands of a person on the ground, the conditions may have changed drastically. Thus, some type of sampling approach is needed which collects data at or near the time of satellite data acquisition to be related by cluster analysis or some other type of estimation based on the satellite data.

One approach which might be applicable to the SCS information needs is to collect data over some type of grid pattern. Collection of data for enough grid points and collection of biomass (or other information) for a large enough unit at each point to minimize within sampling unit variation would allow estimation through a poststratification approach with the strata based on the satellite imagery. Satellite data has not proven to be easily integrated into SCS's conventional range site and condition surveys, nor to the point sample used in SCS national inventories but it is an approach of great current interest.

Since there will not usually be "field" boundaries in rangeland areas it will not be possible to match data as precisely as in the SRS crop acreage approach or the Forest Service approach. Rectification of one pixel accuracy or registration at one pixel accuray if repetitive coverages are interpreted should be adequate in light with the type of ground data available. As with most other USDA applications registration or rectification needs for new sensors would continue to be in terms of one pixel accuracy rather than a specification in terms of absolute meters.

Sampling vs. Whole Frame Studies

One topic of interest to individuals concerned with registration and rectification is differences in requirements for sampling approaches versus whole frame studies. From my viewpoint of USDA requirements I feel that the answer is contained in the examples cited. For estimation purposes when whole frame estimates are created in the SRS approach or when FAS desires to make estimates for areas without corresponding ground data positional accuracy of one pixel is sufficient. However, when sampling approaches are used such as the SRS matching of ground data with corresponding satellite data for training or the USFS matching of various ground data items with satellite data, positional accuracy is more critical and one-half pixel or greater accuracy is needed. These accuracy requirements are relative to the purposes for which the data are used and should be thought of as related to the resolution of each sensor and not normally as absolute measures of ground distances.

Need for Standardized Concepts

As a closing note I would like to comment on observations from the communications during the past two years and particularly from the past few weeks in preparing for this workshop. Disagreement in definition of terms was already addressed in the opening of the paper. Even within the use of a particular definition I think there is considerable misunderstanding.

Although the term "RMS" error as in "40 meters RMS" is widely used, I would question if all people using it have the same concept of how to calculate RMS error and I feel from discussions many users are misunderstanding what is meant by a certain result. At least as used by the Statistical Reporting Service RMS error is a confidence interval statement that two-thirds of all pixels will be within plus or minus that distance from "true" location where true location may come from another data scene or from map locations. Since so much emphasis has been placed on this RMS concept some data users may believe that "all" data are within this RMS bound. SRS has adopted a procedure of calculating a second accuracy measure, the R-90 criterion, which is the radius of a circle containing 90 percent of the deviations of pixels from "true" locations. This is felt to convey more information about the accuracy of registration or rectification than just the RMS calculation. In the Forest Service example above, the data users are interested in knowing how precisely 95 percent of all points are registered which is essentially a distance equal to twice the RMS measure.

If this workshop can publicize procedures for properly measuring or calculating positional accuracy and can educate users as to proper interpretation of accuracy statements, it will have accomplished a great deal.

REFERENCES

Since little is documented in U.S. Department of Agriculture publications on registration and rectification requirements an alternate approach is to provide a list of references for more information about applications of the various Agencies. Below are listed individuals who can be contacted for the remote sensing approachs mentioned in this paper.

Foreign Agriculture Service - Bobby Spires, Chief, Analysis Branch, Foreign Commodity Condition Assessment Division, Foreign Agriculture Service, 1050 Bay Area Blvd., Houston, Texas 77058.

U.S. Forest Service - Edgar Chapman, Cartographer, Nationwide Forestry Applications Program, U.S. Forest Service, 1050 Bay Area Blvd., Houston, Texas 77058.

Soil Conservation Service - Bill Hance, Soil Conservationist, Inventory and Monitoring Staff, Soil Conservation Service, 12th & Independence Avenue, S.W., 5241 South Building, Washington, D.C. 20250.

Statistical Reporting Service - Rich Allen, Chief, Remote Sensing Branch, Remote Sensing Branch, Statistical Reporting Service, 12th & Independence Avenue, S.W., Room 4832 South Building, Washington, D.C. 20250.

USDA REGISTRATION/RECTIFICATION REQUIREMENTS

APPLICATION	STATUS	GROUND DATA	INFORMATION REQUIREMENTS	ACCURACY DESIRED
FOREIGN CROP MONITORING	IN OPERATION*	NONE	CONTINUOUS EVALUATION OF CROP ACREAGES AND CROP STRESS FOR SAMPLE SEGMENTS	± 1 PIXEL
DOMESTIC CROP ACREAGE ESTIMATES	FULL STATE RESEARCH	CROPS OR LAND USE BY FIELDS IN SAMPLE SEGMENTS	CLASSIFICATION OF ALL PIXELS IN ENTIRE SCENES	± 1 PIXEL
			MATCHING OF GROUND DATA AND SATELLITE DATA FOR TRAINING	± 1/2 PIXEL
FORESTLAND INVENTORIES	PILOT TEST	SOILS, TOPOGRAPHY AND LAND USE BY SAMPLE SEGMENTS	OVERLAY OF SEVERAL DIFFERENT TYPES OF INFORMATION	± 20 METERS
RANGELAND CONDITION ASSESSMENT	PROPOSED RESEARCH	OBSERVATIONS FOR SAMPLE PLOTS	EVALUATION OF BOTH CONDITION (LONG RANGE) AND CURRENT BIOMASS	± 1 PIXEL

* CURRENT OPERATION INVOLVES NO REGISTRATION OR RECTIFICATION EFFORTS

4.3 NEEDS FOR REGISTRATION AND RECTIFICATION OF SATELLITE IMAGERY FOR LAND USE AND LAND COVER AND HYDROLOGIC APPLICATIONS

Leonard Gaydos
U.S. Geological Survey
240-8 Ames Research Center
Moffett Field, California 94035

ABSTRACT

Many land use and land cover and hydrologic applications require the use of satellite imagery and data. Maps and aggregations are made from the data which might exist in concert with other data in a geographic information system. Users have basic needs for registration and rectification of satellite imagery related to specifying, reformatting, and overlaying the data. Presently, each user must accomplish these tasks independetly because the present data pre-processing system is unreliable. These data are sufficient for users who must expand much effort in registering data. These users have requirements concerning projection, pixel size, resampling, and accuracy, and most would be satisfied with data that met the standards proposed, but not consistently achieved, for the present system.

APPLICATIONS

Users of satellite imagery for land use and land cover or hydrologic applications generally are interested in interpreting land use and land cover from the data to produce maps and aggregations, inputting the data into geographic information systems, detecting changes over time, and using derived data in a predictive fashion (ORI, 1979). Ancillary data is important in every step, and the ability to incorporate such data into the analysis process directly increases utility for such applications as inventorying, managing, and planning. The hydrologic application is really a subset of the more general land use and land cover applications. Frequently, particular categories of land use and land cover affecting the hydrologic budget (such as irrigated agricultural land) are mapped and utilized in hydrologic models (much like geographic information systems) with other data sets.

Those users interested in areas at least as large as multiple counties make most use of the present generation of satellite imagery. We'll focus on one prospective user, the U.S. Geological Survey (USGS) to illustrate needs most other users can be expected to have.

USGS began a program in 1974 to map land use and land cover for the entire Nation, to digitize the resulting polygons, and to make the data available for use in geographic information systems. Although present satellite data have not been used as primary source material, data from improved sensor packages may prove more useful. In any case, satellite data can be expected to play a role in identifying areas in need of updating (Milazzo, 1980), and Landsat digital data have proved valuable in regions where other source material is lacking (Morrissey and Ennis, 1981).

The Water Resources Division of USGS has a need to map specific categories of land use and land cover as an indirect estimator of water use. Field measurements and ancillary data are used to determine the average amount of water used for each hectare of a given land use and land cover. The resulting data are used in combination with other layers of data such as recharge and discharge rates and present saturated thickness of an aquifer to predict future saturated thickness given alternative water use plans. A hydrologic model is used for this application in much the same way that a geographic information system might be used to relate multiple layers of data.

BASIC NEEDS

Land use and land cover and hydrologic applications users have basic needs for registration and rectification of satellite imagery: (1) the users must be able to locate data when given geographic coordinates or to find geographic coordinates given data coordinates; (2) it must be possible to reformat the data to fit given map projections; and (3) scenes of the same area from different times must overlay each other.

Presently, each user solves these problems independently with different degrees of success and at varying costs. Typically the user first finds a set of 30 or more control points for a Landsat scene that can be identified on the imagery and on the largest scale maps available. Methods differ somewhat. Some users identify control points from a digital display. Others print grayscales for areas surrounding likely control points on a lineprinter and correlated them with topographic maps. Map coordinates are determined either through measurement with a latitude/longitude or Universal Tranverse Mercator (UTM) coordinates. Second- or third-degree polynomials are computed by analyzing the control points and discarding those inaccurately determined. These polynomials are used as a calibration file to reference the data. Other data can then be registered to the Landsat base through the calibration file even though that base might not actually be itself registered to a map.

For display of Landsat data as a map, though, additional processing is required. Typically the Landsat data will be registered to a map base by specifying a calibration, desired projection, size of final pixel, and resampling scheme. This precision reformatting is a computation-intensive procedure, and not every user is able to accomplish it.

Utilizing more than one Landsat scene, either to make use of temporal data in an analysis or to detect change with time, requires registration of one scene to another. Again there are many ways to accomplish this task. Some users use a modified version of the control point procedure used to register a scene with a map. A digital display or grayscales are used to find control points on each scene, and calibration is established based on a polynomial. A less labor-intensive method is to use autocorrelation techniques, sometimes combined with gradient identification techniques, on a computer. This automatically finds control points that

can then be edited. In addition to the labor-saving advantages, such systems frequently are able to find many more control points than the analyst is willing to find, say 200 rather than 50. Errors are usually less with more control After the equations are established, one scene is considered the primary scene, and the other is "rubber-sheeted" to fit it, another intensive computation job. Though many users are interested in using multitemporal data for analysis, not everyone can carry it out, given the procedures required today.

PRESENT LIMITATION

The techniques outlined to solve present registration problems have been around for at least 5 years. EDIPS data have been around for 2 1/2 years. The same procedures used before EDIPS to solve registration problems are as necessary today as they were before EDIPS became available. There was great hope that the Master Data Processor (MDP) at Goddard would alleviate many of the problems and provide reliably corrected data. The Landsat data corrected with ground control points (GCP) chosen from 1:24,000-scale maps would be less than one pixel for 90 percent of the pixels in a scene. The Landsat Data-Users' Handbook also specified that the temporal registration offsets between two Landsat scenes having the same path-row location would be less than 0.5 pixel for 90 percent of the pixels in a scene (U.S. Geological Survey, 1979).

Those expectations are not being met. The U.S. Department of Agriculture (USDA) compared registration quality of data from the MDP with their existing techniques and found that though they could not rely on it presently, they could use data from the MDP as a starting point for an algorithm that will automatically register their segment data to the Landsat data (Graham and Luebbe, 1981). The Digital Mapping of Irrigated Cropland Technique Testing project found it necessary to manually find control points for 36 scenes in 1981 because results of testing those Landsat scenes from the High Plains with assessment ratings of three or more where an average of no closer than ten pixels from their expected locations (Koch, 1981).

The same Technique Testing project found that not only was it necessary to find control points for scene to scene registration (multitemporal), but there was more rotation of one scene with respect to another with data from he MDP than there had ever been before. The increase in rotation requires much more computer memory for the "rubber sheeting" algorithm. On the positive side, EDIPS data seemed to correlate better than the old x-format, presumably because of the cubic convolution resampling. This improvement was also noted by the California Irrigated Lands Technique Testing project (E. Bauer, oral commun., 1981).

REQUIREMENTS

The present registration of Landsat data products is insufficient for the needs of land use and land cover and hydrologic applications users. Much time and effort is expended in referencing the data by map coordinates,

precision correcting it to fit maps, and overlaying multitemporal scenes. These steps could be simplified considerably and even eliminated for some applications if data was really available in registered form. User demands in this area are not extreme. It is fair to presume that those users presently dissatisfied with data registered by the MDP would be quite happy with data that was registered as well as they are able to obtain themselves.

Users with the ability to perform their own geometric corrections would like Landsat data to come with information on image geometry (like listings of ground control points) sufficient for facilitating geometric corrections (ORI, 1979). This is probably the most common demand heard. Users would like listings of control points. With them they could perform their own corrections, check out the accuracies of the system-corrected data, or use them as a base for adding additional points when warranted.

Those users who would like system-corrected data are divided on questions of projection, rotation, pixel size, resampling, and accuracy. Let's look at each question, one at a time.

All users will not be satisfied with data in just one standard projection, such as the Space Oblique Mercator (SOM) or Hotine Oblique Mercator (HOM). Users of satellite imagery for land use and land cover applications commonly use the data in combination with maps and other data layers. These maps can be cast on a variety of projections, such as the UTM, Albers Conical Equal Area, or polar Stereographic. What is needed is the ability to convert data from one projection to another. USGS does have a package of computer routines, in Fortran, designed to permit the transformtion of coordinate pairs from one map projection to another (U.S. Geological Survey, 1981). Data could be made available in one or two standard projections with software available to the users to convert to other projections, or the list of available projections could be expanded for the standard product with the user specifying his choice.

Most users would prefer land use and land cover data that are geometrically corrected before delivery to them to be rotated to North. Though arguments can be made that rotation is not really necessary, the fact remains that when working with maps, and other data levels derived from maps, rotated data is a pleasure and unrotated data is a pain. There is a dilemna with respect to this question. When working with an entire Landsat scene or multiple scenes, a rotated data set is substantially larger than its unrotated counterpart. When working with a map quadrangle, though, rotated data fit just right, and substantially more data are needed to get the quadrangle coverage from the unrotated set. So it really depends on the application and the size of the area of concern. The question of rotation should really be an option for the user. This would satisfy all.

Three pixel sizes seem to vie for attention. The 57-meter square delivered with EDIPS seems to garner no real harsh feelings. Users understand that 57 meters is the resampling interval along a scan line

and they understand the logic of choosing that for the resampled pixel. There are perhaps stronger arguments to be made for going to a 50-meter square pixel since it would correspond quite nicely to UTM coordinates and be compatible with the cell size of the USGS land use and land cover data in the grid cell form. There are also those who would like to see 60-meter pixels which would be easier to compare with 30-meter thematic-mapper data.

There has also been much disagreement over resampling. Most users who do their own geometric corrections tend to use simple nearest neighbor, mostly because of cost considerations. Cubic convolution does appear to provide smoother looking data. It does so by increasing the variability of the pixel values making the data harder to compress and perhaps adversely affecting the accuracy of classification algorithms that utilize variance. Much of what resistance there is to convoluted data is probably due more to unfamiliarity with it than to other factors.

The question of accuracy is probably the single most important issue. At a minimum, users would like to know what the average accuracy of a particular product is. This is important above all else. If it is reasonable to achieve only 10-pixel accuracy for a given scene, because many 15-minute maps had to be used, the user needs to know. He can then determine whether that accuracy is sufficient for his application and improve upon it if necessary or possible. Perhaps the greatest disappointment from the AgRISTARS evaluation of data registration was the poor correlation that was found between accuracy and assessment ratings (Graham and Luebbe, 1981).

There are three distinct accuracies the user must worry about. The first involves the referencing problem. It may be necessary to extract pixels that lie within polygons digitized from a map. Most users would tell you that for this they require root-mean-square (RMS) accuracies at least as good as 1 pixel. This can be achieved, however, in two stages. The first might reference the data to within several pixels, while the second mist use local fit to achieve the sub-pixel accuracy desired.

For fitting the data to a map, the real consideration is scale. The National Map Accuracy Standard for horizontal accuracy is 0.02 inches at scales smaller than 1:20,000 (Thompson, 1979). This translates to 254 meters at 1:500,000, 127 meters at 1:250,000, and 51 meters at 1:100,000. Judging from past performance it seems reasonable to expect precision-corrected Landsat data to fall somewhere between the standards for 1:500,000- and 1:250,000-scale maps. This should be quite acceptable for most users.

In a geographic information system environment, the resolution of the coarsest unit determines the effective resolution of the entire system. Since land use and land cover data are usually at a finer resolution than other data layers, such as soils, problems with inaccurate registration of a few pixels are not especially critical on the whole. In hydrologic

C-2

applications over multi-State regions, land cover data from Landsat may be at the finest resolution of the system even though it is reported for areas as large as 1 square mile. Misregistration could be critical in particular cases, though. Identifying residential land use within a specified slope interval computed from digital elevation models of 15-meter resolution would require very good, sub-pixel registration. Registration becomes most critical when it come to overlaying data collected from the same point at different times. The California Irrigated Lands Technology Transfer project attains a 0.2 pixel RMS error for multitemporal registration (Wall and others, 1981). Error tolerance depends mostly on environment and repetition. Larger errors can be tolerated if land use and land cover features are large and if only two dates are being overlaid. Those same errors become intolerable when the features are smaller (more boundary pixels) and when more scenes are being overlaid. In general, most users would be quite pleased with the error limits proposed for EDIPS, that is, 0.5 pixel temporal registration offset.

SUGGESTIONS

Most users are puzzled by the lack of quality registration coming out of the MDP. This has limited some users without access to their own geometric correction and overlaying algorithms and has increased costs substantially for the others. It is hoped that a result of the Registration and Rectificaton Workshop will be an improvement in the accuracy of MDP products. One critical element in any procedure to accurately register satellite imagery to maps is selection of ground control points. Thousands of control points have been picked by Landsat analysts in the past. Perhaps a way can be found to accept contributions of GCP's from the users into the MDP library. There they would augment those already in the library, increasing the number of points available for each scene and the reliability of registration.

SUMMARY

Reliable registration of satellite imagery would greatly increase the use of such data for land use and land cover and hydrologic applications. While some users can and do accomplish their own registration, most cannot. The inability to work with registered data results in the loss of the temporal dimension, production of inferior map products, and difficulty in using ancillary data that is registered. While sampling strategies satisfy users from some disciplines, land use and land cover are commonly interested in completing "wall to wall" surveys and producing map products.

Land use and land cover and hydrologic applications users have definite demands for registered satellite imagery. While more variety with respect to options is desirable, products which meet the standards proposed for EDIPS would be welcomed. One addition that most users mention is a listing of control points that can be used to check accuracy of a particular product or as a starting point for refinement. Satisfaction of those requirements would greatly improve the utility of satellite imagery for land use and land cover and hydrologic applications.

ACKNOWLEDGMENTS

Though the opinions expressed in this paper are solely the responsibility of the author, comments on registration and rectification issues were solicited from the following individuals for consideration in preparing this paper:

Rob Aanstoos, Texas Natural Resources Information System
William Acevedo, Technicolor Graphics Services, Inc.
Hal Anderson, State of Idaho Water Resource Divsion
Ethel Bauer, NASA-Ames Research Center
Rick Heimes, USGS Water Resources Divsion
John Jensen, University of South Carolina
Armond Joyce, NASA-NSTL-Earth Resources Laboratory
Richard Sigman, USDA-Economics and Statistics Service
Page Spencer,,Bureau of Land Management
Gail Thelin, USGS-National Mapping Division
Bob Wrigley, NASA-Ames Research Center

REFERENCES

Graham, M. H., and Luebbe, R. C., 1981, An evaluation of MSS p-format data registration: National Aeronautics and Space Administration NSTL/ERL-197, 57 p.

Koch, C. S., 1981, An evaluation of G-format data registration for the High Plains 1980 project: Technicolor Graphics Service, Inc. report, Ames Research Center, 3 p.

Milazzo, V. A., 1980, A review and evaluation of alternatives for updating U.S. Geological Survey land use and land cover maps: U.S. Geological Survey Circular 826. 19 p.

ORI, Inc., 1979, Multispectral resource sampler summary report: Multispectral resource sampler workshop, Ft. Collins, Colorado.

Thelin, G. P., Johnson, T. L., and Johnson, R. A., 1981, Mapping irrigated cropland with Landsat for the High Plains Aquifer in Satellite Hydrology: William T. Pecora Symposium, 5th, Sioux Falls, South Dakota, June 11-15, 1979, Proceedings, p. 715-721.

Thompson, M. M., 1979, Maps for America: U.S. Geological Survey, 265 p.

U.S. Geological Survey, 1979, Landsat data users handbook, revised edition: U.S. Geological Survey.

U.S. Geological Survey, 1981, Computer documentation general cartographic transformation package: U.S. Geological Survey.

Wall, S. L., Thomas, R. W., Brown, C. E., Ericksson, M., 1981, A Landsat-based inventory procedure for the estimation of irrigated land in arid areas: presented at the First thematic Conference, Remote Sensing of Arid and Semi-Arid Lands, Cairo, Egypt, 1981.

N82 28710

4.4 REGISTRATION AND RECTIFICATION NEEDS OF GEOLOGY*

Pat S. Chavez, Jr.

Geologic applications of remotely sensed imaging encompass five areas of interest. These include: enhancement and analysis of individual images; work with small-area mosaics of imagery which have been map-projection rectified to individual quadrangles; development of large-area mosaics of multiple images for several counties or states; registration of multitemporal images; and data integration from several sensors and map sources. Examples for each of these types of applications are summarized in Tables 1 - 5.

Individual image work (Table 1) has been primarily applied for medium-scale structural mapping and surface geology delineation. Small-area mosaics (Table 2) have been developed primarily for structural analysis also, but the rectified image can be considered a map product. Both optical (i.e., photographic) and digital rectification and edge matching have been undertaken. Large-area mosaics (Table 3) have been undertaken to provide geologists with regional views that display major tectonic features. Until recently, most of this work has involved digital processing on subsampled Landsat scenes (i.e., a resolution of 200 meters) or optical processing for photomosaics. Temporal processing (Table 4) has been applied to several imaging sensors to detect changes over time associated with vegetation seasonality and of dynamic phenomena such as ocean currents or ice flows. The last area of concern is data integration (Table 5), in which a variety of remotely sensed and ancillary data are map projected and overlain to assist in the analysis of geologic structure. In data integration studies, satellite images form a limited but essential contribution to the overall analysis. As the various data types are being overlaid, the accuracy of image reprojection to a given map projection and scale is of paramount importance.

In summary (see Table 6), geologists have first-order geometry corrections with 1 to 250,000 scale. For the geologists, if you take care of aspect ratio, earth rotation, variable scanning of the mirrors, things you can do automatically, probably 60% of the time that is acceptable. But if geologists are going to do very detailed lithology and lineament mapping, you need to go to ground control points. For satellite ephemeris corrections, we have tried several of those techniques and it never seems to give the accuracy needed, probably because we haven't been able to obtain the ephemeris information for that image. Digital correlation techniques already exist; this is what the MDP is using and now more recently the Purdue and JPL teams are using with FFT techniques. For correction techniques, we look at image to map and image to image. If you go from an image to one map and then another, the geologist may want to convert from a UTM to an orthographic or other projection. This brings out the question: should we really do the Landsat geometry corrections right at the beginning at MDP or should you just supply the coefficient to the user so he can adjust the coefficients if he would really like to map projection 2 instead of map 1. This would reduce having to resample the data twice.

*Edited oral presentation.

One of the things that I feel may still need improvement is the accuracy in the terms of pixels rather than meters. If you are working on a 1:250,000 scale you could get typically with Landsat ±1 or 2 pixels. With the Thematic Mapper, of course, the same distance would be more pixels but now we are going to be working with 1:50,000 and 1:100,000 scale maps, so again the ±1 or 2 pixels will probably be sufficient for the geologist. In other words, if what I am mapping has accuracy within the width of my pencil line, that's all I need. For digital-mozaicking accuracy though, I think that the geologists will complain when they see a mismatch of one pixel, even if it falls within their accuracy criteria from one image to the other. Right away they start worrying that the area of mismatch may be a lineament, and mapping isn't as accurate as it should be. They don't realize that its still within ±80 or 90% of the particular need that they ask for.

We talked a little about band-to-band registration problems. Again, I would like to suggest that maybe somebody ought to investigate the idea of taking the individual bands, trying some of the autocorrelation techniques used to select ground control points, and registering an individual band to your map, and extending your autocorrelation from band to band for further correction. Finally, I mentioned the geometry vs radiometry and topographic displacement. Goddard has its ground control point library, and perhaps they could include some of the new DTM 30-meter topographic data into their correlation? Perhaps this could be added as another data set for topography.

Table 1.

EXAMPLES OF INDIVIDUAL IMAGE WORK

° SAN FRANCISCO PEAKS AREA
- STRUCTURAL MAPPING
- SELECTION OF OPTIMUM RATIO COMBINATION BY STATISTICAL METHODS

° DENVER/AUTOLINER PROJECT
- STRUCTURAL ENHANCEMENT IN DENVER AREA
- DEVELOP AN AUTOMATIC LINEAR MAPPING TECHNIQUE

° OFFICE OF INTERNATIONAL GEOLOGY
- SAUDI ARABIA
  - STRUCTURE
  - MATERIAL COVER
- MOROCCO AND TUNISIA
  - MATERIAL COVER
  - HYDROLOGY

Table 2.

EXAMPLES OF SMALL-AREA MOSAICS (QUADRANGLES)

(DIGITAL AND/OR OPTICAL)

° ALASKA (13 1°x2° QUADS FROM LANDSAT MSS/1974-76)
- DIGITAL MOSAICS
- STRUCTURE AND MATERIALS MAPPING

° GRAND CANYON (4 LANDSAT MSS IMAGE MOSAICS/1978)
- DIGITAL MOSAIC DONE BY NASA/GODDARD
- USGS FLAGSTAFF DID THE FALSE AND SIMULATED NATURAL COLOR PRODUCTS AFTER ATMOSPHERIC SCATTERING CORRECTIONS
- MOSTLY OVERVIEW OF THE CANYON AREA AND FOR COMPARISON WITH TOPO MAP

° 1:250K SAUDI QUADS (10 1°x2° QUADS FROM LANDSAT MSS/1979-80)
- DIGITAL MOSAICS
- STRUCTURAL MAPPING
- BLACK AND WHITE BASE MAP FOR GEOLOGIC MAPPING

° SONAR (GLORIA SONAR IMAGES OF THE ATLANTIC/1980)
- OPTICAL MOSAIC OF 30-40 TRACKLINES
- DIGITAL MOSAIC OF 3-5 TRACKLINES
- PRIMARILY FOR STRUCTURE; BUT SOME MATERIAL TYPES

° RADAR (AIRBORNE AND SATELLITE/1979-PRESENT)
- G. SCHABER, ET AL (SAN FRANCISCO PEAKS AND DEATH VALLEY)
- WALTER BROWN, ET AL/JPL

Table 3.

EXAMPLES OF LARGE-AREA MOSAICS

(STATES AND/OR COUNTRIES)

° NEVADA (1973-74)
- 32 LANDSAT MSS IMAGES
- DIGITAL

° SAUDI ARABIA (1978-81)
- 260 LANDSAT MSS IMAGES
- OPTICAL MOSAIC OF DIGITALLY PROCESSED IMAGES
- STRUCTURE AND BLACK AND WHITE BASE MAP

° FLORIDA
- APPROXIMATELY 15 LANDSAT MSS IMAGES/USGS-RESTON
- OPTICAL MOSAIC

° ARIZONA
- APPROXIMATELY 20 LANDSAT MSS IMAGES/JPL
- DIGITAL MOSAIC

° NORTH AMERICA PLATE MOSAIC (NAM)
- PROPOSED PROJECT OF APPROXIMATELY 2200 LANDSAT MSS IMAGES
- DIGITAL/OPTICAL/HYBRID
- STRUCTURE PLUS HIGH-QUALITY DIGITAL MOSAIC DATA BASE

Table 4.

EXAMPLES OF TEMPORAL PROCESSING

° LANDSAT MSS
- FLAGSTAFF AREA - MONITOR/DETECT VEGETATION CHANGES FOR SOILS TYPE INFORMATION AND SOIL EROSION
- C. ROBINOVE ET.AL. - ALBEDO MONITORING IN ARID LANDS (REGISTERED APPROXIMATELY 20-25 LANDSAT MSS IMAGES)

° RADAR/SEASAT
- ASCENDING VS DESCENDING ORBITS FOR GEOMETRY AND TOPOGRAPHIC INFORMATION BASED ON VIEWING DIRECTION DIFFERENCE
- SEA-ICE DYNAMIC AND ICE-FLOE TRACKING

° HCMM
- OCEAN PATTERN AND LAND AREAS
- THERMAL INERTIA MAPPING (K. WATSON AND A. KAHLE, ET.AL.)

Table 5.

DATA INTEGRATION (MULTI-SENSORS AND MULTI-MAP SOURCES)

° REDWOODS PROJECT (1976-77)

- DIGITIZED COLOR U-2 FOR ENHANCEMENTS AND VEGETATION OVER MAP
- GEOLOGY MAP
- PROXIMITY MAP
- TOPO/SLOPE MAP

PURPOSE: GENERATE A DERIVATIVE MAP THAT REPRESENTED THE LANDSLIDE/EROSION POTENTIAL BASED ON THE INTEGRATED DIGITAL DATA SETS.

° CEMENT FIELD (1979-80)

- GAMMA-RAY SPECTROMETRY - 4 PARAMETERS
- AEROMAGNETICS
- MULTI-FREQUENCY RESISTIVITY
- GRAVITY
- LANDSAT MSS
- COLOR U-2
- GEOLOGY
- TOPOGRAPHY

PURPOSE: EVALUATE VISUALLY AND STATISTICALLY THE CORRELATION AMONG THE MEASURED VARIABLES OVER A KNOWN SURFACE AND NEAR-SURFACE GEOCHEMICAL ALTERATION PATTERNS. IN THE STUDY AREA USED, ANOMALOUS GEOCHEMICAL AND GEOPHYSICAL SIGNATURES HAD BEEN PREVIOUSLY DOCUMENTED. IT WAS AN AREA WHERE HYDROCARBON MICROSEEPAGE HAD INDUCED THE ALTERATIONS.

TABLE 5.(continued)

° OCEAN BOTTOM DATA SET (FAMOUS AREA/1980-81)

- BATH
- MAGNETIC
- GRAVITY
- PRESENTLY ADDING SONAR

° MULTI-SENSOR

- MSS/SEASAT
- MSS/RBV
- FUTURE - MSS/RBV/TM/SPOT

TABLE 6 .

SUMMARY

° VARIOUS TYPES OF GEOMETRIC CORRECTION TECHNIQUES EXIST
- FIRST-ORDER CORRECTION (I.E., AUTOMATIC CORRECTIONS ONLY)
- GROUND CONTROL POINT (GCP) CORRECTIONS
- SATELLITE EPHEMERIS CORRECTION
- DIGITAL CORRELATION TO ALREADY CORRECTED IMAGE

° CORRECTION TECHNIQUES CURRENTLY IN USE
- IMAGE TO MAP
- IMAGE TO IMAGE
- IMAGE TO MAP 1 TO MAP 2

° IMPROVEMENT IS STILL NEEDED IN THE FOLLOWING AREAS
- ACCURACY VS COST
- BETTER EPHEMERIS DATA FOR MORE ACCURATE CORRECTION
  - THIS WILL GREATLY IMPROVE THE USE OF THE IMAGES BECAUSE MORE AUTOMATIC AND EASIER TO USE IN MOSAIC
  - AN ABSOLUTE MUST FOR SEA-ICE MONITORING TYPE PROJECTS
- MULTI-SENSOR AND MULTI-RESOLUTION DATA INTEGRATION
- NEED A GOOD FRONT END (I.E., RECEIVING STATION) GEOMETRY CORRECTION TO GET GOOD IMAGE-TO-IMAGE MATCHING FOR DIGITAL AND/OR OPTICAL MOSAICS. CURRENTLY THE COST PER IMAGE FOR A GOOD DIGITAL MOSAIC IS FROM $800 TO $2500 PER IMAGE; NEED TO GET THIS DOWN TO $200

° ACCURACY
- DEPENDS OF THE RESOLUTION/PIXEL SIZE OF THE IMAGE BEING USED
- GENERALLY FOR VISUAL INTERPRETATION ±1.5 PIXEL ACCURACY IS SUFFICIENT (I.E., WIDTH OF A PENCIL LINE AS GORDON SWANN WOULD SAY)
- FOR DIGITAL MOSAICS THE ACCURACY NEEDED IS MORE LIKE ± 0.5 PIXEL

Bibliography

Chavez, P.S., Jr., and Soderblom, L.A., 1974, Simple high speed digital image processing to remove quasi-coherent noise patterns, in American society of Photogrammetry Symposium, Washington, D.C., 1974, Proceedings: Falls Church, VA, p. 595-600.

Eliason, E., Chavez, P.S., Jr., and Soderblom, L.A., 1974, Simulated true color images from ERTS data: Geology, v. 5, no. 2, p. 231-234.

Albert, N.R.D., and Chavez, P.S., Jr., 1975, computer-enhanced Landsat imagery as a tool for mineral exploration in Alaska, in First W.T. Pecora Memorial Symposium, Sioux Falls, SD, October 1975: U.S. Geological Survey Professional Paper 1015, p. 193-200.

Chavez, P.S. Jr., October 1975, Atmospheric, Solar, and M.T.F. corrections for ERTS digital imagery, in American Society of Photogrammetry Symposium, Phoenix, 1975, Proceedings: Falls Church, VA, p. 69-69a.

Berlin, G.L. Chavez, P.S., Jr., Grow, T.E., and Soderblom, L.A., 1976, Preliminary geologic analysis of southwest Jordan from computer enhanced Landsat 1 image data, in American Society of Photogrammetry Symposium, Washington, D.C., 1976, Proceedings: Falls Church, VA, p. 545-563.

Chavez, P.S., Jr., Berlin, G.L., and Acosta, A.V., 1976, Computer processing of Landsat MSS digital data for inear enhancement, in Second W.T. Pecora Memorial Symposium, Sioux Falls, SD, October, 1976, Proceedings: Sioux Falls, SD.

Rangland, T., and Chavez, P.S., Jr., 1976, The Earth Resources Observation in Second W.T. Pecora Memorial Symposium, Sioux Falls, SD, October, 1976, Proceedings: Sioux Falls, SD.

Chavez, P.S., Jr., Berlin, G.L., and Mitchell, W.B., 1977, Computer enhancement techniques of Landsat MSS digital images for land use/land cover assessments, in Sixth Remote Sensing of Earth Resources Symposium, Tullohoma, TN, March 1977, Proceedings: Tullahoma, TN, p. 259-275.

Robinove, C.J., and Chavez, P.S., Jr., 1978, Landsat albedo monitoring for an arid region, in AAAS International Symposium on Arid Region Plant Resources, Lubbock, TX, 1978.

Condit, C.D. and Chavez, P.S., Jr., 1979, Basic concepts of computerized digital image processing for geologists: U.S. Geological Survey Bulltein 1462.

Chavez, P.S., Jr., O'Connor, J.T., McMacken, D.K., and Eliason, E., 1979, Digital image processing techniques of integrated image and non-image data sets, in Thirteenth International Symposium on Remote Sensing of Environment, Ann Arbor, MI, April, 1979, Proceedings: Ann Arbor, MI, Environmental Research Institute of Michigan, p. 439-454.

Chavez, P.S., Jr., Leeds, A., and Crawforth, J., 1979, Design of a very mini image processing system, in Second U.S. Geological Survey Computer Symposium, Denver, CO, April, 1979: Abstract.

Chavez, P.S., Jr., 1980, Automatic shading correction and speckle noise mapping/removal techniques for radar image data, in Report of the Radar Geology Workshop, Snowmass, CO, July, 1979: JPL Publication 80-61, p. 251-262.

Eliason, P.T., Donovan,T.J., and Chavez, P.S., Jr., 1980, Integration of geological, geochemical, and geophysical spatial data of the Cement oil field, Oklahoma test site, in Sixth W.T. Pecora Memorial Symposium, Sioux Falls, SD, April, 1980, Proceedings: Sioux Falls, SD.

Chavez, P.S., Jr., and Bauer, B., 1980, An automatic optimum kernal-size-selection technique for edge enhancement: Accepted for publication in Journal of Remote Sensing of Environment.

Chavez, P.S., Jr., and Eliason, P.T., 1980, The use of Landsat digital data for variable haze mappings: U.S. Geological Survey, Flagstaff, AZ, unpublished report, 10 p.

Chavez, P.S., Jr., Watson, R.D., Henry, M.E., and Theisen, A.F., 1980, Digital processing techniques for small digital arrays (FLD data set): in Report of the applications of Luminescence Techniques to Earth Resource Studies Workshhip, Lunar and Planetary Institute, Houston, TX, p. 50-54.

Eliason, P.T., Soderblom, L.A., and Chavez, P.S., Jr., 1980, Extraction of topographic and spectral albedo information from multispectral images: Submitted for publication in Journal of Remote Sensing of Environment.

Chavez, P.S., Jr., and Sanchez, E., 1981, Digital combination of Landsat and SEASAT images: Submitted for publication in Journal of Photogrammetry and Remote Sensing.

Teleki, P., Roberts, D., Chavez, P.S., Jr., Somers, M.L., and Twichell, D., 1981, Sonar survey of the U.S. Atlantic Continental Slope; Acoustic characteristics and image processing techniques, in 13th Annual Offshore Technology Conference, Houston, TX, May, 1981, Proceedings: Houston, TX, p. 91-102.

Chavez, P.S., Jr., October, 1980, Preliminary image processing results of the ice flow movement using SEASAT radar images: U.S. Geological Survey, Flagstaff, AZ, unpublished report, 10 p.

Kozak, R. Berlin, G.L., and Chavez, P.S., Jr., 1981, SEASAT's imaging radar system: Journal of Remote Sensing of Enviornment, November, 1981, 4 p.

Berlin, G.L., Schaber, G.G., Kozak, R., and Chavez, P.S., Jr., 1981, Observation of the Grand Canyon with a SEASAT radar image: Accepted for publication in Journal of Remote Sensing of Environment.

Robinove, C.H., Chavez, P.S., Jr., Gehring, D., and Holmgren, R., 1981, Arid land monitoring using Landsat albedo difference images: Journal of Remote Sensing of Environment, vol. 11, no. 133, 1981, p. 133-156.

Chavez, P.S., Jr., Berlin, G.L., and Sowers, L.B., 1981, Statistical method for selecting Landsat MSS ratios: Special Issue of Journal of Applied Photographic Engineering, Fall, 1981, (in press).

Sowers, L.B., Sanchez, E.M., Chavez, P.S., Jr., and Morgan, J.O., 1981, Saudi Arabia Landsat film mosaic, in Seventh W.T. Pecora Memorial Symposium, Sioux Falls, SD, October, 1981, Proceedings (in press): Sioux Falls, SD.

Sanchez, E.M., Sowers, L.B., Chavez, P.S., Jr., Edwards, K., Eliason, E. M., Eliason, P.T., 1981, Mosaicking techniques applied at the Flagstaff image processing facility, in Seventh W.T. Pecora Memorial Symposium, Sioux Falls, SD, October, 1981, Proceedings: Sioux Falls, SD.

4.5 Data Registration and Integration Requirements

for

Severe Storms Research

John T. Dalton
Interactive Systems Development Branch
Information Extraction Division
Goddard Space Flight Center

November 1981

Presented at the NASA Workshop on
Registration and Rectification

1. Introduction

Severe storms research is characterized by temporal scales ranging from minutes (for thunderstorms and tornadoes) to hours (for hurricanes and extra-tropical cyclones). Spatial scales similarly range from tens to hundreds of kilometers, depending on the phenomenon being observed.

Sources of observational data include a variety of ground based and satellite systems. As one would expect, requirements for registration and intercomparison of data from these various sources are a function of the research being performed and the potential for operational forecasting application of techniques resulting from the research.

This paper presents an overview of the sensor characteristics and processing procedures relating to the overlay and integrated analysis of satellite and surface observations for severe storms research. It is based on a review of the literature, discussions with meteorologist researchers in the Troposphere Branch of Goddard's Laboratory for Atmospheric Sciences, and on experience in the development of the Atmospheric and Oceanographic Information Processing System (AOIPS).

2. Severe Storm Data Sources

Data sources include geostationary satellites, polar orbiting satellites, radar, aircraft, balloons, and meteorological models. Satellite, aircraft, and radar data are frequently in image form, while the remaining sources and information derived from satellite imagery are either in the form of gridded fields or station observations. This section surveys the major data sources, identifying the information provided and the spatial and temporal characteristics.

2.1 Satellite sources - Geostationary Orbit

The GOES Visible and Infrared Spin Scanning Radiometer [1, 2] (VISSR) provides visible imagery showing cloud structure and patterns, and infrared imagery showing surface and cloud top temperature. A full earth image is generally scanned every 30 minutes, however, limited area north-south scans may be commanded at intervals as frequent as 3 minutes. Analysis of sequences of these images provides meansurements of cloud motion winds and storm growth rates. Spatial resolution is nominally 1 km visible and 8 km IR at the subsatellite point, but degrades away from that point due to curvature of the earth's surface. The IR resolution is approximately 10 km, for example, at 40° latitude. Wind and cloud height observations derived from VISSR are essentially randomly spaced corresponding to locations where cloud features can be identified.

An improved sensor based on the VISSR - the VISSR Atmospheric Sounder [3] (VAS) is currently being operated in a research/evaluation mode. A total of 12 IR channels provide measurements of temperature and humidity integrated over different layers of the atmosphere. When operated in Dwell Sounding mode, all 12 channels are scanned for a selected north-south extent. Because of multiple spin averaging to improve the signal to noise of the radiances, an area the size of the U.S. requires approximately 3 hours to image. Four IR channels may be selected by ground command to scan

at VISSR rates (30 minutes for full earth). This multispectral imaging mode provides time sequenced imagery of temperature and water vapor patterns and motion. Like wind fields derived from VISSR, temperature and humidity profiles derived from VAS are generally randomly spaced observations.

Earth location information for the VISSR and VAS data is derived from interactive identification of landmark locations in visible imagery. The initial method used was to fit Kepler orbital elements to direct observations of satellite position and to fit the parameters for spacecraft attitude and sensor geometry to landmark observations.[4,5] In 1975, techniques were developed[6,7] to derive both orbit and attitude state from image landmarks. Chebyshev polynomials are now used to model spacecraft position and image-sun angle as a function of time. This allows predictive parameters to be generated and thus permits earth location of image features immediately after acquisition. The Chebyshev coefficients have been transmitted by NOAA in the image line documentation since 1977.

The VAS navigation procedure correlates prestored 16 x 16 image chips to locate landmarks. Orbit, attitude and camera biases are estimated using an iterative weighted least squares technique.

Comparison of image locations derived using this model with NOAA landmark observations yields the following statistics for residuals:[8]

	mean	σ
pixel	-0.0055	1.335
line	0.0192	1.58

Using 20 landmark observations per day for a 3 day period allows navigation parameters to be extrapolated for 48 hours with 3 pixel accuracy. The mean pixel and line error vs. prediction interval is shown in Figure 1.

2.2 Satellite sources - Polar Orbit

Sensors on-board polar orbiters typically repeat coverage at 12 hour periods. Because this is much longer than time scales of severe storm dynamics, this source of data is not as heavily utilized as the GOES sensors. The primary uses have been model initialization and comparison, extraction of parameters not available from geostationary sensors, and comparison with geostationary observations. Two sensor systems will be summarized here for illustration and comparison.

The Electrically Scanning Microwave Radiometer (ESMR) on Nimbus-6 provides radiometric measurements in two bands for two polarizations. The instrument scans in a 70° area ahead of the spacecraft motion with a constant 50° incidence angle with the earth's surface. Nominal resolution is 20 km cross-track and 45 km along-track. Multispectral classification techniques are used to identify areas of rainfall.[9]

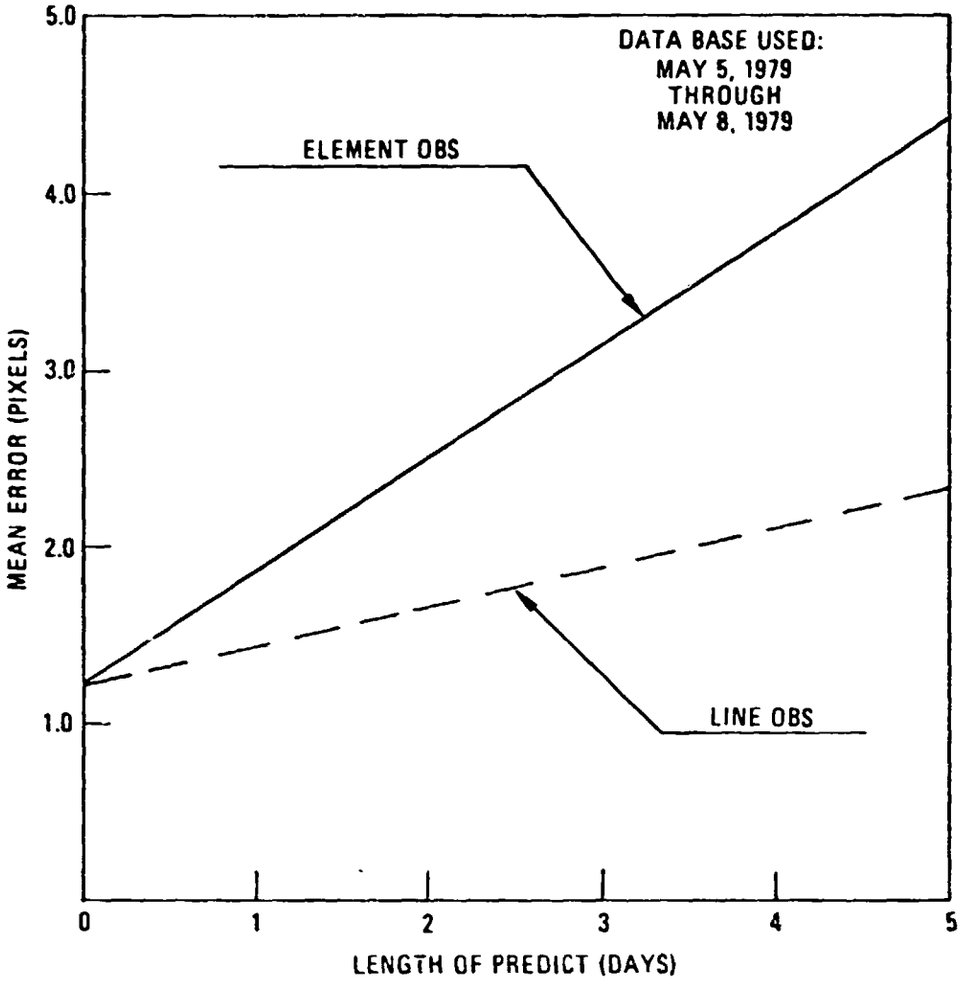

Figure 1. Line and pixel navigation prediction error for GOES VAS.

Four instruments on the TIROS-N and NOAA-6 satellites provide visible and infrared imagery along with sounding radiances.[10]

The Advanced Very High Resolution Radiometer (AVHRR) scans a 1650 km swath in 4 visible and infrared bands. The 1.1 km IFOV is oversampled by a factor of 1.362 to produce 2048 samples per line at approximately 800 meter separation. NOAA generates latitude/longitude values every 40 pixels (51 points per line).

The High Resolution Infrared Radiation Sounder (HIRS/2) scans a 2240 km swath in 20 infrared bands. The 56 step scan produces IFOV's of 17.4 km at nadir, degrading to 58.5 km (cross-track) by 29.9 km (along-track) at maximum scan angle. NOAA generates latitude/longitude values for each scan position.

The Stratospheric Sounding Unit (SSU) and Microwave Sounding Unit (MSU) scan in 8 and 11 steps respectively, resulting in IFOV's exceeding 120 km.

2.3 Aircraft and Ground Based Observations

Aircraft flights are used to measure smaller scale cloud properties and to test new sensors. The scanning resolution depends on the instrument and aircraft altitude. The Cloud Top Scanner, for example, has a 100 meter cross track resolution and a 200 meter along-track resolution. Aircraft navigation data is used to define image georeferencing parameters.

Ground based digital radar provides measurements of rainfall intensity and, for doppler radars, velocity. Digital returns are oriented along radial scans with varying range, range resolution, and azimuth angle resolution. The Norman, Ok. doppler radar for example has a range of 456.2 km, range gate resolution of 0.6 km, and azimuth angle resolution of approximately 0.8^{o}.[11] Elevation angle is varied to provide measurements at different altitudes.

Rawinsonde balloons provide measurements of temperature, altitude, dewpoint and winds at 40 mandatory pressure levels from over 100 stations in the U.S. every 12 hours.

3. Registration Requirements

Data registration processing for severe storms studies tends to have both multi-temporal and multispectral aspects. As mentioned in the discussion of the VISSR, multi-temporal imagery from a single sensor is frequently used to extract measurements of atmospheric motion and cloud growth. The resulting observations are often registered and overlayed on visible imagery from a single time for comparison with cloud features and are registered and integrated with other sources (e.g., ground based observations) for comparison or integration with models. Examples of multi-source image registration include GOES-west to GOES-east for direct stereo cloud top measurements, and digital radar to GOES visible and IR for comparison of rainfall and doppler velocities with cloud structure. These multi-source observations from different times are then registered to produce time lapse displays and temporal analyses. Because of its frequent coverage, its ability to show mesoscale features, and the computional time required to remap sequences of images to a common projection, the GOES imagery is generally used as the

reference coordinate system or map base for these analyses. Because of its relative importance, the accuracy and remapping considerations of GOES sensors will be addressed further in the next subsection. Next, some considerations involving point source and gridded field registration will be discussed. Finally, in the next section, the current multi-source combinations will be summarized.

3.1 GOES Data Registration

As described in Section 2.1, the absolute navigation accuracy from current VISSR and VAS landmark processing is on the order of 1 to 2 pixels (1-3 km). Errors may be introduced by:

- operator errors in the identification and correlation of landmarks,
- geometric irregularities in the image, and
- differences between the oblate spheroid model and the actual earth's surface.[12]

For registration of successive image frames, relative errors are typically on the order of a single pixel. In measurement of cloud drift winds, this equates to an error of approximately 0.5 m/sec for 30 minute interval data and 3 m/sec for 5 minute interval data.

Stereo measurements of cloud top heights are made by remapping 512 x 512 image sectors from one GOES satellite to the projection of another. The orbit/attitude coefficients define a (latitude, longitude) to (line, pixel) remapping function and its inverse. This is used to generate a remapping grid, with bilinear interpolation used to relate corresponding locations between grid points. Absolute georeferencing errors are reduced by shifting registered images to align cloud shadows and other features. The resulting relative error is on the order of a $_2$ pixel, with a resulting absolute cloud height error on the order of 0.5 km.

Digital radar data is registered to GOES Visible and IR imagery through a two step process. Data in radial scan orientation (B scan) is first resampled to an earth latitude, longitude grid. Plane earth, low elevation and short range approximations are used where possible to reduce computation time in transforming from the radar to earth coordinate system. These approximations introduce an error on the order of 0.5 km (one half a GOES visible pixel). Next, the image in this earth latitude, longitude projection is remapped to the GOES projection. Bilinear interpolation is used to compute positions between user specified grid points (usually at 20 pixel spacing).[11]

Polar orbiter data is not generally registered to GOES data for severe storms observations, partially due to the disparate time scales and partially due to the representation of the polar orbiter image location information as latitude, longitude values at sampled locations along scan lines. The latter makes the (line, pixel) to (latitude, longitude) transformation trivial, but makes the inverse transformation difficult to solve. It is therefore easier to register data using the polar orbiter image as a base.

3.2 Point Source and Gridded Field Registration

Point source or station observations (e.g., winds from VISSR, soundings from VAS, and rawinsondes) have known locations and can easily be overlayed on maps or GOES imagery. However, further analysis and comparison with image features frequently requires gridded fields for contouring or diagnostic (e.g., divergence) computation. Furthermore, integrated analysis of multiple parameters requires that all parameters be represented in the same grid locations. A number of techniques are used to interpolate between point source observations to compute values at intermediate grid points. These techniques include weighting values by inverse distance within a search area, eliminating points that are shadowed by closer points, and interactive schemes that recompute weights based on residual errors between original point values and values interpolated from the gridded field. The selection of technique and algorithm parameters affects the degree to which the gridded field represents features in the data.

4.0 Summary and Recommendations

Current multi-source and multi-temporal registration requirements are summarized below:

Multi-temporal

- GOES VISSR and VAS image frames to first image of a sequence
- Station observations and gridded fields to GOES image loops and to map projections

Multi-source

- GOES VISSR/VAS - west satellite projection to east satellite projection (or the reverse)
- Digital radar to GOES VISSR/VAS
- Station observations and gridded fields to GOES VISSR/VAS

Because the GOES image projection generally serves as a common base, registration accuracy requirements are generally 1 km (1 visible pixel).

Registration of the above data for research case studies generally allows sufficient time for the remapping process. For nowcasting applications as will be performed on the Centralized Storm Information System (CSIS),[13] the registration and overlay must be performed in minutes.

While the above capabilities for data registration are fairly powerful, limitations still exist:

(1) Absolute errors on GOES VISSR image are as high as 6 pixels. It is not clear whether improved models or procedures can improve this. Furthermore, non-linearities are observed in short interval images that are not found in 30 minute data and are therefore not modeled in the navigation function.

(2) Stereo GOES image pairs are currently offset interactively to compensate for absolute navigation errors. Registration using relative control points in the two images may improve the registration accuracy and thus the accuracy of cloud height measurements.

(3) The incorporation of a new data source (e.g., a polar orbiting sounder) into an analysis requires the development of additional software to identify and extract image control points and to perform the necessary resampling and remapping to the reference map projection. It is also extremely difficult to experiment with map projections, resolutions, and resampling functions. An interactive "geographic information system" is needed that allows selection of map projection, resolution, data sources, and resampling function for each source. Image georeferencing function implementations are needed for different data sources that embody approximations for computational efficiency while maintaining required geographic accuracy. Finally, the system interface should provide for straightforward addition of new sources in terms of format and image location parameters.

References

1. A. F. Hasler, W. C. Skillman, W. E. Shenk, and J. Steranka, "In Situ Aircraft Verification of the Quality of Satellite Cloud Winds over Oceanic Regions", Journal of Applied Meteorology, Vol. 18, No. 11, November 1979.

2. A. F. Hasler and R. F. Adler, "Cloud Top Sturcture of Tornadic Thunderstorm from 3 minute Interval Stereo Satellite Images Compared with Radar and Other Observations", Conference on Radar Meteorology, April 1980.

3. H. Montgomery, "VAS Instrumentation for Future GOES Mission", Geosynchronous Meteorological Satellite Data Seminar, GSFC X-931-76-87, March 1976.

4. C. T. Mottershead and D. R. Phillips, "Image Navigation Geosynchronous Meteorological Satellites", Preprints of Conference on Aerospace and Aeronautical Meteorology and Symposium on Remote Sensing from Satellites, pp. 260-264, 1976.

5. Dennis Phillips and Eric Smith, "Geosynchronous Satellite Navigation Model", University of Wisconsin, Janurary 1974.

6. C. E. Velz, "Orbit and Attitude State Recoveries from Landmark Data", Proceedings of AAS Astrodynamics Specialist Conference, paper No. AAS 75-058, July 1975.

7. A. J. Fuchs, C. E. Velz, and C. C. Goad, "Orbit and Attitude State Recoveries from Landmark Data", Journal of Astronautical Sciences, 1975, pp. 369-381.

8. R. Nankervis, D. Koch, H. Sielski, D. Hall, "Absolute Image Registration for Geosynchronous Satellites", GSFC, 1979.

9. E. Rodgers, H. Siddingaiah, A. Chang, E. Wilheit, "A Statistical Technique for Determining Rainfall over Land Employing Nimbus-6 ESMR Measurements", Fourth NASA Weather and Climate Program Science Review, January 1979.

10. NOAA Polar Orbiter Data (TIROS-N and NOAA-6) Users Guide (Preliminary Version), NOAA National Climatic Center, Satellite Data Services Division, December 1979.

11. L. Chen, M. Faghmous, and K. Ghosh, AOIPS RADPAK System Description and Users Guide, General Software Corporation, GSC-TR8102, August 1981.

12. A. F. Hasler, "Stereographic Observations from Geosynchronous Satellites: An Improtant New Tool for the Atmospheric Sciences", Bulletin of the American Meteorological Society, Vol. 62, No. 2, February 1981.

13. Centralized Storm Information System (CSIS) Implementation Plan, University of Wisconsin Space Science and Engineering Center, Madison, Wisconsin, May 1981.

4.6 OCEANOGRAPHIC SATELLITE REMOTE SENSING: REGISTRATION, RECTIFICATION, and DATA INTEGRATION REQUIREMENTS

David A. Nichols
Jet Propulsion Laboratory

INTRODUCTION

Oceanographic remote sensing is still in its beginning stages of development. Results from the early meteorological satellites suggested that parameters of oceanographic interest, such as sea surface temperatures, might readily be obtained by satellite remote sensing. The accuracy of the data, however, was found to be unacceptable. Later instruments, such as those flown on Seasat[4], demonstrated the feasability of obtaining nearly all-weather observations of wind speed and direction, wave height, sea surface temperature and elevation. These data, along with those obtained by the latest generation of weather satellites, appear to be of much greater utility. The relatively limited experience with these systems, however, places much of oceanographic remote sensing at a stage where results are still being verified and evaluated. Calibrated geophysical parameters are available for many of the data items, but the quality and significance of these observations is only now beginning to be understood.

There are many reasons why oceans remote sensing has lagged behind meteorological and terrestrial applications. They cannot all be addressed here, but a significant impediment has been the lack of appropriate tools for acquiring, processing and analyzing remotely sensed data. Until very recently only a few oceanographic institutions had any semblance of an image processing capability - a capability which is mandatory for processing and viewing image data and extremely useful for processing and displaying nonimage data. This lack of computerized tools for remotely sensed data processing, especially data integration, has been an impediment to algorithm development and sensor verification. The lack of appropriate mechanisms for acquiring the data continues to cause problems but is currently being addressed, to a limited degree, by the Ocean Pilot System[1].

Firm data integration requirements are difficult to pin down. Operational applications are in the best position to dictate data integration requirements, but operational oceanographic applications usually require real- or near-real-time data. Data integration services, which are generally quite time consuming, are therefore precluded. For this reason, data integration is largely a problem pertinent to research oceanography and requirements of research projects vary widely in the requirements area. With the launch of Seasat in 1978 and with the improved accuracy and availability of data from meteorological satellites, ocean remote sensing is entering a period in which the necessary analysis tools are being built and investigators are becoming more familiar with the various sensor systems. This should lead to more investigator concern with data integration requirements for scientific and operational purposes.

Table 1 presents a summary of the primary satellite sensors of interest to oceanography. (See also Wilson[5].) Since microwave sensors are so prevalent, resolving the different IFOVs and subsatellite coverages becomes extremely difficult. All presently operating oceanographic satellites primarily contain imaging-type sensors. This makes image processing an important tool for present-day oceanographic studies.

TABLE 1

Summary of sensors of primary interest to oceanographers

SATELLITE	SENSOR	TYPE	CHANNELS	IMAGING/ NONIMAGING	IFOV	PRIMARY GEOPHYSICAL PARAMETERS
Seasat GEOS-3	Radar Altimeter (ALT)	Active	13.5 GHz	Nonimaging	2.4-12 km (depends on Sea State)	Wave height Wind speed Sea surface height
Seasat NIMBUS-7*	Scanning Multi-Channel Microwave Radiometer (SMMR)	Passive	6.6 GHz 10.7 GHz 18.0 GHz 21.0 GHz 37.0 GHz (Vertical & horizontal polarity)	Imaging (Low rate)	120 x 79 km 74 x 49 km 43 x 28 km 38 x 25 km 22 x 14 km	Sea surface temp. Wind speed Water vapor Liquid water
Seasat	Seasat-A Satellite Scatterometer (SASS)	Active	14.6 GHz	Nonimaging	16 - 23 km x 36 - 93 km highly variable geometry	Wind Speed Wind Direction
Seasat	Synthetic Aperture Radar (SAR)	Active	1.275 GHz	Imaging	~25 meters Dependent on Ground Processing	Wave Spectra Sea Ice
Nimbus-7*	Coastal Zone Color Scanner (CZCS)	Passive	.433-.453 .510-.530 .540-.560 .660-.680 .700-.800 10.5-12.5	Imaging	.825 km	Chlorophyll concentrations Ocean Color Diffuse attenuation coefficient
NOAA-6/7* TIROS-N	Advanced Very High Resolution Radiometer (AVHRR)	Passive	0.58-0.68 .725-1.1 3.55-3.93 10.5-11.3 11.5-12.5	Imaging	1.1 km Channel 1 slightly less	Cloud cover Sea surface temperature

NOTE: Nimbus-7 and NOAA-6 and 7 are the only currently operational satellites

* NOAA-6 and TIROS-N contain only 4 channels

REQUIREMENTS

Data integration requirements for oceanographic remote sensing[1,6,7] can be placed in several categories. Comparison of one observation with another at the same geographic location is important as it is in all disciplines. Observations must be earth-located and interpolated in order to either initialize or test numerical models. Observations must be earth-located to measure magnitude and motion of features. Finally, observations must be located, interpolated, and map-projected in order to provide maps depicting two-dimensional distributions.

Comparison of observations is an important aspect of not only disciplinary research but also sensor validation. Observations of a physical phenomenon from a given sensor need to be compared with observations of the same phenomenon from other sensors which may be on the same satellite, on a different satellite or on an aircraft platform. High-rate observations, such as AVHRR sea surface temperatures (1 pixel - 0.8 km) need to be compared with other observations of the same parameter from a low-rate sensor such as Seasat SMMR (1 pixel - 18 x 28 km).

The different IFOV sizes and shapes and sensor coverages on even the same satellite make observations difficult to compare (See Table 1). Added to this is the fact that the ocean is a dynamic system so that comparisons of observations taken at different times (even a few hours apart) require temporal interpolation as well as spatial interpolation before valid comparisons can be made.

Correcton of one sensor with data from another leads to an additional integration requirement. A single sensor is often incapable of making all the measurements necessary to derive a particular geophysical parameter. For example, to make efficient path-length corrections to the Seasat Altimeter sea surface elevation measurements, Seasat SMMR water vapor content estimates are used where available. The SMMR is also used to adjust scatterometer (SASS) returns for atmospheric attenuation effects. If an outside correction source is on a different satellite or even in an entirely different form (e.g., map form) the data integration problem becomes even more acute.

Feature identification, measurement and movement tracking requires earth-located data. Examples of these operations are found in the current warm ring analyses[8,9] being performed at several institutions. Satellite projections do not allow distance measurements in the image in line and sample coordinates. A transformation from line and sample to geographic coordinates (latitude/longitude) must be obtained and used. It is also necessary to compute this transformation to measure feature movement through time. The dynamic ocean system precludes simple scene/scene registration and simple differencing.

The two-dimensional display of sensor observations implies mapping. Users are accustomed to reading maps with specific orientations, projections, and cartographical characteristics. Satellites have yet to provide maps directly which satisfy these predictions. In fact, many satellite projections are so distorted that it is unreasonable to expect investigators to become accustomed to them. It becomes necessary, therefore, at some stage of analysis, to place the data into a suitable map projection and create a map using conventional cartographic methods (albeit automated).

Mapping of imagery data seems fairly straightforward. However, it is also important to create maps which are based on data from nonimaging sensors such as the Seasat Altimeter[3]. (See Figure 1.) These data are, in general, randomly spaced. For a number of reasons, a particular sample may be missing or unreadable. Interpolation techniques for establishing a reasonable value are needed. Alternatively, cartographic techniques are required for indicating missing values, yet providing an easily readable map. Oceanographers are concerned not only with two-dimensional distributions but also with three-dimensional distributions shown either synoptically, time averaged, or as a time continuum. The only effective way to display the four-dimensional information, as the latter requirement implies, is via animation. The art and science of computer graphics provides the technological base for animation. It is necessary, though, to map-project, register, temporally and spatially interpolate, and reformat the data to take advantage of that technology.

Positional accuracy requirements for oceanography are not as stringent as for terrestrial remote sensing but are more in line with meteorological applications. Using present navigation (earth-location) techniques for polar-orbiting image data sets[2], accuracies are adequate for all but micro- and fine-scale studies. Open-ocean positional confidence is probably within 5 kilometers with accuracy being within a kilometer near landmarks. These accuracies are adequate for macro- and mesoscale studies. Additional positional accuracy in open-ocean areas would enable much more activity in fine-scale research. Table 2 presents the spatial scales associated with various classes of oceanographic research.

RESEARCH	FEATURE SIZE
macroscale	global
mesoscale	10-1000 km
fine-scale	2-5 km
microscale	< 1 km

TABLE 2

Comparison of oceanographic research areas and spatial scales.

AREAS FOR RESEARCH AND DEVELOPMENT

Data integration is a problem for oceanography just as for any other discipline. Areas where progress is needed include technique development and evaluation, understanding requirements, and packaging techniques for speed, efficiency and ease of use. Some specific topics for futher research and development are presented below.

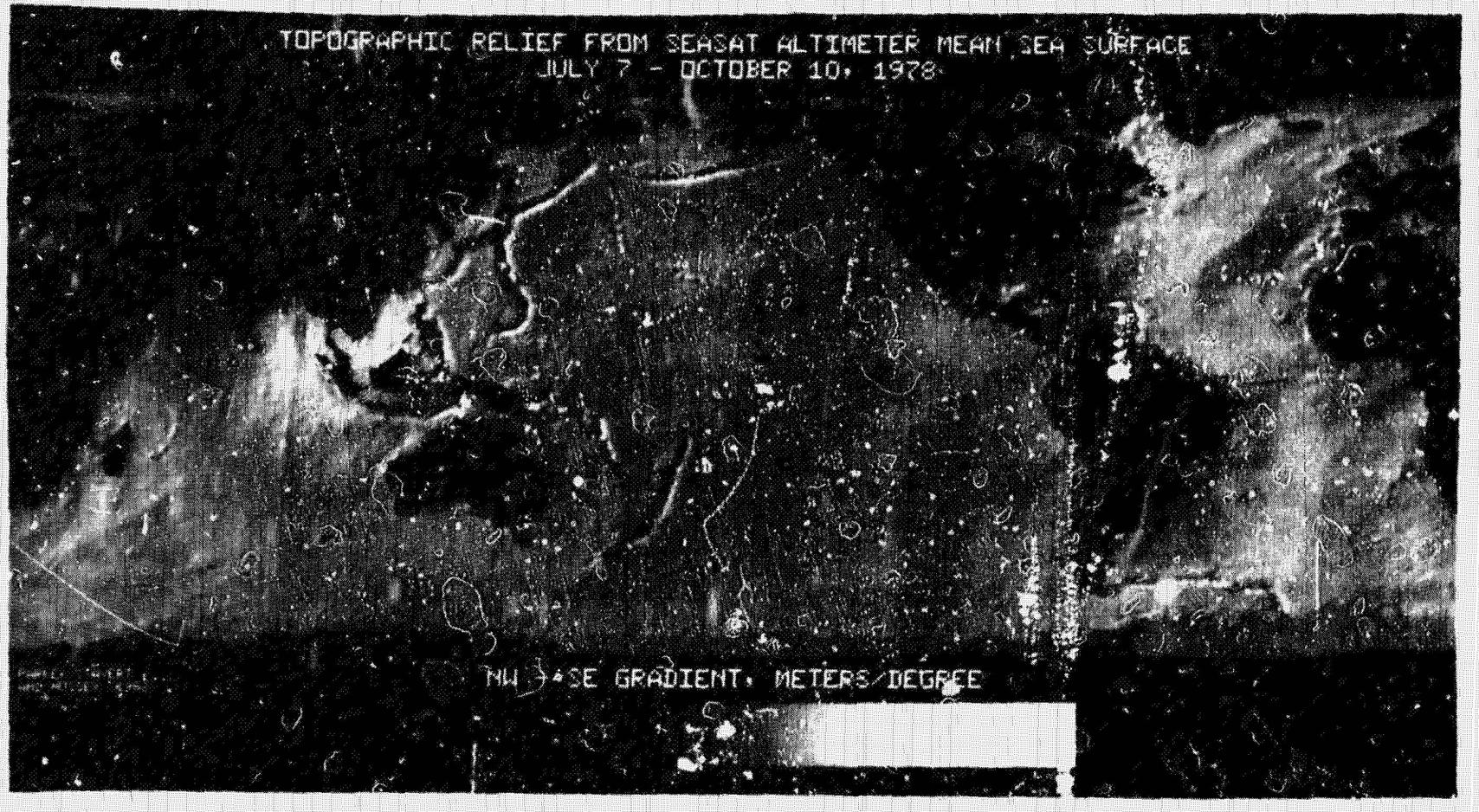

Figure 1

Shaded relief map of sea surface elevation constructed from Seasat Altimeter data

Source: M. Parke, JPL

TECHNIQUE EVALUATION AND DEVELOPMENT

- Evaluate techniques for establishing geophysical values in areas of missing data.
- Evaluate techniques for temporal interpolation.
- Compare and evaluate alternative navigation strategies.
- Develop algorithms for automated coastline detection and correlation with vector-coded coastline data (e.g., World Data Banks I and II).

FURTHER DEVELOPMENT OF REQUIREMENTS

- Define spatial scale requirements for fine-scale studies.
- Define requirements for band-to-band registration of multiband imagery.
- Define requirements for multisensor data integration, where sensors may be on the same satellite, a different satellite, or on aircraft and satellites.
- Define data integration requirements for operational applications.

PACKAGING AND SYSTEM DESIGN

- Produce a well-organized, efficiently accessed, coastline and landmark file for use in interactive adjustments to navigation parameters.
- Develop automated methods of acquiring, managing, and utilizing orbital parameters and clock adjustments provided by tracking facilities.
- Develop analysis systems with user-friendly interfaces enabling researchers to routinely perform data integration tasks in a short period of time. These systems would also provide the basis for evaluating new integration techniques as they are developed in research activities.
- Provide transportable software so that the minimum amount of effort has to be expended in duplicating data integration capabilities at various sites. This is important because the research nature of oceanographic remote sensing data integration implies decentralized activities. Also, the wide variety of sensors of interest suggests that centralized data integration capabilities will not exist, at least until full-scale disciplinary data systems are built.

REFERENCES

1) JPL, (1980), "Oceanic Pilot System User Functional Requirements Version I", Jet Propulsion Laboratory, D. B. Lame and S. E. Pazan, preparers, Internal Doc. #715-77, August.

2) ---- (1981), "User's Manual For Preliminary Satellite Image Processing: Extraction, Calibration, and Location", Scripps Satellite - Oceanographic Facility, SID Reference No. 81-36, October.

3) Chelton, Dudley B., K. J. Hussey, and M. E. Parke, (1981), "Global Satellite Measurements of Water Vapor, Wind Speed and Wave Height", Nature, Vol. 294, pp 529-532, Dec. 10.

4) Born, G. H., J. H. Dunne, and D. B. Lame, (1979), "Seasat Mission Overview", Science, AAAS, June, Vol. 204, #4400.

5) Wilson, W. Stanley, (1981), "Oceanography From Satellites?", Oceanus, Woods Hole Oceanographic Institution, Vol. 24, #3, pp 10-16.

6) NASA, (1980), "OSTA Data Systems Planning Workshop, Part II: Technical Summary", ADS Study Office, Draft February 22.

7) Fujimoto, Brad, (1981), "User Requirements for NASA Data Base Management Systems, Part One: Oceanographic Discipline", NASA, Jet Propulsion Laboratory, JPL pub. 81-50, June 15.

8) Lai, D. and T. Richardson, (1977), "Distribution and Movement of Gulf Stream Rings", Journal of Physical Oceanography, Vol. 7, pp 670-683.

9) Gordon, H. R. and D. Clark, J. Brown, D. Brown, R. Evans. (1982), "Satellite Measurement of Phytoplankton Pigment Concentration in the Surface Waters of a Warm Core Gulf Stream Ring", Journal of Mining Research, forthcoming

5.0 PRESENTATIONS ON SPACE SEGMENT ERRORS

5.1 SUMMARY

It was the purpose of the space segment errors analysis to first give a brief overview of the individual sensor system design elements considered to be a priori components in the registration and rectification process; and second, provide an analysis of the potential impact of error budgets on multitemporal registration and side-lap registration. The presentations reviewed the properties of scanner, MLA, and SAR imaging systems. Each sensor displays internal distortion properties which to varying degrees make it difficult to generate on orthophoto projection of the data acceptable for multiple-pass registration or meeting national map accuracy standards. Each sensor also is affected to varying degrees by relief displacements in moderate to hilly terrain. Nonsensor related distortions, associated with the accuracy of ephemeris determination and platform stability, also have a major impact on local geometric distortions. It was for this reason that a review of platform stability improvements expected from the new Multi-Mission Spacecraft series and improved ephemeris and ground control point determination from the NAVSTAR/ Global Positioning Satellite systems were reviewed.

5.2 SPACEBORNE SCANNER IMAGING SYSTEM ERRORS

Arun Prakash (General Electric)

INTRODUCTION

There are various stages and forms of error in a spaceborne scanner imaging system. The instrument, in this case consisting of the spacecraft and its sensors, is designed to behave in a nominal or ideal way. In real operating conditions, there are deviations from this nominal behavior. These deviations are a source of error not only as independent entities but because of the interdependence of the various components of the instrument. Thus, deviation from design of one parameter may cause another to display nonoptimal behavior.

The deviations mentioned above are large enough that if they are ignored in subsequent processing on the ground, the resulting images will be distorted and misregistered to unacceptably high levels. Therefore, direct or indirect measurement of deviations in instrument performance is necessary. Inaccuracies in measurements form a source of error which ultimately filter through to the output image along with ground processing errors.

In this paper we will discuss errors due to deviation from ideal instrument performance and due to the measurement system. The discussion will be within the Landsat-D system framework which consists of the spacecraft and two scanner type sensors—the Thematic Mapper (TM) and the Multispectral Scanner (MSS) [1,2].

Whatever the source of error in the instrument, when it propagates through to the image the error can be classified as either radiometric error or geometric error. On ground, it is difficult to distinguish between these two forms of error but from the point of view of the instrument, there is no difficulty in making this classification. In this paper we discuss only those instrument components which contribute to geometric error, because radiometric error is a function of parameters that are largely independent of the instrument being a scanner type or not.

Geometric error implies lack of accurate knowledge of the position of a sample. To place a detector sample of the spacecraft sensor precisely on ground, one needs to know the time the sample was taken, the position of the spacecraft, its orientation (in inertial space) and the orientation of the sensor body with respect to the spacecraft all at that same time. These are the platform or spacecraft components of the imaging system that need to be known. In addition, the sensor characteristics and dynamics need to be known for all time. Other important components which will not be specifically discussed here are earth shape, spin, atmospheric effects, etc.

The next section discusses the platform errors and Section III covers the sensor errors. For convenience, Table 1 shows the units often used interchangeably in describing the errors.

II. PLATFORM ERRORS [7,8,9,11]

With the exception of spacecraft jitter, all platform errors vary slowly (low-frequency error) with respect to the time required to collect data for

one image. The direct effect of these errors on the image is a shift or registration error as opposed to distortion of features within an image. We now discuss the four components of platform error individually, remembering that the Landsat-D System framework is assumed.

Time [7]

The spacecraft clock is updated once every 24 hours from the ground. The accuracy of the updated time is ±3 milliseconds. In a 24-hour period, the clock can also drift by a maximum of ±17 msecs. Thus a maximum of ±20 msec inaccuracy can build up in the spacecraft clock This time error is essentially a bias for any one image and may be treated as a spacecraft or image position knowledge uncertainty.

Ephemeris [7,8,9]

The nominal spacecraft orbit parameters and deviations from them are shown at the bottom of Table 2. At the top of the table is shown the error incurred in measuring the spacecraft ephemeris. This is the measurement error incurred when ephemeris information is uplinked from the ground. In the GPS modes, these errors would reduce substantially. The along-track and cross-track position error directly results in an image registration error, whereas the altitude deviation causes the ground projected pixel size to vary.

Attitude [7,8,9,10,11]

The nominal attitude of the spacecraft implies geocentric pointing of the sensor optical axis. For the Landsat-D TM, the attitude errors are shown in Table 3, along with jitter errors (which are high-frequency attitude errors). The spacecraft attitude control is in error by 36 arc sec [1]. This is a low-frequency error, as shown. The TDRSS antenna drive interacts with the spacecraft structure and causes attitude/jitter error of the magnitude shown. It should be noted that most of this error is in the lower-frequency range and can be measured by the gyros.

High-frequency jitter in the spacecraft is caused by the scanners themselves. Odd harmonics of the scan mirror frequency (7 Hz for the TM and 13.62 Hz for the MSS) are fed back to the sensors through the spacecraft structure. An angular displacement sensor (ADS) is used to measure this jitter on the TM sensor. In Table 3, the baseline and the worst case design values for jitter in the roll, pitch, and yaw axis is given. Error in ADS and DRIRU (dry rotor inertial reference unit) calibration causes measurement error in attitude/jitter.

Alignment [7,8]

The spacecraft assumes a predetermined alignment between the pointed axis and the master reference cube in order to achieve proper pointing. This predetermined alignment can, however, be achieved to within only a certain tolerance, and the real alignment can be measured to only a certain accuracy. The values are shown in Table 4. Another error source in alignment is the fact that it does not remain constant. There is a dynamic component to it caused mainly by thermal bonding due to spacecraft temperature changes. The static error component of alignment results in the sensor pointing away from nominal and is

equivalent to an attitude error. The dynamic component has a time constant that is large enough (about 360 secs) that the resulting error over one image is essentially constant. Both result in image registration errors.

Table 5 shows the approximate geometric errors (in meters) in knowledge of the position of an image due to platform errors. These errors are essentially constant for one image and therefore result in image misregistration. The attitude error shown here is the result of the low-frequency (<2-Hz) attitude errors. Higher-frequency attitude errors (jitter) affect the scan profile and will be dealt with in the next section. Note that the alignment error can be extremely large but postlaunch calibration will reduce this error substantially.

III. SENSOR ERRORS [5,6,8,9]

In this section errors in the sensor are discussed. Some of these errors are a result of platform errors such as spacecraft altitude or jitter. Others are errors in the sensor itself. Specific errors will be discussed with respect to the TM and the MSS will be indicated. As background, the article by Blanchard and Weinstein [3] on the TM design provides a good review of the essential design components of a scanner imaging system.

One advantage of a scanning sensor over nonscanning kinds is that object plane scanning can be used. This simplifies the performance requirements for the rest of the optical system by requiring the telescope to operate at only very small field angles. Moreover, the same zone of each element is used at all scan angles which eliminates many of the major problems of off-axis imaging. The scanning mechanism, however, is also a major source of error in these sensors. Ideally, the samples from all the scans should form an evenly sampled grid on the ground. Deviations from this idealization must be measured in real time so that appropriate ground processing can be applied. In order to understand these deviations, schematics of the MSS and TM sensor mechanisms are shown in Figures 1 and 2.

The MSS design is relatively straightforward. Fiber optics are used to transmit the focused image energy to the detectors. There are four bands with six detectors per band. Sampling of the detector outputs is done only during a scan mirror forward scan. The reverse scan is used to bring the mirror back to its initial position only.

The TM, on the other hand, does its imaging during both forward and reverse scans. Due to the relative velocity between the Earth and the spacecraft in the in-track direction, the forward and reverse scans when projected to earth are skewed to each other. Another scan mirror (the Scan Line Corrector) that opposes the relative in-track motion, is used to compensate for this effect. The TM has seven bands and a total of 100 detectors. These detectors are directly placed on the focal plane; thus fiber optic relays with their attendant losses are bypassed. Spacing between bands is naturally larger in such a design -- up to 183 samples maximum (compared to a maximum of six samples for the MSS). Scan profile repeatability and precise timing is therefore critical for accurate band-to-band registration.

The mirror mechanism that does the scanning is a major source of error in these sensors -- for the TM, this means the scan mirror and the scan line

corrector mirror. During active scan (when imaging is done) the scan mirror design dictates that no torques act on it. Under these conditions, the scan mirror moves at a constant angular velocity in inertial space. This velocity is predetermined by design. The scan line corrector mirror is also designed to scan with a constant angular velocity opposing the in-track velocity of the spacecraft with respect to the Earth. The design of the scan line corrector angular velocity is based on the spacecraft altitude and velocity.

Deviations from design conditions of the scan mechanism result in in-track and cross-track efforts. We will discuss these errors in terms of the scan profiles.

Cross-Track Profile

These are the profile errors in the scan mirror motion. Again, the TM is used as a base to describe the errors. Two kinds of errors occur. Design conditions of torque-free inertial motion result in evenly spaced samples on ground (ignoring the earth curvature effects and slant range effects) and a linear mirror angle versus time plot (profile). Due to small residual torques, however, a nonlinear profile is actually achieved. This means that the mirror motion is faster or slower than nominal and results in ground sample spacings that are uneven. Cross-track profile nonlinearity of the scan line corrector also adds to the total cross-track profile linearity. However, the scan line corrector nonlinearity is largely in the in-track direction.

The other error is called line length error, and refers to deviations that occur in total active scan time with respect to the nominal of 60743 usec. The sources of this error are the control system, spacecraft jitter in the roll axis, and interaction of the two. The sensor scan mirror control system responds very well to jitter caused by itself but poorly to external jitter sources.

The cross-track profile nonlinearity and the line length are dynamic error sources and must be measured in flight. Line length is easily measured by clock counts taken from start to end of scan. The scan mirror cross-track profile for the TM is modeled as a six-term power series with time as the independent variable. It has been shown by extensive tests [6] that the variation in the profile can be accurately modeled by updating the first-order and second-order terms of the power series. This requires knowledge of first-half and second-half scan times which are measured by a clock on the spacecraft. Time is normalized using line length and jitter data.

Table 6 shows the magnitude of along scan (or cross-track) errors.

Along-Track Profile

The ground projected scan profile (i.e., the envelope of the projection of all detectors of a band on ground during one complete scan) should ideally be rectangular, with each scan starting where the last left off. The real ground projected scan profile doesn't follow this simple geometry. Gaps between scans (underlaps) and scan overlaps are present for a number of reasons.

The projected size of a pixel is directly related to the distance between the detector and look point on the Earth's surface. At the spacecraft design altitude of 705.3 km, a detector (42.5 μradians) projects to ground as a 30-meter square pixel. The slant range being larger than the nadir, the scan profile is wider at the ends than it is in the center. This effect is called the bow-tie effect and results in a small scan overlap at the scan ends and an underlap at scan center.

Spacecraft altitude variations (696 km to 741 km) affect the scan profile in two ways. First, as described above, it causes a scan overlap/underlap. The second error is due to spacecraft velocity variations as a result of altitude deviations. The scan line corrector mirror rate design is based on the spacecraft velocity. When the latter changes, the scan line corrector compensation is no longer correct. The forward and reverse scans then are skewed to each other.

Spacecraft jitter in the yaw and pitch axis also shows up in the ground projected scan profile. High-frequency jitter causes underlap/overlap to vary across the scan. See Table 7 for numerical values for scan gap error.

The profiles of the scan mirror and scan line corrector mirrors in the in-track direction is a fixed function known a priori, and, though it does make the ground projected scan profile deviate from the rectangular case, it is a constant, known deviation.

Knowledge of imaging geometry along with measurement of the parameters mentioned above (which cause in-track scan nonlinearities) allows one to accurately describe the scan shape and position of samples on the ground. The next step is to define an algorithm to perform image resampling under the conditions, which will not be discussed in this paper.

Other sources of error in the sensor are detector alignment and the electronics. These errors are relatively small in comparison to the scan nonlinearities. They are summarized in Table 8 and will be briefly discussed. The effective focal length (EFL) of the optical system determines the dimensions of the projection of the detector on ground. Because the image is scanned across the detector arrays, the EFL is also responsible for the system transfer function. Tolerances must be tight if the real sampling is to mimic the design transfer function characteristics. Values for the EFL fabrication and measurement tolerances are shown, as is deviation of EFL.

The spacing between detector arrays for the different bands determines the band-to-band image spacing. Alignment between detector arrays must be within strict tolerance limits or band-to-band registration will suffer.

Vibration of the detector layout causes band-to-band error for band-to-band vibration and also overlap/underlap error for vibration within any one band. The electronics of the system introduces errors too. Detector response nonuniformity is one reason. The filter response and timing errors are other causes. The vibration and detector/electronics responses cause distortions within an image.

This overview of spaceborne scanner imaging system errors shows the sensitivity of image errors to spacecraft component errors and also the interdependance

of the imaging system components. As more sophisticated imaging systems are developed, with greater resolution capabilities and stricter accuracy requirements, the need to understand and model these error sources becomes more important [4].

Table 1. **UNITS**

TM PIXEL = 42.5 μ RAD = 8.77 ARC-SEC ⇒ 30 METERS AT 705.3 KM

MSS PIXEL = 117.2 μ RAD = 24.17 ARC-SEC ⇒ 82.7 METERS AT 705.3 KM

1 μ RAD ⇒ .71 METER AT 705.3

1 ARC-SEC ⇒ 3.4 METER AT 705.3

1 ARC-SEC = 4.85 μ RAD

Table 2. **EPHEMERIS ACCURACY AND VARIATION**

- ORBIT SUPPORT COMPUTING DIVISION EPHEMERIS ERROR

	(1σ AFTER 2 DAYS)	
	POSITION (METERS)	VELOCITY (METERS/SEC)
ALONG TRACK	500*	.163
CROSS TRACK	100	.065
RADIAL	33	.650*

*GSFC SPEC

- VARIATION FROM NOMINAL
  - ALTITUDE (705.3 KM ORBIT): 696 TO 741 KM OVER EARTH; RANGE OF 19 KM OVER ANY FIXED LATITUDE
  - CROSS TRACK: ± 4 KM AT THE EQUATOR
  - INCLINATION: 98.21 ± .045 DEGREES

- SPACECRAFT CLOCK ACCURACY ± 20 MILLISECONDS

Table 3.

ATTITUDE/JITTER ERROR (AT THE TM)

FREQUENCY RANGE	ERROR MAGNITUDE (ARC-SEC)		COMMENT
0 - 0.01 Hz	36 (1σ)		ALL AXES, ATTITUDE CONTROL ERROR
0.01 - 0.4 Hz	10 (1σ)		ALL AXES, TDRSS ANTENNA DRIVE ERROR
0.4 - 7 Hz	0.3 (1σ)		ALL AXES, TDRSS ANTENNA DRIVE ERROR
	BASELINE MODEL (.01 DAMPING)	WORST CASE DESIGN	
>7 Hz	R 0.93 (1σ)	20.0 (PEAK)	ADS LIMIT IS 50 ARC-SEC
	P 0.20 (1σ)	. (PEAK)	LIMITS JITTER GAP TO LESS THAN ONE PIXEL
	Y 0.30 (1σ)	16.8 (PEAK)	LIMITS JITTER GAP TO LESS THAN ONE PIXEL
ADS CALIBRATION REQUIREMENT		3% ERROR	.5 ARC-SEC (1σ) USED IN ERROR BUDGETS
DRIRU CALIBRATION REQUIREMENT		3% ERROR	.5 ARC-SEC (1σ) USED IN ERROR BUDGETS
ATTITUDE DATA PROCESSING REQUIREMENT		1% ERROR	.5 ARC-SEC (1σ) USED IN ERROR BUDGETS

ADS: ANGULAR DISPLACEMENT SENSOR
DRIRU: DRY ROTOR INERTIAL REFERENCE UNIT
TDRSS: TRACKING AND DATA RELAY SATELLITE SYSTEM

Table 4. **STATIC ALIGNMENT**

- **ALIGNMENT REQUIREMENTS**
  - **ALIGNMENT BETWEEN ACS AXIS AND POINTED AXIS WITHIN 1.25 DEGREES (3σ)**
  - **POINT THE AVERAGED AXES OF THE MSS AND TM**
  - **ALIGNMENT KNOWLEDGE ACS TO TM OPTICAL AXIS ROLL = .10, PITCH = .21, YAW = .21 DEGREES (3σ)**
- **POST LAUNCH ESTIMATION OF SPACECRAFT STATIC ALIGNMENT WILL BE PERFORMED**

ACS: ATTITUDE CONTROL SYSTEM

DYNAMIC ALIGNMENT

- **SPACECRAFT TEMPERATURE CHANGES CAUSE ALIGNMENT CHANGES**
  - **EXAMPLE: 1 DEGREE GRADIENT ACROSS THE INSTRUMENT MODUL CAUSES A 12 ARC-SEC ACS TO TM ALIGNMENT CHANGE. (GODDARD ANALYSIS)**

Table 5.

GEOMETRIC ERROR IN SYSTEMATIC CORRECTION DATA (APPROXIMATE)

ERROR SOURCE	CROSS TRACK (METERS 1σ)	ALONG TRACK (METERS 1σ)
EPHEMERIS	100	500
TIME		80
ATTITUDE	123	123
ALIGNMENT	427*	855*
TOTAL (ROOT-SUM-SQUARE)	455 (25 PIXELS 90%)	1001 (55 PIXELS 90%)

*SUBSTANTIAL REDUCTION WILL OCCUR AFTER POSTLAUNCH CALIBRATION

Table 6.

SCAN MIRROR PROFILE

- SCAN MIRROR ALONG SCAN NONLINEARITY DEFINED BY 5TH-ORDER POLYNOMIAL
  - NOMINAL NONLINEARITY 35 MICRORADIAN
- ALONG SCAN PROFILE VARIATIONS
  - ± 10 MICRORADIAN WANDER OVER 2000 SCANS
  - ± 50 MICRORADIAN SHIFT DUE TO A VIBRATION EVENT
  - ± 200 MICRORADIANS WORST CASE SHIFT
- ALONG SCAN CORRECTION
  - LINEAR CORRECTION MEASURED BY SCAN TIME
  - SECOND-ORDER CORRECTION MEASURED BY MIDSCAN TIME
  - JITTER MOVES INERTIAL START, MID, END SCAN POSITIONS
- CROSS SCAN PROFILE MUST BE CORRECTED

NOTE: ALL ANGLES ARE IN OBJECT SPACE

Table 7. **SCAN GAP** ERROR**

ALTITUDE VARIATION	JITTER	TM UNDERLAP/OVERLAP
696 – 741 KM FOR 705.3 ORBIT 713 KM TM DESIGN ALTITUDE	LESS THAN 1 PIXEL	0.2 PIXEL (SPEC)

END SCAN GAP

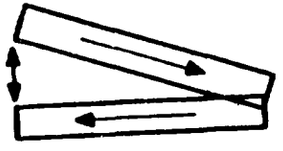

EARTH LOCATION	WORST CASE END SCAN GAP IN PIXELS*
NORTHERN HEMISPHERE	-0.7 TO 0.8
45°N	-0.4 TO 0.6
EQUATOR	-0.2 TO 0.8
45°S	-0.9 TO 0.1
SOUTHERN HEMISPHERE	-1.6 TO 0.8

WORST CASE GAP RANGE

-2.8 TO 2.0

*INCLUDES SCAN WIDTH, SCAN LINE CORRECTOR AND BOWTIE EFFECTS

**GAP < 0 : OVERLAP
= 0 : NOMINAL
> 0 : UNDERLAP

Table 8. Summary of Error Sources

Error Source	Magnitude		
		µrad (90%)	
Effective Focal Length (EFL)	Band	Across-Track	Along-Track
EFL Measurement and Fabrication	1 to 4	2	2
	5 to 6	2	2
	5 to 1	2	2
EFL Deviation	2 µrad (max)		
Focal Plane Tolerance	0.4 µrad (max)		
Detectors			
		µrad (90%)	
Detector Array Alignment Accuracy	Band	Across-Track	Along-Track
	1 to 4	3	3
	5 to 6	31	31
	5 to 1	6	6
Band-to-Band Vibration	1 to 4	1.5	1.5
	5 to 6	1.5	1.5
	5 to 1	1.5	1.5
One-Band Vibration	2.6 µrad random error (90%) in tests.		
Detector Response Nonuniformity	1 to 5	2	2
	5 to 6	8	8
	5 to 1	2	2
Filter Response - Forward to Reverse Scan	Bands 1-5 and 7	1.3 IFOV offset	
	Band 6	5.2 IFOV offset	
Filter Response - Bands 1-5 and 7 to Band 6	3.0 IFOV offset		

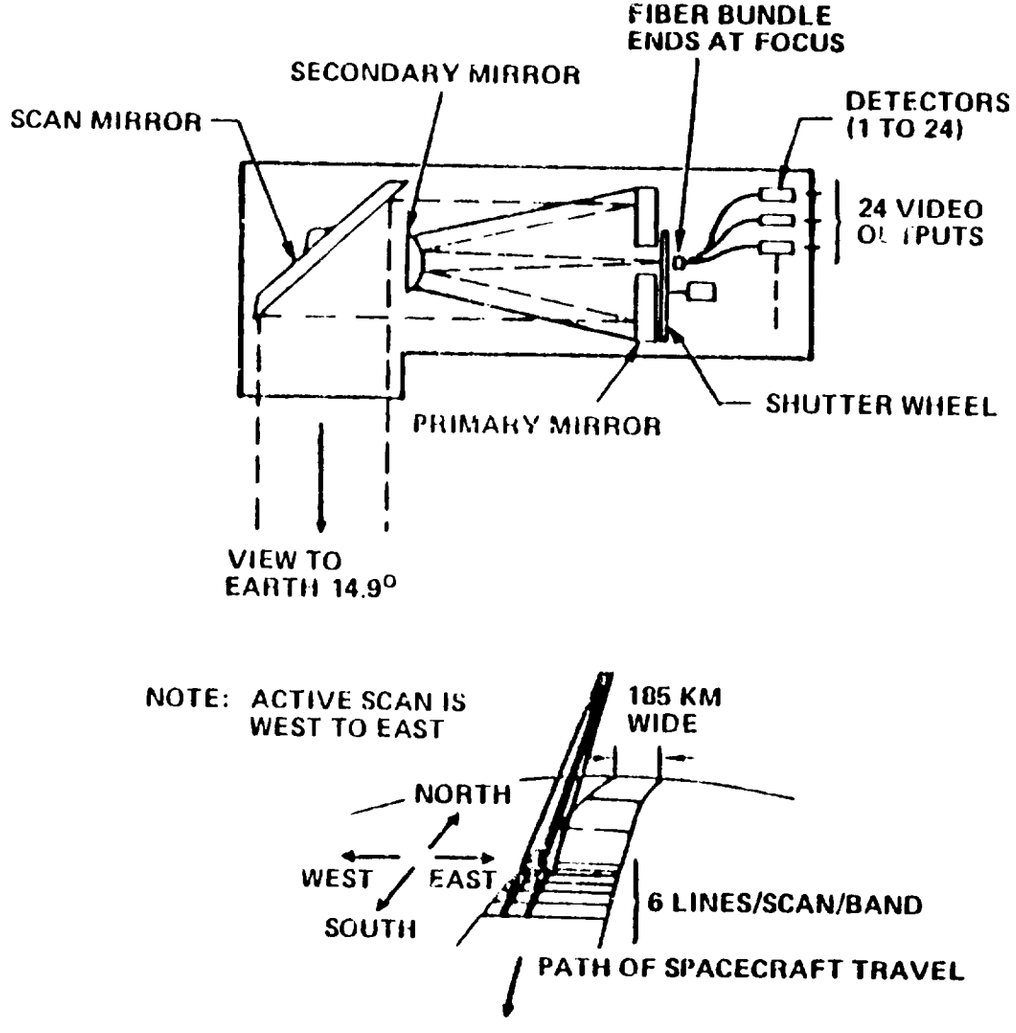

Figure 1. Multispectral Scanner

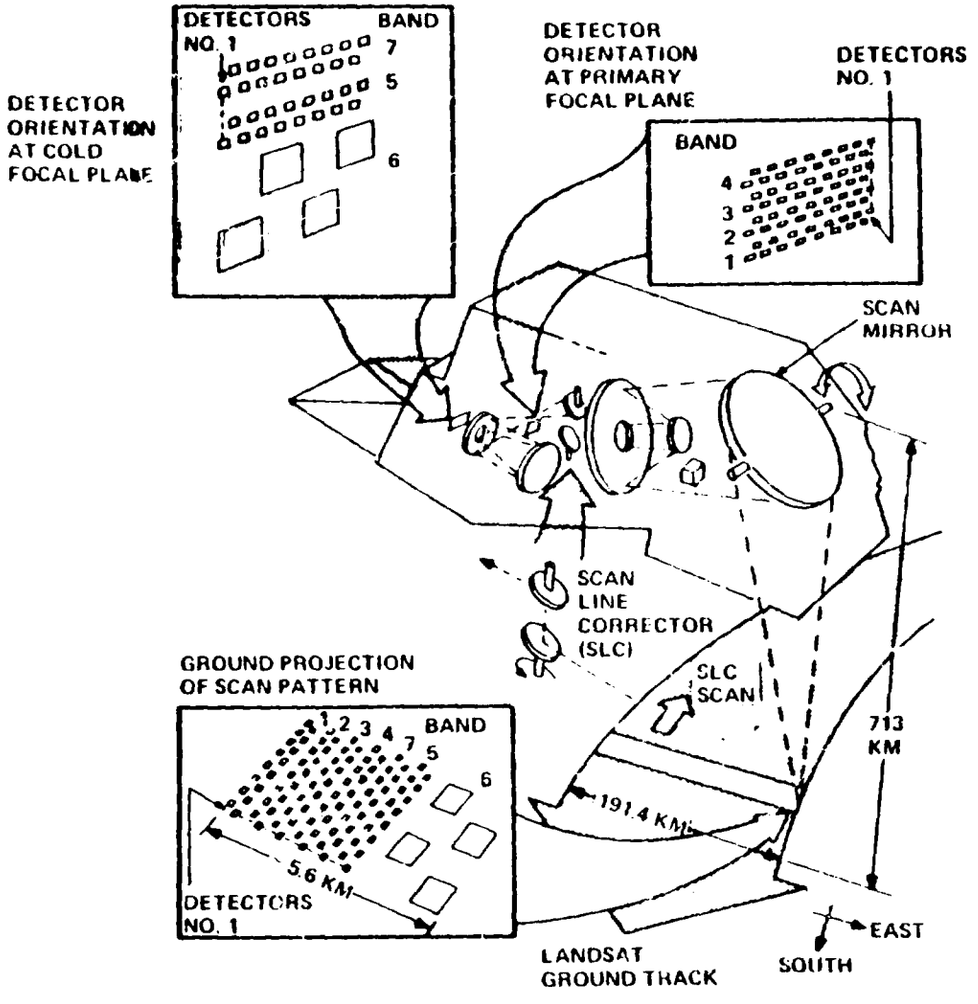

KEY GEOMETRIC FEATURES

- SCAN MIRROR
  - BI DIRECTIONAL CROSS-TRACK SCANNING
  - DATA AVAILABLE TO GROUND:
    - SCAN START TIME
    - SCAN DIRECTION
    - FIRST HALF-SCAN TIME ERROR
    - SECOND HALF-SCAN TIME ERROR
- SCAN LINE CORRECTOR
  - PROVIDES IN TRACK SCANNING
- TWO FOCAL PLANE ASSEMBLIES
- INSTANTANEOUS FIELD OF VIEW (IFOV)
  - BANDS 1-5, 7: 42.5 μrad (30 METERS)
  - BAND 6: 170 μrad (120 METERS)

Figure 2 . Thematic Mapper

REFERENCES

1. V.V. Solmonson, P.L. Smith, Jr., A.B. Park, W.C. Webb, and T.J. Lynch, "An Overview of Progress in the Design and Implementation of Landsat-D Systems", IEEE Trans. on Geoscience and Remote Sensing, Vol. GE-18, No. 2, pp. 137-146, April 1980.

2. T.C. Aepli and W. Wolfe, "Landsat-D the Next Generation System", Western Electronic Show and Convention, Sept. 18-20, 1979.

3. L.E. Blanchard and Oscar Weinstein, "Design Callenges of the Thematic Mapper", IEEE Trans. on Geoscience and Remote Sensing, Vol. GE-18, No. 2, pp. 146-160, April 1980.

4. Roger A. Holmes, "Processing System Techniques for the 80's", Proceedings of the 7th Intl. Symp. on Machine Processing of Remotely Sensed Data, Session II.C. Preprocessing and Systems, pp. 140-145, June 23-26, 1981.

5. A. Prakash and E.P. Beyer, "Landsat-D Thematic Mapper Image Resampling for Scan Geometry Correction", Proceedings of the 7th Intl. Symp. on Machine Processing and Remotely Sensed Data, Session II.C. Preprocessing and Systems, pp. 189-200, June 23-26, 1981.

6. Hughes Aircraft Company, Thematic Mapper Detailed Design Review Package, Hughes No. D4596-SCG 80201R, June 1978.

7. A. Prakash, Landsat-D System Geometric Error Budget, General Electric Co., PIR 1K50-LSD-784B, March 20, 1981.

8. General Electric Company, Landsat-D Thematic Mapper Image Processing System Design Review, Oct. 6-7, 1981.

9. General Electric Company, Landsat-D Multispectral Scanner Image Processing System Design Review, Oct. 6-7, 1981.

10. General Electric Company, Landsat-D Jitter Review, May 20-21, 1980.

11. T.C. Aepli, Approach to Geometric Performance Improvement, General Electric Company, PIR 1K51-LSD-684.

A5 N82 28714

5.3 THEMATIC MAPPER PERFORMANCE*

Jack Engle, Santa Barbara Research Corp

Just a brief overview, if some of you aren't familiar with how the thematic mapper primarily differs from MSS. The spatial resolution is the key improvement where the TM has 30-meter resolution and the MSS has 80-meter resolution. For the agricultural users, this should provide an ability to accurately classify 10-acre fields with the TM versus 70-acre fields with the MSS data. As far as spectral resolution, there are six reflected light bands in the thematic mapper. Two of those bands are of basically a new spectral region out in the the near IR, the shortwave IR region, 1.55 to 1.75 microns and 2.08 to 2.35 microns as opposed to MSS's four reflected light bands. The other four thematic mapper reflected light bands in the visible portion of the spectrum are designated to enhance the classification capability. They are much more ideally selected from a spectral standpoint, narrow spectral bands more optimally selected to enhance classification accuracy. The TM also has better signal-to-noise ratio performance and radiometric sensitivity, and in order to obtain that we have had to increase the size of the optics, basically a 16-inch telescope as opposed to an 9-inch telescope in MSS. We've increased the scan efficiency through the use of bidirectional scanning, which gives us a scan efficiency of 85% versus 45% with the multispectral scanner, and more detectors per band, 16 versus 6. We also have greater encoding resolution in our multiplexer, 8-bit resolution versus 6 bits for MSS.

One of the features that is of particular interest is the scan profile and the registration capability. Certainly the scan profile is more linear than was obtained in the MSS, and for a large selection of the users, the imagery could be used without resampling and I think satisfy many of the needs that I've heard expressed today. As far as geometric accuracy or scan profile, a typical Landsat D MSS scan profile exhibits nonlinearities on the order of five instantaneous fields of view. For the MSS, with 80-meter resolution, those were on the order of 500-microradian nonlinearities in the scan profile.

The thematic mapper profile data, on which, as I indicated, we are still doing some final refinements in the processing, is our measured forward scan profile, as shown in Figure 1. You can see the peak nonlinearity in the scan has a magnitude of about 30 microradians. The rms nonlinearity I believe is on the order of 10 microradians. The reverse scan profile has a slightly different shape (Figure 2). It's not quite as linear as the forward scan, but it's well characterized. The peak nonlinearity in the reverse scan as measured in our vacuum tests just prior to delivery was about 60 microradians. Each figure would have to be flipped end for end in order to see how they register in object space. Note also that they are both plotted on a time scale instead of an object space scale.

As far as the overlap/underlap characteristics, Figure 3 summarizes the various contributors to the overlap/underlap effects within the system. We have chosen to optimize the scanning parameters at 712.5-km altitude and an average 40° north latitude where most of the scenes of interest appear to be located

*Edited oral presentation.

throughout the world. As the scanning parameters were optimized for that altitude and latitude, the resultant underlap and overlap of about 3.4 and -3.4 microradians occurs (Figure 4).

The bow-tie effect (Figure 4) is basically due to the path length over the scan angle. From one end of the scan to the other this contributes an overlap effect of about 6.5 microradians at the end of scan. Scan mirror performance has these contributions. Basically, within the prime focal plane, we have a maximum over/underlap of about 7.3 microradians, and with the bow-tie effect included we have a maximum overlap of about 11.1. For the cooled focal plane, we have 7.9 with a maximum overlap of 10.5. Our requirement is 8.5 microradians neglecting the bow-tie effect so we're fairly well within our requirements. Basically, the altitude variations globally sort of wash out or certainly dominate the overlap/underlap performance on a global scale.

As far as band-to-band registration, we chose the band-to-band registration between bands 5 and band 1 which are the furthest separated bands within the thematic mapper (Figures 5 and 6). The nominal band spacing is 146 instantaneous fields of view and the dynamic registration measured at 30 points in the scan profile is as plotted with a typical, an average registration of about 145.95. Our requirement is that the prime and cool focal planes be registered to within .3 of an instantaneous field of view and about the nominal band separation. So we are well within our requirement on a dynamic registration basis between the prime and cooled focal planes. All the other spectral bands, with respect to band 1 are more closely registered.

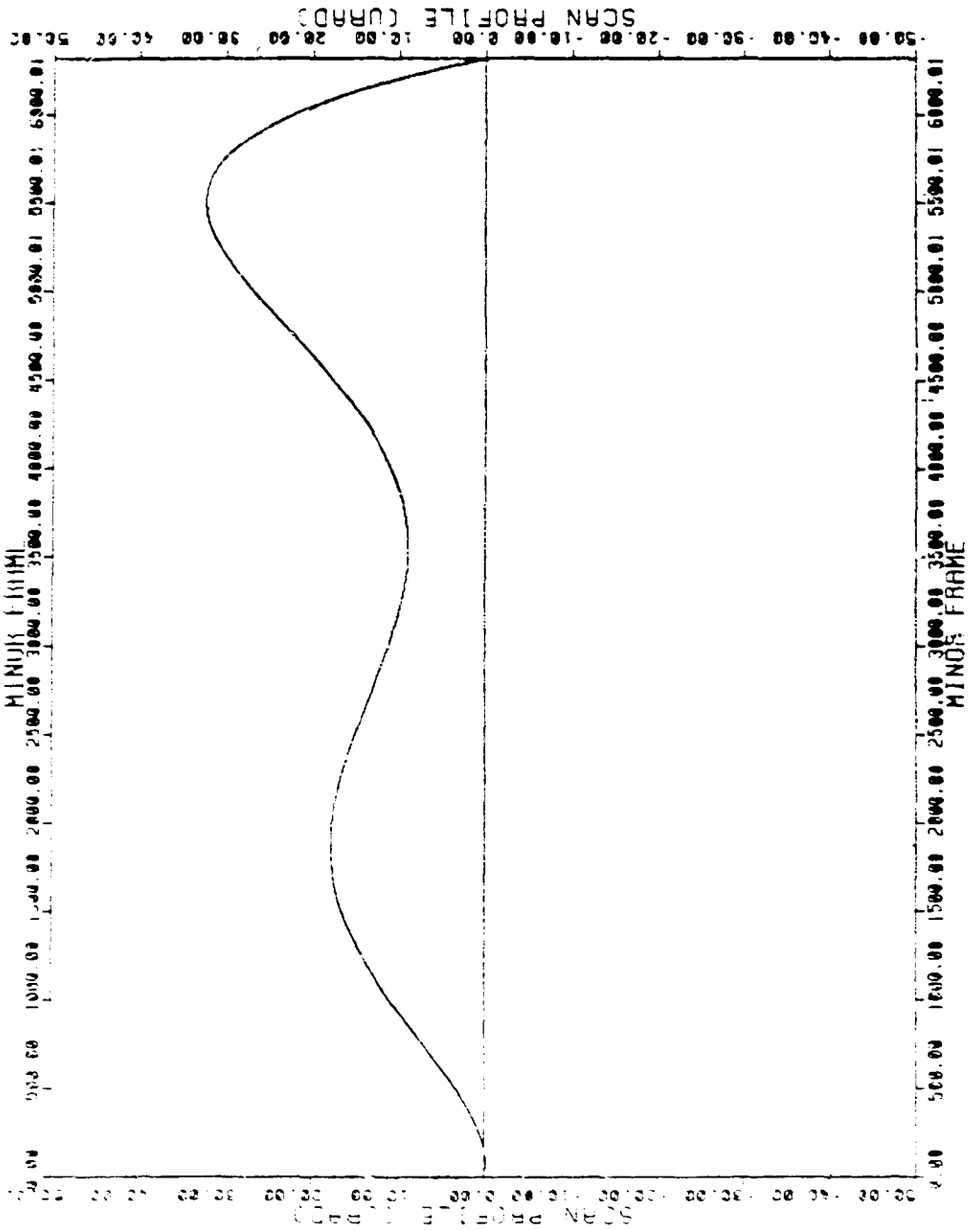

Figure 1. Forward Scan Profile

Figure 2. Reverse Scan Profile

SOURCE		PROTOFLIGHT UNDER	PROTOFLIGHT OVER	PROTOFLIGHT RANDOM*
NOMINAL ORBIT AND SCAN PARAMETERS**		3.4	-3.4	
BOW TIE EFFECT		0.0	6.5	
SMA				
SM CROSS AXIS MOTION		2.0	2.0	1.0†
SM PERIOD VARIATION		2.6	1.3	0.0
VIBRATION				0.5
RADIOMETER				
NON-IDEAL SLC SCAN		2.0	2.0†	0.2
EFL DEVIATION				
TELESCOPE		-1.0	1.0	
RELAY OPTICS		4.3††	4.3††	
DETECTOR IFOV SIZE		-5.4††	+5.4††	
VIBRATION		-1.7†††	+1.7†††	1.4
TOTAL	PFPA	7.3	11.1	1.8
	CFPA	7.9	10.5	
SPECIFICATION			8.5	
EFFECT OF ORBITAL ALTITUDE VARIATIONS BETWEEN 45°N AND 45°S LATITUDES		22.0	15.7	

*1 SIGMA
**ALTITUDE = 712.5KM
VELOCITY = 6821 KM/SEC
SCAN PERIOD = 142.925 MSEC

†OVER FULL TEMPERATURE RANGE
†† AFFECTS COOLED FOCAL PLANE ONLY
††† AFFECTS PRIME FOCAL PLANE ONLY

11/81

Figure 3. Overlap/Underlap (3.2.7.2) (microradians)

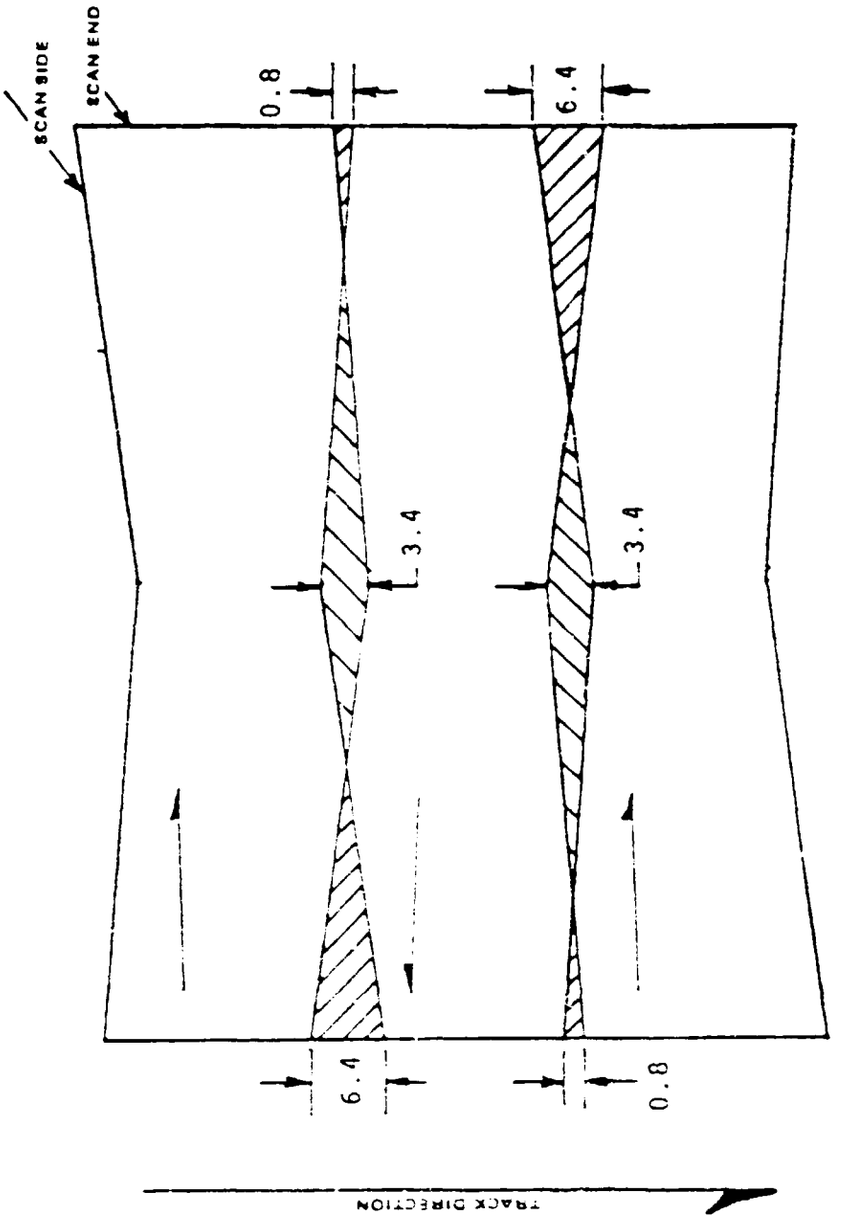

Figure 4. Overlap/Underlap With Bow-Tie Effect

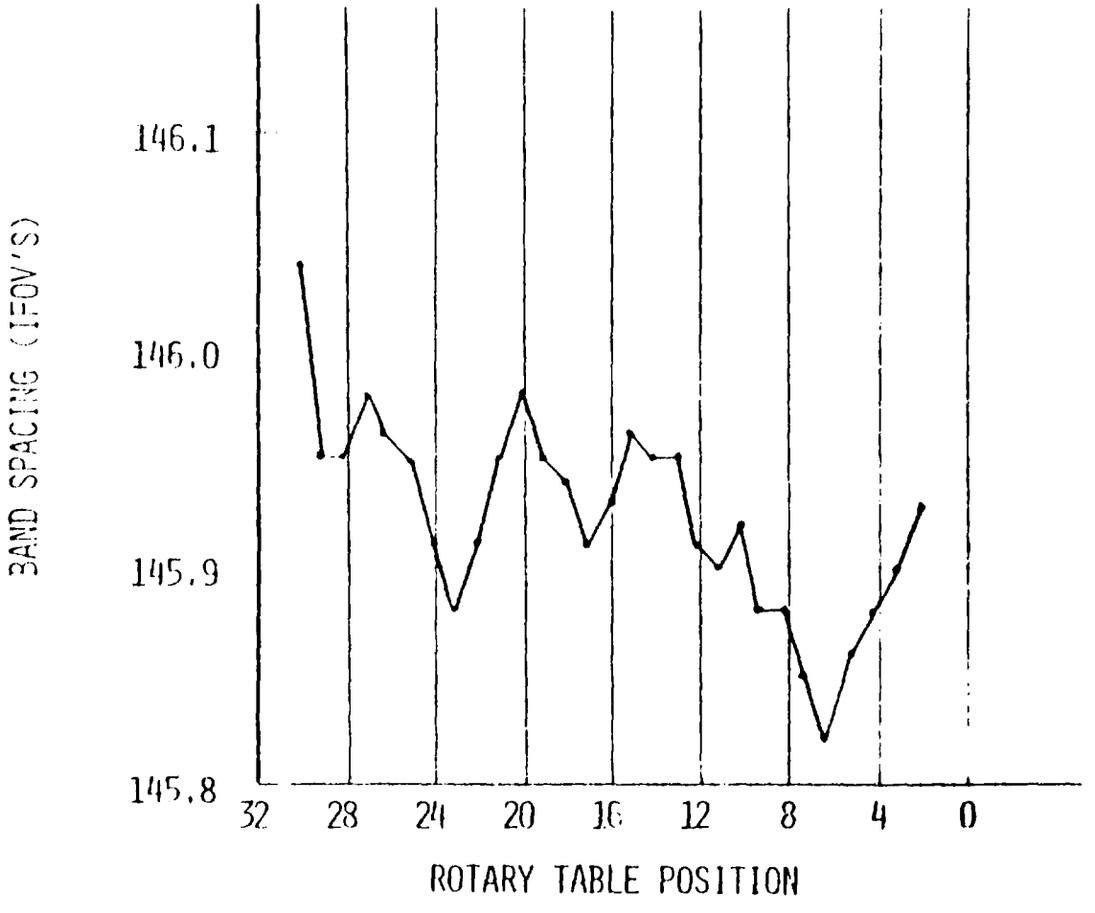

Figure 5. Dynamic Band-to-Band Registration (Along Scan)

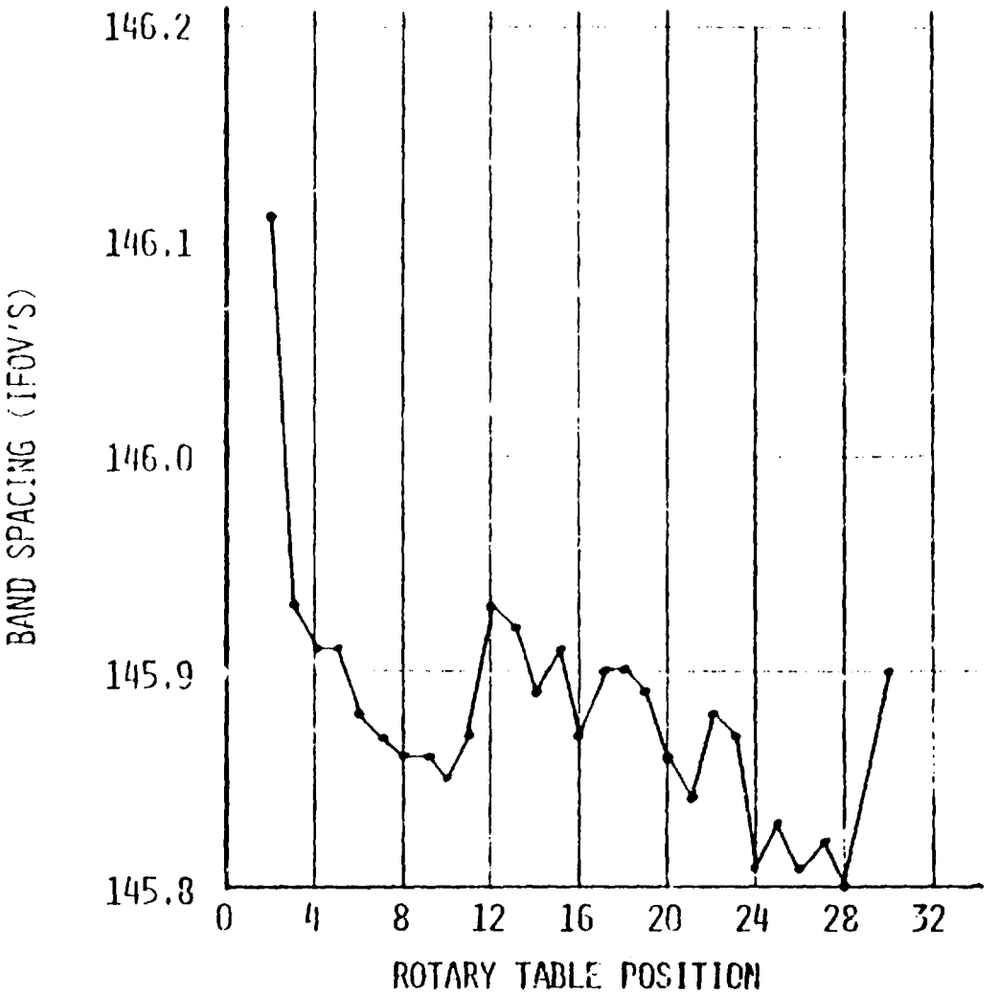

Figure 6. Dynamic Band-to-Band Registration (Along Scan)

5.4 SCANNER IMAGING SYSTEMS, AIRCRAFT

Stephen G. Ungar
NASA/Goddard Institute for Space Studies

With the advent of advanced satellite-borne scanner systems, the geometric and radiometric correction of aircraft scanner data has become increasingly important. These corrections are needed to reliably simulate observations obtained by such systems for purposes of evaluation. This paper reviews the causes and effects of distortion in aircraft scanner data and discusses an approach to reduce distortions by modelling the effect of aircraft motion on the scanner scene.

Causes of Distortion

Both the location of an observation (or pixel) on the ground and the target area (footprint) contained within the instantaneous field of view (IFOV) of the sensor system are governed by the following three factors: aircraft position; aircraft attitude; and sensor system can angle. Terrain relief may interact with aircraft/scanner geometry to further complicate determination of pixel position and footprint in planar coordinates. For purposes of this discussion, we shall address only cases in which the terrain effects are negligible.

During the acquisition of a single scan line, the scan pattern on the ground is largely a function of the scan geometry convoluted with the attitude of the aircraft. It is convenient to

characterize an aircraft's attitude (orientation) in terms of a fusilage axis and a wing axis. The fusilage axis passes from tail to nose through the aircraft's center of gravity. The wing axis passes through the center of gravity parallel to the wing surface. The orientation of the fusilage axis is expressed in spherical polar coordinates as follows: the angle of rotation east of north about a vertical axis (clockwise rotation looking down at aircraft) is called heading (ϕ); the angle of the nose above the horizontal is called the pitch (θ). An additional angle, roll (ρ), is required to specify the final orientation of the wing axis and is measured by the degree of clockwise rotation of the aircraft about the fusilage axis looking towards the nose. Since the aircraft scanner systems treated here rotate in a plane perpendicular to the fusilage axis, roll can be combined with the scanner orientation to determine the effective scan angle. The scan angle (ψ) is the look angle of the sensor measured clockwise from a direction mutually perpendicular to the fusilage and wing axis (i.e., the nadir direction for an aircraft in level flight). Therefore, the effective scan angle may be expressed as ($\psi_e = \rho + \psi$).

Given the altitude of the aircraft and the coordinates of the nadir point below the aircraft, the position of the instantaneous viewpoint on the ground can now be located in terms of the attitude parameters. Table 1 presents the detailed formulas required for making this calculation. "h" is the altitude of the aircraft above the ground, X_o and Y_o are the coordinates at aircraft nadir.

We have selected a coordinate system in which the positive x-direction is east and the positive y-direction is south in order to conform to conventions found in most image processing systems.

Impact of Aircraft Motion

In principle, both the attitude and position of the aircraft changes during the acquisition of a scan line. However, contemporary scanner systems actively gather image data only during a time interval of approximately 12 to 28 percent of the scan period. Typical scan periods range from 0.05 to 0.1 seconds. Therefore, in practice, changes in aircraft attitude may be considered negligible during the active portion of the scan. The forward motion of the aircraft will introduce skew in the scan line pattern which amounts to approximately one-tenth pixel displacement at the end of the scan line for contemporary systems. This corresponds to an angle of about 0.01 degrees. A viable geometric correction scheme need only update the aircraft's position once per scan line, specifying the aircraft coordinates at $\psi = 0$.

Rectification of Scanner Data

Table 1 outlines a method for rectifying aircraft scanner observations in cases where reliable navigational data is available. As previously discussed, the first half of the table relates the planar coordinates of the pixel to the navigational parameters for a given nadir location (X_o, Y_o). The remainder of Table 1 describes an integration scheme for updating the nadir position during the course of the flight. The scheme is valid for situations in which navigational data is available at time intervals wnich are com-

parable or less than the scan period. The values of all navigational parameters including aircraft velocity may be estimated at the center of each scan ($\psi = 0$) by cubic interpolation as indicated in Step 2. Finally, the aircraft nadir displacement in both the x and y-directions between scans may be calculated as indicated in Step 3. For roll-compensated systems, the scan mirror moves with a constant "inertial" velocity and Δt represents the period of ($\psi_e = \rho + \psi$). Under these circumstances, the solutions to the equations in Table 1 are equivalent to assuming $\rho = 0$ at all times and dropping that term out of the analysis.

Simulated Flight

The impact of variations in flight parameters on aircraft scanner imagery can best be illustrated by simulating a flight over a geometrically regular pattern and varying the flight parameters in a controlled way. The simulated scanner system selected for this study is patterned after NASA's NS001 scanner system flown onboard a C130 aircraft. Nominal flight and scanner parameters are given in Table 2. Simulated flights are conducted over a checkerboard pattern consisting of half mile square sections (approximately 800 meters x 800 meters). Figures 1(A-L) show the results of such flights with flight parameters deviating from the nominal values as specified. The left portion of each figure displays the scan system pattern projected on the ground as follows: the "footprint" for each observation along every 90th scan line is represented as a plotting point; in addition, the footprints of observations on every scan line are plotted at

10 degree intervals (from -50 to +50 degrees). The scanner "image", consisting of radiometric values of the simulated checkerboard terrain, is displayed in scanner coordinates (pixel position, scan line) to the right of its corresponding ground pattern.

For agricultural applications, it is instructive to draw an analogy between the checkerboard squares and field boundaries. Figure 1(A) represents an ideal case of the aircraft flying from north to south, parallel to field boundaries, with all parameters fixed at constant altitude. The foreshortening of fields at the edges of the flightline is due to the oblique look angle at the ends of the scan. In Figure 1(B), we introduce a drift (v_x component) in the aircraft motion while keeping the heading (orientation) of the aircraft north-south (in positive y-direction). Motion of this sort occurs in situations where aircraft flying at fixed headings are subject to substantial constant cross winds. The drift component introduces a skew in north-south field boundaries caused by the shift in x value of the nadir coordinates along the aircraft ground track. Figure 1(C) illustrates a flight with heading 20 degrees west of south as opposed to due south. This produces a flight pattern identical to that of Figure 1(A), but rotated with respect to field boundaries. The accompanying image shows the typical S-shaped distortion in the field boundaries that is so characteristic of linear features in aircraft scanner data. This occurs because the road sections are no longer aligned with the scan direction, although the

distortion is still in the scan direction. Figure 1(D) portrays the impact of the aircraft flying in a banked position. The scan center ground track is displaced 20 degrees to the west of the aircraft nadir ground track. Many aircraft scanner systems, including the NS001, are "roll-compensated" to maintain the scan center along the aircraft nadir ground track.

Many of the distortions in scanner imagery result largely from *variations* in orientation of the aircraft during the flight. For example, a change in pitch results largely in a fixed displacement along the ground track such that the aircraft is looking somewhat ahead of where it normally would. In addition, each scan covers a somewhat wider swath on the ground. However, variations in pitch results in distortions such as those displayed in Figures 1(E) and 1(H). In Figure 1(E), the pitch varies linearly from 0 degrees at the start of the flight segment to 20 degrees at the end. The most apparent effect is the widening coverage in the scan direction as the flight progresses. In addition, the changing pitch angle contributes to increasing the effective ground velocity beyond v_y. Thus the distance between scan lines is increased, resulting in a squeezing of fields in the y-direction on the scanner image. Figures 1(F) and 1(G) display the impact of similar type variations in heading and drift, and in roll. In particular, Figure 1(F) shows the combined effect of a 10 degree linear variation in heading and a 10 degree linear variation in aircraft tracking angle due to drift.

In general, aircraft motions are more complex than can be adequately represented by a linear variation over the course of the flight. Typically, motion will be oscillatory in nature, since it is generally desirable to correct departures from nominal flight parameters. Figures 1(H) through 1(L) portray the effects of sinusoidal variations in selected flight parameters. In Figure 1(H) the aircraft nose pitches up to a maximum angle of 20 degrees and then is brought back down, passing through the horizontal, to a negative pitch angle of 20 degrees and finally back to horizontal flight by the end of the flight segment. The scan pattern near the center of the flight segment indicates that, although the aircraft is moving forward the center line of the scanner moves backward because of the variation in pitch resulting in a prolonged viewing period for areas on the ground at this point in the flight. This is clearly seen by field distortions in the accompanying image. Figure 1(I shows the result of similar variation in heading. The turning of the aircraft can cause the edges of the scan line to move backward with respect to forward motion of the aircraft during portions of the flight segment. This can result in a rather distorted image since the same area on the ground may be viewed more than once during the flight segment. In effect, at the time the aircraft is experiencing its maximum change in heading, it may be considered as moving perpendicular to a radius of curvature lying along the scan direction. Ground areas near the center of curvature will be observed repeatedly while the edge of the scan, beyond the radius of the curvature, will be covered in reverse

direction (from south to north) during that portion of the flight segment. As the variation in heading is reduced the normal forward motion of the aircraft will force the scan coverage at the edge to once again proceed from north to south doubling back over the area covered. In fact, some areas near the edge of the scan line may be observed as many as three times during the course of the flight segment. This creates a rather significant problem in attempting to recapture or correct for radiometric values, even in the situations where the scanner geometry is well-known.

As can be seen in Figure 1(J), variations in the aircraft tracking angle equal to those occurring in Figure 1(I) can be obtained by varying the drift angle. The scan center ground track in Figure 1(I) is identical to that of 1(J). However, in 1(J) the orientation of the aircraft is maintained constant and the scan pattern is consequently much simpler, with no crossing of scan lines. Figure 1(K) displays a situation in which the heading and drift are varying simultaneously in a manner such that the tracking angle variation is identical to that of Figures 1(I) anf 1(J). Once again, it is difficult to establish a one-to-one mapping between actual ground coordinate radiometric values and the values which appear in the scanner image. Figure 1(L) portrays a sinusoidal variation in roll angle, beginning from level flight, banking to 20 degrees below the horizon in the west, and returing to level flight. In this instance, the flight segment is flown in the time equal to the half period of the sinusoidal variation.

In summary, if sufficient navigational information is available, aircraft scanner coordinates may be related very precisely to planimetric ground coordinates using the approach outlined in Table 1. However, the potential for a multi-value remapping transformation (i.e., scan lines crossing each other), adds an inherent uncertainty, to any radiometric resampling scheme, which is dependent on the precise geometry of the scan and ground pattern.

TABLE 1

AIRCRAFT SCANNER GROUND PATTERN EQUATIONS

$$X = X_o + h \tan\theta \sin\phi - h(\tan(\rho+\psi)/\cos\theta)\cos\phi$$

$$Y = Y_o - h \tan\theta \cos\phi - h(\tan(\rho+\psi)/\cos\theta)\sin\phi$$

$$X_o(t+\Delta t) = X_o(t) + \int_t^{t+\Delta t} v \sin(\phi+\delta)\,dt$$

$$Y_o(t+\Delta t) = Y_o(t) - \int_t^{t+\Delta t} v \cos(\phi+\delta)\,dt$$

where: X_o, Y_o = nadir coordinates

Δt = scan period	ρ = roll
θ = pitch	ψ = scan angle
ϕ = heading	h = altitude
δ = drift	v = ground speed

UPDATING X_o, Y_o WITH NAVIGATION DATA (NERDAS)

(1) Find nearest observation times from NERDAS

$t_i \le t \le t_{i+1}$ where: $i = \text{INT}\{(t-t_o)/f+1\}$

f = frequency of observation

(2) Obtain values for each scan by cubic interpolation

$$Z(t) = \sum_{n=0}^{3} a_n t^n$$

where: Z represents $[\theta, \phi, \delta, \rho, h, \text{or } v]$

using NERDAS values for $Z(t_i)$ $i-1 \le k \le i+2$

solve for a_n $n = 0, \ldots 4$

(3) Calculate nadir displacement between scans assuming

$$\int_t^{t+\Delta t} Z\,dt = \sum_{n=1}^{4} \frac{a_{n-1}}{n}\left\{(t+1/f)^n - t^n\right\}$$

where: Z represents $v \sin(\phi+\delta)$ or $-v \cos(\phi+\delta)$

and a_n is determined by technique used in step (2)

TABLE 2

SIMULATED NS001 FLIGHT
NOMINAL FLIGHT PARAMETERS

DRIFT	$\delta_0 = 0°$
HEADING	$\phi_0 = 180°$
PITCH	$\theta_0 = 0°$
ROLL	$\rho_0 = 0°$
GROUND SPEED	$V_G = 280$ KNOTS
ALTITUDE	$H = 25{,}400$ FEET
SCAN ANGLE	$-50° < \Psi < 50°$
SCAN FREQ.	$F = 15$ RPS
IFOV	$\Omega = 2.5$ MR

FIGURE 1 (A - C)

SIMULATED FLIGHT-SCANNER GROUND PATTERN AND IMAGE

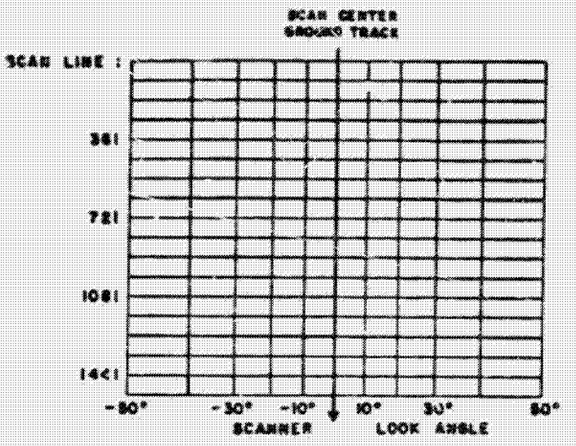

(A)

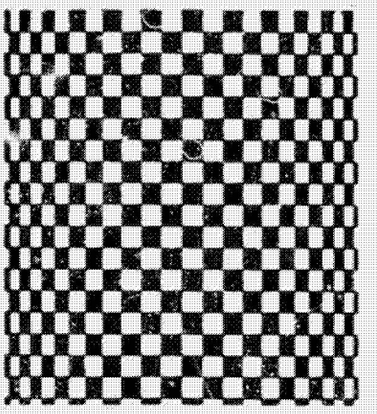

Nominal flight parameters

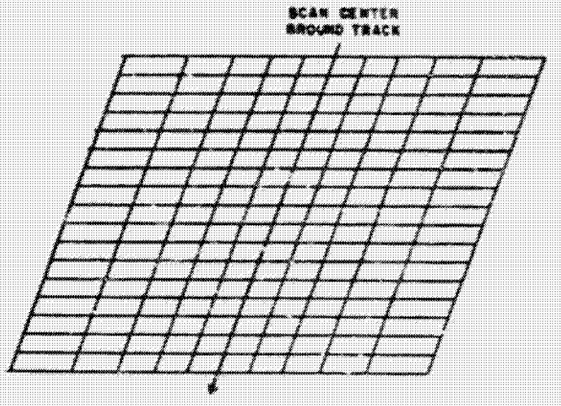

(B)

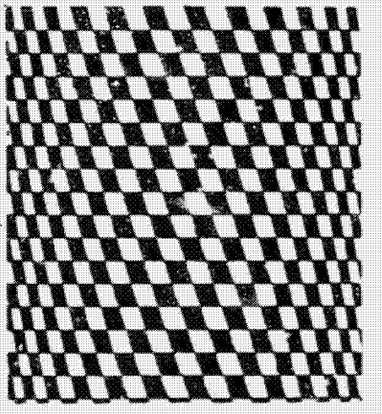

20° change from nominal drift ($\delta = \delta_0 + 20$)

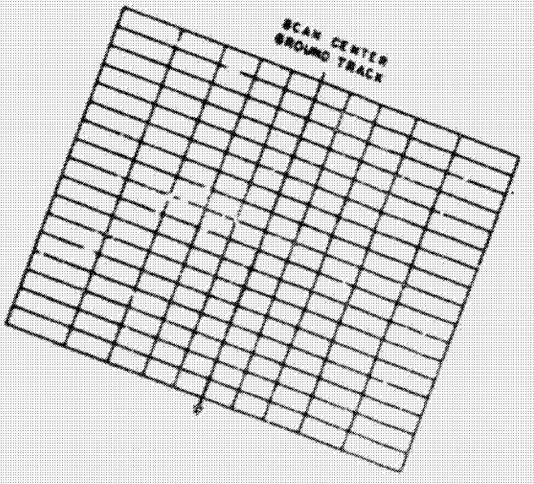

(C)

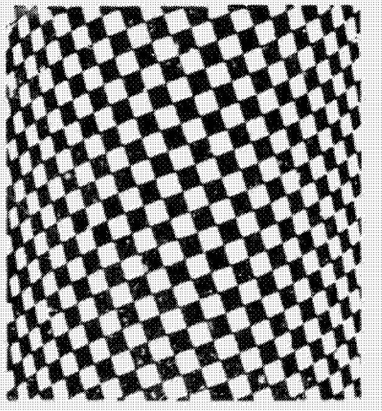

20° change from nominal heading ($\phi = \phi_0 + 20$)

FIGURE 1 (D - F)

SIMULATED FLIGHT-SCANNER GROUND PATTERN AND IMAGE

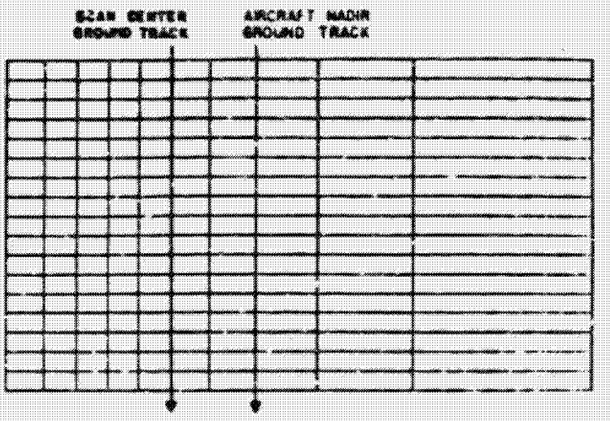

(D)

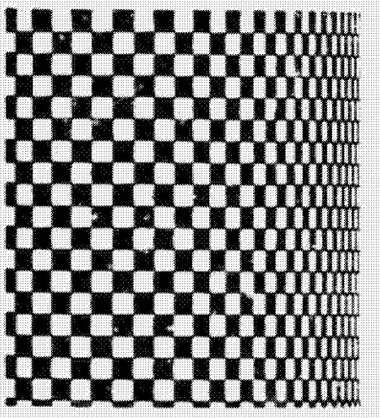

20° change from nominal roll ($\rho = \rho_0 + 20$)

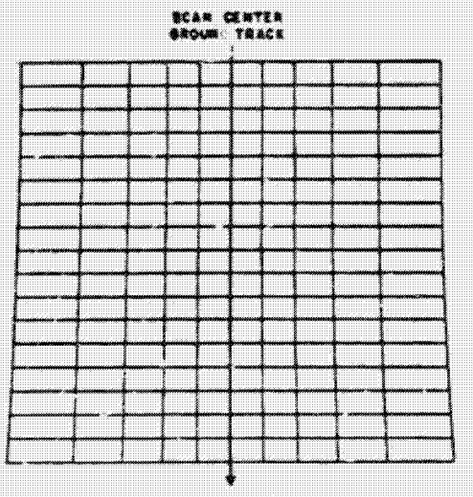

(E)

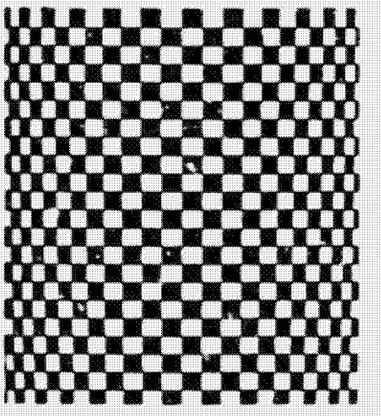

20° linear variation in pitch ($\theta = \theta_0 + 20\alpha t$)

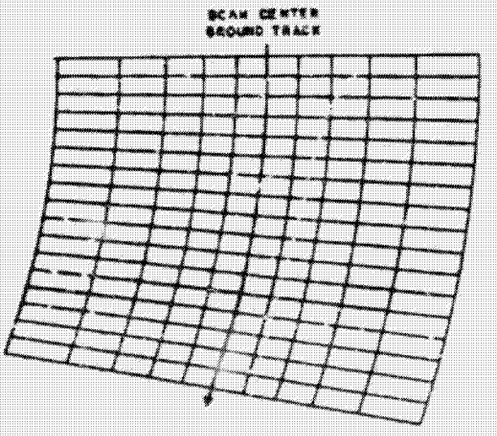

(F)

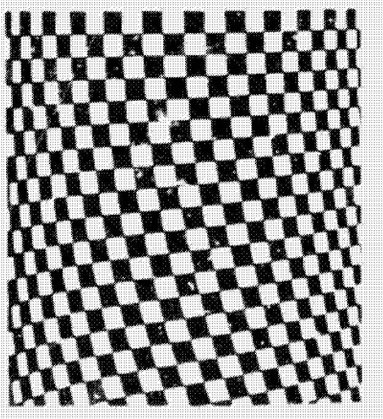

10° linear variations in heading and drift

FIGURE 1 (G - I)

SIMULATED FLIGHT-SCANNER GROUND PATTERN AND IMAGE

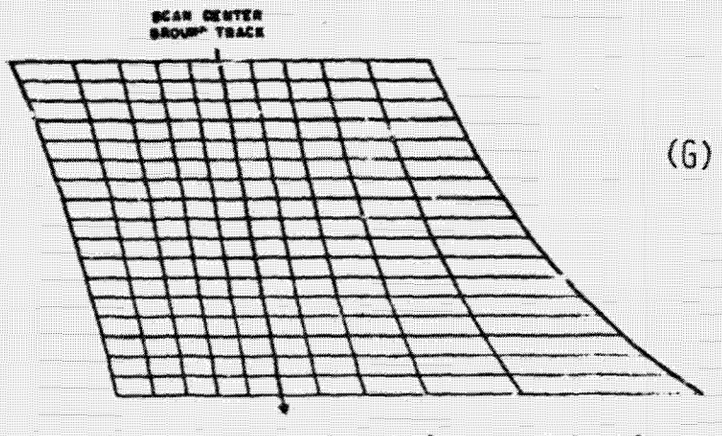

(G)

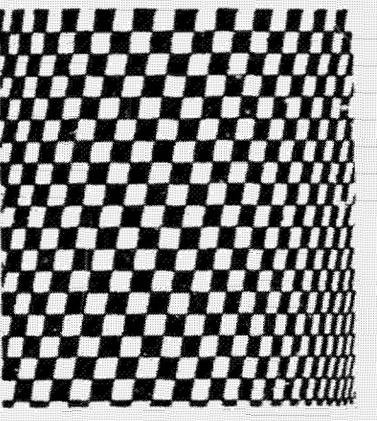

20° linear variation in roll ($\rho = \rho_0 + 20\alpha t$)

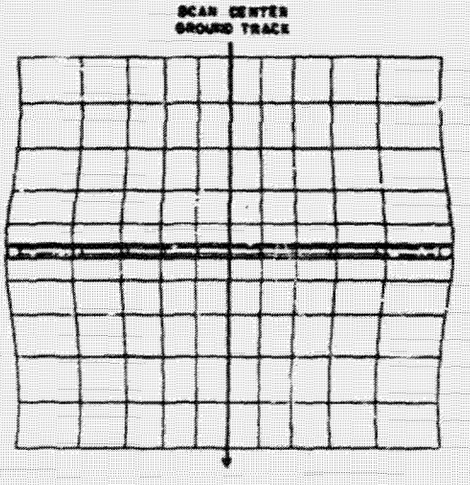

(H)

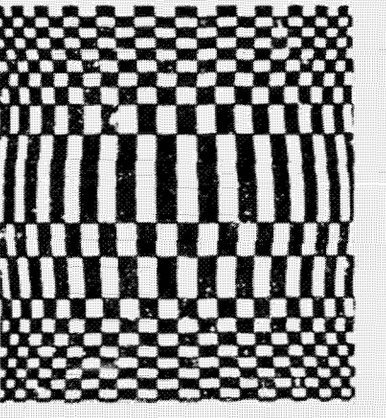

20° sinusoidal variation in pitch ($\theta = \theta_0 + 20 \sin \omega t$)

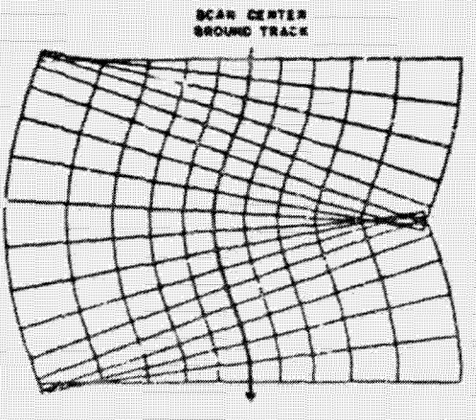

(I)

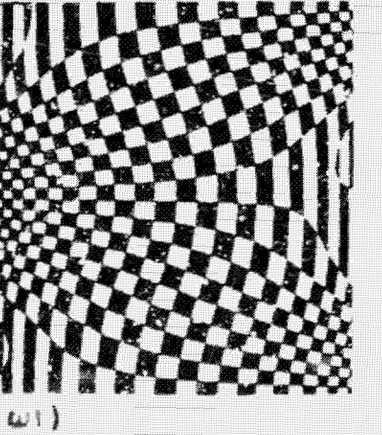

20° sinusoidal variation in heading ($\phi = \phi_0 + 20 \sin \omega t$)

FIGURE 1 (J - L)

SIMULATED FLIGHT-SCANNER GROUND PATTERN AND IMAGE

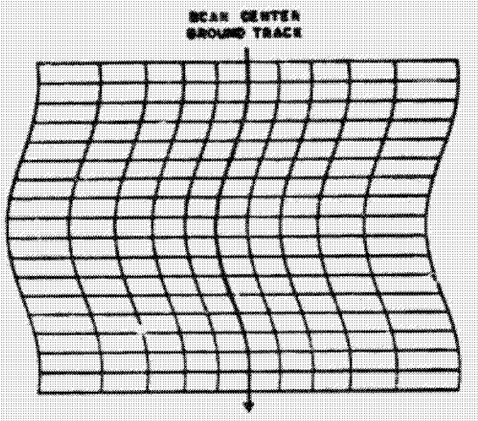

(J)

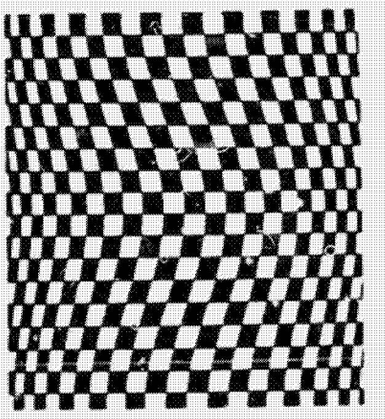

20° sinusoidal variation in drift ($\delta = \delta_0 + 20 \sin \omega t$)

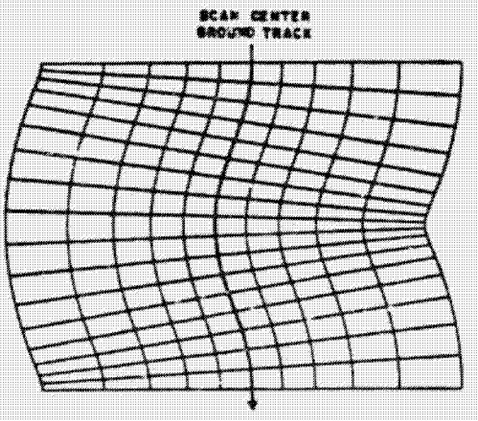

(K)

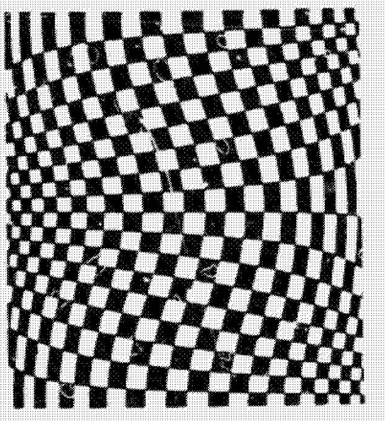

10° sinusoidal variations in heading and drift

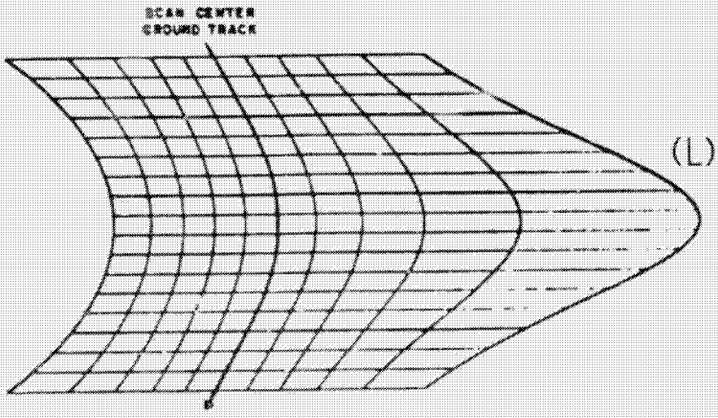

(L)

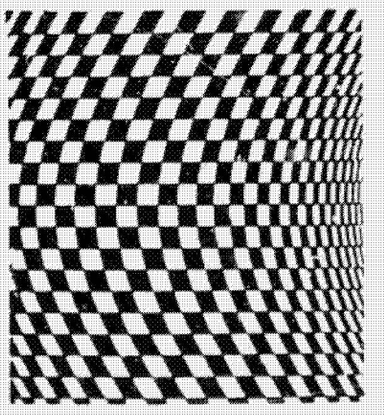

20° sinusoidal variation in roll ($\rho = \rho_0 + 20 \sin \omega t$)

N82 28716

5.5 MLA IMAGING SYSTEMS*

Ken J. Ando, NASA Headquarters

MLA is the abbreviation for "Multispectral Linear Array." Within NASA, MLA has evolved to become the generic term for the sensor concept and technology associated with solid-state electronically scanned linear arrays operating in the pushbroom mode for resource observations. The overall program objective is to develop the enabling technology and instrument/mission definition phase for the application of advanced solid-state sensors for future experimental remote sensing missions. The approach being taken is to develop complementary multiyear efforts at GSFC and JPL. GSFC will concentrate upon focal plane development, instrument concept/design development, mission studies, and service requirements; JPL is concentrating on development of an imaging spectrometer technology and a Shuttle sortie mission definition.

There is a heavy emphasis on technology. The technologies that we are developing are the shortwave infrared focal plane technology, primarily mercury-cadmium-teluride, platinum-silicide, visible chips, the optics, passive radiators -- all the critical technology acquired for the implementation of an MLA system. We are also developing instrument concepts and we are doing this through a number of Phase A studies. In addition, we have support activities. Primarily we are trying to define what the requirements are from a science standpoint, and what the user requirements are, and how can we best utilize this technology. We are in the process of forming a science working group. And finally, we are looking into various concepts and scenarios for missions for validation of the technology.

I want to mention the fact that besides the MLA activity there are other complementary technology efforts within NASA. There is the information adaptive system effort which is being funded by OAST. This is an effort to develop and demonstrate a breadboard for on-board signal processing MLA-type data. Specifically, this breadboard process will correct all the MLA data at the 80- to 90-megabyte range, and, in addition, generate all the geometry correction factors such that it can be resampled on the ground. The input will be the ephemeris information, the attitude control information and the thermal data from which the resampling coefficients will be calculated. There are two other activities, one called TIRA (Thermal Infrared Ray)--an effort which has been under way for about two years to develop an 8- to 12,000-micron element linear array. Finally there is another activity -- TIMS (Thermal Infrared Multispectral Scanner): this is an effort to develop a 6-channel imaging spectrometer radiometer for aircraft utilization. I might mention that the scanner will be delivered to JPL for calibration, then in the June-July time frame it will be flown on the Lear 23 Jet out of NSTL.

One of the areas that we're looking at is the possibility of some sort of a Shuttle experiment. Originally, our major interest was in some sort of a free-flyer; however, with the budget uncertainties we felt that a Shuttle-type mission might be a viable and perhaps a more realistic alternative as a precursor for a full-up experimental mission utilizing a free-flyer. What I have summarized here are some of the objectives, technology validation objectives,

*Edited oral presentation.

and some research objectives. It turns out that there are some problems utilizing the Shuttle for this type of research. Primarily the Shuttle does not have a very adequate pointing system. The way we think we can circumvent that is to utilize some of the pointing modules which are currently under development with NASA. One of them is the IPS, and I understand there is another pointing module which is being developed by Langley. By tilting the Shuttle about 45° and looking simultaneously at the stars, we think we can both track and get ACS information in addition to imaging on the ground.

Figure 1 provides a comparison between MLA and other Earth observation imaging systems. There are three types of techniques to generate imagery. There is the conventional scanner -- the mechanical scanner -- which scans back and forth across the ground with the spacecraft providing the motion and the scan in the in-track direction. The next level of scanner beyond this, which is strictly mechanical, is the MLA approach which is basically a linear array which provides electronic scan in the cross-track direction and the orbital motion provides the scan in the in-track direction. The key here is the fact that the pushbroom-type scanner provides simultaneous imaging in the cross-track direction -- it maintains perspective in one direction at least. If you go to a conventional framing camera like a 35-mm camera, the perspective is imaged silmultaneously in both directions -- the conventional framer. Again, NASA examples are the return beam videcon and the large format camera -- which is a film camera. What I want to summarize here are some of the pushbroom-type scanners which have been proposed and one which is actually in the hardware stage. The imaging spectrometer (Figure 2) is an approach which JPL is developing and basically is an approach wherein a slit, which corresponds to one line on the ground, is simultaneously imaged in a number of spectral bands. The slit is dispersed by the defraction grading and then reimaged onto the area ray. The advantage is that you have inherent registrations because of the fact that you are imaging only the slit and all the colors simultaneously. The other advantage is the fact that by programming the array you can arbitrarily change both the spectral path and the center frequencies.

As far as the potential advantages of the pushbroom mode of imaging with the MLA, one of the limitations of the mechanical scanner is the question of scanner linearity. With an electronic scanner like the MLA, for all intents and purposes, there is no linearity because of the fact that you are electronically scanning as opposed to mechanically scanning. One of the advantages is that you simultaneously image a line--all the pixels in one line--so that there is less than a jitter problem--because you have literally frozen the line in time and space. There is no high-frequency jitter component variation from pixel to pixel because you don't scan across the line, you simultaneously image it. The other advantage is the fixed geometry, and again that provides the true perspective in cross- ack direction and that potentially will reduce the geometric correction requirements and resampling requirements simply because of the fact that the detector geometry was fixed. The other attribute is the fact that since the scan is electronic, you can change them and program them; for example, if you have orbit anomally, you can presumably change the scan rates dynamically such that you don't have the overlap-underlap problem. Finally, inherent band-to-band registration is possible. One of the reasons why we are insisting on obtaining band-to-band registration and one of the requirements of the definition study is that band-to-band registration be less than 1/10 of a pixel. This requirement is made because, for example, if you have a 15-meter pixel and a misregistration of 1/10 of a pixel, then the best

you can do as far as the error in the ratios is of the order of 2%. We are currently involved in an instrument definition study, and we have four contractors studying alternative instrument configurations. One of the things that's come out of the studies is the fact that it's going to be very, very difficult to mechanically register each of the bands to less than 1/10 of an IFOV.

What the Table 1 chart does is compare the results of mounting a Fairchild Loreors and the MLA requirements. As you can see, it looks like it's possible to get to 1/10 of an IFOV, but this is the current state of the art in terms of the physical location and mounting of chips to form a contiguous array.

I just want to quickly touch on two considerations as far as misregistration is concerned. One is the impact of the Earth's rotation (see Figure 3). If you have a displacement of the array in the focal plane -- let's say you have a six-linear array focal plane consisting of six-linear arrays with integrated filters, the physical displacement between band one and band six had to be less than 20 IFOVs. The impact of the rotation of the Earth is shown in Figure 3. There are two ways to compensate for the misregistration and that is to introduce a yaw and a pitch in the direction opposite the westerly rotation of the Earth. The other is to simply change the heading, and reduce the velocity vector associated with the rotation of the Earth. Another consideration -- and this one is equally applicable to scanners and to pushbroom arrays -- is the effect of off nadir viewing and the geometric consideration (Figure 4). As you view off nadir, obviously what happens is that you get panorama effect. You get geometric distortion, but in addition, there's a resolution and a scale change. I might add that the field of views currently being considered for the MLA is $\pm$7-1/2 to 15 degrees. It turns out that the pushbroom array, because of the fact that it simultaneously images, has an advantage. By maintaining perspective, it turns out that there's a slight geometric distortion advantage to the pushbroom over the scanner. But as you can see if you point off nadir, there's a significant change in the perspective which we call the panorama effect. That impacts the problem associated with absolute geolocation and misregistration because any attitude change will result in a considerably larger uncertainty in terms of registration and geolocation off nadir than on nadir. So to summarize some of the issues associated with off nadir viewing, any system we're going to consider in the future will have the capability to point off nadir. The reason we'd like to go to off-nadir pointing is to increase the temporal visitation. For example, with SPOT, their 26-day overpass cycle is reduced to one to five days by a $\pm 26^{\circ}$ off-nadir viewing capability. From the research standpoint, there are additional desirable features of off-nadir pointing. These include the ability to investigate atmospheric effects, adjacency effects, and calibrate the atmosphere. A key issue for the conference to be concerned with as far as off-nadir pointing is the possibility of registering a nadir scene with an off-nadir scene, given the geometric distortions and the other problems associated with off-nadir viewing.

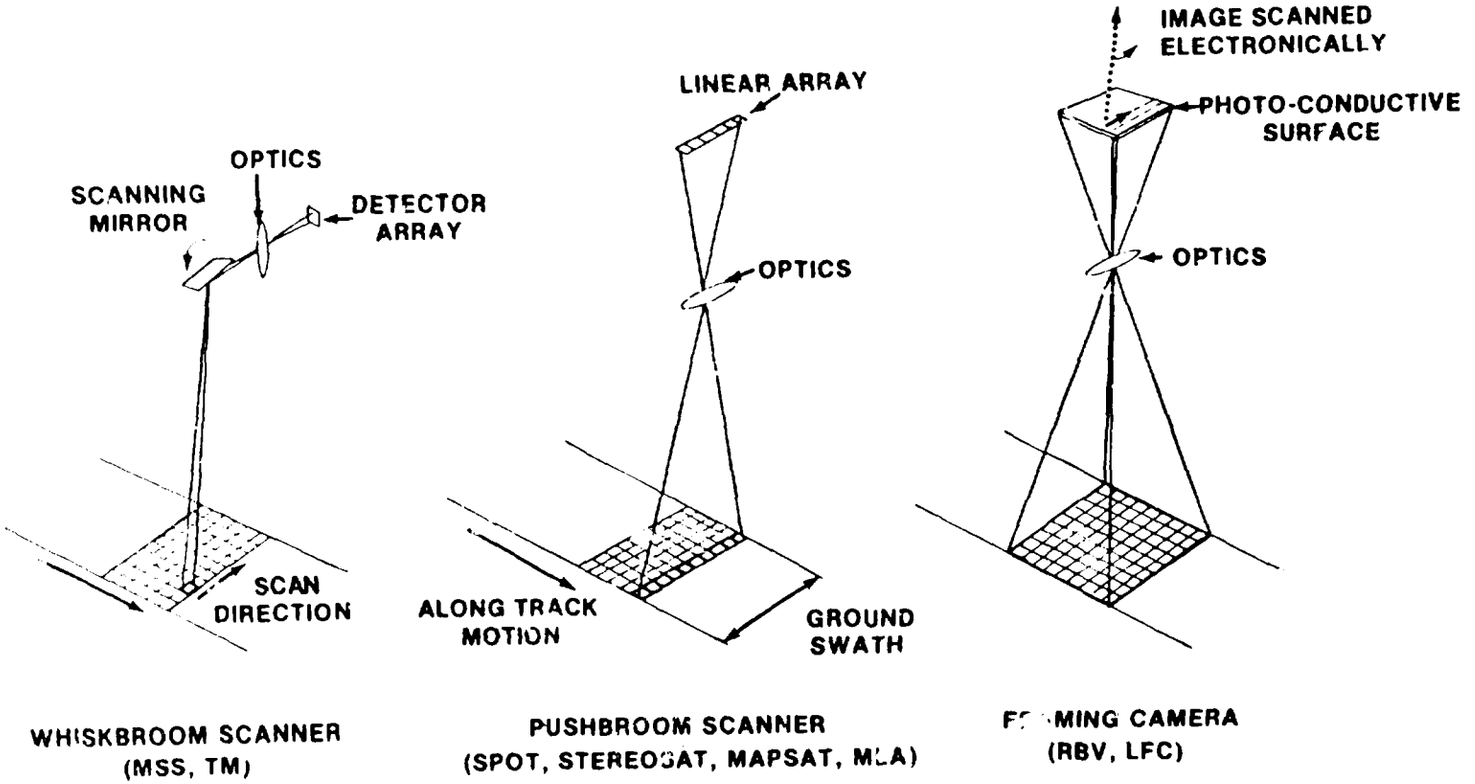

Figure 1. Comparison of Scanning Systems for Earth Observations

NASA HQ E-R82-201 (1)
11-13-81

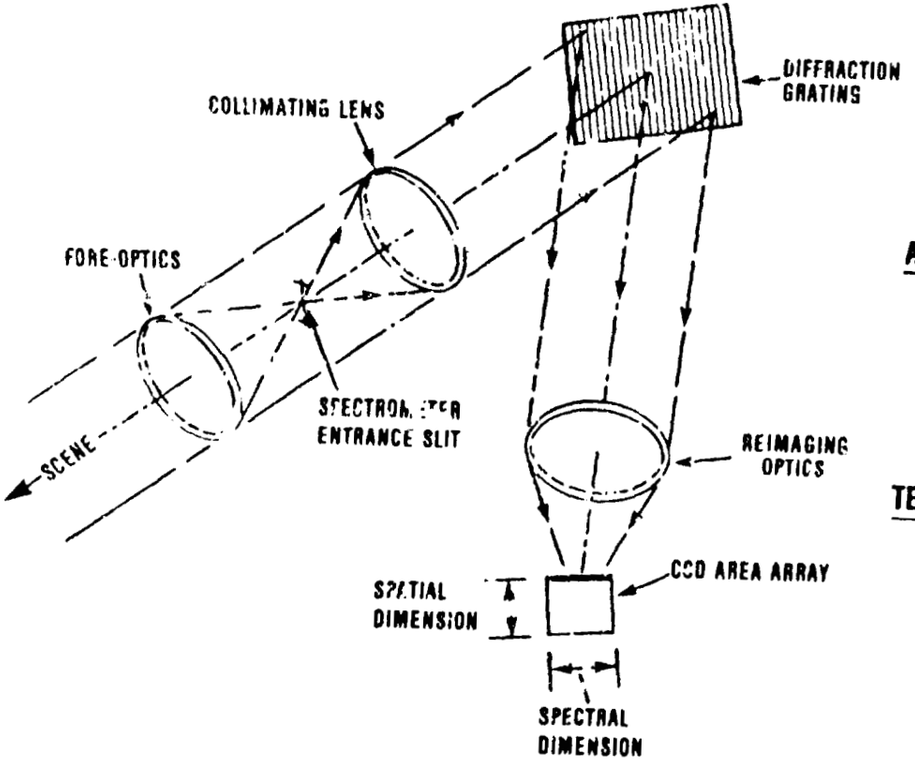

CONCEPT

- SPECTRAL DISPERSION OF LINE IMAGE VIA DIFFRACTION GRATING
- LINE IMAGE SCANNED IN ORTHOGONAL DIRECTION IN "PUSHBROOM" MODE BY SPACECRAFT MOTION

ADVANTAGES

- INHERENT REGISTRATION OF ALL SPECTRAL CHANNELS
- ELECTRONICALLY PROGRAMMABLE SPECTRAL AND SPATIAL RESOLUTION

TECHNOLOGY DRIVERS

- AREA ARRAY DETECTORS—SWIR
- FOCAL PLANE
- WIDE FIELD OPTICS
- ON-BOARD DATA PROCESSING
- FOCAL PLANE COOLING

Figure 2. Imaging Spectrometer

Table 1. COMPARISON OF LOREARS FOCAL PLANE MOUNTING RESULTS WITH MLA REQUIREMENTS

PARAMETER	LOREORS	MLA
LINEAR X	± 2μ (1)	± 1.3μ
ROTATION θ (ONE CHIP)	± 4"/20.48 MM (2)	± 1.3μ/26.62 MM
STRAIGHTNESS (FOUR CHIPS)	± 8μ/82 MM (3)	± 1.3/106 MM

(1) ACTUAL "X" ALIGNMENT ACHIEVED FOR LOREORS
2 BUTTS - NO DETECTABLE ERROR
2 BUTTS - 2μ APART
1 BUTT - 4μ APART (DEEMED ADEQUATE - REMOVAL AND REALIGNMENT NOT WARRANTED

(2) WITHIN ± 3μ

(3) WITHIN ± 3μ

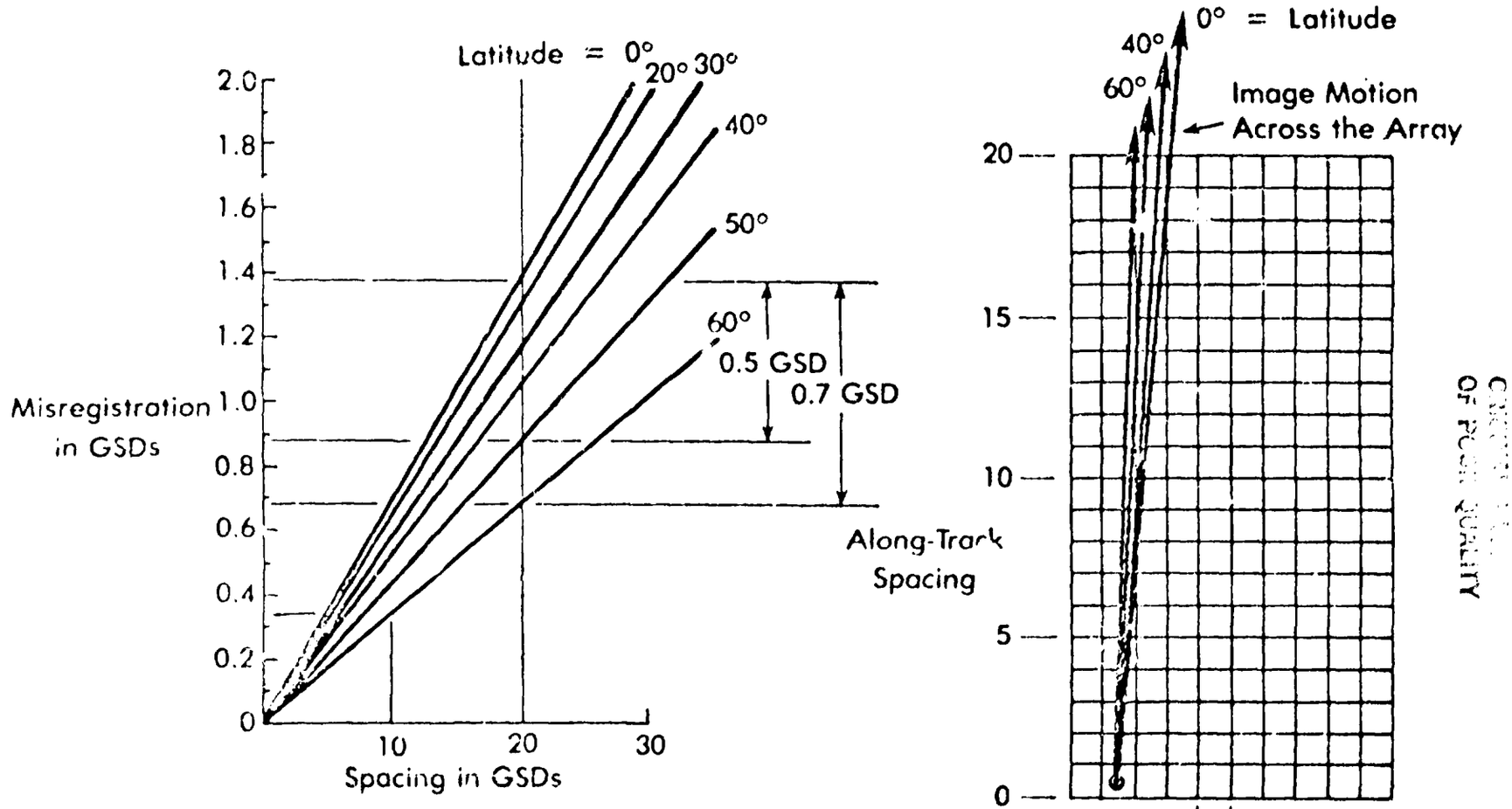

Array Normal to Ground Track Direction Error in Cross Track Direction Only $X \leq 1.4$ GSD

Figure 3. Misregistration Due to Earth Rotation

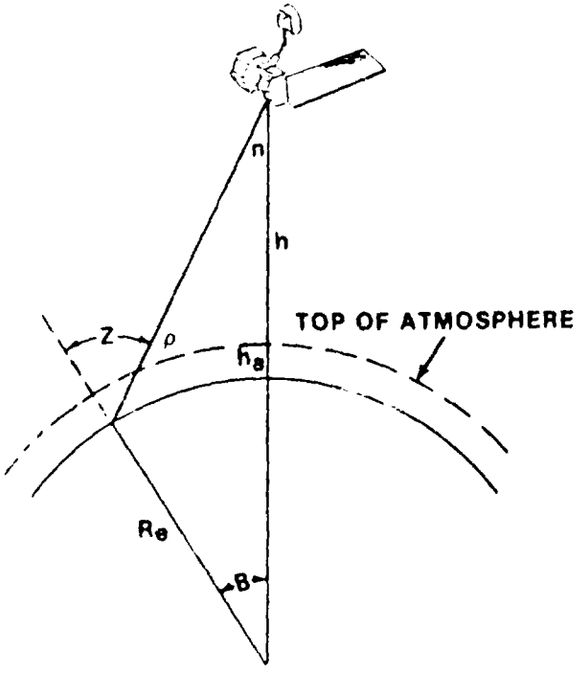

SATELLITE VIEWING GEOMETRY

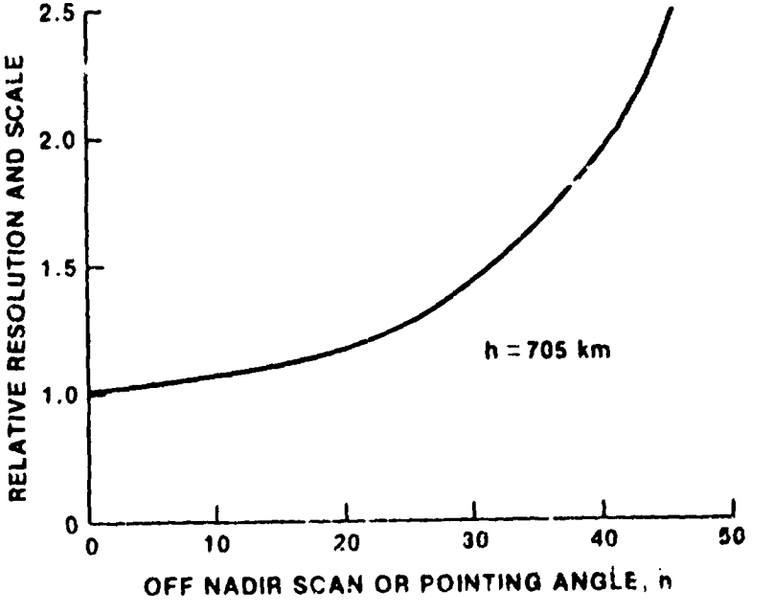

- CHANGE IN RESOLUTION/SCALE
- INCREASED ATTITUDE, EPHEMERIS SENSITIVITY
- RADIOMETRIC CHANGE

NASA HQ ER82-280 (1)
11-13-81

Figure 4. Off Nadir Viewing Geometric Considerations

MLA Bibliography

Multispectral Linear ARRAY (MLA) Phase A Definition Study, JPL Document No. 725-29, July 11, 1980. Jet Propulsion Laboratory, Pasadena, Calif. (JPL internal document.)

Multispectral Linear ARRAY (MLA) Phase A Definition Study, NASA/GSFC Interim Report, July 11, 1980.

MLA Instrument Definition Study, Mid-Term Review Briefing Books, September 9-14, 1981 (NASA/GSFC Contracts #NAS5-26588-through NAS5-26591), Eastman Kodak, Ball Aerospace, Honeywell, and SBRC.

Application of Solid-State Array Technology to an Operational Land-Observing System, JPL Technical Report No. 715-82, dated October 31, 1980. Jet Propulsion Laboratory, Pasadena, Calif. (JPL internal document.)

Preliminary Sterosat Description, NASA, JPL Report No. 720-33, 1979. Jet Propulsion Laboratory, Pasadena, Calif. (JPL internal document.)

J. Wellman, "Technologies for the Multispectral Mapping of Earth Resources", 15th International Symposium on Remote Sensing of Environment, Ann Arbor, MI, May 1981.

J.M. Driver and D.H. Tang, "Earth Applications Orbit Analysis for a Shuttle-Mounted Multispectral Mapper," AAS/AIAA Paper 81-182, AS/AIAA Astrodynamics Specialist Conference, Lake Tahoe, Nevada/August 3-5, 1981.

J.M. Driver, "A Flexible Approach to an Operational Land Observing System," AIAA Paper 81-0315, AIAA 19th Aerospace Science Meeting, January 12-15, 1981, St. Louis, MO.

"MLA/Beam Splitter Design Study", Perkins-Elmer Corporation, Report No. 15184, September 15, 1981 NASA/GSFC Contract NAS5-25608.

S.W. Wharton, J.R. Irons and F. Huegel, "LAPR: An Experimental Pushbroom Scanner," Photogrammetric Engineering and Science, Vol. 57, No. 5, 631 (1981).

Conceptual Design of an Automated Mapping Satellite System (MAPSAT), Final Technical Report, Jan. 12, 1981 ITEK Optical Systems, ITEK Corporation.

A.P. Colvocoreses, "Proposed Parameters for Mapsat", Photogrammetric Engineering and Remote Sensing, Vol. 45, No. 4, 501 (1979).

K. Nummedal, "Wide-Field Imagers--Pushbroom or Whiskbroom Scanners", Proceedings SPIE, Vol. 226, 1981, pp. 38-52.

D.C. Smith and R.H. Howell, "Visible and Infrared Sensors for Earth Resource Observation in the '80's" AAS/AIAA paper, October 20-23, 1980, Boston, MA.

R. Welch, "Measurement from Linear Array Camera Images", Photogrammetric Engineering and Remote Sensing, Vol. 46, No. 3, 315 (1980).

L.L. Thompson, "Remote Sensing Using Solid-State Array Technology", Photogrammetric Engineering and Remote Sensing, Vol. 45, No. 1, 47 (1979).

T.J. Brown, F.J. Corbett, T.J. Spera and T. Andrada, "Thermal IR Pushbroom Acquisition and Processing", Proc. SPIE Symposium, 1981.

T.J. Brown, Development of an Earth Resource Pushbroom Scanner Utilizing a 90-element 8-14 micron HgCdTe Array", Proc. SPIE Technical Symposium East, Vol. 226, Washington, D.C., April 7-11, 1980.

T.J. Brown, "Image Processing Hardware and Software for the 90-element IR/CCD/MOX Field Test Instrument", Proc. SPIE Technical Symposium West, Vol. 253, San Diego, CA, July 28-August 1, 1980.

R. Welch and W. Marke, "Cartographic Potential for a Spacecraft Line-Array Camera System: Sterosat", Photogrammetric Engineering and Remote Sensing, Vo. 47, No. 8, 1173 (1981).

On-Board Image Registration Study, Final Report, January 31, 1979, TRW, Redondo Beach, Calif., NASA/GSFC Contract no. NAS5-23725.

C.C. Schnetzler, On the Use of Off-Nadir Pointing for Increasted Temporal Resolution of Earth Observing Satellite Systems, NASA Technical Memo 82139, may 1981, NASA/GSFC.

Y.J. Kaufman and R.S. Fraser, The Effect of Finite Field Size on Classification and Atmospheric Correction, NASA TM83818, September 1981, NASA/GSFC, Greenbelt, MD.

Multispectral Resource Sampler (MRS) Workshop, Summary Report of Workshop held May 31-June 1, 1979, Colorado State University, ORI Report dated June 1979, Boulder,

5.6 GEOMETRIC AND RADIOMETRIC DISTORTION IN SPACEBORNE SAR IMAGERY*

J.C. Curlander

Jet Propulsion Laboratory
California Institute of Technology
4800 Oak Grove Drive
Pasadena, California 91109

*Invited Paper - NASA Workshop for Registration/Rectification for Terrestrial Applications, November 17-19, 1981, Leesburg, Virginia

I. INTRODUCTION

Synthetic aperture radar (SAR) [1,2] is a side-looking sensor capable of very fine along-track resolution. This characteristic, in addition to its all-weather monitoring capability, makes it an attractive instrument for generating space imagery. A SAR typically operates in a spectral region (1-10 GHz) that complements most optical scanners (LANDSAT). In this region, the subsurface sensing depth is much greater and the reflectance properties of imaged terrain objects are different [3]. A SAR will therefore collect a complementary set of "terrain signatures" that when registered with other spectral data can greatly facilitate the interpretation of remotely sensed imagery. But before multisensor data can be properly registered, the various types of distortion inherent in SAR imagery must be quantitatively analyzed. This requires an understanding of the properties of the sensor as well as the data processing system used in the image formation.

The production of quality imagery from spaceborne SAR data requires extensive processing of the raw echo data. This procedure is more complex than previously used for aircraft SAR imagery due to the large increase in sensor altitude. The correlation procedure must compensate not only for undesirable spacecraft motion, but also for target motion resulting from Earth curvature and rotation [4,5]. To simplify this procedure, approximations are often made that can result in both geometric and radiometric distortion in the image product. Furthermore, the viewing geometry of the SAR and the characteristics of the data collection system will also introduce distortion into the imagery. Precise registration of SAR imagery with other types of remotely sensed imagery requires the

identification of these distortions and the development of post-processing techniques to rectify them. Furthermore, considering the large quantity of data, it is desirable that these post-processing techniques be automated and designed to interface directly with the image processor to generate a geometrically and radiometrically correct product without supervision or operator interaction.

This paper will summarize what is currently known about these distortions and describe the development to date of unsupervised post-processing rectification techniques. The geometric distortion can be divided into two categories. The first catagory consists of distortion derived from the radar viewing geometry. This includes such effects as ground range nonlinearities, radar foreshortening and radar layover. The second category consists of distortions introduced during the data processing. These distortions result from approximations made during the correlation such as in estimation of the target phase history, or compensation for the earth rotation. The processor induced distortions will obviously depend on the specific correlation algorithm used for image formation. This paper generally addresses the effects on the image product resulting from assumptions during the processing and it specifically considers distortions inherent in digital imagery produced by the digital image processor at JPL [6].

II. SAR REVIEW

This section is intended as a brief tutorial on SAR system characteristics and processing techniques. Basic system parameters are introduced that are relevant to understanding the sensor and processor induced distortion to be discussed in subsequent sections. Interested readers will find an excellent treatment of various characteristics of SAR in a recently published collection of papers [7].

2.1 SAR Sensor Characteristics

The viewing geometry for a SAR in the imaging mode is illustrated in Figure 1. The sensor moves along a predetermined orbit track radiating energy in the form of pulses and receiving the backscattered signal. This data is either recorded on film for later optical processing or is transmitted on a downlink to a tracking station where it is digitized and recorded on high-density tape for digital processing. The antenna pointing direction is normal to the flight path and its orientation with respect to the spacecraft is normally fixed. Two important system parameters are the antenna look angle θ, defined as the angle of the antenna beam with respect to nadir direction, and the slant range R, the distance from the sensor to the imaged target area. The radar antenna range beamwidth β_r and the spacecraft altitude H, determine the cross-track dimension of the radar footprint.

The radar transmitter is typically designed to operate in a frequency region between L-band and X-band, thus permitting cloud and fog penetration. The pulse repetition frequency (PRF) of the radar and the spacecraft velocity determine the azimuth (along-track) resolution. This is typically designed

to be several times higher than the range (cross-track) resolution so that the azimuth return can be divided into several looks for incoherent summation to reduce the speckle noise. The range resolution is determined by the spectral bandwidth of the transmitted pulse. Coded pulses such as a chirp waveform are typically used to achieve the maximum resolution for a given level of transmitter power [8]. During the image processing these pulses must be compressed to a point response. Imperfect compression can result in both reduced resolution and range sidelobes in the image.

2.2 SAR Processor Characteristics

Processing raw echo data into finished imagery essentially consists of the following four steps (15):

(1) Range pulse compression;

(2) Doppler parameter estimation;

(3) Azimuth correlation; and

(4) Speckle reduction.

2.2.1 Range Pulse Compression

The purpose of this step is to compress the time dispersed radar transmitted pulse into an impulse. A chirp function is the radar pulse waveform typically used because of its focusing capability in an optical SAR processor. The key to attaining an adequate signal-to-noise ratio is transmission of a wide-band pulse and use of the data processor to compress this pulse. The range resolution can be approximated by

$$\rho_R = \frac{c}{2W} \tag{1}$$

where c is the speed of light and W is the pulse bandwidth. Spaceborne SAR requires unusually large pulse compression ratios compared with aircraft radar to achieve fine image quality.

2.2.2 Doppler Parameter Estimation

Formation of the synthetic aperture is critically dependent on accurate estimation of the phase delay history of the return echo signal. This phase delay can be approximated by [9]

$$\phi(t) = \phi(0) + 2\pi\left(f_d t + \frac{1}{2}\dot{f}_d t^2\right) \tag{2}$$

where $\phi(0)$ is the phase at t=0, f_d is the Doppler frequency shift of the echo data, and $\dot{f}_d$ is the Doppler rate, both evaluated at t=0. These two parameters, f_d and $\dot{f}_d$, can be estimated based on the orbit and attitude data. If an accurate ephemeris is not available, these estimates can be used as initial predicts and further refined by evaluation of certain characteristics in the resultant imagery. Details of these refinement techniques, termed autofocusing for $\dot{f}_d$ and clutterlock for f_d, can be found in the literature [9,10].

2.2.3 Azimuth Correlation

One of the primary features of SAR is its very high resolution. As previously discussed, fine range resolution is achieved by transmission of a wide bandwidth pulse and compression of this pulse in the data processor. A high azimuth resolution is achieved by coherent processing of echo data from

successive radar pulses. The azimuth correlation operation essentially simulates a very narrow effective beamwidth in the azimuth direction by coherently adding the returns of several radar echoes. This operation is performed on range compressed data and involves shifting the phase reference function given in (2) and summing the resultant detected echo data.

The complexity of the azimuth correlation is increased by the range migration of the target as it passes through the antenna beam. This migration consists of a range walk term which is directly proportional to the elapsed along-track time and a range curvature term, which is proportional to the square of the along-track time. To compensate for the fact that the target transverses may range resolution elements, the input data is resampled before the phase reference function is applied. After phase detection, the return from each pulse over the length of the synthetic aperture is summed to obtain a refined estimate of the target's brightness. If the returns are added over the full aperture, a single-look full resolution image is produced. If the aperture is divided into sections, several single-look reduced resolution images are produced. For example, two single-look images can be produced by dividing the phase reference function in half and processing the first and second portions of the target response separately. The single-look images are then added incoherently as described in the next section to obtain a multiple-look image.

2.2.4 Speckle Reduction

Coherent processing of radar echo data is used to achieve very fine along-track resolution, but this same processing also makes the images

susceptible to speckling effects. Basically, speckling results from scattering of non-uniformly distributed reflectors within a resolution cell during the period the cell is within the antenna beam. The speckles are signal dependent and therefore act like multiplicative noise. Techniques for speckle suppression essentially fall into two main categories: 1) averaging several reduced resolution images produced from independent looks; and 2) filtering a full-resolution single-look image to smooth the speckle.

The multiple-look overlay technique is typically used for image production because it can achieve a satisfactory level of speckle reduction with a minimal amount of additional computation [11]. To produce multiple looks, the phase reference function is divided into segments during azimuth correlation. Each segment is applied to the appropriate portion of the return echo data to produce a reduced resolution single-look image of the target area. The single look imagery is then registered and averaged to produce a multi-look product with reduced speckle noise.

The speckle can also be reduced by filtering a single-look high resolution image [12]. Smoothing algorithms have been devised based on the local statistics of the noise. In general, these filters can achieve a greater speckle reduction for a given resolution product then the multiple-look overlay technique, but because of the additional computational load, this approach is not feasible for large-scale image production.

C - 3

III. GEOMETRIC DISTORTION

SAR imagery is subject to several types of geometric distortion that must be corrected before the imagery can be properly registered with other sensor data. These distortions can be classifed into two main categories: 1) sensor derived distortion, and 2) processor derived distortion.

3.1 Sensor Derived Distortion

The geometric distortions classified in this category are mainly derived from the viewing geometry of the radar. Design parameters such as the sensor altitude, look angle, and range beamwidth are critical in determining the degree of distortion in the imagery. In most cases, post-processing will be required to correct these distortion effects.

3.1.1 Ground Range Nonlinearity

Perhaps the most predominant distortion in a spaceborne SAR image is the ground range nonlinearity. This effect results from the fact that each pixel represents a constant slant range distance rather than uniform ground spacing. Figure 2 illustrates the type of distortion inherent in a slant range projection. Features in the near range of a slant range image are compressed with respect to the far range. For example, a circle in the far range would have the appearance of an ellipsoid in the near range of the image. To project the image in a ground range format, the ground distance represented by each pixel in the slant range projection must be determined from

$$\Delta x = \frac{\Delta r}{\sin\phi} \tag{3}$$

where Δr is the slant range pixel spacing and ϕ is the incidence angle of the radar beam at the target. The slant range spacing is constant and is given by

$$\Delta r = \frac{c}{f_s} \tag{4}$$

where c is the speed of light and f_s is the sampling frequency. The maximum frequency is limited by the range bandwidth. For SEASAT SAR, this frequency was 45.53 MHz producing a slant range spacing of 6.59 m.

The incidence angle, ϕ, can be related to the beam elevation angle, θ, by trigonometric means as follows (Figure 3)

$$\phi = \sin^{-1}\left[\frac{(H + R_e)\sin\theta}{R_e}\right] \tag{5}$$

where R_e is the radius of the earth, H is the spacecraft height and θ, the look angle, is given by

$$\theta = \cos^{-1}\left[\frac{R^2 + (H + R_e)^2 - R_e^2}{2R(H + R_e)}\right] \tag{6}$$

The relationships for ϕ and θ in (5) and (6) have been derived assuming a smooth spherical surface with a radius equal to the radius of the earth at the target. Since the incidence angle is a function of the terrain, equation (5) is ony approximate for a rough surface. This could result in an error in the ground range projection.

3.1.2 Radar Foreshortening [13]

Radar foreshortening is the variation in apparent size of identical features at different slopes with respect to the sensor. The effect for terrain sloping toward the radar is an increase in the effective incidence angle. Terrain sloping toward the radar will therefore appear elongated with respect to terrain sloping away from the sensor. This is illustrated in Figure 4. Since terrain features are recorded as a function of the slant range distance from the sensor, slope ab is mapped into a'b' in the image plane while bc is mapped into b'c'. Although ab and bc are identical in length, b'c' will be more than three times larger than a'b' in the image. Quantitatively stated the elongation (or shortening) factor is given by

$$\frac{a'b'}{ab} = \sin (\theta - \beta_s) \tag{7}$$

$$\frac{b'c'}{bc} = \sin (\theta + \beta_s) \tag{8}$$

where β_s is the surface slope and θ is the look angle. Thus for a look angle similar to the terrain slope, the foreshortening effect is most severe.

The foreshortening can be corrected if the radar altitude and look angle are known and a terrain map of the target area is available. One technique to correct the foreshortening is as follows [14]: A digital topographical map is illuminated from the same angle that the radar used to generate the original foreshortened image. This can be routinely done using a radar simulation program. The resultant movement of each pixel in the simulated image is recorded. This image is then registered to the actual radar image

and the inverse of this movement is applied. The result of this type of process is shown in Figure 5. Note that the presence of certain geological features becomes readily apparent. This technique, although capable of producing an image without foreshortening, is a tedious process which requires exact registration of the simulated image with the actual radar image. In addition, this technique requires a priori terrain information for the imaged area which may not be available.

3.1.3 Radar Layover [13]

Radar layover is a distortion inherent in all radar imaging of irregular terrain. It results from an image pixel being placed in its cross-track location based on its range from the sensor. If the target area contains features with steep slopes, the top of the feature can be at a closer range than the bottom. This effect is shown in Figure 6. It is especially severe when features of appreciable level relief appear in the near range.

3.1.4 Earth Rotation

The earth rotation effect is common to satellite scanning systems where the scan lines are gathered serially in time while the earth's surface is rotating during the imaging period. This results in the near edge of the image being skewed with respect to the nadir track of the satellite as shown in Figure 7a. This effect, known as range walk or range migration can be compensated by resampling the echo data during the image processing. Figure 7b shows the outline of an image frame after data resampling to compensate for the range walk. The stairstep edge is an artifact of the multiple-look overlay process and does not result in any discontinuities within the frame.

3.2 Processor Derived Distortion

The distortions generated during image formation are obviously dependent on the specific processing algorithm. Generally, approximations made in determining the phase reference function will result in a skewed image. This section discusses some typical approximations and the resultant distortions.

3.2.1 Earth Curvature and Rotation

In the previous section, the range walk effect that results from the Earth rotation was described. This rotation in conjunction with the Earth curvature can also result in an image skew in the azimuth direction. This skew occurs during the image formation process. As previously discussed, to process raw echo data into imagery the Doppler frequency and frequency rate must be determined. The rotation and curvature of the earth, however, result in a complex Doppler response that is a function not only of target latitude but also depends on target position within the swath. A plot of Doppler frequency as a function of swath position and latitude is shown in Figure 8. It is extremely difficult to design a processor that adapts to the varying frequency without introducing reduced image resolution resulting from misregistration during the multiple-look overlay. As an alternative to precise tracking of the Doppler frequency during the processing, an optimum f_d is selected for the entire image frame and the resultant skew is corrected in the post-processing. This skew resulting from the Doppler mismatch is essentially in the azimuth direction as shown in Figure 9. The amount of skew is dependent on the difference between the actual Doppler response of each target and the f_d used in the processing and is given by

$$\Delta N_{az} = \frac{\Delta f_d}{f_d} \cdot \frac{PRF}{L} \tag{9}$$

where PRF is the pulse repetition frequency, L is the number of looks, Δf_d is the Doppler frequency mismatch, $\dot{f}_d$ is the Doppler rate and ΔN_{az} is the azimuth displacement in pixels. Note that since the iso-Doppler lines are nearly linear, a linear correction can be used to deskew the image. For a 100 km swath width as in SEASAT SAR, a typical skew is $\Delta N_{az} \simeq 150$ pixels or 2.5 km, which corresponds to a skew angle of 1.5 degrees.

3.2.2 Sensor Parameter Shift

The eccentricity of the spacecraft orbit requires adjustment of the sensor parameters at certain intervals during the orbit. This can result in either a discontinuity, or variation of the pixel resolution within an image frame. A sharp discontinuity in the image results from a shift in the delay of the pulse sampling window. This parameter shift is made in the data collection system to maintain the optimum signal-to-noise ratio in the sampled echo data. If the pulse sampling window were not adjusted as the spacecraft altitude changed, this window would not center on the portion of the signal with the strongest return and the resulting imagery would be degraded. The effect on an image produced from data collected during a sampling window shift is to displace one part of the image in range with respect to the other, resulting in a line of discontinuity across the frame.

Another parameter requiring adjustment based on variation in the spacecraft orbit is the pulse repetition frequency (PRF). The PRF is adjusted to prevent pulse mixing or range ambiguities. An upper limit on the PRF is set to avoid interference between successive pulses. This limit is dependent on the range swath width which is in turn a function of spacecraft altitude. A lower limit on the PRF is determined by the resolution and

azimuth ambiguity requirements. This bound is also dependent on the spacecraft orbit. To keep the PRF within these bounds, it must be adjusted according to variation in the spacecraft height. Certain frames therefore may contain pixels of mixed resolution if the PRF was adjusted during that frame's data collection period.

3.3 Radiometric Characteristics

Registration of a SAR image to an optically sensed image or another SAR image can present a difficult problem since the apparent brightness of an image pixel is critically dependent on the relative position of the sensor. A small change in the aspect angle can significantly alter the appearance of a scene as shown in Figure 10. Furthermore, SAR imagery is corrupted by both speckle and thermal noise, pulse compression sidelobes, ambiguity responses and weak signal suppression effects [6]. With proper radar and processor design, the effects of most of these distortions on the final image product can be minimized. The image degradation resulting from speckle noise is greatest in coherent imagery of terrain with a surface roughness comparable to the wavelength of the illumination [15]. The speckle can be reduced by summarion of looks or filtering at the cost of pixel resolution.

When attempting to register SAR imagery from two adjacent passes for the purpose of constructing a mosaic, the distortion resulting from speckle can cause misregistration. This results from the fact that for a small change in the sensor position (4 km for SEASAT) the speckle noise in the resultant imagery is totally independent. Therefore, from one pass to the next a feature may be distorted differently resulting in a poor correlation between the two frames. An additional factor that can cause image misregistration between two adjacent passes is a phenomenon called specular point

migration illustrated in Figure 11. This effect occurs when a feature with a varying slope is imaged from two different sensor positions. The apparent position of a feature changes relative to other features within the frame because the point of maximum reflectivity of that feature occurs at a slope perpendicular to the radar beam. This effect can also result in apparent misregistration of features in SAR imagery.

IV. CURRENT PROGRESS IN REGISTRATION/RECTIFICATION OF SAR FREQUENCY

Many of the geometric and radiometric distortions present in digitally processed SAR imagery do not occur in optically sensed imagery. The effect of these distortions on image resolution, rectification and ultimately mosaicking have not been fully investigated. To date very few mosaics have been constructed with digital SAR imagery and at present no comprehensive studies have been conducted to investigate the feasibility of generating unsupervised mosaics.

The SAR processing research group at Jet Propulsion Laboratory has laid the ground work for development of an unsupervised mosaicking procedure and plans to implement this procedure within the next year. Recently completed is an algorithm capable of determining the absolute location of an image pixel without the aid of ground reference points [6]. This algorithm utilizes information provided by the spacecraft ephemeris and characteristics of the sensor data collection system to predict the latitude and longitude of an arbitrary image pixel. Tests have shown this technique has an accuracy of better than 200 m for SEASAT SAR data. The target location uncertainty is primarily dependent on the accuracy of the spacecraft position and velocity provided by the ephemeris and the validity of the assumed geoid in the target area.

The capability for unsupervised pixel location is a prerequisite for automated rectification and mosaicking of SAR imagery. With informtion on both the sensor and target position, the parameters for slant range to ground-range conversion can be determined as well as the Doppler shift in the echo

data. Using this information and the image processing parameters, it is a simple procedure to conduct range and azimuth interpolation to remove the ground range nonlinearity and azimuth skew distortions. An algorithm has been developed at JPL to correct these distortions for digitally cor- d SEASAT imagery. A preliminary version of this algorithm has been plement utilizing the hardware architecture of the digital processor. This hardware configuration, shown in Figure 12, was designed both for efficiency and economy [17]. The host computer is a Systems Engineering Laboratory 32/77 which features very rapid I/O data transfers. Attached to the host are three Floating Point Systems AP120b array processors and four 300 Mbyte discs. The image data is transferred from disc to the array processors through the host. Each AP operates simultaneously on a separate area of the image and returns the rectified product to the host to be merged and transferred to disc. It is anticipated that with proper design this approach can rectify a 6000 x 6000 pixel frame which covers a 100 x 100 km ground area in under 30 minutes. This approach is compatible with the image processor and could be easily incorporated into the image production procedure.

A preliminary version of this algorithm is currently operating at JPL. It utilizes a single AP and makes some simplifying assumptions in generating the rectification parameters. The current operating time for a full frame is 80 minutes. The output has been resampled to 12.5 m spacing in both the range and azimuth dimensions. As a result of approximation, the rectified product still contains some residual skew. Tests show approximately a 200 m registration error across a 100-km frame. The expected registration error using a more exact version of the algorithm is less than 50 m or about 2 pixels.

Following completion and test of the rectification algorithm, studies are planned to investigate the feasibility of generating unsupervised image mosaics. Imagery from parallel passes as well as ascending and descending passes will be examined. Statistics will be compiled on the correlation of common features as well as the misregistration between geometrically corrected images from two adjacent passes. Automated feature detection techniques are also being considered to locate suitable tie points.

Obviously much work remains to be done with regard to rectification and registration of SAR imagery. It is clear that digitally correlated imagery offers distinct advantages over optical imagery such as: reproducible processing, large inherent dynamic range and highly accurate pixel location. The refinement of these techniques utilizing SEASAT SAR data will provide insight into the design of future sensor systems to optimize the registration and rectification accuracy.

ACKNOWLEDGEMENT

This paper presents the results of one phase of research carried out at the Jet Propulsion Laboratory, California Institute of Technology, under Contract No. NAS7-100, sponsored by the National Aeronautics and Space Administration. The author wishes to thank C. Wu for his assistance in the preparation of this paper.

REFERENCES

[1] L.J. Cutrona, "Synthetic Aperture Radar," Radar Handbook M.I. Skolnik, ed., McGraw-Hill, New York, 1970, Chapter 23.

[2] W.M. Brown and L.J. Procello, "An Introduction to Synthetic Aperture Radar Theory," IEEE Spectrum, pp 55-62, Sept. 1969.

[3] J.D. Lent and G.A. Thorley, "Some Observations on the Use of Multiband Spectral Reconnaissance for the Inventory of Wildland Resources," Remote Sensing of the Environment, Vol. 1, pp 31-46, 1969.

[4] J.C. Kirk, "A Discussion of Digital Processing in Synthetic Aperture Radar," IEEE Trans on Aero and Elec Systems, Vol. AES-11, No. 3, pp 326-337, May 1975.

[5] C. Wu, "A Digital System to Produce Imagery from SAR Data," AIAA System Design Driven by Sensors Conference, Paper No. 76-968, Pasadena, California, Oct. 1976.

[6] C. Wu, B. Barkan, B. Honeycutt, C. Leary and S. Pang, "An Introduction to the Interim Digital SAR Processor and the Characteristics of the Associated SEASAT SAR Imagery," Publication 81-26, Jet Propulsion Laboratory, Pasadena, Calif, Apr. 1981.

[7] J.J. Kovaly, ed., Synthetic Aperture Radar, Artech House, Inc., Dedham, Mass., 1978.

[8] C.E. Cook and M. Bernfeld, Radar Signals, Academic Press, New York, 1967.

[9] J.C. Curlander, C. Wu, D. Held and F. Li, "Estimation of Doppler Parameters for Spaceborne Synthetic Aperture Radar Processing," in preparation.

[10] R.E. Morden, F. Powell, "SAPHIRE Design and Development," Paper GERA-2177, Rev. A, Goodyear Aerospace Corp., Arizona Division, Litchfield Park, Arizona, Sept. 1977.

[11] L.J. Porcello, N.G. Massey, R.B. Innes, J.M. Marks, "Speckle Reduction in Synthetic Aperture Radars," Journal of the Optical Society of America, Vol. 66, No. 11, pp 1305-1311, Nov. 1976.

[12] J.S. Lee, "Speckle Analysis and Smoothing of Synthetic Aperture Radar Images," Computer Graphics and Image Processing, Vol. 17, pp 24-32, 1981.

[13] A.J. Lewis and H.C. MacDonald, "Interpretive and Mosaicking Problems of SLAR Imagery," Remote Sensing of the Environment, Vol. 1, pp 231-237, 1970.

[14] M. Naraghi, W. Stromberg and M. Daily, "Geometric Rectification of Radar Imagery Using Digital Elevation Models," submitted to Photogrametric Engineering and Remote Sensing.

[15] J.C. Dainty, ed., Laser Speckle and Related Phenomena, Springer-Verlag, Berlin, 1975.

[16] J.C. Curlander and W.E. Brown, Jr., "A Pixel Location Algorithm for Spaceborne SAR Imagery," Proceedings of the 1981 International Geoscience and Remote Sensing Symposium, Washington, D.C., pp 843-851, June 1981.

[17] C. Wu, B. Barkan, W. Karplus, and D. Caswell, "SEASAT Synthetic Aperture Radar Data Reduction Using Parallel Programmable Array Processors," Proceedings of the 1981 International Geoscience and Remote Sensing Symposium, Washington, D.C., pp. 541-548, June 1981.

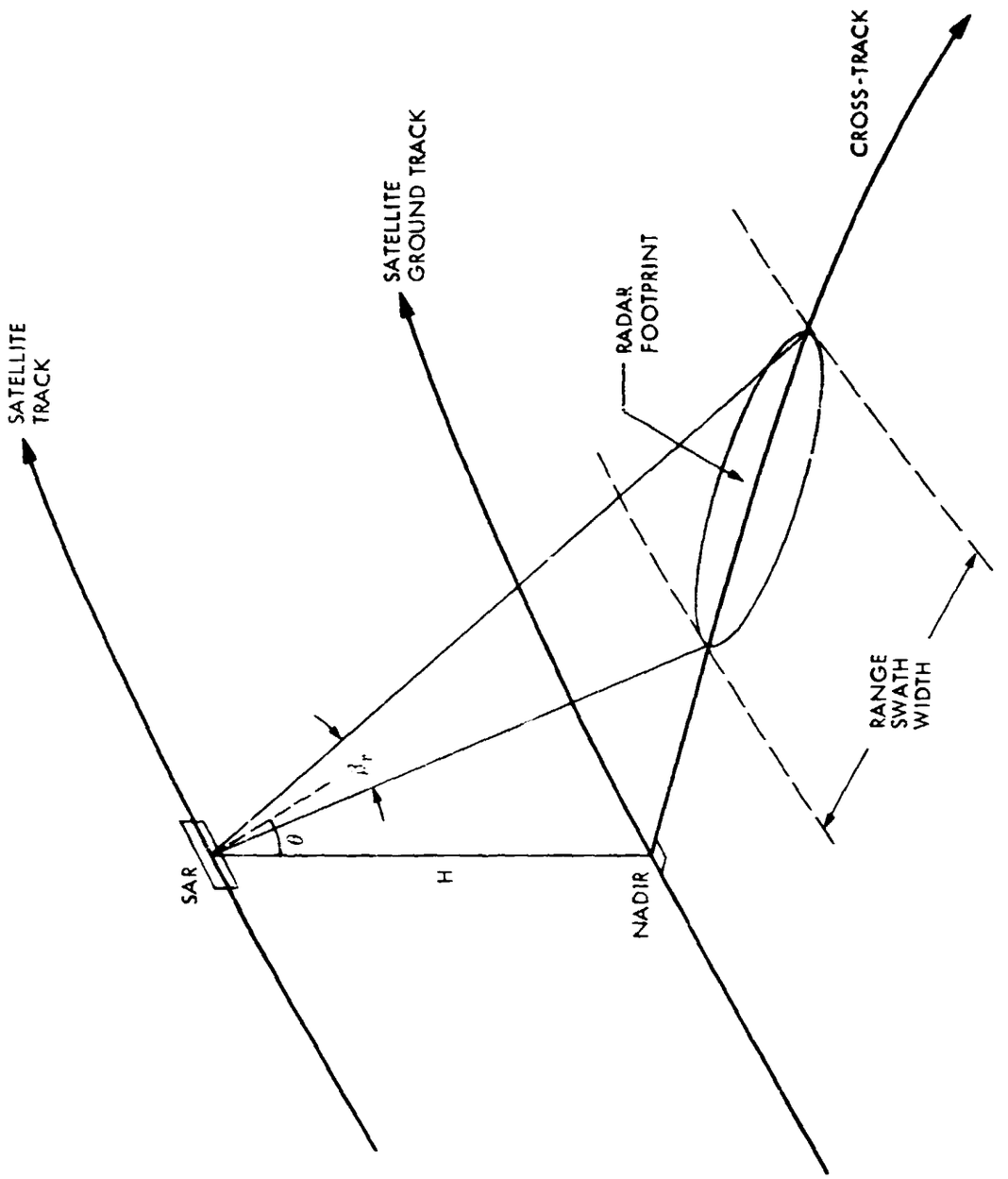

Figure 1. Viewing geometry for a typical side-looking synthetic aperture radar

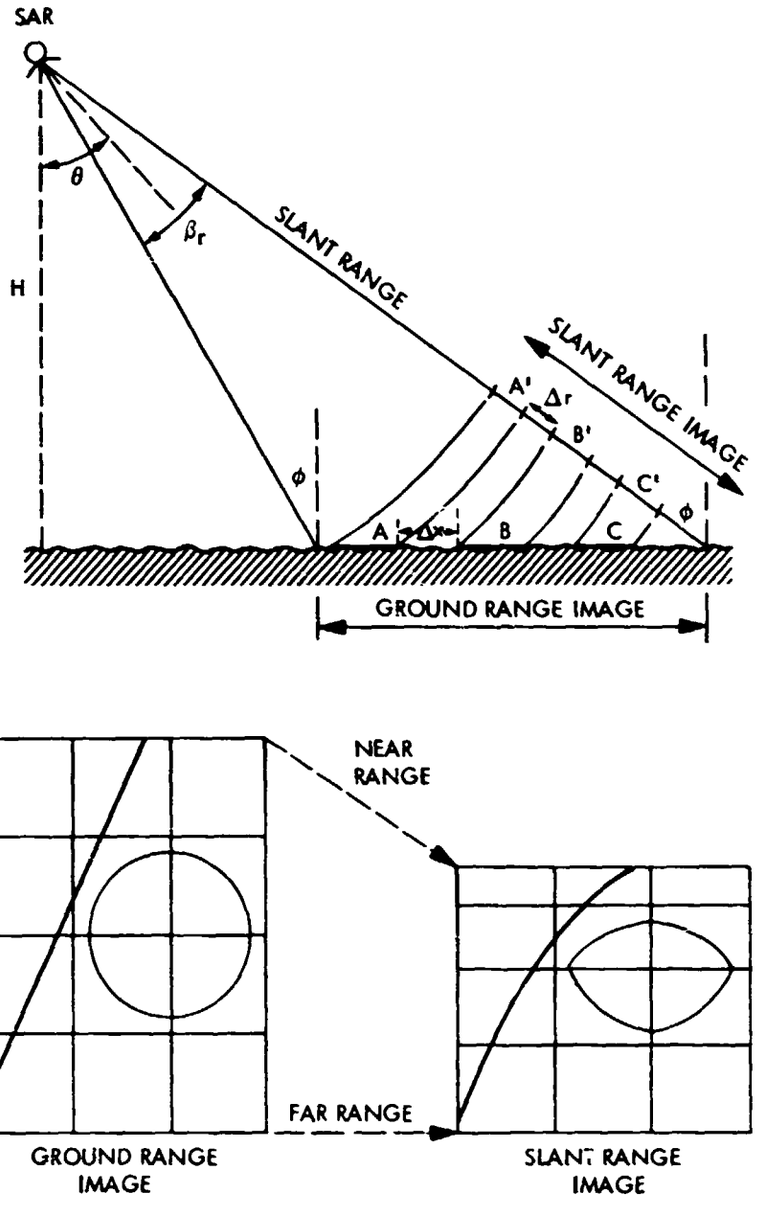

Figure 2. Slant range to ground range nonlinearity inherent in all side looking radar systems. Near range features are compressed relative to far range features because of change in incidence angle, ϕ.

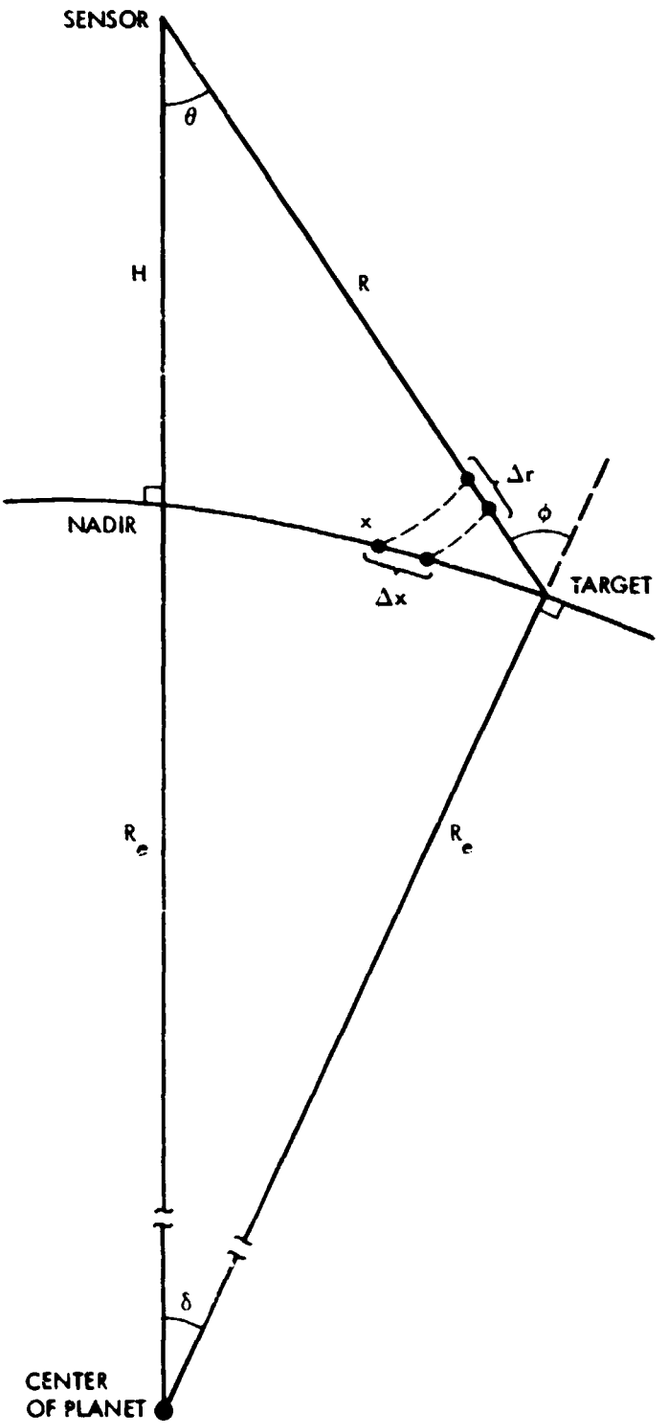

Figure 3. Relationship between look angle, θ and incidence angle ϕ for a smooth spherical planet surface.

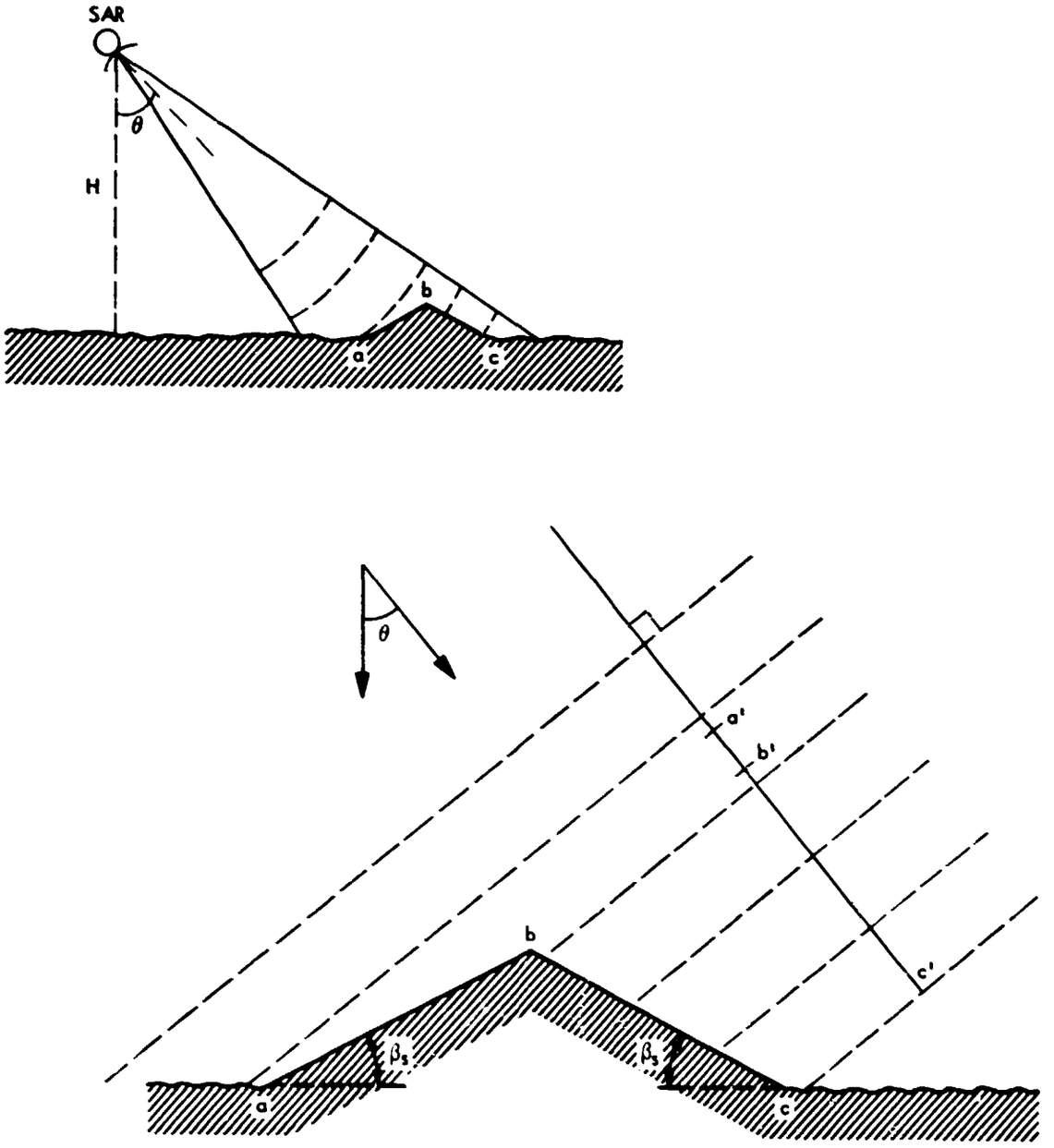

Figure 4. The radar foreshortening effect causes slopes inclined toward the radar to appear shorter than those inclined away from the radar.

a

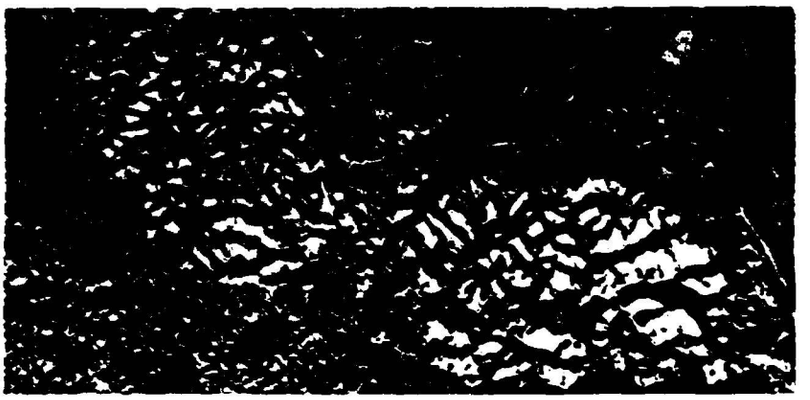

b

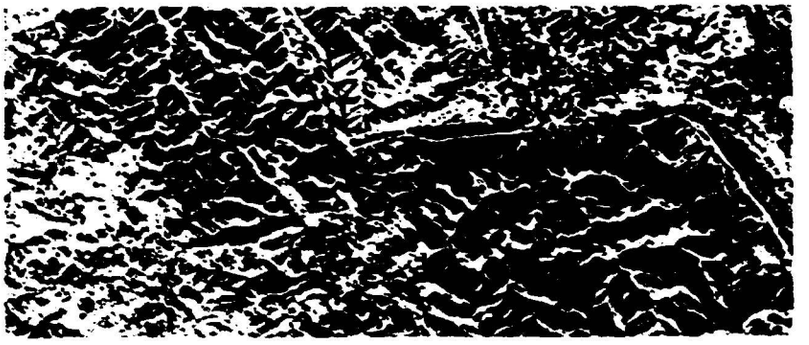

c

Figure 5. Results of compensation for radar foreshortening using digital terrain model. a) Simulated radar image from topographical map, b) Corrected SEASAT image, c) Original SEASAT image. Note the enhancement of fault lines not evident in original image (Naraghi, 1981).

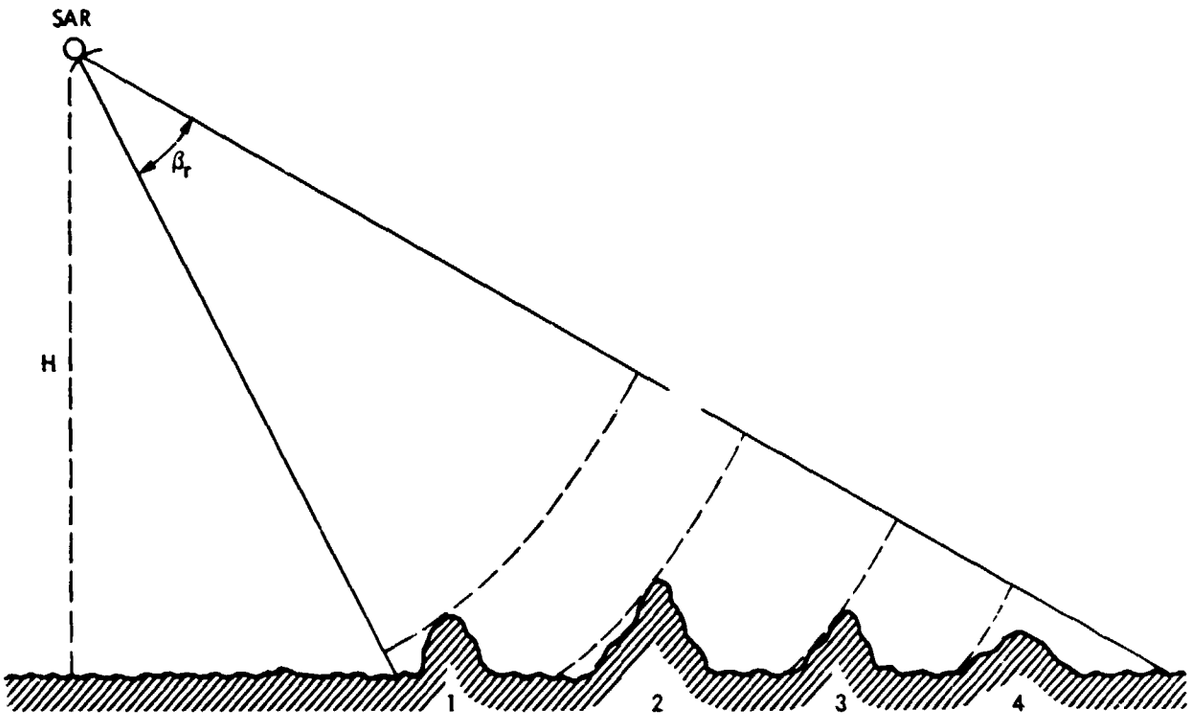

Figure 6. Radar layover is a function of the terrain slope and the slant range to the target. Layover occurs when the surface feature slope exceeds the look angle. Signal scattered from the top of features 1 and 2 will be placed at a nearer cross-track position in the image than signal scattered from the bottom.

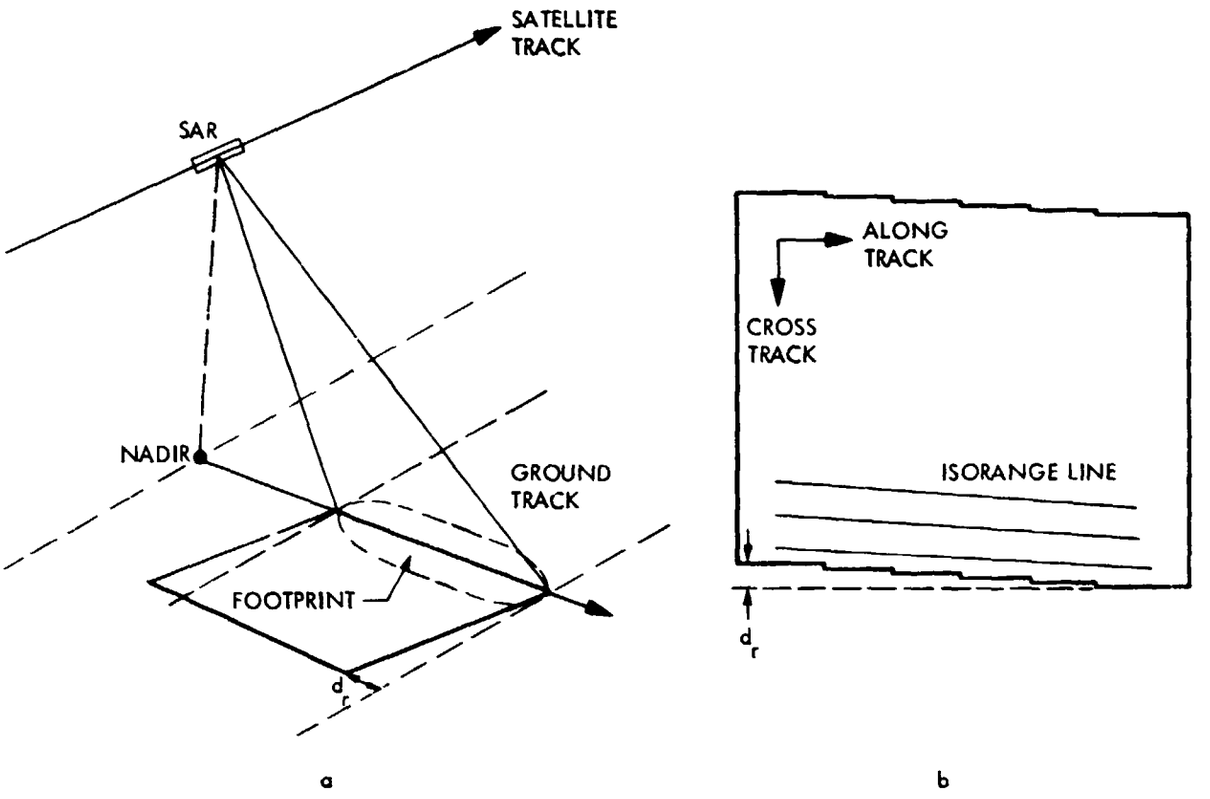

Figure 7. Range migration of the ground track resulting from earth rotation during the imaging period is shown in a. The range skew distance is given by $d_r = V_e \cdot \Delta t$ where V_e is the velocity of the earth and Δt is the imaging time for the frame. The cross track skew shown in b is applied during the image formation.

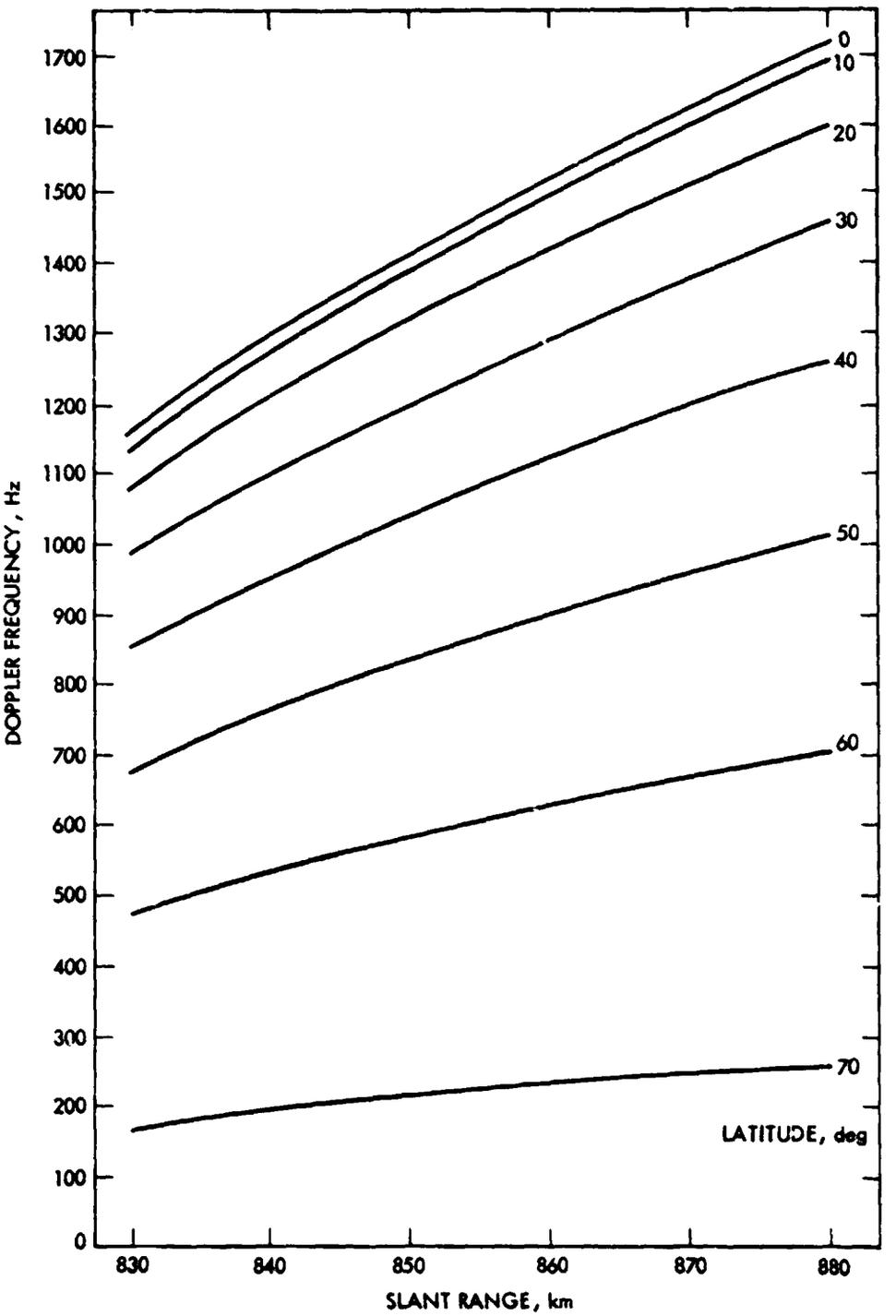

Figure 8. Plot of Doppler frequency as a function of swath position and latitude. Nominal values for SEASAT SAR were assumed for spacecraft in descending mode (Wu, 1981).

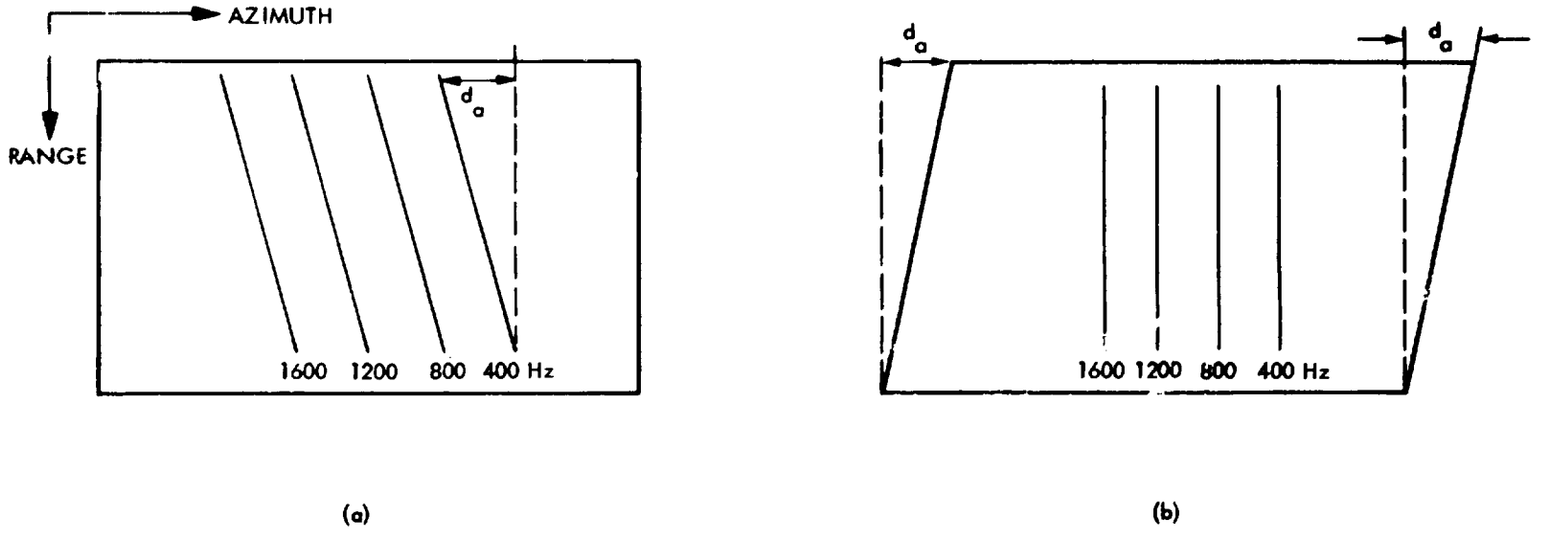

Figure 9. Azimuth skew resulting from Doppler frequency mismatch during processing. a) Image frame without azimuth skew illustrating orientation of iso-Doppler lines. b) Skewed image showing azimuth displacement d_a. Note: Processor assumes uniform f_d across swath resulting iso-Doppler lines aligning with cross-track direction.

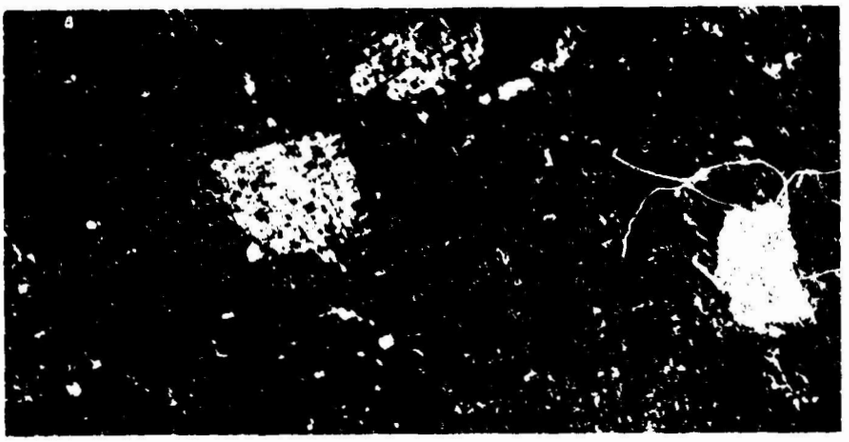

a

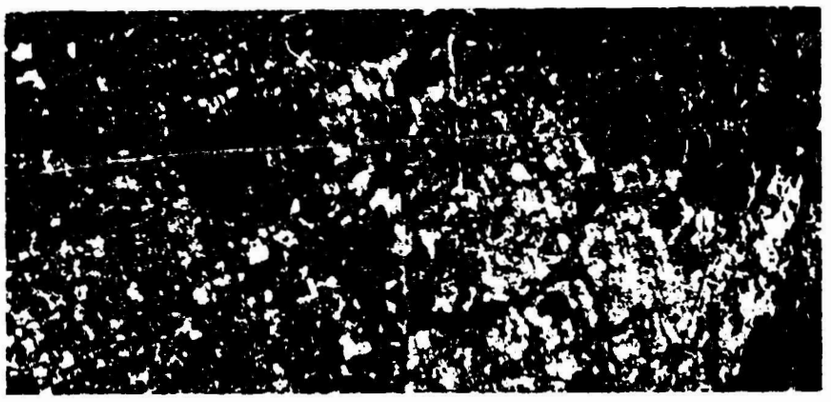

b

Figure 10. Effect of radar aspect angle on the apparent brightness of target. Figure 10a was imaged during a descending mode and Figure 10b during an ascending mode

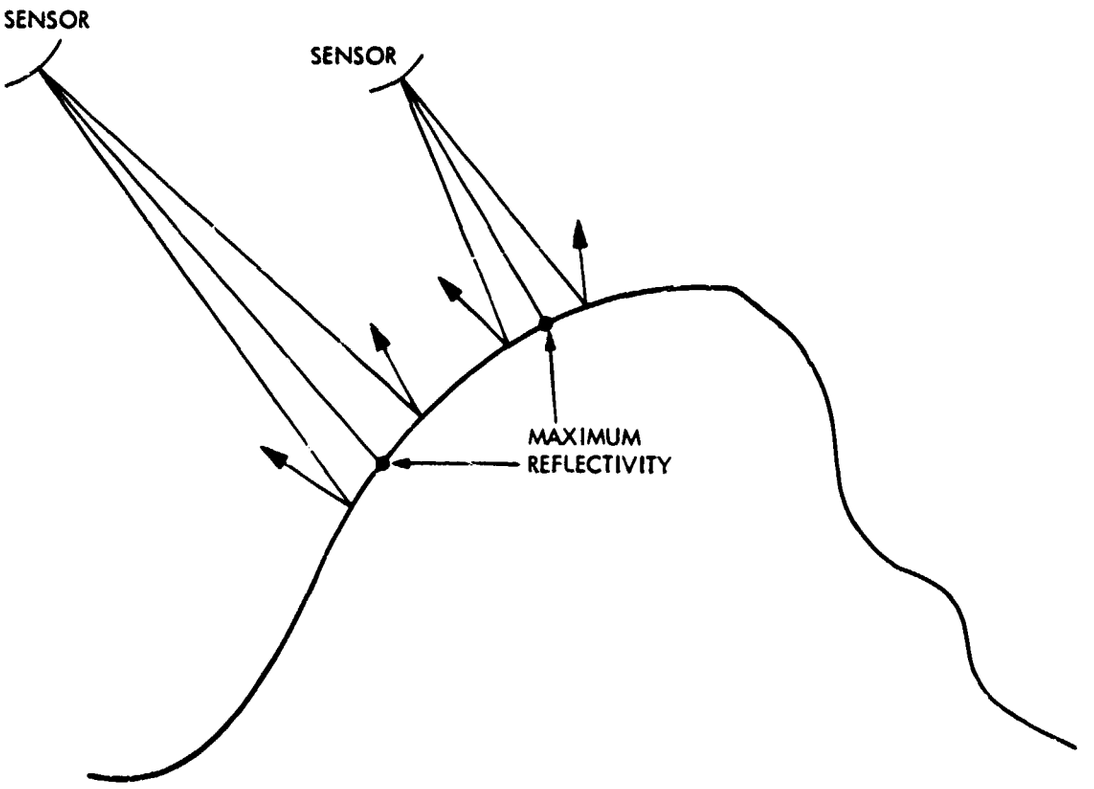

Figure 11. Specular point migration results when sensor images the same feature from two different positions. Point of maximum return is dependent on target slope and may vary relative to other features within the frame.

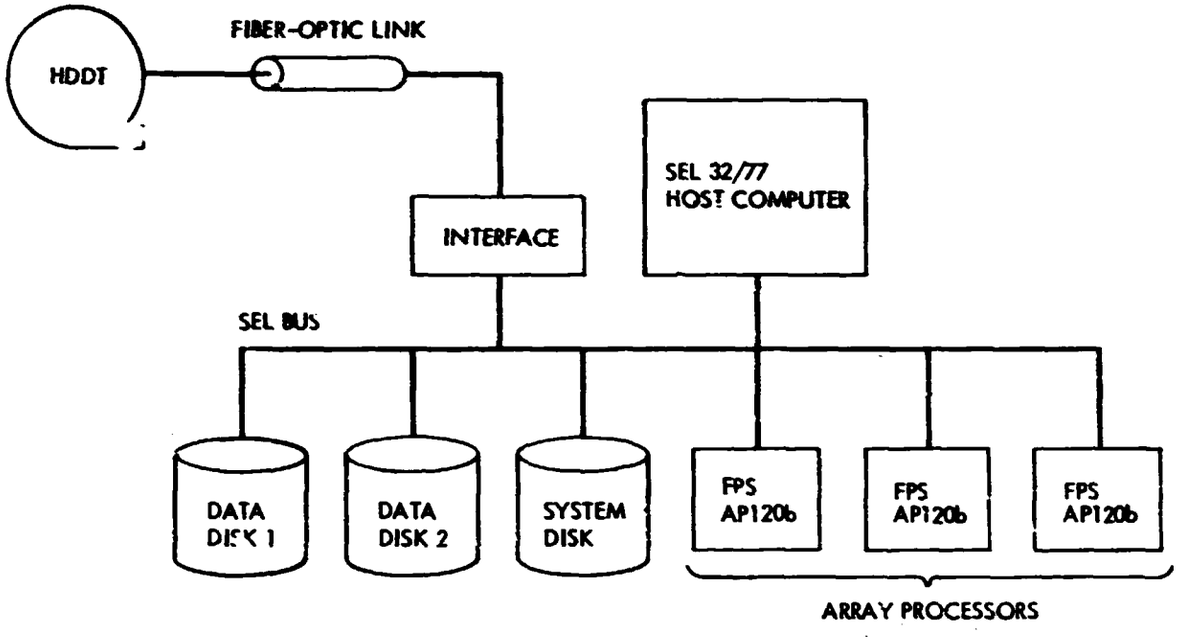

Figure 12. Block diagram of digital processing system at Jet Propulsion Laboratory. Data is recorded on high density digital tape (HDDT) at the tracking station. It is received at the processing facility via an optical link and recorded on disk for processing (Wu, 1981).

N82 28718

5.7 SPACECRAFT INDUCED ERROR SOURCES*

H. Heuberger, GSFC

I'm going to say a few words about spacecraft induced error sources, basically attitude errors on the Landsat spacecraft, the 1, 2, 3 and D, and ephemeris errors from various tracking systems.

First, I want to talk about the attitude control system and attitude measurement system on Landsat-2 (actually 1, 2, and 3 as they are basically the same). Table I reviews the kind of attitude information we had to work with on those three spacecraft. The attitude control system uses horizon scanners and gyros to solve for pitch and roll directly, and once those are brought in, there is a gyro in the roll/yaw plane; knowing the roll and the rate from that gyro, you can solve for yaw and bring the yaw error in.

TABLE I

Landsat-2 Attitude Control and Measurement

- Attutude Control System (ACS)
  - Horizon scanners and gyros provide pitch and roll error sensing
  - Rate Measurement Package (RMP) in roll/yaw plane used to determine yaw error
  - Pointing Control = 0.1 deg
  - Pointing Stability = 0.01 deg/s
- Attitude Measurement Sensors (AMS)
  - Independent of ACS
  - Horizon scanners fore and aft determine pitch and roll
  - Yaw assumed proportional to roll
  - Measurement accuracy = 0.1 deg
  - Horizon scanners susceptible to atmospheric effects (e.g., cold clouds)

The specification on the platform is a pointing control of .1° and stability of .01° per second. Now on that spacecraft the measurement system or what we actually know about the attitude is independent of the control system. We have infrared horizon scanners for pitch and roll. There's nothing though that gives us the yaw error so we assume it's proportional to roll. Basically because of the way the control system solves for yaw, we have the same specification there of .1°.

What people are really seeing is quite a bit worse because the infrared horizon scanners are susceptible to cold clouds etc. Depending on who you listen to, .5° is not unusual -- even possibly 1°. I've heard numbers like that. On the last slide, I'll translate all these numbers into what an image error would be from that type of attitude error.

*Edited oral presentation.

Table II reviews the situation on Landsat-D. It is the same as the previous Landsats for course acquisition and there's a fine sun sensor that's used for transition and the nominal mode is star trackers and gyros. Star trackers and the gyro information are filtered to update quaternians and actually the star trackers are used to update the gyro drift. We have a much improved system here, as we have pointing accuracy advertised as .01° and very good stability, and from talking to different people, that's the specification and it seems to be that it will be achievable. In fact, we may do quite a bit better than that by a factor of 2 or something. On Landsat-D, the attitude measurements come from the control system Kalman filter and the DRIRU.

TABLE II

Landsat-D Attitude Control and Measurement

- o Same as Landsat-2 for coarse acquisition
- o Fine sun sensor used for transition to fine acquisition
- o 2 star trackers and 6 gyros (3-axis redundant) used to update quaternians
- o Pointing accuracty = .01 deg
- o Pointing stability = 10^{-6} deg/s
- o Attitude measurements from control system Kalman filter and DRIRU
  - Quaternians every 4.096 s
  - Gyro measurements every 64 ms

Table IIIa reviews the ephemeris. I'm not contrasting Landsat 1, 2, and 3 against D because basically they're the same class of spacecraft. It depends on what type of data you have to work with for ephemeris error. Now some of these numbers you've already seen from the GE people, in fact some of these numbers come off GE's slides. The altitude variation is due to earth oblateness and variations in eccentricity etc. Along-track variation is not by itself too important because the spacecraft is basically following the same ground path. Dr. Prakash said four kilometers cross-track; I got 5 kilometers from the people who are responsible for the orbit control. That's probably the most important number there. If Mr. Billingsly was talking about relief displacement, that's the kind of number we would be looking at for relief displacement, if you were 5 kilometers off on your look angle there.

With conventional processing, and operational processing of the Goddard network and standard network, we generally can get around 100 meters in ephemeris error. This is definitive, as you get 24 hours of data and do a least squares fit to orbit or doppler data and do a batch fit or sequential filter. You can characterize errors pretty reliably and usually find 100 meters or better. Orbit predicts (a second method) generally represent what is uplinked to the spacecraft. They claim these are 2-day predicts; I would think they would be more like 1-day predict numbers. Five-hundred meters after 2 days is doing pretty good; I would say 1 day or somewhere in there. All of these numbers are 1-sigma numbers and it depends on who you talk to and what your assumptions are.

Table IIIb looks at tracking systems of the future. On Landsat D, using TDRSS data and from simulations and error analysis, we find out we can do about the same that we do now—processing 24 hours of TDRSS data may get you 90 meters,

TABLE IIIa

Landsat-D Orbit Variations and Ephemeris Accuracy

- o Variations from nominal
  - Altitude (705.3 km nominal)
    - 696 to 741 km over earth
    - 19 km variation over fixed latitude
  - Along track: ± 95 km
  - Cross track: ± 5 km at equator
  - Inclination: 98.21 ± .045 deg
- o Conventional Processing Ephemeris Error (GSTDN Data)

	Operational Post Processing	Orbit Predicts
Along track	100 m	500 m
Cross track	30	100
Radial	20	35
RSS	105	510

you might do slightly better generally, but it's about the same measures as using the ground tracking. The really good news is the GPS, the Global Positioning System, which is a system of DOD satellites and navigational development satellites, which will significantly reduce ephemeris errors. As a result, the combined attitude and ephemeris errors, as shown in Table IV, are expected to experience better than an order of magnitude improvement over the previous Landsats.

TABLE IIIb

Landsat-D Ephemeris Accuracy (cont.)

- o Ephemeris Error with TDRSS

	Definitive Orbits
Along track	80 m
Cross track	30
Radial	25
RSS	90

- o Ephemeris Error with GPS

	4 nds. Inview	Poor Visibility
Along track	10 m	50 m
Cross track	6	25
Radial	4	20
RSS	12	60

TABLE IV

Attitude/Ephemeris Scene Distortions

Along/Cross-Track Error (MET)

Distortion Source	Landsat-2 AMS GSTDN Tracking	Landsat-D ACS GPS
ATTITUDE		
Pitch	1570/-	123/-
Roll	- /1585	- /125
Yaw	160 / -	124 / 125
EPHEMERIS		
Along Track	100 / -	10 / -
Cross Track	- / 30	- / 6
Radial	- / 3	- / -
RSS	100 / 30	10 / 6

N82 28719

5.8 NAVSTAR/GLOBAL POSITIONING SYSTEM*

M. Ananda, The Aerospace Corporation

The Global Positioning System (GPS) has been developed to provide highly precise position, velocity, and time information to users anywhere in the neighborhood of earth and at any time. The GPS, when fully operational, will consist of 18 satellites in six orbital planes. These satellites will be at about 20,000 km altitude with a 12-h period and the orbits will be inclined to 55°. The satellites will transmit L_1 (1575.42-MHz) and L_2 (1227.6-MHz) signals. Navigation information such as the emphemeris of the satellites and satellite clock model parameters and the system data are superimposed on these radio signals. Any GPS user, by receiving and processing the radio signals from the constellation can instantaneously determine navigation information (position and velocity parameters) to an accuracy of about 15 m in position and 0.1 m/s in velocity. This radio navigation system is primarily developed for utilization by the Department of Defense. However, there exists a broad spectrum of civil users who would benefit from this system.

The GPS system has three separate segments. One is the space segment, which is the satellite itself, then what we call a control segment, which is responsible for providing the information to the satellite, and the third is the user segment. The user segment includes individual user MANPAC or automobiles, trucks, ships, aircrafts, and satellites. With regard to program history, originally the Navy was responsible for initiating a navigation system, the TRANSIT program--and it is still operational now. They have five satellites and the accuracy is reasonable. The GPS mission program was a preliminary study which the Navy originated and 621-B was a program the Air Force initiated; they were subsequently combined and became the Global Positioning System. During the program evolution there are three phases: (1) the concept validation phase, (2) the full-scale engineering development and testing (present phase), and (3) full operation capability. In Phase I we had four satellites and two planes; in Phase II we have 6 satellites; however, one of the satellites is not functioning properly because of the on-board clock. It is not giving the accuracy we need. In Phase III we will eventually have 18 satellites and this will be a different satellite than what we have now.

Let's briefly look at the space segment. Once we have 18 satellites, each satellite will be in a 12-hour period at 20,000 km altitude. (Figure 1). Current clock accuracy is about $1{:}10^{-13}$ to $5{:}10^{-14}$. Clock performance is extremely good even though the design specifications show only $2{:}10^{-13}$. We have two L-band frequency signals, L-1 and L-2, at 1.2 GHz and 1.5 GHz, and we also have an L-3 but that's not a user oriented band, it is used for a specific purpose. We may use that L-3 which is a cross-link capability from one satellite to another satellite.

Now the concept of getting navigation information from the GPS satellites. The satellites will provide signals from which you can, if you have a receiver, get range information and simultaneously if you can get full range information properly distributed in the sky, you can determine your own position and the bias in your clock. If your clock is not as precise as the satellite clock, you can determine instantaneously our precision plus the timing bias.

*Edited oral presentation.

If you have the range rate information in addition to the range information you can also determine the velocity if you are a user. The accuracy we are currently broadcasting (Figure 2) we would get is 15 meters of spherical distributed error for all these types of users, whether a MANPAC, an automobile, ship, aircraft or Shuttle. When you deviate from 800-1,000 km altitude, like Landsat, your accuracy will be improved because of some of the errors are associated with atmospheric modeling.

In comparison of navigation systems (Figure 3), the GPS is a navigation system purely based upon radiometric measurements. There are a quite a large number of navigation systems in existence. Currently, LORAN-C, OMEGA, INS, TACAN, TRANSIT—these are all radio based navigation systems. The TRANSIT is probably closer to GPS because it has a global capability; however, the accuracy degrades in between orbits. GPS provides the same accuracy globally everywhere anytime. That's the key point. In other systems the errors are fairly large and obviously there is a lot of lost information you will not receive. GPS is a very simple concept and versatile, and obviously, a very expensive system also. For user equipment, as I said earlier, you need to have four satellites simultaneously visible. Simultaneous in the sense that you don't need to have a four-channel receiver in order to do it; you can do it sequentially. However, the four satellites have to be available to the user and the constellation is designed to be able to achieve at least four satellites at any given time, anywhere near the earth.

The performance of the user system depends upon several things (Figure 4). The vehicle environment -- of concern in particular to defense related problems and constellation geometry -- is very geometry dependent and dependent on the dynamics of the vehicle and the way the ionosphere and troposphere are modeled. The ionosphere can be monitored better if you have a two-channel receiver because you have two frequencies going in and separated in frequencies so we can calibrate real time. For a single receiver, we have provision in the navigation message which will provide some kind of table for modeling the ionospheric effects. It may not be very accurate, but sufficient for that type of user.

Reviewing the error budget (Figure 2), true navigation error is a product of what we call GEODOFF, that is, geometry delusion of precision. If you multiply the GEODOFF times the user equivalent range error component you get the navigation error. The GEODOFF data varies from one place to another place and the best GEODOFF is 2 or 2.2. So if the satellite dependent range error is multiplied by 2.2, it would give you around 15-meter accuracy, which is the total of the various error sources. The satelite clock is minus 13 over a 24-hour period and we update once in 10-hours. Each clock will have a different elapsed time because the update time will be different for each satellite. A single satellite will be visible once or twice a day from a given ground control station. Another interesting element is that if you use GPS in a relative mode for a relative navigation, all these errors tend to cancel out. So the only error you will be left with is a user related error of approximately 2 meters. Most of the civilian types of purposes can be used in a relative mode depending on what your particular application is. For that reason, we have what we call for security purposes selective availability, so we cannot guarantee any user the real accuracy the system would provide. However, the degraded accuracy would be available to everyone. We don't know what the degraded accuracy is or whether it will be opted; those decisions are to be made

at a much higher level, but we have the ability to introduce whatever error we want. However, that will not affect a user using a relative mode.

- USERS NAVIGATE IN RELATIVE COORDINATES USING THE SAME SATELLITES

- ERRORS THAT DISAPPEAR	NORMAL THREE SIGMA	THREE SIGMA WITH *
• IONOSPHERIC	6.9	6.9
• TROPOSPHERIC	6.0	6.0
• EPHEMERIS PREDICTION	7.5	353.0
• CLOCK STABILITY	8.1	353.0
• SV PERTURBATIONS	3.6	3.6
RSS	14.85	500
- REMAINING ERRORS		
• RECEIVER NOISE	4.5	4.5
• MULTIPATH	3.6	3.6
• OTHER	1.5	1.5
RSS	6.0	6.0

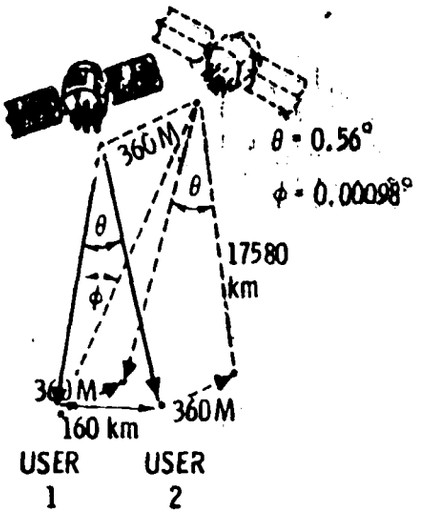

*Degraded clock and ephemeris

Figure 1. Relative Navigation

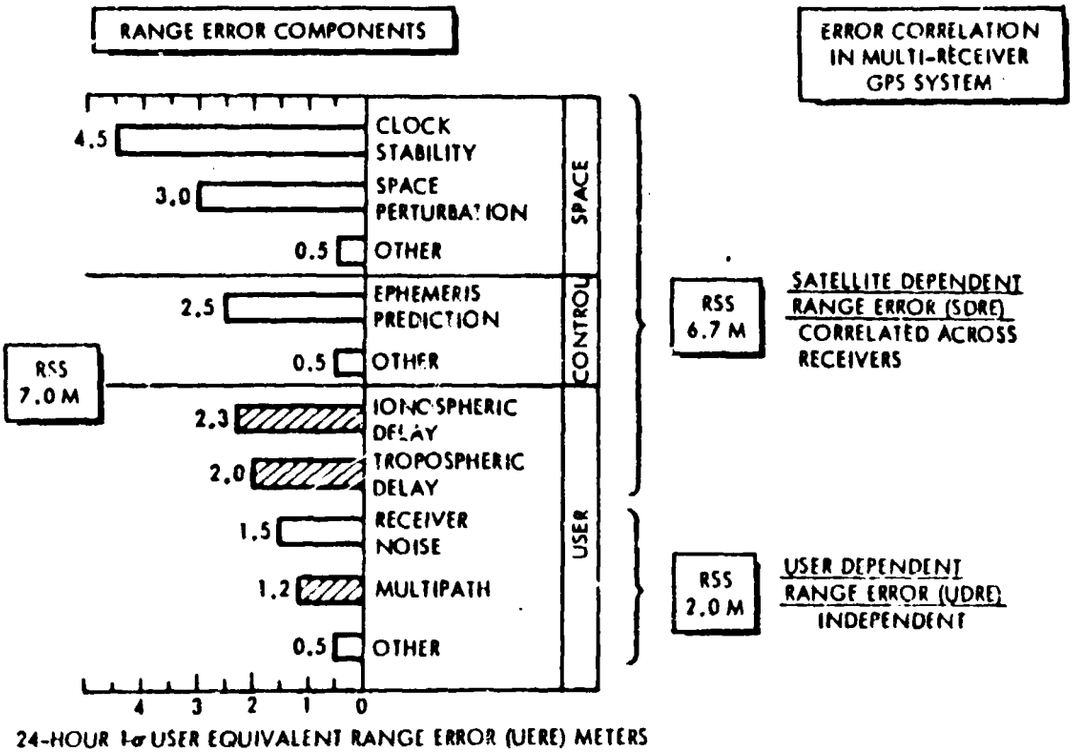

Figure 2. User Equivalent Range Error Budget

System	Position Accuracy (m)	Velocity [illegible]cy (m/sec)	Range of Operation	Comments
GPS	15 (SEP) 3-D	0.1 (RMS per axis)	Worldwide	Operational worldwide with 24-hour all-weather coverage.
Loran-C (Note 1)	180 (CEP)	No velocity data	U.S. Coast, Continental U.S., Selected Overseas areas	Operational with localized coverage. Limited by skywave interference.
Omega (Note 1)	2,200 (CEP)	No velocity data	Near global (90% coverage)	Currently operational with localized coverage. System is subject to multi-path errors.
Std INS (Note 2)	1,600 max after 1st hour (CEP)	0.8 after 2 hr (RMS per axis)	Worldwide	Operational worldwide with 24-hour all-weather coverage. Degraded performance in polar areas.
TACAN (Note 1)	400 (CEP)	No velocity data	Line of sight (present air routes)	Position accuracy is degraded mainly because of azimuth uncertainty which is typically on the order of ±1.0 degree.
Transit (Note 3)	200 (CEP)	No velocity data	Worldwide	The interval between position fixes is about 90 minutes. For use in slow moving vehicles

NOTES:
1. Federal Radio Navigation Plan, July 1980
2. ENAC-77-IV, Characteristic for a Moderate Accuracy Inertial Navigation System, August 1979
3. Journal of the Institute of Navigation, Volume 27, No. 2, Summer 1979

Figure 3. Navigation System Comparison

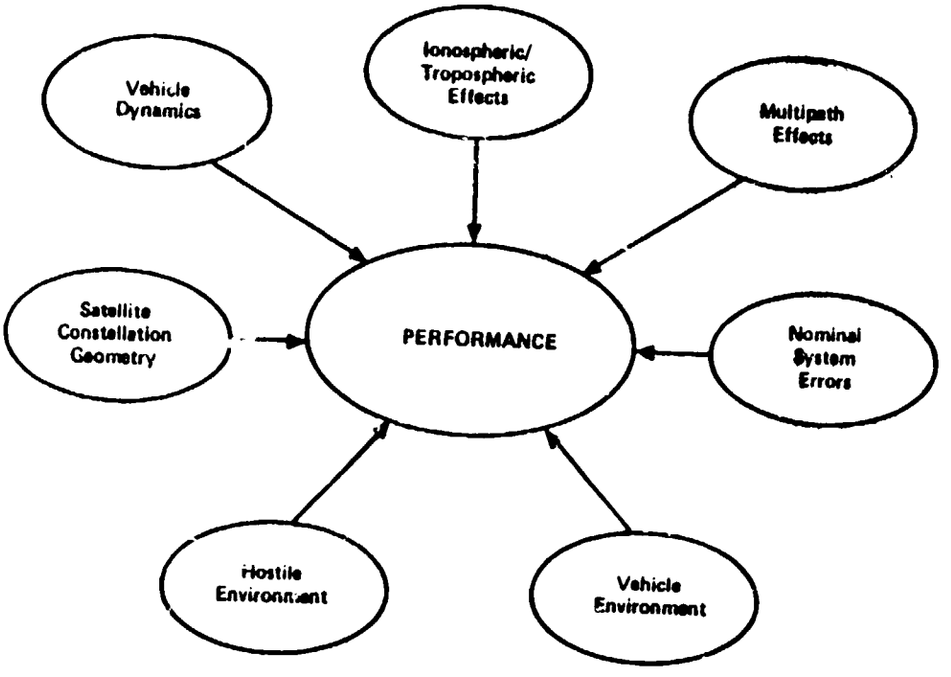

Figure 4. UE Set Performance

OMIT

6.0 PRESENTATIONS ON GROUND SEGMENT ERRORS

6.1 SUMMARY

The position papers on ground segment errors reviewed the underlying theory for essential elements in the rectification process and also reviewed positional accuracy standards. Geodetic control can be characterized as well established in developed countries but having somewhat more poorly developed networks in many other parts of the world. Furthermore, it is frequently difficult to obtain geodetic information in many countries as it is considered of strategic value and each country has a different datum upon which it bases its horizontal control. As a result, rectifying spacecraft to a particular map projection within map accuracy standards must be considered on a case-by-case basis for most areas of the world.

National Map Accuracy Standards (NMAS) apply to both horizontal and vertical position error. A fundamental relationship between spatial resolution, x-y positional error, and vertical elevation error points out that vertical resolution capability is twice the nominal spatial resolution for a stereographic pair of images. Thus, a 5-meter IFOV resolution system could provide 10-meter elevation contour interval data. This fact combined with national map accuracy criteria would indicate that a 15-meter resolution system could achieve 1:50,000 NMAS planimetrically but only 1:250,000 NMAS for topographic mapping.

The review of map projections illustrated salient points. First, all projections distort the real condition extant on the spherical earth in some way. As a result, each map must compromise size, shape, or area. The smaller the scale, i.e., the larger the region being displayed on a map, the more apparent these distortions become. Most maps in use today are based on lines of longitude, or meridians, and therefore are oriented north/south and east/west. The Space Oblique Mercator projection in use with Landsat MSS data is based upon the nadir track of the spacecraft, a convention which eases computational considerations. However, because of the nadir tracks' continuous positional changes with each overpass, this projection undergoes continuous variation, resulting in its not being adopted by the majority of the map-base oriented users.

N82 28720

ORIGINAL PAGE IS
OF POOR QUALITY

6.2 GEODETIC CONTROL*

J. Gergen, NOAA
Horizontal Networks Div

Geodetic Control nets are built over time depending on the resources available. In the U.S. the situation around 1900 looked like Figure 1. You had a translation scheme along the east coast, you had some activity around the great lakes, and the major accomplishment of 25 to 30 years was the Transcontinental Arch of Triangulation. So that was the first time when people even knew how far it was from one coast to the other one. By 1931 (Figure 2), the situation had changed to a rather nicely developed pattern with the arch of triangulation going North, South, East, and West. You see in Figure 2 extremely large triangles, and the basic principle of triangulation observations is that one measures the angles in a triangle and occasionally one measures a distance between two points, a side of a triangle. By that you can compute the coordinates and resolve all the unknowns in the triangle and get coordinates. If you have a starting value, you can build upon that as you go along. The accuracies that are involved depend very much on how frequently you update your distance, because that is the most degrading effect. By 1946 the situation in North America looked like Figure 3: a highly developed system in the conterminous United States with hardly anything in Canada, some attempts to do something in Alaska, and a development in Mexico by virtue of the Inter-American Geodetic Survey. By 1946 the number of points reached over a 100000 in the U.S. The situation as it stands today, looks like Figure 4. In the conterminous U.S. it has grown to an inventory of about 250,000 points. Canada has also made progress; there is significant progress in Alaska, and one should expect much more in Alaska with the current developments in energy. The control net has been pushed all the way through the Central American Republics into the northern part of South America with all of the connections to islands.

The instruments that are used to build a horizontal network have been primarily the theodolites and they are considered part of the classical arsenal of instrumentation. We can measure directions with the theodolites to a standard error of about 6/10 of a second. We now have electronic distance measuring instruments which can measure distances most accurately to 1 part in a million of the distance. We make satellite doppler observations which give us point positions with accuracies of standard deviations of level of less than 1 meter. In recent years, inertial survey systems have been developed and they are primarily used for identification purposes. For the future, there will be Global Positioning Satellites, but in our concept it will come down to standard deviations between 2 and 4 centimeters. That is the difference from the 15-meter and 6-meter deviations mentioned before. The point is we have more time, we don't need it instantaneously. We can sit there at the station for a number of hours and that will improve the accuracy. Furthermore, we will use GPS only in a relative mode because we have 200,000 points already. We can put one receiver at a known point, and then relatively position any other point within 200 km from the first point, to this kind of accuracy.

The relative and absolute accuracies of the U.S. horizontal network are shown in Figure 5. We distinguish between several orders of accuracy. The first order is the most precise one, it has direct accuracy of 1 in a 100,000 and

*Edited oral presentation.

the others just decrease to 1 in 5,000. What is more interesting possibly for this audience is the absolute accuracy of the U.S. network which is on the North American datum of 1927. The accuracy in the absolute sense is about 15 meters, and that is due to the existing distortions in the network. We are actively working now on a project that will give the North American Datum in 1983, where all positions will be known to about 1/2 meter. That 1/2 meter refers to the worst; we contemplate just 4-5 centimeters precision for some of the best points in the network.

For the U.S. network on the 1927 datum, all points are related to a mathematical surface which is an ellipsoid placed in space many many years ago, in such a way that there is an offset with respect to the Geocenter of 22 meters in x, 157 meters in y, 176 meters in z. These numbers are not to be looked at as errors, but they are very well known numbers. Still, we will move the mathematical surface from one point to another point because when this was done originally no one knew where the earth's geocenter was. But today because of satellites it is very easy to determine where the Geocenter is. The most significant datum defined by the Defense Department was the world generic system of 1972. We know these numbers that relate to the U.S. datum, but we also know these numbers for the other datums. Figure 6 gives an example of the major datums in the world and what these shifts to the Geocenter are, but you see that these numbers vary depending on how these datum were defined to begin with. The thing that needs to be remembered is that one cannot apply one philosophy to all datums and assume that they are all consistent in the same coordinate system. Each of them is a separate coordinate system, and in order to make one earth coordinate we have to take all of these datums and shift them to one common place, and the most logical common place today is the geocenter. International meetings have agreed that the geocenter makes sense. The International Association of geodesy has defined the geodetic reference system of 1980 as a geocentric system.

The availability of geodetic information within the U.S. is the responsibility of the National Geodetic Survey and the information is freely available in this country. That is not the case in general. Other countries have looked at geodetic activities very much in terms of their military establishment. As a consequence the information is generally unavailable because these countries classify the information. However, there are old publications that you can find that show what these datums look like, and give you some idea of what the accuracy is. There are international units of measure in geophysics national reports that one can consult, and one can read between the lines and see for example the Peoples Republic of China has a network that is similar to ours in terms of accuracy or you can obtain it from the geodetic organizations that are inclined to make that information available. For the accuracies that we can estimate relative between two points, the worst that you can find is 1 in 5,000. That is due to the instrumental errors because you are dealing with an accuracy only from one point to another 2-3 miles away. However, when you look at these in terms of an absolute reference (where is this vis-a-vis the geocenter?) then of course you can have errors as high 200 meters. Some of the datums in other continents are much weaker in terms of the way they were constructed, and the instrumentation that was used, so you may very well get to that number.

In general, if one gets some coordinates, either latitude or longitude or some other types of coordinate system derived from latitude and longitude any place

on the Earth, one cannot immediately assume that that's part of the same coordinate system that we have in the U.S. The Doppler Survey System today is allowing us to make exact determination of what these changes and what the errors actually are. An example of this problem is the Universal Transverse Mercator projection. The UTM coordinate system is a way to represent coordinates if you don't want to deal with latitudes and longitudes. Basically the system divides the Earth up into sixty zones and the center meridian for Zone 1 is at longitude 180° east. The scale along the central meridian assumes a false easting of 500,000. Now what's important is that this is not a universal transverse Mercator in an absolute sense. Its universal within a particular datum. It should be possible to compute, if you know the information world-wide, all your coordinates and put all them into one datum, a Geoscentric Datum and then you can transform all these points a given projection. Then you have indeed a universal projection. All of this is done by the military, but I don't know of an inventory of coordinates world-wide that is consistent from all these points of view. The problem is not only in the position of the mathematical surfaces, but also the size and shape. When you bring in the size and shape, the semimajor axis of the reference elipsoid and the flattening, you get just as many combinations of datums; there are hundreds of datums world-wide each of which look at the problem from their own point of view. Basically, the characteristic of geodetic control is that it is in direct proportion to the technological development of the countries involved [1,2]. World-wide you find good coverage in terms of geodetic control in the U.S., in western Europe, and in Japan. You find less than full coverage even in the Soviet Union and South America, and Asia and so forth in other large areas.

References:

1. NASA, Directory of Observation Station Locations, GSFC, Greenbelt, MD.

2. NAD Symposium, Proceedings. The Canadian Surveyor, vol. 28, No. 5, 1974.

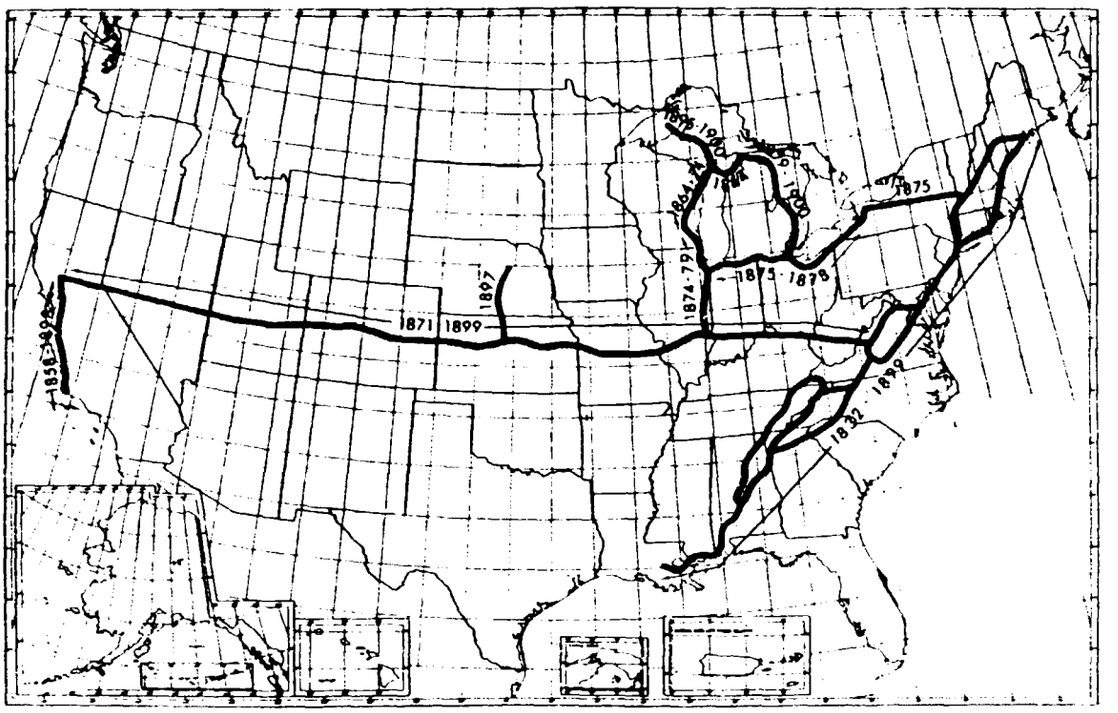

Figure 1. U.S. Horizontal Network 1900

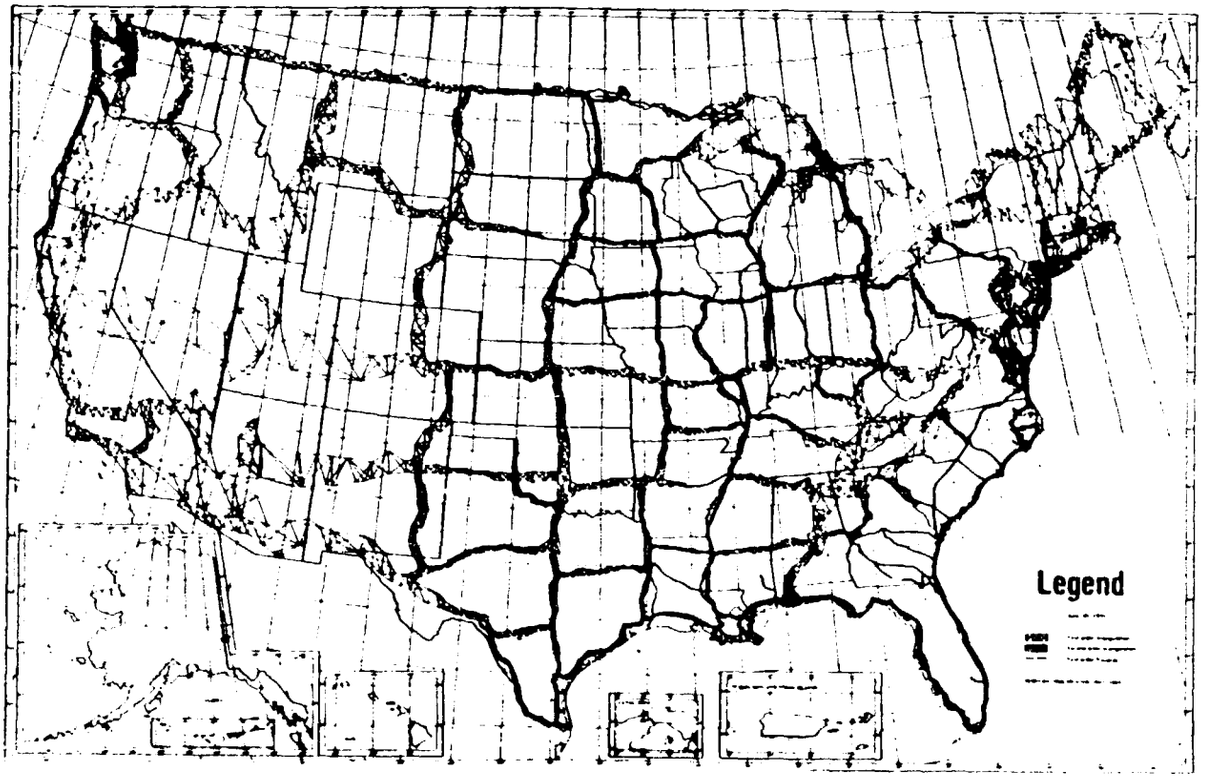

Figure 2. U.S. Horizontal Network 1931

Figure 3. North American Datum 1946

Figure 4. North American Datum 1981

Relative Accuracy
between directly connected adjacent points

First order	Second order		Third order	
	Class I	Class II	Class I	Class II
1:100,000	1:50,000	1:20,000	1:10,000	1:5,000

Absolute Accuracy

- NAD27 15m
- NAD83 0.5m

Figure 5. U.S. Horizontal Network

	Shifts to Geocenter		
	ΔX(m)	ΔY(m)	ΔZ(m)
1. North American	−22	157	176
2. European	−84	−103	−127
3. Tokyo	−140	516	673
4. Arc 1950	−129	−131	−282
5. Indian	293	697	228
6. Australian	−122	−41	146
7. South American	−77	3	−45
8. Pulkovo	—	—	—
9. South Asia	21	−61	−15

Figure 6. Major Geodetic Datums

N82 28721

6.3 MAP ACCURACY REQUIREMENTS: THE CARTOGRAPHIC POTENTIAL OF SATELLITE IMAGE DATA*

R. Welch, University of Georgia

The topic of this presentation is map accuracy requirements. I am going to try to relate map accuracy requirements to the cartographic potential of satellite image data. The objectives are to consider, first, if resolution will be adequate for the identification of control and for the compilation of map products. Then, second, to define map accuracy standards and to determine the potential for meeting these standards with image data from the film camera, scanner and linear array systems of the 1980s.

Cartographic products fall into a variety of classes. We have topographic maps that are concerned with planimetric information and elevations or heights. We have thematic maps, which might be used for geology, vegetation, water, or to display these subjects. We have digital elevation maps that would be produced from digital terrain data, and finally we have image maps. In terms of satellite applications, we've dealt primarily with thematic maps and with image maps, and in the future we would like to be able to develop some digital terrain models and topographic map products.

Table 1

EARTH SATELLITE PROGRAMS--1980s

SATELLITE	SENSOR	IFOV	SWATH
Shuttle/Spacelab (1982)	Film Cameras (LFC, MC)	5m*	225 km
Landsat-D (1982)	Mechanical Scanner (TM)	30	185
SPOT (1984)	Line Array (HRV)**	20	60
MOS (1985)	Line Array (MESSR)	50	200
Stereosat (?)	Line Array**	15	61
Mapsat (?)	Line Array**	10-30	185

*Equivalent IFOV
**stereo

We would like to be able to develop an array of points for which we know the X, Y, and Z coordinates and then interpolate from these points the contours or the elevations. I might point out that the accuracy with which we interpolate may be a problem here. In addition, sensor resolution must be considered.

Table 1 summarizes the terrain imaging satellite programs for the 1980s. It is important to note the Shuttle/Spacelab film cameras. These film cameras have an equivalent IFOV of about 5 m and represent the baseline against which the other sensor systems will have to be compared.

*Edited oral presentation.

The conventional 1:250,000 scale map contains contours and considerable planimetric detail. One can see the outline of towns, the different classes of roads, and the vegetation patterns. This is typical of a 1:250,000 scale map product. Now, I'll talk about well-defined points. By well-defined points I mean the intersection of roads or where a bridge crosses a river, things of this nature. Well-defined points don't exist in any great frequency in undeveloped areas, so this is a problem if we are going to extract control from maps.

With the Skylab Earth Terrain camera photograph we can detect the highways, the urban development, the airfields and so on. This is about the best resolution data that we've had to-date and is representative of what we will get with the Shuttle cameras. This is our baseline information. How good a map can we prepare with an approximate equivalent 5 m IFOV? Well, we can prepare quite a good map as a matter-of-fact. We can delineate the outlines of the urban areas, we can show most of the roads, we can pick-up the vegetated areas, we can obtain quite a bit of information. If we go to the map compiled from a RBV image of Landsat-3, it in no way compares to a 1:250,000 scale map, nor does it compare in any way to a map which was compiled from the Skylab photography. So if we're talking about Thematic Mapper data which may be of slightly better resolution than the RBV, it's very unlikely that we're going to be able to compile maps in the traditional sense of the word.

Now, what are U.S. National Map Accuracy Standards (NMAS, Table 2)? First of all we can divide them into horizontal and vertical accuracy standards. For horizontal accuracy, the U.S. standards say that 90% of well-defined points should be plotted at the map scale to within $\pm$ 0.5 mm of the correct position. For example, if we have a map scale of 1:100,000, the bridges, road intersections, and so on, must be correct to $\pm$ 0.5 mm on the map. Thus, we can say that 90% of the points must be within $\pm$ 0.5 mm on the map and $\pm$ 50 m on the ground. For spot heights, 90% of the elevations that are determined from contours shall be correct to within one-half the contour interval. Thus, if we have a contour interval of 100 m, ninety percent of the interpolated elevations should be correct to within $\pm$ 50 m.

Table 2

U.S. NATIONAL MAP ACCURACY STANDARDS

A. HORIZONTAL - 90% OF WELL-DEFINED POINTS SHALL BE PLOTTED (AT THE MAP SCALE) TO WITHIN $\pm$ 0.5 mm OF THEIR CORRECT POSITION, e.g.,

MAP SCALE = 1:100,000
$\pm$ 0.5 mm AT MAP SCALE = $\pm$ 50 m ON GROUND

THUS, 90% OF POINTS MUST BE WITHIN $\pm$ 0.5 mm ON THE MAP AND $\pm$ 50 m ON THE GROUND.

B. VERTICAL - 90% OF THE ELEVATIONS DETERMINED FROM CONTOURS SHALL BE CORRECT TO WITHIN 1/2 THE CONTOUR INTERVAL (C.I.), e.g.,

C.I. = 100 m

THUS, 90% OF ELEVATIONS REFERENCED TO CONTOURS SHALL BE CORRECT TO WITHIN $\pm$ 50 m.

In terms of horizontal accuracy now, let us introduce root mean square error (RMSE). By RMSE we mean that 68% of the points tested lie within the specified distance from the correct grid coordinates (Figure 1). For example, if the RMSE is ± 15 m, 68% of the points tested lie within ± 15 m of the correct location. For the 90% confidence level specified by NMAS, we must multiply 15 m by 1.65 which yields ± 25 m. Next, we want to determine the largest scale map (which is really what we want to know) that can be compiled from these data and still meet NMAS. As Figure 1 notes, the largest scale map compatible with horizontal errors of ± 25 m at the 90% level of confidence is 1:50,000.

Figure 2 reviews vertical accuracy (Z). If the $RMSE_Z$ is ± 15 m, that means 68% are to be within that value. But NMAS state that 90% of interpolated Z-values must be correct to within one-half the contour interval. So statistically, the closest contour interval which will meet NMAS is 3.3 times the $RMSE_Z$, or 50 m in this instance. From this discussion we can make the general observation that elevations are the problem, not the planimetric positions.

Figure 3a notes areas of the world with poor map coverage, and it is precisely these areas where satellite data are going to be most useful. These are also areas that have poor control nets.

Figure 3b indicates the standard contour intervals associated with maps around the world. The 1:50,000 scale maps normally have a 20 m contour interval. The contour intervals found on 1:100,000 scale maps range from 20 to 50 m and those on 1:250,000 maps from 50 to 100 m. If you are going to talk about compiling topographic maps at these scales, you have got to be able to meet the accuracy standards for elevations. For example, with a 1:100,000 scale map. planimetric accuracy requirements mean ± 50 m at 90% or ± 30 m RMSE. A 50 m contour interval requires an $RMSE_Z$ of ± 15 m.

The other subject which we have to consider is ground control and I'd like to make these points. First, ground control is normally required to establish the exterior orientation of the sensor system. Second, ground control will consist of well-defined points within the image data set for which the X, Y, Z terrain coordinates are known. Third, most ground control to be used to rectify satellite image data will be obtained from existing topographic map bases. Thus, the accuracy of the source maps may be an important factor (Table 3). Fourth, in the absence of ground control there must be an external means of establishing the X, Y, Z coordinates of the spacecraft or sensor system: e.g., orientation data from a star tracker and position and time from the NAVSTAR GPS. As satellite data are likely to prove most useful for mapping areas with poor control, the external means of determining spacecraft position, sensor attitude and time are extremely important.

Table 3

ACCURACY OF GROUND CONTROL POINTS OBTAINED FROM MAPS MEETING NMAS

SCALE OF MAP	HORIZONTAL RMSE	CONTOUR INTERVAL	(C.I./3.3-C.I./2)
1:250,000	75 m	100 m	30-50 m
1:200,000	60	100	30-50
1:100,000	30	50	15-25
1:50,000	15	20	6-10
1:25,000	7.5	10	3-5

Future sensors will employ MLA technology in which a line array is pushed over the earth and there is a time element involved. You are not recording the entire frame at one instant in time. You are recording one line of data at a time. There are several sources of error with MLAs. We have pointing, attitude stability, satellite velocity, measurement precision and accuracy, reliability of ground control, earth curvature refraction, processing equipment, adjustment procedures, and relief displacement.

Pointing and attitude control are a major problem. If we are going to map we require stereo coverage, and most of the stereo systems such as Mapsat or Stereosat are going to take coverage with a forward-looking camera and with an aft-looking camera. The time interval between the fore- and the aft-looking coverage is on the order of 90 to 100 seconds (B/H = 1.0). During that 90- to 100-second period, the attitude of the spacecraft has to be very stable. If one assumes for the moment that we have a combined error due to pointing errors and attitude errors on the order of five seconds of arc, the error in X,Y is $\pm$ 10 m and the Z error is going to be about $\pm$ 20 m. The elevation component is the critical aspect, and attitude control is absolutely essential.

A hypothetical combination of errors is reviewed in Figure 4. Given the assumption that sensor attitude is maintained to five seconds of arc, the errors in X,Y and in Z are about $\pm$ 10 m and $\pm$ 20 m respectively. Let's also assume we have a measurement or correlation error equivalent to a half of a pixel. That's about $\pm$ 8 m. Additional miscellaneous errors may equal another $\pm$ 10 m. If we combine these errors by taking the square root of the sum of the squares, we obtain $\pm$ 15 to $\pm$ 20 m for planimetry, and about $\pm$ 25 m for spot heights. The largest scale map that we can reproduce from such data, working in even increments, comes out to about 1:100,000 scale and the contour interval that meets NMAS is on the order of 100 m.

In conclusion then, I think that we can say that, first of all, for topographic mapping at scales of 1:100,000 and larger, an IFOV of 10 m or less will be required, as will geometric accuracies of $\pm$ 20 m or better. Secondly, the film cameras to be employed on the shuttle missions will provide baseline data against which the scanner, line array and radar systems can be evaluated. Third, automated mapping will require error-free image data. Thus, in my opinion, it appears reasonable to emphasize satellite positioning and attitude control rather than to rely solely on the availability of dense ground control and on costly image processing techniques to create rectified image data sets. Finally, satellite systems which provide data meeting rigorous topographic mapping requirements will also satisfy the accuracy requirements for thematic mapping.

ROOT MEAN SQUARE ERROR (RMSE) -68% OF POINTS TESTED LIE WITHIN THE SPECIFIED DISTANCE WITH REFERENCE TO THE CORRECT GRID COORDINATES, e.g.,

RMSE = $\pm$ 15 m

THUS 68% OF THE POINTS TESTED LIE WITHIN $\pm$ 15 m OF THE CORRECT LOCATION.

FOR A 90% CONFIDENCE LEVEL AS SPECIFIED BY NMAS, IT IS NECESSARY TO MULTIPLY THE RMSE BY 1.65, e.g.,

+ 15 m x 1.65 $\approx$ + 25 m

THUS, THE LARGEST SCALE MAP WHICH CAN BE COMPILED AND STILL MEET NMAS IS:

$$\text{MAP SCALE FACTOR} = \frac{\text{RMSE} \times 1.65}{0.5}$$

$$= \frac{25000 \text{ mm}}{0.5 \text{ mm}}$$

$$= 50{,}000$$

FIGURE 1. HORIZONTAL ACCURACY (X,Y)

e.g. $RMSE_Z = \pm$ 15 m (68%)

NMAS STATE 90% OF ELEVATIONS TO $\pm$ 1/2 C.I.

STATISTICALLY,

$$\text{C.I.}_{\text{NMAS}} = 3.3 \times RMSE_Z$$

$$= 3.3 \times 15$$

$$= 50 \text{ m}$$

THUS, THE CLOSEST C.I. WHICH CAN BE COMPILED TO MEET NMAS IS 50 m

FIGURE 2. VERTICAL ACCURACY

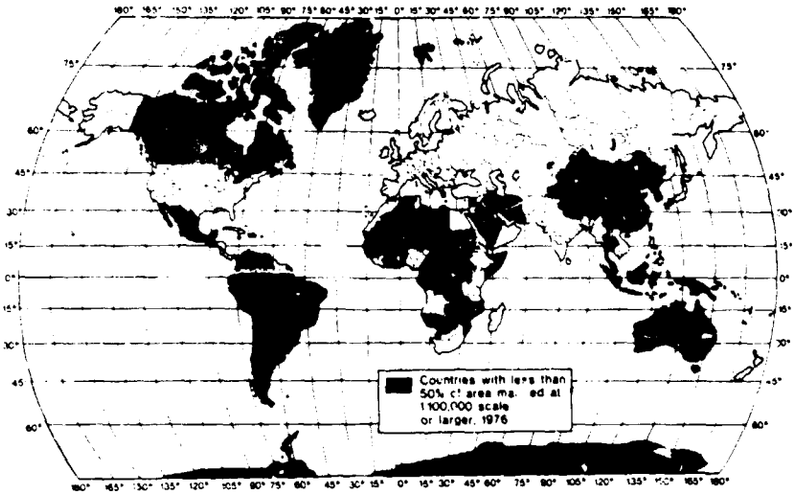

Figure 3a. The shaded areas represent countries or regions with 50 percent or less of their area mapped at 1:100,000 scale or larger in 1976 (United Nations, 1976).

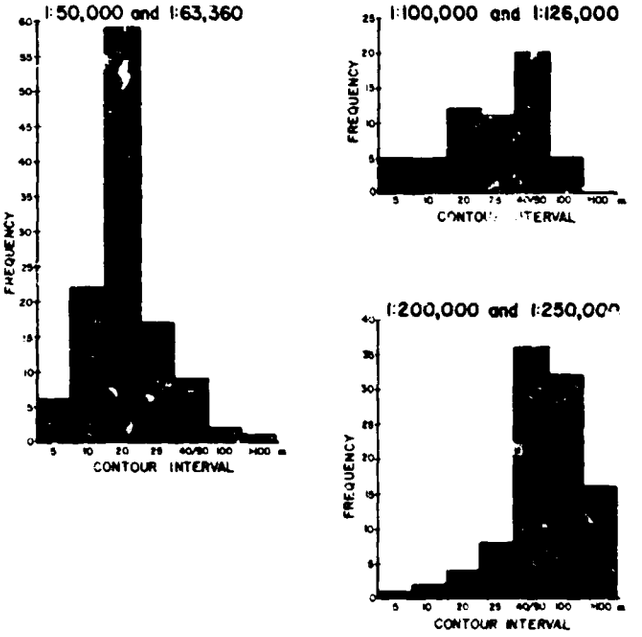

Figure 3b. Histograms of contour intervals for topographic maps at scales of 1:50,000, 1:100,000, and 1:250,000 (United Nations, 1976).

SENSOR ATTITUDE - ± 10 m IN X, Y
(e.g. ± 5 sec) ± 20 m in Z

MEASUREMENT ERROR - ±1/2 PIXEL (e.g. + 8 m) in X, Y, Z

MISCELLANEOUS ERRORS - ± 10 m IN X, Y, Z
(DUE TO GROUND CONTROL, PROCESSING, REFORMATTING, RESAMPLING, ADJUSTMENT PROCEDURES ETC.

$$RSME_{X, Y} = \sqrt{10^2 + 8^2 + 10^2}$$

$$\approx \pm 15 - 20 \text{ m}$$

$$RSME_Z = \sqrt{20^2 + 8^2 + 10^2}$$

$$\approx \pm 25 \text{ m}$$

MAPPING CONSIDERATIONS

$$\text{MAP SCALE FACTOR}_{X, Y} = \frac{20 \times 1.65}{0.5}$$

$$= \frac{33\ (000)}{0.5}$$

$$= 66{,}000 \approx \underline{100{,}000}$$

$$\text{C.I.}_{\text{NMAS}} = 3.3 \times 25$$

$$= 83 \approx \underline{100 \text{ m}}$$

FIGURE 4. COMBINATION OF ERRORS (Based on H = 800 km, IFOV = 15 m)

Bibliography:

American Society of Photogrammetry, 1980, Manual of Photogrammetry, Fourth Edition, Falls Church, VA.

Baudoin, A. and Kirsner, D., 1979, "Terrain Modeling and Geometric Corrections Using the SPOT Satellite," Proceedings of the Thirteenth International Symposium on Remote Sensing of Environment, Environmental Research Institute of Michigan, Ann Arbor, pp. 537-556.

Chapman, W. H., 1974, "Gridding ERTS Images," Proceedings, ACSM Fall Convention 1974, pp. 15-19.

Colvocoresses, A. P., 1975, "Evaluation of the Cartographic Applications of ERTS-1 Imagery," The American Cartographer, Vol. 2, No. 1, pp. 5-18.

Defense Mapping Agency, 1972, Production Specifications for Joint Operations Graphics + Series 1501 and Series 1501 Air, Scale 1:250,000, DMA, Washington, D.C.

Derenyi, E. E., 1981, "Skylab in Retrospect," Photogrammetric Engineering and Remote Sensing, Vol. 47, No. 4, pp. 495-499.

Doyle, F. J., 1973, "Can Satellite Photography Contribute to Topographic Mapping?" USGS Journal of Research, Vol. 1, No. 3.

Doyle, F. J., 1979, "A Large Format Camera for Shuttle," Photogrammetric Engineering and Remote Sensing, Vol. 45, No. 1, pp. 73-78.

Ducher, G., 1980, "Cartographic Possibilities of the SPOT and Spacelab Projects," Photogrammetric Record, Vol. 10, No. 56, pp. 167-180.

Fitzpatrick-Lins, K., 1978, "Accuracy of Selected Land Use and Land Cover Maps in the Greater Atlanta Region, Georgia," USGS Journal of Research, Vol. 6, No. 2, pp. 169-173.

Gustafson, G. C. and Loon, J. C., "Updating the National Map Accuracy Standards," Proceedings, American Congress on Surveying and Mapping, 41st Annual Meeting, Washington, D.C., February 22-27, 1981, pp. 466-482.

Helava, U. V. and W. E. Chapelle, 1972, "Epipolar-Scan Correlation," Bendix Technical Journal, Vol. 5, No. 1, pp. 19-23.

Itek Corporation, 1981, "Conceptual Design of an Automated Mapping Satellite System (MAPSAT)." Final Report Excerpt System Overview, Contract No. 14-08-0001-18656, February 3, 1981.

Jet Propulsion Laboratory, 1979, Preliminary Stereosat Mission Description, NASA/JPL Report 720-33, May 30, 1979 (JPL internal document).

Konecny, G. and Pape, D., 1981, "Correlation Techniques and Devices," Photogrammetric Engineering and Remote Sensing, Vol. 47, No. 3, March 1981, pp. 323-333.

McEwen, R. B. and Asbeck, T. A., 1975, "Analytical Triangulation with ERTS," Proceedings, American Society of Photogrammetry, pp. 490-503.

Panton, D. J., 1978, "A Flexible Approach to Digital Stereo Mapping," Photogrammetric Engineering and Remote Sensing, Vol. 44, No. 12, pp. 1499-1512.

Petrie, G., 1970, "Some Considerations Regarding Mapping from Satellites," Photogrammetric Record, Vol. 6, No. 36, pp. 590-624.

Tham, P., 1968, "Aerial Map Accuracy in Photogrammetry," Sartryck ur Svensk Lantmateritidskrift, No. 2, pp. 161-172.

Thompson, M. J., 1979, Maps for America, U.S. Government Printing Office, Washington, D.C. 20402.

United Nations, 1970a, "Inventory of World Topographic Mapping," World Cartography, Vol. X, pp. 27-96.

_____, 1970b, "The Status of World Topographic Mapping," World Cartography, Vol. X, pp. 1-23.

_____, 1976, "The Status of World Topographic Mapping," World Cartography, Vol. XIV, pp. 3-70.

U.S. Bureau of the Budget, 1947, United States National Map Accuracy Standards, revised June 17, 1947, 2 pp.

Welch, R. and Lo, C. P., 1977, "Height Measurements from Satellite Images," Photogrammetric Engineering and Remote Sensing, Vol. 43, No. 10, pp. 1233-1241.

Welch, R., 1980, "Measurements from Linear Array Camera Images," Photogrammetric Engineering and Remote Sensing, Vol. 46, No. 3, pp. 315-318.

Welch, R. and Marko, W., 1981, "Cartographic Potential of a Spacecraft Line Array Camera System," Photogrammetric Engineering and Remote Sensing, Vol. 47, No. 8, pp. 1173-1185.

Welch, R., 1981, "Spatial Resolution and Geometric Potential of Planned Earth Satellite Missions," Proceedings, Fifteenth International Symposium on Remote Sensing of Environment, ERIM, Ann Arbor, MI, pp. 1275-1283.

6.4 MAP PROJECTIONS FOR LARGER-SCALE MAPPING*

John P. Snyder
U.S. Geological Survey
National Center, Stop 522
Reston, Virginia 22092

ABSTRACT

After decades of using a single map projection, the Polyconic, for its mapping program, the U.S. Geological Survey now uses several long-established projections for its published maps, both large and small scale. For maps at 1:1,000,000-scale and larger, the most common projections are conformal, such as the Transverse Mercator and Lambert Conformal Conic. Projections for these scales should treat the Earth as an ellipsoid. In addition, the USGS has conceived and designed some new projections, including the Space Oblique Mercator, the first map projection designed to permit low-distortion mapping of the Earth from satellite imagery, continuously following the groundtrack. The USGS has programmed nearly all pertinent projection equations for inverse and forward calculations. These are used to plot maps or to transform coordinates from one projection to another. The USGS is also publishing its first comprehensive map projection manual, describing in detail and mathematically all projections used by the agency.

INTRODUCTION

The U.S. Geological Survey was created in 1879, and detailed large-scale mapping of the country soon became one of its primary objectives. It has relied heavily over the years on the former U.S. Coast and Geodetic Survey (USC&GS, now the National Ocean Survey) for guidance on map projections. Until the late 1950's, only the Polyconic projection was used for the primary USGS mapping product, i.e., large-scale quadrangle maps.

The Polyconic projection was apparently invented and certainly promoted by Ferdinand Rudolph Hassler, the first head of what was to become known as the Coast and Geodetic Survey. In the 1950's, the USGS quadrangle projection was changed to the Lambert Conformal Conic and the Transverse Mercator projections, which had been adopted by the Coast and Geodetic Survey in the 1930's for the State Plane Coordinate System. The development of standardized zones based upon the Universal Transverse Mercator and the polar Stereographic led to USGS use of these projections. In addition to these, the regular Mercator, the Oblique Mercator, the Albers Equal-Area Conic, and the Azimuthal Equidistant have been used for other larger-scale mapping by the USGS and other agencies. Although authors and organizations variously define large-

*Note: This paper is adapted with several modifications from one by the author published in the Proceedings of the 1981 ACSM Fall Technical Meeting.

and intermediate-scale mapping, for the purposes of this paper, the term "larger scale" will apply to scales larger than 1 to 2 million.

When the space age added its impact to mapping, classical projections (Mercator, Lambert Conformal Conic, and Stereographic) were chosen for the mapping of the Earth's Moon, three other planets, and a number of other natural satellites. Some projections, especially the Space Oblique Mercator, originated within USGS to assist mapping from satellite imagery.

TYPES OF PROJECTION

Before describing the projections themselves, I'd like to review briefly the different types. Equal-area or equivalent projections of the globe are used especially by geographers seeking to compare land use, densities, and the like. On an equal-area projection, such as the Albers Equal-Area Conic, a coin laid on one part of the map covers exactly the same area of the actual Earth as the same coin on any other part of the map. Shapes, angles, and scale must be distorted on most parts of such a map, but there are usually certain lines on an equal-area map as well as on other types of projections, along which there is no distortion of any kind. These so-called "standard lines" may be a meridian, one or two parallels, lines which are neither, or not a line but a point.

More commonly used in larger-scale mapping are conformal (orthomorphic) projections such as the Transverse Mercator and the Lambert Conformal Conic. The term means that they are correct in shape, but, unlike the term "equal area," the conformal principle applies only to each infinitesimal element of the map. Angles at each point are correct, and consequently the local scale in every direction around any one point is constant, so the map user can measure distance and direction between near points with a minimum of difficulty. Conformal maps may also be prepared by fitting together small pieces of other conformal maps which have been enlarged or reduced; non-conformal projections require reshaping as well. When the region consists of more than a small element, distortion in shape as well as area becomes appreciable. This is especially serious with the most famous conformal projection -- the Mercator -- because of its widespread use in classrooms, especially in the past. Because there is no angular distortion, all meridians intersect parallels at right angles on a conformal projection, just as they do on the Earth. "Standard lines" may also be applied to a conformal map to eliminate scale and area distortion along these lines and to minimize distortion elsewhere.

Some map projections, such as the Azimuthal Equidistant, are neither equal-area nor conformal, but linear scale is correct along all lines radiating from the center, along meridians, or following other special patterns. In addition, there are compromise projections, almost entirely restricted to small-scale mapping, which are used because they balance distortion in scale, area, and shape.

Projections are often classified by the type of surface onto which the Earth may be mapped. If a cylinder or cone that has been placed around a globe is unrolled, we have the concept of cylindrical or conic projections, such as the Mercator or Lambert Conformal Conic, respectively. If the axis of the cone or cylinder coincides with the polar axis of the globe, the projection has equally spaced straight meridians, parallel on the cylindrical projections and converging on the conics. The parallels intersect the meridians at right angles, being straight on the cylindricals and concentric circular arcs on the conics. The spacing of the parallels is seldom projective. A plane laid tangent to the globe at the pole leads to polar azimuthal projections, such as the polar Stereographic, with the parallels mapped as arcs of concentric circles and meridians as equally spaced radii of the circles. Scale remains constant along each parallel of latitude on a regular cylindrical, conic, or polar azimuthal projection, but it changes from one latitude to another. Directions of all points are correct as seen from the center of an azimuthal projection.

If the cylinder or cone is secant instead of tangent to the globe, the projection conceptually has two lines instead of one which are true to scale. Wrapping the cylinder about a meridian leads to transverse projections. By placing a plane tangent to the Equator instead of a pole, equatorial aspects of azimuthal projections result. Tilting the cylinder, cone, or plane to relate to another point on the Earth leads to an oblique projection, and the meridians and parallels are no longer the straight lines or circular arcs they were in the normal aspect. The lines of constant scale are correspondingly rotated.

THE EARTH AS AN ELLIPSOID

For maps at scales smaller than 1:5,000,000, and which cover regions larger than the United States, the distortions from mapping the spherical Earth on flat paper are much greater than the slight additional corrections needed to compensate for the ellipsoidal shape of the Earth. These corrections may then usually be ignored. The ellipsoid should be, and normally is, used for large-scale mapping of small areas, or for long narrow strips. For such areas, the flattening of the round Earth usually produces less distortion than the use of the sphere instead of the ellipsoid.

A shift from one ellipsoid to another has a negligible effect, even on large-scale maps, upon the projected shapes and positions of meridians and parallels. A greater effect is the translation of latitude and longitude for all points on a map, due to a change in datum, that changes the position of the ellipsoid relative to the Earth. For this reason, the notation in the corner of USGS quadrangles stating "North American Datum 1927" or "1983" is as important as the parameters of the map projection in defining the basis of these maps.

PRINCIPAL PROJECTIONS

Polyconic Projection

About 1820, Hassler began to promote the easily constructed Polyconic

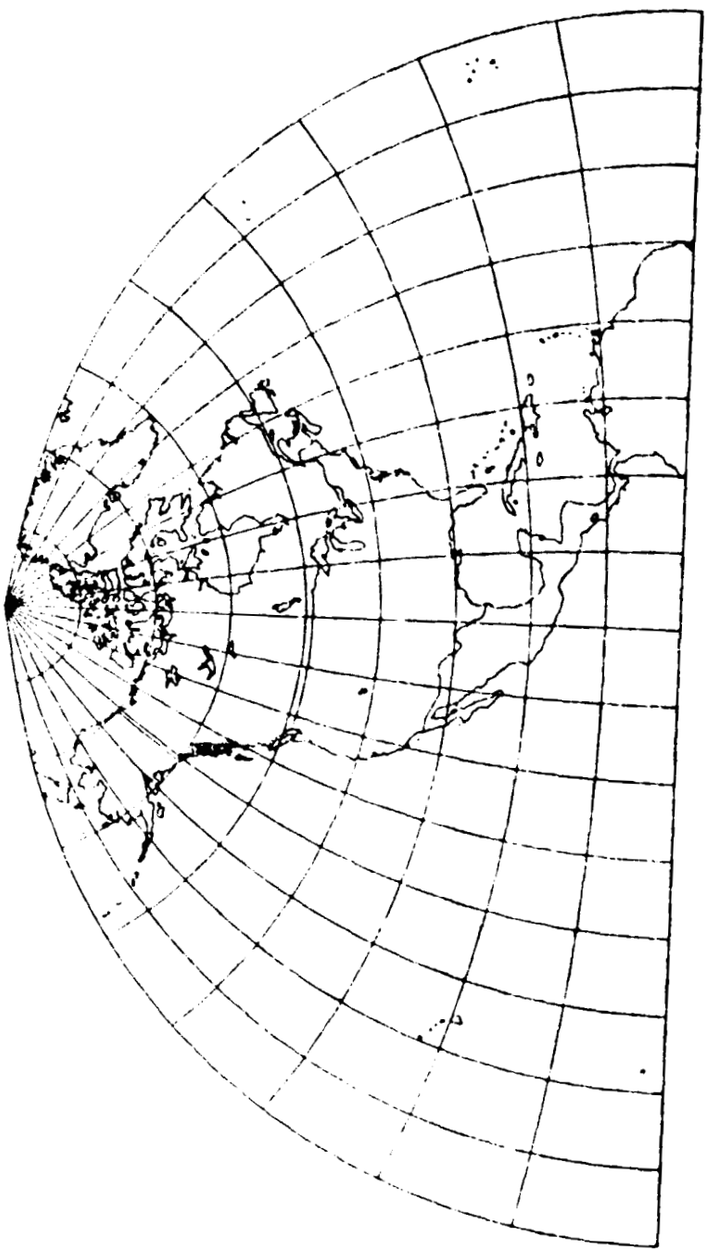

Polyconic Projection

projection as the basis of large-scale mapping. The USGS used this projection for the earliest quadrangles, only changing in the 1950's to other projections, although relabeling the map legend lagged considerably behind the change. The Polyconic is neither equal-area nor conformal. For 7-1/2- and 15-min. quadrangles, however, the distortion is negligible. Along the central meridian, it is free of distortion. Each parallel is also true to scale, but the other meridians are too long, and constantly change scale. The projection is not recommended for maps of considerable east-west extent and, in fact, should not be seriously used for any new maps in view of other projections available.

The parallels of latitude are circular arcs spaced at their true distances along the central meridian, but with radii equal to the length of the element of a cone tangent at the particular parallel. The projection receives its name from the fact that each cone is different. Meridians are marked on each parallel at the true distances, but the meridians are complex curves connecting these points. Lines of constant scale run roughly parallel to the central meridian, but they are curved.

Mercator Projection

The Mercator projection is the most well known of all. It was presented by Mercator for navigational purposes in 1569, because rhumb lines, or lines of constant compass bearings, are plotted as straight lines. This is still the most justifiable use of the projection for a map of regions away from the Equator. It is a normal cylindrical projection, on which the lines of constant scale are straight and run parallel to the Equator. On the Mercator, the scale increases away from the Equator.

The USGS has used the Mercator projection for maps of part of the Pacific Ocean, of Indonesia, and for portions of each of the outer bodies mapped to date, from our Moon to the satellites of Saturn. In some cases, the chosen scale applies to standard parallels placed symmetrically north and south of the Equator. The shape of the map does not change. The scale along the Equator could still be called correct if the stated scale of the map were slightly decreased.

Transverse Mercator Projection

Rotating the cylinder of the Mercator so that it lies tangent (or secant) along a meridian of the globe leads to the very important conformal projection called the Transverse Mercator. The central meridian, the Equator, and each meridian 90° from the central meridian are straight lines. All other meridians and parallels are complex curves. For the sphere and normally for the ellipsoid, the central meridian has a constant scale, but this is usually reduced from the nominal map scale to balance errors in measurement over the rest of the map. The lines of constant scale are straight lines parallel to the central meridian for the sphere, and nearly straight for the ellipsoid. When the scale factor along the central meridian is reduced, the lines of true scale are symmetrical with respect to the central meridian.

ORIGINAL PAGE IS
OF POOR QUALITY

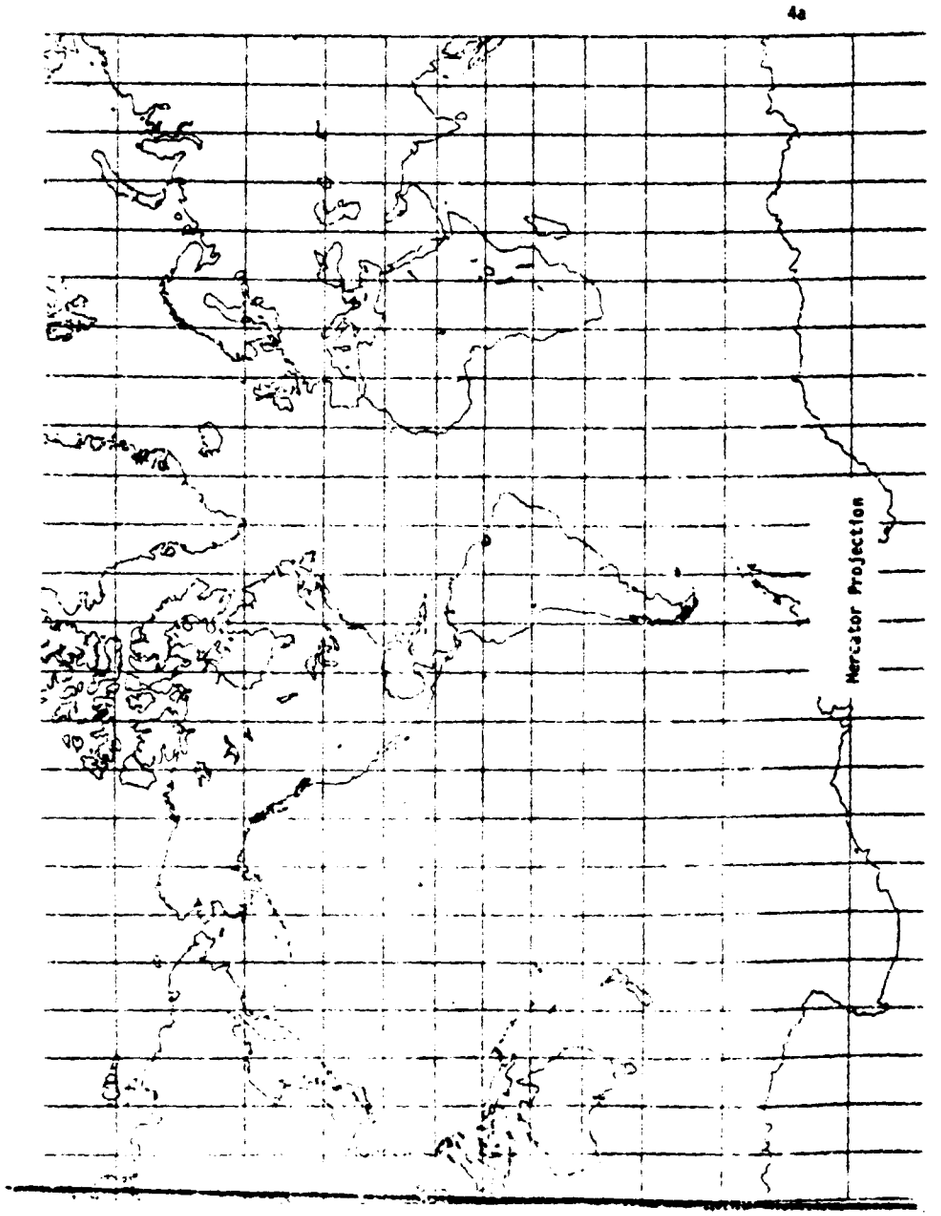

Lambert presented the spherical projection in 1772, but Gauss and later Krüger developed the mathematics for the ellipsoidal form. The projection was almost ignored until the 20th century, when it was adopted for much of the topographic mapping in Europe under the name Gauss-Krüger, and in the United States for the State Plane Coordinate System of States predominantly north and south in extent and for the Universal Transverse Mercator or UTM projection and grid system. The UTM has two special restrictions: (1) The central scale factor is 0.9996, and (2) the Earth is divided into sixty zones, each 6° of longitude wide, with the central meridians placed at every sixth meridian beginning with the 177th West. (There are minor exceptions.)

When USGS stopped using the Polyconic projection for large-scale quadrangle maps, the Transverse Mercator was adopted for maps of areas where it was used for the State Plane Coordinate System. (Recent metric quadrangles are based upon the UTM). In the State Plane Coordinate System, each zone follows county boundaries and is designed to restrict scale variation over the map to one part in ten thousand. The USGS uses the predominant zone for the projection of quadrangles which cross county boundaries. The central scale reductions, which change between zones, vary from 1:160,000 to 1:10,000. Central meridians have been individually selected for each zone.

Equations in series form are used for the Transverse Mercator calculations for the ellipsoid. These are limited to a 6° to 8° band of longitude and cannot be safely extrapolated for use over a whole continent. Simpler closed formulas can then be used if the Earth is assumed to be a sphere. To extend the ellipsoidal form a greater distance from the central meridian, much more complicated formulas are available.

When USGS converted from the Polyconic projection, with a central meridian on each quadrangle, to the State Plane Coordinate System, this included employing the central meridian and other parameters used for the new zone. The discrepancies in measurements on the Polyconic and the Transverse Mercator forms of the same 7-1/2- or 15 min. quadrangle depend especially upon the distance of the quadrangle from the central meridian of the zone. The new quadrangles can be mosaicked for the entire zone.

The 1:250,000-scale 1 x 2 quadrangle series covering 49 of the States was originally to be cast on the UTM. When the Army Map Service prepared these, the UTM central scale factor of 0.9996 was used, but the central meridian of the quadrangle itself was used in place of that of the UTM zone. These central meridians agree with those of the UTM zones for only one-third of the quadrangles. East-west mosaicking within a UTM zone thus cannot be achieved with the existing maps, which are now being updated and distributed by USGS. As these areas are remapped, they are being recast with the UTM central meridians.

Oblique Mercator Projection

A cylinder may be placed around the sphere so that it is tangent along a great circle which is neither a meridian nor the Equator. In this case, the Oblique Mercator may be conceptually projected for conformal mapping of a region chiefly

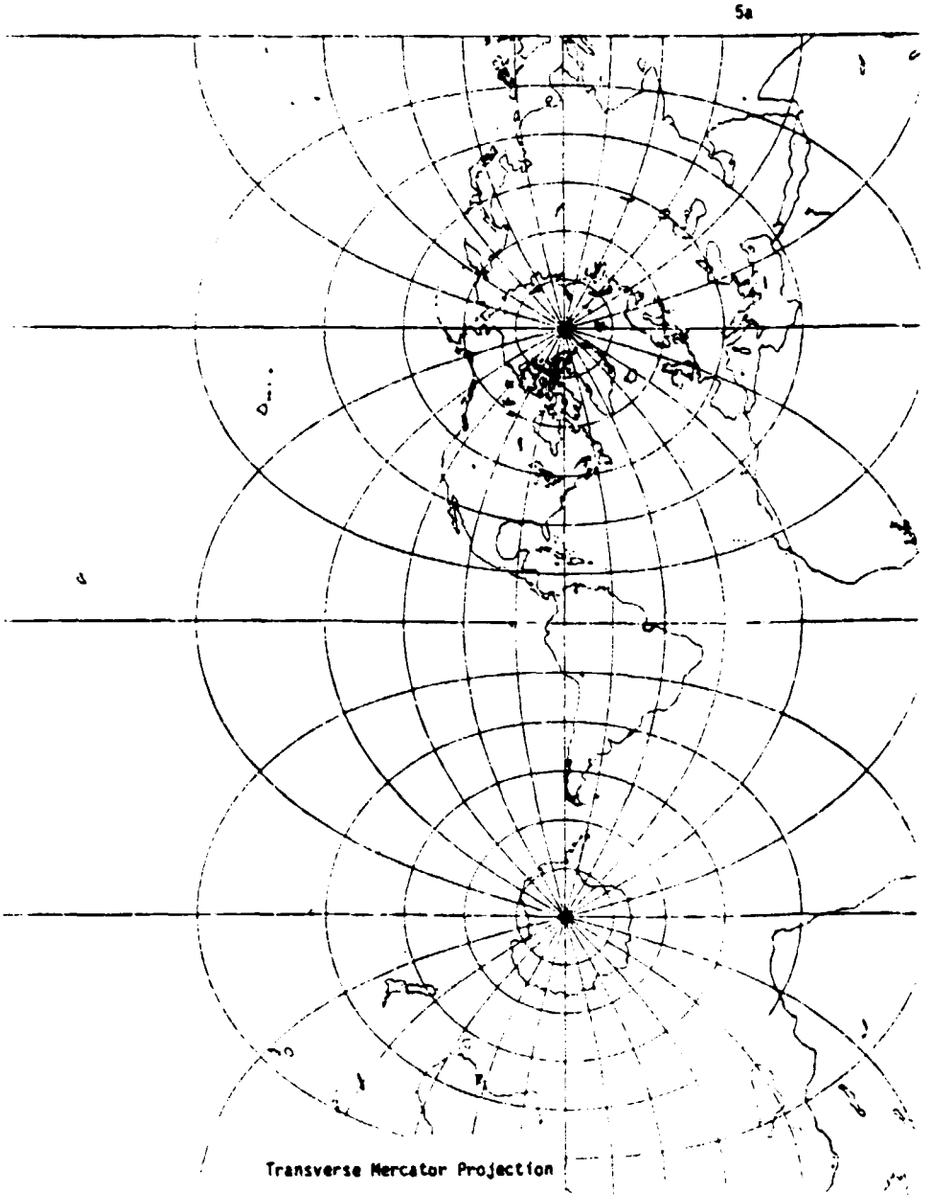

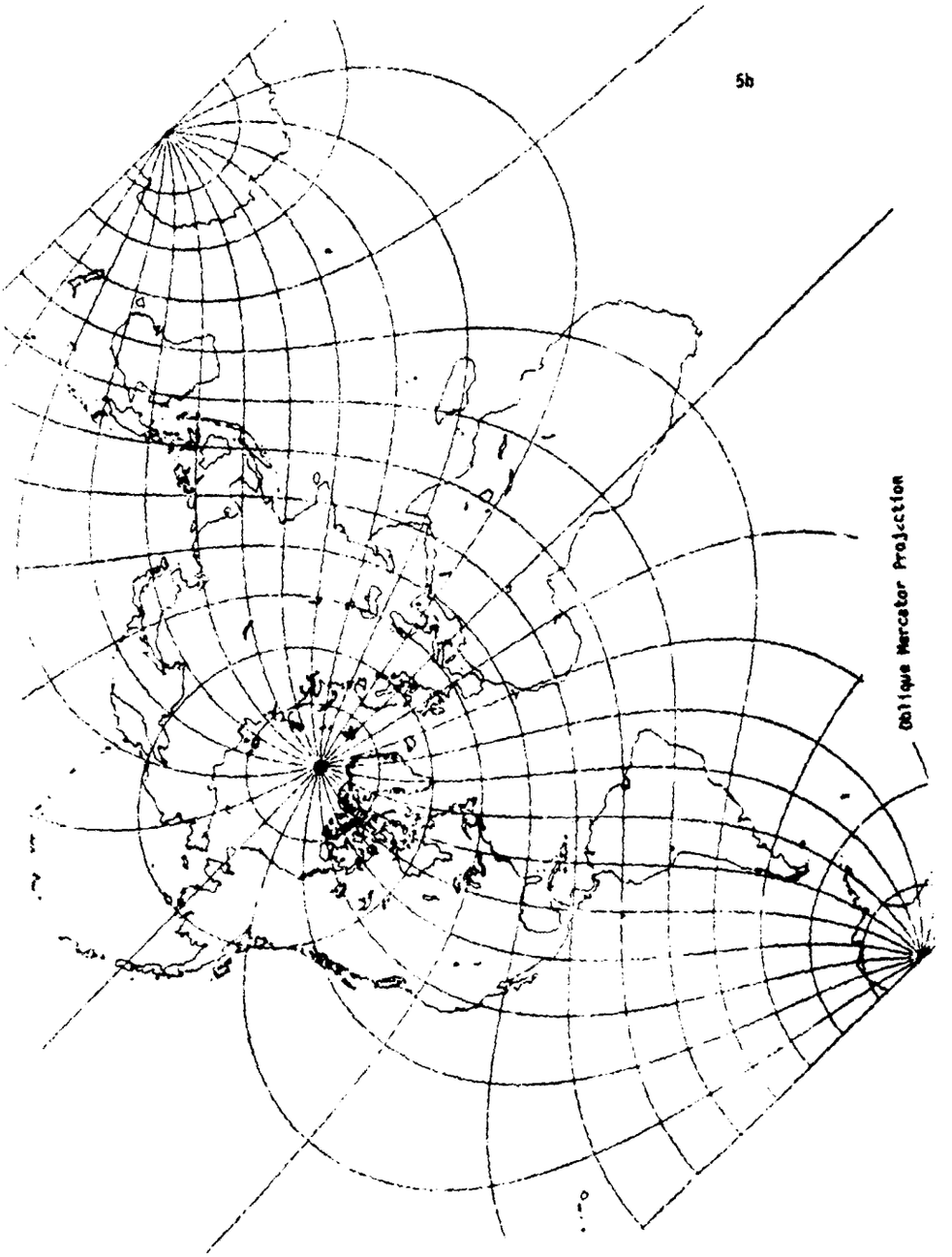

extending along this great circle. Nearly all meridians and parallels are complex curves. Here the lines of constant scale run parallel to the oblique great circle path, which may have a reduced scale. Its topographic use by USGS is confined to the State Plane Coordinate System of the southeast extension of Alaska and to the mapping of Landsat data from 1978 to the present, prior to implementation of the Space Oblique Mercator projection on Landsat D. There are several ways of adapting the Oblique Mercator to the ellipsoid, although none is ideal because either the central line does not remain at a precisely constant scale or conformality is not precise. Hotine's adaptation, which is exactly conformal, is used in these USGS applications.

Space Oblique Mercator Projection

Among the more complicated projections is the Space Oblique Mercator, conceived by A.P. Colvocoresses of USGS in 1973 and mathematically implemented in 1978. It is intended specifically for the continuous mapping of imaging from satellites such as Landsat for which a rudimentary form was used 1975-1978. The more accurate form is to be used for Landsat D. The groundtrack for the satellite is held true to scale, and mapping is made basically conformal. Because of the relative motion of Earth and satellite, the groundtrack is curved, and appears almost sinusoidal on the map. Formulas have been published in summarized form, and very recently with detailed derivations as USGS Bulletin 1518. It is designed for use with the ellipsoidal Earth, and with circular or elliptical satellite orbits.

Cassini Projection

A non-conformal transverse cylindrical projection called the Cassini was used for British topographic mapping until about 1920, when it began to be replaced with the Transverse Mercator. On the Cassini, scale is true along the central meridian and along lines on the map perpendicular to the central meridian. In a direction parallel to this meridian, scale is constant, but it is increasingly too large as the distance from the meridian increases. Thus shape, angles, and area are distorted. It may also be cast obliquely. The projection was used for Landsat from 1972 to 1975, but is hardly used at present.

Lambert Conformal Conic Projection

Nearly all the States predominantly east and west in extent use the Lambert Conformal Conic as the projection for the State Plane Coordinate System. It was therefore adopted by USGS for post-1950 quadrangle mapping of these areas. This projection, presented by Lambert in 1772, maps parallels as concentric circular arcs and the meridians as equally spaced radii of those circles. One pole is at the center of the circles, while the other pole is at infinity. The parallels are more closely spaced between the normally two standard parallels, which have no distortion.

For the USGS map of the conterminous United States, the standard parallels are 33° and 45° N., and USGS has made base maps of each of the 48 States using these standard parallels at a scale of 1:500,000. The base maps therefore

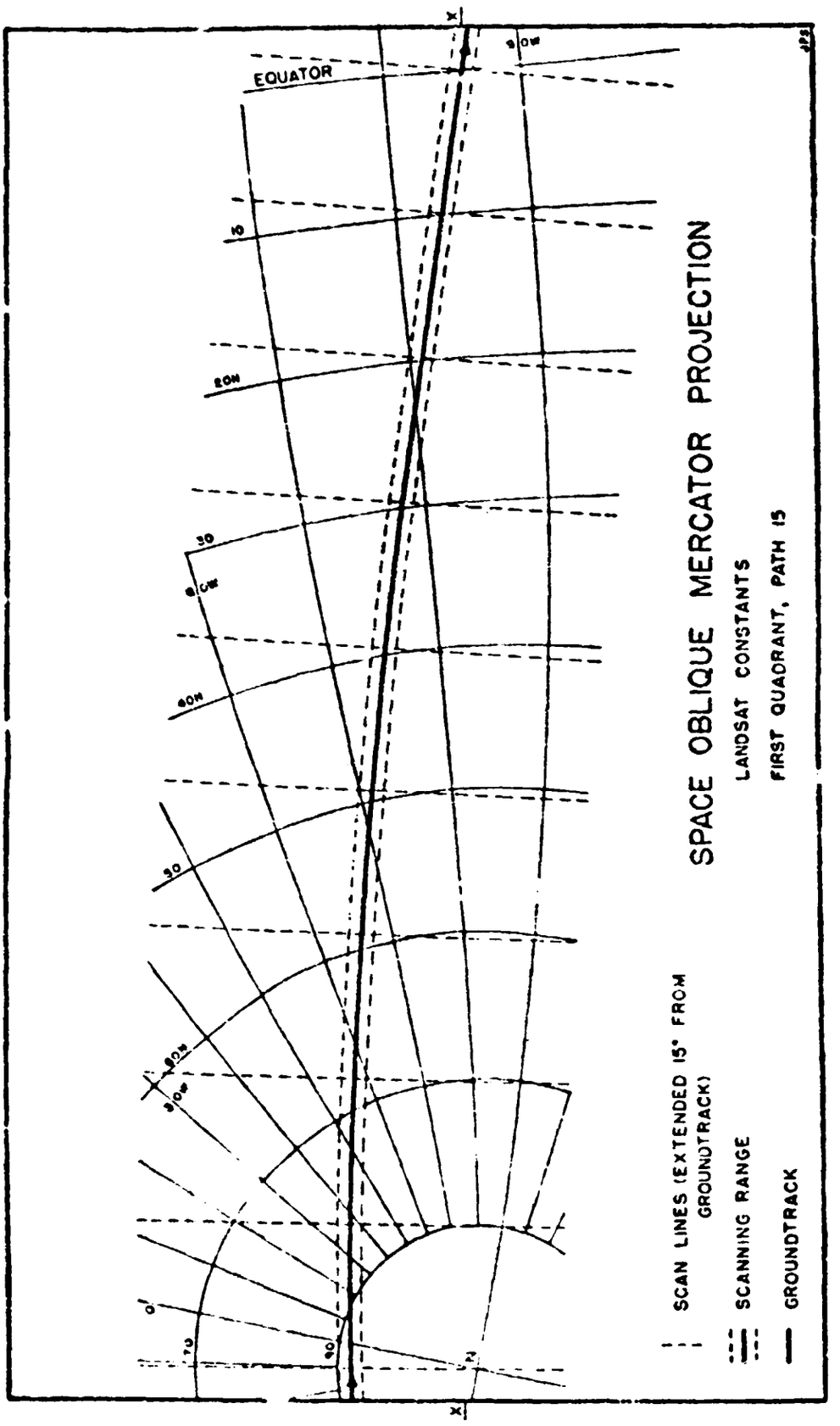

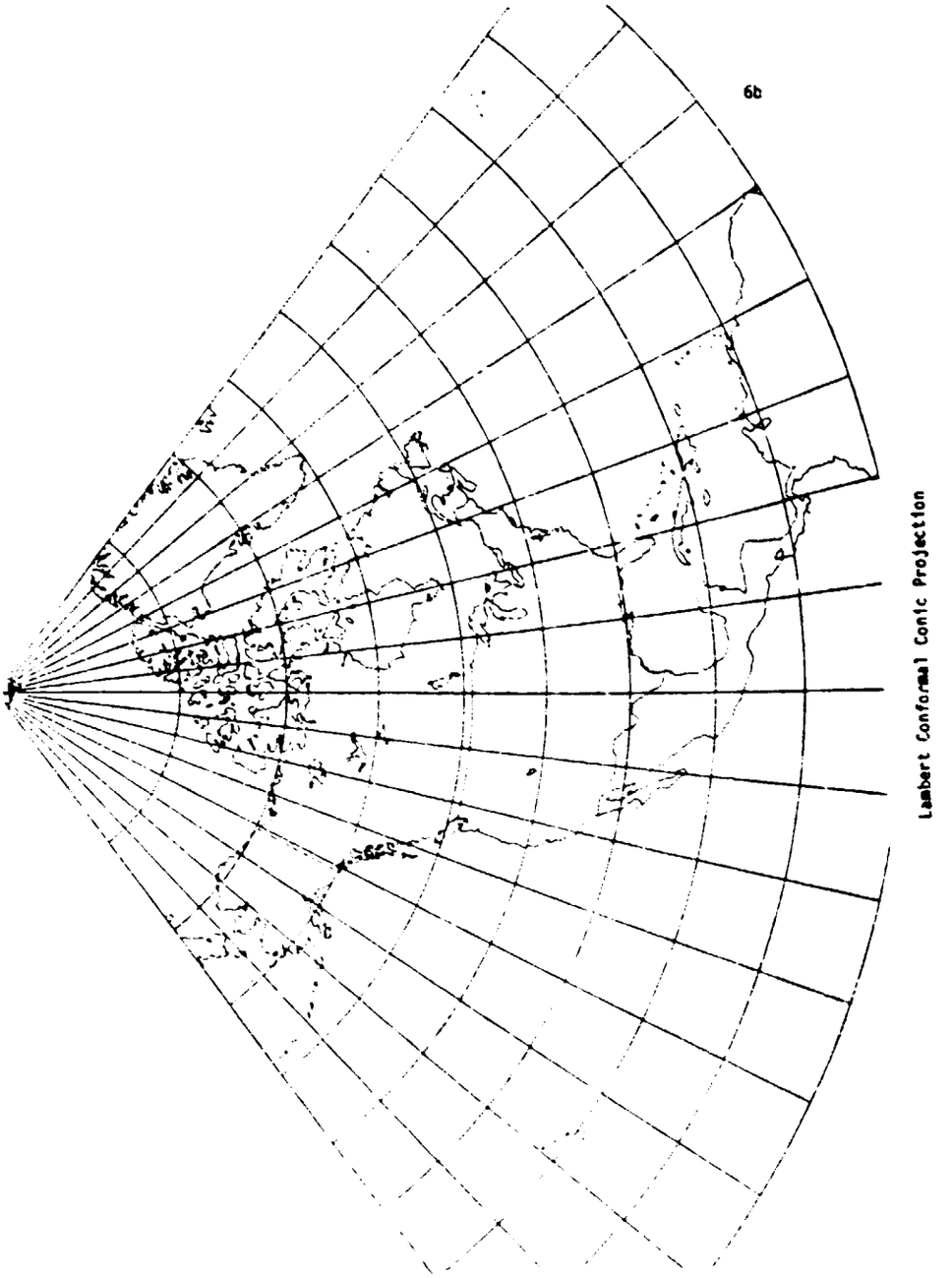

match along the boundaries. Each zone of the State Plane Coordinate System has its own standard parallels. These are the parameters used for USGS quadrangles which have been produced on this projection; thus, quadrangles edge-match within the zone.

The Lambert is also used for the map sheets of the International Map of the World series at a scale of 1:1,000,000. The projection for these sheets was changed from a Modified Polyconic in 1962.

Albers Equal-Area Conic Projection

The Albers Equal-Area Conic is probably seen more than the Lambert Conformal Conic as the projection for maps of the United States and its larger regions. In 1805, Albers showed that by proper spacing of the parallels on a conic projection, there is no area distortion, and along one or two standard parallels there is no scale or angular distortion. The projection was nearly dormant until Oscar S. Adams of USC&GS began encouraging its use for equal-area maps of the United States in the early part of the 20th century.

Adams's tables of coordinates for the 48 States are based upon standard parallels of 29-1/2° and 45-1/2° N. It should be noted that the United States on the Albers projection cannot be distinguished from a Lambert Conformal Conic version if the projection is not identified, except by careful measurements. Like the Lambert, the Albers, which is the equal-area counterpart, has concentric arcs of circles for parallels, and equally spaced radii as meridians. The parallels are not equally spaced, but they are farthest apart in the latitudes between the standard parallels and closer together to the north and south. The pole is not at the center of the circles, but is normally an arc itself.

Scale along any given parallel is constant, as on the Lambert, with scale too small between the standard parallels, and too large beyond them. The scale along the meridians is just the opposite, to maintain equal area. While Adams recommended that standard parallels be placed one-sixth of the displayed length of the central meridian from the northern and southern limits of the map, this is empirical. The standard parallels may be selected in other ways.

Since meridians intersect parallels on the Albers at right angles, it may at first be thought that there is no angular distortion. It exists, however, for any angle other than that between the meridian and parallel, except at the standard parallels.

Stereographic Projection

For larger-scale maps of polar regions, the Stereographic projection is commonly used. This is a perspective projection of the sphere onto a tangent or secant plane. The point of perspective lies on the opposite side of the globe. For the sphere, the Stereographic is both perspective and conformal. For the ellipsoid, it may be one or the other, but not quite both; in practice, it is used conformally in every case. All great and small

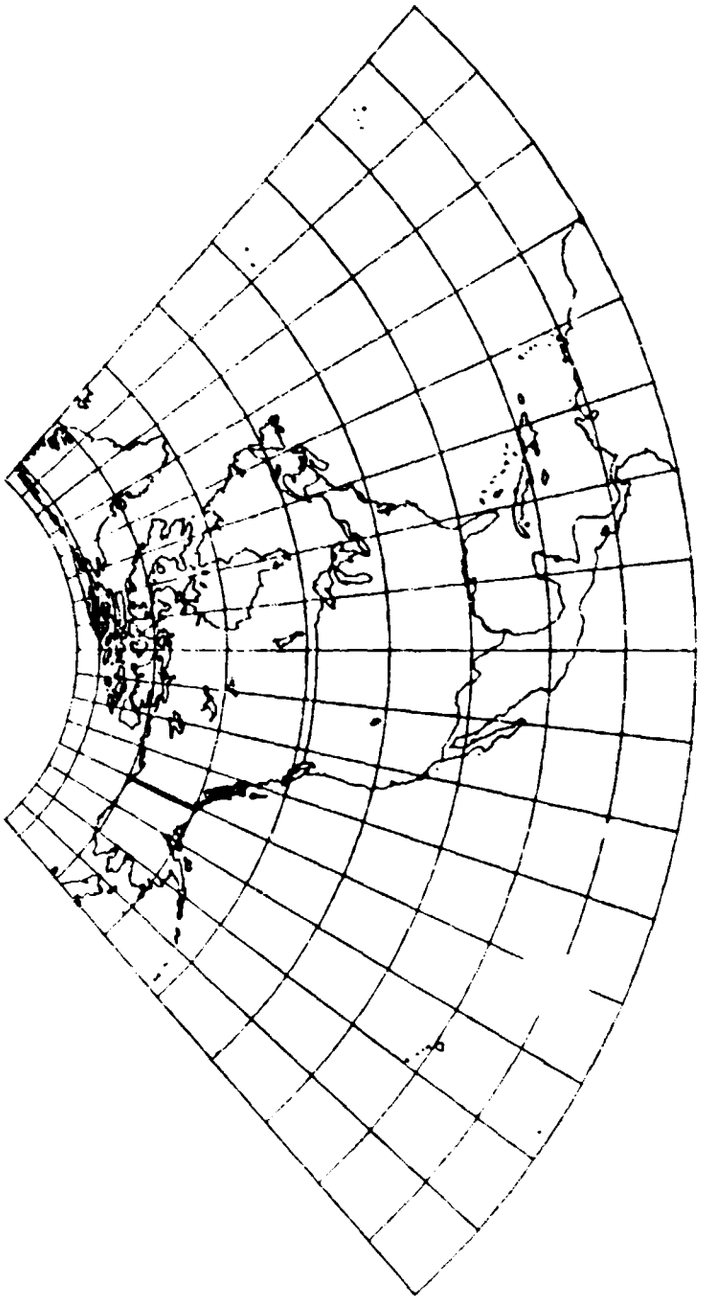

Albers Equal-Area Conic Projection

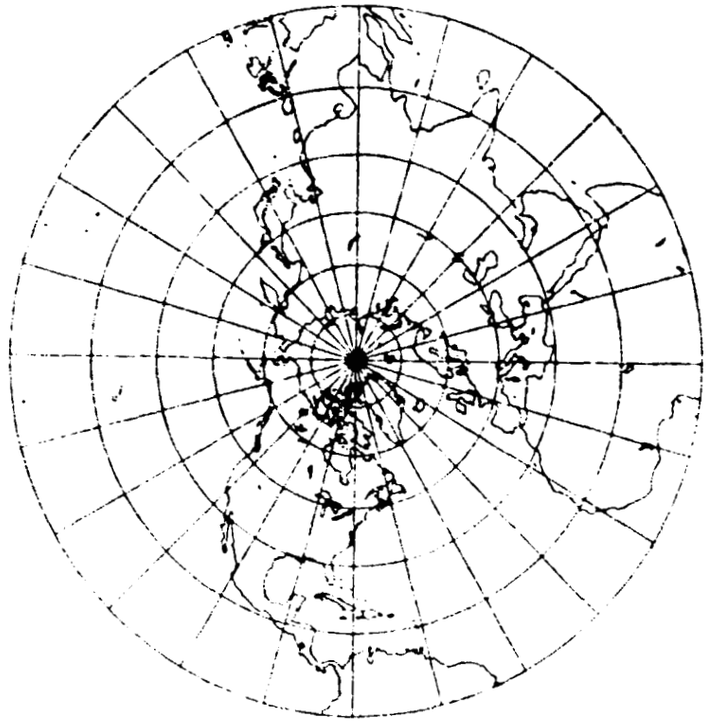

Polar Stereographic Projection

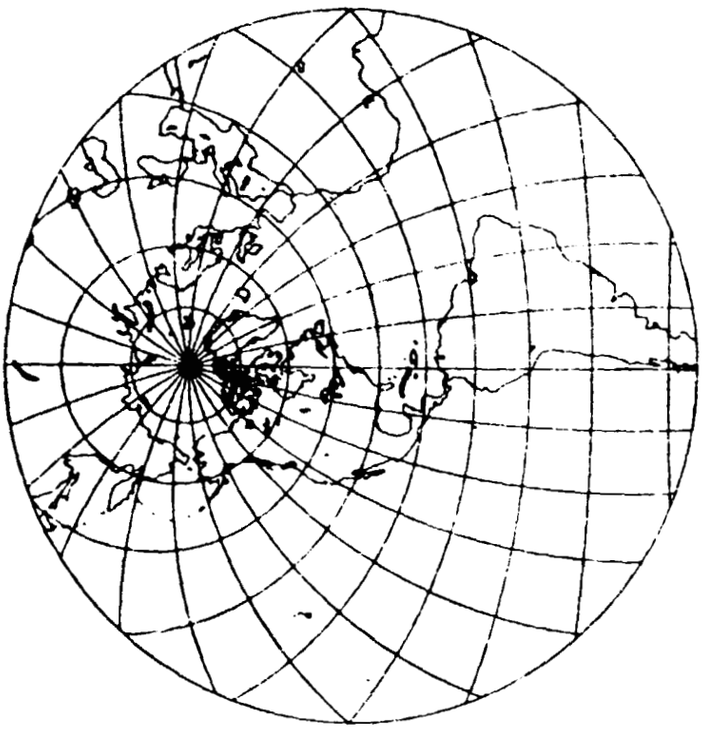

Oblique Stereographic Projection

circles on the sphere are shown as circles or straight lines on the map. This includes all meridians and parallels.

The Stereographic is also azimuthal, and lines of constant scale are circles centered on the projection center. In the polar aspect, a parallel other than the pole is therefore often made true to scale to balance scale variation. The USGS has used the projection for maps of the entire Antarctic continent as well as for 1:250,000-scale quadrangles of portions. It is also used for polar portions of the International Map of the World, and for portions of extraterrestrial bodies centered at the poles or at basins elsewhere on the bodies.

Azimuthal Equidistant Projection

Familiar to many air-age atlas users is an azimuthal projection which shows both distances and directions correctly from the chosen center of the map, whether the North Pole or a major city. Scale in other directions varies, and is too great except at the center; therefore shape and area are distorted. In addition to several spherical applications, the Azimuthal Equidistant projection has been used in the ellipsoidal form for the Plane Coordinate System of Micronesia, for which each major island provides a center for one of the zones.

Because of the increasing digitization of data from and onto many different maps, most of these as well as several other map projections have been programmed by USGS in both forward and inverse form, to transform geodetic coordinates into rectangular coordinates, and vice versa. A bulletin describing in detail all projections which have been used by USGS, including numerical examples of formulas, is soon to be published. We hope that such analyses of both the past usage and capabilities of map projections will serve the public at large as well as our own mapping development.

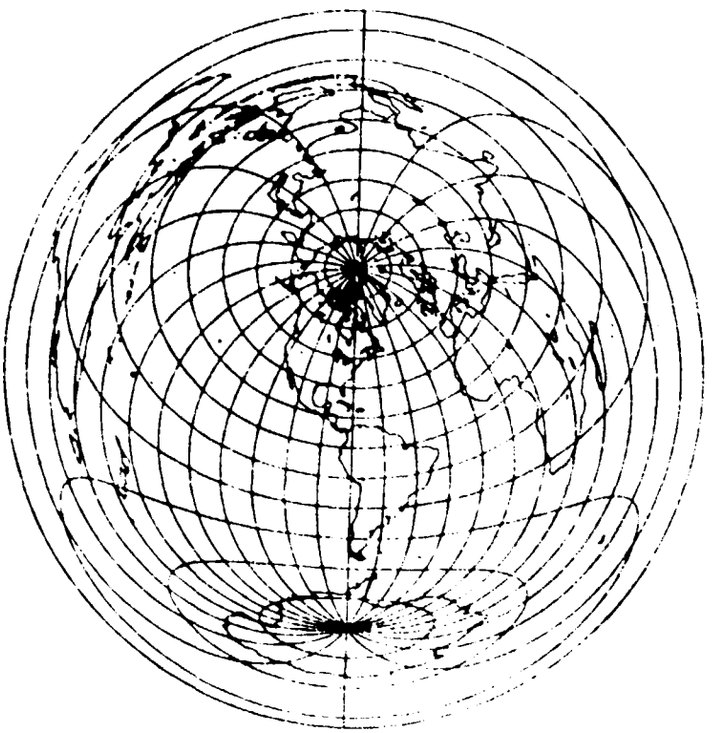

Oblique Azimuthal Equidistant Projection

7.0 PRESENTATIONS ON PROCESSING AND VERIFICATION

7.1 SUMMARY

For each working group, position papers were given to survey the state of the art in applications techniques and anticipated requirements and focus the workshop discussion. Three papers discussed ways to improve procedures for identifying and matching ground control points (image sharpness, feature extraction, inter-image matching). Three papers reviewed the procedures and essential elements in rectifying images for registration and map reprojection (photogrammetric and computational aspects of remapping and resampling). Two papers used case studies to illustrate the complex, multiple-component character of error characterization/error budget analysis and verification procedures used for spaceborne imaging sensor systems.

7.2 A DISCUSSION OF IMAGE SHARPNESS*

Paul Anuta, Purdue University

There has been a great deal of work done on image sharpening, image filtering and related areas. It is a very large field of activity with hundreds of references which you could site in this area. The image sharpness problem can be perceived in terms of the block diagram in Figure 1. Basically a scene is viewed by a sensor, and the sensor has some sort of function which is a non-point observing function. It's a function that gathers energy from some region around a point in the scene. That energy is integrated and is contributed to each point or each sample that is taken of the scene. The samples become the pixels, and the pixels are assembled together into the digital image. Each one has some blurr or some of what is called the point's spread function creating the value of information or data that you see in each pixel. Then the sensor and electronic part of the system acts on that signal out of the sensor and perhaps adds more blurring, more loss of resolution to the system. Finally, sampling and quantization of the data produce their effects. You sample the signal at some rate and create the ditigal image from that. The sampling or digitizing process puts the continuous voltage or whatever you have into a number of discrete binary levels, and you have another error introduced there.

After quantization you end up with the digital array of numbers known as the remote sensing image. It should be noted that the point spread function of the atmosphere is something in addition that causes blurring of the image at the point the sensor sees it.

The terminology of the imaging process often creates confusion. Table 1 summarizes the definitions frequently used. The only term or function that I feel comfortable with is the point spread function, the function which describes what an infinitely small source in the scene would look like in the image. The image is spread by the optics and by the other effects in these systems to produce the final image. How that is affected by the system is what we call the point spread function.

The point spread function is a two-dimensional function describing how a point is blurred in the scene. The IFOV we take as a number; a single number telling you what the resolution or size of the point spread function is. That can be any functional derivation of the PSF and we like to use the gaussian point spread function due to the mathematical ease of applying it, and we feel it relatively well expresses the imaging system. Effective field of view and resolution field of view is something to be discussed in the panels later in trying to define what those mean. They describe the imaging aperture associated with the imaging process.

The point spread function is what we use to describe what's going on in the imaging process and that can include the filter-like effects of the sensor, actual optical effects, and perhaps the atmospheric effects also. Right along with that is a function called the modulation transfer function which is the Fourier transform of the point spread function (Figure 2). It is the frequency domain representation of the blur properties of your system. That is

*Edited oral presentation.

what you seek to find for an imaging system. It's what defines the sharpness, what will result in the particular image sharpness that you have, and the problem then is to figure out what to do about that. Is it a satisfactory characteristic for your system? If it isn't, what do you do to compensate for the effects of that? How do you sharpen the image that you have other than building a whole new sensor that has a sharper optical characteristic? Can you mathematically process the imagery to improve the sharpness?

Some other terms are shown in Figure 3; these include the edge spread function, the one-dimensional version of the point spread function which tells you how the response will look going over an edge in one direction in an image. Then there is the term resolution, defined as the number of black and white square bars that can be discerned from a particular unit distance in an image. Accoutance is another term I'm not familiar with but related to the slope of the edge spread function. We have not used that in any of our work.

Defining the point spread function or the sharpness of an image is done after the system is built and in the platform. That is a hard job; you normally do that in the laboratory by special test panels, scenes that you use to evaluate the system. Once it's in orbit, trying to check it out you need to to find optics in the scene that will simulate line or point sources so that you can measure what those blurr function are. You usually assume separable point spread functions so that lines in one direction or another can be used to estimate that function. If it's not symmetric, you have a problem like the computer-aided tomography problem where you're trying to image the solid by using projections and you have to define lines at many different directions and use techniques of tomography to try and estimate the point spread function.

One can look at an image as a one-dimensional sequence of stair-step changes that is convolved with the point spread function in the imaging process as the sensor scans across the scene and produces a smooth or blurred version of the scene (Figure 4). The idea is to try and get back the original image or original signal. The output is the convolution of h, the point spread function and the image called x there. It would appear that a simple division in the frequency domain takes the Fourier transform of these functions. This becomes a simple division to remove the effect of h and you would get x back. But it doesn't work out that easily. There are noise effects, and there's the problem of zero's of the point spread function in the frequency domain causing discontinous points in the solution. And it turns out to be a rather tricky problem to try and do this. And a great deal of literature is in existence on attacking this problem.

There are problems with the inverse in that as 1/h(f) goes to zero, you have singularities, you find ghosts can be created, artifacts in the restored image due to the combination of these problems of taking the inverse, noise effects and quantization. Quantization can amplify the effects of noise and there is more to that problem than initially meets the eye. Therefore, we form a model that describes the way you want to take a look at the problem and set up the mathematical representation of the model, and then define the means of solving for the filter you want which would be here.

Background References or Sharpness

Rosenfeld and Kak, Digital Picture Processing, Academic Press, New York, N.Y., 1976.

W.K. Pratt, Bibliography on Digital Image Processing and Related Topics, U.S.C. Report 453, Sept. 1973. University of Southern California, Los Angeles, Calif.

IEEE Proceedings, Special Issue on Digital Image Picture Processing, Vol. 60, No. 7, July 1972.

T. Huang, W. Schreiber and O. Tretian, "Image Processing," Proceedings of IEEE, Vol. 59, No. 11, Nov. 1972, pp. 1586-1609.

H.C. Andrews, "Digital Image Processing," Proceedings of IEEE. Vol. 63, No. 4, April 1975, pp. 693-708.

N.Y. Chu and C.D. McGillem, "Methods and Performance Bound for Constrained Image Restoration," LARS Technical Report 061678, Purdue University/ LARS, LaFayette, Indiana, 1978.

R.H. Dye, "Restoration of Landsat Images by Discrete 2-D Deconvolution," 10th Michigan Symposium, ERIM, Ann Arbor, Michigan, Oct. 1975.

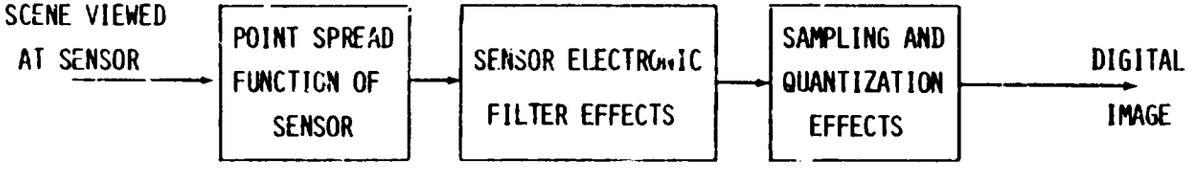

OTHER FACTORS

POINT SPREAD FUNCTION OF ATMOSPHERE

ATMOSPHERIC SCATTERING

Figure 1. Factors Related to Sharpness

TABLE 1.

TERMINOLOGY OF THE IMAGING APERTURE

IFOV -- Instantaneous Field of View

Aperture shade of sensor optics

PSF -- Point Spread Function

Overall transfer function due to all sensor and environmental factors

EFOV -- Effective Field of View

RFOV -- Resolution Field of View

- Point Spread Function -- $h(x,y)$. The function which expresses the output of an imaging system for a point source input.

- Modulation Transfer Function -- $M(u,v)$. The function which expresses the frequency response of the imaging system. It is the magnitude of the Fourier Transform of $h(x,y)$. The transform is called the Transfer Function:

$$H(u,v) = \int_{-\infty}^{\infty}\int_{-\infty}^{\infty} h(x,y)\, e^{-j2\pi(ux + vy)}\, dx\, dy$$

$$= \left|H(u,v)\right| e^{j\Phi(u,v)}$$

$$\text{MTF} \longrightarrow M(u,v) = \left|H(u,v)\right|$$

The phase transfer function is $\Phi(u,v)$

Figure 2. Measures of Image Spatial Quality

- Edge Response -- Expresses response to step inputs. Expressed by Edge Spread Function (ESF).

- Resolution -- Classical definition is minimum width of black and white bars which can be distinguished. Stated in terms of line pair width or line pairs per unit distance. This is qualitative definition.

  Another definition is the half amplitude width of the PSF.

- Acutance -- A measure of edge sharpness in output image. Can be expressed as the average slope of the Edge Spread Function.

$$\frac{1}{H_E(B)-H_E(A)} \int_A^B \left(\frac{D\,H_E}{DY}\right)^2 DY$$

Figure 3. Edge Spread Function: One-Dimensional Version of PSF

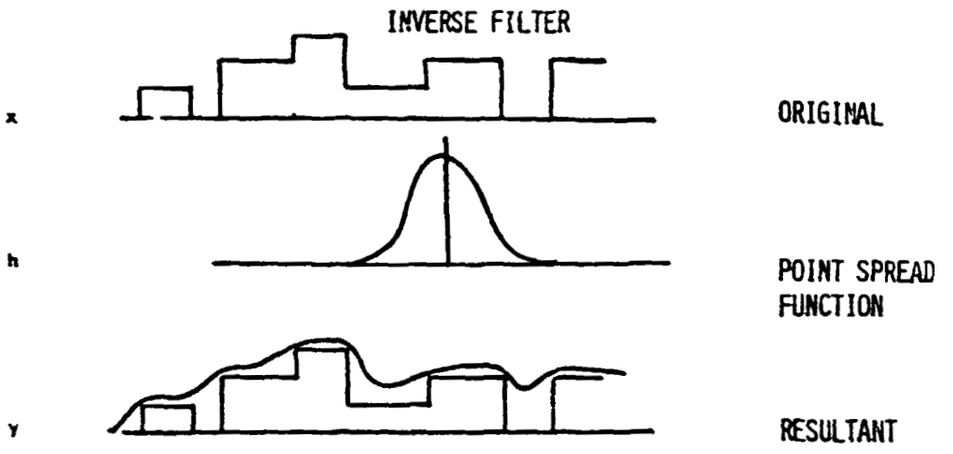

CAN WE RECOVER ORIGINAL?

$$y = h * x$$

$$Y = H \cdot X$$

$$X = \frac{Y}{H}$$

$$x = y * h^{-1}$$

$$h^{-1} = \mathcal{F}^{-1}\left\{\frac{1}{H}\right\}$$

Figure 4. Inverse Filter Concepts

7.3 THE DIGITAL STEP EDGE

Robert M. Haralick

Departments of Electrical Engineering and Computer Science
Virginia Polytechnic Institute and State University
Blacksburg, Virginia 24061

Abstract

We use the facet model to accomplish step edge detection. The essence of the facet model is that any analysis made on the basis of the pixel values in some neighborhood has its final authoritative interpretation relative to the underlying grey tone intensity surface of which the neighborhood pixel values are observed noisy samples.

Pixels which are part of regions have simple grey tone intensity surfaces over their areas. Pixels which have an edge in them have complex grey tone intensity surfaces over their areas. Specifically, an edge moves through a pixel if and only if there is some point in the pixel's area having a zero crossing of the second directional derivative taken in the direction of a non-zero gradient at the pixel's center.

To determine whether or not a pixel should be marked as a step edge pixel, its underlying grey tone intensity surface must be estimated on the basis of the pixels in its neighborhood. For

this, we use a functional form consisting of a linear combination of the tensor products of discrete orthogonal polynomials of up to degree three. The appropriate directional derivatives are easily computed from this kind of a function.

Upon comparing the performance of this zero crossing of second directional derivative operator with Prewitt gradient operator and the Marr-Hildreth zero crossing of Laplacian operator, we find that it is the best performer and is followed by the Prewitt gradient operator. The Marr-Hildreth zero-crossing of Laplacian operator performs the worst.

I. Introduction

What is an edge in a digital image? The first intuitive notion is that a digital edge occurs on the boundary between two pixels when the respective brightness values of the two pixels are significantly different. Significantly different may depend upon the distribution of brightness values around each of the pixels.

We often point to a region on an image and say this region is brighter than its surrounding area, meaning that the mean of the brightness values of pixels inside the region is brighter than the mean of the brightness values outside the region. Having noticed this we would then say that an edge exists between each pair of neighboring pixels where one pixel is inside the brighter region and the other is outside the region. Such edges are referred to as step edges.

Step edges are not the only kind of edge. If we scan through a region in a left right manner observing the brightness values steadily increasing and then after a certain point observe that the brightness values are steadily decreasing we are likely to say that there is an edge at the point of change from increasing to decreasing brightness values. Such edges are called roof edges.

It is, therefore, clear from our use of the word edge that edge refers to places in the image where there appears to be a jump in brightness value or a local extrema in brightness value

derivative. Jumps in brightness values are the kinds of edges originally detected by Roberts (1965). Relative extrema of first derivative in a one dimensional form is used by Ehrich and Schroeder (1981) and in an isotropic two-dimensional suboptimal form by Marr and Hildreth (1980).

In some sense this summary statement about edges is quite revealing since in a discrete array of brightness values there are jumps, in the literal sense, between neighboring brightness values if the brightness values are different, even if only slightly different. Perhaps more to the heart of the matter, there exists no definition of derivative for a discrete array of brightness values. The only way to interpret jumps in value or local extrema of derivatives when referring to a discrete array of values is to assume that the discrete array of values comes about as some kind of sampling of a real-valued function defined on a bounded and connected subset of the real plane R^2. The jumps in value or extrema in derivative really must refer to points of high first derivative of f and to points of relative extrema in the second derivatives of f. Edge detection must then involve fitting a function to the sample values. Prewitt (1970), was the first to suggest the fitting idea. Heuckel (1971, 1973), Brooks (1978), Haralick (1980), Haralick and Watson (1981), Morgenthaler and Rosenfeld (1981), Zucker and Hummel (1979), and Morgenthaler (1981) all use the surface fit concept in determining edges.

Edge finders should then regard the digital picture function as a sampling of the underlying function f, where some kind of random noise has been added to the true function values. To do this, the edge finder must assume some kind of parametric form for the underlying function f, use the sampled brightness values of the digital picture function to estimate the parameters, and finally make decisions regarding the locations of discontinuities and the locations of relative extrema of partial derivatives based on the estimated values of the parameters.

Of course, it is impossible to determine the true locations of discontinuities in value or relative extrema in derivatives directly from a sampling of the functions. The locations are estimated by function approximation. Sharp discontinuities can reveal themselves in high values for estimates of first partial derivatives. Relative extrema in first directional derivative can reveal themselves as zero-crossings of the second directional derivative. Thus, if we assume that the first and second partial derivatives of any possible underlying image function have known bounds, then any estimated first or second order partials which exceed these known bounds must be due to discontinuities in value or in derivative of the underlying function. This is basis for the gradient magnitude and Laplacian magnitude edge detectors. However, edges can be weak but well localized. Such edges, as well as the strong edges just discussed, manifest themselves as local extrema of the deriva ve taken across the edge. This idea

for edges is the basis of the edge detector discussed here.

In this paper, we assume that in each neighborhood of the image the underlying function f takes the parametric form of a polynomial in the row and column coordinates and that the sampling producing the digital picture function is a regular equal interval grid sampling of the square plane which is the domain of f. As just mentioned, we place edges not at locations of high gradient, but at locations of spatial gradient maxima. More precisely, a pixel is marked as an edge pixel if in the pixel's immediate area there is a zero crossing of the second directional derivative taken in the direction of the gradient. Thus this kind of edge detector will respond to weak but spatially peaked gradients.

The underlying functions from which the directional derviatives are computed are easy to represent as linear combinations of the polynomials in any polynomial basis set. That polynomial basis set which permits the independent estimation of each coefficient would be the easiest to use. Such a polynomial basis set is the discrete orthogonal polynomial basis set.

Section II discusses the polynomials. In section II.1 we discuss how to construct the one dimensional family of discrete orthogonal polynomials. In section II.2 we discuss how arbitrary two dimensional polynomials can be computed as linear combinations of the tensor products of one dimensional discrete

orthogonal polynomials. In section II.3, we discuss how the discretely sampled data values are used to estimate the coefficients of the linear combinations: coefficient estimates for exactly fitting or estimates for least square fitting are calculated as linear combinations of the sampled data values.

Having used the pixel values in a neighborhood to estimate the underlying polynomial function we can now determine the value of the partial derivatives at any location in the neighborhood and use those values in edge finding. Having to deal with partials in both the row and column directions makes using these derivatives a little more complicated than using the simple derivatives of one dimensional functions. Section III discusses the directional derivative, how it is related to the row and column partial derivatives, and how the coefficients of the fitted polynomial get used in the edge detector. In section IV we discuss the statistical confidence of the estimate of edge existence and the edge angle. In section V we show results indicating the superiority of the directional derivative zero-crossing edge operator over the Prewitt gradient operator and the related Marr-Hildreth zero-crossing of the Laplacian operator.

II. The Discrete Orthogonal Polynomials

These polynomials are sometimes called the discrete Chebychev polynomials (Beckmann, 1973). In this section we show

how to construct them for one or two variables and how to use them in fitting data.

II.1 Discrete Orthogonal Polynomial Construction Technique

Let the index set R be symmetric in the sense that r∈R implies -r∈R. Let $P_n(r)$ be the n^{th} order polynomial. We define the construction technique for discrete orthogonal polynomials iteratively.

Define $P_0(r) = 1$.

Suppose $P_0(r),\ldots, P_{n-1}(r)$ have been defined. In general, $P_n(r) = r^n + a_{n-1}r^{n-1} + \ldots + a_1 r + a_0$. $P_n(r)$ must be orthogonal to each polynomial $P_0(r),\ldots,P_{n-1}(r)$. Hence, we must have the n equations

$$\sum_{r\in R} P_k(r)(r^n + a_{n-1}r^{n-1} + \ldots + a_1 r + a_0) = 0,\ k=0,\ldots,n-1 \quad (1)$$

These equations are linear equations in the unknown $a_0,\ldots,a_{n-1}$ and are easily solved by standard techniques.

The first five polynomial functions formulas are

$$P_0(r) = 1$$

$$P_1(r) = r$$

$$P_2(r) = r^2 - \mu_2/\mu_0$$

$$P_3(r) = r^3 - (\mu_4/\mu_2)r$$

$$P_4(r) = \frac{r^4 + (\mu_2\mu_4-\mu_6)r^2 + (\mu_2\mu_6-\mu_4^2)}{\mu_0\mu_4-\mu_2}$$

where

$$\mu_k = \sum_{s\in R} s^k$$

II.2 Two Dimensional Discrete Orthogonal Polynomials

Two dimensional discrete orthogonal polynomials can be created from two sets of one dimensional discrete orthogonal polynomials by taking tensor products. Let R and C be index sets satisfying the symmetry condition $r\in R$ implies $-r\in R$ and $c\in C$ implies $-c\in C$. Let $\{P_0(r),\ldots,P_N(r)\}$ be a set of discrete polynomials on R. Let $\{Q_0(c),\ldots,Q_M(c)\}$ be a set of discrete polynomials on C. Then the set $\{P_0(r)Q_0(c),\ldots,P_n(r)Q_m(c),\ldots,P_N(r)Q_M(c)\}$ is a set of discrete polynomials on RXC.

The proof of this fact is easy. Consider whether $P_i(r)Q_j(c)$ is orthogonal to $P_n(r)Q_m(c)$. when $n \neq i$ or $m \neq j$. Then

$$\sum_{r \in R} \sum_{c \in C} P_i(r)Q_j(c)P_n(r)Q_m(c)$$

$$= \sum_{r \in R} P_i(r)P_n(r) \sum_{c \in C} Q_j(c)Q_m(c).$$

Since $n \neq i$ or $m \neq j$ one or other of the sums must be zero.

Examples:

Index Set	Discrete Orthogonal Polynomial Set
$\{-1/2, 1/2\}$	$\{1, r\}$
$\{-1, 0, 1\}$	$\{1, r, r^2 - 2/3\}$
$\{-2/3, -1/2, 1/2, 3/2\}$	$\{1, r, r^2 - 5/4, r^3 - 41/20r\}$
$\{-2, -1, 0, 1, 2\}$	$\{1, r, r^2 - 2, r^3 - 17/5, r^4 + 3r^2 + 72/35\}$
$\{-1, 0, 1\} \times \{-1, 0, 1\}$	$\{1, r, c, r^2 - 2/3, rc, c^2 - 2/3, r(c^2 - 2/3), c(r^2 - 2/3), (r^2 - 2/3)(c^2 - 2/3)\}$

Figure 1 and 2 show some of the window masks used for the 3 x 3 and 4 x 4 cases.

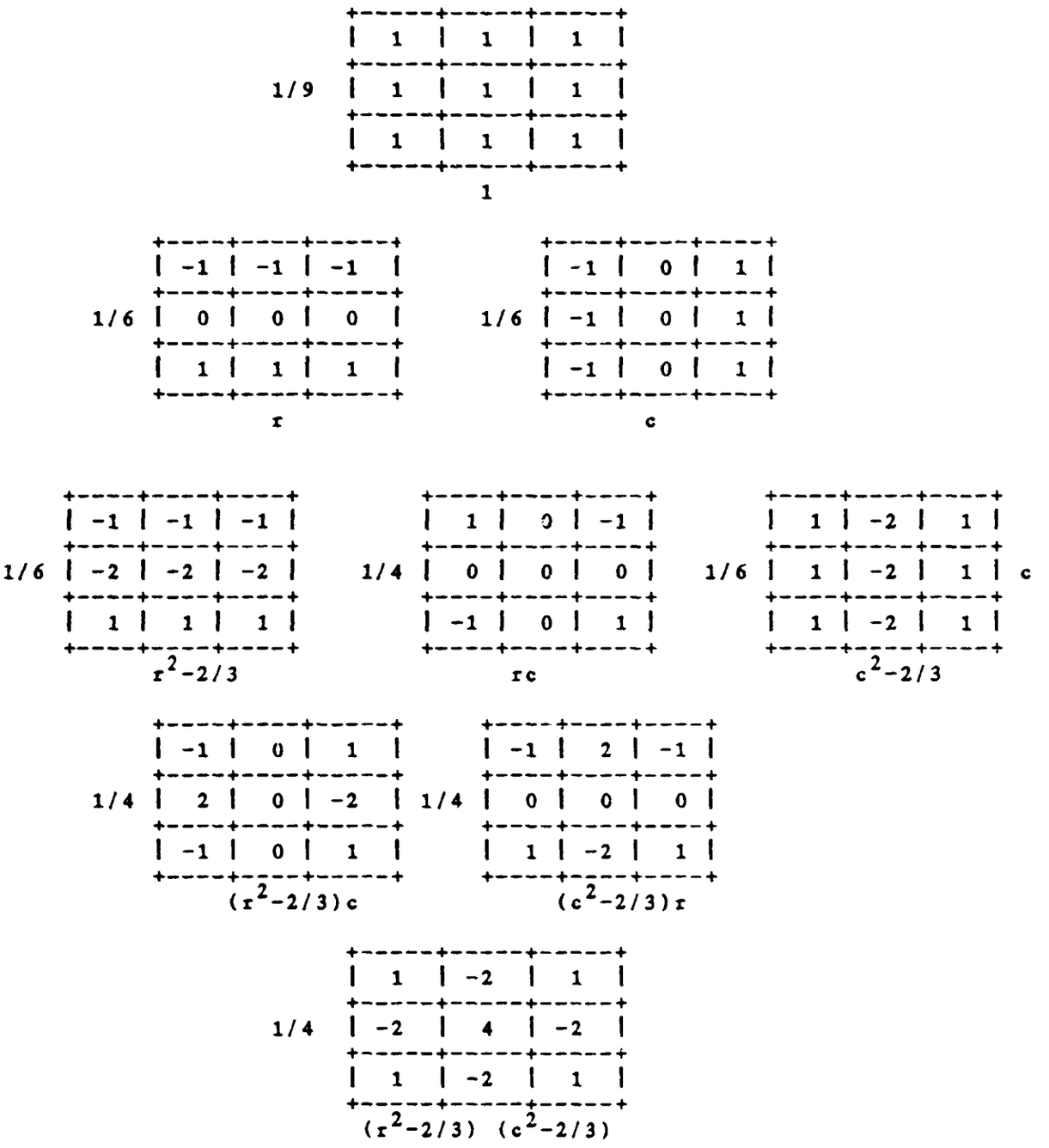

Figure 1 illustrates the 9 masks for the 3x3 window

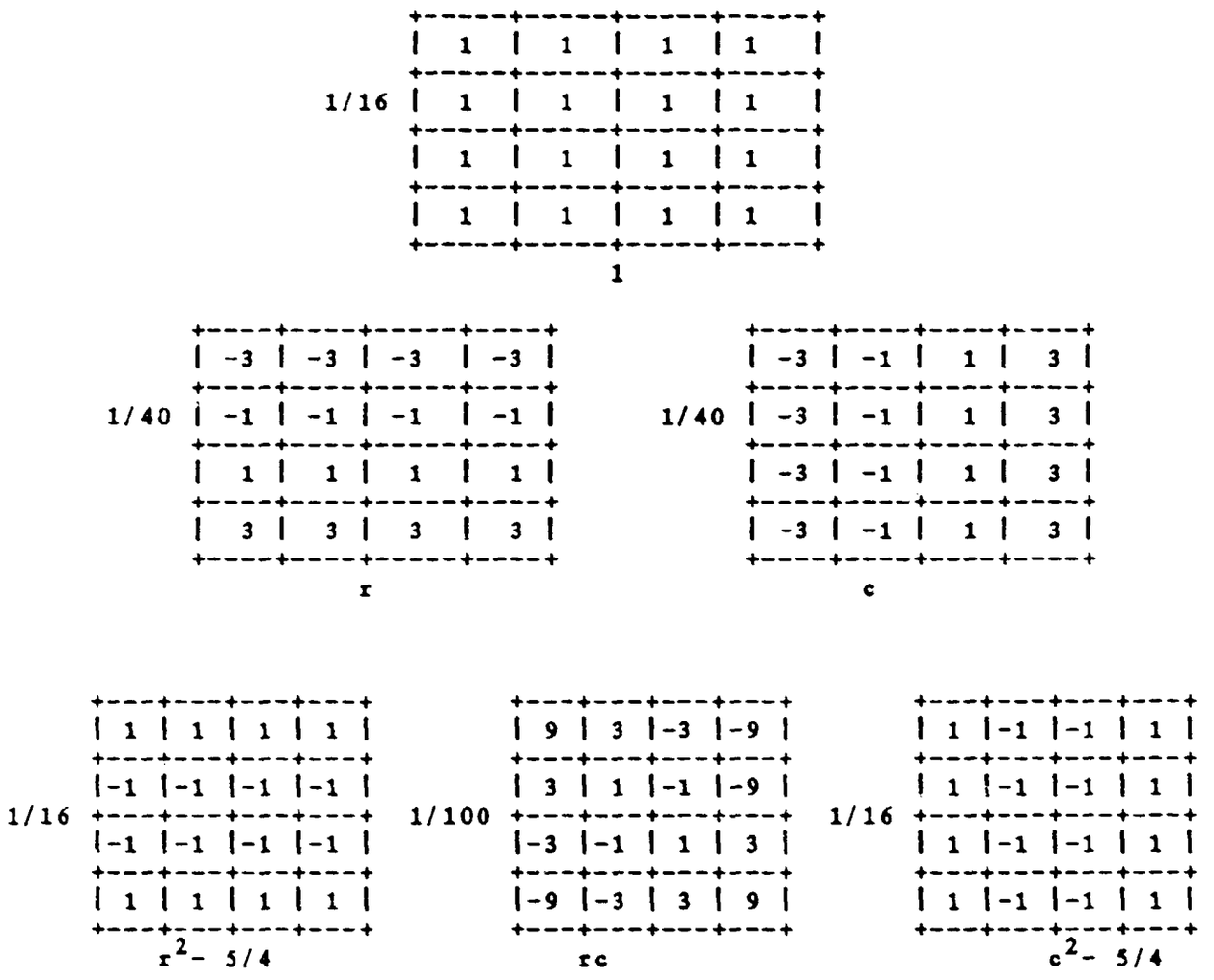

Figure 2 illustrates the masks used to obtain the coefficients of all polynomials up to the quadratic ones for a 4x4 window.

II.3 Fitting Data With Discrete Orthogonal Polynomials

Let an index set R with the symmetry property $r \varepsilon R$ implies $-r \varepsilon R$ be given. Let the number of elements in R be N. Using the construction technique, we may construct the set $\{P_0(r),\ldots,P_{N-1}(r)\}$ of discrete orthogonal polynomials over R.

For each $r \varepsilon R$, let a data value d(r) be observed. The exact fitting problem is to determine coefficients $a_0,\ldots,a_{N-1}$ such that

$$d(r) = \sum_{n=0}^{N-1} a_n P_n(r)$$

The orthogonality property makes the determination of the coefficients particularly easy. To find the value of some coefficient, say a_m, multiply both sides of the equation by $P_m(r)$ and then the sum over all $r \varepsilon R$.

$$\sum_{r \varepsilon R} P_m(r) d(r) = \sum_{n=0}^{N-1} a_n \sum_{r \varepsilon R} P_n$$

Hence,

$$a_m = \sum_{r \in R} P_m(r)d(r) \; / \; \sum_{r \in R} P_m^2(r) \qquad (2)$$

The approximate fitting problem is to determine coefficients $a_0,\ldots,a_K$, $K \leq N-1$ such that

$$e^2 = \sum_{r \in R} [d(r) - \sum_{n=0}^{K} a_n P_n(r)]^2$$

is minimized. To find the value of some coefficient, say a_m, take the partial derivative of both sides of the equation for e^2 with respect to a_m. Set it to zero and use the orthogonality property to find that again

$$a_m = \sum_{r \in R} P_m(r)d(r) / \sum_{r \in R} P_m^2(r) \qquad (3)$$

The exact fitting coefficients and the least squares coefficients are identical for $m = 0,\ldots,K$.

Fitting the data values $\{d(r) | r \in R\}$ to the polynomial

$$Q(r) = \sum_{n=0}^{K} a_n P_n(r)$$

now permits us to interpret Q(r) as a well behaved real-valued function defined on the real line. To determine

$$\frac{dQ}{dr}(r_0)$$

we need only to evaluate

$$\sum_{n=0}^{N} a_n \frac{dP_n}{dr}(r_0)$$

In this manner, any derivative at any point may be obtained. Similarly for any definite integrals. Beaudet (1978) uses this technique for estimating derivatives employed in rotationally invariant image operators.

It should be noted that the kernel used to estimate a derivative depends on the neighborhood size, the order of the fit, and the basis functions used for the fit. Figure 3 illustrates one example of the difference the assumed model makes. This difference means that the model used must be justified, the justification being that it is a good fit to the data. In particular, a not sufficiently good justification for

using first order models is that first order partial derivatives are being estimated.

Assumed Model	Kernel Mask for Row Derivative
$g(r,c)=a_{00}+a_{10}r+a_{01}c$	$1/6 \begin{bmatrix} -1 & -1 & -1 \\ 0 & 0 & 0 \\ 1 & 1 & 1 \end{bmatrix}$
$g(r,c)= a_{00}+a_{10}r+a_{01}c$ $a + a_{20}(r^2-2/3)+a_{11}rc +a_{02}(c^2-2/3)$ $+ a_{21}(r^2-2/3)c + a_{12}(c^2- 2/3)r$	$1/2 \begin{bmatrix} 0 & -1 & 0 \\ 0 & 0 & 0 \\ 0 & 1 & 0 \end{bmatrix}$

Figure 3 illustrates that the assumed model does make a difference in the kernel mask used to estimate a quantity such as row derivative.

III. The Directional Derivative Edge Finder

We denote the directional derivative of f at the point (r,c) in the direction α by $f_\alpha'(r,c)$. It is defined as

$$f_\alpha'(r,c) = \lim_{h\to 0} \frac{f(r+h\sin\alpha, c+h\cos\alpha) - f(r,c)}{h} \qquad (4)$$

The direction angle α is the clockwise angle from the column axis. It follows directly from this definition that

$$f_\alpha'(r,c) = \frac{\partial f(r,c)}{\partial r} \sin\alpha + \frac{\partial f(r,c)}{\partial c} \cos\alpha \qquad (5)$$

We denote the second directional derivative of f at the point (r,c) in the direction α by $f_\alpha''(r,c)$ and it quickly follows that

$$f_\alpha'' = \frac{\partial^2 f \sin^2\alpha}{\partial r^2} + \frac{2\partial^2 f \sin\alpha \cos\alpha}{\partial r c} + \frac{\partial^2 f \cos^2\alpha}{\partial c^2} \qquad (6)$$

Taking f to be a cubic polynomial in r and c which can be estimated by the discrete orthogonal polynomial fitting procedure, we can compute the gradient of f and the gradient

direction angle at the center of the neighborhood used to estimate f. Letting f be estimated as a two dimensional cubic

$$\begin{aligned} f(r,c) = {} & k_1 + k_2 r + k_3 c \\ & + k_4 r^2 + k_5 rc + k_6 c^2 \\ & + k_7 r^3 + k_8 r^2 c + k_9 r c^2 + k_{10} c^3 \end{aligned} \tag{7}$$

we obtain α by

$$\begin{aligned} \sin\alpha &= k_2/(k_2^2 + k_3^2)^{.5} \\ \cos\alpha &= k_3/(k_2^2 + k_3^2)^{.5} \end{aligned} \tag{8}$$

At any point (r,c), the second directional derivative in the direction α is given by

$$\begin{aligned} f_\alpha''(r,c) = {} & (6k_7 \sin^2\alpha + 4k_8 \sin\alpha\cos\alpha + 2k_9 \cos^2\alpha)r \\ & + (6k_{10} \cos^2\alpha + 4k_9 \sin\alpha \cos\alpha + 2k_8 \sin^2\alpha)c \\ & + (2k_4 \sin^2\alpha + 2k_5 \sin\alpha \cos\alpha + 2k_6 \cos^2\alpha) \end{aligned} \tag{9}$$

We wish to only consider points (r,c) on the line in direction α. Hence, $r=\rho\sin\alpha$ and $c=\rho\cos\alpha$. Then

$$f_\alpha''(\rho) = 6[k_7\sin^3\alpha + k_8\sin^2\alpha\cos\alpha + k_9\sin\alpha\cos^2\alpha + k_{10}\cos^3\alpha]\rho + 2[k_4\sin^2\alpha + k_5\sin\alpha\cos\alpha + k_6\cos^2\alpha] = A\rho + B \tag{10}$$

If for some ρ, $|\rho| < \rho_0$, $f_\alpha''(\rho) = 0$ and $f_\alpha'(\rho) \neq 0$ we have discovered a zero-crossing of the second directional derivative taken in the direction of the gradient and we mark the center pixel of the neighborhood as an edge pixel.

IV. Statistical Analysis

In this section we show how the randomness of the noise induces a randomness in the least squares coefficients and then how the randomness of the least squares coefficients induces a randomness in the estimated gradient value, the estimated angle of the gradient, and the estimated location of the zero-crossing.

IV.1 General Model

We let p_n, $n=1,\ldots,N$ denote the names of the discrete orthonormal basis functions, η denote the independent and identically distributed noise, and g denote the gray tone intensity function. Under this model, the observed image can be

written as

$$g(r,c) = \sum_{n=1}^{N} a_n \, p_n(r,c) + \eta(r,c) \tag{11}$$

where $$\sum_{r,c} p_n(r,c) \, p_m(r,c) = \begin{cases} 0, & n \neq m \\ 1 & n = m \end{cases}$$

and the least squares estimates $a_1', \ldots, a_N'$ for the unknown coefficients $a_1, \ldots, a_n$ are given by

$$a_n' = \sum_{r,c} g(r,c) \, p_n(r,c) \tag{12}$$

Substituting the formula for $g(r,c)$ into the equation for a_n' and simplifying results in

$$a_n' = a_n + \sum_{r,c} p_n(r,c) \, \eta(r,c) \tag{13}$$

clearly showing that a_n' has a deterministic part and a random part, the randomness being due to the noise. We assume that the noise is independent normal having mean 0 and variance σ^2. Therefore, the estimated coefficient a_n' has mean a_n, variance σ^2 and is uncorrelated with every other coefficient:

$$E\,[a_n'] = a_n$$

$$E\,[a_m'\,a_n'] = a_m a_n,\ m \neq n$$

$$E\,[a_n'^2] = a_n^2 + \sigma^2$$

$$V\,[a_n'] = \sigma^2$$

The residual error e is defined as the difference between the observed values and fitted values. It too is a random variable.

$$e(r,c) = g(r,c) - \sum_{n=1}^{N} a_n'\,p_n(r,c) \qquad (14)$$

$$= \sum_{n=1}^{N} (a_n - a_n')\,p_n(r,c) + \eta(r,c)$$

It is not difficult to see that at each (r,c), the residual error has mean zero and is uncorrelated with each estimated coefficient a_n' since

$$E\,[a_n'\,e(r,c)] = 0$$

After some algebraic substitutions and manipulation, the total residual error, S^2, can be written as

$$S^2 = \sum_{r,c} e^2(r,c) = \sum_{r,c} \eta^2(r,c) - \sum_{n=1}^{N} (a_n - a_n')^2 \qquad (15)$$

Thus, if the noise is assumed normal and there are K pixels in a window

$$\sum_{r,c} \eta^2(r,c)/\ \sigma^2 \text{ has } X_k^2,$$

a chi-squared variate with K degree of freedom,

$$\sum_{n=1}^{N} (a_n - a_n')^2/\sigma^2 \quad \text{has } X_N^2$$

which makes $\sum_{r,c} e^2(r,c)$ have X_{k-N}^2

IV.2 Estimating the First Partials

If the discrete orthogonal basis functions are polynomials then each first partial derivative at (0,0) in the row and column directions is given as some linear combination of the estimated coefficients. Furthermore, the linear combination for the row partial will be orthogonal to the linear combination in the

column partial. Letting the coefficients of the linear combination for the row partial be $s_1,\ldots,s_N$ and the coefficients of the linear combination for the column partial be $t_1,\ldots,t_N$, where

$$\sum_{n=1}^{N} s_n^2 = \sum_{n=1}^{N} t_n^2 = k,$$

we have,

$$\mu_r = \sum_{n=1}^{N} s_n a_n$$

$$\mu_c = \sum_{n=1}^{N} t_n a_n$$

as the true but unknown values of the row and column partials. The estimates are

$$\mu_r' = \sum_{n=1}^{N} s_n \, a_n'$$

$$\mu_c' = \sum_{n=1}^{N} t_n \, a_n'$$

and they have mean and variance given by

$$E[\mu_r'] = \mu_r$$

$$E[\mu_c'] = \mu_c$$

$$V[\mu_r'] = \sigma^2 k$$

$$V[\mu_c'] = \sigma^2 k$$

$$E[\mu_r' \mu_c'] = \mu_r \mu_c$$

Hence, the estimates for the row and column partial derivatives are uncorrelated.

IV.3 Hypothesis Testing For Zero Gradient

To see the effect of the randomness on the estimate of the gradient magnitude, consider testing the hypothesis that $\mu_r = \mu_c = 0$. This hypothesis must be rejected if there is to be a zero-crossing of second directional derivative. Under this hypothesis,

$$\frac{\mu'^2_r + \mu'^2_c}{k\,\sigma^2}$$

has a X^2_2 distribution.

The total residual error normalized by the noise variance, S^2/σ^2, has a X^2_{K-N} distribution. Hence

$$\frac{(\mu'^2_r + \mu'^2_c)/2}{k\,S^2/(K-N)}$$

has a $F_{2,K-N}$ distribution and the hypothesis of $\mu_r = \mu_c = 0$ would be rejected for suitably large values.

IV.4 Confidence Interval For Gradient Direction

To see the effect of the randomness on the estimate of the direction of the gradient, consider the relationships portrayed in figure '. The axes are the row and column partials μ_r and μ_c. The direction angle θ of the gradient is given by

$$\cos\theta = \mu_r/(\mu_r^2 + \mu_c^2)^{1/2}$$
$$\sin\theta = \mu_c/(\mu_r^2 + \mu_c^2)^{1/2} \qquad (16)$$

The center of the circle is at the estimate (μ_r', μ_c'). Upon substituting the estimates μ_r' and μ_c' for μ_r and μ_c, we obtain the estimated direction angle θ' by

$$\cos\theta' = \mu_r'/(\mu'^2_r + \mu'^2_c)^{1/2}$$
$$\sin\theta' = \mu_r'/(\mu'^2_r + \mu'^2_c)^{1/2} \qquad (17)$$

From a Bayesian point of view, the area of the circle represents the conditional probability that the unknown (μ_r, μ_c) lies within a distance R from the observed (μ_r', μ_c') given that the variance of μ_r' and μ_c' is known and equal to $k\sigma^2$. Assuming a normal distribution for the noise, this conditional probability is $q = 1-e^{-R^2/2k\sigma^2}$ Hence, if probability q is given, the corresponding radius R is

$$R = k\,\sigma\,[-2\,\log(1-q)]^{1/2} \qquad (18)$$

To determine a confidence interval for θ of the form $\theta' - \Delta \leq \theta \leq \theta' + \Delta$, we have from figure 4 that

$$\sin^2\Delta = \frac{k\,\sigma^2(-2\,\log(1-q))}{\mu'^2_r + \mu'^2_c} \qquad (19)$$

Note that the 2Δ confidence interval length depends on the probability q of the circle confidence region for (μ_r, μ_c) and the unknown noise variance σ^2. Although σ^2 is not known, we do know S^2 which has a $\sigma^2 X^2_{K-N}$ distribution. We can handle the problem of ths unknown σ^2 by determining a joint confidence region for (μ_r, μ_c) and σ^2 (Foutz,1981). Taking p to be the probability that a chi-squared random variable with $K-N$ degrees of freedom has an observed value greater than $X^2_{K-N,p}$ we have the confidence interval $[0, S^2/X^2_{K-N,p}]$ for σ^2 having at least probability p. Replacing σ^2 in equation (19) by $S^2/X^2_{N-K,p}$ we obtain

$$\sin^2\Delta = \frac{k\, S^2(-2\log(1-q))}{X^2_{K-N,p}\,(\mu'^2_r + \mu'^2_c)} \qquad (20)$$

A confidence interval for θ having at least probability pq is then $(\theta' - \Delta, \theta' + \Delta)$.

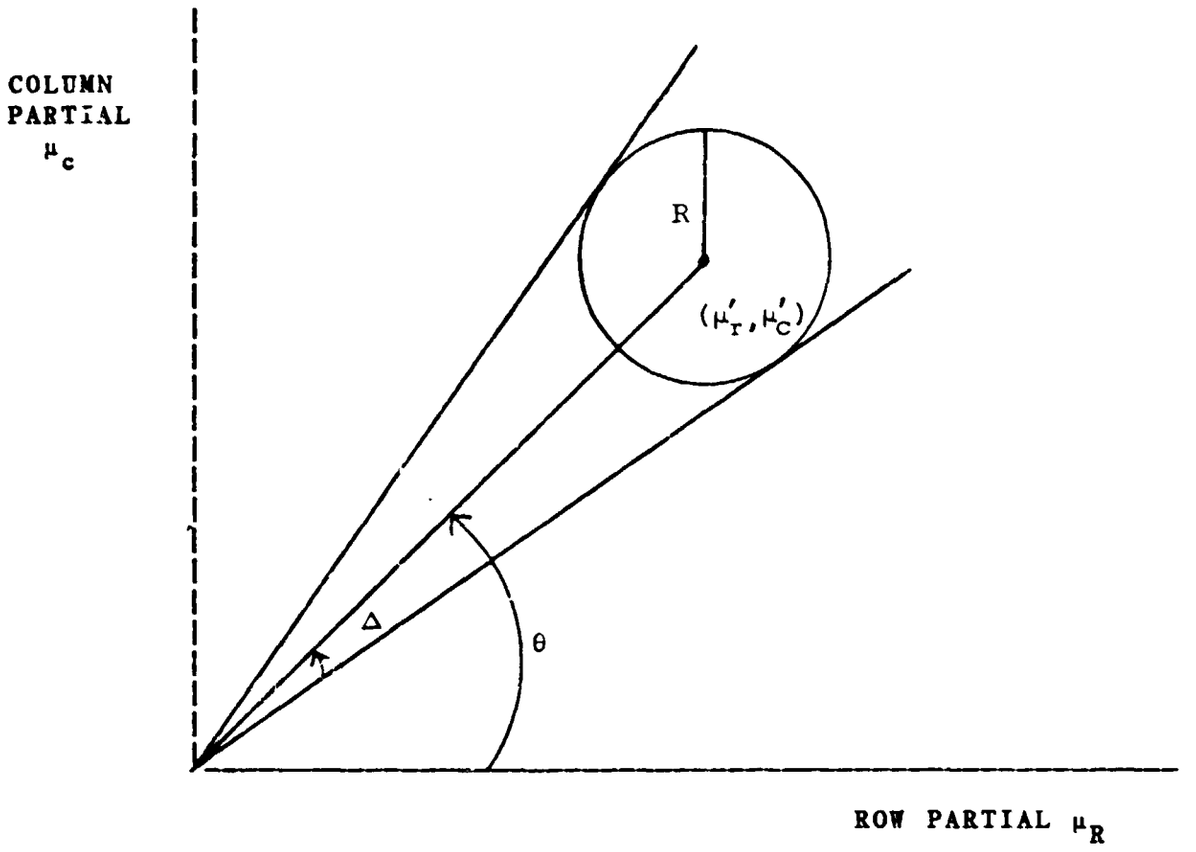

Figure 4 illustrates the geometry of the confidence interval estimation for the edge angle.

IV.5 Edge Hypothesis Testing

In this section we first take the edge direction α to be a fixed constant. We let μ_A and μ_B be the expected values of the random variables A and B appearing in equation (10). The null hypothesis is that an edge exists. The null hypothesis is satisfied if for some ρ, $o \leq \rho \leq d$, $\mu_A\rho + \mu_B = 0$.

The observed random variables are A, B, and the residual fitting error S^2. The bivariate random variable $\begin{pmatrix} A \\ B \end{pmatrix}$ is normal having mean $\begin{pmatrix} \mu_A \\ \mu_B \end{pmatrix}$ and covariance $\sigma^2 \begin{bmatrix} k_A & 0 \\ 0 & k_B \end{bmatrix}$ where k_A and k_B are known constants. For a window of K pixels and a cubic fit, S^2/σ^2 has a X^2_{K-10}.

From this it follows that

$$Z(\mu_A,\mu_B) = \frac{[(A-\mu_A)/k_A]^2 + [(B-\mu_B/k_B{}^2)]/2}{S^2/(K-10)}$$

has an $F_{2\ K-10}$ distribution.

We define $R = \{(x,y) \mid$ for some ρ, $o \leq \rho \leq d$, $x\rho + y = 0\}$ Then the null hypothesis is rejected at the p significance level if

$$\min_{(\mu_A,\mu_B) \in R} Z(\mu_A,\mu_B)$$

is larger than $F_{2\ K-10\ 1-p}$.

An edge strength probability can be defined by q where q satisfies

$$\min_{(\mu_A,\mu_B)\in R} Z(\mu_A,\mu_B) = F_{2\ k-10\ q}$$

Of course the edge direction α is not fixed. But we do have a confidence interval for it. And for each value of α in the confidence interval, the random variable $A(\alpha)$ and $B(\alpha)$ can be computed and the null hypothesis tested. If for all α in the confidence interval the null hypothesis is rejected, then the existence of an edge is also rejected.

In practice, we can perform a non-exact hypothesis test selecting only the left end, middle, and right end values of α from its confidence interval. If for each of these three values of α the null hypothesis is rejected, then the existence of an edge is also rejected.

V. Experimental Results

To understand the performance of the second directional derivative zero-crossing digital step edge operator we examine its behavior on a well structured simulated data set and on a real aerial image. For the simulated data set, we use a 100x100 pixel image of a checkerboard, the checks being 20x20 pixels. The dark checks have gray tone intensity 75 and the light checks

have gray tone intensity 175. To this perfect checkerboard we add independent Gaussian noise having mean zero and standard deviation 50. Defining the signal to noise ratio as 10 times the logarithm of the range of signal divided by RMS of the noise, the simulated image has a 3 db signal to noise ratio. The perfect and noisy checkerboards are shown in figure 5.

Section V.1 illustrates the performance of the classic 3x3 edge operators with and without preaveraging compared against the generalized Prewitt operator. Section V.2 illustrates the performance of the Marr-Hildreth zero-crossing of Laplacian operator, the 11x11 Prewitt operator, and the 11x11 zero-crossing of second directional derivative operator. The zero-crossing of second directional derivative surpasses the performance of the other two on the twofold basis of probability of correct assignment and error distance which is defined as the average distance to closest true edge pixel of pixels which are assigned non-edge but which are true edge pixels.

V.1 The Classic Edge Operators

The classic 3x3 gradient operators all perform badly as shown in figure 6. Note that the usual definition of the Roberts operator has been modified in the natural way so that it uses a 3x3 mask.

Averaging before the application of the gradient operator is considered to be the cure for such bad performance on noisy

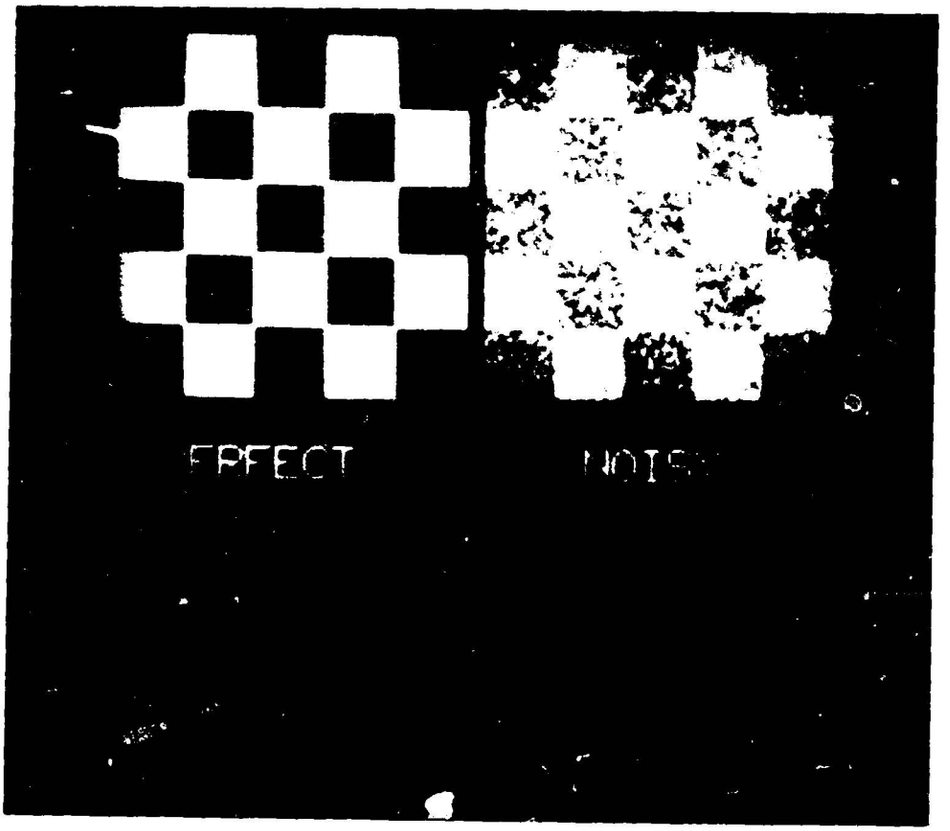

Figure 5 illustrates the noisy checkerboard used in the experiments. Low intensity is 75 high intensity is 175. Standard deviation of noise is 50.

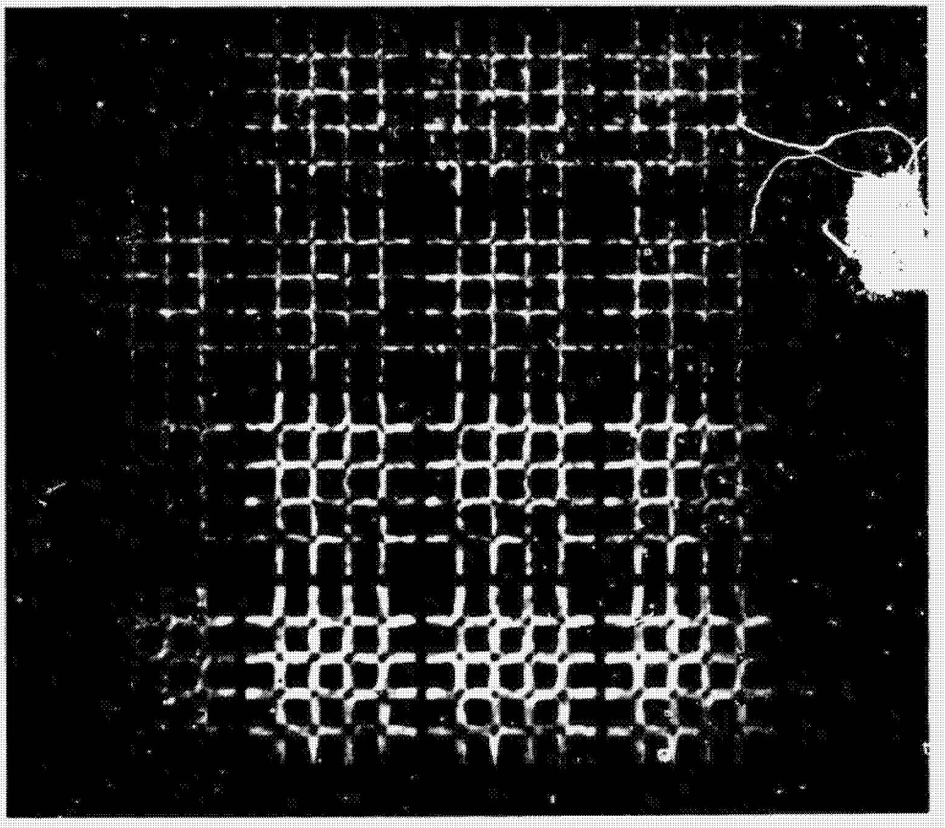

Figure 6 illustrates the 3x3 Roberts, Sobel, Prewitt, and Kirsch edge operators with a box filter preaveraging of 1x1, 3x3, 5 5 and 7x7.

images (Rosenfeld and Kak, 1976). Figure 6 also shows the same operators applied after a box filtering with a 3x3, 5x5, and 7x7 neighborhood sizes.

An alternative to the preaveraging is to define the gradient operator with a larger window. This is easily done with the Prewitt operator (Prewitt,1970) which fits a quadratic surface in every window and uses the square root of the sum of the squares of the coefficients of the linear terms to estimate the gradient. (A linear fit actually yields the same result for the polynomial basic function. A cubic fit is the first higher order fit which would yield a different result.) This is illustrated in figure 7. A 3x3 pre-average followed by a 3x3 gradient operator yields a resulting neighborhood size of 5x5. Thus in figure 7 we also show the 3x3 preaverage followed by a 3x3 gradient under the 5x5 Prewitt and we show the 5x5 pre-average followed by the 3x3 gradient under the 7x7 Prewitt. The noise is higher in the pre-average edge-detector. For comparison purposes the 5x5 Nevatia and Babu (1979) compass operator is shown alongside the 5x5 Prewitt in figure 8. They give virtually the same result. The Prewitt operator has the advantage of requiring half the computation.

It is obvious from these results that good gradient operators must have larger neighborhood sizes than 3x3. Unfortunately, the larger neighborhood sizes also yield thicker edges.

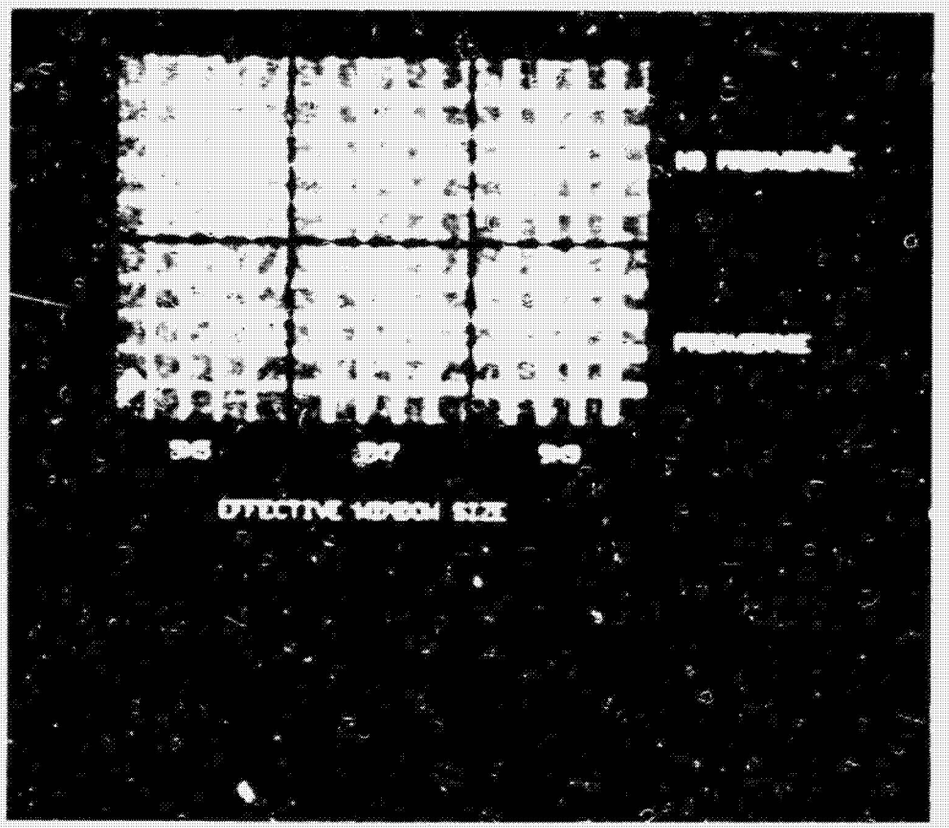

Figure 7 illustrates the Prewitt Operator done by using a least squares quadratic fit in the neighborhood versus doing preaveraging and using a smaller fitting neighborhood size. The no preaveraging results show slightly higher contrast.

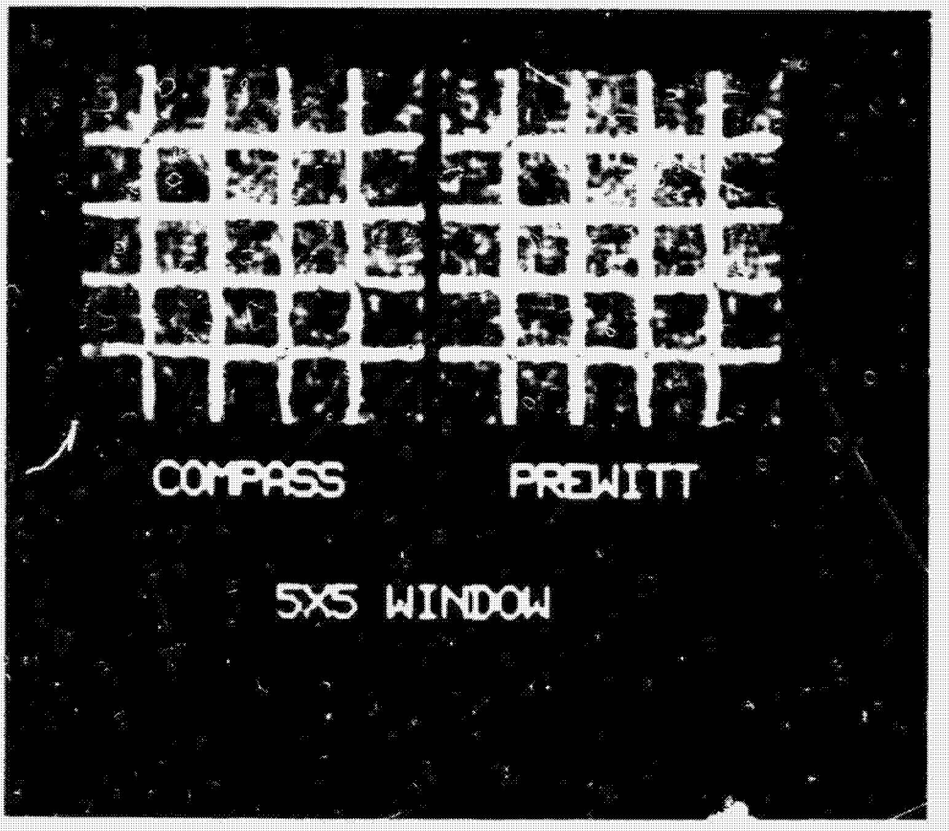

Figure 8 compares the Nevatia and Babu compass operator with the Prewitt operator in a 5x5 neighborhood.

To detect edges, the gradient value must be thresholded. In each case, we chose a threshold value which makes the conditional probability of assigning an edge given that there is an edge equal to the conditional probability of there being a true edge given that an edge is assigned. True edges are established by defining them to be the two pixel wide region in which each pixel neighbors some pixel having a value different from it on the perfect checkerboard. Figure 9 shows the thresholded Prewitt operator (quadratic fit) for a variety of neighborhood sizes. Notice that because the gradient is zero at the saddle points (the corner where four checks meet), any operator depending on the gradient to detect an edge will have trouble there.

V.2 The Second Derivative Zero Crossing Edge Operators

Marr and Hildreth (1980) suggest an edge operator based on the zero crossing of a generalized Laplacian. In effect, this is non-directional or isotropic second derivative zero crossing operator. The mask for this generalized Laplacian operator is given by sampling the kernel

$$1 - k\frac{r^2+c^2}{\sigma^2} e^{-1/2\frac{r^2+c^2}{\sigma^2}}$$

at row colum coordinates (r,c) designating the center of each pixel position in the neighborhood and then setting the value k so that the sum of the resulting weights is zero. Edges are

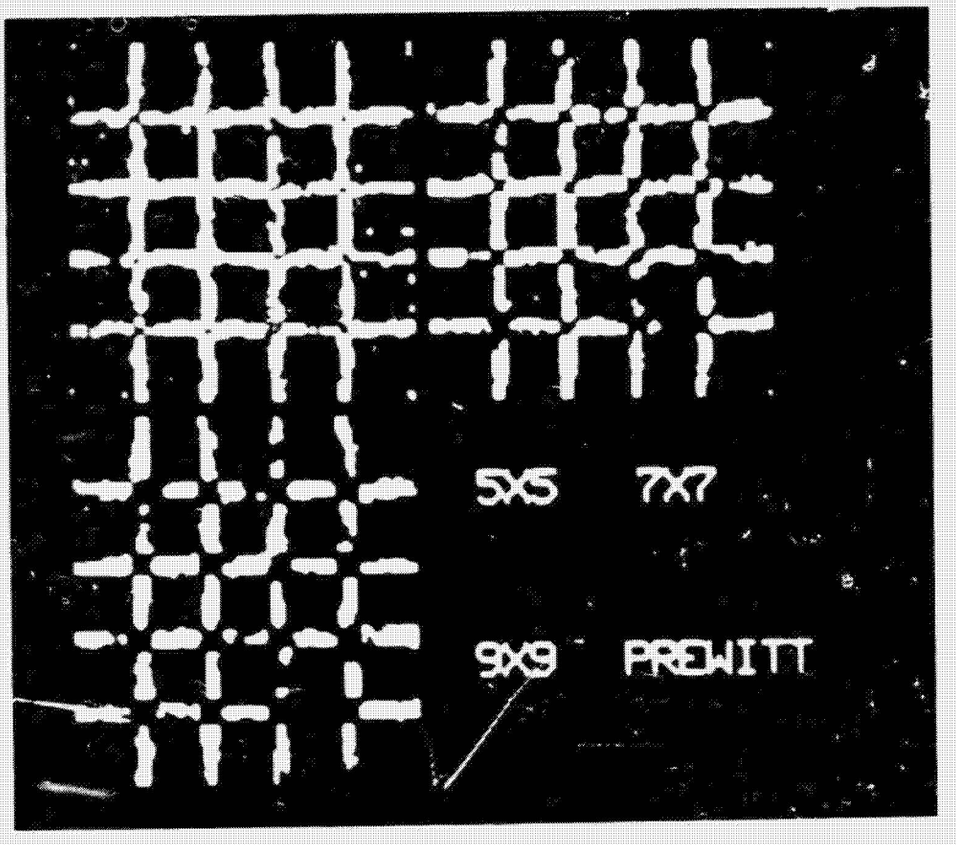

Figure 9 illustrates the edges obtained by thresholding the results of the Prewitt operator.

detected at all pixels whose generalized Laplacian value is of one sign and one of whose neighbors has a generalized Laplacian value of the opposite sign. A zero-crossing threshold strength can be introduced here by insisting that the difference between the positive value and the negative value must exceed the threshold value before the pixel is declared to be an edge pixel. Figure 10 illustrates the edge images produced by this technique for a variety of threshold values and a variety of values for σ for an 11 by 11 window. It is apparent that if all edge pixels are to be detected, there will be many pixels declared to be edge pixels which are really not edge pixels. And if there are to be no pixels which are to be declared edge pixels which are not edge pixels, then there will be many edge pixels which are not detected. Its performance is poorer than the Prewitt operator.

The directional second derivative zero crossing edge operator introduced in this paper is shown in figure 11 for a variety of gradient threshold values. If the gradient exceeds the threshold value and a zero-crossing occurs in a direction of $\pm$ 14.9 degrees of the gradient direction within a circle of one pixel length centered in the pixel, then the pixel is declared to be an edge pixel. This technique performs the worst at the saddle points, the corner where four checks meet because of these being a zero gradient there.

Table 1 shows the comparison among the Prewitt operator and the directional and the Marr-Hildreth non-directional second

ORIGINAL PAGE
BLACK AND WHITE PHOTOGRAPH

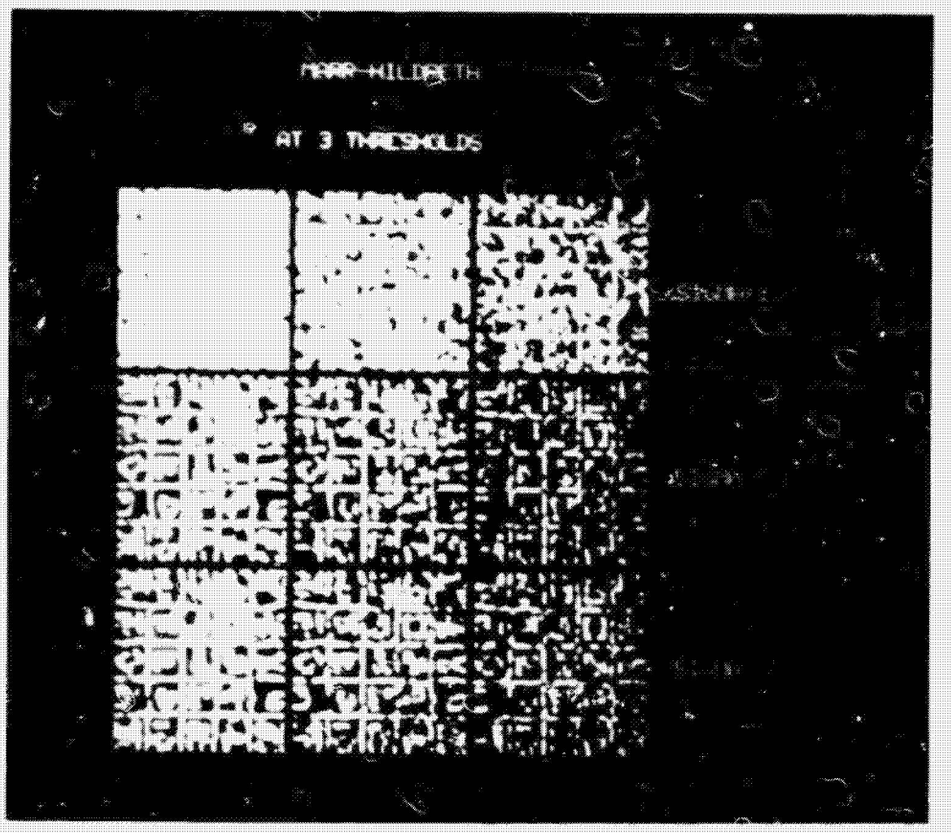

Figure 10 illustrates the edges obtained by the 11x11 Marr-Hildreth zero-crossing of Laplacian operator set for three different zero-crossing thresholds and three different standard deviations for the associated Mexican hat filter.

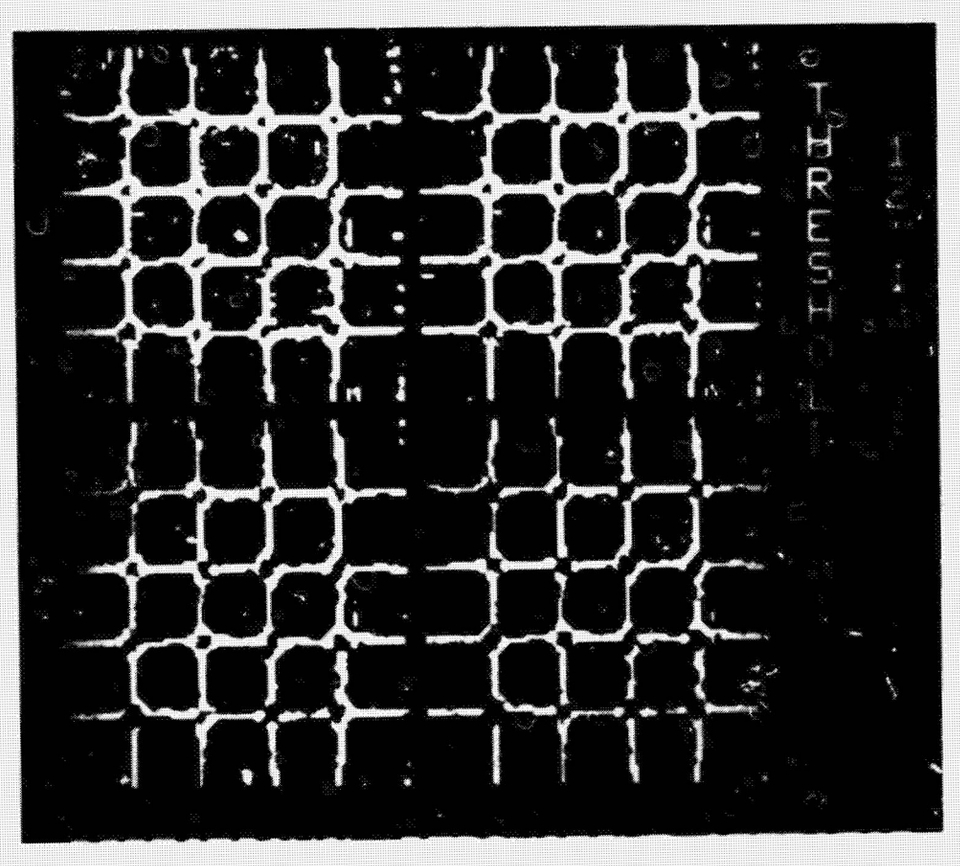

Figure 11 illustrates the directional derivative edge operator for 4 different thresholds.

derivative zero crossing edge operators. The threshold used is, as before, the one equalizing the conditional probability of assigned edge given true edge and the conditional probability of true edge given assigned edge. It is clear that the performance of the directional derivative operator is better than the Prewitt operator and the Marr-Hildreth operator, both on the basis of the correct assignment probability and the error distance which is the average distance to closest true edge pixels of pixels which are assigned non-edge labels but which are true edge pixels.

Figure 12 shows the corresponding edge images of the 11x11 Prewitt operator using a cubic fit rather than a quadratic fit, the 11x11 Marr-Hildreth operator, and the 11x11 directional derivative zero-crossing operator. The thresholds used are the ones to equalize the conditional probabilities as given in Table 1. A visual evaluation also leaves the impression that the directional derivative operator produces better edge continuity and has less noise than the other two.

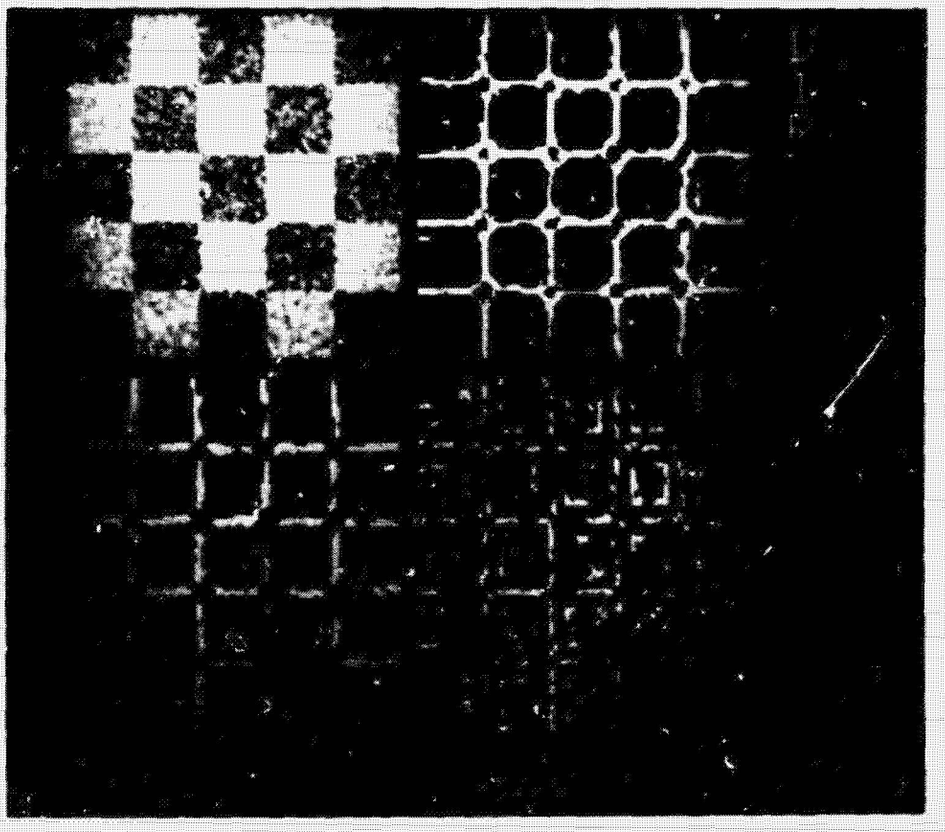

Figure 12 Compares the directional derivative edge operator with the Marr-Hildreth edge operator and the Prewitt edge operator. The thresholds chosen were the best possible ones.

For the case of constant variance additive noise, thresholding on the basis of the hypothesis test of section IV.3 yields essentially the same results as simply thresholding the gradient value.

Figure 13 illustrates the second directional derivative zero crossing operator on an aerial image which has been median filtered and then enhanced by replacing each pixel with the closer of its 3x3 neighborhood minimum or maximum. The technique is so good that it is possible to determine region boundaries essentially by doing a connected components on non-edge pixels. Figure 13b shows the cleaned edge image which is obtained by doing a connected components on the non edge pixels, then removing all pixels whose region has fewer than 20 pixels. The resulting boundaries are given as pixels which have a neighbor with a different label than its own.

Initial raw edges which leave gaps in a region boundary will in effect make the regions merge in the connected components step. Thus the small number of missing boundaries is surprising. To be sure, we are not advocating connected components as an image segmentation technique. The fact that it works as well as it does is an indication of the strength of the edge detector.

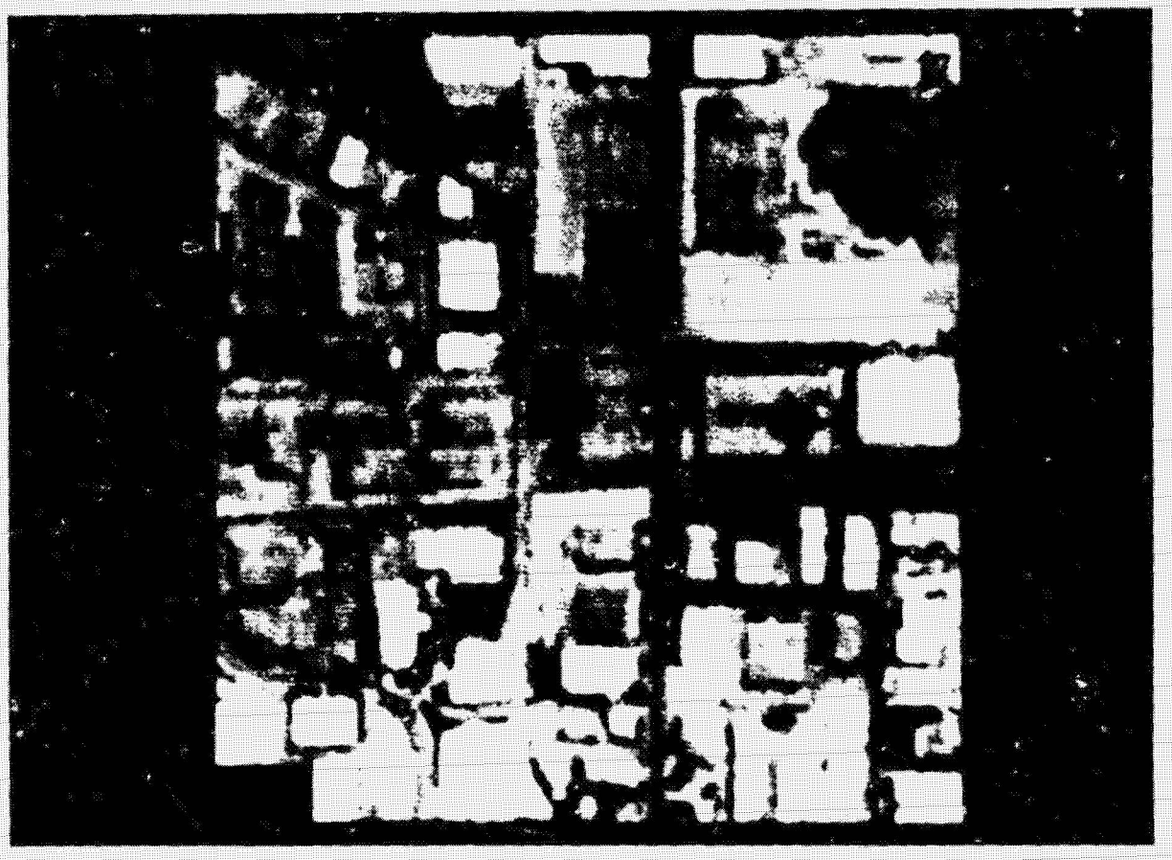

Figure 13a illustrates an aerial photograph.

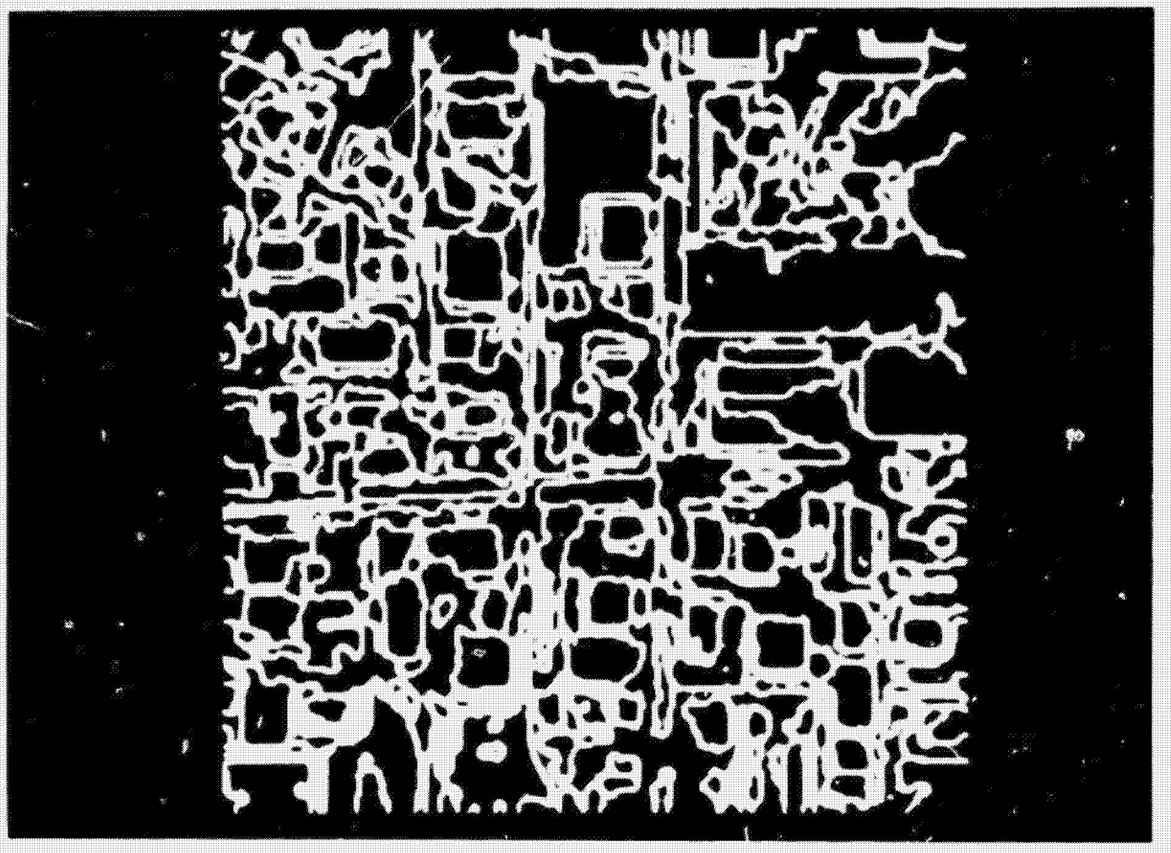

Figure 13b illustrates the directional derivative edges obtained from the aerial photograph by first 3x3 median filtering, then replacing each pixel by the closer of its 3x3 neighborhood minimum or maximum, then taking the directional derivative edges using a 7x7 window, then doing a connected components on the non-edge pixels, and removing all regions having fewer than 20 pixels, and then displaying any pixel neighboring a pixel different than it as an edge pixel.

	Prewitt	Marr-Hildreth	Directional Derivative
Parameters	Gradient Threshold = 18.5	Zero-crossing Strength = 4.0 σ = 5.0	Gradient Threshold=14.0 ρ = .5
P(AE|TE)	.6738	.3977	.7207
P(TE|AE)	.6872	.4159	.7197
Error Distance	1.79	1.76	1.16

Table 1 compares the performance of three edge operators using an 11x11 window on the noisy checkerboard image. Thresholds are chosen to equalize, as best as possible, P(AE|TE), the conditional probability of assigned edge given true edge and the conditional probability, P(TE|AE) of true edge given assigned edge. The error distance is the average distance to closest true edge pixels of pixels which are assigned non-edge but which are true edge.

VI. Conclusions

We have argued that numeric digital image operations should be explained in terms of their actions on the underlying gray tone intensity surface of which the digital image is an observed noisy sample. We called this model, the facet model for digital image processing and showed how the facet model can be used to estimate in each neighborhood the underlying gray tone intensity surface.

We described a digital step edge operator which detects edges at all pixels whose estimated second directional derivative taken in the direction of the gradient has a zero crossing within the pixel's area. We discussed the statistical analysis of this technique, illustrating how to determine confidence intervals for the direction of the gradient and how this [illegible] determines a confidence interval for the placement of the zero-crossing

We have compared the performance of the directional derivative zero crossing edge operator with that of the classic edge operators, the generalized Prewitt gradient operator, and the Marr-Hildreth zero crossing edge operator. We found that in both the simulated and real image data sets the directional derivative zero crossing edge operator had superior performance.

We have illustrated that for good performance it is important to use larger neighborhood sizes than 3x3 and have shown that better results are achieved by defining the edge operator naturally in the large neighborhood rather than pre-

averaging and then using a smaller neighborhood edge operator on the averaged image.

There is much work yet to be done. We need to explore the relationship of basis function kind, (polynomial, trignometric polynomial etc.), order of fit, and neighborhood size to the goodness of fit. Evaluation must be made of the confidence intervals produced by the technique. The technique needs to be generalized so that it works on saddle points created by two edges crossing. A suitable edge linking method needs to be developed which uses these confidence intervals. Ways of incorporating semantic information and ways of using variable resolution need to be developed. An analogous technique for roof edges needs to be developed. We hope to explore these issues in future papers.

REFERENCES

Peter Beckmann, Orthogonal polynomials for Engineers and Physicists The Golem Press, Boulder, Colorado 1973.

Paul Beaudet "Rotationally Invariant Image Operators" 4th International Joint Conference on Pattern Recognition, Tokyo, Japan, November 1978, p579-583.

M.J. Brooks "Rationalizing Edge Detectors" Computer Graphics and Image Processing, Vol 8, 1978 p277-285.

Roger Ehrich and Fred Schroeder, "Contextual Boundary Formation by One-Dimensional Edge Detection and Scan Line Matching" Computer Graphics and Image Processing, Vol 16, 1981, p116-149.

Robert Foutz, Personal communication, 1981.

Robert Haralick, "Edge and Region Analysis For Digital Image Data" Computer Graphics and Image Processing, Vol. 12, 1980 p60-73.

Robert Haralick and Layne Watson, "A Facet Model for Image Data" Computer Graphics and Image Processing, Vol 15, 1981, p113-129.

M. Hueckel, "A Local Visual Operator Which Recognizes Edges and Lines" J. Assoc. Computing Machinery Vol 20, 1973, p634-647.

M. Hueckel, "An Operator Which Locates Edges in Digitized Pictures" J. Assoc. Computing Machinery, Vol 18, 1971, p113-125.

David Marr and Ellen Hildreth, "Theory of Edge Detection" Proc. Royal Society of London, B, vol 207, 1980, p187-217.

David Morgenthaler, "A New Hybrid Edge Detector" Computer Graphics and Image Processing, vol 16, 1981, p166-176.

David Morgenthaler and Azriel Rosenfeld, "Multidimentional Edge Section by Hypersurface Fitting" IEEE Transactions on Pattern Analysis and Machine Intelligence, Vol PAMI-3, no 4, July 1981, p482-486.

Ramokaut Nevatia and Ramesh Babu, "Linear Feature Extraction and Description" Computer Graphics and Image Processing, Vol 13, 1980, p257-269.

Judith Prewitt, "Object Enhancement and Extraction" Picture Processing, and Psychopictories (B. Lipkin and A. Rosenfeld Ed.), Academic Press, New York, 1970, p75-149.

L. G. Roberts " Machine Perception of Three-Dimensional Solids" in Optical and Electrooptical Information Processing, J.T. Trippett et. al., Eds, MIT Press, Cambridge, Mass, 1965, p159-197

Azriel Rosenfeld and A. Kak Digital Picture Processing, Academic Press, New York, 1976.

Steve Zucker and Robert Hummel, "An Optimal Three-Dimensional Edge Operator" Pattern Recognition and Image Processing Conference, Chicago, August 1979, p162-168.

7.4 INTER-IMAGE MATCHING

A Tutorial Presented to the NASA Working Group on Image Registration and Rectification

Robert H. Wolfe, Jr.
IBM Federal Systems Division
Houston, Texas

Richard D. Juday
NASA Johnson Space Center
Houston, Texas

November 18, 1981

FOREWORD

This paper was invited to provide a review of the portion of the registration process relating to determining relative positions of reference and registrant images at a set of locations within the images and embodiment of those positions in a reference-to-registrant mapping function. There was an unfortunately short time available between request and conference date, and as a result the review is not as thorough as the authors would have liked to have given. We are most familiar with the processing of earth observations from Landsat, and have concentrated our review on the processing of Landsat data by the Master Data Processor (MDP) at the Goddard Space Flight Center (GSFC), the registration processor installed at the Johnson Space Center (JSC), the registration process used in the DAM (detection and mapping) Package in conjunction with a Corps of Engineers project to map surface water, the registration process used by the LACIE processor at GSFC, and the sequential similarity detection algorithm (SSDA) used by IBM/Houston in the evaluation of the LACIE processor imagery. Our review slights the body of information available from military research, in which shape recognition and artificial intelligence play a prominent part. In that field, there is interest in finding objects that have changed position with respect to a fixed background, or monitoring changes in aspect for guidance, and there is often limited interest in spectral development. Our own field of concentration involves images in which considerable spectral development has taken place (observations are made throughout a crop year for agricultural applications), although for the most part the scene's basic geometrical shape is unchanged. To some extent field boundaries change from year to year, but this is usually a small enough effect so as not to interfere with the registration process. In the presence of spectral development, one does not ordinarily correlate between images on the radiance measurement making up the parent image, but instead relies on a derivative feature (in our case, edges) that one hopes will be stable despite spectral development. We defer the discussion of extracted feature selection to other papers being presented at this workshop, noting in passing that we are most familiar with the edge-detection algorithm implemented in both the MDP and the JSC registration processor. This paper further concentrates on automated interimage correlation; the manual techniques involved in the DAM Package and other systems are a fundamentally different technology. First, of course, the points of correspondence

between images are manually determined. Second, the interpretation is normally done on radiance images transformed into visual presentations. And finally, the manual techniques are typically done on a point basis with only contextual involvement of the neighborhood around the point designated as being in correspondence. In the image comparisons discussed in this paper, measures of similarity are made over areal extents of subsets of the parent images, as opposed to points.

Introduction

Interimage matching is the process of determining the geometric transformation required to conform spatially one image to another. In principle, the parameters of that transformation are varied until some measure of "difference" between the two images is minimized or some measure of "sameness" (e.g., cross-correlation) is maximized. The number of such parameters to vary is fairly large (six for merely an affine transformation), and it is customary to attempt an a priori transformation reducing the complexity of the residual transformation or subdivide the image into small enough match zones (control points or patches) that a simple transformation (e.g., pure translation) is applicable, yet large enough to facilitate matching. In the latter case, a more complex mapping function is fit to the results (e.g., translation offsets) in all the patches. The methods reviewed have all chosen one or both of the above options, ranging from an a priori along-line correction for line-dependent effects (the "high-frequency correction") to a full sensor-to-geobase transformation with subsequent subdivision into a grid of match points.

There is, of course, a correct geometric transformation to apply, but it is unknown (otherwise, an empirical image matching process would be unnecessary); thus, some sort of model must be assumed whose parameters can be solved for by correlation of offset-fitting. Commonly, a portion of the geometric model is established a priori based on external data such as preflight measurements. If that portion is incorporated in an a priori transformation, then the demand for fidelity in the overall model becomes an issue of tradeoffs between the a priori geometric correction and the residual correction to be determined by matching. For example, if one know the geometric transformation is affine with an unknown translation, one might let the image matching function solve for the whole affine transformation, risking the introduction of errors into the affine coefficients, or apply the affine transformation a priori and solve only for translation. Thus, in addressing the various parts of image matching in the following sections, we must also consider their interaction with portions of the overall geometric correction process which otherwise might be regarded as beyond the scope of this paper. The utility of an a priori transformation is also manifested in another way. Data gathered from prior registrations can be used to bias the a priori correction. Such "experience" data might be gathered by

analyzing ensembles of prior registrations such as associated acquisitions (different dates, same scene) or associated geometry (e.g., different subscenes, same frame). Such experience data are then included in the data base.

The following sections logically divide, according to the above precepts, into (1) a consideration of correlation techniques, (2) examination of other matching methods, (3) a discussion of determining the translational offset from the correlation, (4) a consideration of the residual geometric model and how to determine it, and (5) a summary of techniques going beyond the assumption implicit in the previous sections that match points have been established to allow correlation for translational offsets only. Throughout these discussions we make reference to the registration processor recently installed at JSC, note experimental results pertaining to that system as appropriate, and note general limitations and areas deserving further study.

Image Correlation

Suppose that an a priori correction has been applied or patches are defined small enough that any residual geometric error worthy of consideration is pure translation. Matching, then, consists of determining the translational offset of one subimage from another "reference" subimage corresponding to the same scene. The most common form of matching is some sort of cross-correlation technique. The "image" referred to is the actual radiance image or a feature-space image such as an edge or gradient image. In principle the cross-correlation of two acquisitions of the same scene should resemble the autocorrelation displaced by the same amount as one image from the other. Since the peak of the autocorrelation function must occur at the origin, the peak of the idealized cross-correlation then measures the displacement. In practice, the acquisitions differ because of instrument, atmosphere, and other environmental noise and because the scene may have changed appearance due to seasonal, weather, or cultural changes. Thus, the cross-correlation only approximates the autocorrelation, and the peak may not be well-defined. Another argument for the cross-correlation peak measure is that it minimizes the sum-square-difference between the two images. This measure of cross-correlation can be normalized (to be between -1 and 1) by two techniques summarized in Figure 1. The "template matching"[1] alternative utilizes only the pixel values from the search area, whereas the "classical" alternative

utilizes both images. The pixel values indicated are after subtraction of the image means. For binary edge images, whose pixel values are either 0 or 1, rigor fails in the following sense. Strictly speaking, the means of the 0's and 1's should be subtracted before summing; however, considerable gain in computation speed is achieved if the coincidences and numbers of 1's are summed directly.

The correlation techniques just described are employed in several production registration systems. The Master Data Processor (MDP)[2,3], the GSFC baseline system for Landsats 2 and 3, basically performs the "classical" cross-correlation on the radiance image. As a functional equivalent, Fourier techniques are used; that is, the reference and search areas are transformed by the standard FFT algorithm, one of the transforms is multiplied by the complex conjugate of the other, and the result is inverse-transformed by FFT. A slight variance is effected in the denominator by subtracting the local mean (mean over portion of search area overlayed by reference) from the search area's pixels, rather than the mean of the whole search area. The latter is used in the numerator in conformance with the classical formula. The GSFC LACIE Registration Processor[4] employed the template matching algorithm on binary edge images, and the same scheme was used in an evaluation of that processor.[5] Both classical and template matching algorithms are provided for binary edge correlation in the JSC Registration Processor.[6,7] The classical option has been chosen for production processing.

The matching policy discussed above is based on minimizing the sum-square-difference. The sequential similarity detection algorithm (SSDA)[8] is based on minimizing the sum-absolute-difference. However, rather than summing over all pixels, the SSDA selects at random a subset of pixels to sum. Summing stops when a present threshold is reached, and the number of pixels needed for that sum is noted. Then, the correlation maximum occurs at the same point as the maximum of the numbers of pixels required (because the sum-absolute-difference is smallest there requiring the most pixels to reach the threshold). The utility of the SSDA lies in its reduction in computation by utilizing only partial sums whose computational rigor is less, the smaller the correlation is. Thus, the bulk of the computation is devoted to correlation samples showing promise with little effort wasted on low values. The SSDA was also used[9] this time on the

radiance images, in the performance evaluation of the GSFC LACIE Registration Processor. The correlation was normalized by dividing the pixels of each image by their standard deviation before correlating.

The design of the SSDA illustrates a primary concern in standard cross-correlation, viz diminishing the number of required computations. In general, methods to address that issue have focused on devoting the bulk of the computations to the region around the appropriate extremum. Such a method, well-suited to binary edge correlation, was used in the GSFC LACIE Registration Processor[4] and for coarse acquisition in the JSC Registration Processor. First, cross-correlation is done only for offsets every fourth row and every eighth column. The mean and standard deviation of the results are computed, and thrice the latter is added to the former to generate a rejection threshold. Next, an approximate correlation is computed at every offset but with only pixel values from every third row and third column included in the sums in Figure 1 (thereby reducing the computation by about a factor of nine). If, at a given displacement, the resulting approximate correlation value exceeds the rejection threshold, the sums are repeated using every pixel value. In binary edge correlation the peak is generally fairly sharp, and only a very small fraction of the correlation samples exceed the threshold, thereby sparing a considerable amount of computation. This method, used for a segment-level correlation (8 x 10 km portion of a Landsat MSS frame), proved very effective in the GSFC and JSC Processors.

The foregoing discussion assumes the geometric difference between the compared patches is pure translation. This assumption may not be valid, which raises the question of how geometric distortion (other than translation) affects the cross-correlation function. The effect has been studied for standard cross-correlation (i.e., for minimizing the sum square difference) where one patch is distorted linearly (rotation, scale change, shear distortion) from the other.[10,11,12] The results indicate that linear distortion effectively blurs the cross-correlation function by applying a running average over the ideal nondistorted counterpart, where the dimensions of the averaging filter are proportional to the degree of distortion. This conceptual averaging does not apply to the noise present, so that the signal-to-noise ration (SNR) is effectively reduced. Also, the area around the peak is effectively flattened somewhat, making the peak search less accurate, and the peak-to-background (or peak-to-sidelobe) ratio is distorted

(these subjects are discussed in a subsequent section). The magnitude of these effects is greater, the greater the patch size, because the geometric distortion becomes larger. Thus, choosing a smaller patch decreases the effects of geometric distortion, but the SNR is also decreased with fewer pixels. Some compromise is generally required, as is discussed in a later section.

The effects of geometric distortion on binary edge correlation could be drastic in certain cases. For example, a scale difference might prevent overlaying edge features on opposite sides of a patch at the same time. Thus, rather than smearing the correlation function, as described above, it could divide into several peaks. This kind of problem has not been identified in typical patch correlation, but it has been suspected of degrading the full sample-segment correlation used in the GSFC LACIE and JSC Processors. One solution to the problem (at least for coarse correlation) might be to resample the images to a coarser grid by use of a low-pass or median filter before edge detection. Then, the geometric distortions are reduced relative to the pixel spacing or, equivalently, effective edge "thickness."

Other Techniques for Image Offset Matching

Several other matching techniques, though not yet implemented in large-scale registration, deserve mention as potentially applicable. The Cluster Reward Algorithm (CRA)[13] conceptually analyzes the bivariate histogram of the two images at each displacement. A measure is established characterizing the definition of pattern in the histogram, e.g., a measure of clustering. At the offset denoting an image match the histogram should show a relatively high image-to-image correlation by exhibiting clusters. The technique has been applied to several sample-segment-size (about 8 x 10 km) scenes with notable success.

The point-matching technique[14,15], though designed primarily for target arrays such as star fields, might find application to binary edge images. The method minimizes a geometric distance measure between points (say, edge pixels in the two images) rather than minimizing radiometric or feature differences. A variation[15] of the method ascribes weights to the point-pairs according to how well they associate in the matching. This technique is iterative with first

a matching, then a comparison of the distance spanned by each point-pair to the estimated common displacement for assigning a weight, then a weighted match, etc.

The use of normalized cross-correlation for minimization of sum-square-differences or sum-absolute-differences described in the previous section can also be viewed as an application of maximum-likelihood classification in which the measurement sets are distinguished by translational offset (analogous to pixel number in spectral classification), the channels of information are the pixels in the search overlay area (analogous to the bands in spectral classification), and the classes are Match and Non-match (analogous to classes, e.g., crop species, in spectral classification). In the spatial case, however, it is known a priori that only one measurement set should be classified as a Match (if the match scene is unique) corresponding to the single correct translational offset. Analogous to spectral classification a Bayes technique has been applied[16] to spatial matching. The probability of misacquisition (match lock-on to the wrong point), expressed as the Bayes risk is minimized by maximizing the a posteriori probability of a correct match (i.e., the probability that there is a match at an offset, given the particular pixel values in the overlay region for that offset). The a posteriori probability is estimated in principle by least squares by assuming it is a linear function of the pixel values. In fact, that probability should exceed 1/2 only at the match offset which provides a direct means for identifying a probable misacquisition (a posteriori probability never exceeds 1/2). The method is conveniently implemented by Fourier transformation techniques. The a posteriori probability, though assumed linear in the pixel values above, can be expressed as a linear combination of any functions of the measurements, as deemed appropriate to the application. The case of a second-order relation has been investigated[17], and trials on synthesized data indicate improvement over the maximum likelihood alternative offered by cross-correlation.

The methods described in this section should be considered as new candidates for interimage matching. They must be integrated with the various feature selection methods (e.g., the Cluster Reward Algorithm makes no sense with binary edge images, while the point pattern matching technique is especially suited to such images). The methods should be tried on a representative set of sensor data and evaluated for applicability to different sensor types, scene types, season, sensor-to-sensor differences, etc.

Offset Determination

The cross-correlation techniques for image matching presumes that the position of the maximum or minimum of the correlations or difference function characterizes the translational offset between the two images. The true offset might be in between pixel centers so that the correlation peak lies between correlation samples. To achieve subpixel accuracy in a given patch, some form of interpolation is needed. Several alternatives have been developed, as we discuss in this section. These techniques lend themselves to estimating the accuracy of peak location and to evaluating certain measures for establishing pass/fail status, and we address this subject also.

As an alternative to peak interpolation for subpixel accuracy, a number of patches can be defined, the peak can be determined to the nearest sample, and the subsequent mapping function fit to the numerous peak offsets can be relied upon to yield subpixel accuracy. This approach is predicated on the assumption that a random position error is introduced by choosing a sample position rather than interpolating. This method was used in matching images produced by the GSFC LACIE Processor for the purpose of evaluating the performance of that processor[5,9]. Secondary peaks were also identified and compared to the primary peak. A measure of decline away from the peak was established in terms of averages of correlation samples in concentric rings extending out from the peak. If the peak was not strong enough relative to the secondaries or the decline was too shallow, that zone was rejected in the mapping function fit.

A straightforward means of interpolating for the peak consists of fitting a surface function to the cross-correlation samples in the vicinity of the peak and evaluating the peak location analytically. The MDP and JSC Registration Processor[6,7] use a bivariate polynomial (i.e., containing terms $x^M y^N$, $MN \leq$ polynomial order). The MDP uses a fourth-order polynomial on a 5 x 5 neighborhood around the peak and also evaluates the curvature at the peak as a measure of the breadth of the correlation peak. The smaller the curvature is, the larger is the uncertainty in locating the peak. The MDP uses the minimum curvature on the surface and the height of the peak as rejection criteria.

The JSC Registration Processor allows any order polynomial up to and including fourth order, but the latter has been used mainly, with the lower orders being studied[18] for applicability. The fit neighborhood size can also be varied[18], but a 5 x 5 has been used in production. The peak is located by the use of the MDP algorithm, and the curvature matrix is used, in lieu of the curvature itself, in a variational approach to express the peak uncertainty covariance in terms of the covariance of uncertainty in the polynomial fit coefficients. Since the bivariate polynomial is fit by least squares, the coefficient uncertainty covariance can be estimated from the fit residuals. Often, relatively few points are fit, compared to the number of coefficients solved for (25 points for a 5 x 5 neighborhood, as compared to 15 coefficients for a fourth-order polynomial), and little confidence can be placed in the uncertainty estimate. To circumvent this problem, the user may supply an a priori fit variance of the fit uncertainty rather than determining it from the residuals. The a priori variance can be established by tests on representative data, whereby the a priori variance can be adjusted to make the estimated peak uncertainty agree with the observed peak displacement errors. Preliminary tests[18] established a value for early production in the JSC Registration Processor. A peak-to-background ratio is also established by subtracting from the correlation peak value the mean of samples away from the peak and then dividing by the standard deviation of those samples. The subtraction was included to compensate for the fact that the edge image means are not subtracted out in binary edge correlation.

Rather than establishing the order of the bivariate polynomial a priori, successive orders could be tried and the RMS residuals compared. When that error falls significantly and then starts tapering off, whatever order has been used at that point is adopted as the fit. As an attempt to sidestep the issue that a good model of the cross-correlation is not really at hand, this approach follows the rationale that a good representation lies somewhere between a simple model and a fit, with no remaining error, to every point, as a sufficiently high-order polynomial would do. Choosing an intermediate order, as outlined, attempts to balance a lack of understanding of the general form of the cross-correlation function with the knowledge that errors do exist in the data which makes forcing a perfect fit unwarranted. This problem of model uncertainties is encountered again in the section dealing with the mapping function.

Functions other than a bivariate polynomial can be fit to the cross-correlation samples. A bivariate gaussian function is an obvious choice; however, its use has not come to our attention. One registration application[19] chose an elliptical cone. The orientation of the cone was also a solution variable. Although surface fitting has been the commonest method of peak interpolation, it is by no means universally accepted. A principal criticism with that method involves the sensitivity of the intersample peak location to the particular form of the fitting function.

As an alternative to surface fitting, the peak can be assumed to lie at the centroid of the correlation neighborhood[20]. That is, the peak location is computed as the weighted sum of neighboring sample locations, with the correlation values serving as weights. Analogous to the peak uncertainty or surface curvature mentioned earlier, a corresponding measure of the breadth of the peak can be computed as the moment of gyration[21] or simply as the second moment of the correlation distribution (just as the centroid is the first moment). Unfortunately, little more can be said about this method at this time. It would be interesting to compare the centroid and surface fit methods for a representative set of correlation sample arrays.

Another method of peak location takes advantage of cross-correlation by Fourier techniques. The offset in the spatial domain corresponds to a non-vanishing phase in the frequency domain. In fact, if the cross-correlation function were symmetric about its peak, the phase function would directly specify the offset (since phase introduced by non-symmetry would vanish). One approach[22] transforms the phase portion of the correlation transform back to the spatial domain wherein the peak is located. The spatial result was noted to resemble closely a delta function so that subpixel peak location seems viable. The peak location was facilitated by using the inverse transform operation directly to compute a finer grid of spatial samples around the indicated peak than would normally be obtained from Fast Fourier Transform (FFT) algorithms. If indeed the transformed phase function is consistently nearly a translated delta function, then in the frequency domain the phase should be proportional to the spatial displacement. Thus, the phase vs frequency points can be fit by a straight line forced to pass through the origin, and the slope gives the translational displacement. However, somehow the possibility of non-symmetry may need to be accounted for. Preliminary results[18] have shown that binary edge correlations, for example, do exhibit nonsymmetry.

This section closes by returning to the issue of estimating peak location uncertainty or sharpness. The schemes described above can be categorized basically into curvature at peak, second moment of correlation samples around peak, and rate of decline away from peak. Any of these sharpness measures can be used to compare with a rejection threshold or to construct a weight for use in the mapping function fit. In the latter case the weight would be lower, the broader the peak lobe is. The weight is given directly by a peak uncertainty estimate (as the inverse of the uncertainty covariance). As mentioned earlier, a fixed a priori surface fit variance should probably always be used to estimate the peak uncertainty when fitting bivariate polynomials so that effectively its variance is directly related to the curvature. The sharpness measures can also be computed for the autocorrelation function to give an idea of the intrinsic clarity of the image. This application has been implemented as well in the JSC Registration Processor.

Residual Mapping Model

If the approach of the previous sections has been adopted, viz. local translational mismatches are determined at an array of control points, some means is needed to distribute the corrections for those mismatches over the regions in between the control points. Toward that end, a geometric transformation function is to be formulated in terms of the measured displacements. The nature of that function depends upon one's confidence in the measured mismatches versus one's understanding of the geometrical or physical processes causing the mismatch. If the control point translations are expected to contain errors, and the nature of the geometric distortions is well understood, then some sort of error minimization or maximum likelihood estimation technique is utilized. On the other hand, if the data are highly trusted and the model is unknown, some form of "rubber sheeting" technique is employed (analogous to curve-smoothing in one dimension). These alternatives are addressed below. The case that the model is understood is discussed first, with a breakdown into a geometry-based model (e.g., platform attitude error, trajectory error, etc.) and a sensor-based model (e.g., scan irregularities, band-to-band offsets, etc.). Then, the rubber sheet approach is considered. If uncertainty is associated with both the measurements and the model the attack is not so clear. This situation is considered briefly along with the situation that some measure of confidence in the model is available and the control point data are being used to improve it. It is well established that cross-correlation will occasionally result in an erroneous translational offset, and if such an error goes undetected it can ruin the mapping fit. The section ends with a description of several methods for identifying and handling such outliers.

Geometric errors are generally modeled as time varying satellite attitude and altitude errors. The MDP[3] assumes for MSS processing that the Landsat yaw, pitch, and roll can be modeled as third-order functions of time over the dimensions of a double frame (about 340 km of downrange). Similarly, the altitude variations are modeled as linear in time. The resulting 14 coefficients are solved for by weighted least squares utilizing both control point offsets and the less-precise attitude/altitude data available from Landsat's attitude measurement system (AMS) and ground tracking. The weights are set up a priori based on past experience in control point location accuracies and in AMS and

ground tracking accuracies. Hence, the control point weights are considerably larger than the others so that if many control point offsets are utilized the solution is essentially based on them. However, if few or none are available the AMS and ground tracking data do contribute appropriately to the solution. To handle the fact that the AMS data are poor for estimating the constant portion of the model (biases), a scheme is implemented to allow devoting the control point data to estimating the attitude biases, while the other measurements are utilized for rates and higher-order coefficients. Nominally, this scheme is employed only if a very few control points are available. Also, the attitude biases from a good solution (one with control points) are carried over to the next frame if that frame has insufficient control points (nominally, less than two). A weight associated with that carry-over is propagated in a manner that makes it decay with time, in order to model the growth in uncertainty of the biases as the satellite moves further away from the estimation point. This whole approach is predicated on the measurement errors being normally-distributed, an assumption which breaks down if one or several of the control point offsets are erroneous. To overcome that problem, the MDP has been tested with the threshold number of control points for triggering the bias estimation scheme raised to 15 from the nominal value of unity.[23] Hopefully, such a large number of control points will contain enough good offsets to overwhelm any erroneous ones. Another approach to eliminating the outliers is discussed later.

A TRW study[24] has adopted the same model as the MDP except for assuming a constant altitude deviation. The coefficients were evaluated by Kalman filtering. ERIM's geometric correction process also models the geometric errors as yaw, pitch, and roll, with pitch and roll assumed linear and yaw assumed constant over the area of interest.[25]

The GSFC LACIE processor models the geometric error (after the more-complicated a priori transformation) as pure translation over the dimensions of its 8 x 10-km sample segments. Performance evaluation[5,9] of that system indicated that, although specifications were met, there was a residual error that appeared to be affine. Thus, the JSC Registration Processor has adopted an affine model. A weighted least squares solution is made in which the weights are the reciprocals of the peak uncertainty standard deviations estimated from the correlation surface fit. At user option, default weights can be substituted if the correllation

surface fit fails in its estimation process, or weights can be eliminated altogether. A preliminary evaluation[26] of the JSC Processor has indicated that an affine model is adequate; that is, observed residual distortion does not show any systematic effect associated with an incomplete geometrical description. The success of the affine model lies in the fact that the JSC Registration Processor is only removing residual distortion left by the MDP. The a priori geometric correction has taken care of map projections, sensor geometry, and sensor line effects as characterized by the MDP data (a priori modeling constants and attitude/altitude solution).

Sensor effects can also be modeled and solved for by use of the acquired scenery. Alternatively, they can be assumed static, determined from a priori data, such as laboratory or flight tests, and then used in the a priori geometric correction. Landsat MSS effects include scan nonuniformity, band-to-band offset, "staircasing" caused by simultaneity of six scan lines, and line-by-line offsets due to sampling delays and changes in scan speed. The MDP, GSFC LACIE Processor, and JSC Registration Processor all assume a static model for those effects. All effects are assumed constant, except for the scan speed and scan nonuniformity. The latter is modeled as a third-order polynomial in position with the line (i.e., sample number). The coefficients were determined prior to implementation in the registration systems. The scan speed is assumed to have a fixed relation to the number of samples actually obtained in a scan line (line length majority). Although this model seems fairly good in normal circumstances, it breaks down for Landsat 3 when the MSS sample initiation fails (the "late line start") because the correct line length majority is not available. A model has been installed in the GSFC processing line to estimate the line length majority from the number of samples in the partial line. The resulting line length majority is used by both the MDP and the JSC Registration Processor. An inaccurate line length majority is manifested as a line jitter over portions of the image, and indeed a jitter is sometimes apparent as irregular field boundaries in some Landsat 3 agricultural scenes (especially at lower lattitudes where field boundaries tend to be parallel to lines and columns of pixels). An error of one in the line length majority will result in a misregistration of up to one pixel or about 58 m in MSS imagery. The possibility of variations in scan nonuniformity can also not be ruled out as the cause. These anomalies merit further investigation. Techniques for line-to-line registration to straighten field boundaries should be

considered, if for no other purpose than clarifying operational scan characteristics.

The sensor geometrical model for the Landsat RBV is considerably simplified by the presence of reseau marks on the face of the Vidicon tube. Also, the satellite attitude model is simplified by the fact that a whole frame is gathered at one instance, hence, for one value of roll, pitch, and yaw.

The rubber sheet approach to geometrical modeling assumes the form of the model is poorly understood. Whatever is the correct model, it should be possible to express it as a bivariate polynomial (e.g., assume a Taylor series). Thus, a common rubber sheet technique fits a polynomial to the array of control point offsets. The JSC Registration Processor and the GSFC Digital Image Rectification System[27] can utilize polynomials, the former to fourth order and the latter to second order. The principal concern is generally what order to use, although omission of certain terms may also be considered (such as sample-dependent terms if distortions seem to be from line to line). A sufficiently high order will fit all control points with dubious results in between. If the points are known rigorously to contain no error, then fitting all the points is reasonable, and the problem becomes one of selecting an interpolating function with suitable behavior between the points. Generally, the control points are assumed to have errors so that fitting them rigorously at the risk of inter-point error is not particularly suitable. A compromise is often achieved by trying a progression of successively higher-order polynomials and tracking the decrease of the error, expressed as the RMS of fit residuals. Assuming the idea that lower order is better for inter-point behavior, the fit is chosen for which the error has dropped substantially from lowest order but for which little error reduction is apparent at higher orders.

Another rubber sheet approach effectively spatial-filters the "sampled" offsets at the control points, thereby distributing the offsets over areas between the control points. This approach parallels the reconstruction of a two-dimensional analog signal from its samples by cubic or sinc convolution. The filter might be derived from maximum likelihood considerations such as a Kalman filter. This approach might be reduced to any desirable scale by reducing the size of control points while increasing their density so that a fairly

high-frequency matching process could be designed. When sensor resolution becomes good enough, atmospheric turbulence will be discernible as high-frequency distortion for which such a high-frequency geometry-matching filter would be appropriate.

Sometimes, the model may be partially known before control point information is acquired; that is, a priori values for the model parameters are available with an associated covariance characterizing the level of confidence. Then, the control point offsets provide additional information which can be used to improve the estimates of the model parameter. A Bayes approach is utilized. Simply stated, a least squares solution is performed on the control point offsets, and a weighted average of the results with the a priori estimate is computed. The weights are the inverses of the respective covariances normalized by matrix premultiplication by the inverse of the sum of the covariance inverses. This approach has been implemented in the JSC Registration Processor to account for the fact that it follows the MDP. Since the MDP has already geometrically corrected the data, the a priori values for the residual mapping function are zero. The covariance of the MDP's attitude/altitude solution is provided, and, after transformation to the covariance of a local (8 x 10-km sample segment) affine geometrical model, it serves as the a priori covariance. The JSC Processor performs its own least squares solution and utilizes its and the a priori covariances to average its solution with zero (the MDP's value). The appropriate expressions are summarized in Figure 2. Effectively, the result down-weights the JSC Processor's solution according to the size of the MDP covariance, with greater attenuation the smaller the MDP covariance. It must be borne in mind that all this theory is predicated on the MDP's and JSC Processor's error sources being normally-distributed. A crude compensation (shrinkage) is provided, as shown in Figure 2, in case they are not normally-distributed.

Unfortunately, control point correlations tend to either work reasonably well, or they are very bad. Thus, unless false fix detection is very good, erroneous control point offsets will be interspersed among the good ones. One straightforward approach to eliminating the outliers simply compares the residuals after the least squares fit to a preset threshold, or a threshold scaled by the estimated covariance. This technique was used in the GSFC LACIE Processor evaluation[5,9]. Control points with residuals greater than three standard deviations

were discarded, and the least squares solution was repeated. The new residuals were again tested, and the procedure was repeated until no more failures were noted.

Another approach performs a least squares solution with one control point omitted. Similarly, another solution is made with the first control point returned but a second omitted, and the process is repeated to yield as many solutions as there are control points. The post-solution residual for each omitted control point may then be examined for rejection, or a weighted combination of all the solutions may be made, with the weights related to the post-solution residuals.

Finally, a robust estimation[28] technique can be utilized in which the control point error is assumed to come, not from a normal distribution, but from a distribution with long tails which characterize the possibility of "outliers." Just as least squares is a maximum likelihood estimator for a normal distribution, maximum likelihood estimators can be formed for other longer-tailed distributions. A number of such solution techniques exist.[28] They down-weight measurements with large errors, while sacrificing a small amount of efficiency (i.e., not being quite as good as least squares) when the measurement errors really are normally-distributed. To our knowledge, none of these techniques have been explored for image matching.

Sizing and Placement of Control Points

The method of inter-image comparisons reviewed here involve the distributing of a number of patches within each image (the reference image and the registrant image). The patches are chosen small enough that the inter-image shifts within them may be considered to be purely translational; that is, scale, skew, and other interimage distortions have negligible effect when compared to the translation, viewed on the scale of the patch. Translation we will regard as zeroth order, amounting to a constant bias in the functions that relate coordinate values in one image to coordinate values in the other. Similarly, scale, rotation, and skew are first order distortions, and keystoning, etc., are higher order. In the zeroth order, coordinates $\underline{x}$ in the reference image and $\underline{y}$ in the registrant image are related

$$(x_i - y_i) = b_i \quad ,$$

while to first order they are related

$$(x_i - y_i) = \sum_j a_{ij} y_j + b_i \quad .$$

So, it is seen that the above description of the order corresponds to the order of the polynomial in the equations relating the coordinates. The essence of registration is to specify the mapping between the reference and registrant images, which is done in either "rubber-sheeting" form or by modeling. The latter uses rigid descriptions of the sensor geometry to permit an economy in describing the interimage coordinate relationship. So, rather than describing the coordinate relationship in the form above, coefficients are often drawn that relate the coordinates through platform ephemerides and known sensor geometries. This section interrelates with the previous one via economic and accuracy considerations; an optimum mapping method will require the fewest control patches to establish the desired degree of accuracy, since there is a high cost per correlation patch.

Number, location, and size of the patches used for control points is a very important consideration in the design of a registration system, from both economic and accuracy standpoints. A large part of the registration computation load is proportional to the number of the patches and to the second power of the patch dimension, so it behooves one to minimize the number and individual size of the patches. At the same time the interaction of the spatial distribution of the patches with the remapping model will affect the accuracy of the registration; so the location of the population of patches is a consideration to be combined with their number. One patch gives a single estimation of the translational correspondence between the images in the vicinity of the patch. If it be assumed that errors are not systematic in the estimation of that translational correspondence, more patches (in a neighborhood) are better in that the errors will tend to cancel. However, although there is no conceptual difficulty with having patches overlap, there is a limit to the number of functionally independent patches that can be drawn from any image. That number puts an upper limit to the tendency for growth to larger number of patches in order to have statistical cancellation of errors.

There is a tradeoff in the determination of the optimum size of a correlation patch that is dependent on the accuracy with which the a priori corrections can account for the encountered misregistration. Consider first a purely translational misregistration. As the size of the patch gets larger, there is more picture structure within it; although the value of the correlation peak is not affected, at translational locations off the peak there will be (generally) lower cross-correlation values due to the larger amount of structure within the window. The result is an enhancement of the peak-to-background ratio (the value of the peak correlation divided by the correlation in the general vicinity), enabling increased sensitivity in detecting a peak and perhaps increased accuracy in determining the location of the peak.

Now, however, consider the ramifications of first-order departures from the condition in which there are only translational offsets between the images being registered (i.e., suppose there are skew and scale differences as well as translation). In the position in which the true centers of the patches being correlated are coincident (that is, the position one would want to find as a result of the cross-correlation process), picture structure towards the edges of the patches will be relatively displaced by scale and skew differences. In contrast to the translation-only situation, the correlation in this case is reduced as the size of the image is increased. But the presence of effects other than translational offsets does not mandate the use of the smallest possible patch--one pixel!--because the correlation is at its noisiest there. For a binary extracted feature on which correlation is being done, the correlation takes on only the values zero or one for the one-pixel patch, and it would be impossible to locate a peak. So one determines an optimum patch size by considering a reasonable envelope for the distortions (beyond translational) that one expects, and works out the spatial range over which they would cause significant displacements for the translationally-correct position.

Where appropriate by necessity of increased registration accuracy, a reentrant technique is possible. In that technique, patches of the original images are extracted and run through the correlation process. The resulting remapping for the whole image is then used to reextract the correlation the correlation patches, which can now be at least first-order corrected for the modeled distortions. The patches are extracted from the input imagery by

resampling onto a grid derived from the first registration process, and consequently larger patches, with potential for increased accuracy, may be drawn. The cost of such a reentrant technique is not necessarily to double the computation time, inasmuch as a coarser registration job is enabled for the first pass.

As mentioned earlier, the strategy for location of the correlation patches is important. In the case of the MDP, there is a scattering of patches amounting to approximately 0.1% of the scanned area (say 10 patches of 32 x 32 pixels within a frame of 3596 x 2983 pixels). In order for this small a correlated area to control the overall registration accuracy to an acceptable level, the patches must be located efficiently so as to exercise reasonable control over the entire image. Further, the modeling of the scanner behavior between control points becomes of paramount importance. In the other extreme, the JSC Registration Processor actually uses something over 100% of the area of the registrant image, when it is taken into account that the patches overlap slightly (about 7 pixels/line).

The registration of two images logically breaks into two philosophically different kinds of operations--the determination of the mapping of the coordinate grid of the reference image into the coordinates of the registrant image onto that remapped grid of the reference image. The mapping process is guided by the selection of patches within which interimage comparisons give the local estimate of the mapping (typically just the translational characteristics are determined on an area small enough that translation is the dominant effect over the size of the patch). Since considerable computation effort goes into the interimage comparisons done on the patches, and since the accuracy of the overall registration depends linearly on the accuracy with which a single patch is compared between images, and also since the model, usually driven by the translational offsets determined at the patches, will be more tightly and accurately determined with a "sufficient" number and distribution of patches, it is very important that the following qualities are achieved in the location of the control patches.

1. The comparison method allows an accuracy of interimage comparison at least as good as the registration accuracy desired for the whole process. Otherwise one must use a superfluity of control patches and hope that they

contribute independent measurements, with error cancellation, to the remapping model.

2. The model being driven by the control patches is sufficiently highly detailed to account for the entire behavior of the relative geometry in between control points.

3. The locations of the control points are chosen to interact sensitively with the modeling geometry. For example, if a sinusoidal component to the interimage geometry is hypothesized, one would not want control points (the centers of the patches) placed at uniform one-period separations within the image. If they were, aliasing would have the result of a sinusoidal relative geometry look the same as a translational offset.

This section discusses some aspects of location of control points (taken as the centers of their control patches).

Let the registration of Image 1 to Image 2 be defined as the mapping of the coordinates (i,j) in Image 1 to the coordinates (k,l) in Image 2 (i.e., we will do only the geometric portion of the problem).

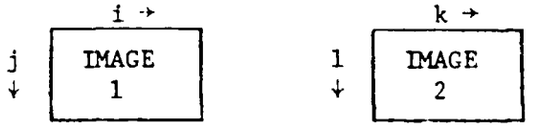

Suppose the "true" relationship is given by F_1 and F_2

$$i = F_1(k,l) \qquad j = F_2(k,l);$$

let them be estimated as a result of the interimage correlation and modeling by

$$f_1 = \hat{F}_1, \qquad f_2 = \hat{F}_2 .$$

Then the root-mean-square registration error (RMSE) is

$$\text{RMSE} = \sqrt{\frac{1}{\text{area}} \iint_{\text{image}} [(F_1-f_1)^2 + (F_2-f_2)^2]\,dA}$$

where $\iint_{\text{image}}$ is the integral over the area of the image, and various assumptions are included regarding orthogonality of the coordinate axes, sameness of scale on those axes, etc. Further, suppose the mapping f_1 and f_2 to be derived according to some sensor/platform model, or according to other limitations on the complexity such as a mapping of no higher order than affine, and that the mapping f_1 and f_2 is determined by a finite number of control points within the images. If the images are not initially pathologically misregistered, we may reasonably express the mapping by beginning with the simplest of mappings,

$$f_1(k,l) = k \ , \qquad f_2(k,l) = l$$

and then include the deviations g_i,

$$f_1(k,l) = k + g_1(k,l), \qquad f_2 = l + g_2(k,l).$$

This slightly complicates the expression for RMSE but facilitates the analysis of sensitivity with respect to control point location. Translational offsets are written

$$\begin{aligned} g_1(k,l) &= a_o \\ g_2(k,l) &= b_o \end{aligned} \quad ;$$

affine mappings have the general form

$$\begin{aligned} g_1(k,l) &= a_o + a_1 k + a_2 l \\ g_2(k,l) &= b_o + b_1 k + b_2 l \end{aligned} \quad ;$$

keystoning is modelable by the inclusion of a cross term,

$$\begin{aligned} g_1(k,l) &= a_o + a_1 k + a_2 l + a_3 kl \\ g_2(k,l) &= b_o + b_1 k + b_2 l + b_3 kl \end{aligned} \quad ,$$

etc.

We consider a control point established between the images. Let $\underline{t}(k_1 l)$ be the derived estimate of the "true" offset between the images, and let Σ be the estimated covariance of the estimate $\underline{t}$.

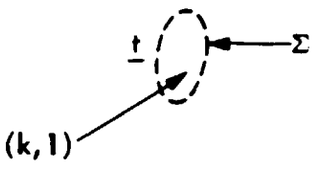

By a method unspecified here (so as to preserve generality), the set of control points {km, lm, $\underline{t}$m, Σm} is then used to generate the mapping functions g_1 and g_2. Let us make some simplifying assumptions:

1. The method of obtaining g_1 and g_2 will work with any number of control points (e.g., no control points gives g_1 and g_2 identically zero, one control point allows a translational solution, etc.).

2. The method of obtaining g_1 and g_2 is tractable to linearization.

3. A priori estimates of Σ are available (they might be in the form

$$\Sigma_{ap} = \text{diag}(\sigma_1^2, \sigma_2^2) \text{ or } \Sigma_{ap} = \sigma^2 I \ .$$

4. The a priori estimates of Σ are independent of location.

5. The a priori estimates of g_1 and g_2 are zero. (Otherwise the image could be adjusted according to the a priori estimates so that this would be true.)

We are now in position to find the sensitivity of the mapping functions g_1 and g_2 to the location of a single control point, that sensitivity being a function of location of control point in the reference image and of location in the registrant image. The sensitivity can be converted into an rms value by integration over the registrant image, as will be seen, and thus an ideal location of the first control point is specified.

Defining $\underline{y} = \begin{pmatrix} i \\ j \end{pmatrix}$, $\underline{x} = \begin{pmatrix} k \\ l \end{pmatrix}$, we have used the set $\{\underline{x}, \underline{t}, \Sigma\}$ to produce the (vector) function $\underline{g}$ such that

$$\underline{y} = \underline{g}(x) + \underline{k}.$$

The fact that the variation in, say, the first coordinate of $\underline{y}$ is given by

$$\delta y_1 = \frac{\partial g_1}{\partial x_1} \delta x_1 + \frac{\partial g_1}{\partial x_2} \delta x_2$$

leads us to the vector variation in $\underline{y}$

$$\delta \underline{y} = \underline{\underline{J}} \, \delta \underline{x} \ ,$$

in which $\underline{\underline{J}}$ is the Jacobian matrix

$$\begin{pmatrix} \frac{\partial g_1}{\partial x_1} & \frac{\partial g_1}{\partial x_2} \\ \frac{\partial g_2}{\partial x_1} & \frac{\partial g_2}{\partial x_2} \end{pmatrix} \equiv \underline{\underline{J}} \ .$$

The covariance in $\underline{y}$ is calculated from Σ_x, the covariance in $\underline{x}$, as follows.

$$(\delta\underline{y})(\delta\underline{y})^T = (\underline{\underline{J}}\,\delta\underline{x})(\underline{\underline{J}}\,\delta\underline{x})^T$$
$$= \underline{\underline{J}}\,\delta\underline{x}\,\delta\underline{x}^T\,\underline{\underline{J}}^T \ .$$

Taking expectation values, and assuming that the expectation of $\delta\underline{x}\,\delta\underline{x}^T$ is as estimated from the considerations of the cross-correlation surface for the point,

$$\Sigma_y = E\{(\delta\underline{y})(\delta\underline{y})^T\} = \underline{\underline{J}}\,E\{(\delta\underline{x})(\delta\underline{x})^T\}\,\underline{\underline{J}}^T$$
$$\Sigma_y = \underline{\underline{J}}\,\Sigma_x\,\underline{\underline{J}}^T$$

which will be a non-constant function of $\underline{y}$ inasmuch as the partials forming $\underline{\underline{J}}$ are not constant. The trace of Σ_y gives, as a function of $\underline{y}$, the squared registration uncertainty. We can average over the image and take the square root.

$$\text{RMSE} = \sqrt{\frac{1}{\text{area}} \iint_{\text{image}} \text{tr}\,\Sigma_y \, dA} \ .$$

Alternatively the trace can be taken after integration (the operations communite):

$$\text{RMSE} = \sqrt{\frac{1}{\text{area}} \text{tr}\left(\iint_{\text{image}} \Sigma_y \, dA\right)} \ .$$

Note that the RMSE so calculated is a function of $\underline{x}$, the location of the first control point. If a priori values for Σ_x and $\underline{t}\,(\underline{x})$ are used (the latter being zero), we have an a priori estimate of the sensitivity, measured in terms of coordinates in the image, as a function of location of the first control point. Fixing the location of the first control point at the location that minimizes RMSE, then an exactly similar procedure leads to the location of the best place to position the second control point. The RMSE should monotonically decline as the number of optimally-placed control points increases, and the system designer can quit adding control points when the anticipated accuracy has gotten to requirement level.

It is true that the placement of n control points by this technique will (probably) not produce as good accuracy as n points placed optimally as an ensemble. The algorithm for determining that optimal ensemble position, however, is a substantially more complicated one. The following relaxation technique is such an algorithm. The n points are placed according to some scheme in the image, and RMSE is calculated in the general manner as described above. The position of the first point is permitted to vary about its original location, and RMSE is observed; the location is altered until a minimum of RMSE against first-point-location is found. Then, the second is allowed to vary, and its minimum location found. Similarly through the set of n control points, and the procedure is iterated for all the control points again until each point is at a minimum. But, even this relaxation technique guarantees only a relative minimum, for small deviations of control point location. The sequential technique is likely to require more points to achieve a given level of anticipated accuracy than the minimum number meeting the requirements with the relaxation technique, but the sequential technique is, as mentioned earlier, more tractable.

This problem, optimizing locations of control points, is analogous to the statistical problem of selecting a set x_i at which to evaluate the associated set y_i, the combination to drive a regression between x and y. It has proven more practical to select an oversupply of x_i's and drop members one at a time according to a utility criterion, until the required performance would fail if any further members were dropped. A practical scheme for location of control points could proceed similarly.

All too often, a desired control point location, even with the allowance of small deviations around it, will not contain picture structure to permit sufficiently accurate cross-correlation. The strategy for control point location should be robust against failure to find proper structure at a subset of the ideal control point locations. An iterative scheme is envisioned, in which that failure would send one back to the image to obtain another set of control points.

These techniques seem clearly impractical for one-shot application. The amount of time spent in the computations could better have been spent in getting on with the registration problem by casting an overkill of control points into the image, and just proceeding. The application for such techniques is in a

production environment, where the fewest control points with the most advantageous effect is desired. Using the remapping model and the a priori estimates of the covariance, a general optimal strategy for control point location is drawn. The covariance estimation is done either entirely without prejudice ($\Sigma_{ap} = \sigma^2 I$), or if a large number of images are to be registered against a single base image (as in the authors' case, multitemporal agricultural images of certain ground areas), that base image can be investigated for the estimations of Σ.

To the authors' knowledge, this sort of optimal placing of control points has not been done. The MDP uses hand-picked control points with control in any given frame of Landsat data coming from not only that frame but from adjacent frames as well. In the LACIE Processor[4], there was essentially only a single point, the entire image; translational registration alone was done, with nearest-neighbor resampling following translational correlation done on whole-segment basis. An experiment[19] associated with the LACIE Processor utilized five control points placed at the corners and center of the image. In the DAM Package[30], manual control points are selected with admonishments to spread them out well in the image being registered. In the JSC Registration Processor[6,7], the control points are placed on a uniform grid, the patch size and spacing relating so as to cause overlap. In the "automatic" registration system[31] for the LACIE ground truth segments, control points are initially placed on a uniform grid, with small deviations allowed in order to find a suitable correlation peak. In all the processors with which the authors are familiar, it has been the practice to follow one's instincts rather than to code in a sophisticated patch location algorithm. The success of those processors indicates the efficacy of the less-elaborate methods, but it remains possible to make algorithmic improvements to permit sufficient accuracy with minimum computation load.

Non-Control Point Methods

The previous sections dealt with the step-wise manner of first matching images within local patches or control points and then fitting the full mapping function to the resultant array of point-shifts. Although the complexity of straightforward multidimensional correlation (say, in translation, rotation, scale change, etc.) generally makes it prohibitive, a fortuitous property of affine distortions under Fourier transformation has given rise to such a method[32]

which may show promise. It is shown that even with affine distortions (i.e., rotation, scale change, and skew or shear distortion, in addition to pure translation) the translation maps into a phase factor in the frequency domain, and the modulus of the transform function exhibits a similar, affine distortion. This fact, coupled with the fact that typical agricultural scenery shows considerable spatial structure, facilitates the use of Fourier transforms for matching in an easier way than with the images themselves. The structure of agricultural scenes generally casts the major portion of the spectral energy (i.e., transform modulus) along two nearly-perpendicular axes, corresponding to the presence of rectangular field and road structure. In that case the axes of the two transformed images can be sought out by searching for lines of maxima, and the matching need only occur over the axes, rather than over the whole domain. The rotation and skew are determined by rotating corresponding axes into coincidence, and scale changes are determined by matching energy distributions along the axes. Once the linear portion of the affine transformation has been determined (wholly from the modulus), the translation is determined from the phase.

The method was used successfully[32] to determine rotation and skew distortion in airborne scanner data. It is not certain that modulus-matching along the axes for scale change determination is sensitive enough to give a good scale solution because the modulus probably changes far more slowly along an axis than traverse to it. This question should be addressed and the method tried on other data types and scene types before further conclusions are drawn. At present, the method does seem applicable to agricultural images in which only translation, rotation, and skew are present.

Summary and Conclusions

A number of image correlation, match offset determination, control point placement, and geometrical modeling techniques are in use today, but there is still considerable ground to cover. There appears to have been little effort in interchanging methods, e.g., trying different offset determination techniques with each matching technique, etc. Perhaps the greatest potential for correlation improvements lies in increased computational efficiency and speed. Several new matching techniques appear to show promise, but they need to be tested on a wider range of image data. There is room for improvement in the robustness of

offset determination schemes. The various schemes need to be compared when used with representative data. Improved techniques for identifying false fixes without rejecting good fixes are seriously needed.

Methods of modeling sensor anomalies such as late line start perturbations need further investigation. Is the current MSS scan nonuniformity model adequate, or does it change with time? More attention to the degrading effects of geometric distortion on cross-correlation is needed by evaluating tradeoffs between patch size and iterative registration. Control point placement techniques need to be compared in terms of overall performance; particularly, the adaptive placement scheme described earlier needs to be tested. Robust estimation techniques should be investigated for their applicability to registration.

TEMPLATE MATCHING:

$$\frac{\sum_{\text{WINDOW}} (\text{REFERENCE PIXELS}) \times (\text{SEARCH PIXELS})}{\sum_{\text{WINDOW}} (\text{SEARCH PIXELS})^2}$$

- FOR EDGE IMAGES:

$$\frac{\text{NO. OF COINCIDENCES}}{\text{NO. OF SEARCH EDGES}} \approx P(\text{SEARCH PIXEL=EDGE} \mid \text{REF. PIXEL=EDGE})$$

"CLASSICAL" CORRELATION:

$$\frac{\sum_{\text{WINDOW}} (\text{REFERENCE PIXELS}) \times (\text{SEARCH PIXELS})}{\left[\sum_{\text{WINDOW}} (\text{REFERENCE PIXELS})^2 \times \sum_{\text{WINDOW}} (\text{SEARCH PIXELS})^2\right]^{1/2}}$$

- FOR EDGE IMAGES:

$$\frac{\text{NO. OF COINCIDENCES}}{\sqrt{\text{NO. OF REF. EDGES}}\ \sqrt{\text{NO. SEARCH EDGES}}}$$

$$= \sqrt{P(\text{SEARCH=EDGE} \mid \text{REF=EDGE}) P(\text{REF=EDGE} \mid \text{SEARCH=EDGE})}$$

Figure A. Normalization Options For Registration Cross-Correlation

A-PRIORI (MDP) MAPPING FUNCTION:

MAPPING = NULL

COVARIANCE $\underline{C}_M$ = MDP COV. OF REG. + MDP COV. OF REF.

RESIDUAL MAPPING FIT:

MAPPING ≈ AFFINE $\quad \underline{X}_R = (\underline{A}^T \underline{W} \underline{A})^{-1} \underline{A}^T \underline{W} \underline{Y}$

COVARIANCE $\underline{C}_R = (\underline{A}^T \underline{W} \underline{A})^{-1}$

COMBINATION OF FIT AND A PRIORI

$$\underline{X} = (\underline{C}_M^{-1} + \underline{C}_R^{-1})^{-1} \underline{C}_R^{-1} \underline{X}_R$$

$$\underline{C} = (\underline{C}_M^{-1} + \underline{C}_R^{-1})^{-1}$$

CAN INSERT ADDITIONAL SHRINKAGE α

$$\underline{X} = (\alpha \underline{C}_M^{-1} + \underline{C}_R^{-1})^{-1} \quad \underline{C}_R^{-1} \underline{X}_R$$

$$\underline{C} = (\alpha \underline{C}_M^{-1} + \underline{C}_R^{-1})^{-1}$$

Figure B. Weighted Incorporation of Residual Mapping Fit

References

1. W. K. Pratt, Digital Image Processing, Wiley, New York, 1978.

2. R. Bernstein, "Digital Image Processing of Earth Observation Sensor Data," IBM J. Res. Develop., 20, 40-56 (1976).

3. "MSS Data Processing Description," IBM Federal Systems Division report, Contract NAS5-22999, November 1978.

4. G. J. Grebowsky, "LACIE Registration Processing," in The LACIE Symposium, Proceedings of the Technical Sessions, 87-97, July 1979.

5. T. Kaneko, "Image Registration Accuracy Evaluation by an Edge Method," IBM memorandum to NASA JSC, Contract NAS9-14350, June 4, 1976.

6. "ERSYS Registration Subsystem Level C Requirements," AgRISTARS Report SR-I1-00203, Contract NAS9-14350, JSC No. 17620, September 24, 1981.

7. "ERSYS Registration Subsystem Detailed Design Specification," AgRISTARS Report SR-I1-04154, Contract NAS9-14350, JSC No. 16946, September 25, 1981.

8. D. I. Barnea, and H. F. Silverman, "A Class of Algorithms for Fast Digital Image Registration," IEEE Trans. Computers, C-21, 179-186 (1972 - reprinted in Digital Image Processing for Remote Sensing, edited by R. Bernstein, IEEE Press, Wiley, New York, 1978, pp. 138-145).

9. T. Kaneko, "Evaluation of Landsat Image Registration Accuracy," Photogrammetric Engineering and Remote Sensing, 42, 1285-1299 (1976).

10. H. Mostafavi and F. W. Smith, "Image Correlation with Geometric Distortion Part I: Acquisition Performance," IEEE Trans. Aerospace and Electronic Systems, AES-14, 487-493 (1978).

11. H. Mostafavi and F. W. Smith, "Image Correlation with Geometric Distortion Part II: Effect on Local Accuracy," IEEE Trans. Aerospace and Electronic Systems, AES-14, 494-500 (1978).

12. T. L. Steding and F. W. Smith, "Optimum Filters for Image Registration," IEEE Trans. Aerospace and Electronic Systems, AES-15, 849-860 (1979).

13. C. D. Kuglin and W. G. Eppler, "Map-Matching Techniques for use with Multispectral/Multitemporal Data," in Image Processing for Missile Guidance, Proc. SPIE, 238, 146-155 (1980).

14. D. J. Kahl, A. Rosenfeld, and A. Danker, "Some Experiments in Point Pattern Matching," IEEE Trans. Syst. Man. Cybernet., SMC-10, pp. 105-116 (1980).

15. S. Ranade and A. Rosenfeld, "Point Pattern Matching by Relaxation," Pattern Recognition, 12, 269-275 (1980).

16. T. C. Minter, Jr., "Minimum Bayes Risk Image Correlation," in Image Processing for Missile Guidance, Proc. SPIE, 238, 200-208 (1980).

17. T. C. Minter, Jr., private communication, November 1981.

18. A. G. Wacker, R. H. Wolfe, Jr., and R. D. Juday, to be published.

19. E. W. Cordan, Jr., and B. W. Patz, "An Image Registration Algorithm Using Sampled Binary Correlation," in Proc. 1979 Machine Processing of Remotely Sensed Data Symposium, 202-212 (1979).

20. Canadian Centre for Remote Sensing (A. G. Wacker, private communication) April 1981.

21. N. Chu, private communication, 1980.

22. J. J. Pearson, D. C. Hines, Jr., and S. Golosman, "Video-Rate Image Correlation Processor," in Application of Digital Image Processing, Proc. SPIE, 119, 197-205 (1977).

23. G. J. Grebowsky, private communication, November 1981.

24. S. S. Rifman, A. T. Monuki, and C. P. Shortwell, "Multi-Sensor Landsat MSS Registration," in Proc. Thirteenth International Symposium on Remote Sensing, 245-258 (1979).

25. R. Dye, presentation to NASA JSC, 1979.

26. R. H. Wolfe, Jr., presentation to NASA JSC, July 1981.

27. P. Van Wie and M. Stein, "A Landsat Digital Image Rectification System," in Proc. Symposium on Machine Processing of Remotely Sensed Data, 4A-18 - 4A-26 (1976).

28. R. V. Hogg, "Statistical Robustness: One View of Its Use in Applications Today," The American Statistician, 33, 108-115 (1979).

29. M. L. Nack, "Rectification and Registration of Digital Images and the Effect of Cloud Detection," Proc. Fourth Annual Machine Processing of Remotely Sensed Data Symposium, 12-23 (1977).

30. E. H. Schlosser, "Detection and Mapping Package, Vol. 3: Control Network Establishment," Johnson Space Center document JSC-11379, June 1976.

31. "'As-Built' Design Specification of the Automatic Registration System for the Cartographic Technology Laboratory," LEMSCO Report 15904, Contract NAS9-15800, JSC No. 17017, December 1980.

32. R. A. Emmert and C. D. McGillam, "Multitemporal Geometric Distortion Correction Utilizing the Affine Transformation," in Proc. Conference on Machine Processing of Remotely Sensed Data, 1B-24 - 1B-32 (1973 - reprinted in Digital Image Processing for Remote Sensing, edited by R. Bernstein, IEEE Press, Wiley, New York, 1978, pp. 153-161).

7.5 PHOTOGRAMMETRIC ASPECTS OF REMAPPING PROCEDURES*

Edward M. Mikhail, Purdue University

The presentation will discuss aspects specific to photogrammetry, particularly photogrammetric control generation. In order to avoid having this talk be more or less tutorial, I will, at the end of the talk, make the discussion relevant to remote sensing data reduction.

Referring to Figure 1, the outline, I will briefly go through several aspects of photogrammetry, including a classical definition of rectification which existed in photogrammetry for many years and then show how it changed to fit the context of what we do at present with remote sensing data. Since I was specifically asked to discuss triangulation, or at least ground control generation photogrammetrically, I'll be talking a little bit about that and then I will go into the MSS aircraft data work that we've been doing at Purdue at least in my area of engineering for over seven years. At the end, I hope to have time to offer some conclusions.

There are broad definitions for photogrammetry. However, as shown in Figure 2, I'm going to concern myself here with extracting information from photographs and images that are of metric quality. Fundamentally a photograph or an image, no matter which way it is acquired, is basically a two-dimensional representation of a three-dimensional space. This is shown schematically in Figure 3 for a frame photograph. If we do not take this fact into consideration, we are likely to have problems, and I'm sure many of us have had that.

In order to recover the information about the object, we basically are going in the direction from where the data was acquired back into the object, and the only way we can get the information correctly is to do one of two things. Either to assume that the object is an average plane like it was desired yesterday by Fred Billingsly, or we would have to have an external source of information about the object itself, such as having a digital elevation model as I will mention a little bit later.

Obviously an alternative to that, which is a typically photogrammetric solution, is to have more than one ray, and there was a question, at least one raised yesterday as to what the impact of having more than one image record is on the accuracy. I will show some results on that as well later on. Figure 4 is a schematic of three conjugate rays from three frame photographs.

Rectification, classically, was related specifically to a reprojection, and, in the context of a frame photograph, we assume that it is a perspective projection of a three-dimensional space, as shown in Figure 5, the original photograph was oriented not necessarily with the optical axis of the camera pointing downward. And what we would like to do is to get another equivalent vertical photograph through a transformation. The new equivalent photograph would represent a mean plane in the terrain itself. An extension to this is referred to as differential rectification in photogrammetry and requires having more than one photograph. Figures 6, 7 and 8 show schematics in which the terrain is represented with small segments, each of which is differential-

*Edited oral presentation.

ly rectified, that is to say, now parallel to the datum and then placed properly so that the elevation effect has been taken into account. This is the procedure that produces the orthophotos as is known in photogrammetry. The equivalent to that is to consider a single image, either a frame perspective photograph segmented into small patches or, in the case of the MSS imagery, to consider each of the pixels as if it were a segment. And if you have a digital elevation model, and if you want a full rectification in the photogrammetric sense, then you can merge these two together, and you can properly locate each one of those elements back relative to the terrain datum. I want to say that as far as map projection is concerned, that does nothing other than to change the frame of reference of the data. It has absolutely nothing to do with the fact that you are going either from three-dimensional to two-dimensional or multiple two-dimensional back to three-dimensional. The map projection is strictly a means of projecting the surface onto a map. So it's not the same thing at all.

Now, we move on to the triangulation, which is the procedure for getting control. There is quite a lot of detail that I should go through but I cannot, due to lack of time. There are different types of procedures for triangulation as shown in Figure 9. For our purposes here, the one most commonly used technique is analytical triangulation where a large number overlapping images can be simultaneously reduced in such a manner as to produce very high accuracy control. The idea is to have multiple rays for every point on the terrain for which you require the X, Y, and Z location, as shown in Figure 10, and for each of those rays, you write the proper equations. And then you reduce the entire set of multiple rays simultaneously in one analytical reduction method. Before you do that, you need to have at least estimates for the unknowns you sought for.

Figures 11 and 12 show situations which are rather idealized for a typical block of 20 aerial photographs, and the corresponding structure of normal equations used to derive supplementary control. The lower half of Figure 9 indicates that analytical triangulation has reached a very high degree of sophistication. Everything that enters the mathematical model is considered a stochastic variable including the ground control that is externally obtained by ground means. And you will enter the image coordinates as observable with their a priori known covariance matrices. All the possible systematic errors that occur are corrected according to the best models available. Control requirements are: for the horizontal control, you need it around the perimeter; for the vertical control, you need it well distributed through the block.

Figure 13 shows what are called the colinearity equations. Those are for frame photographs but can be modified for a continuous strip camera which is the exact equivalent of the pushbroom linear array; it can be modified for panoramic photographs and also for the multispectral scanner imagery.

So we have the mathematics to go from regular photogrammetric reduction to MSS reduction. In fact, we have done all that at Purdue, including the block adjustment of MSS data. I will show you some results if I have a chance at the end.

What do we do if we have several hundred photographs and for each of the photographs, there are six unknowns. We end up with a very large system of linear equations, actually they are originally nonlinear, but are linearized. We

take advantage of the characteristics of the normal equation structure which is very sparsely populated by nonzero elements as shown in Figure 17. We also take advantage of techniques of folding parts of this matrix in such a way that we end up with only a subset of the unknowns, and it gives us a banded bordered structure of matrices which are relatively efficiently reduced.

So what do we get from the analytical triangulation scheme? Well, we will basically get X, Y and Z for all points of interest for which we had input image coordinates, based on a skeleton of control points around the perimeter and a few in the center. As regards accuracy, working with frame photography, and this of course may probably look out of context here, we can go down to three micrometers at the plane of the image for the control that we have obtained from aerial photography (Figure 9).

The last section of this talk briefly covers work we did at Purdue. Three papers, listed as references, will briefly be discussed. Figure 14 shows the detailed outline for the first paper, essentially a survey paper giving the mathematical models we use when we actually deal with MSS images as if they were photogrammetric blocks of photographs. The idea is that for each one of the locations of the sensor you would have nominally six parameters describing its location and attitude. This would lead to six parameters per pixel if we treat the problem in a vigorous manner, which would lead to a very large number which would be impossible to reduce (see Figure 15). For the case of the pushbroom scanner, we have six parameters for each line. For practical purposes we segment the image, and consider each segment as if a photograph had six elements (X_c, etc.). We then consider each of those elements as if it were a function of time. There is a large number of possibilities with which we actually model the exterior element and I have several of those already mentioned in those papers. There are two basic techniques: either to specifically model everything we know about the sensor, or to use some interpretive technique in order to get the information.

Another important aspect is to consider whether we want to work with only single images which have the limitation of considering only horizontal (or X, Y) information, or we will work with the block adjustment which then gives us also the Z. In consideration of the Z, there are two ways of looking at this problem: either using the remote sensing data for mapping purposes, or for the purpose of merging the MSS information to other sources of data, which would require only rectification. You want to rectify it but not use it for mapping as such. So everything Roy Welch said yesterday was to meet map accuracy standards as if the MSS or its equivalent (whatever the sensor used) actually does the topographic mapping at appropriate scale. What I am saying here is related to the need to rectify the data so that you may derive other types of information from it.

Figure 16 shows the single coverage results. One of the things that we did is to take a strip of MSS imagery and segment it, write constraints between segments so that continuity is preserved. As the number of segments increases, the check, or what ever measures you have for accuracy, would improve up to a certain point and after that, of course, it levels off because the degrees of freedom are reduced (see Figure 17). Using real data from three sidelapping strips, the Z is indeed recoverable (see Figure 18). I don't know if the gentleman who asked the question yesterday regarding the use of stereo is here or not but he was wondering what would happen if you use overlapping imagery.

This not only produces the Z but it also improves the recovery of horizontal coordinates by 40 and 60% as shown in Figure 19. There are other aspects of this work, namely that you could adapt techniques from the block adjustment of photographs to be used with MSS. Notably, we have used geometric constraints such as points lying on straight lines (e.g., roads). The use of such constraints can replace the need for control, or if used in addition to control, can lead to improved accuracy.

In conclusion, we feel, in photogrammetry, that we were not really heeded as much as we ought to have been; there's a wealth of information, a wealth of technology that is useable with remote sensing imagery. Everything I've said here, of course, relates to aircraft MSS data which is the one thing I had continued to work with. We have not the equivalent thing with Landsat for obvious reasons It was a tremendous jump to go from the micrometer level to the 80-meter resolution, so I stayed with the aircraft.

I feel that I have just scratched the surface as far as the actual remapping topic. However, I hope that this with reference papers will give you a good idea of what can be gained when photogrammetric technology is considered when rectifying and/or registering remote sensing data.

Bibliography

E.M. Mikhail and J.C. McGlone, "Current Status of Metric Reduction of (Passive) Scanner Data", Invited Paper, Commission III (WG III-1) 14th Congress of the International Society for Photogrammetry, July 13-25, 1980, Hamburg, FDR.

J.C. McGlone and E.M. Mikhail, "Accuracy, Precision and Reliability of Aircraft MSS Block Adjustment", paper submitted for publication in Photogrammetric Engineering and Remote Sensing, 1982.

C.J. McClone and E.M. Mikhail, "Geometric Constraints in Multispectral Scanner Data", paper to be presented at the 1982 Annual Convention of the American Society of Photogrammetry.

OUTLINE

- INTRODUCTION
  - * Photogrammetry
  - * Rectification
- PHOTOGRAMMETRIC TRIANGULATION
  - * Purpose
  - * Procedures
  - * Analytical Triangulation
  - * Adaptation to MSS
- METRIC REDUCTION OF SCANNER DATA
  - * Mathematical Models
  - * Applications to Spacecraft Data
  - * Applications to Aircraft Data
- CONCLUSIONS

Figure 1. Remapping Procedures Overview

- PHOTOGRAMMETRY

  * Metric Information from Photographs and Images

  * Image is 2-Dimensional Representation of 3-Dimensional Object Space

  * Recovery of 3-Dimensional Object From a Single Image is Not Possible

    Unless: 1) Assumptions Made About Object

    2) Additional Object Information Available

  * Recovery of 3-Dimensional Object From Two or More Overlapping Images

- RECTIFICATION

  • Transformation of One Frame Photo to Another

  • Differential Rectification

    * Single Photo and DTM

    * Overlapping Photos → Orthophoto

  * Considerations for Remote Sensing Images

Figure 2. Introduction

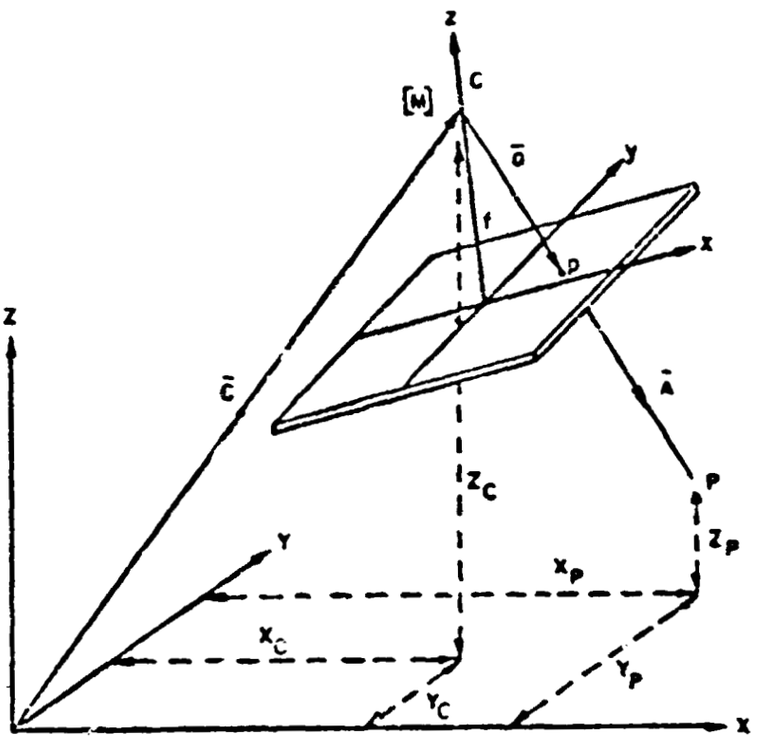

Figure 3. Object Space and Exterior Orientation

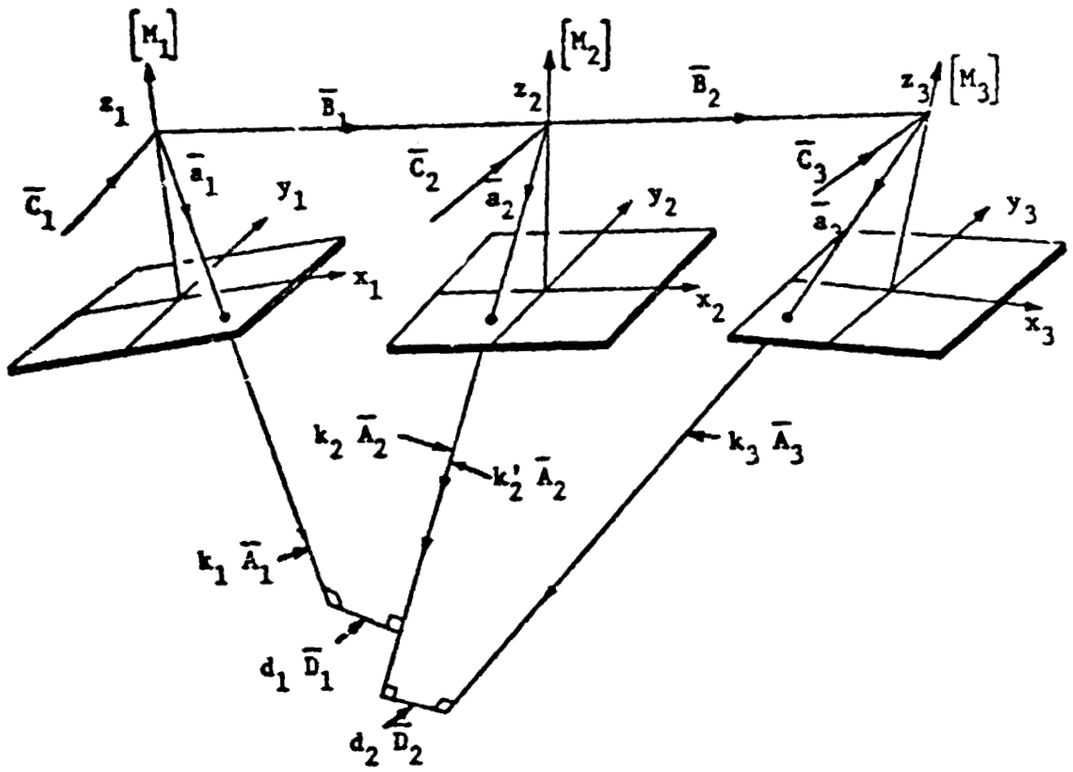

Figure 4. Scale Restraint Equation

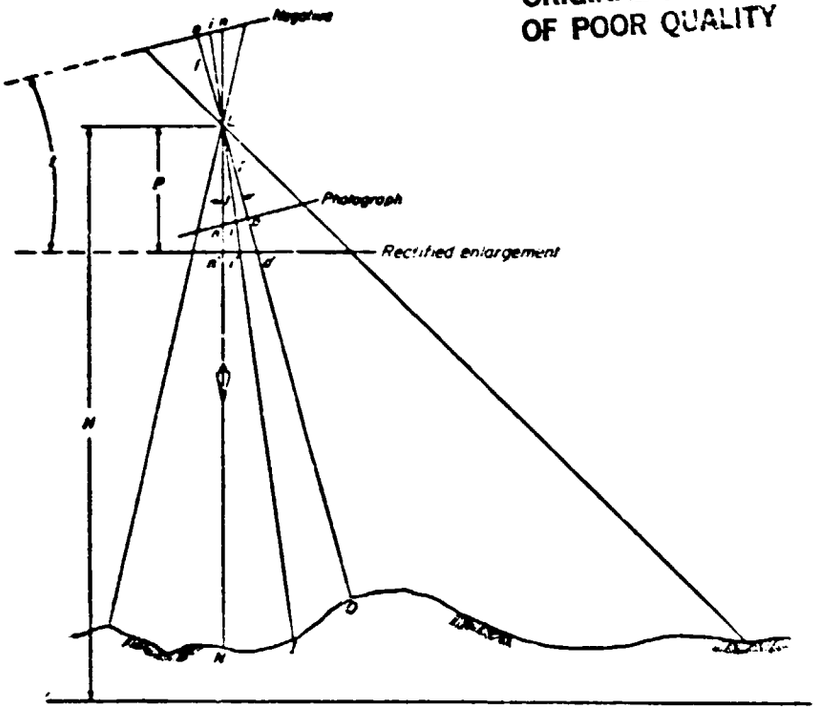

Figure 5. Tilted photograph and rectified enlargement.

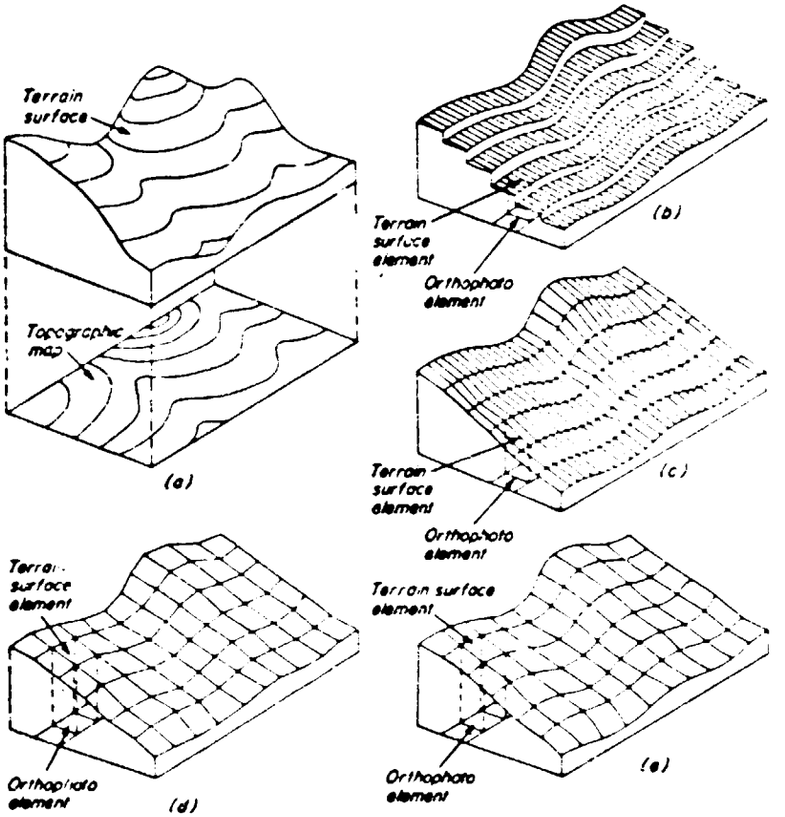

Figure 6. Methods of differential rectification (a) Terrain and corresponding contour map (b) Fixed line element strip rectification (c) Rotating line element strip rectification (d) Plane area element rectification (e) Curved area element rectification. After Edmond, Bendix Technical Journal, Vol. 1, No. 2, 1968.

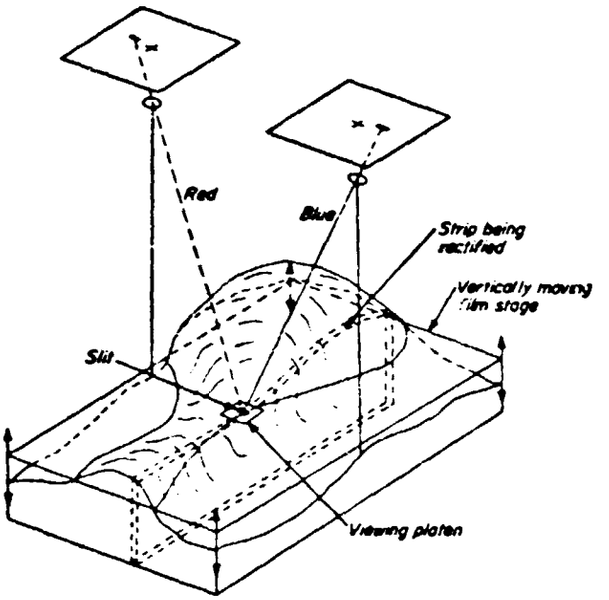

Figure 7. Fixed line element rectification.

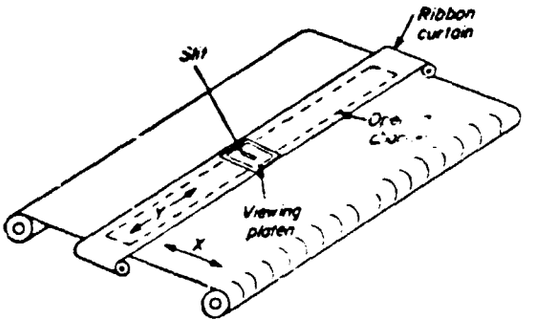

Figure 8. Curtain used to cover film exposure in line element rectification.

- PURPOSE: To Generate Extensive Control Net From Overlapping Photographs and a Few Control Points

- PROCEDURES: Analog Semi-Analytical Analytical
  Choice Accuracy Requirements
  Photography Characteristics
  Equipment

- ANALYTICAL TRIANGULATION

  * Most Sophisticated

  * Can Reduce Large Number of Photos Simultaneously

  * Need: * Image Coordinates - Their Σ
    * Models For Corrections For Systematic Errors
    * Approximations For Unknowns
    * Horizontal Control Along Block Perimeter
    * Vertical Control Distributed Throughout Block

  * Method: * Use Unified Least Squares Where all Variables are Considered Stochastic

  * Result: * All Sensor Parameters - Their Σ
    * All Ground Coordinates - Their Σ

  * Extension: * Extended Mathematical Models For Self-Calibration
    * Use of Geometric Constraints

  * Accuracy: * Fraction of Flying Height (H/20,000 and Better)
    * Given σ at Photo Scale (Down to 3 μm)

- ADAPTATION OF TRIANGULATION TECHNIQUES TO MSS

Figure 9. Photogrammetric Triangulation

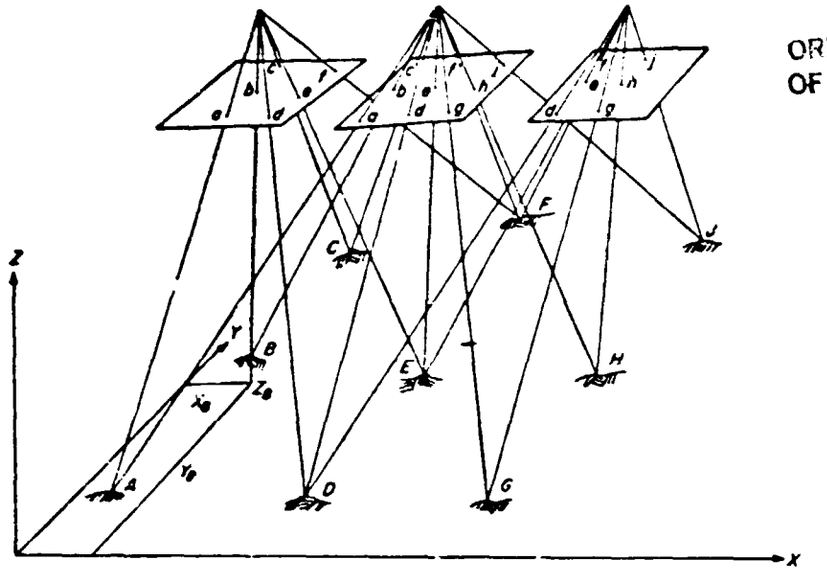

Figure 10. Numerical models to be numerically joined by analytic aerotriangulation.

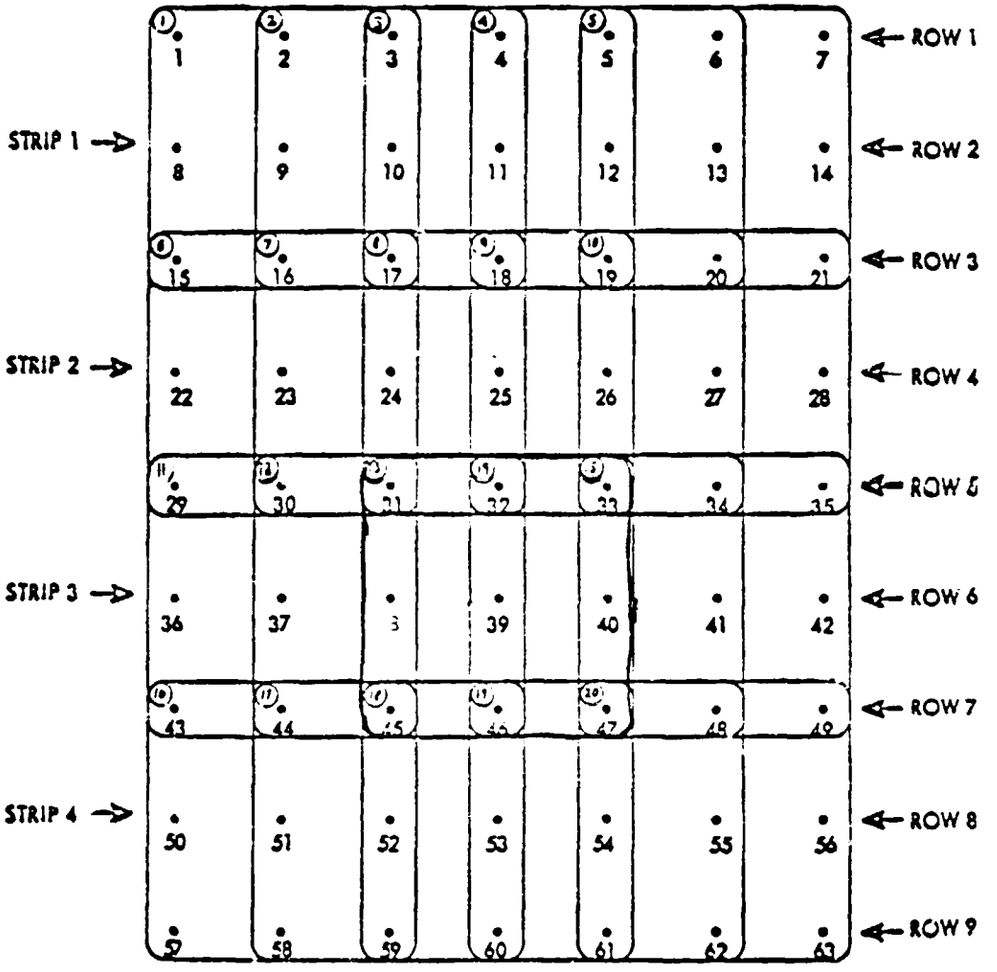

Figure 11. Arrangements of Points in Block of 4 Strips with 5 Photos Per Strip

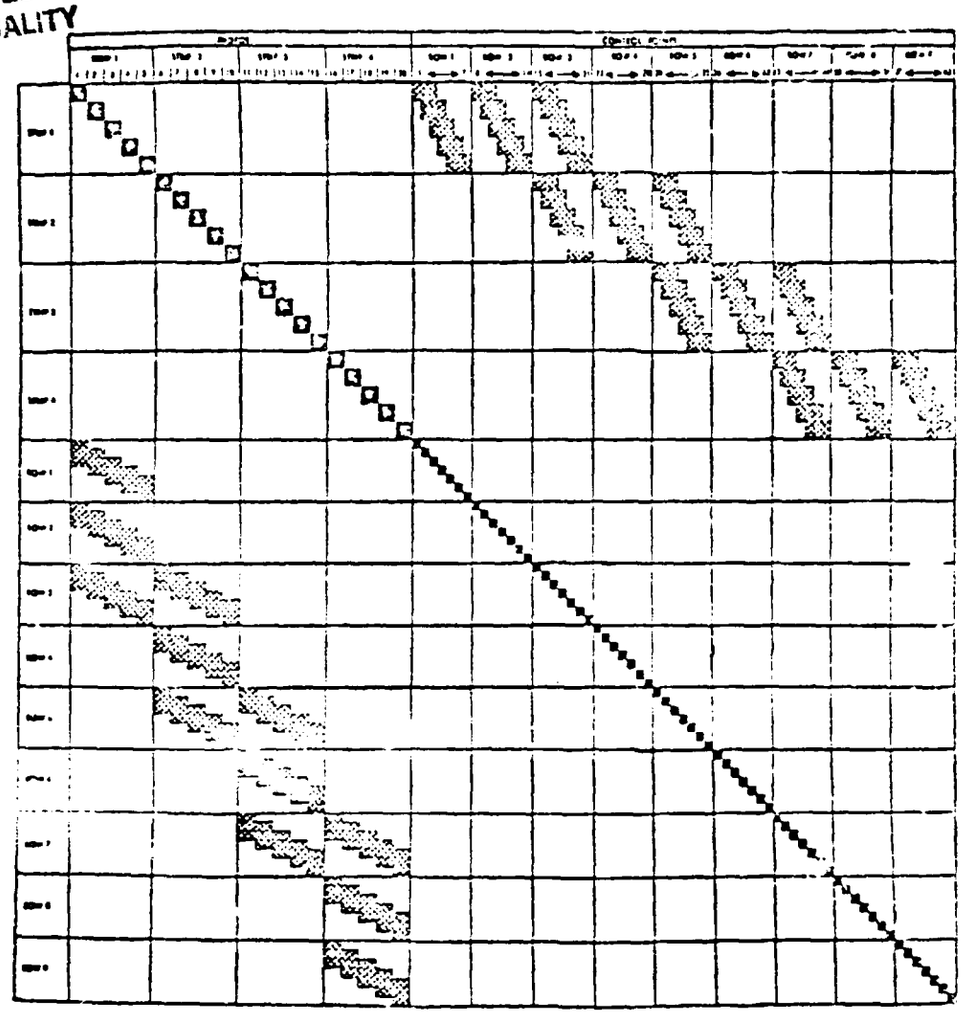

Figure 12. Normal Equation Matrix Arising From Application of Collinearity Equations to a 4 Strip - 20 Photo Block

$$\bar{a} = \begin{cases} (x_p - x_o) = k\left[m_{11}(X_P - X_C) + m_{12}(Y_P - Y_C) + m_{13}(Z_P - Z_C)\right] \\ (y_p - y_o) = k\left[m_{21}(X_P - X_C) + m_{22}(Y_P - Y_C) + m_{23}(Z_P - Z_C)\right] \\ -f \qquad\quad k\left[m_{31}(X_P - X_C) + m_{32}(Y_P - Y_C) + m_{33}(Z_P - Z_C)\right] \end{cases}$$

$$(x_p - x_o) = -f\left[\frac{m_{11}(X_P - X_C) + m_{12}(Y_P - Y_C) + m_{13}(Z_P - Z_C)}{m_{31}(X_P - X_C) + m_{32}(Y_P - Y_C) + m_{33}(Z_P - Z_C)}\right]$$

$$(y_p - y_o) = -f\left[\frac{m_{21}(X_P - X_C) + m_{22}(Y_P - Y_C) + m_{23}(Z_P - Z_C)}{m_{31}(X_P - X_C) + m_{32}(Y_P - Y_C) + m_{33}(Z_P - Z_C)}\right]$$

Figure 13. Collinearity Equations

INTRODUCTION

BASIC MATHEMATICAL MODELS

- PARAMETRIC MODELS
  - ORBIT MODELING FOR SPACECRAFT IMAGES
  - POLYNOMIAL MODELING
  - HARMONICS
  - AUTOREGRESSIVE MODELS
- INTERPOLATIVE MODELS
  - USING GENERAL TRANSFORMATION
  - WEIGHTED MEAN
  - MOVING AVERAGES
  - MESHWISE LINEAR
  - LINEAR LEAST SQUARES PREDICTION

APPLICATIONS TO SPACECRAFT DATA

APPLICATIONS TO AIRCRAFT DATA

ADJUSTMENT OF MULTISERIES DATA

CONCLUSIONS

Figure 14. Current Status of Metric Reduction of (Passive) Scanner Data

PARAMETRIC MODELS

BASED ON LINEARIZED FORM OF COLLINEARITY EQUATIONS

EXCESSIVE NUMBER OF SENSOR/PLATFORM PARAMETERS

REPLACE SOME OR ALL OF THE SIX PARAMETERS

(X_c, Y_c, Z_c, ω, ϕ, κ per pixel, line, or segment)

BY FUNCTIONS.

FOR ORBITAL CASE: REPLACE X_c, Y_c, Z_c BY FUNCTIONS OF THE SIX ORBITAL PARAMETERS

OR USE A LINEAR SEQUENTIAL ESTIMATOR (KALMAN FILTER)

FOR AIRCRAFT CASE: REPLACE PARAMETERS BY POLYNOMIALS AND SEGMENT RECORDS - USE CONSTRAINTS

(COULD USE HARMONICS)

FOR EITHER CASE: USE AUTOREGRESSIVE MODEL (GAUSS-MARKOV PROCESS)

Figure 15. Basic Mathematical Models

INTERPOLATIVE MODELS

GENERAL TRANSFORMATION

- 4 - PARAMETER
- 6 - PARAMETER
- 8 - PARAMETER
- GENERAL POLYNOMIAL (RUBBER SHEET)

WEIGHTED MEAN — WEIGHT DECREASES AS DISTANCE BETWEEN POINT AND REFERENCE INCREASES (NEW PARAMETER ESTIMATION FOR EACH POINT)

MOVING AVERAGES

MESHWISE LINEAR

(TRIANGULAR OR RECTANGULAR MESHES - LINEAR ESTIMATION)

LINEAR LEAST SQUARES PREDICTION

(ESTABLISH COVARIANCE FUNCTION)

Figure 15. (continued)

METHOD	STRIP 1 X	STRIP 1 Y	STRIP 1 XY	STRIP 2 X	STRIP 2 Y	STRIP 2 XY	STRIP 3 X	STRIP 3 Y	STRIP 3 XY	STRIP 4 X	STRIP 4 Y	STRIP 4 XY
COL. 1 SEC.	1.57	2.03	1.80	2.70	2.19	2.45	7.33	9.66	8.58	4.10	4.24	3.90
" 2 SEC.	1.51	1.68	1.59	2.57	1.82	2.19	3.69	5.17	4.49	4.23	3.76	3.34
" 3 SEC.	1.42	1.36	1.39	2.70	1.37	2.04	2.89	3.08	2.99	4.16	4.01	3.63
P.POLY 1 SEC.	1.58	2.01	1.79	2.68	2.38	2.53	7.33	8.71	8.05	4.09	4.32	4.21
2 SEC.	1.51	1.69	1.60	2.57	2.18	2.37	3.66	4.74	4.24	4.18	3.16	3.71
3 SEC.	1.42	1.37	1.40	2.71	1.36	2.03	2.89	3.15	3.02	3.33	3.40	3.49
W. MEAN	1.56	1.23	1.41	3.27	1.52	2.55	3.05	4.44	3.81	3.75	2.91	3.36
M. AVG.	1.32	2.04	1.72	2.74	1.95	2.38	2.62	3.91	3.33	5.33	3.58	4.54
MESH. LINEAR	1.35	2.26	1.86	2.50	2.42	2.46	4.35	4.82	4.59	4.23	7.55	6.18
G. MARKOV, 1ST	1.18	1.44	1.32	2.65	2.33	2.20	2.43	2.80	2.62	3.66	3.77	3.72
	H=1500M, 0.006 RAD 1550 LINES 30 CONT PTS 60 CHK PTS			H=1500M 0.006 RAD 1400 LINES 23 CONT PTS 9 CHK PTS			H=900M, 0.006 RAD 1970 LINES 36 CONT PTS 35 CHK PTS			H=900M, 0.006 RAD 2700 LINES 26 CONT PTS 25 CHK PTS		

Figure 16. Single Coverage Data (E/M), Check Point RMSE (Pixels)

Figure 17. Positional Check Variance Vs. Number of Sections
(Piecewise Polynomial Case P_2 Applied to Flight Penn 1.)

STRIP	1			2			3			4		
	X	Y	Z	X	Y	Z	X	Y	Z	X	Y	Z
1	24.4	31.6	-	25.0	17.7	-	21.6	13.1	-	16.1	12.9	-
2	16.2	24.2	-	16.6	19.4	-	14.4	13.3	-	14.3	11.4	-
3	16.1	23.6	-	11.6	24.5	-	10.0	24.0	-	9.7	23.9	-
POOLED	19.9	27.3	-	19.4	20.5	-	16.73	17.4	-	13.9	16.9	-
1 & 2	20.1	31.0	55.8	21.0	17.7	53.4	17.9	12.5	36.2	14.3	12.5	27.4
2 & 3	16.8	29.3	92.0	11.8	25.2	81.2	10.6	20.0	66.1	9.9	19.8	64.2
POOLED	18.7	30.3	77.2	17.5	21.3	67.1	15.1	16.2	54.2	12.6	16.1	50.4
1,2,3	18.6	29.2	69.2	17.5	18.5	53.5	15.2	13.7	36.4	11.9	14.9	37.5

CONTROL POINTS 44 X,Y 44 Z

CHECK POINTS 53 X,Y 25 Z

H = 3050 M, IFOV = 0.0025 RAD, 1450 LINES EACH

Figure 18. Single and Multiple Coverage Data (Mc/M), Checkpoint Root Mean Square Error (M), Number of Sections

NUMBER OF STRIPS	NUMBER OF RAYS 1		2			3		
	X	Y	X	Y	Z	X	Y	Z
1	16.7	17.4	-	-	-	-	-	-
2	17.3	16.5	11.5	15.8	54.2	-	-	-
3	18.8	14.4	10.3	12.8	41.3	8.9	11.5	27.3

Figure 19. Check Point Root Mean Square Error For Single and Multiple Ray Points

N82 28727

7.6 COMPUTATIONAL ASPECTS OF REMAPPING DIGITAL IMAGERY

Albert L. Zobrist
Jet Propulsion Laboratory
Pasadena, CA 91103

1. Introduction

One of the advantages of automated cartography is that map data stored in the digital computer can be plotted or displayed at any scale or projection by recomputing the coordinates of the data. This is especially easy in the case of vector (graphics) data but in the case of digital image (raster) data, remapping is a more difficult operation. Examples of the remapping of digital imagery would include rectification of a Landsat MSS to an orthographic or Mercator projection, warping of one image to register with another, or rotation, scale, or aspect changes of a digital image. Inputs consist of the digital image and geometric control information. Control information can

include scanner location and pointing, ground truth, and the map transformation. Digital remapping consists of two major steps. First, a distortion model is computed from the control information. Second, the image is warped according to the distortion model.

The first step involves traditional mathematical techniques of estimating a surface from sample points. Several approaches persist because of varying needs of different applications. The second step involves highly specialized computational methods for efficient warping of large images according to a geometric distortion model. Use of general purpose computers and array processors for this task will be covered. Data processing error will be discussed for each modelling/warping approach.

2. Determination of geometric distortion model

Mathematically, a geometric distortion is a mapping from the plane to the plane. The mapping is usually one-to-one and continuous but there may be discontinuities. Orthogonal components of the mapping (the x and y coordinates) are independent and each can be viewed as a surface over the plane. For a point p, the value of the x-distortion surface at p specifies how far the data at p must move in the x direction in the remapping. Some simple geometric distortions are used to rotate images or change pixel size. In this case the general transformation is called affine or linear and the x and y components are planes. Map coordinate conversions (for example UTM to Transferse Mercator) are given by formulas which can also be viewed as distortion surfaces over a plane. Singularities and zone boundaries are not a problem here but are dealt with in sectioning images for a data base.

A more complex geometric distortion problem is the "rubber sheet" case where a set of control points relating the input to the output is known. A number of techniques are known for generating surfaces to fit the control points and give a distortion model over the entire surface. Some are general in nature: polynomial fit, nearest-neighbor interpolation, finite element method, and the method of potential functions. These are used in cases where there is no need or desire to use a priori knowledge of the nature of the geometric distortion. If one knows (from physical considerations) the general functional form of a distortion, then there are methods (least squares, Kalman filtering, etc.) of fitting the functional form to the observations. Table 1 compares some basic properties of these methods.

The most complex distortion models arise from sensor geometry correction. Taking the Landsat MSS to be a basic example, the raw data are perturbed by earth rotation, mirror scan nonlinearity, spherical earth, variations in platform altitude, roll, pitch, and yaw. Most of these components can be modelled by continuous functions, but one component, the line-to-line skew induced by earth rotation is discontinuous at every sixth line. Furthermore, the distortion model is no longer a simple function but a composite of several functions that are applied in order. The first correction function calculates uniform sample spacing in orthographic or Mercator projection along single scan lines. Then a second correction function moves entire lines according to the sensor and earth rotation skew for each line. A third correction for map projection could now be performed if desired. Two basic techniques for model fitting are in common use today. The first is to use nominal values for spacecraft location, etc., and produce a corrected product which has slight deviations from a perfectly mapped product. Note that the largest deviation is a simple lateral

translation, which can be fixed later by a single point observation. The second technique is to fit the model according to control points determined by external means. These methods are covered in other reports in this workshop.

3. Representation of geometric distortion model

Digital computation requires that the geometric distortion be represented in an efficient manner. Three methods are covered here. The first method is to leave the model in its functional or natural form. Model fitting provides coefficients or data for a subroutine F which can be invoked at a point p to give the distortion F(p). The second method is to convert the model to a gridded approximation. A rectangular grid a_{11}, a_{12}, ..., a_{21}, ..., a_{mn} is set up and the subroutine F is calculated at these points. The values a_{ij} and $F(a_{ij})$ are stored in a data structure so that the value F(p) can be generated by interpolation in an efficient manner. The third method is a highly specialized one for scanner type data such as MSS. In cases where some components of F are functions of one variable (separable components) a "dope vector" can be set up to represent the shift. As an example, the mirror scan nonlinearity is a function of position along a scan line only. A dope vector of the same length as a scan line can represent this correction on a per pixel basis. Earth skew offset and sensor readout delay can be represented by a dope vector with a per line lookup. Both of these corrections are "along track", that is, in the direction of scanning. It is possible to have dope vectors for across track corrections as well, if needed.

Direct computation of F for each pixel is a slow method, although it may be helped by array processor techniques. Gridded representation offers great

speedup simply because a 50 x 50 grid, for example, requires a factor of 3072 times fewer evaluations of F than a 2400 by 3200 image would by direct computation. Gridding introduces a data processing error, however (see later section on error). In general, discontinuous functions and functions which are not approximated well by interpolation on a grid are poor candidates for gridding. Dope vectors can only be used on separable functions, of course.

A special strategy for MSS involves a combination of dope vectors for the discontinuous and highly nonlinear elements of F and a gridded approximation for the remainder. Evaluation at F(p) would involve several table lookup operations in the dope vectors followed by the grid interpolation.

4. Large image warping computation

Regardless of method, the remapping of a digital image can be an enormous computation. For example, an MSS input contains over seven megabytes of data per spectral band and yields over ten megabytes of data for 57-meter square pixels. Executing ninety machine instructions per output pixel at one microsecond per instruction would occupy about 16 minutes of processor time. Yet this slim number of cycles must accomplish the following:

(1) For each output pixel, calculate the location of the input point that maps to it (the inverse of the mapping).

(2) For each output pixel, calculate the pixel value based on interpolation of input pixel values neighboring the input point.

(3) Buffer the input and output so that a reasonable main memory region can accommodate the calculation without excessive disk head motion or file rereading.

Computational aspects of these steps for an ordinary digital computer will be covered in order.

The first step requires that for an output pixel location p and an inverse mapping F that F(p) be calculated. If F is a composite function, then each component must be calculated in order. Functions represented by formula are evaluated by their subroutine. There are some opportunities for speeding up function evaluation, for example, by use of table lookup for parts of a function (such as a cosine). Another example is incremental evaluation where

$$F(x + dx) = F(x) + G(x,dx)$$

and G(x,dx) is faster to compute than F(x). A concrete example of this is

$$\cos(x + dx) = \cos x \cos dx - \sin x \sin dx$$

so for uniform dx a cosine can be calculated with two multiplies and an add, assuming that sin x is maintained in a similar fashion. The incremental evaluation can even be an approximation if care is taken to restart with an exact evaluation frequently enough to limit the error to an acceptable range. Functions represented by a grid are amenable to a much faster treatment. Within each grid cell an incrementing scheme can be set up consisting of

$F(x_o,y_o)$	an initial point
Δx	
Δy	increments
Δxy	

which allow for recalculation of F for a series of increments in the x direction

$$F(x + dx,y) = F(x,y) + \Delta x$$

and for a move to the next line of output

$$F(x,y + dy) = F(x,y) + \Delta y$$

$$\Delta x = \Delta x + \Delta xy$$

This corresponds to bilinear interpolation on the grid. If non-uniform increments are needed because of function composition, additional multiplications b dx and dy will be required. When dope vectors are used it is usually accurate enough to use the correction value from the nearest pixel. As an example, the along-track correction for an across track dope vector is

$$F(x,y) = x + D(\text{round } (y))$$

One special problem arises from discontinuities in the mapping function. For purposes of pixel value interpolation, it is necessary to know about local discontinuities in the neighborhood of F(x,y). Hence for cubic spline interpolation for MSS a point (x,y) maps into four locations for four lines which are offset from each other. Fortunately in this case, the samples are uniformly spaced (Figure 1).

The second step of warping computation is the actual interpolation for the output pixel value from the neighboring input. Methods for this are discussed elsewhere in the workshop.

The third problem involves the allocation of limited main storage to storage of a part of the raster input so that the raster output can be computed efficiently. Two previous methods did not work well for large or highly rotated input rasters (for example 3000 x 3000 rotated 11°). Method 1 stores a band of raster lines internally as shown in Figure 2. Because of rotation an output line will only have a short intersection with this band. Therefore, it is only possible to calculate an extremely large number of short

output segments which must be written to disk and later reconstructed into the output raster. The later reconstruction involves excessive disk head motion for large cases. If the raster is n by n and available storage is fixed, then the length of calculated segments is $O(1/n)$, the number of cells is $O(n^2)$, hence the number of short segments is $O(n^3)$ and disk head motion will increase by this factor under a simple reconstruction scheme. Method 2 avoids the reconstruction of short segments by storing all of the input raster in the neighborhood of an output line. But because the stored input area is not a band, the input file must be reread as many times as there are plateaus in the lower part of the stored area. The thickness of the stored area is $O(1/n)$ and the length of the line is $O(n)$ hence the number of rereads of the input data set is $O(n^2)$. Since the amount of data is $O(n^2)$ the disk head motion will increase by $O(n^4)$. The new method developed computes a uniform vertical band of optimal width in the output by storing a corresponding swath of input. The output segment width is independent of n hence disk motion depends on the number of times the input has to be read which is $O(n)$ times amount of data yielding $O(n^3)$. The reconstruction stage is $O(n^2)$. Thus method 2 is unsuitable for large cases and methods 1 and 3 appear the same. A closer analysis reveals that method 1 forces a head motion for sequential passes over the data which minimizes head motion and rotation latency. Methods 1 and 3 are implemented in the VICAR routines LGEOM and MGEOM respectively, and method 2 was reported by H. K. Ramapriyan (1977).

Unusual approaches to this problem have been proposed. One is to resample horizontally, rotate the image 90° and then resample vertically (which is horizontal after rotation). Good methods for 90° rotation are available

(Twogood and Ekstrom, 1976). Resampling techniques and experimentation are reported by Friedmann (1981).

5. Data processing error

Image registration and rectification error analysis is the subject of another report in this workshop. Therefore, model errors will not be considered here. Data processing error includes only the error introduced in the following ways:

(1) errors in calculation of the inverse mapping F(x,y)

(2) errors introduced by interpolation on a grid or dope vector representation of F(x,y)

(3) errors in the location of neighboring pixels of F(x,y) for input to the interpolation scheme.

There may also be error in the interpolation scheme, but this is not a location error. With regard to the three errors, note that a 1/10 pixel error on a 3000 x 3000 image requires an accuracy of one part in 30,000. Gridding methods are the most difficult to hold within such an error budget. One component of grid error is the deviation of the bilinear surface from the model surface. A second component is accumulative error in the incrementing scheme described in the last sections. Both of these errors are controlled by keeping the grid size small. The accumulative error necessitates the use of computer arithmetic with greater precision than 32- or 36-bit floating point.

6. References

Ramapriyan, H. K. (1977), "Data handling for the geometric correction of large images," IEEE Transactions on Computers, vol. C-26, no. 11, pp. 1163-1167.

Twogood, R. E., and M. P. Ekstrom (1976), "An extension of Eklundh's matrix transposition alogirthm and its application in digital image processing," IEEE Transactions on Computers, vol. C-25, no. 9, pp. 950-952.

Friedmann, D. E. (1981), "Two-dimensional resampling of line scan imagery by one-dimensional processing," Photogrammetric Engineering and Remote Sensing, vol. 47, no. 10, pp. 1459-1467.

Table 1. Characteristics of Some Common Surface Fitting Methods

PROPERTIES OF SURFACE / METHOD	CONTINUOUS	DIFFERENTIABLE	EVALUATES AT INPUT POINT	WELL BEHAVED NO MESAS
TRIANGULATION	YES	NO	YES	YES
INTERPOLATION r^{-1}	NO	NO	YES	YES
INTERPOLATION r^{-p}	NO	NO	YES	NO
POLYNOMIAL FIT	YES	YES	NO	NO
POTENTIAL FUNCTION	YES	YES	YES	?
SPACECRAFT MODEL	YES	YES	NO	YES

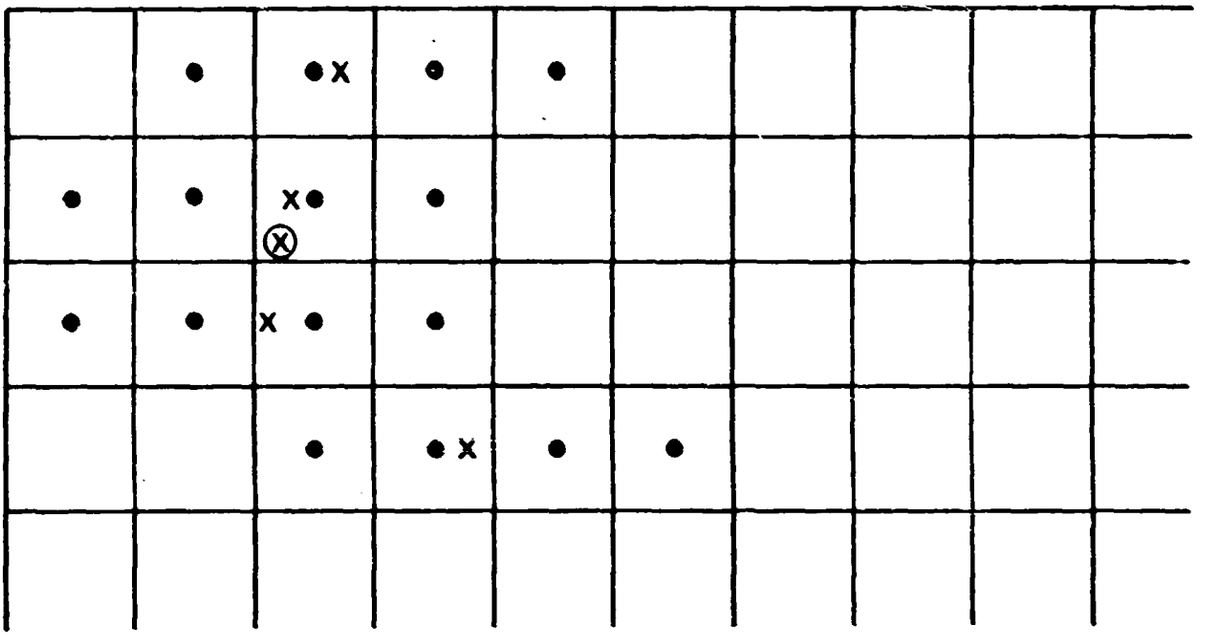

⊗ INVERSE MAPPED LOCATION OF OUTPUT PIXEL

x CENTERS OF INTERPOLATION ALONG A LINE

• INPUT PIXELS USED IN BI-CUBIC SPLINE INTERPOLATION

Figure 1. Interpolation in the Presence of Discontinuities in Input Data Along a Line

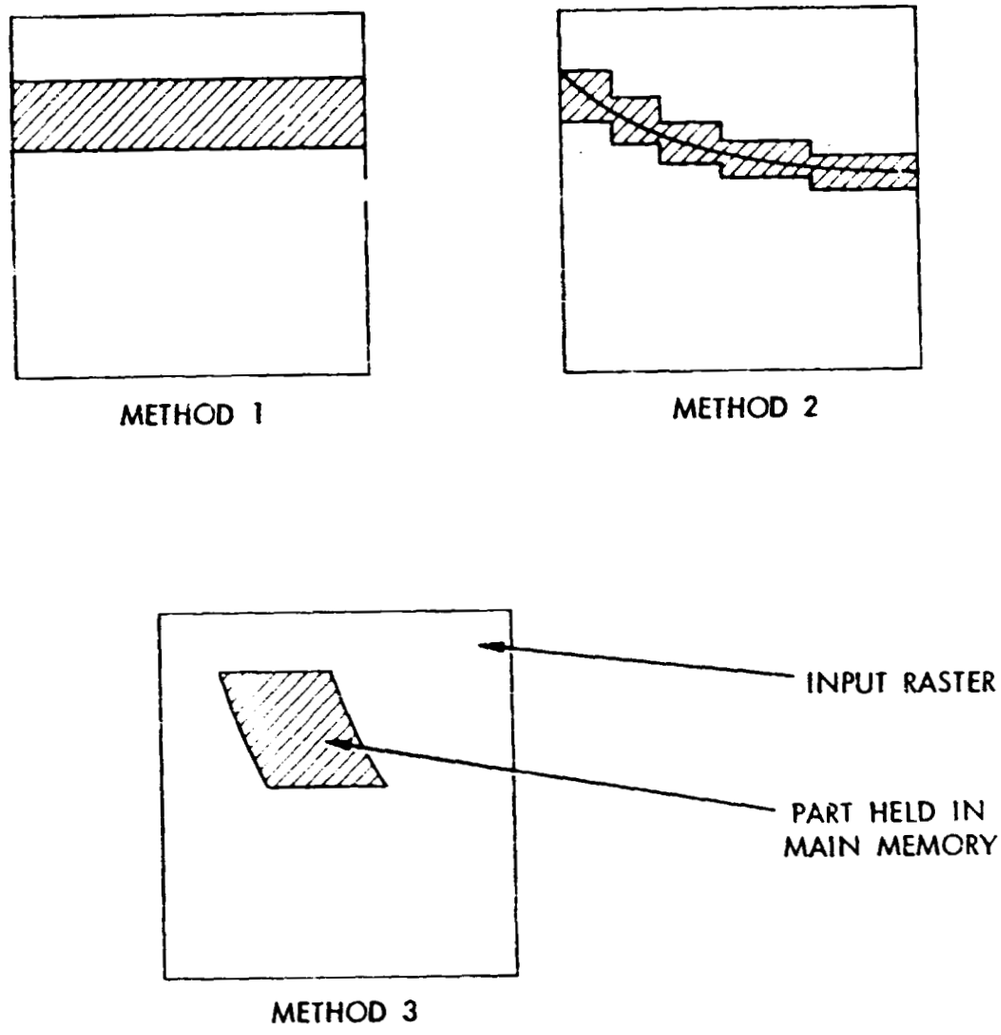

Figure 2. Diagram of Allocation Schemes for Main Memory for Large Image Warping Computation

7.7 A QUANTITATIVE ASSESSMENT OF RESAMPLING ERRORS

Robert H. Dye

Applications Division
The Environmental Research Institute of Michigan
Ann Arbor, Michigan, 48107

INTRODUCTION

Applications associated with digital geographic imagery are subject to great diversity in required cell size, cartographic projection, etc. The need for resampling remote sensing scanner data is evident in all but the most undemanding cases. Past efforts [1] have shown that proper resampling of such data is dependant in important ways on the detailed knowlege of the original scanner's effective point-spread function and to the desired point-spread function of the resampled data. When both of these are known, it is relatively straightforward to compute the resampling coeffients which do the best job of approximating the shape and position of the synthesized point-spread function.

It is useful, however, to recognize that regardless of the rationale used to generate interpolation coefficients and apply them as a linear filter on a subset of the local data the result can be viewed as a synthesis of a new point spread function which is itself a linear combination of shifted positions of the original psf.

The resulting synthesized psf can be compared with an ideal psf located at various interpixel positions and any differences observed as errors.

ERROR MODEL

It is assumed that imaging scanners of interest are adequately modeled as a linear operator on the upwelling radiance and that additive noise is introduced. (The LANDSAT MSS does deliberately introduce a non-linear compression prior sampling but this effect is approximately removed in subsequent ground processing.) Thus, the scanner to be modeled is given by

$$y = Ax + n \qquad (1)$$

where x is a vector representing the two-dimensional upwelling radiance, A is a matrix describing the two-dimensional shape and location of the psf associated with each pixel sampled. The noise vector n is then added to produce the data vector y which can represent either all of the pixels in an image or only those in a locality of interest.

It should be noted that the dimensionality of x is very much greater than that of y in order to permit the A matrix to represent the subpixel detail of the point spread functions and the effect of the dimensionality reducing sampling process.

When an interpolation algorithm is used in the resampling process it is normally intended to estimate the data value that might have been obtained from a psf positioned at an intermediate location between the existing samples.

The desired result of the resampling process thus can be given by

$$z = Bx \qquad (2)$$

where B is a new spatial responsivity matrix with the point spread functions positioned correctly on the desired output grid and the vector z represents the resampled data. Note that the width and shape of the psf's in B need not be the same as that of the original scanner when it is desireable to alter the spatial resolution of the data as well as the location.

Restricting the interpolation process to a linear filter operating on the available data leads to an approximation of the desired scanner in (2) given by

$$\hat{z} = Cy$$

or

$$\hat{z} = (CA)x + Cn \qquad (3)$$

in which the interpolation coefficients C and the original psf matrix combine to produce a new psf matrix CA having spatial resolution properties which can be either better or worse than the original depending on the method used to determine the coefficients.

Any differences between the desired scanner (2) and the achieved scanner (3) can be regarded as an error given by

$$e = z - \hat{z} \qquad (4)$$

The mean squared error is easy to compute and relatively easy to defend as a performance criterion particularly for processes such as classification which may be sensitive to radiometric errors. The mean squared error

$$E = \langle e'e \rangle \qquad (5)$$

can be evaluated by substituting (2),(3), and (4) into (5). The result, after the elimination of terms with expected value of zero is

$$E = \text{Trace}\,[CA\langle xx'\rangle A'C' - 2CA\langle xx'\rangle B' + B\langle xx'\rangle B' + C\langle nn'\rangle] \qquad (6)$$

This expression, when evaluated for various rules and interpixel positions yields the data shown in Table 1. The rules used were nearest-neighbor, bilinear, cubic convolution, and least square. The LANDSAT along-scan psf was used for matrix A and a rectangular psf with a width of 50 meters was chosen for the desired psf matrix B. A signal-to-noise ratio of ten was selected which established a ratio of 100 between the signal covariance matrix <xx'> and the noise covariance matrix <nn'>. Finally, to restrict the error determination to the case of very fine local detail the subpixel correlations were set to zero by use of scalar matrices for <xx'> and <nn'>.

The numbers tabulated are relative errors, giving a maximum of 100 for the worst possible case of no corresponance at all between psf matrices (CA) and B. The relative error is defined as

$$r.e.= 100\ SQRT(E/2B'\langle x'x\rangle B) \qquad (7)$$

The algorithms for generating coefficients for the first three interpolation rules are well known and will not be repeated here. The least square coefficients are obtained from

$$C= B\langle xx'\rangle A'[A\langle xx'\rangle A'+\langle nn'\rangle]^{-1} \qquad (8)$$

In the table, positions 1 and 17 correspond to the cases of the desired psf falling exactly on one of the original data samles. All others are located at interpixel locations differing by multiples of 1/16 of a pixel.

All four methods show the worst error near the center of the interpixel interval where a narrow psf is the most difficult to synthesize- that it is not the exact center is due to the asymmetry introduced by the lowpass presampling filter used in the LANDSAT MSS.

It is recognized that all of the errors might be regarded as undesirably large. Had the sampling rate been even slightly better than the 56 meters used the errors for LS would have been substantially reduced while the errors for the other methods would, of course, remain unchanged.

To explore in the other direction, the case of wider synthesized psf's may be considered. Such resolution-reducing resampling would be the preferred method for the generation of large area, small scale images. As the desired psf is increased in width the errors for all four methods would decrease until an approximate match with the original psf is reached. After this the LS error would continue to decrease while the other three errors would increase again because of their failure to synthesize a psf suited to the resampling interval.

As should be expected NN, BL, and CC all have the same error at positions 1 and 17 since all three merely reproduce the original data when no interpolation is required. By contrast, the LS solution has synthesized a psf more closely approximating the desired psf and hence exhibits a smaller error. The largest error occurs for NN at position 8, where the psf is not only the wrong shape and width but also in the wrong place by a half pixel. Perhaps it could be observed that the BL and CC algorithms do rather well for procedures which provide no opportunity introduce information about the original and desired psf's and the signal and noise statistics.

Another measure of image quality is the modulation transfer function. Although the MTF is merely the magnitude of the Fourier Transform of the psf and hence carries less information than the psf itself, it frequently invoked when image quality is considered. The normalized width at the half amplitude of the MTF at positions 1 and 8 for each resampling scheme is shown in Table 2. It can be seen that LS shows a broader MTF than the other methods for both positions and that both BL and CC have degraded MTF's at the midpixel location.

[1] R. Dye, "Restoration of LANDSAT Images by Discrete Two-Dimensional Deconvolution", Proceedings of the Tenth International Symposium on Remote Sensing of the Environment. ERIM, Ann Arbor,MI, October 1975.

TABLE 1. RELATIVE ERRORS FOR VARIOUS INTERPIXEL POSITIONS

POSITION	NN	BL	CC	LS
1	40.1	40.1	40.1	34.6
2	41.4	41.8	40.7	35.9
3	43.1	43.4	41.5	37.4
4	45.3	44.9	42.4	38.7
5	47.7	46.1	43.2	39.8
6	50.4	47.0	43.8	40.4
7	53.2	47.5	44.1	40.6
8	56.0	47.7	44.2	40.2
9	49.8	47.5	43.9	39.4
10	47.1	47.0	43.4	38.2
11	44.6	46.1	42.7	36.8
12	42.5	45.1	41.9	35.3
13	40.9	43.9	41.1	34.1
14	39.8	42.6	40.5	33.2
15	39.3	41.5	40.0	33.0
16	39.4	40.6	39.9	33.3
17	40.1	40.1	40.1	34.3

TABLE 2. RELATIVE WIDTHS OF MODULATION TRANSFER FUNCTIONS

POSITION	NN	BL	CC	LS
1	100.0	100.0	100.0	142.6
9	100.0	76.6	95.0	127.8

N82 28729

7.8 GEOMETRIC ERROR CHARACTERIZATION AND ERROR BUDGETS*

Eric Beyer, General Electric

This discussion describes the procedures used in characterizing geometric error sources for a spaceborne imaging system, and uses the Landsat-D Thematic Mapper ground segment processing as the prototype. It should be noted that software has been tested via simulation and is currently going through tests with the operational hardware as part of the operational system evaluation prelaunch, so that we can thoroughly characterize this system with respect to its geometric performance before we launch it. In addition, there is a substantial effort, both on the part of General Electric and NASA-Goddard in postlaunch evaluation of this data. With respect to geometric performance and radiometric performance the requirements for this system are being taken very seriously.

There are two requirements for Landsat-D Thematic Mapper as well a[s] pro-cessing, which relate to the geodetic accuracy. Figure 1 displays t[he] ac-cess whereby we can match back to a standard map as well as provide tempor[al] reg-istration, and band-to-band. There are some significant caveats in these areas which are important to the users. For one, Landsat is not a mapping system, we don't view it that way. We are providing a system that will meet certain geodetic rectification requirements if we are provided maps that have no errors in them. That obviously is not the case. Therefore, much of the attention in Landsat-D has been directed towards temporal registration. That is we want to be sure that we are self-consistent, that our images will overlay with high accuracy.

The requirements for geodetic registration is .5 pixel, again with its major caveat, and there is another caveat which has to do with adequate numbers of ground control points. One other that says this is to be done without consideration of topographical variations. Thus, this is the performance expected if you have a flat earth for temporal registration and the ground track and attitude control of the spacecraft were exactly repeatable past to past. There has been very little concern about band-to-band accuracy with the multispectral scanner, mostly because due to its design it has exceedingly good band-to-band accuracy. Once you get the focal plane base plate properly designed along with the scanning mechanism, there is very little opportunity for band-to-band misregistration with the MSS. The Thematic Mapper has a much larger spread to its detectors and much larger time between various bands being imaged, so there is much more opportunity for band-to-band registration errors. As Jack Engel has pointed out, the current instrument has very good band-to-band accuracy. There are features in the ground processing that will significantly improve that. For the Thematic Mapper after processing, it should be possible to achieve something well down below a 10th of a pixel band-to-band accuracy.

The single scene accuracy requirement can be characterized as:

*Edited oral presentation.

0.3 PIXEL TEMPORAL (90%) X

$$\frac{42.5 \text{ RAD}}{\text{PIXEL}} \times \frac{(1\ )}{1.645(90\%)} \times \frac{\text{SINGLE SCENE}}{2 \text{ TEMPORAL}} = 5.48 \text{ RAD } (1\ )$$

$$= 3.9 \text{ METER } (1\ )$$

We are essentially dealing then with the Gaussian-type error performance, so I can convert one-to-one sigma by the Gaussian transformation 90% to one sigma for temporal registration. Given we do our processing down to the point where the errors are uncorrelated from scene to scene, we are roughly talking about a factor or square root of two for a single scene. That translates to 5.5 microradian, a little more than an arc second, four meters total error budget. All errors have to be significantly smaller than that. At 30 meters with subpixel accuracy specified this way we have an extremely challenging job.

Figure 2 describes the Landsat-D processing system. The characteristics of the Thematic Mapper and the Spacecraft and the Tracking Data Relay Satellite Systems on that spacecraft provide essentially all constraints of spacecraft design. You don't have much flexibility in spacecraft design. We first looked at the Thematic Mapper as a big MSS and we are going to process it as an MSS. We started down that path about three years ago doing error analysis and every time we would examine in detail some of the errors we were horrified. It finally got to the point were we were about 3 pixels temporal registration and growing. At that point in time, we went to the Landsat-D project and said something has to be done, either the specs have to be changed or we have to redesign the processing system, from a system point of view. That was the first test of that 0.3 pixel, and it would have been much easier at that point in time to say 0.3 pixel was not really required. That requirement has, however been maintained. What I am going to describe now is an overview of the changed design, which essentially we've been going through the last two years.

In our attempt to meet the registration goals, we had to get involved in the workings of the Thematic Mapper. We had to get in there and really understand how that worked and apply our processing directly to the inner workings of that instrument. We could not hold the platform steady to an arc second or a fraction of an arc second to achieve a 1-arc-second total error budget. The solution there was to measure. We installed a small angular displacement 3-axis package on the Thematic Mapper; it cannot be mounted any place else on the spacecraft because of structural dynamic effects. It's one draw back is that it is essentially a high-pass device, and the electronics we build for it has a band of 2 Hz to 125 Hz; it does not capture the low-frequency end. That shortcoming was alleviated by incorporating some of the hardware that was already on the spacecraft, namely the attitude control drivers which have a bandwidth of somewhere just above 0 Hz to 2 Hz nominally. An onboard computer performs functions of sampling the gyros as part of its attitude control function; it estimates the gyro drift, gives us initial attitude estimates, and it is the source of an ephemeris if the GPS system is giving the ephemeris to the OBC, which then sends it down to us, and sometimes an uplink of ephemeris also comes to us for ground processing through the onboard computer. A formatter was added, which is essentially a piece of hardware that takes samples of the angular displacement sensor and sends it down on a telemetry link called payload correction data. That data set is all the information external to the

Thematic Mapper needed to perform Thematic Mapper Processing, both radiometric and geometric.

There are certain pieces of additional data that are very important. We know that the scan mirror is not perfectly repeatable in the Thematic Mapper. That was determined after extensive testing by Hughes of the Thematic Mapper scan mirror mechanism. In order to characterize the scan mirror it was determined that more than just the starting and end locations were needed. We needed an evaluation point in the middle of the scan. So the data that is sent down is the scan start time, which allows us to coordinate the scan mirror positions with all the other measurement systems on the spacecraft. The scan direction first-half second-half scanner essentially tells us how the scan profiles are behaving in time. In the ground processing, we extract the scan information out of the wideband data. Payload correction processing is the process that takes the scan mirror information, as well as all the other attitude and ephemeris related information, and generates systematic correction data which will essentially remove all the high-frequency internal distortions when applied to the imagery. At that point of time we have not captured some significant low-frequency errors relating to ephemeris alignment, time, errors, and low-frequency attitude errors. Those are captured by ground control points (Figure 3) used to adjust the data and to derive what we call geodetic correction data, which is an identical form, but improved values (see Figure 4).

In the meantime, off-line, there is a very high speed reformating and radiometric correction applied to the imagery in parallel to generate what we call archive imagery. Archive imagery is available as a product for the TM; it includes reformatted imagery with the data appended to it. The next step in processing is to actually perform the resampling based on this product for the TM; it includes reformatted imagery with the data appended to it. The next step in processing is to actually perform the resampling based on this data. We do the mapping from the input space to the map coordinate outboard space.

Figures 5 and 6 describe the error budget. In review, systematic correction data is data which does the mapping from input space to output space, but control points have not been included. Control points remove some very large errors, but they are low frequency. Ephemeris uses the worst case, a 2-day predict to which we had to design. This time is the result of the $\pm$ 20 millisecond clock or absolute time. Attitude control as .01° effective meters, 1 sigma, is an alignment which is a rather large number. This is essentially a fixed bias, and I know here that with minimal amounts of processing, that number can be reduced very substantially in ground processing and indeed that will be done. But immediately after launch, we could have alignment errors that large. So we are talking about rather large uncertainty here, so there is no hope of knocking all of these down to anything less than that without using ground control points. The ground control point processing is substantially different than previous processing for ground control points in its estimation technique in that it is a common filter smother-type processing. We have developed both noise models and dynamic models for all these errors and they are included in the processing. The advantage of doing that is that we can develop the processing technique that is significantly less sensitive to control point distribution. One of the major problems that plagues many of the current processing systems is that if you have to have an extremely good distribution of control points, you better not have any control points that

are in serious error because it will substantially affect polynomial fits. With this technique we have a very graceful degradation in performance as we change the locations into non-optimal positions and we can propagate through extended periods that don't have control points. So if there is a group of scenes that have a number of control points at the top, then ten scenes later a number of control points, we are not necessarily going to meet our accuracy requirements in between, but we can come very close to it, as we can verify performance by propagating these errors, via the dynamic models of the filter smoother estimation technique.

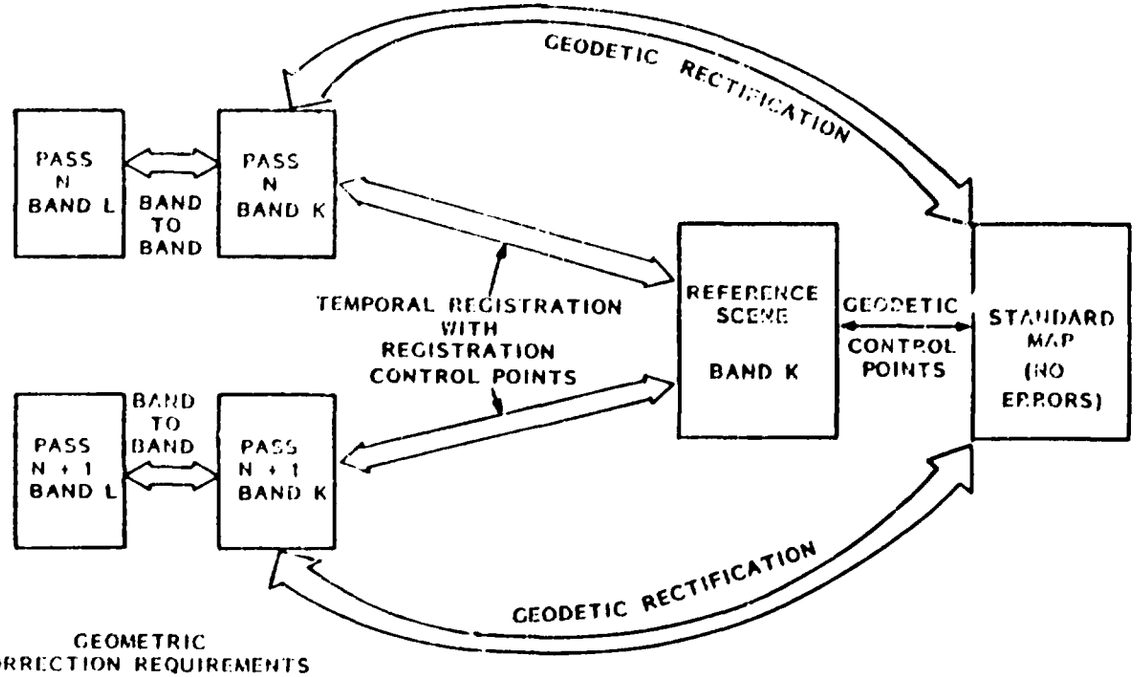

GEOMETRIC
CORRECTION REQUIREMENTS
90% OF THE TIME

GEODETIC	0.5 PIXEL
TEMPORAL	0.3 PIXEL (REGISTRANT TO REFERENCE)
BAND-TO-BAND	0.3 PIXEL

Figure 1.. Geometric Accuracy Specifications

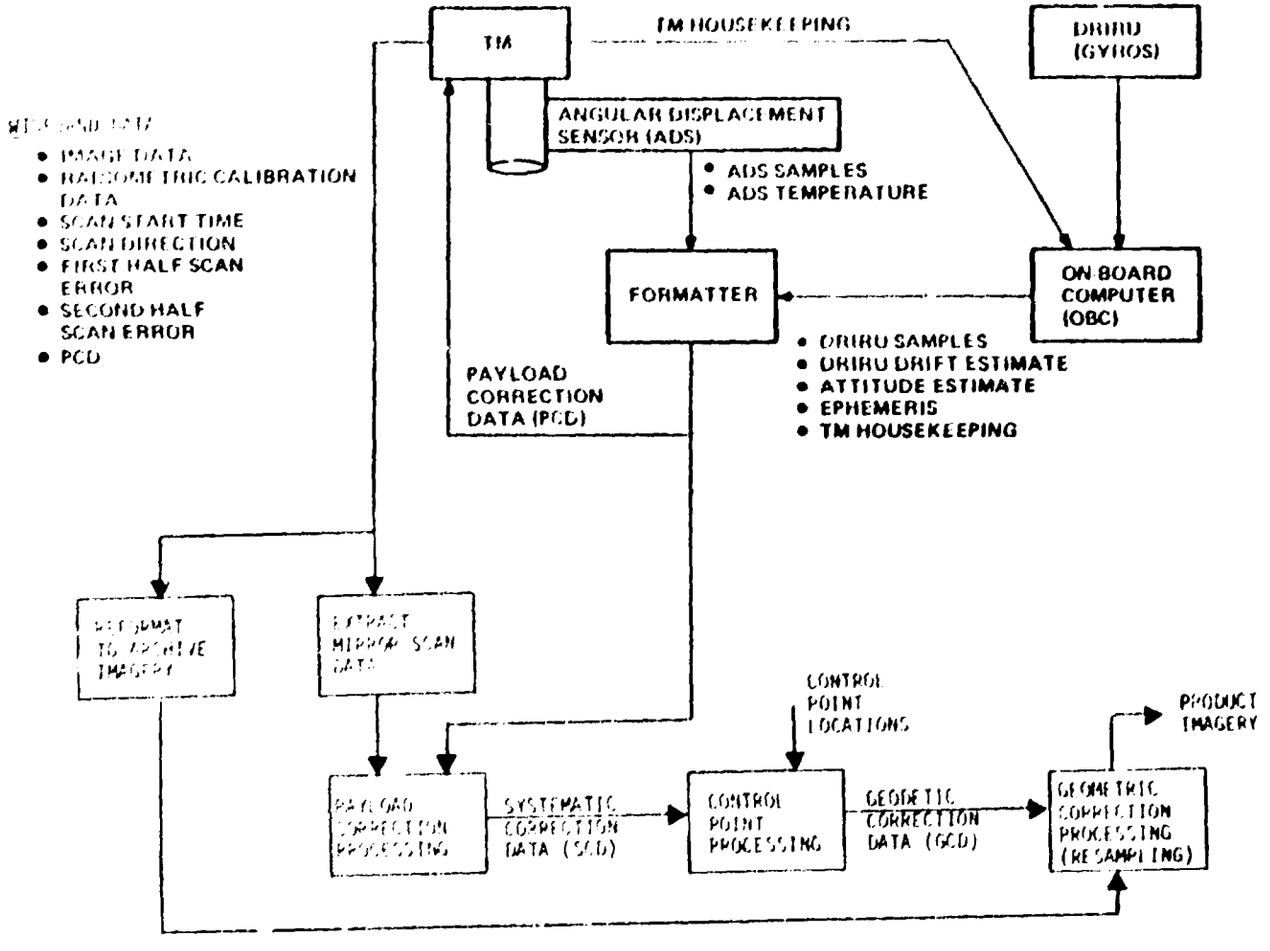

Figure 2. Thematic Mapper Geometric Correction

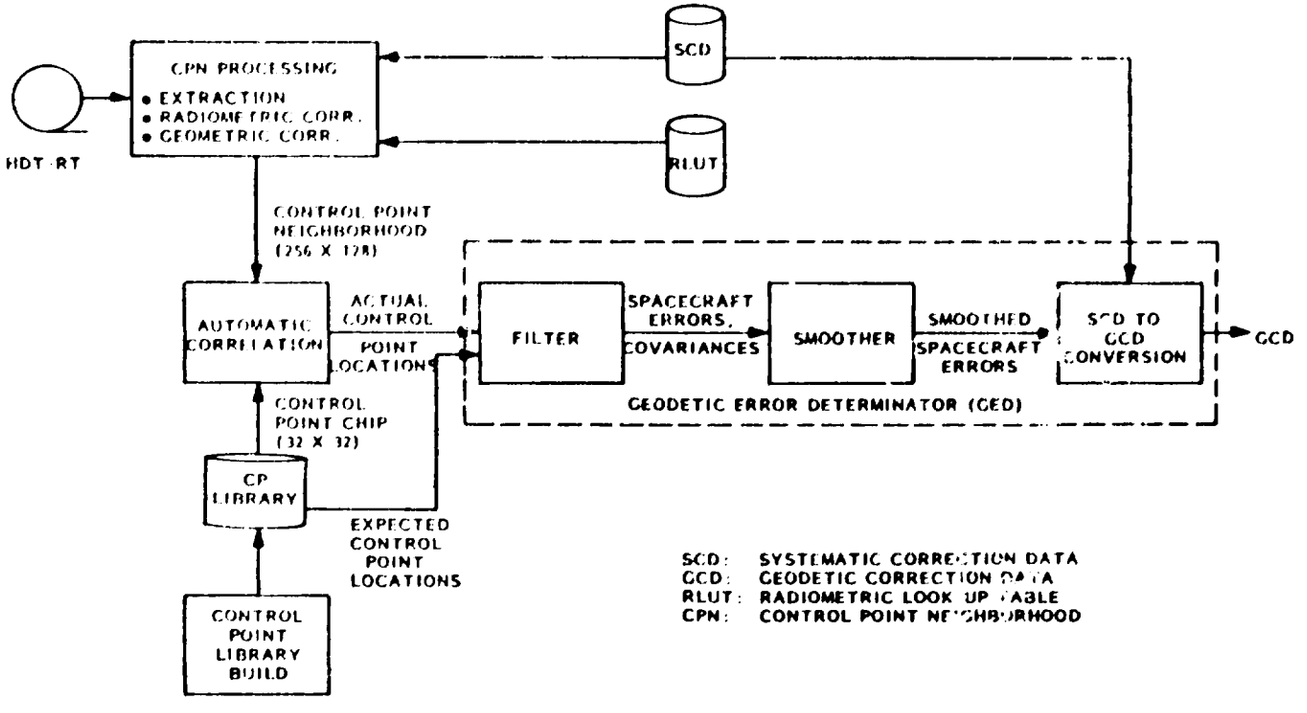

Figure 3. Control Point Processing

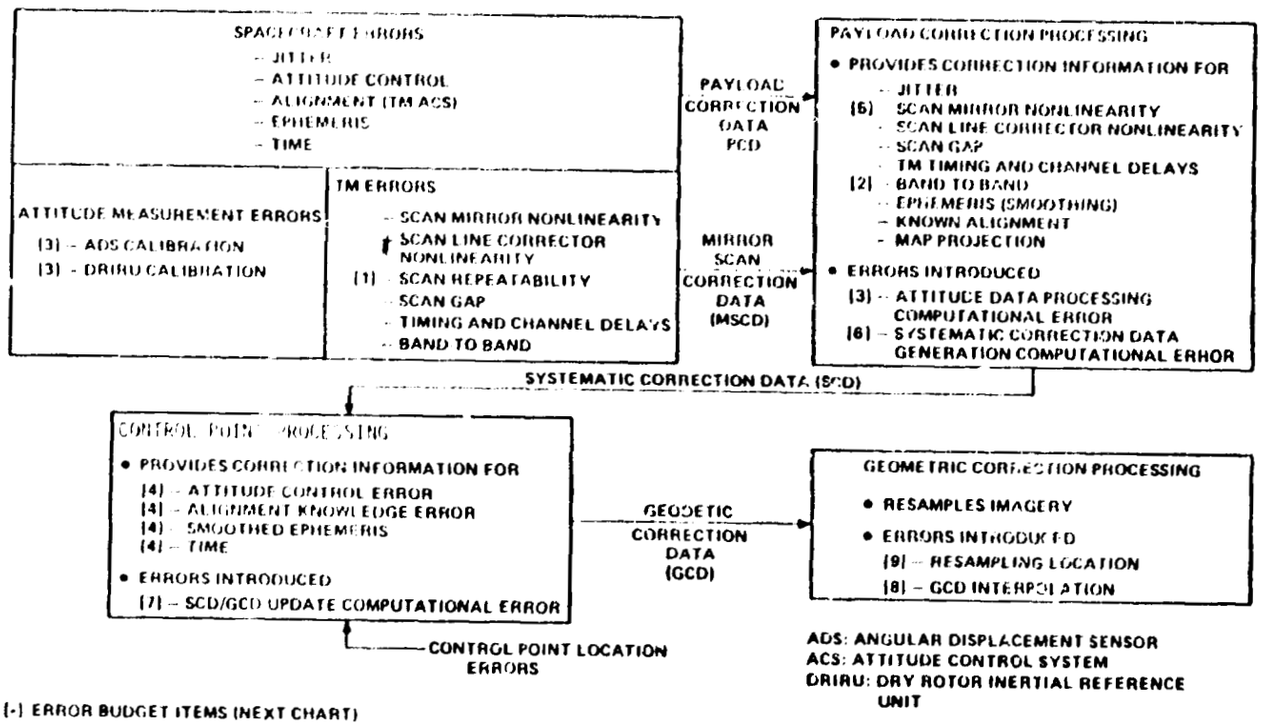

Figure 4. Thematic Mapper System Geometric Errors

ERROR SOURCE	CROSS TRACK ERROR*	ALONG TRACK ERROR*	ITEM NUMBER (PREVIOUS CHART)
• THEMATIC MAPPER			
– SCAN REPEATABILITY	$.165\sqrt{2}$	$.165\sqrt{2}$	1
– BAND TO BAND	$.048\sqrt{2}$	$.039\sqrt{2}$	2
• SPACECRAFT			
– JITTER	$.094\sqrt{2}$	$.094\sqrt{2}$	3
– ATTITUDE, EPHEMERIS, ALIGNMENT, TIME RESIDUAL	.165	.165	4
• GROUND PROCESSING			
– SCAN NONLINEARITY CORRECTION	$.082\sqrt{2}$	0	5
– SYSTEMATIC CORRECTION DATA GENERATION	$.055\sqrt{2}$	$.055\sqrt{2}$	6
– CONTROL POINT PROCESSING	$.055\sqrt{2}$	$.055\sqrt{2}$	7
– GCD INTERPOLATION	$.055\sqrt{2}$	$.055\sqrt{2}$	8
– RESAMPLING LOCATION	$.014\sqrt{2}$	$.014\sqrt{2}$	9
• TOTAL (ROOT-SUM-SQUARE)	.369	.348	
• SPECIFICATION	.3	.3	

*RESIDUAL ERROR AFTER PROCESSING

Figure 5. Thematic Mapper System Temporal Registration Error Budget In Pixel (42.5 Microrad) 90%

ERROR SOURCE	CROSS TRACK (METERS 1σ)	ALONG TRACK (METERS 1σ)
EPHEMERIS	100	500
TIME		80
ATTITUDE	123	123
ALIGNMENT	427*	855*
TOTAL (ROOT-SUM-SQUARE)	455 (25 PIXELS 90%)	1001 (55 PIXELS 90%)

*SUBSTANTIAL REDUCTION WILL OCCUR AFTER POSTLAUNCH CALIBRATION (205 METERS (1σ))

Figure 6. Geometric Error In Systematic Correction Data (Approximate)

N82 28730

7.9 GEOMETRIC VERIFICATION

Gerald J. Grebowsky
Goddard Space Flight Center

Before proceeding with a discussion of geometric verification methods, a brief review of present Landsat data formats will clarify how both geodetic location and registration capabilities were defined. Since February 1979, Landsat multispectral scanner (MSS) data has been processed through the master data processor (MDP). The definition of the fully processed output image arrays (P-tape products) was intended to facilitate both geodetic location and temporal registration of image pixels. The world reference system (WRS) nominal image centers defined in degrees and integer minutes of latitude and longitude were selected as the reference points in output images. Framing of MSS images was defined to locate the WRS nominal image center on the center line (line 1492) of the output array. The phasing of the geometric resampling process was defined to locate the WRS center exactly on a pixel (not necessarily the center pixel) of the center line. Finally, at the WRS pixel the orientation of the center line relative to rectangular map coordinates was specified for each WRS.

By the above definitions, the geodetic location of pixels in a P-tape image lie on a 57 x 57 meter grid rotated by a specific angle (about the WRS pixel identified in P-tape header) relative to the rectangular coordinates of the map projection used. Two images for a given WRS can be registered by simply shifting one of the arrays in the along scan line direction to account for the difference in pixel locations of the WRS center.

As an aside, fully processed output arrays for return beam vidicon (RBV) data were defined as 19 x 19 meter grids overlaying the MSS grids (3 x 3 array of RBV pixels for each MSS pixel). A pixel and line number referencing each RBV subframe relative to a WRS pixel are given in the header of an RBV P-tape. This definition of RBV arrays was intended to provide a registration capability between RBV and MSS.

The accuracy of a P-tape image is a function of the geometric modeling which determines where image data are located in the P-tape array. Since there is only one geometric model used in the MDP, geometric location accuracy depends on the absolute accuracy of the model and registration accuracy is determined by the stability of the model. Due primarily to inaccuracies in data provided by the Landsat attitude measurement system (AMS), desired accuracies are attainable only by using ground control points (GCP) and a correlation process.

Control points consist of 32 x 32 arrays of MSS data with locations defined by latitude and longitude. When maps are available, the locations are derived from the maps and both location and registration accuracy will be improved. Without maps, locations are derived from a reference P-tape image using the array location definition previously discussed. In these cases only the stability of the geometry and, therefore, the registration accuracy is improved.

The performance specifications for MSS P-tape data were .5 pixel (per axis) geodetic location and .3 pixel (per axis) registration. In the development of the MDP, this specification was taken with reference to input pixel instantaneous field of view (IFOV) of approximately 80 meters. In terms of the 57 meter pixel spacing of output P-tape arrays, these specifications convert to .7 pixel (per axis) geodetic location and .4 pixel (per axis) registration. This performance requires successful correlation of 20-25 well distributed control points in an MSS image. The geodetic location specification also requires the control points to have location errors less than 35 meters (rms) relative to refence maps.

The verification of system performance with regard to geodetic location requires the capability to determine pixel positions of map points in a P-tape array. Verification of registration performance requires the capability to determine pixel positions of common points (not necessarily map points) in 2 or more P-tape arrays for a given WRS scene. It should be noted that registration measurements will identify changes in location, while the difference between location measurements yields the registration error. Thus an accurate geodetic location verification provides registration data and registration verification can provide location data if one of the P-tapes has been verified geodetically. This relationship offers the opportunity for alternate (or mutually checking) implementations for verification of geometry.

Since the building of a GCP library for the MDP consisted of accurately identifying the locations of 32 x 32 MSS arrays relative to maps, the library build function demonstrated a method for location verification. The location funtion was accomplished by a manual overlay of a map feature and a cathode ray tube (CRT) display of MSS data. The overlay was accomplished using a Bausch and Lomb zoom-transfer scope which provides an optical superposition of 2 inputs through a binocular viewer. The inputs were a CRT display of MSS data (scaled according to available map scale) and the actual map with a feature identified. The manual overlay of the superimposed binocular view consisted of simply moving the map to give the best fit to the displayed MSS data. The specific point on the map for which latitude and longitude had been defined was then identified by moving a cursor on the CRT display. The cursor position identified the center of the 32 x 32 GCP array to be stored in the MDP library and the fractional pixel location of the defined latitude and longitude within the 32 x 32 array.

Using this technique f r geodetic location verification is straightforward. For a selected map feature, the expected pixel and line number location in a P-tape image can be calculated from the latitude and longitude using the appropriate map transformation and rotation of coordinates previously described. This calculated location identifies the area of MSS data to be displayed on the CRT. The cursor position after manual superposition identifies the measured pixel and line number location of the map feature. The location error is simply the difference between the expected and measured locations.

An improved version of this technique can be developed by converting the selected area of a map to a digital video signal and combining the map and MSS displays directly onto the CRT display. A short study by IBM demonstrated that this superimposed display facilitates the manual overlay function.

Techniques for registration verification can be more varied and automated since map data are not required. Although correlation of common features would be possible, edge detection and correlation of arbitrary areas is probably preferable. Goddard's Large Area Crop Inventory Experiment (LACIE) processor used edge detection and matching to extract sample segments (117 lines, 160 pixels) registered to a reference segment. This system met its specified registration goal of 1 pixel (rms). However, all LACIE extractions were verified by manually comparing film images of the extracted segments with the reference segment and a small percentage were rejected due to registration errors. This experience demonstrated the need for a manual backup test. Rather than using film images, a CRT display with the capability to flicker between 2 test areas is recommended for verification testing. This manual mode would not have a strict accuracy requirement since it would only be used to assure that a correlation should exist.

One additional lesson can be learned from the LACIE System. During the development effort, experiments showed that edge data of a single MSS band were not necessarily invariant with seasonal changes. In fact, edges appearing in one band for one season occasionally appeared in another band for another season. This effect lead to the use of composite edge images using MSS bands 5 and 7. Similar considerations may be required in a registration verification system.

Although automated verification methods are highly desirable, manual processes are presently necessary when dealing with maps and advisable for verifying registration correlations. Manual processes offer an additional verification capability in terms of exposing higher frequency distortions in image data. Automated correlation functions produce mean results for the areas correlated and may be insensitive to registration errors in smaller areas.

The implementation of a verification system will depend on the number of measurements required per image and the number of images to be verified. In turn, these requirements depend on user expectations implied by performance specifications. The final question is: which of the following verification levels are required by data users?

a) 100 percent of pixels in an image within specifications

b) Less than 100 percent, but some minimum percent of pixels in an image within specifications

c) A probability that an image meets specification

REGISTRATION

8.0 SYSTEMS PRESENTATIONS AND DISCUSSION PAPERS

8.1 SUMMARY

In response to the workshop call for additional papers that represent recent thinking on the problem of registration and rectification, ten papers were received. Three were concerned with the impact of misregistration upon the overall information content (i.e., utility) of data being used for models based on multitemporal analysis, particularly for croptyping. Five papers were concerned with the problem of accurately determining spacecraft attitude in near-earth orbits and the resultant impact on precise registration and rectification of terrestrial imagery. Two papers proposed spaceborne imagery systems that would serve multiple roles by incorporating multiple resolutions and view angles, each imaging component being optimized for a different function. This contrasts with the current approach toward a single general purpose sensor. Four papers proposed ways to improve attitude control, either through improved engineering of future spacecraft and ephemeris instrumentation, or through enhanced techniques for ground segment processing of control points.

8.2 MISREGISTRATION'S EFFECTS ON CLASSIFICATION AND PROPORTION ESTIMATION ACCURACY*

R. Juday and F. Hall, Johnson Space Center

The estimates of crop type and acreage (proportion estimation) are undertaken in the AgRISTARS program by registering multiple date acquisitions of small subareas of Landsat scenes (termed segments), and applying multispectral analysis to them. An important contribution to errors in classification and acreage estimates is misregistration between multiple acquisitions. The relationship can be expressed as:

$$\mathrm{VAR}(\hat{A}) = \sum_i \omega_i \sigma_i^2$$

σ_i^2 = VARIANCE OF ACREAGE ESTIMATE FOR iTH STRATUM

ω_i = WEIGHT WHICH DEPENDS ON STRATUM SIZE

$$\sigma_i^2 = (\omega_i)^2 \sum_j \sigma_{js}^2 + \sigma_{jc}^2 + \sum_{j \neq k} \mathrm{COV}(\hat{P}_j \hat{P}_k)$$

σ_{js}^2 = VARIANCE RESULTING FROM SAMPLING

σ_{jc}^2 = VARIANCE RESULTING FROM SAMPLE SEGMENT PROPORTION ESTIMATES

$\hat{P}_i$ = PROPORTION ESTIMATE IN iTH SEGMENT

The particular series of operations applied are shown diagrammatically in Figure 1. The spectral data brought in with ancillary data are transformed into the Kauth-Thomas space, where features are extracted. The Kauth-Thomas greeness is a function of time for multiple acquisitions. It is approximated in functional form with various parameters and the vector of these parameters and its distribution within the segment you are working with is decomposed so that its overall distribution function is approximated a posteriori. The a priori probabilities given class and spectral vector that describe a class are the parameters that give you the estimate of the area and crop type. The ancillary data is the place where you bring in the fact that you are working in a specific area, thereby limiting the variety of possible crop choices.

Figure 2 illustrates the taking of a Landsat feature vector and deriving the brightness and the greeness. A procedure derives certain parameters that describe the time at which a crop begins to green up, and the steepness with respect to which the curve moves off the soil line is a function of time; time being a characteristic difference between some of the crops that we're trying to differentiate. This kind of procedure is sensitive to absolute radiometry to perhaps a larger extent than some researchers maybe are interested in with regard to maintaining radiometric fidelity in the resampling process. Figure 3 illustrates the procedure whereby a scene is broken into various strata. There are distribution functions within each strata for the spectral measurement vectors via a procedure called CLASSY. CLASSY breaks the curve down to

*Edited oral presentation.

several distributions which are assumed unimodal and normal. This is the place at which the proportion estimates fall out. In the process of doing this, the mixture pixels along the boundaries of the segments create confusion. Registration error looks something like a mixture pixel. If there is misregistration, and a given address for a pixel jumps across the boundary, it acts as a noise, and in the multitemporal sense will tend to confuse crop discrimination.

Figure 4 presents the expression of pure and mixed pixel contributions to classification error. Knowing full well that we have mixture pixels, and if you can parameterize the problem in terms of your estimate of a crop that has found its truer pixels, the equation can be applied to derive a final proportion estimate. The variance in the estimate of the crop proportion in mixed pixels is typically larger than the variance of the estimate of the crop that is in pure pixels. You would like to have q, which is the proportion of the scene which is in pure pixels, to be a larger number so as to reduce the overall variance. That, of course, is done in one way by going to smaller pixels and in another by having better registration accuracy so that you don't have the multitemporal jumping of pixels. Now the quantity q will approach a number that is limited by the spatial resolution of the system as the registration error declines. There is a point at which you cannot drive q to be a larger number with increasing registration accuracy and that declining gain determines the point at which for any particular analysis technique, it is not practical to expend more effort in trying to get better.

For any given sensor IFOV geometry, you can derive typical populations of fields and you can plot histograms of the number of fields against field size and you can draw different histograms for the different kinds of crops that, according to your ground truth, go into making up the population examined. Dave Pitts and Gothem Badhwar have published some results for representative samples in the growing regions of the U.S. that are of significance to us (Figure 5). As a function of the resolution element, the IFOV of the sensor, according to those kinds of histograms in Figure 5, can draw the proportion of pure pixels in a given crop (Figure 6). This is the quantity which you would like to drive up. The TM will have a resolution that is considerably smaller, so the proportion of pixels that are pure in any given area will be larger. You can draw an analogy between the misregistration error as acting much the same as an increased resolution IFOV and expect that things will go in the same direction although we have some doubts that you can draw an exact equivalence there because there is some difference in behavior.

This is a workshop and not a symposium so I am not presenting a final result. At this point we do have a program underway to come up with quantitative numbers for the results for the effect of the misregistration error. Also, we are tending to work mostly on the multitemporal aspects of misregistration at this point. Band-to-band misregistration has similar effect, but, in our particular application, it's a less dynamic kind of an affect. We built a registration system at JSC to a point when it was clear that the one pixel registration accuracy that the LACIE processor was giving us was only marginally adequate for the LACIE technology, and with AgRISTARS we needed something better. The MDP, being a full-frame system, does not concentrate as heavily its computation power on an individual pixel. We set ourselves a goal of 2/10 pixels as the registration accuracy that we would like to get to. This was based on the arbitrary criteria that what you would like is 50% of the multi-

temporal energy to come from a common area on the ground. When you do that, it's really amazing how strictly that ties down the registration accuracy that you think you would like to get to. When you begin talking about registration at that accuracy you uncover all sorts of things that you didn't have to think about previously. As Figure 7 illustrates, the difficult problem to determine is the registration accuracy that you want analytically when you overlay one aperture over another. For pixel A and pixel B, the portion of the clear aperture is a function of the position of the pixel B, given pixel A is fairly easy to calculate. But when you begin to add other pixels that complicates your clear aperture upon adding a third aperture, given a position of the first two is some value on the ramp. It is highly nonlinear and this gets worse when you go to two dimensions, and when you get nonsquare IFOVs, and when you have a variation of response within a IFOV. Our plan is to pursue a Monte Carlo approach in assuming a misregistration error and model its distribution through the process.

In conclusion, it should be noted that we do not have a quantification of misregistration's effect on our analysis at levels better than we currently achieve. Synthetic data is one approach; extrapolations obtained by deregistration is another. Registration accuracy requirements are difficult to specify a priori. "More is better"; everyone's an expert. Extrapolation to the performance expected from better registration is risky, and highly dependent on analysis techniques. The proper arena for testing is one's own applications analysis.

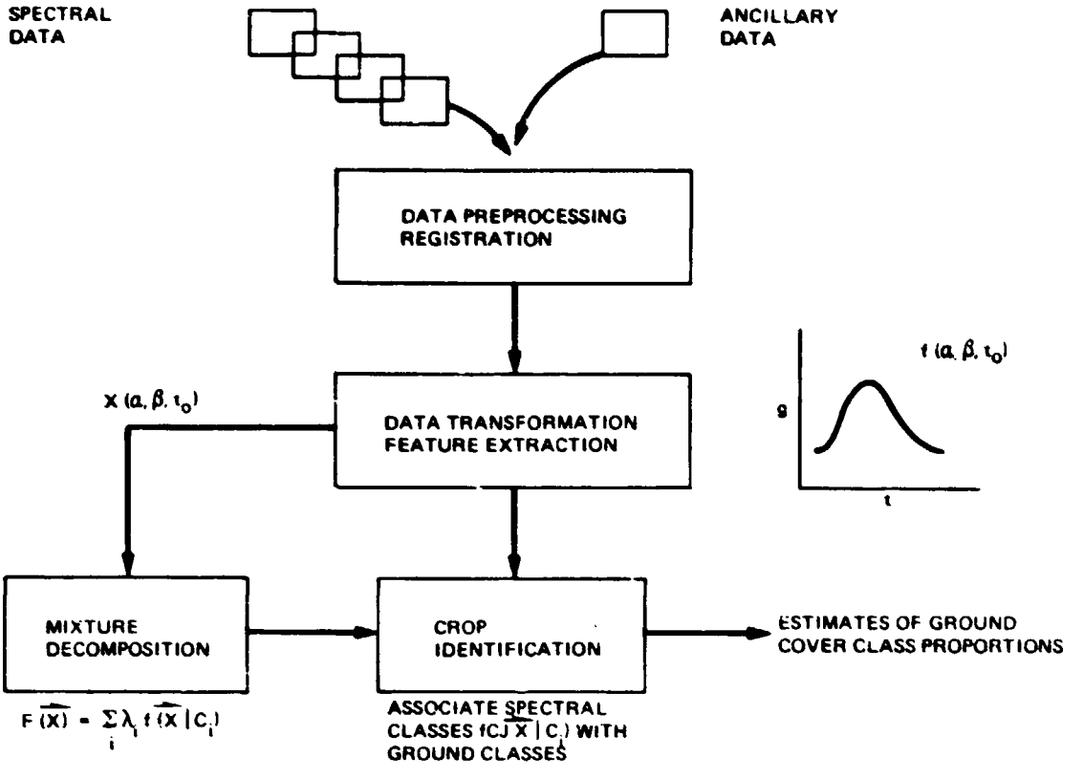

Figure 1. Crop ID/Proportion Est.

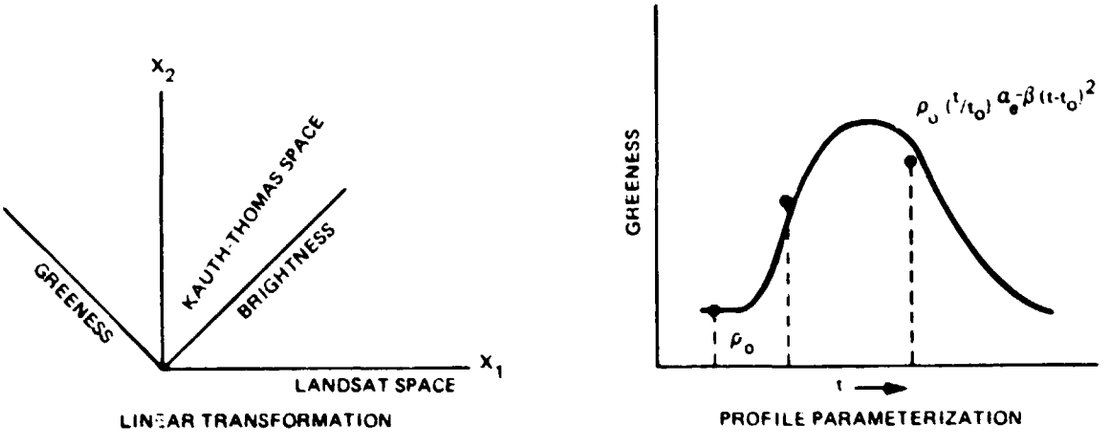

Figure 2. Data Transformation/Feature Extraction

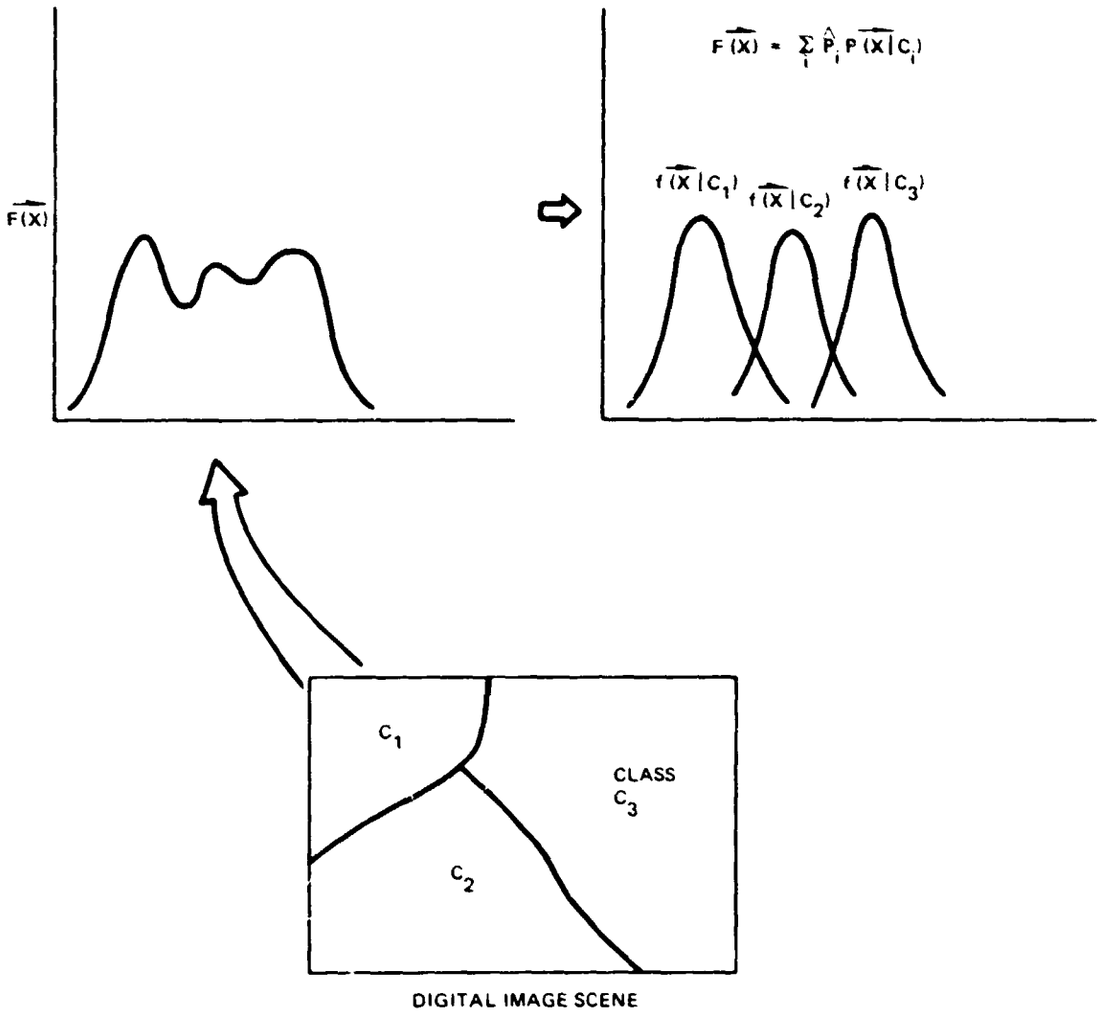

Figure 3. Mixture Decomposition Estimation

$$P = qP_o + (1-q)P_m$$

P = PROPORTION ESTIMATE FOR SCENE FOR CROP

P_o = ESTIMATE OF CROP PROPORTION IN PURE PIXEL AREA

P_m = ESTIMATE OF CROP PROPORTION IN MIXED PIXEL AREA

q = PROPORTION OF SCENE IN PURE PIXELS

$$\text{VAR } P = q^2\sigma_o + (1-q)^2\sigma_m^2 + 2q(1-q)\sigma_{om}$$

$\sigma_o^2 = \text{VAR } (P_o)$

$\sigma_m^2 = \text{VAR } (P_m)$

$\sigma_{om} = \text{COV } (P_oP_m)$

Figure 4. Pure and Mixed Pixel Error Contributions

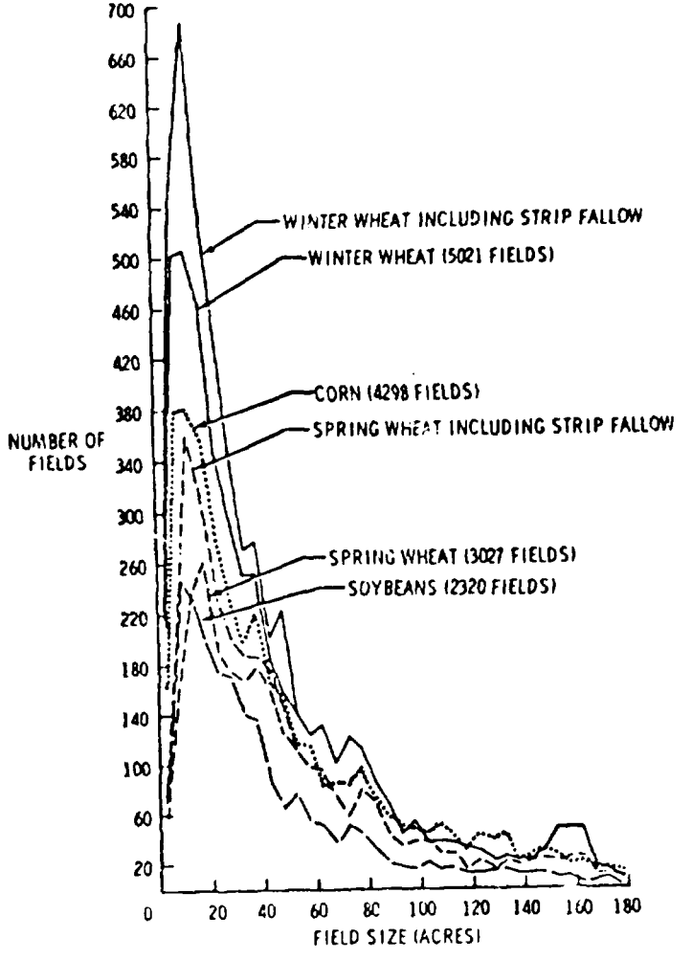

FIGURE 5 Field size distribution for winter wheat, corn, soybeans, spring wheat, winter wheat including strip fallow, and spring wheat including strip fallow.

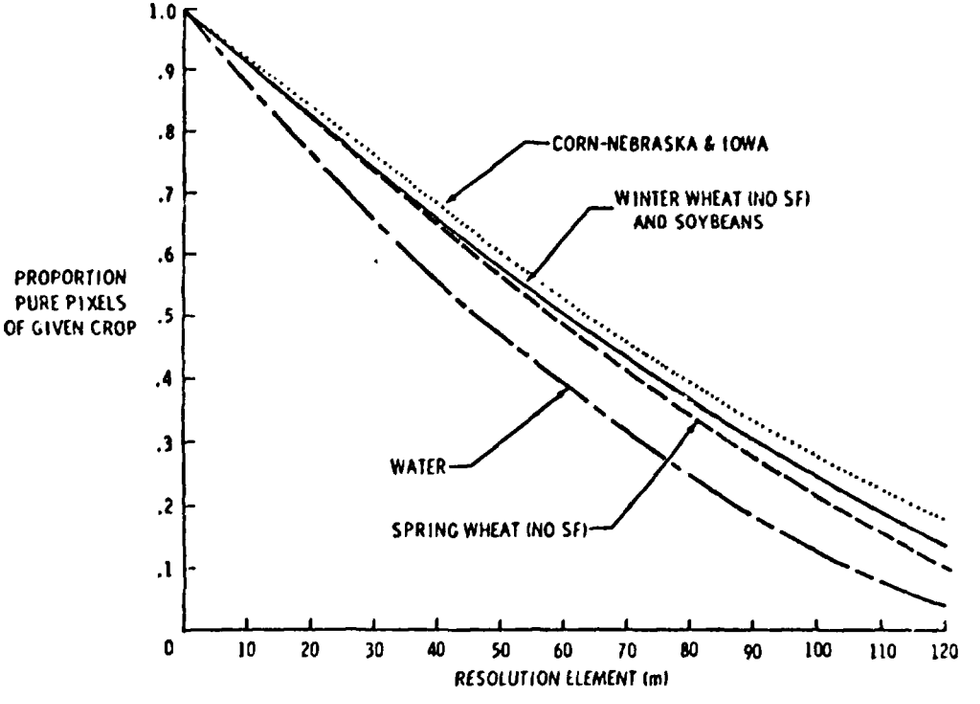

FIGURE 6 Proportion of a crop in pure pixels as a function of sensor resolution.

- ANALYTIC METHOD IS TOUGH

  CONVOLUTION OF TWO APERTURES:

  |--------| A

  |--------| B

  CLEAR APERTURE

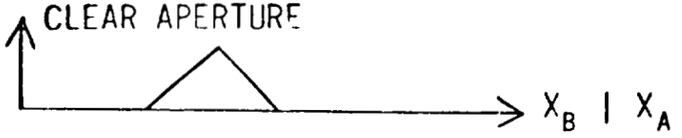

  ADD A THIRD:

  CLEAR APERTURE

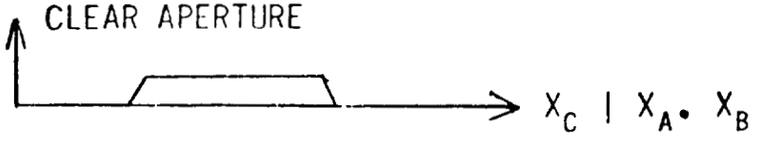

  NON-LINEAR EVEN FOR IDEAL APERTURES.

  COMPLICATES WITH Z-D. NON-SQUARE IFOV's

- PLAN TO PURSUE MONTE CARLO

Figure 7. Effects of Resampling Upon Multiple Overlays

8.3 DATA VS. INFORMATION: A SYSTEM PARADIGM

Fred C. Billingsley
Jet Propulsion Laboratory, California Institute of Technology
Pasadena, California 91109

This is a paper about thinking.
It may not seem to be, but it is.
As such, it won't give any answers.
But it should give you some ideas.

In the justification stage of any new system, the proponent is usually asked to provide some sort of Benefit/Cost analysis. Because, for a data system, there is no value in the data per se, justification must be found in the benefits in the use of the data. If, as is usually the case, the instrument or system designer is not a "user", his recourse is to survey the user community to obtain some sort of consensus on the utility. The generally unsatisfactory nature of the resuls is reflected in the large number of times the users are surveyed, resurveyed, and re-resurveyed. Something must be missing, or the answers would have been found.

The thrust here is not the justification of the system itself, but rather the justification of the selection of the various technical parameters which the system must meet. This justification (i.e., optimum parameter tradeoff) must be done in relation to the ability of the user to turn the cold, impersonal data into a live, personal decision or piece of information.

Therein, of course, lies the sleeper: the data system designer requires data parameters, and is dependent on the user to convert his information needs to these data parameters. This conversion will be done with more or less accuracy, beginning a chain of inaccuracies which propogate through the system, and which, in the end, may prevent the user from converting the data which he receives into the information he requires. The concept to be pursued will be that errors will occur in various parts of the system, and, having occurred, will propogate to the end. Modeling of the system may allow an estimation of the effects at any point and the final accumulated effect, and may provide a method of allocating an error budget among the system components.

Inaccuracies will be considered to be of two types, which may be stated in terms of transfer functions for each of the system components considered: 1) Calibration--the difference between the stated transfer function and reality; 2) Uncertainty--the error bars around each stated function and measurement.

This paper presents the results of one phase of research performed by the Jet Propulsion Laboratory, California Institute of Technology, sponsored by the National Aeronautics and Space Administration under Contract NAS7-100.

We begin by modeling an information system as shown in Figure 1. The forward model is required to convert units of information to units of required data, and answers the question "What set of measurements will best carry (i.e., allow the best derivation of) the information?" This box provides the set of measurement "requirements" to the measuring system, which responds with a set of real measurements which will hopefully be somewhat near to the desired set. However, the data system may have an inaccurate or uncertain transfer function, so that the set of apparent measurements presented to the information model deviate further from reality. It is with this set that the user attempts to derive his information, using the Information Model.

Evaluation of the system takes place in two levels as suggested in Figure 2. Note that the evaluation (and, therefore, the design) of a total information system is the joint responsibility of the user and the data system designer, as model boxes under the cognizance of each are involved. The data system designer cannot be held for the inadequacies/uncertainties in either the forward or the information models, although he is deeply interested in the validity of each.

Care must be taken in designing the models, and the systems which they represent. Figure 3 applies to both models and systems. At the low end of complexity, the system may only provide a nominal solution to the information problem (A), and so the potential errors due to the design may be quite large. But at least, (B), the data can be obtained. At the other extreme, a complex model (D) can produce the desired results quite precisely, if only the data required for the solution could be obtained (C). If it can be identified, the saddle point, (E), is the optimum complexity to design to. In the case of registration of Landsat, for example, the saddle point may be found to be at the 0.5-1.5 pixel level, fairly broad, with the moderate gains obtained with very complex processing being very costly or the requisite complex data (e.g., world-wide GCPs) being unobtainable, or at the low complexity end, simple processing producing only moderate registration accuracy.

SYSTEM DESIGN

We will be concerned primarily with the data system design. This includes the choice of the parameters (e.g., spectral bands, resolution, etc.), the exactness with which they must be maintained, the calibration process including the availabilty of required ancillary data, data latency, and the uncertainties associated with each of these items. This must be done in the context of the complete information system. The data system block is diagrammed in Figure 4.

Two approaches may be taken to the data system design: 1) Optimize the data system by minimizing the summation of the deviations of the delivered products from the desired measurements; 2) Optimize the total information system by minimizing the decreases in obtainable information (by the users) due to deviations in the desired measurements from the requested set. One of these approaches is used implicitly, if not explicitly, in any system design. They do not necessarily lead to the same choice of parameters.

Thus, the data system design model for 1) is diagrammed in Figure 5. It can be seen that this is a linear programming problem. The loss function to be minimized is the (weighted, according to the importance of the various disciplines) sum of the deviations in the data delivered from each discipline request. The parameters available to the designer are the sensor bogie parameters, anticipated interference factors (such as sensor vibrations, ground altitude relief displacements, orbit uncertainties, etc.), the ability to measure these, the calibration forward model (i.e., how do we plan to remove the errors?), data system procedures, availability/accuracy of calibration references, and the procedures used to rectify (apply the calibrations). To properly choose between the parameters, coefficients pertaining to the sensitivity of results to variations in each parameter and to the importance of the various parameters are required. (For example, how important to Discipline A is the difference between prompt registration to 1 pixel vs. delayed registration to 0.3 pixel; how important are these relative to overlay matching or to absolute geodetic location, and how important is Discipline A in the total scheme of things?) These coefficients, if available at all, will generally be only poorly known. Note, however, that if they are not explicitly stated, they will be assumed by the data system designer with or without affirmation by the discipline users. A caveat to the users!

In approach 2), the user and his forward and information models are explicitly treated, as demonstrated in Figure 6. In this case, the information system design must take into account the effect of the real data on the information conversion in the information models, recognizing that it will be different from the desired data and will be accompanied by the accumulated uncertainties. In addition to the set of data system parameters, available also are potential changes in the forward and information models (e.g., the user may have to do things differently than first planned if the anticipated real data is too divergent from the data desired or if it will be accompanied by too large errors.) In an informaton-driven system, the information losses allowed will place tolerances on the real data. This requires that the information model be accompanied with a sensitivity analysis. The information/forward model linear programming optimization will allow the user to trade off the various desired parameters requested, allowing for the anticipation of data realities and the influences of the other disciplines on the total information system outcome.

Again, a caveat to the users--this procedure, usually implicit, requires the choosing of sensitivity coefficients, also usually implicit. The user with particularly sensitive requirements had best make his needs known!

Just as the various errors propagate to the end ("downstream"), in an information-driven system the tolerances will propagate upstream. The implication is that, in contrast to the normal single-thread system which requires ever-tighter tolerances in the earlier stages, it may be possible for certain users to pick off data earlier in the data stream before errors have had a chance to accumulate, and for them to do their own processing. This may relieve error tolerances on the remainder of the system.

In addition to the sensitivity coefficients for a single parameter, cross coefficients may be important in analyzing the tradeoffs. Four examples of interdependency of variables are sketched in Figure 7. For example, with Variable A being spatial resolution and Variable B being data rate: Case I (upper left), a user may have lots of computer capability, so that data quantity is no problem, but increasing resolution improves things up to a point after which (say) scatter in the data decreases his performance. In Case IV (lower right) a smaller user finds the same type of resolution optimization, but total data quantity hurts, so that at some point the increase of data with resolution becomes the limiting factor.

As a second example, let the variables be ability to register (in pixels) vs. the pixel size, and let us consider three cases: 1) user doesn't care about registration at all, because he is only looking at a single image; 2) desired geodetic location (in, say, meters) is constant regardless of resolution because the user must register to GCP at the same location accuracy independent of resolution; this user requires that the per pixel registration get better as the pixels get larger; 3) for overlay purposes, the same fractional pixel accuracy is required regardless of the pixel size. These are sketched in Figure 8, together with a hypothetical system peformance. The heavy line in Figure 8 indicates the ridge of optimum performance from the user point of view. The intersection of the anticipated system performance with the user ridge indicates the design optimum.

It is realized that the bogie parameters, sensitivity coefficients, and cross-sensitivity coefficients required to do a quantitative system optimization will generally not be available. Nevertheless, these are implicitly defined in the system designer's mind. He will make a mental evaluation of the user forward and information models, and try to decide which parameters are important and which can be slighted, and then proceed to the data system design. Much fundamental research remains to be done to define the forward and information user models and to obtain the sensitivity factors, to allow these to be used in a quantitative total information system design.

SYSTEM ANALYSIS

Somehow the system design is arrived at, the sensor built and data delivered. The user must then work with whatever data is now available, together with its errors. At that point he has only the information model to vary--that is, he will do whatever necessary to derive the desired information. We will leave him to his troubles, and consider the data system itself. The task at this point is to evaluate the system performance (see Figure 9).

The normal desire in designing a system is that each function be a 1:1 translation, with a change in dimensions only, until finally the "correct measurement" is the same as the "desired measurement". We will therefore model each function as "somewhat linear, with a bias" (figure left), but let the output be produced with some uncertainty (figure right). For a linear system with the input having any possible value with equal probabilty, the probability that the output has a value in a certain range is found by convolving the probability density function of the error with that of the

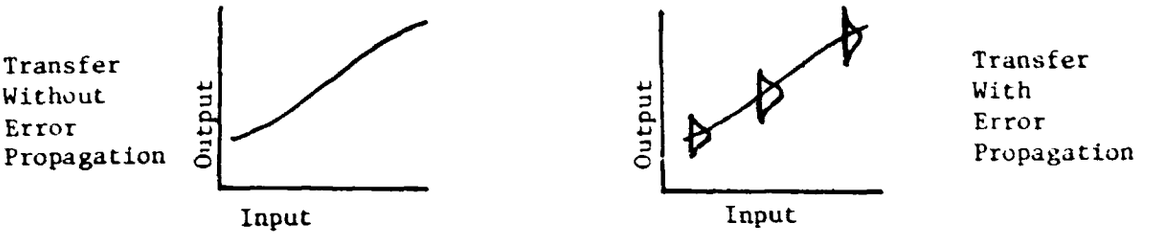

signal, and integrating between limits representing the range of interest. (Note that the probability distribution function of the error is equivalent, in one dimension, to the point spread function of the image case. The symbol h will therefore be used.) Define the "gain" of each stage as Output/Input = a, so that for a two stage system,

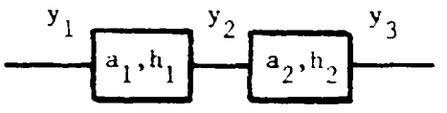

$$y_2 = a_1 y_1 * h_1$$

$$y_3 = a_2 y_2 * h_2 = (a_1 y_1 * h_1)\, a_2 * h_2$$

For constant total system gain $a_1 a_2$, minimum error occurs when $a_1 \gg a_2$. This leads to the engineers' old rule of thumb: put as much gain ahead of any noise sources as possible.

If the error sources are Gaussian, the convolutions become root-mean-square additions. However, in the registration case, it is not yet clear whether the error sources are Gaussian, so the RMS addition must be used wih caution. It is also not clear whether an RMS statement of the errors is the one most useful to the user in evaluating the system performance. For example, it may be more important for the user to know where the displacement errors occur (worse in areas of high relief and predictable in direction) than it is for him to know an RMS value (which in itself may be suspect).

It should be noted that a statement of the errors occurring in various parts of the system is of marginal use by itself unless, perhaps, one or more is glaringly bad. Not until the system model is built (implicitly or explicitly) can the error propagation be estimated. During system design, the propagation estimate is used to establish tolerances on the components, and during evaluation it will be used with the actual expected errors to check performance and to identify critical error contributors. After the contributing error sources and their interactions are identified, the following questions may be asked of each source and of the system as a whole:

* What is the intended component performance?
* What is the component actual expected performance?
* How may the performance be verified?
* What correction methods are available for system use?
* What correction methods are available for user use?
* How well can the correction methods potentially work?
* How well may the correction methods actually work?

* How do inaccuracies propagate through the system?
* How do uncertainties propagate through the system?
* Where are the major inaccuracy or uncertainty sources?

Finally, it is to be expected that there may be breakdowns during operation, or that there may be operational problems in performing the component functions. Considering probability of correct operation as a system criterion, the following questions are pertinent:

* What slack is there in the design to allow for problems?
* If a problem occurs, will the system fail catastrophically or gracefully?
* What is the probability that the system will remain up (within specs) for X% of the time?
* How hard does the system seem to be to operate?
* What potential for operator errors are present?
* Are work-arounds for various envisioned errors defined?
* How friendly are the system interfaces to the users?
* Where are the operational bottlenecks?
* Are there any serious single-point failure points?

FINAL POINTS

It can be seen that the various "User Requirements Surveys" have not asked the right questions, or at least have not asked the questions within a milieu to allow the user to respond with the coefficients required by the system designer. The most recent system survey by GSFC has taken a step in the right direction by presenting to the users several potential systems among which the users were to indicate the relative usefulness. But the necessary grossness of the differences prevents any fine tuning of the parameters.

It is not clear that this fine tuning is even possible, given the diversity of users within each discipline, let alone among the disciplines. No plateaus of, say, registration accuracy, have been found beyond which there is a marked loss of utility of the data. The loss of utility with poorer performance has not, perhaps cannot, be stated for the various disciplines. And the aggregation of the losses will produce a loss curve with a gradual slope, with no cliffs.

In the long run, it may well be found that all of the potentially obtainable information is already in the user surveys which are available and that users really cannot define their coefficients, much less anticipate the coefficients of others. This is the "low complexity" end of the spectrum. In this case, th advances in system performance will be more technology driven, and the users must make of it what they will. (In any event, once a system is designed, this is the situation.) It then remains to the system personnel to define what data quality results at various points in the system, and hopefully to allow the users to obtain data of various quality to suit their needs. The system error model will be used to do the evaluation, identify and remove successive error predominant sources, to provide ever-better data to the users, and to serve as a source of information for subsequent systems.

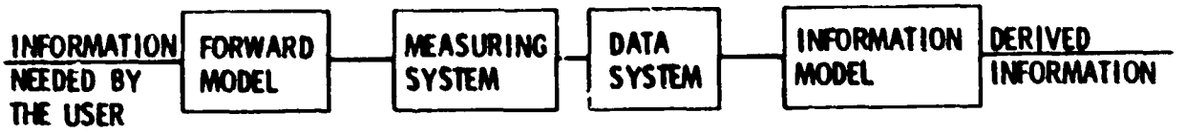

Figure 1. Information System Overall Block Diagram

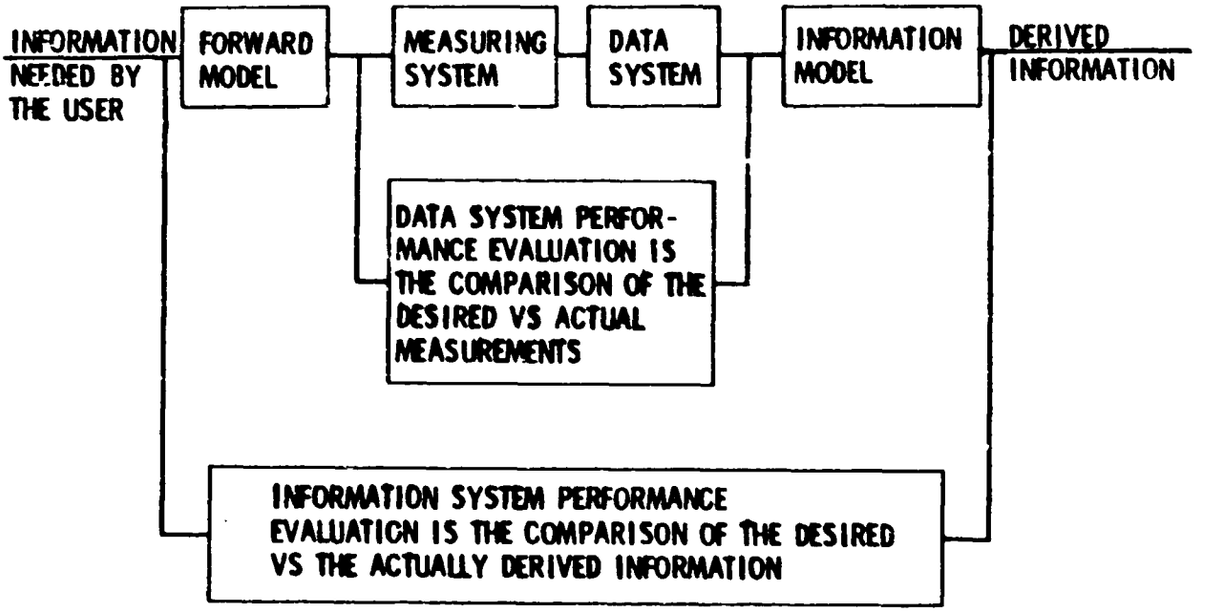

Figure 2. Performance Evaluation at Data System or Information System Level

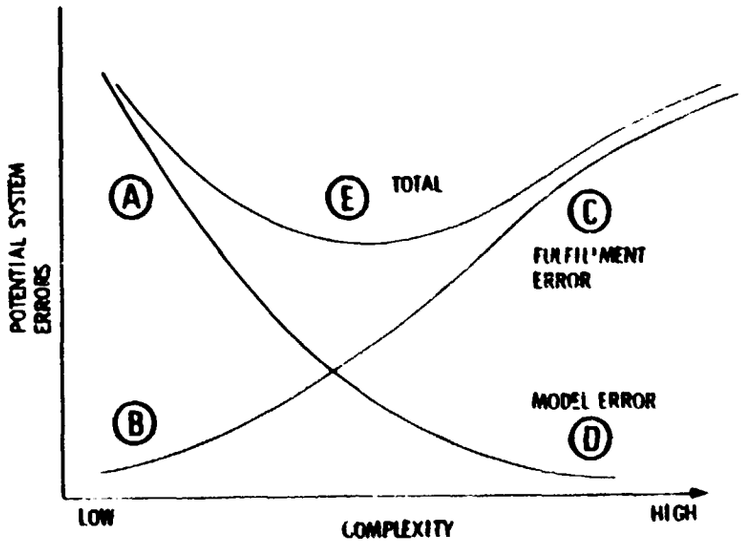

Figure 3. Model and System Complexity Optimization

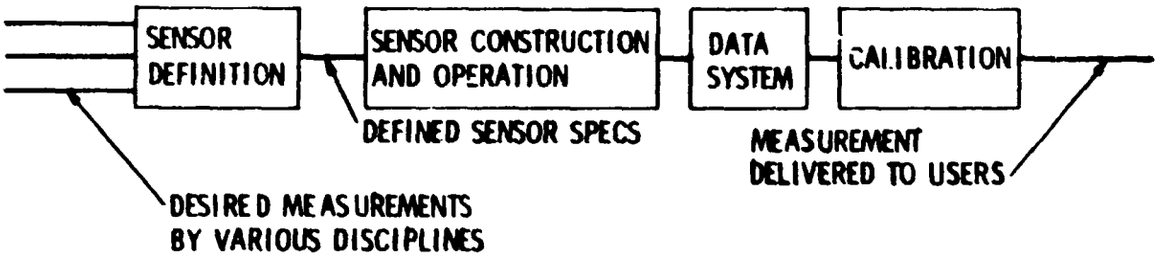

Figure 4. Data System Block Diagram

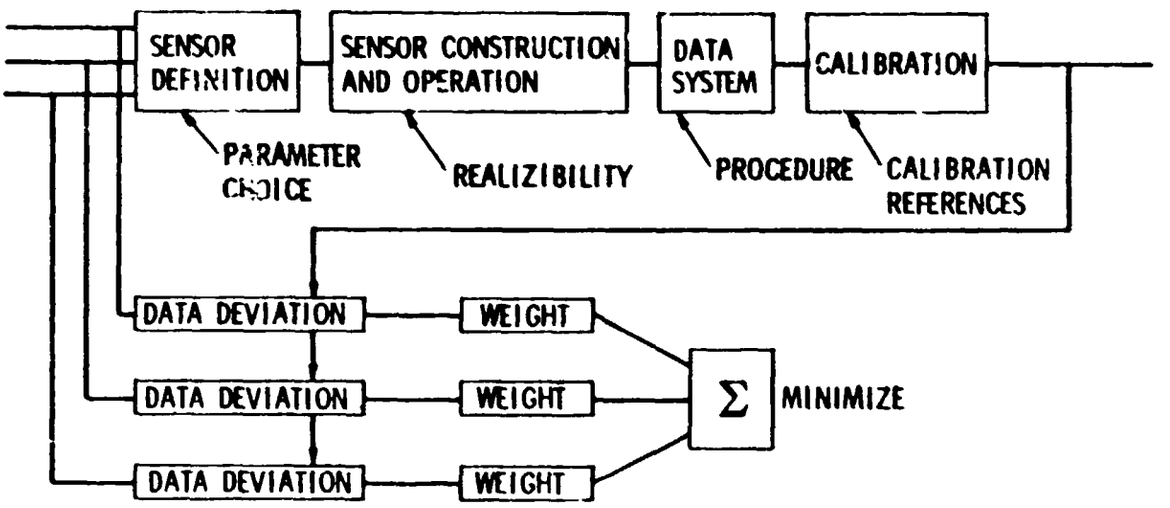

Figure 5. Design Model for Data System Optimization

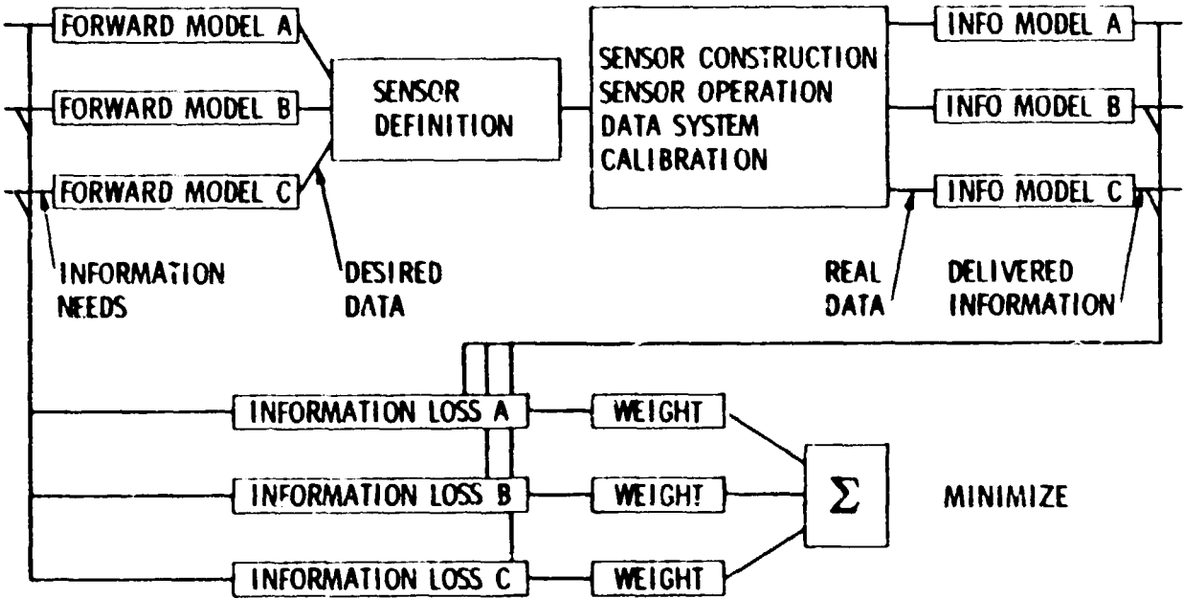

Figure 6. Design Model for Information System Optimization

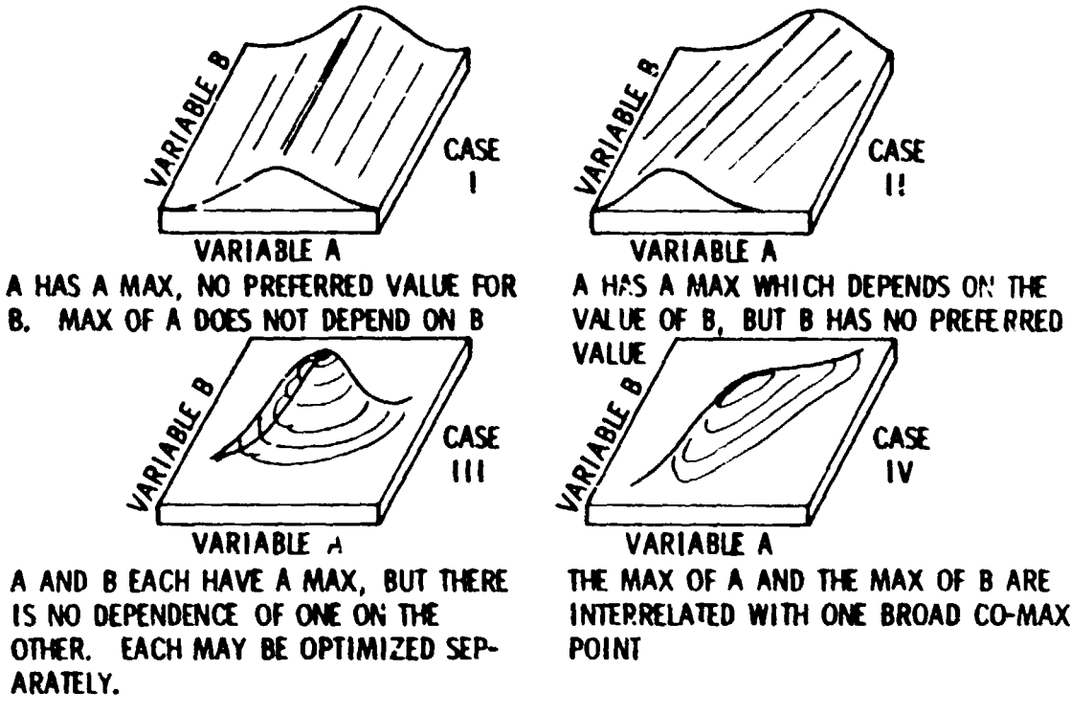

Figure 7. Interaction of Sensitivity Coefficients

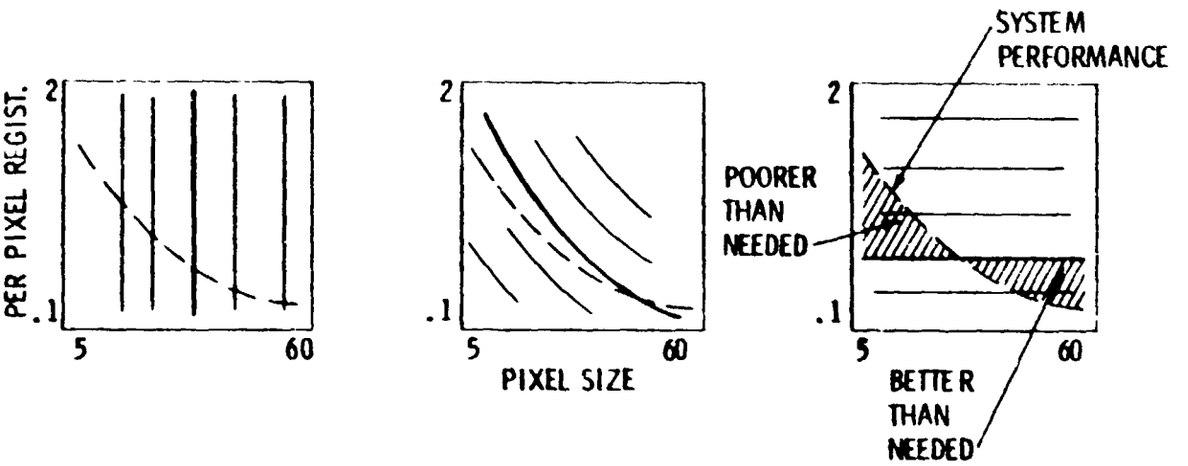

Figure 8. System Operating Point Selection

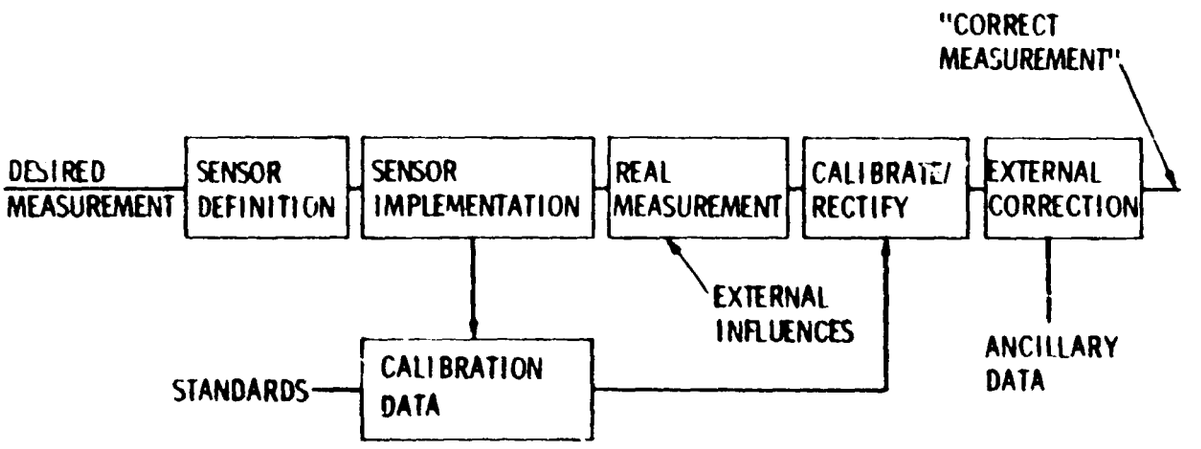

Figure 9. System Error Budget Model

N82 28733

8.4 MODELING MISREGISTRATION AND RELATED EFFECTS ON MULTISPECTRAL CLASSIFICATION*

Fred C. Billingsley

Jet Propulsion Laboratory, California Institute of Technology
Pasadena, California 91109

INTRODUCTION

Spectral analysis generally takes the form of multispectral classification in which the classification is done by comparing the sample measurement vector to the statistics of the set of known material vectors (training statistics) representing all possible classes, and by using one of several decision methods, determining which of the knowns it most nearly matches.

The problem pursued will be the effects of misregistration on the accuracy of multispectral classification in answer to the question:

> What are the effects on multispectral classification accuracy of relaxing the overall scene registration accuracy from 0.3 to 0.5 pixel?

The misregistration is but one of a group of parameters (noise, class separability, spatial transient response, field size) which must all be considered simultaneously. The thread of the argument (which will be discussed in detail below) is this: any noise in the measurements (due to the scene, sensor, or the analog to digital process) causes a finite fraction of measurements to fall outside of the classification limits. For field boundaries, where the misregistration effects are felt, the misregistration causes the border in a given (set of) band(s) to be closer than expected to a given pixel, so that the mixed materials in the pixels causes additional pixels to fall outside of the class limits. Considerations of the transient distance involved in the difference in brightness between adjacent fields, when scaled to "per pixel", allows the estimation of the width of the border zones. The entire problem is then scaled to field sizes to allow estimation of the global effects.

This approach allows the estimation of the accuracy of multispectral classification which might be expected for field interiors, the useful number of quantization bits, and one set of criteria for an unbiased classifier.

---

*This paper presents the results of one phase of research performed at the Jet Propulsion Laboratory, California Institute of Technology, sponsored by the National Aeronautics and Space Administration under Contract NAS7-100.

CONCLUSIONS

The following briefly stated conclusions are developed in detail in the body of the report.

- o The difference between 0.3-and 0.5-pixel misregistration is in the noise for multispectral classification.
- o Precision users may have to reregister image segments anyway, making extreme registration precision by the system of less importance.
- o Interpolation algorithm choice is relatively unimportant, provided a higher-order interpolator is used.
- o If small fields are important, small pixels are more important than sensor noise contributions.

In addition, several observations result:

- o System registration to 1-2 pixels should satisfy users of film products.
- o There is a grey area of 0.5 to 1-2 pixels in which the requirements for high precision are not well justified.

THE BASIC MODEL

The expected effect of misclassification may be estimated by a simple first-order approach, because the differences in classification accuracy between the many classification schemes and conditions that have been tested are overshadowed by the vagaries in the data and assumptions in the classification process, so that higher order analysis will contribute little additional understanding.

Consider first the probability of correct identification of a field interior pixel. Field interiors are nonuniform because of the combined effects of sensor noise, scaled to equivalent reflectivity ($NE\Delta\rho$) and inherent nonuniformities in the field itself. The overall brightness distribution is considered to be Gaussian - this is approximately true for field interiors, although the distribution deviates considerably toward bimodal for mixed materials at field borders.

The combined effect of these various noise sources produces a finite probability of misclassification. (Figure S-1) The first-order estimate considers the total variance caused by the scene, sensor and quantization as compared to the defined class size limits, however these are determined. Similar, but relatively second-order, effects may be expected with a higher order analysis. Proper classifier training, resulting in accurate limits, is essential (Hixson et al, 1980).

For simplicity, and because of the later desire to misregister one (or more) of the bands, the discussion will assume that spectral bands as sensed will be used, and that for recognition, the unknown pixel must fall between

appropriate limits in every band tested. Therefore, brightness outside of a limit in any one band is sufficient for rejection, so that we need to consider only one band at a time.

The probability of a sample being within the class limits can be derived by assuming that an ensemble of clean signals from a series of areas of the same material can be anywhere within the quantizing range with uniform probability, but that individual samples are perturbed by the Gaussian noise with a distribution equal to σ . The probability distribution of the signal plus noise is found by convolving the probability distribution of the signal with that of the noise. The probability of correct class assignment (i.e., the pixel is within the class limits) is then found by integrating the probability distribution between appropriate class limits (Friedman 1965). The result of this calculation is shown in Figure S-2. In the useful range of β ($3 < \beta < 7$), the curve can be approximated by

$$\beta \log P = -0.40$$

where P = probability of correct classification, and

$$\beta = \frac{\text{class size}}{\sigma_{\text{scene}}}$$, with class size and σ_{scene} in the same units.

Sources of noise will be the scene itself and the sensor, both assumed to be random for this analysis. The root mean square (rms) sum is taken to give the total effective noise. A number of pixel measurements may be averaged together to reduce the noise before classification. This final noise figure may be compared to the width of the class to give β , from which the probability P of correct classification may be estimated. This leads to the Classification Error Estimator, Fig. S-3.

As an example, consider a scene having a field-interior variation of 3%, to be viewed with a sensor having a total noise figure of 1%. The total effective noise seen by the classifier (upper left) will be the rms sum of these, or 3.16%, which for a total 0-255 digital number (dn) range, would be 8.1 dn. If the class width (determined by the classifier algorithm) is 25 dn (right center) the $\beta = 3.1$, giving $P = 0.742$ (right lower). If this P is not accurate enough for the analysis, several pixels must be averaged(right upper): a 2x2 averaging will raise β to 6.2, giving a new $P = 0.86$.

Considering β in this way allows an estimation of the total noise permissible as it affects the attainable classification accuracy. If the amount of scene noise to be encountered in a given classification task can be estimated, the allowable extra noise from the sensor and quantization can be specified by estimating the loss of accuracy of the classification caused by quantization error. This leads to an estimate of the number of bits which will be useful.

Define the perfect sensor as having no random noise nor quantization error (i.e., an infinite number of bits). This will define (for nxn pixels averaged)

$$\beta_o = \frac{\text{class size} \cdot n}{\sigma_{\text{scene}}} \qquad \text{and} \qquad P_o = 10^{-0.4/\beta_o}$$

For the real sensor, $\beta<\beta_o$ because of the finite σ_{sensor} and $\sigma_{quantization}$.

The new probability of correct classification P is related to P_o by:

$$P = P_o(\beta/\beta_o)$$

A plot of the loss in classification accuracy vs. P_o is given in Figure S-4, for the parameter families β/β_o and $\sigma_{sensor}/\sigma_{scene}$. Noise allocation starts with defining the desired P_o and ascertaining that the required β_o can be obtained. Definition of the allowed ΔP determines (e.g., from the graph) the allowed $\sigma_{sensor}/\sigma_{scene}$. An estimation of the scene noise for which the other conditions apply allows the calculation of the total sensor noise allowed. The final step is to partition this noise between sensor random noise and quantization noise.

For example, let the desired P_o = 85% and allow no more than 2% loss due to the total sensor noise. The no-sensor-noise β_o must be ≥ 5.7 to give P_o. Then, from Figure S-4, the allowed $\sigma_{sensor} = 0.6 \cdot \sigma_{scene}$. If the scene has a σ_{scene} = 2%, the allowable σ_{sensor} = 0.6x2% = 1.2%, which must be partitioned between NE$\Delta\rho$ and the quantization noise. For NE$\Delta\rho$ = 1%, the allowable $\sigma_{quant} = \sqrt{1.2^2 - 1^2}$ = 0.66%, which can be met by 6-bit quantization.

Two observations are important here: (1) Increasing the number of bits of quantization produces improvements which asymptotically approach zero, as each successive bit reduces the step size by a factor of 1/2. (2) A scene having as little as 2% variation is a very uniform scene. Since this noise is rms'd with the sensor noise, it will overwhelm any but a very noisy sensor. Therefore, for purposes of multi-spectral classification, more than six bits would seem to be unnecessary.

EDGE EFFECTS

To this point, the analysis is based on pixels well inside uniform fields and well away from field boundaries. A number of experimenters have spent appreciable time discovering that classification accuracy falls off at boundaries due to what has become known as the mixed-pixel effect. We will start at that point and attempt to model the effect to allow us to quantify our expectations.

We assume as a starting point that all the spectral bands used in classification, whether obtained from one date or series of dates, are in perfect registration. This means that when the pixel grids from each band are aligned the data contents (field borders, roads, all features) are also aligned - note that this is more than simply having all internal distortions removed, which is all that most geometric rectifications accomplish. Misregistration will (later) be considered as the lack of alignment of the pixel grids; because the computer can only work with pixel grids, aligning these pixel grids appears to the computer as a shift in the boundaries. We will assume that training samples are accurate and that class limits have been set from these by the classifier chosen. The classification is modelled as follows: signature shifting in any individual band will tend to cause misclassification, so that the situation may be treated one band at a

time. The effects of pixel mixture in all bands may then be rms'd together if desired. The entire analysis simplifies to the consideration of the transient intensity shift across field boundaries as compared to the class limits and the noise components of the measurement.

The first step in analyzing the spatial extent of pixel mixing across borders is to estimate the shape and extent of the transient intensity shift. If the impulse response functions or the modulation transfer functions (MTFs) of the various components (and, hence, the entire system) are known, a precise transient response may be calculated. For example, the specifications for the Thematic Mapper for Landsat D call for a 2% to 98% time equivalent of about 2 pixels implying a 10%-90% transient response of about 1.3 pixel. The practical result of this is that the "infinitely sharp" edges of the real scene will be softened by the filtering effect of the scanning aperture (assumed to be rectangular and having uniform response) and it is this softened transient response which is sampled. Interpolation required for registration will cause some further softening, and the use of any of the competent higher-order interpolation functions (sinx/x, TRW cubic convolution, modified cubic convolution, other splines) will have minor effects of the rise time. A total τ_{10-90} (transient response from 10% to 90%) of 1.5 pixels with no ringing will be used as a surrogate global value.

The transient situation across a border is sketched in Fig. S-5. We are concerned here with the decrease in probability that a given pixel will have a value within the class limits as that pixel moves toward the boundary, as shown in Figure S-6. The analysis only needs to determine the area under the normal curve (assuming the noise is Gaussian) between the limits as determined by the classification class size and the offset from the "field interior value" caused by the mixture. The important scaling involved is the amount of signal shift caused by the transient total shift T, as related to the desired class size S, for a given β . The left portion of Figure S-7 reflects this shift in brightness (vertical axis) as it affects the area within the class (the probability of recognition).

The transient rise distance estimated for the Thematic Mapper has very close to a Gaussian shape and a $\tau_{10-90} = 1.5$ pixel. The amount of brightness shift is the difference between the brightness of the field under consideration and the adjacent field which is causing the shift. The important intensity relation is the magnitude of this shift, T, as related to the size S of the class being tested by the ratio T/S. These curves, for various T/S, are combined with the probability curves of the previous discussion in Figure S-7. From this may be estimated the loss in probability in classification of pixels near borders.

BIAS IN FIELD SIZE ESTIMATION

It can be appreciated that several things are happening simultaneously: If the lower limit of field B and the upper limit of field A have a gap between, pixels "lost" by field B will not be picked up by field A, and will be considered unknowns and not be counted in either field. The lost pixels will be some interior pixels, due to insufficient β , and a large number of near-border pixels, resulting in apparent field size loss. Only if the lower limit of field B and the upper limit of field A are coincident will pixels lost from one field be picked up by the other, and vice versa, to give

complete account of all pixels. For the field size estimator to be unbiased, the loss-and-pickup in both directions must cancel; that is, on the average the true border must be located. The total effect will depend on the ratio of the number of border pixels to the number of field-interior pixels, and hence is a function of the field shape and size.

This leads directly to the required algorithm for field size estimation: First divide the scene into blobs, each of which is sufficiently uniform, and with closed boundaries. Then for each blob (field) determine the average brightness for all the interior pixels which are safely away from the border. For each segment of the border, the correct field edge decision level is midway (in σ's) between the average brightness of the two fields on either side. After the borders are located using this criterion, the field interiors may be reclassified using the classification limits as determined from the training samples.

EFFECTS OF MISREGISTRATION

In preparation for estimation of the misregistration effects, an analysis will first be made of the expectations of registered data and the sensitivity to the various parameters estimated. The starting model used has rectangular fields aligned with the pixel grid. Pixels are grouped into four zones: 1) Interior (i)-those with centers 2 or more pixels inside borders, 2) Inner border (ib)-pixels with centers 1-1/2 pixel inside borders, 3) Outer border (ob)-pixels with centers 1/2 pixel inside borders, 4) Exterior border (xb)-pixels outside the borders, with centers 1/2 pixel outside. Estimates of classification accuracy for each zone are obtained from Figure S-7. The total estimate of classification accuracy is the sum of pixels in each zone multiplied by the corresponding zone accuracy estimate. Later, the field will be misregistered, changes in the number of pixels in each zone calculated, and the probabilities again summed. The following parameters are required:

- r - the field shape ratio, length of long side/length of short side
- T - transient brightness difference between field being considered and its neighbor
- S - decision class size
- τ - transient distance for 10% to 90% response
- β - class size S/σ of Gaussian noise

The following global values selected for the parameters are considered to be representative:

- r = 2
- T/S = 1 to 5
- τ = 1.5 pixels
- β = 3 to 5

After the parameters r, T/S, τ, and β are selected, the resultant (from Fig. S-7) probabilities are substituted for the brightnesses in the various zones to produce a "probability image" aligned with the desired output pixel grid. The probability assigned to a pixel at a given location represents the probability that that pixel will have a brightness falling within the classification limit determined by the classifier, for the given spectral

band. The total probability of correct classification is given by

$$P = \frac{1}{rn_1^2}\left[p_i n_i + p_{ib} n_{ib} + p_{ob} n_{ob} + p_{xb} n_{xb}\right]$$

where n_1 is the field width (short side) in pixels, and n_i, n_{ib}, n_{ob}, n_{xb} are the number of pixels in the various zones. Using these values, the global estimate of the probability of correct classification with no misregistration is given Figure S-8 for three values of T/S. The predominant effect is the pixel mixture (the effect of T/S). As expected, this is worst for small fields (n_1 small) because of the larger percentage of border pixels for these fields. Note that for T/S = 1, decision level midway between brightnesses of adjacent fields, no probability loss occurs, even with small fields. Unfortunately, this desirable condition cannot be systematically obtained.

MISREGISTRATION OF CONGRUENT FIELDS

The initial model for misregistration is a displacement of d pixels, equal in both x and y. The result of this misregistration is that some area is lost from the external border, causing a further classification accuracy decrease. The misregistration loss as seen by the external border loss is given by

$$\Delta P = p_{xb}\left[d\,\frac{r+1}{r}\,\frac{1}{n_1} + (4d - d^2)\frac{1}{n_1^2}\right]$$

The basic character of this misregistration loss term is $1/n_1$, so that it will have a slope approximately equal to -1 on a log-log plot vs n_1. The precise results depend critically on the values of p_{xb} estimated for the p_{xb} from Figure S-7:

T/S	β	$\tau = 1$	$\tau = 1.5$	$\tau = 2$
1	3	.10	.14	.20
	5	.02	.025	.07
	7	0	.01	.04
2	3	0	0	0
	5	0	0	0
	7	0	0	0

Using these values, the loss ΔP due to displacement misregistration is plotted in Figure S-9 for various parameter combinations.

MISREGISTRATION DUE TO NON-CONGRUENCE

1.) SIZE AND RATIO (ASPECT) CHANGES

Size and aspect ratio changes can come about from several causes such as scan velocity or altitude changes, and if uncompensated can cause additional

misregistration errors. Progressive mis-registration from a point of accurate registration will be caused by both causes (Figure S-10a); the modeling of this effect considers first that size changes $N = n'/n$ will cause a shift in points n to points n' both vertically and horizontally, and then that changes in aspect ratio will cause further shifts in the horizontal position of vertical borders by changing the field shape ratios by the factor $R = r'/r$. The resulting shifts are:

$$\Delta n_v = (N - 1)\, n_v \quad \text{and} \quad \Delta n_h = (NR - 1)\, rn_v$$

For analysis, this shift will be divided around the borders symmetrically as optimum field registration is accomplished (Figure S-10b). Two cases must be distinguished (using scan velocity as a surrogate cause):

Case I: A slow scan decreases pixel spacing and puts more pixels into a given field. When these are placed into the output grid, the field appears stretched. The field as defined by the other (correct) bands now covers only part of the stretched field, so that the classification tends to see only interior pixels, and the accuracy will increase, ultimately reaching the field-interior accuracy. The sizes of the border errors are:

$$e_1 = \frac{1}{2}(N - 1)\, n_1 \quad \text{and} \quad e_2 = \frac{1}{2}(NR - 1)\, rn_1$$

Case II: A fast scan has the opposite effect, causing the field to appear smaller and the analysis pixels defined by the other bands now include more exterior pixels. The classification accuracy will decrease.

For fast scan, the smaller apparent field covers an area expressed as a fraction f_i of the total:

Fractional Areas:

$$f_i = \frac{r'(n_1')^2}{rn_1^2} = RN^2 \qquad \text{(Interior)}$$

$$f_{xb} = \frac{2Nn_1 + 2NRn_1 r + 4}{rn_1^2} \qquad \text{(External Border)}$$

The total expected probability is

$$P_{tot} = f_i P_i + f_{xb} P_{xb} \cdot$$

Since the external border pixels are now included within the analyzed field, but with a low probability, the fractional area RN^2 represents approximately the fraction of the basic field-interior accuracy to be expected. Since the total size shrinkage (in pixels) is small for small n_1, only larger n_1 need be considered, and the $1/n_1^2$ term may be dropped.

This allows P_{tot} to be approximated for r = 2 by:

$$P_{tot} \approx RN^2 p_i + \frac{3}{n_1} p_{xb}$$

For large fields, the probability is seen to be independent of field size, and only weakly dependent (because of low p_{xb}) for small sizes.

2.) WAVY BORDERS AND MULTIPLE ACQUISTIONS

For single-band analysis, with borders distorted so that there are pixels both inside and outside of the analyzed area, some pixels will have increased probabilities of correct classification and some will have less. The decrease in probability across border is (very) approximately linear, so that the (signed) average displacement will model the effect.

For multi-band analysis, those pixels having a low probability of classification will have the largest effect as the net probability at each pixel location is the product of the probabilities obtained for each acquisition (band). In this case the rms displacement will produce a better model of the effects.

SOME OBSERVATIONS

I. ON BASIC CLASSIFICATION

- The total noise figure (compared to the class size in a given determination) controls β, and in turn controls the maximum attainable classification accuracy. However, for practical range of $3 < \beta < 7$, increasing β has only a moderate effect.
- Because of this, if small fields are most important, the reflected energy might be more profitably divided into smaller pixels, even at the expense of $NE\Delta\rho$. As this will cause an increase in data rate, optimum coding should be investigated. The possible noise introduced in reconstructing the data will cause some further decrease in the overall effective $NE\Delta\rho$ and so decreases β. But since there is smaller sensitivity to β than to $1/n_1$, there should be a net gain in utility.
- Increasing the number of bits of quantization produces improvements which asymptotically approach zero, as each successive bit reduces the step size by a factor of 1/2.
- A scene having as little as 2% variation is a very uniform scene. Since this noise is rms'd with the sensor noise, it will overwhelm any but a very noisy sensor. Therefore, for purposes of multi-spectral classification, an extreme number of bits would seem to be unnecessary.

II. ON EDGE EFFECTS

- For accurate field size estimation, the decision brightness must be halfway between the brightnesses of the fields on either side of a given boundary. This means that classifiers set for material identification will in general produce errors in field size. But the

field-interior brightness is increasingly hard to estimate for small fields because of the fewer interior pixels.

- It is important to keep the transient response distance and the accompanying sample spacing small, to get as many pixels into a given ground distance as possible. Field area errors become large at $n_1 = 5$ or less. The transient distance must also be matched between spectral bands.

III. ON MISREGISTRATION

- For large T/S (i.e., 2 or more) the edge effects are so great that the base probability is drastically affected, and the external border pixels have zero probability of being within the class limits. For this reason, there is no misregistration effect for large T/S.
- Square fields show the most misregistration loss, when scaled to n_1.
- A shape ratio r=2 is believed to be representative.
- Misregistration loss decreases with higher β. However, these losses in general are small to begin with, and the discussion calling for sacrifice of β to gain smaller IFOV (more pixels n_1 into a given field) would seem to override.
- Increase in τ decreases the basic accuracy of edge pixels and also increases the misregistration losses.
- Geometric rectification and registration procedures must not only remove the internal distortions but must also produce pixels on a defined (preferably ground-referenced) grid. Current procedures do not do this. Without this reference grid, users will have to re-interpolate before multi-temporal data can be compared.
- Scale and aspect ratio errors will have only minor effects on moderate-area problems, but they will cause problems in correlating over large distances.
- Altitude relief displacement will require users to use many control points to register images in areas of high relief.
- Unless standard reference grids are established, users requiring registration will have to interpolate every image, even in low relief areas.
- For single-band analysis, the algebraic average of the displacement may be used. For multi-band analysis, with erratic errors in location among the bands, the lowest probability of correct classification holds and the rms of the displacements is appropriate.

AN UNANSWERED QUESTION

This report models the potential misregistration effects on multispectral classification accuracy. It may allow the comparison of the various tests and simulations, and points out the variables which must be reported for those simulations to allow their validation. It does not answer the following question: Given a certain loss in accuracy due to misregistration, how does that damage the ability to use the data analysis results? These evaluations will be discipline dependent, and must be sought separately.

REFERENCE

Friedman, H.D., 1965, On the Expected Error in the Probability of Misclassification, Proc IEEE Vol 53, p. 658.

Hixson, M., Scholz, D., Fuhs, N., Akiyama, T., Evaluation of Several Schemes for Classification of Remotely Sensed Data, Photogrammetric Engineering and Remote Sensing, Vol 46 # 12, Dec 1980, pp 1547-1553.

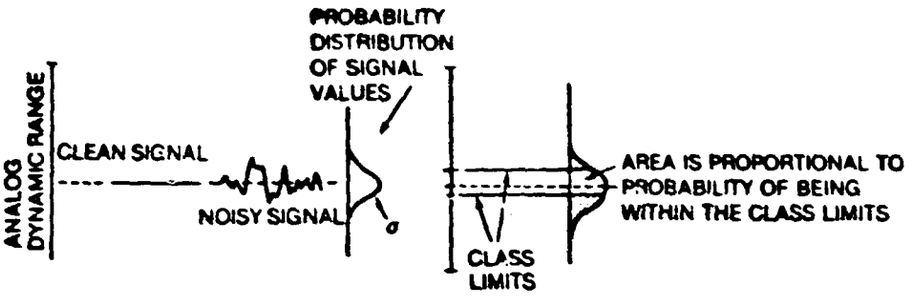

Figure S-1 Effect of Noise on the Probability of Correct Multi-spectral Classification

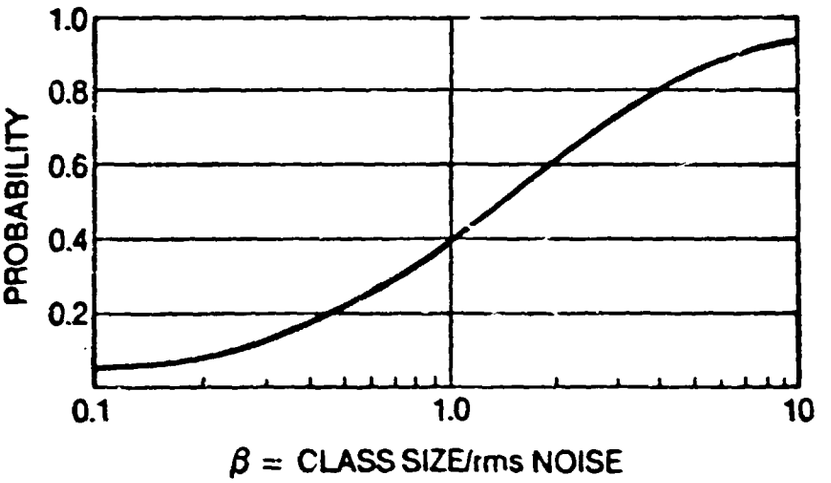

Figure S-2 Given a Signal Uniformly Probable over the Dynamic Range, and Gaussian Noise with standard Deviation = σ . The curve shows the Probability of Correctly Recognizing a class corresponding to the Noise-free Signal as a Function of the Ratio β = class size / σ .

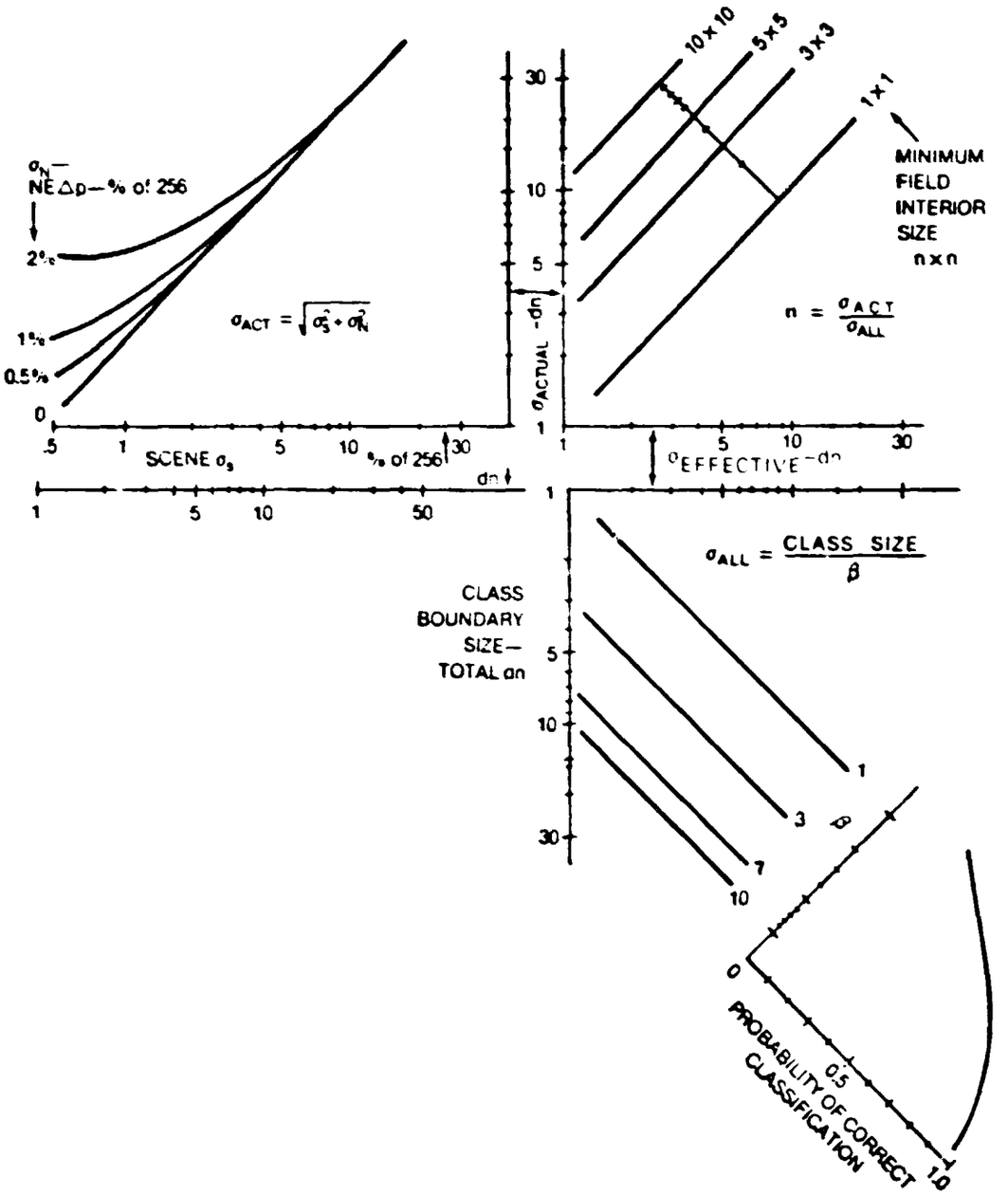

Figure S-3. Classification Error Estimator

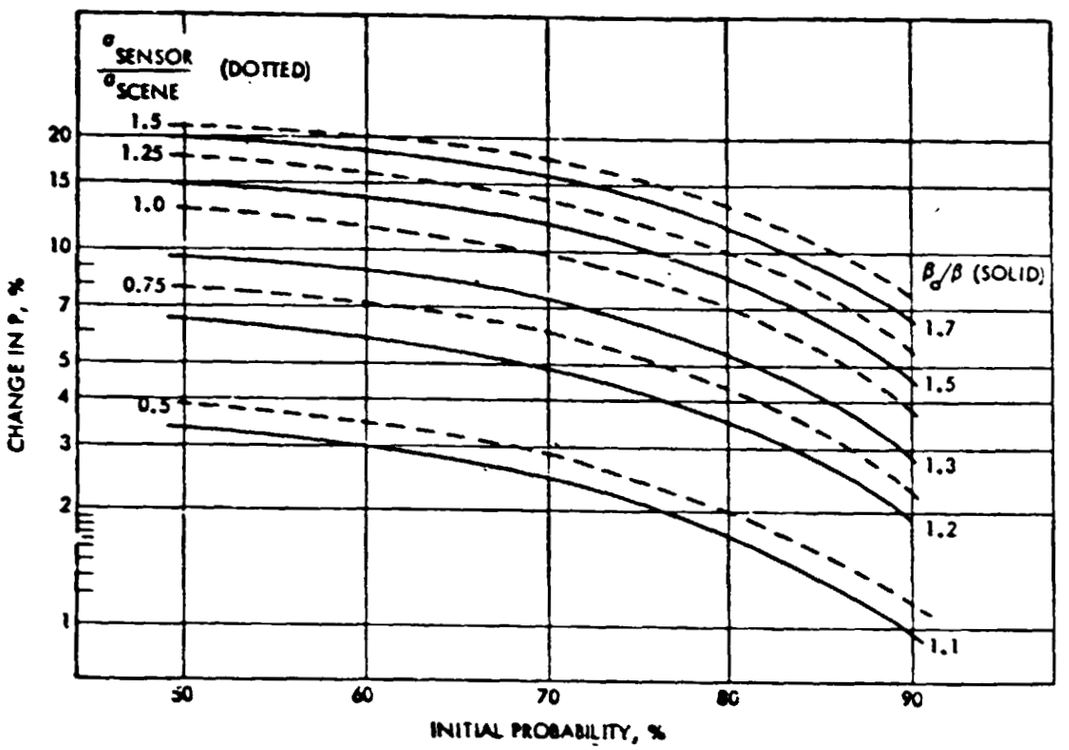

Figure S-4 Loss in Classification Accuracy due to Noise

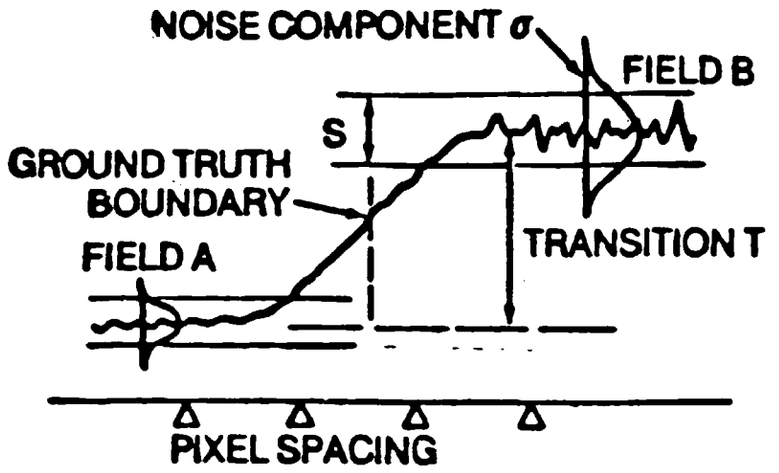

Figure S-5 Cross Section of brightness trace across a boundary between two fields, showing the distance required for the brightness transition.

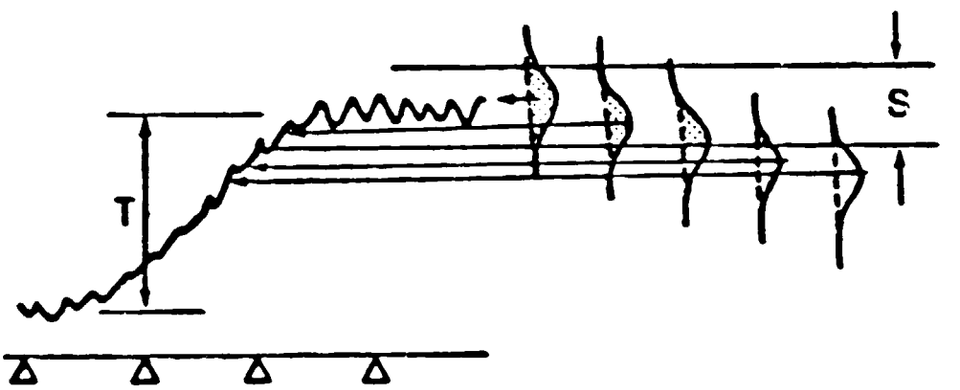

Figure S-6 The distribution of "field" pixels moves down the transition curve as the measurement point moves toward the boundary. The shaded area is the proportion which will be correctly classified.

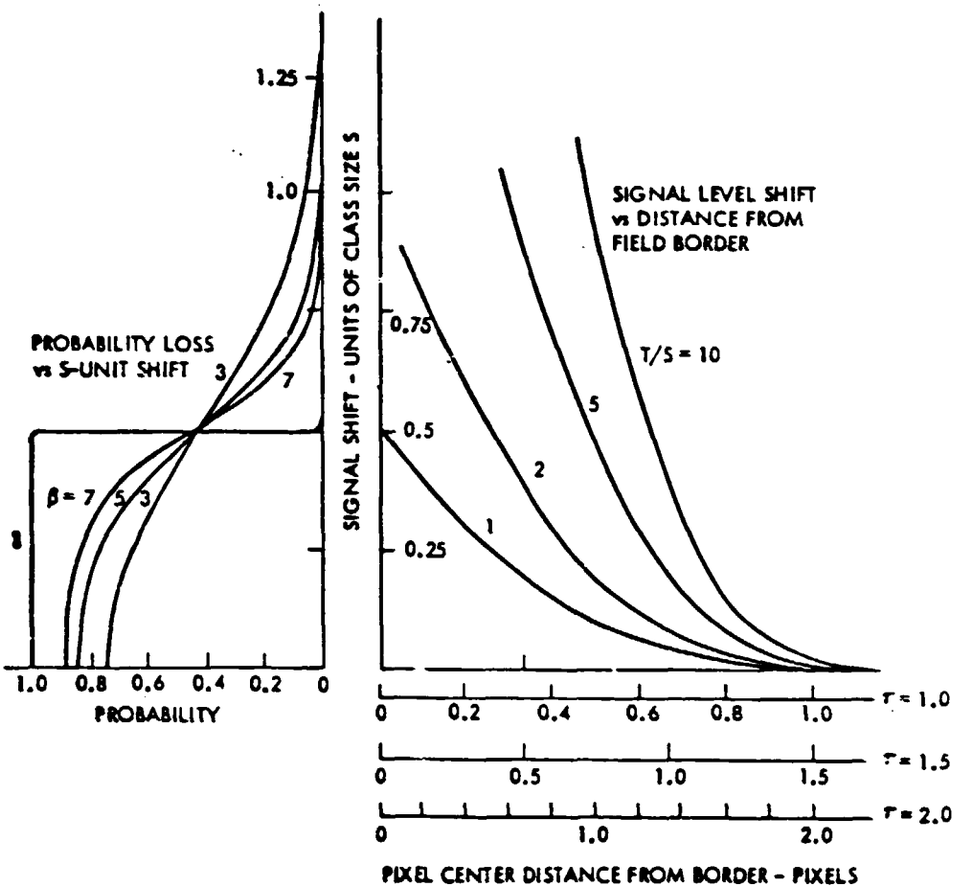

Figure S-7 Combined Curves for Translation of Pixel Distance from Border to Shift in the Brightness (Scaled in Units of Class Size, S) to Probability of Correct Classification.

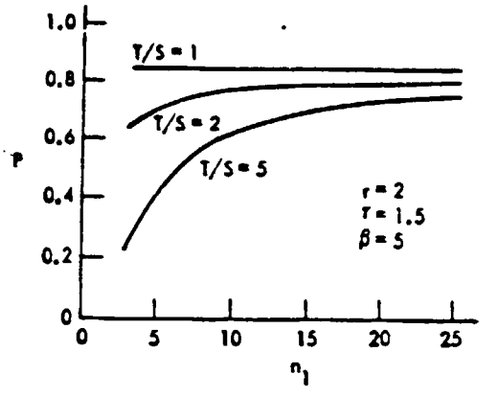

Figure S-8 Probability of Correct Classification using Global Parameters, for Perfectly Registered Pixels. One Spectral Band Only.

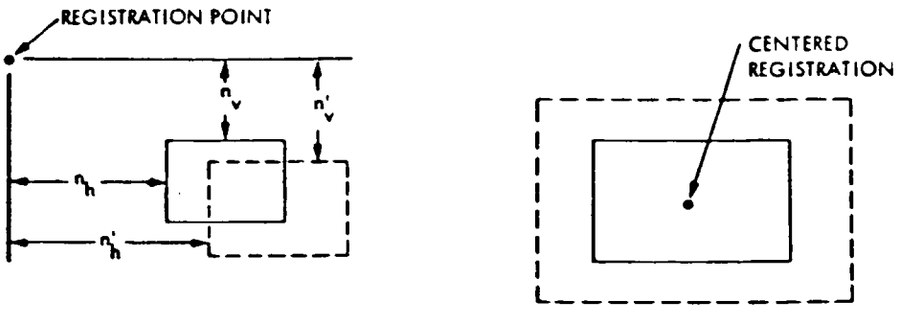

a. GENERAL CASE

b. BEST REGISTRATION CASE (NO TRANSLATION DISPLACEMENT)

Figure S-10 Construction for Estimating Misregistration Caused By Size and Aspect Errors.

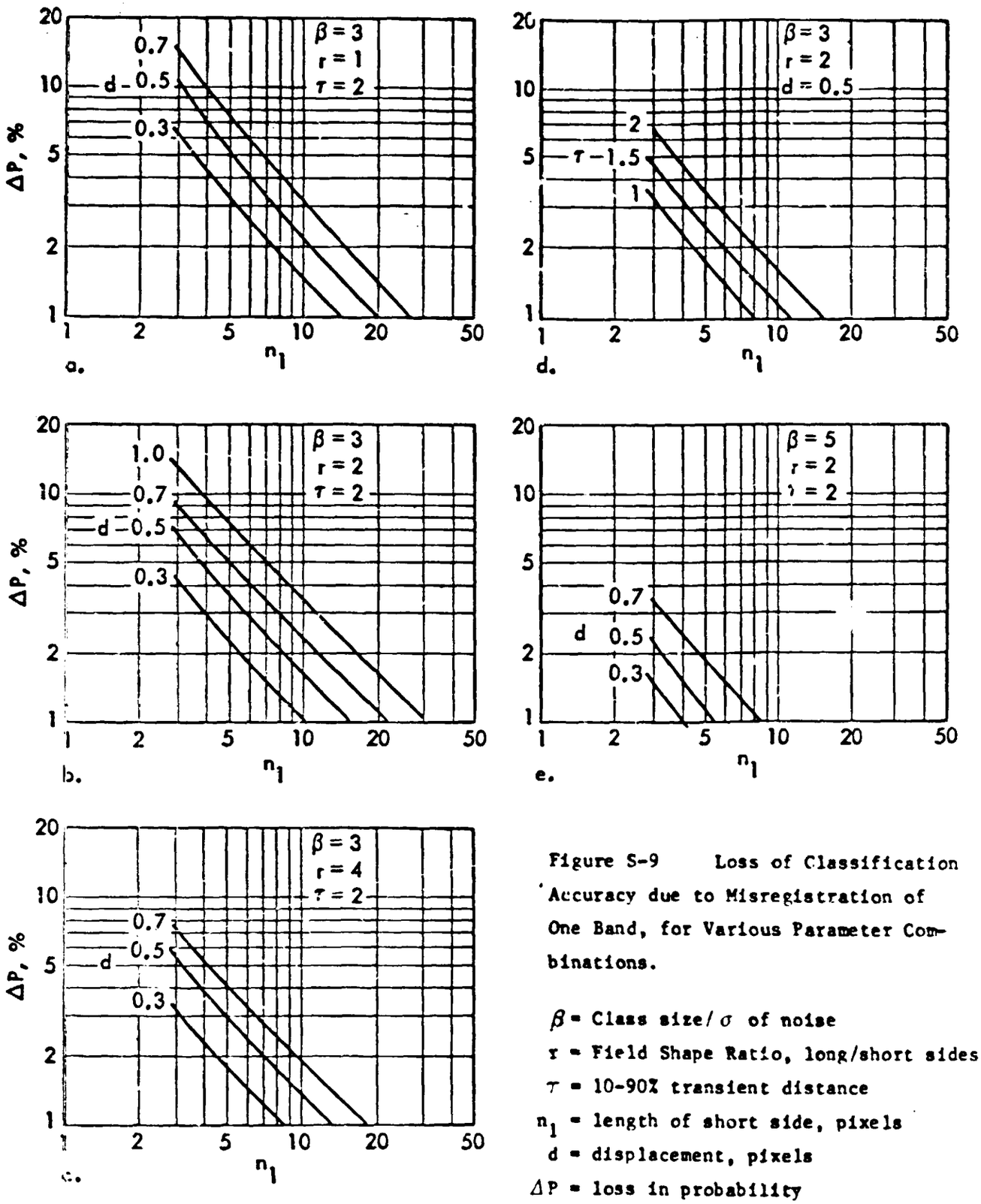

Figure S-9 Loss of Classification Accuracy due to Misregistration of One Band, for Various Parameter Combinations.

β = Class size/σ of noise

r = Field Shape Ratio, long/short sides

τ = 10-90% transient distance

n_1 = length of short side, pixels

d = displacement, pixels

ΔP = loss in probability

D35 N82 28734

8.5 AN AUTOMATED MAPPING SATELLITE SYSTEM*

Alden P. Colvocoresses
U.S. Geological Survey
National Center, Mail Stop #520
Reston, Virginia 22092

Abstract

Throughout the world, topographic maps are compiled by manually operated stereoplotters that recreate the geometry of two wide-angle overlapping stereo frame photographs. Continuous imaging systems such as strip cameras, electro-optical scanners, or linear arrays of detectors (push brooms) can also create stereo coverage from which, in theory, topography can be compiled. However, the instability of an aircraft in the atmosphere makes this approach impractical. The benign environment of space permits a satellite to orbit the Earth with very high stability as long as no local perturbing forces are involved. Solid-state linear-array sensors have no moving parts and create no perturbing force on the satellite. Digital data from highly stabilized stereo linear arrays are amenable to simplified processing to produce both planimetric imagery and elevation data. A satellite, called Mapsat, including this concept has been proposed to accomplish automated mapping in near real time. Image maps as large as 1:50,000 scale with contours as close as 20-m interval may be produced from Mapsat data.

Background

The geometry of stereo mapping photographs, whether taken from aircraft or satellite, is well known and documented. Transforming such photographs into topographic maps is a relatively slow and expensive process that for many critical steps defies automation. Compared to an aircraft, a satellite offers the unique advantages of much greater stability and uniform velocity.

Utilizing these advantages, a sensing system in space can now provide imagery of mapping quality, even though a continuous electro-optical imaging system is used instead of a mapping camera with its inherent high geometric fidelity. The next generation of space sensors will include solid-state linear arrays (fig. 1) that involve no moving parts. By continuous imaging with very high geometric fidelity they will permit, at least in part, the automated mapping of the Earth from space in three as well as two dimensions. The fundamental difference between conventional and continuous stereo methods is illustrated by figure 2.

---

* Approved for publication by Director, U.S.G.S.

At least four papers have been published that relate directly to automated three-dimensional mapping. In 1952, Katz (1) showed how height measurements could be made with a stereoscopic continuous-strip camera. The geometry of such a strip camera and stereo linear arrays is basically the same. In 1962, Elms (2) elaborated on the strip camera concept and indicated its advantages over frame cameras as a possible component of an automated mapping system. In 1972, Helava and Chapelle (3) described the development of instrumentation by which a conventional stereomodel can be scanned using the epipolar-plane* principle, and thus reducing image correlation from a two-dimensional to a basically one-dimensional task.

In 1976 Scarano and Brumm (4) described the automated stereo-mapper AS-11B-X which utilizes the epipolar-scan concept and one-dimensional digital image correlation described by Helava and Chapelle. Thus the concept of reducing photogrammetric data stero correlation from two to one dimension is well established. The cited literature, however does not describe the possibility of imaging the Earth directly in stereoscopic digital form suitable for one-dimensional processing.

Beginning in 1977 a serious effort to define a stereo satellite or Stereosat (5) was undertaken by NASA. The Stereosat concept calls for linear-array sensors, looking fore, vertical and aft, but its principal objective is to provide a stereoscopic view of the Earth rather than to map it in automated mode. There are other ways of obtaining stereo imagery with linear arrays. The French SPOT (6) satellite can look left or right of the track and thus achieves stereo by combining imagery from nearby passes of the the satellite. NASA's Multispectral Linear Array (MLA) concept (7), as so far defined, calls for fore and aft looks through the same set of optics by use of a rotating mirror. However, neither the SPOT nor NASA's MLA approach are considered optimum for stereo mapping of the Earth, as neither is designed to acquire data in continuous form.

Mapsat Geometric Concept

Linear arrays represent a relatively new remote sensing concept. Five papers on this subject were presented at the ASP/ACSM annual convention during March 1978 (8,9,10,11,12). These papers concentrated on detector

*An epipolar plane is defined by two air or space exposure (imaging) stations and one point on the ground.

technology and the application of linear array sensors in a vertical imaging mode. Welsh (13) recently described the geometry of linear arrays in stereo mode, although his error analysis for such a system is based on measurements made from images rather than computations based on the digital data.

By combining the technology of linear arrays, the concept of epipolar-plane scanning, and the experience gained from Landsat and other space sensing systems, Mapsat was defined (14), and its proposed parameters are listed in Table 1. The Mapsat concept was the work of several individuals, but perhaps the single most important contribution was that of Donald Light (verbal communication), then of the Defense Mapping Agency, who first suggested that epipolar planes, as described by Helava (3) and used in the AS-11B-X plotter, could be achieved directly from space and that topographic data might then be extracted in real time. There are several feasible configurations by which linear array sensors can continuously acquire stereo data. It was decided that the system must permit selection from the three spectral bands, provide for two base-to-height ratios of 0.5 and 1.0 and be compatible with the epipolar concept. Figure 3 illustrates the configuration selected to accomplish the stereoscopic as well as monoscopic functions.

Acquiring stereo data of the Earth in epipolar form directly from space is the fundamental geometric concept of Mapsat. The epipolar conditions shown in Figure 4 implies that five points--the observed ground point P, the two exposure stations S_f and S_a, and the two image detectors f and a --lie in a single plane. If this epipolar condition is maintained as the satellite moves along its orbit, every point P observed by detector f in the forward looking array will also be observed subsequently by detector a in the aft looking array. Thus image correlation can be obtained by matching the data stream from detector f with that from a --a one-dimensional correlation scheme. This description applies equally to the use of the vertical with either the fore-or aft-looking array but involves a weaker (0.5) base-to-height ratio than the described use of the fore and aft arrays (base-to-height ratio of 1.0). In practice the data streams from more than one detector may be involved since there will normally be some offset in the path of a given pair of detectors. Moreover under certain conditions, correlation may be improved by a limited expansion of the correlation function to two dimensions.

Because each detector array is looking at a different portion of the Earth at any given time, Earth rotation complicates the epipolar condition. As shown in figure 5, this complication can be overcome by controlling the spacecraft attitude. This description is obviously simplified; further complications involve such factors as the ellipsoidal shape of the Earth, variations in the orbit, spacecraft stability, and even very large elevation differences. The spacecraft position and attitude must be precisely determined by such systems as the Global Positioning System (GPS or NAVSTAR) and frequent stellar referencing. Satellite attitude control involves gyros and inertial wheels, and, when a satellite is free of perturbing forces created by moving (actuated) parts, attitude can be maintained for reasonable periods to the arc-second.

Of course, the sensing system must retain precise geometric relationship to the attitude control system. Defining the correct satellite attitude and the rates in yaw, pitch, and roll to maintain the epipolar condition requires precise mathematical analysis. Two independent analyses, one by Howell of ITEK (15) and the other by Snyder (16) of U.S. Geological Survey, confirm Mapsat's geometric feasibility, and a U.S. patent has been allowed on the concept. Table 2 indicates the maximum deviations from the epipolar condition caused by the various expected error sources. This table is based on a half orbit (50 minutes) which covers the daylight portion to which imagery is basically limited. Attitude rate errors would be considerable if only corrected once every 50 minutes but, as the table indicates, 10-minute intervals based on stellar reference reduce the errors to a reasonable amount. Ten-minute stellar referencing using star sensors as described by Junkins et al., (17), is considered reasonable. Computer programs have been developed that result in the epipolar plane condition being maintained as long as adequate positional and attitude reference data are available and properly utilized. Figure 6 illustrates the simplicity of elevation determination in an epipolar plane which is the key element of Mapsat.

Obviously, the Mapsat concept can be effectively implemented only if stringent specifications regarding orbit, stability, reference, and sensor systems are met. Table 3 lists the Mapsat geometric requirements as defined to date, and each is considered to be within the state of the art.

Mapping Accuracy

By meeting the geometric requirements indicated and achieving stereo correlation, the resulting map accuracy is compatible with scales as large as 1:50,000 and contours as close as 20 m interval based on U.S. National Map Accuracy Standards. Reference 15 covers this analysis in some detail. Such accuracies result from the indicated geometric requirements and the following factors:

- o Linear array detectors are positioned with sub-micron accuracy.
- o Optical distortion effects, when accounted for by calibration, are negligible.
- o Atmospheric refraction, because of the steep look angles, is of a very low order and is reasonably well known; air-to-water refraction is also known where underwater depth determination is involved.
- o Relative timing, which is referenced to data acquisition, is accurate to within the microsecond.
- o Digital stereo correlation, where uniquely achieved, provides three dimensional root-mean-square (rms) positional accuracy to within half the pixel dimension.

These considerations result in relative positional errors for defined points of only 6 to 7m (rms) both horizontally and vertically. This vertical accuracy requires the 1.0 base-to-height ratio. Such accuracy is adequate for the mapping indicated but assumes that control is available for reference to the Earth's figure. As indicated by ITEK (15) and the author (19), control points of 1,000 km spacing along on orbital path will be adequate for such a purpose. Where no control exists the absolute accuracy of the resultant maps, with respect to the Earth's figure, may be in rms error by 50 to 100 m although their internal (relative) accuracy remains at the 6 to 7 m rms level.

Stereocorrelation

The determination of elevations from stereo data requires the correlation of the spectral response from the same point or group of points as recorded from two different positions. In the aerial photography case these two positions are the camera stations, whereas with linear arrays in space the two recording positions are constantly moving with the satellite. In the photography case, correlation is achieved by orienting the two photographs to model the acquisition geometry. Once this is done, correlation can be achieved by the human operator, or the image stereomodel can be scanned and correlated by automated comparison of the signal patterns from the two photographs. A system such as the AS-11B-X (3,4) generates one-dimensional digital data in epipolar planes from the model. In theory, epipolar data should be correlated much faster than that from a system that must search in two dimensions to establish correlation. In practice, the automated correlation of digital data has been only partially successful; and, as Mahoney (18) has recently pointed out, correlation by either manual or automated systems is still a slow and costly process. To date, no one has acquired original sensor data in epipolar form. As, no one can really say how well such data can be

automatically correlated, until a satellite such as Mapsat is flown. Simulation using digitized aerial photographs or linear-array stereo-sensing of a terrain model are relevant experiments worth conducting. However, they will provide only partial answers, since the degree of correlation will depend on the area involved. The characteristics of the Earth's surface, coupled with related conditions, such as the atmosphere and Sun angles, are highly varied; which means that the degree of correlation will also be highly varied. This problem does not imply that the Mapsat concept has not been validated. Having stereo data organized in linear digital form is of obvious advantage to create the three-dimensional model of the Earth's surface. Many areas will correlate in one-dimensional mode, others will require two-dimensional treatment, and still other areas may not correlate at all. By properly defining the satellite parameters and data processing, the correlation function can be optimized and raised well above that obtainable from wide-angle photography systems. For example, digital data can readily be modulated to enhance contrast or edges that make up the patterns on which correlation depends. Photography can also be modulated, but it is far more difficult (and less effective) than digital-data modulation, as film lacks the dynamic range and sensitivity of solid-state detectors. Mapsat will acquire data in an optimum form for automated correlation, which will expedite the precise determination of elevations and create digital elevation data that are becoming a basic tool for many disciplines.

Acquisition Modes and Products

As previously described (.4), Mapsat is designed to be operated in a wide variety of modes. These include variation in resolution (10-m elements on up), spectral bands, swath width, and stereo modes. Such flexibility permits optimum data acquisition without exceeding a specified data-transmission rate that is now defined at 48 megabits per second (Mb/s).

The Earth's surface is highly varied, and data product requirements are likewise highly varied. By varying the acquisition modes and, in turn, producing a variety of products, the data management problem becomes complicated as compared to existing systems such as Landsat which produces only two basic types of data. However, solving this data management problem is a small price to pay for a system that can meet a wide variety of requirements for remotely sensed data of the Earth. Only four primary products are expected from Mapsat as follows:

(a) Raw-data digital tapes from which quick-look images can be displayed in near real time.

(b) Processed digital image tapes calibrated both radiometrically and geometrically to a defined map projection. Such data will be two-dimensional (planimetric) but describe the Earth's radiance (brightness) in multispectral form as is now accomplished by Landsat Multispectral Scanner tapes.

(c) Processed digital tapes, again calibrated both radiometrically and geometrically, but which now describe the Earth's surface in three dimensions (topographically) with an associated radiance value. Such tapes are, in effect, digital elevation data sets of the Earth's surface.

(d) Standardized images, both black-and-white and in color, which include geometric corrections and radiometric enhancements. Such corrections and enhancements will be of recognized general value and of a type that can be performed without undue delay or excessive cost. The images would also be of standardized scale.

From these four basic products, a wide variety of derivatives can be made which include the following:

(a) Black-and-white and multicolor image maps and mosaics at scales as large as 1:50,000, or even 1:25,000 (1:24,000) where map accuracy standards are not required.

(b) Thematic displays and maps involving such subjects as land cover and land use classification.

(c) Maps which depict the Earth's topography by such means as contours (as close as 20-m interval), slopes, elevation zones, shaded relief, and perspective display.

Conclusion

Mapsat will not meet all anticipated remote sensing requirements, and it will in no way replace those air-photo surveys required to meet mapping requirements for scales larger than 1:50,000 and contour intervals of less than 20 m. What it will do, is provide a precise three-dimensional multispectral model of the Earth at reasonable resolution and in digital form. Moreover, the satellite will record the changing responses of the Earth's surface as long as it is in operation.

Mapsat can be built today at what is considered to be a reasonable cost (15) as it is based on available components and technology. Moreover, it is designed for simplified operation and data processing. Assuming that an operational Earth-sensing system will be flown, surely Mapsat is a deserving candidate for such a job.

Mapsat Parameters

- Orbit--Same as Landsat 1, 2 and 3 (919 km alt).
- Sensor--Linear Arrays--Three optics looking 23° forward, vertical and 23° aft. Three spectral bands:

blue green	0.47 - 0.57 um
red	0.57 - 0.70 um
near IR	0.76 - 1.05 um

- Swath--180 km or portion thereof.
- Resolution--Variable--Down to 10 m element.
- Transmission--S (or X) band, compatible with Landsat receivers but with rates up to 48 Mb/s.
- Processing--One dimensional, including stereo.

Table 1

Mapsat Epipolar Condition

Maximum Deviation (±) in Half Orbit--(50 Minutes)

(Meters on the Ground)

	Case 1. Vertical plus For or Aft--B/H = 0.5	Case 2. Fore and Aft--B/H = 1.0
o Optimum condition:	1.3 m	0.3 m
o Attitude errors (yaw and pitch) of:		
10 arc seconds	0.7	1.6
100 arc seconds	5.0	12
o Attitude rate errors of:		
10^{-6} deg./sec.	11 (2)*	22 (4)*
10^{-5} deg./sec.	110 (22)*	230 (46)*
o Elevation differences of:		
1,000 m	2.3	0.5
10,000 m	22	1.8

*( ) Values obtained by 10 minute rather than 50 minute stellar reference intervals.

Table 2

Mapsat Geometric Requirements

- Positional Determination of Satellite--10 to 20 m[1/] in all three axes.
- Pointing Accuracy--Within[2/] 0.1 of vertical.
- Pointing Determination--Within[2/] 5 to 10 arc seconds
- Stability of Satellite--Rotational rates within[2/] 10^{-6} degrees/second.

1/ rms (1σ)
2/ very high probability (3σ)

Table 3

Figure 1

CONVENTIONAL VS. CONTINUOUS STEREO IMAGING MODES

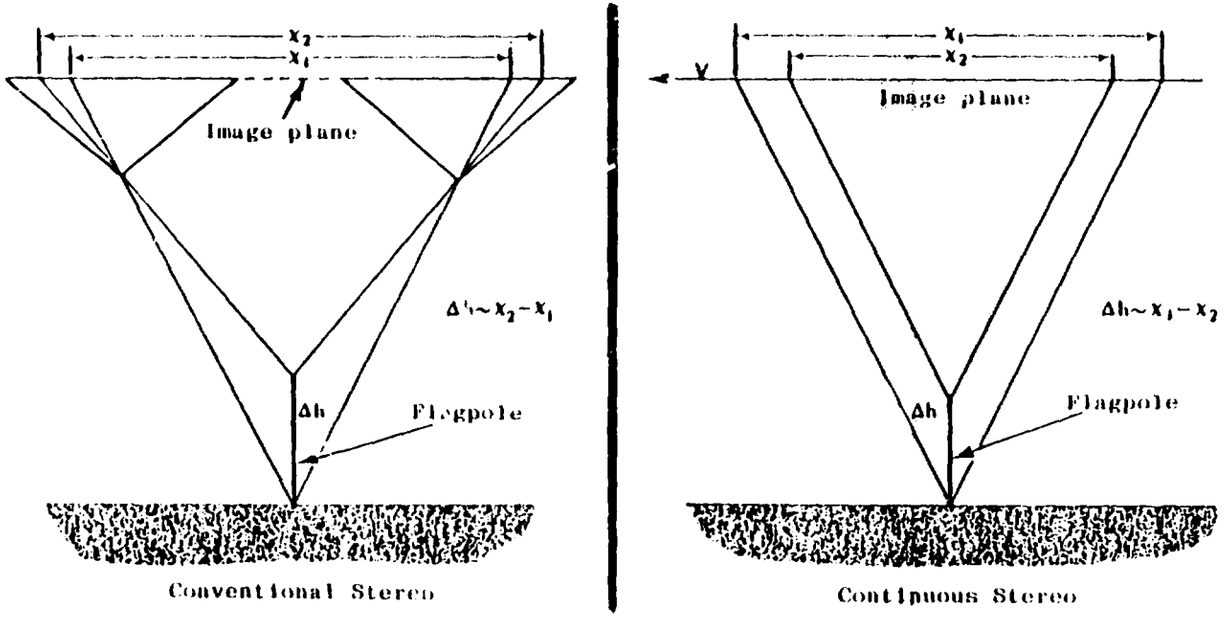

- Both modes resolve elevation differences
- Conventional mode involves discontinuities based on each stereo pair
- Continuous mode involves no discontinuities but requires very stable platform of known uniform velocity (V)
- Conventional mode involves 2 dimensional data processing
- Continuous mode permits 1 dimensional data processing from 2 data sets

Figure 2

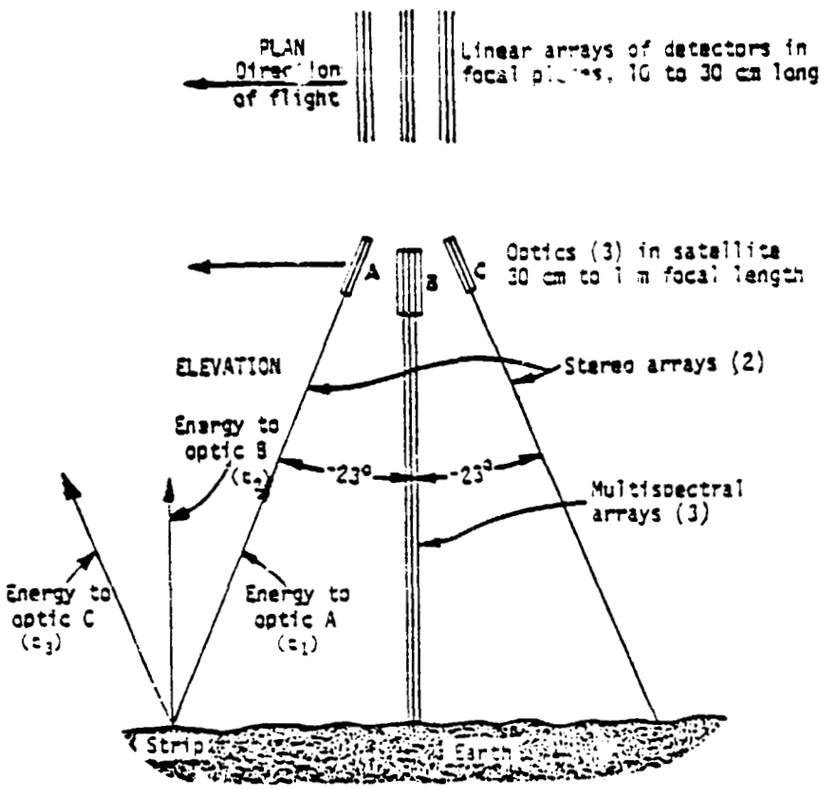

Mapsat Sensor Configuration (not to scale).

Optics A, B, and C are a rigid part of satellite. Optic B senses the same strip 60 seconds after A; optic C, 120 seconds after A. Any combination of A, B, and C produces stereo. Optics A and C are of about 10% longer focal length to provide resolution compatible with optic B.

Figure 1

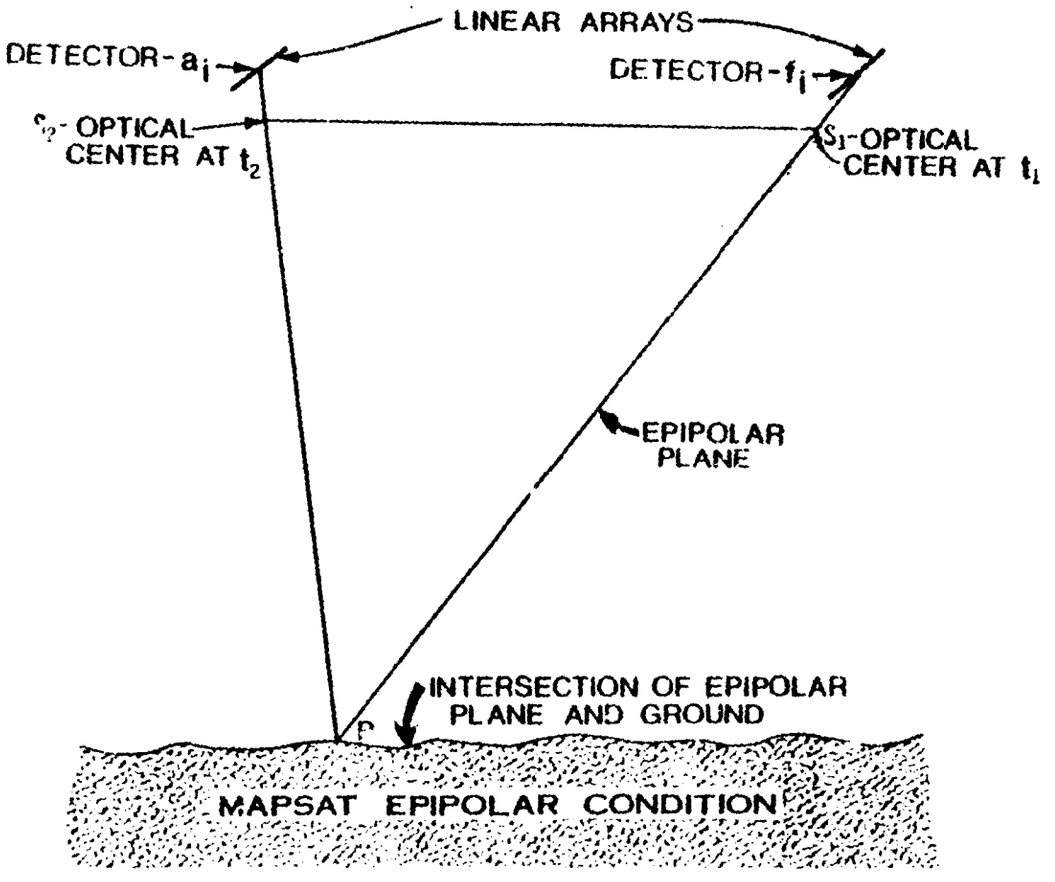

Figure 4

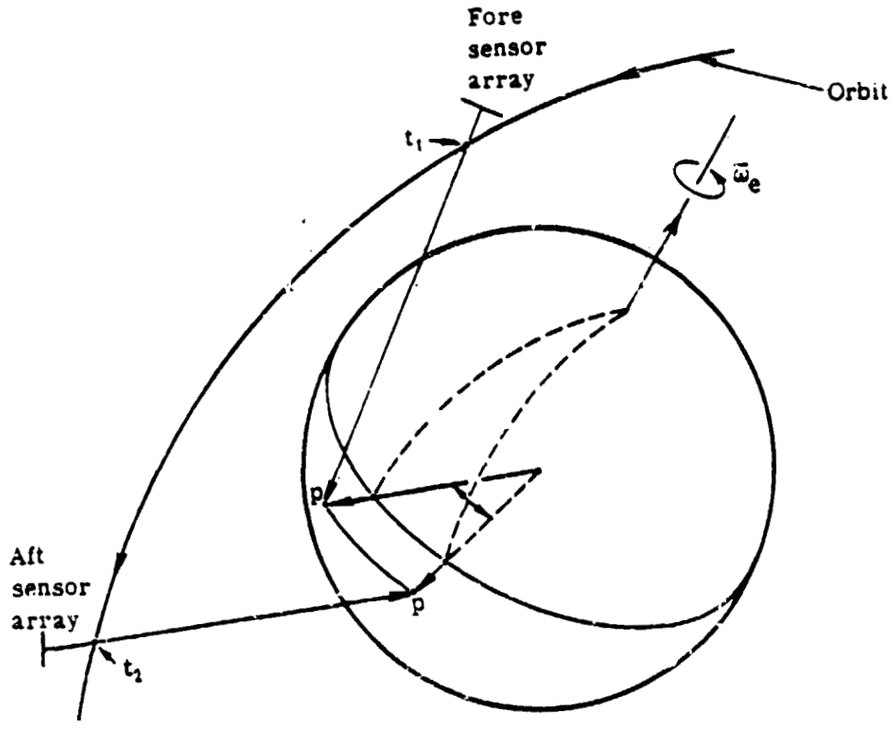

Mapsat Epipolar Acquisition Geometry

Figure 5

Mapsat En'polar Plane Geometry

Elevation difference as a function of time

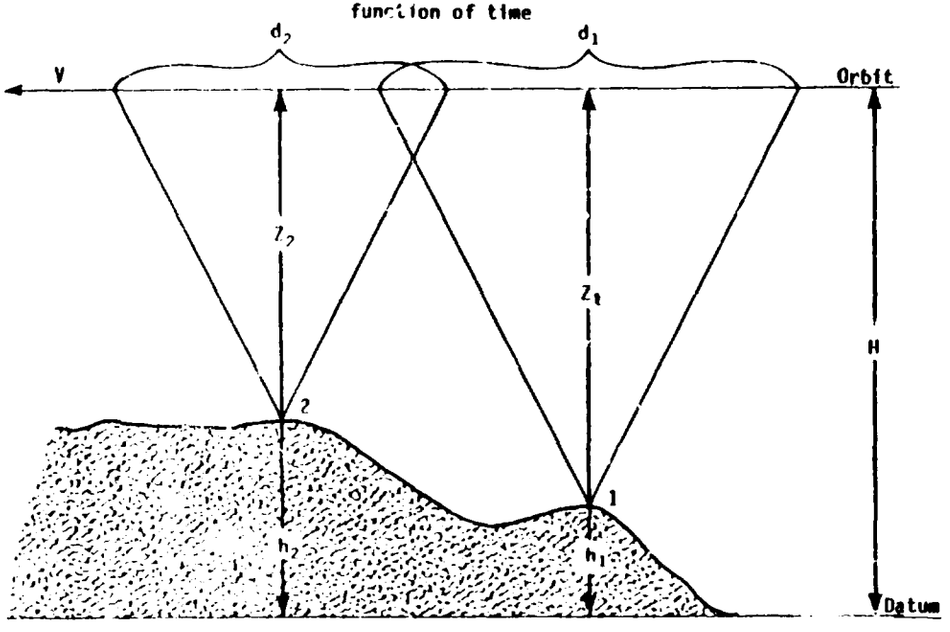

V = satellite velocity (constant)
t_1, t_2 = time to stereo image points 1 and 2

$d_1 = V.t_1$ dist. moved to acquire stereo
$d_2 = V.t_2$ data of points 1 and 2

H = satellite altitude above datum (constant)
h_1, h_2 = elevation of points 1 and 2 above datum
Z_1, Z_2 = distance from orbit to points 1 and 2

k, K = constants
$h_1 = H - Z_1 = H - k.d_1 = H - k.V.t_1$
$h_2 = H - Z_2 = H - k.d_2 = H - k.V.t_2$
$h_2 - h_1 = K.(t_2 - t_1)$

Δh, Δt = elevation and time differences, points 1 and 2

$\Delta h = K.\Delta t$

Figure 6

N82 28735

8.6 Concept for a Multiple Resolution Pushbroom Sensor

Fred C. Billingsley

Jet Propulsion Laboratory, California Institute of Technology
Pasadena, California 91109

Abstract

A general purpose "pushbroom" sensor will have parameters determined by the needs of the majority of potential users. These parameters may not satisfy the needs of certain users: Agriculture requires a very short return visit interval; cartography requires a very small pixel size; Land Use and Geology would be satisfied with moderate resolution and seasonal return times. The aggregate solution of these needs would produce a sensor with extremely high data rates. A sensor concept is proposed which may meet the combined needs without the extreme data rate.

Coverage Requirements

The various disciplines have expressed requirements ranging from 5-day repeat to semi-annual repeat, from 5-meter to 60-meter resolution, various spectral band combinations, and reasonable data rates.[1] Fortunately, all of the requests may not need to be met simultaneously. The various requirements seem to group somewhat as follows:

Agriculture: Revisit interval 5-8 days to pick up emergence and other crop calendar-related events.
- Spatial: High resolution (10-15 m?) to pick up field boundaries; coarser resolution would suffice for field interiors.
- Spectral: Properly placed bands; 4 to 6 probably sufficient.

Mapping: Revisit interval not critical; eventually need complete cloud-free coverage.
- Spatial: 3-10 meter resolution needed for 1:24000 mapping.
- Spectral: The fine resolution may be panchromatic or principal components.

Geology: Revisit interval should be seasonal to pick up variations indicative of the geologic information desired.
- Spatial: No hard requirement; 15 meter is a logical next step.
- Spectral: Perhaps 7 or so bands, placed for soils and rock recognition. Bands probably different than agriculture bands.

Land Use: Revisit interval perhaps seasonally or semiannually.
- Spatial: No hard requirement; 15 meter is a logical next step.
- Spectral: No hard requirement; bands placed for other purposes may suffice.

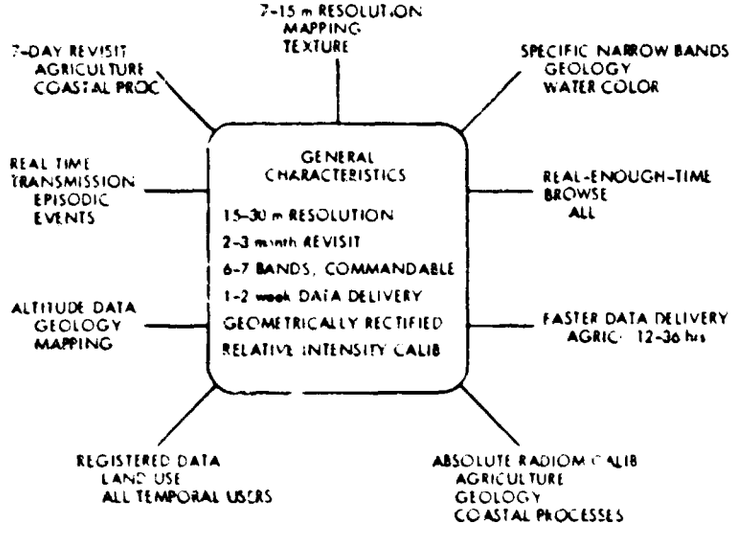

Figure 1. Parameters of a General Purpose Sensor Will Leave the Tall Poles Unsatisfied.

As there are no firm revisit requirements nor firm resolution requirements, a general purpose sensor might be designed to have 15-30 meter resolution, seasonal revisit interval, 6-7 spectral bands. This leaves the agriculture short revisit time and the mapping of fine pixels as major "tall poles" which are not satisfied. Figure 1 illustrates the situation.

C-6

Strawman Solution

A compromise sensor concept is proposed based on the proposition that all tall pole parameters need not be met simultaneously. Specifically, if revisit time can be traded against resolution (short revisit time with low resolution and long revisit time with high resolution), the data rate and quantity can be kept within bounds. Spectral selection will be handled using the imaging spectrometer technique.[2,3]

The revisit time sets the basic parameters:

$$\text{Number of swaths required to cover} = \frac{40{,}000 \text{ (km, earth circumference)}}{\text{Equatorial Spacing (km, = S)}}$$

$$R = \text{Revisit Interval} = \text{Swaths} \times 100 \text{ minutes/swath (approx.)} = \frac{2780}{\text{Eq. Spacing, km}} \text{ days}$$

This gives, for various intervals:

Annual	R = 360	S = 8
Semiannual	180	16
Seasonal	90	32
Monthly	30	96
Weekly	7	411

The actual swath width should be some comfortable amount larger than S to allow for variations in orbit, etc. Considering the potential for orbit control, let the swath width, W, be S + 10 km, rounded to some convenient size.

What now remains is to find an orbit which simultaneously meets the following:

1. Find a suitable orbit which completes its cycles (closes) in about 180 days. The required swath width is about 25 km, which will be covered with 7 1/2 meter pixels.

2. Adjust the basic orbit selection so that a wider swath will close in 2-3 months. Cover this wider swath section with 15-meter pixels. The pixels in the center narrow section may be averaged to form the center part of the wider swath, either on board or on the ground. Let this section be about 60-km width.

3. Further adjust the orbit to allow a still wider swath to cover in about 7 days. The width will be 300-400 km, depending on the revisit time desired. For 8-day maximum intervals (with some intervals shorter), the required width is about 400 km, and for 11-day maximum, the width is about 300 km. Cover the wide swath with 45-60 meter pixels (TBD), and suitably average the pixels in the center sections to form a continuous wide swath.

4. Be sun-synchronous.

Basic Orbit Coverage Periodicity

The basic requirement for periodic coverage is that the nadir trace return to a previously traversed path after some definite period of time, that is, the Rth orbit trace falls on the Nth repetition of the origin (end of the Nth day). This is equivalent to viewing the equator as a continuous arc passing under the ascending node, with the arc measure accumulating indefinitely instead of resetting each day.[4] Note that N and R are both integers.

The N-fold equatorial arc is divided in two ways: into N equal parts and into R equal parts. The smallest division mode which includes both of these is equal to RN if R and N are relatively prime. R and N must be held relatively prime to avoid redundant repeating of the intended closure period.

The orbit repetition parameter Q is the prime descriptor of the coverage pattern. Q is defined as the number of satellite orbit revolutions completed during a single rotation of the earth relative to the satellite plane (approximately equal to the number of revolutions in a day). The value of Q depends primarily on the orbit period, which in turn depends on the satellite altitude. Q is normally expressed in the form

$$Q = I + K/N$$

where I is the number of complete satellite revolutions and K/N is the additional fraction

of a satellite orbit required for a point on the earth to complete one revolution and to reencounter the satellite plane. (Note the parallel between this and the action of the vernier scales used to measure the fractional distance between scale marks.) For a resonant orbit the fraction is zero. The fraction K/N determines the swathing pattern, independent of the integer part of Q, which determines the gross scaling of the orbit advance per orbit.

The design space available is generally in the range of 400-1300 km altitude, which results in a Q range of 13-15. Within this range, sun-synchronism is obtained with orbit inclinations in the range of 97-101 degrees (see Figure 2).

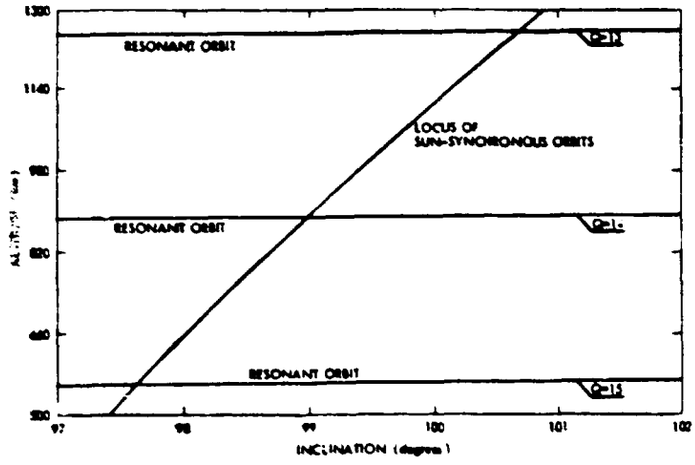

Figure 2. Potential Design for Sun-Synchronous Satellites

The design procedure is to select the K/N to give the desired pattern, and then to select I to correspond to the altitude range desired.

The 6-month, 2-month desire for semiannual and (approximately) seasonal repeat requires that K/N be approximately 1/3. The additional requirement that there be not precise closure until about a year requires that K/N be displaced from 1/3 by a small amount. Because N is the number of days for closure, R = NI + K. Because R, N, and I are integers, K must also be integer, selected so that R and N are relatively prime.

Thus, choose N = 185 for the 6-month period. K must be about 185/3 = 62, approximately. Two patterns, with K = 67 and K = 69, are presented in Figures 3 and 4, which show the desired patterns and with the desired closures of the wide swath giving repeat times of 11 and 8 days, respectively.

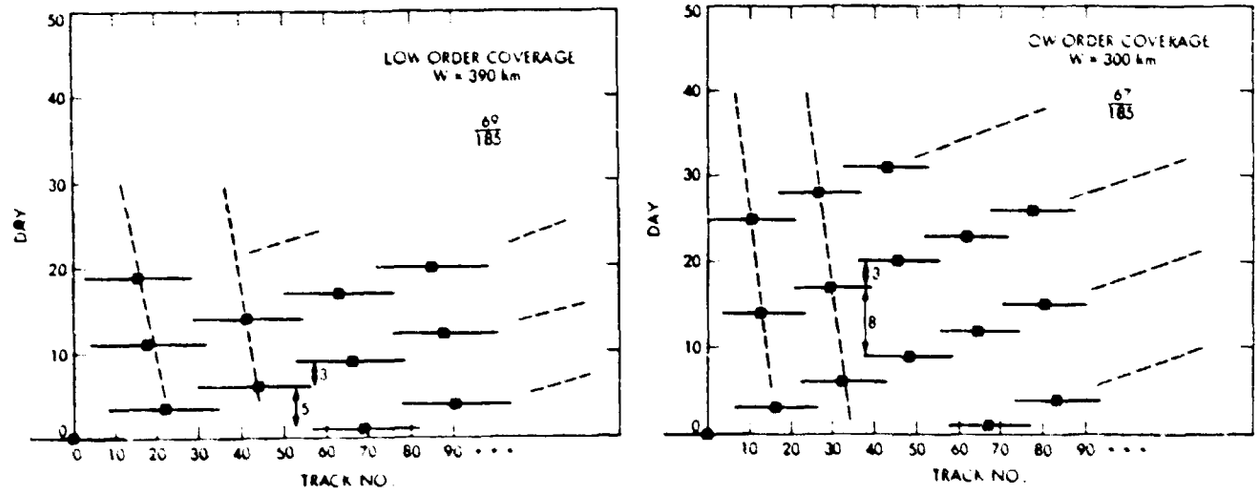

Figure 3. Low Order Coverage Obtained with K/N = 69/185 (left) and 67/185 (right).

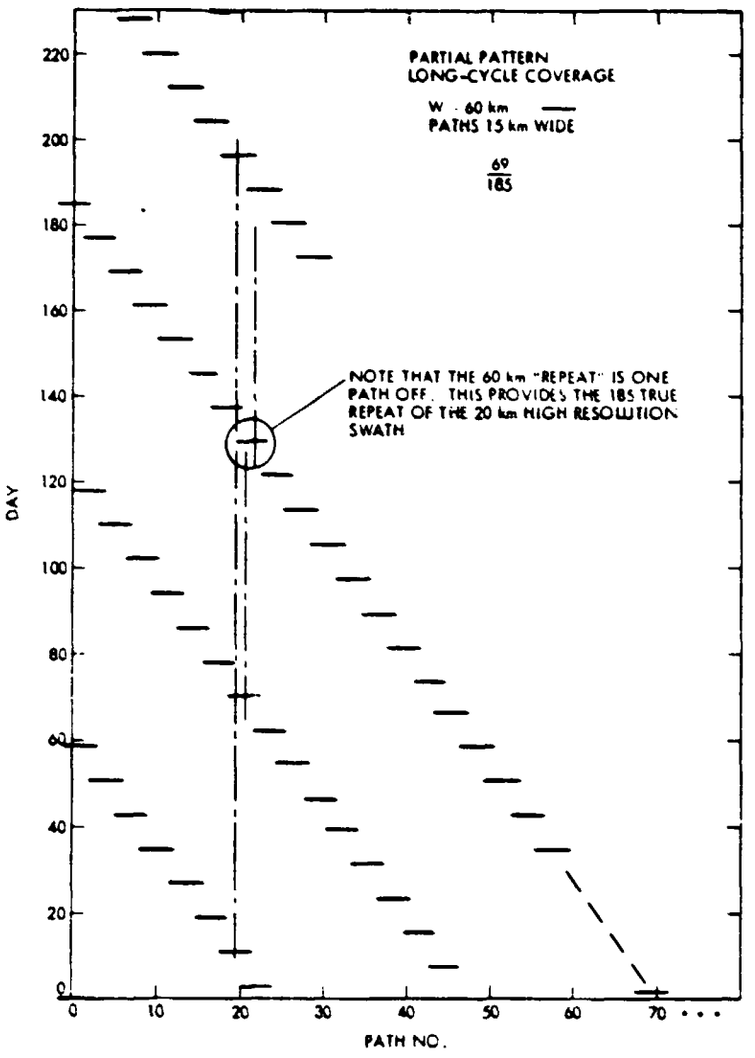

Figure 4. Long Cycle Coverage with K/N = 69/185.

Selecting I in the range of 13-15 sets the altitudes:

I = 13	Altitude = 1145 km	Inclination = 100.0 degrees
14	767	98.5
15	445	97.3

The Sensor

The semiannual closure time chosen results in the basic track separation interval being about 15 km. Thus, the center section should be about 20-25 km wide to allow for orbit variations. The second and outer sections are about 60 and either 300 or 400 km, respectively, to provide the progressively more often repeated coverage while the center section gradually covers the globe once (Figure 5).

If all of the sections are to be panchromatic or to have the same spectral bands, the inner pixels may be averaged to fill in the outer sections. This will reduce the intersensor differences in response which would otherwise be present. At the same time, however, the center pixels will be useful for generating high resolution images, for precision location on maps of the entire swath, for precision location of boundaries in conjunction with the simultaneous lower resolution pixels, and for analysis of texture.

The spectral requirements may be met using a spectrum spread orthogonal to the line of spatial pixel locations.[2] This requires an area sensor array--the long dimension for the

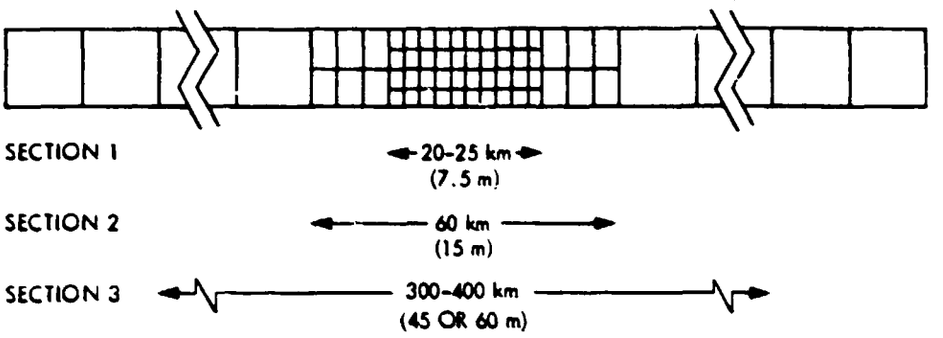

Figure 5. Makeup of the Multiple Resolution Swath Sections

pixels along the swath width, and the short dimension (30 to 60 pixels or so) to sample the spectrum of each of the ground instantaneous fields of view. This approach guarantees spectral band registration, as all pixels are sampled simultaneously.

The area array would image only one 7.5 meter pixel line at a time. The various resolutions and spectral selection would be accomplished with logic on board to minimize data bandwidth requirements. If, for example, the high resolution is desired panchromatically, the inner section pixels would be averaged across the spectral set, but not spatially. They may also be averaged spatially to match the spectral and spatial characteristics of the other sections. Inter-detector differences are reduced in both cases, mitigating some of the deficiencies of the small pixel detectors. At the same time, the on-board processing provides additional flexibility in both the spatial and spectral domains by allowing commandable changes.

The data rate may be kept within bounds by selecting the minimum resolution in the sections to satisfy a given observation, and selecting or synthesizing a small number of required spectral bands from the 30 to 60 available. The specific data rate resulting will depend upon the design parameters ultimately chosen. For example: Consider section 1 (20 km width) to be panchromatic after averaging in the spectral domain, to be used for edge registration, panchromatic texture, and mapping. Section 2 (60 km width) would be seven bands, chosen primarily to provide four bands for agriculture plus three extra bands for geology or other disciplines. Section 3 (300 or 400 km width) would be just the four agriculture bands. With resolutions of 7.5, 15, and 45 meters, the aggregate data rate with 8-bit pixels is about 190 M bit/sec before data compression. Compression in the range of 5:1 may be practical without appreciable data loss, at least for the four-band sections, which would reduce the net data rate by a factor of about 2:1 to 4:1. The data rate will be large, but not intractable.

Potential design altitudes, as discussed above, are 767 or 445 km. These and the desired swath widths, set the angular field required. The angular extent ϕ of a 7.5 meter pixel at these altitudes is 10 or 17 μrad, comfortably above the diffraction limit, although it will push the excellence of the optical design. Practical detectors currently are about 40 μm in size, with some hope of reducing this to 25 μm or so in the future. These two sizes set the required focal length of the lens. Finally, a system with a speed of f:2 to f:4 is visualized, which sets the lens diameter. These combinations are shown in Table 1.

Swath Width km	Alt. km	ϕ pixel km	Field of View deg.	40 μm Detectors Line Length m	40 μm Detectors Focal Length m	40 μm Detectors f:2 Dia. m	25 μm Detectors Line Length m	25 μm Detectors Focal Length m	25 μm Detectors f:2 Dia. m
400	767	9.8	29	2	4.1	2.1	1.33	2.6	1.3
	445	16.9	48		2.4	1.2		1.5	0.8
300	767	9.8	22	1.5	4.1	2.1	1.0	2.6	1.3
	445	16.9	37		2.4	1.2		1.5	0.8

Table 1. Design Parameters for 40 μm and 25 μm Detectors and 7.5 meter pixels.

The requirement for wide field optics for the 300-400 km section is a problem if high resolution is required to the edge of the swath. However, the lower resolution postulated for the outer sections will allow the optics performance to be relaxed at the edge of the

field of view, where the problem is normally the worst. As an alternate, the wide swath portion may be met with a separate sensor. Thus, section 1 and 2 may be met with a sensor covering only 60 km with the 7.5 meter pixels, and a separate sensor covering the wide field 45 meter pixels. Table 2 shows this combination. This approach greatly reduces the optics problem, but requires that the two sensors be accurately boresighted. The two-sensor design has a secondary advantage: at the expense of a higher data rate, and because the wide angle section optics will cover the complete field of view anyway, this section could be implemented with a complete complement of 45 m pixels. Then, as it is redundant to the detectors of section 2, that section could be programmed for different spectral bands than used in section 3.

Swath Width km	Alt. km	¢ pixel km	Field of View deg.	40 μm Detectors Line Length m	40 μm Detectors Focal Length m	40 μm Detectors f:2 Dia. m	25 μm Detectors Line Length m	25 μm Detectors Focal Length m	25 μm Detectors f:2 Dia. m
400	767	58.8	29	0.4	0.75	0.4	0.22	0.43	0.22
	445	101.4	48		0.4	0.2		0.25	0.13
300	767	48.8	22	0.3	0.75	0.4	0.17	0.43	0.22
	445	101.4	37		0.4	0.2		0.25	0.13
60	767	9.8	4.5	0.3	4.1	2.1	0.2	2.6	1.3
	445	16.9	7.7		2.4	1.2		1.5	0.8

Table 2. Design Parameters for 40 μm and 25 μm Detectors, with 45 m pixels for the 300 or 400 km section and 7.5 m pixels for the 60 km section.

Conclusion

A concept for a multiple resolution sensor is presented which, by allowing the various driving parameters to be traded off, may allow satisfaction of several disciplines which are otherwise competing for coverage and spectral and spatial resolution. Although some examples of possible design parameters are given, this is not meant to propose any specific design. Rather, they are given as food for thought. However, they are believed to be representative of the designs possible.

Acknowledgment

This paper presents the results of one phase of research performed at the Jet Propulsion Laboratory, California Institute of Technology, sponsored by the National Aeronautics and Space Administration under Contract NAS7-100.

References

1. G. Vane, F. Billingsley, J. Dunne, "Observational Parameters for Remote Sensing in the Next Decade," SPIE Symposium on Advanced Multispectral Remote Sensing Technology and Applications, Arlington, VA, May, 1982. SPIE Proceedings, Vol. 345.

2. J. B. Wellman, "Technologies for the Multispectral Mapping of Earth Resources," 15th Symposium on Remote Sensing of the Environment, University of Michigan, Ann Arbor, Michigan, May, 1981.

3. J. B. Wellman, J. B. Breckinridge, P. Kupferman, R. Salazar, "Imaging Spectrometer Technology for Advanced Earth Remote Sensing," SPIE Symposium on Advanced Multispectral Remote Sensing Technology and Applications, Arlington, VA, May, 1982. SPIE Proceedings, Vol. 345.

4. J. C. King, "Quantization and Symmetry in Periodic Coverage Patterns with Applications to Earth Observation," AAS/AIAA Astrodynamics Specialist Conference, Nassau, Bahamas, July 1975. GSFC Publication X-932-75-331.

N82 28736

8.7 ATTITUDE TRACKER

Fred C. Billingsley
Jet Propulsion Laboratory, California Institute of Technology
Pasadena, California 91109

Line array sensors produce data which has no inherent geometrical continuity. Hence, any platform attitude variation will be evidenced as a distortion when the data lines are displayed in the normal Cartesian raster. Ancillary sensing is required to establish the platform attitude to allow geometric rectification. This is normally provided by inertial or star reference attitude sensors. However, in the absence of such sensors or if performance of them is degraded, the required attitude information is lost.

A strawman sensor design is proposed which utilizes small image areas on the ground to provide a series of motion vectors with which the platform attitude can be tracked; this allows the distorted image received by the normal image line sensor to be rectified.

THE PROBLEM

Future sensors of the linear array type will return lines of data which are independent in the sense that there is no data tie between them. It is essential for mapping and stereo work that the data lines used for analysis be in precisely the correct geometrical position. If the sensed image lines are not in the correct positions, interpolation or other compensation must be used before analysis. But there is no information in the data as planned to measure the correctness of position; position accuracy depends on platform attitude accuracy for a sufficiently long period. Anticipated spacecraft control parameters will be (marginally) adequate if all is perfect, but there is not much tolerance for degradation, nor any planned way to work around degradations. The use of ground control points will be necessary for precise tie to the ground, but will be clumsy for continued use for the stereo tracking, and, in any event, surveyed ground control points will not be available for many areas. The problem is exacerbated with an aircraft platform due to the ubiquitous attitude instability.

WHAT IS NEEDED

What is needed is a system for analyzing the platform motion as reflected in the ground distortions, which may be used to 1) verify platform stability and 2) provide the data for correcting the geometric aspects of the image lines, either in parallel with the expected good performance of a spacecraft platform or to compensate for degraded performance. Ideally, the system would be useful on board, but ground calculations and correction would be acceptable. Maximum use should be made of the GCPs and the Global Positioning System, but the system should allow (perhaps degraded) use without these.

STRAWMAN SOLUTION

A system for providing the data for self-tracking could be designed as follows: As part of a separate sensor boresighted to the imaging sensor, a set of small square image areas of, say 64 x 64 or 128 x 128 pixels, arranged as sketched (Figure 1) is imaged on to a set of area array detectors. All are read out simultaneously into a set of memories. For each area, the displacement between it and a previous image, taken a few image lines previously is determined. The sequential set of displacement vectors may be used to model the platform attitude variations, and to generate the geometric correction parameters. The related software will have to bridge gaps in the displacement vector sequence due to clouds or other noncorrelation, and to operate in areas of terrain relief.

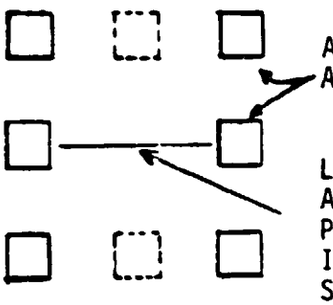

Figure 1. Possible Arrangement of Area Array Sensors

Data analysis follows the well known stereo compilation principles. The effects as seen in normal stereo compilation practice are given in Figures 2 and 3 (from D. H. Alspaugh, "Stereo Compilation and Digitizing," Proc. Latin American Technology Exchange Week, Panama City, May 1979, p. 314).

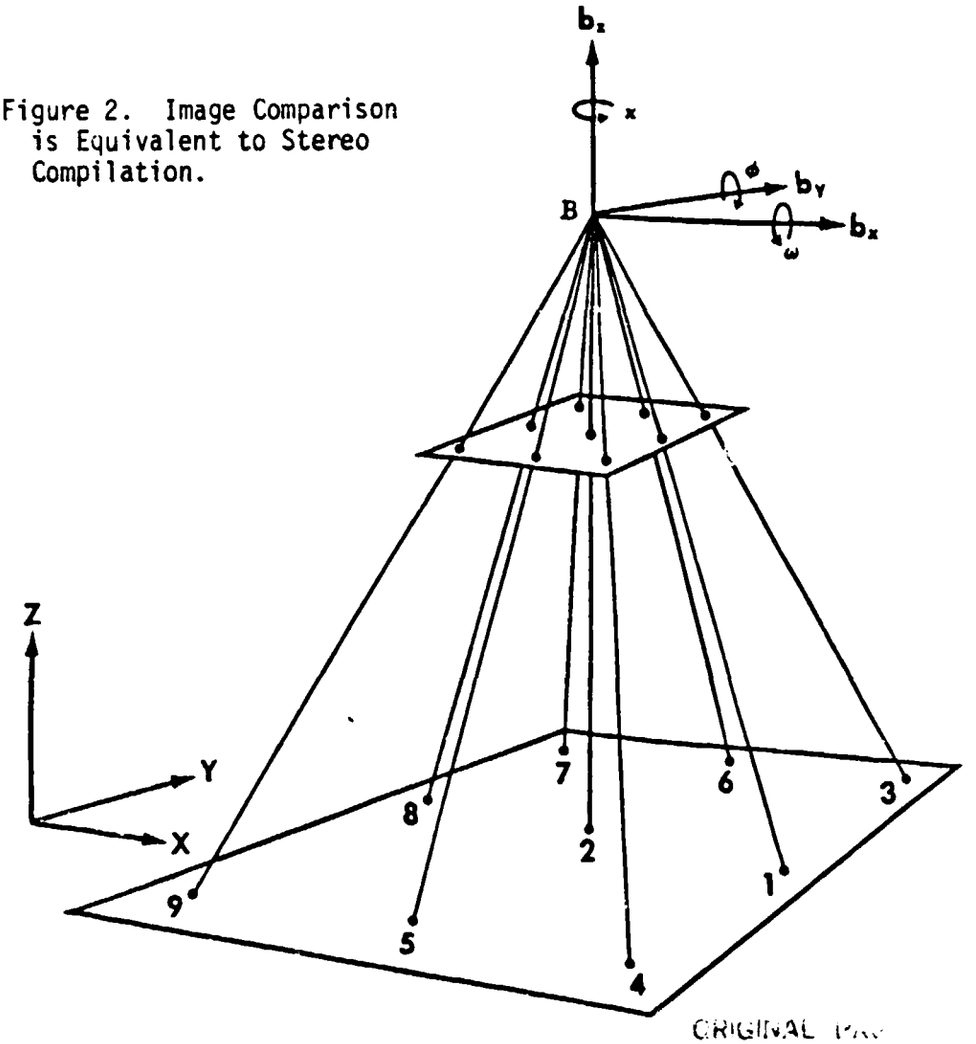

Figure 2. Image Comparison is Equivalent to Stereo Compilation.

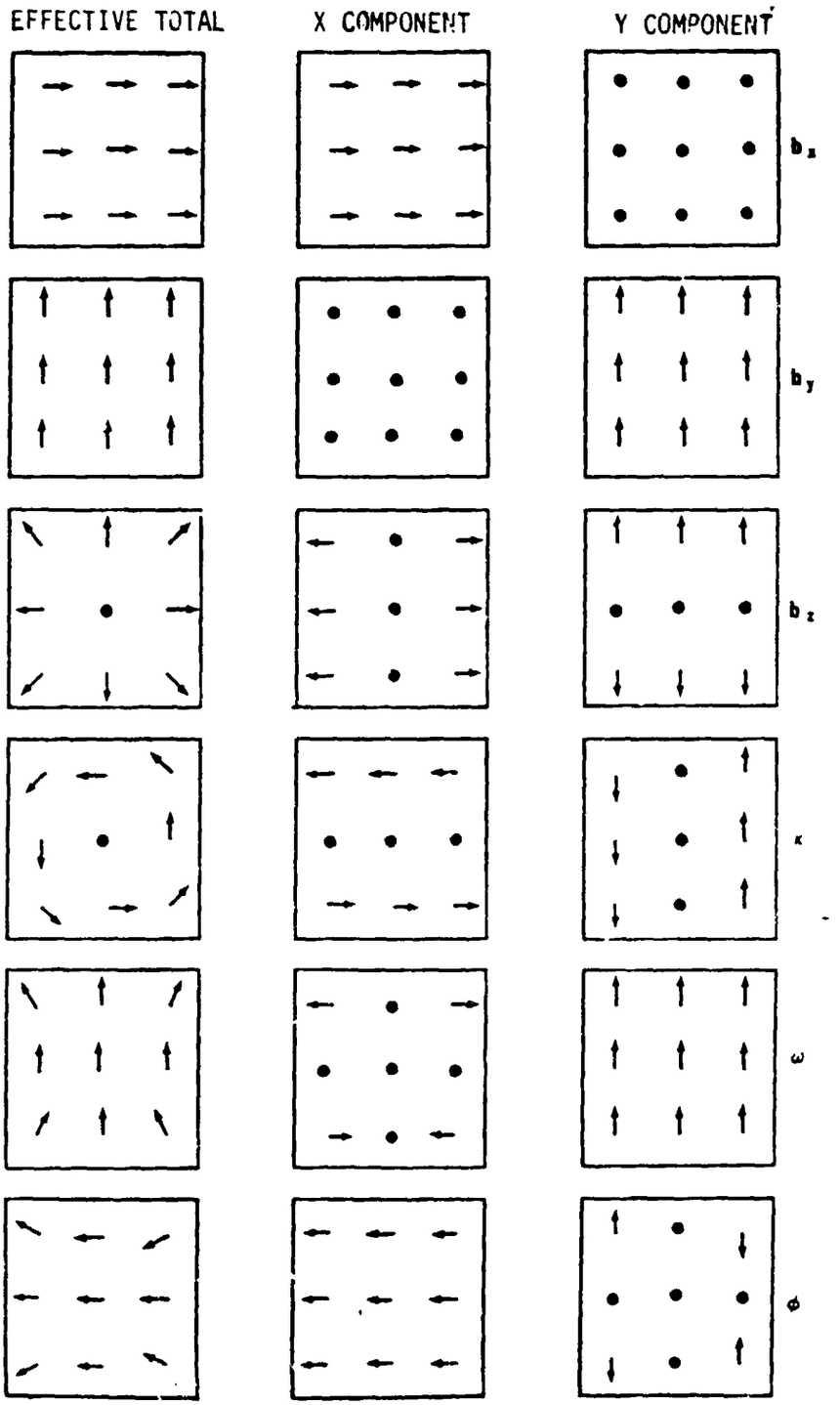

Figure 3. The Image Motion Vector Set as it Reflects Platform Motion

In the eventual instrument, the data processing would be self-contained (Figure 4), so that only the derived attitude parameters would be transmitted or utilized.

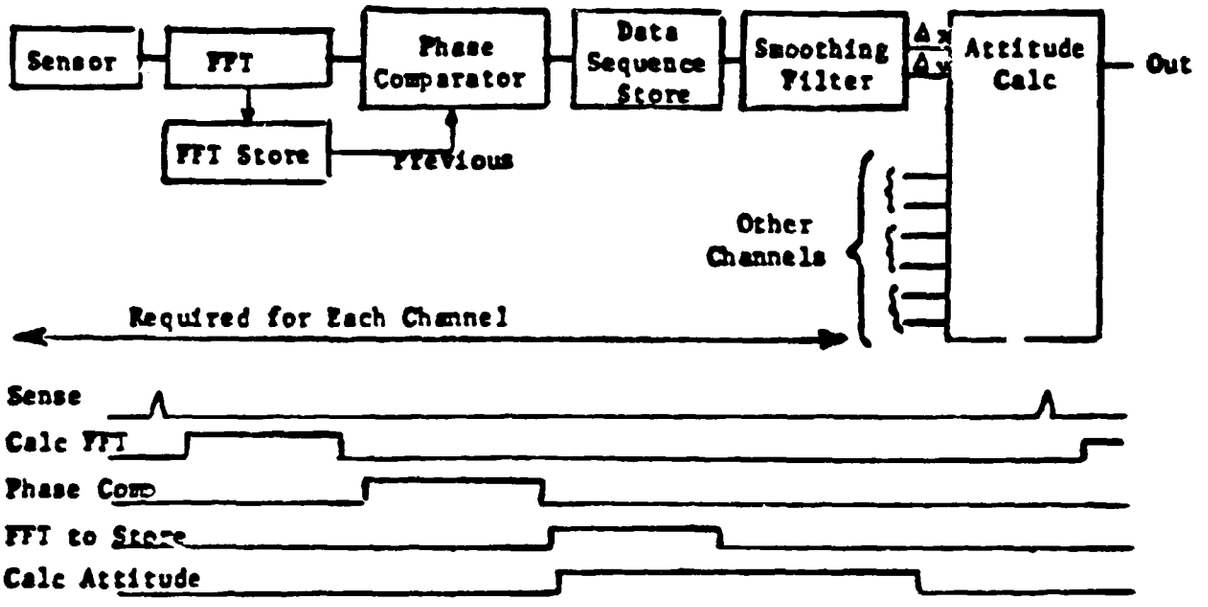

Figure 4. Data Processing Block Diagram and Timing

Lockheed[1 & 2] has built a phase plane comparator, including the FFT, which operates in 1/30 second. Incorporation of this approach could allow this part of the processing to be time-multiplexed.

1. Kuglin, C. D., Hines, D. C., "The Phase Correlation Image Alignment Method," Proc. IEEE 1975 International Conference on Cybernetics and Society, pp. 163-165.

2. Pearson, J. J., Hines D. C., Golosman, S., "Video Rate Image Correlation Processor," SPIE Vol. 119, Applications of Digital Image Processing, IOCC 1977, pp. 197-205.

It may be necessary to incorporate a LIDAR or equivalent sensor to determine the instantaneous altitude.

N82 28737

8.8 A CASE FOR INHERENT GEOMETRIC AND GEODETIC ACCURACY IN REMOTELY SENSED VNIR AND SWIR IMAGING PRODUCTS*

by

Johnie M. Driver**

INTRODUCTION

The multispectral images produced by Landsats 1, 2, and 3 have provided valuable data to a diverse spectrum of users worldwide and there is presently a growing demand for more and better data of this kind. Technologies are under development to satisfy this growing demand -- better detectors, new imaging modes, improved platforms, and innovative utilization techniques. There is a compelling legitimate concern, however, that new data types be mergeable with existing data types. To satisfy this concern, there is a tendency to force new data types to fit existing usage modes with an unnecessary efficiency impairment that can be grossly debilitating with an increasingly large volume of data. This paper argues for image acquisition concepts and processing methods which take proper advantage of new imaging modes and accompanying technologies. The goal is to provide delivery timeliness and throughput efficiencies commensurate with the volume of data acquired.

The inherent inaccuracies in the previous Landsat scanning imaging method rendered extensive image rectification a necessity. By contrast, the inherent linearity in solid state line array imagers shows promise for allowing acquisition of images with inherent geometrical accuracy, leaving platform dynamics as the principal source of error. But new platform developments can potentially provide acceptable stability and pointing accuracy. Hence there is a real prospect for acquiring images with inherent geometrical accuracy at least for certain regions. Platform pointing adequacy, when coupled with adequate orbit state determination, can provide geodetic accuracy as well. Further research is required to determine conditions under which inherently accurate global imagery can be acquired both geometrically and geodetically, and how such imagery can be processed to provide the high volume throughput demanded and the required data mergeability as well.

---

*This paper presents the results of one phase of research carried out at the Jet Propulsion Laboratory, California Institute of Technology, under contract NAS7-100, sponsored by the National Aeronautics and Space Administration.

**Member of the Technical Staff, Mission Design Section, JPL

IMAGING OBJECTIVE

The long-range imaging objective is to provide information adequate to satisfy the perceived operational mission needs. Principal needs relate to quality, timeliness, continuity, coverage, usage diversity, and economy. These needs are discussed at some length in References 1 and 2 and are summarized in Table 1. This paper focuses on "Data Processing Efficiency" as described under the second bullet of Table 1. The imaging system assumed is one which satisfies the remaining requirements except for Thermal IR and Microwave Imagery. The specific imaging objective as relates to this analysis is to acquire images anywhere on the globe which are inherently accurate both geometrically and geodetically. Acquisition of such images will enable efficiencies in processing with consequent relief from timeliness and throughput problems that have plagued Landsats 1, 2, and 3.

SCIENTIFIC IMPORTANCE

Geometrically accurate images are essential to automatic information extraction as well as extraction of bootstrap information, i.e., mission parameters determination from image data. Qualitative (i.e., photointerpretative) use of images, although forgiving, is enhanced by geometric accuracy as is also the capability for quantitative information extraction in a manual mode. Images which are not geometrically correct when acquired (inherently accurate) must be corrected by various time-consuming rectification processes (image line rotation, translation, stretching, warping, etc.). Obtaining images which are inherently accurate offers the following important scientific advantages:

a) Provides timely quick-look information for reconnaissance and episodic events analysis.
b) Provides the potential for onboard information extraction.
c) Avoids the partial loss of spatial and spectral information which resampling typically incurs.
d) Allows timely analysis of a large volume of high-resolution multispectral data which could be totally intractable using conventional processing techniques.

Geodetic accuracy is essential for such processes as multi-temporal comparisons, ground control point improvement, digital mosaicking, automatic inter-image matching, automatic map updating, and map construction to NMA standards. If the acquired images are not inherently accurate geodetically, laborious ground control point fitting must be employed which can be costly and slow indeed when done automatically by correlation techniques, particularly without benefit of a good *a priori* estimated location. With adequate knowledge of platform orbit state and instrument pointing direction, data can be acquired with inherent geodetic accuracy, making possible the scientifically important uses indicated above which would otherwise be too costly to consider on any massive scale.

TECHNICAL FEASIBILITY

The technical feasibility of acquiring inherently accurate images is examined here in terms of a particular mission and imaging system concept and specific functional capabilities. The analysis considers error characteristics (types, sources, and magnitudes) and conceptual compensation modes. The strawman concepts assumed for this analysis are summarized below but are described in greater detail in References 1 and 2.

Mission Concept

A land remote sensing mission is assumed using a free flyer spacecraft launched from WTR into a near-circular sun-synchronous orbit. The spacecraft is assumed to fly at 882-km altitude, orbiting the Earth every 103 min in a contiguous swathing coverage pattern, completing a repeat coverage cycle in 52 days after 729 orbital periods. Surface spacing between adjacent ground tracks occur one day apart, separated by 55 km at the equator and decreasing separation along latitude lines as the cosine of latitude. The 99-deg inclination required for sun-synchronism allows orthographic imaging of all regions of the Earth below 81 deg latitude.

A pushbroom imaging concept (Ref. 2) is used (Fig. 1) to image the land masses of the Earth in the visible and near infrared (VNIR) and short wave infrared (SWIR) spectral ranges. Each image line is formed by 4000 contiguous detector elements arrayed nominally perpendicular to the spacecraft ground track. Image exposure time is adjusted according to spacecraft altitude to form for each pixel a square Ground Instantaneous Field of View (GIFOV). Area array detectors are used to allow a dispersive imaging approach, enabling selective acquisition of multispectral images from any portion of the covered spectral range with high spectral resolution and inherent spectral registration.

Simultaneous utilization of three types of imaging devices is assumed to provide orthographic, stereographic and arbitrary site oblique imaging. Orthographic imagery is provided by the nadir-oriented imaging device. This device will provide a complete and repetitive set of timely and synoptic land area images on a near global scale. This multispectral imaging device will emphasize uninterrupted coverage with high geometric and geodetic accuracy suitable for cartographic use.

For stereographic imagery, the nadir-oriented device is supplemented by two additional instruments, offset fore and aft, to allow continuous monospectral imaging of the terrain from three different vantage points in space. Extremely high inherent geometric and geodetic accuracy for these stereographic imagers is desirable but not crucial. This is due to the comparatively limited data volume these instruments produce and the characteristically retrospective and selective data usage mode expected.

The third imaging device is multispectral and pointable and is used intermittently to provide timely coverage of rapidly changing phenomena at arbitrary imaging sites anywhere on the globe (Ref. 2). With a capability of pointing 55 deg either side of nadir (Fig. 2), the instrument will be

capable of next-day coverage of any point on Earth and next-orbit coverage at high latitudes. Geometric and geodetic accuracy for this instrument, while desirable, is not crucial -- in contrast with the orthographic imager -- since the chief information use depends on its inherent spectral registration instead.

Specific capabilities for these three imaging devices are summarized in Table 2. Table 3 summarizes the expected coverage characteristics.

Error Characteristics

Typical image aberrations include scale variations, displacement, distortion, skew, and rotation. These aberrations are common to all imaging modes, but their relative importance differs from one mode to another. Intraframe, interframe, swath-to-swath, and geodetic registration are affected by these aberrations to varying degrees. The following material discusses the error types, principal causes, and gross magnitudes for each imaging mode and examines inherent accuracy feasibility.

Orthographic Imagery. Table 4 lists the characteristic image aberrations expected for the orthographic imager if no special measures are taken to obtain inherent accuracy. The table shows areas where research is needed to find acceptable error compensation options.

The list in Table 4 is dominated by intraframe errors, the primary determiners of geometric accuracy. Image scale changes of 2.4% typically occur due to altitude variations, driven by the combined effects of gravity harmonics and Earth flattening, hindering one-to-one correspondence of image pixels with predetermined geographic locations. These same altitude changes coupled with velocity variations hinder equilateral pixel dimensions on the ground unless compensated.

Continual platform movement around the pitch axis to maintain a nadir orientation gives rise to keystone distortion in the image, causing a shape like the central portion of an orange slice. This distortion, although worse for wider swath widths, appears entirely negligible for a 60-km swath.

Frame skew occurs when the spacecraft maintains a fixed inertial heading while imaging the rotating Earth. The resultant image is composed of an array of parallelogram-shaped pixels, skewing the frame. This aberration may not pose any serious information extraction problem. The skew can be removed by continuous yawing of the spacecraft as a function of latitude. However, this yaw rotates the image lines and gives rise to nonparallelism which can result in large relative pixel displacements at the image frame edge.

Earth curvature causes image lines to overlap toward the frame edges, particularly for wide swaths. The less than 1% overlap expected due to Earth curvature should not significantly impact image radiometry and is probably negligible. Random distortions can occur within an image frame because of drift, vibration or jitter in the imaging platform or instru-

ment. If drift rates are kept to 10^{-5} deg/s, no serious image impairment should result. However, drift rates as large as 10^{-4} deg/s give cause for concern and would doubtless rule out obtaining inherent geometrical accuracy at the 15-m pixel level except for small swaths.

Significant interframe, swath-to-swath and geodetic errors stem principally from navigation errors, altitude variations, and attitude control inaccuracies. Errors of these types hinder mosaicking, multitemporal comparisons, and map registration. With accurate models and suitable ancillary data, these errors and those above can be compensated if necessary by post-processing. The goal, however, is to obtain inherent accuracy. Hence compensation options are needed onboard the spacecraft so that the received images for the most part are ready for use.

Stereographic Imagery. The principal stereographic image aberrations relate to obtaining interframe registration between a given pair of images from the triplet obtained. The error types, causes and expected magnitudes are shown in Table 5. The scale of one image differs from the other because of differential variations in imaging distance, impairing pixel-to-pixel coincidence between frames. Orbit dynamics, Earth geometric flattening, and attitude control errors, principally around the pitch axis, are the major contributors to stereographic image scale errors. Image displacements hinder inherent frame-to-frame correspondences. Earth rotation is the principal contributor giving rise to a 27-km loss in stereoframe overlap if not compensated (Fig. 3). If compensated by yawing the imaging platform, assuming the focal planes of all three cameras are rigidly fixed relative to the platform, image line rotation occurs (Fig. 4). This line rotation results in non-parallel image lines (4.3 mrad middle-to-offset, 8.6 mrad between offset cameras) as well as a 1.7-km departure from geographical coincidence. In addition, attitude control errors can cause significant interframe displacement errors unless limited by a tighter stability rate requirement. A more detailed analysis of stereographic image aberrations is given in Ref. 3.

Oblique Imagery. All of the generic geometrical imaging error types (intraframe, interframe, swath-to-swath, and geodetic) are found to a significant degree in the oblique imaging mode, particularly for large off-nadir viewing angles and large swath widths. Figure 5 indicates how the image scale changes as a function of off-nadir viewing angle, assuming a fixed imager field of view. The imaging distance variation relates directly to pixel spread alongtrack. The swath width variation shows the combined effects of increasing imaging distance and Earth curvature.

Figure 6 shows the character of the intraimage distortion caused by off-nadir viewing at large angles. It is noted that for sufficiently small swath portions (10-30 km), this keystoning effect can be kept to pixel level across the frame even at large off-nadir angles.

Compensation Options

A stable imaging platform is of fundamental importance to acquiring images with inherent geometrical accuracy. Attitude stability in the

vicinity of 10^{-5} deg/s is needed for 15-m GIFOV in a 60-km frame size. A larger frame size at the same resolution implies a pointing stability which is proportionately more precise. Given inherent geometrical accuracy within the image, pointing accuracy, or at least accurate pointing knowledge, becomes the next sine qua non for geodetic accuracy. When coupled with 10- to 15-m orbit position knowledge, a 0.001-deg pointing accuracy will enable geodetic registration to within one 15-m pixel most of the time.

Beyond the basic platform requirements, many mission parameters impact the attainable accuracy as discussed in the previous section. Figure 7 suggests compensation options for some of the potential image aberrations encountered. The principal cause of orthographic image aberration is the image scale and pixel shape errors caused by orbit altitude variations. Methods and options for orbit altitude control should be investigated thoroughly to assess the potential for error minimization. Successful orbit control, whether through orientation and shaping, restricted region operation, or active propulsion, will benefit all imaging modes. Typical orbit characteristics and expected deviations are explored in Ref. 4-6.

In principle, certain instrument design features can be used to compensate for potential image aberrations. If a practical method is found for dynamic focal length variation, image scale problems could be essentially overcome for all imaging modes. Altitude variations could be tolerated for orthographic imagery, geometrical flattening and orbit dynamics could be compensated for stereographic imagery, and the effects of imaging distance variations for arbitrary site imaging could be ameliorated. If focal plane rotation is feasible, image line rotation in stereographic and orthographic imagery need no longer be a problem. The capability for dynamic variation of image line exposure time could be a very valuable instrument design feature. This feature would allow maintenance of square pixels with consequently greater image regularity and scalability even if the overall image scale changed with altitude. Without variable exposure time, instrument electronics redesign would be required to obtain square pixels and variable resolution at different nominal operating altitudes.

Given sufficiently accurate ancillary data, compensation for various image aberrations could be performed onboard the spacecraft. Processes such as geometrical correction, dynamic scaling, resampling to a map grid and registration to star references are conceivable and could enable inherent geometric and geodetic accuracy in images transmitted to the ground.

If inherent accuracy is not achieved through the various processes discussed above, precise orbit and attitude knowledge can still be transmitted to the ground where various high-powered but costly and slow methods can be used to compensate for remaining image aberrations.

TECHNOLOGY READINESS

The continual progress being made in pertinent technology developments heightens the promise and value of obtaining inherent geometrical and geodetic imaging accuracy. The principal technology is the solid-state imager developments which make possible the acquisition of high resolution

images with high signal-to-noise content and with inherent spatial linearity in a many-element line array. The extensions being made to allow area arrays make possible inherent spectral registration. Obtaining adequate geometrical accuracy onboard offers the hope for optional onboard information extraction with consequent transmission of only the extracted information to the ground.

Pointing platform technology is indicated by the fraction of an arc second stability and accuracy (Ref. 7) promised for the Annular Suspension and Pointing System (ASPS). While these devices are slanted primarily toward inertial pointing needs, extension to a nadir-oriented device with up to an order-of-magnitude degradation would satisfy the principal inherent accuracy needs envisioned here. The Multimission Modular Spacecraft (MMS), which is inherently geared to Earth observation needs (Ref. 8), also shows promise for providing the 10^{-5} deg/s stability needed for inherent geometric accuracy.

Orbit position knowledge to 10 m is targeted for the Global Positioning System (GPS). This accuracy is commensurate with pixel level geodetic accuracy at 15-m GIFOV. Long-term orbit propagation to commensurate accuracies is potentially attainable using precision propagators such as GSFC's GEODYN Program (Ref. 9). The repeating nature of typical Earth observation orbits should allow construction and refinement of specialized geopotential models suitable for orbit prediction to very high accuracies, particularly with refinement of atmospheric drag parameters and continual updates of the modeled atmosphere.

Active orbit control using OMS propulsion on Shuttle missions is probably a viable option for short-term image compensation. Active orbit control using onboard propulsion is not obviously practical for free flyers. The potential for using such an orbit control mode should be determined.

Continual improvements in computing speed, memory, and size minimization increases the options for onboard computation. Imaginative utilization of this capability can also be a strong factor in the acquisition of inherently accurate images.

Overall, the technology readiness is such that attaining inherent geometric and geodetic accuracy in the acquired images is a real possibility and the necessary research and analysis to define more clearly the options and requirements is warranted.

RESEARCH NEEDS

GEODYN Updates

The GEODYN orbit propagator should be modified to compute nadir orientation and orbital position relative to a triaxial ellipsoid rather than an oblate spheroid for improved geodetic accuracy.

Atmosphere Dynamics/Updates

Continuing research in atmosphere modeling is needed to predict more accurately the short-term variations in drag-related parameters. The capability to allow frequent updates to the atmosphere model is warranted. Drag will constitute the major orbit prediction uncertainty for typical low- altitude Earth observation missions.

Geopotential Model Development

Procedures need to be developed for creating in routine fashion specialized geopotential models which take advantage of the repetitive nature of typical Earth observation orbits to improve prediction accuracy. Thus if an orbit is modified to provide a different coverage pattern, a new geopotential model of comparable accuracy will shortly ensue.

Imaging Platform

Research is needed to assure that for both free flyer and Shuttle or Space Platform missions, the capability will exist to provide a 10^{-5} deg/s or better platform stability and pointing control accuracy or knowledge as a minimum to 0.001 deg for a nadir-oriented imaging platform.

Orbit Dynamics

Methods of control for orbit dynamics are needed to define the requirements and limitations on frozen orbits, constant altitude orbits, minimum altitude variation orbits, coverage pattern maintenance, and active orbit shaping using onboard propulsion.

Image Geometrical Characteristics

A detailed investigation is needed to determine the precise geometrical characteristics of acquired images on a representative Earth surface for accurately modeled orbits, showing geographical dependence and the effects of typical off-nominal mission characteristics.

Variable Instrument Parameter Development

There is a potentially high payoff in acquired image quality if dynamic variation of instrument parameters can be implemented in a practical way. Significant research is warranted to find a reliable mechanization for variable focal length for imaging distance compensation on spaceborne telescope-type instruments of the kind envisioned for Earth observation missions. Similarly, a mechanism is needed to provide commanded focal plane rotation one cycle each orbit for thousands of orbital revolutions. This mechanism would be used to maintain image line parallelism in image frames.

Dynamic variation of image line exposure time is simple to implement in principle. However, there are doubtless unforeseen implications in the resulting variation of data acquisition rates and possibly some image

radiometry implications as well. Research is needed to find an acceptable implementation scheme, thus allowing free variation in orbit altitude and image resolution without distortion in pixel shapes.

CONCLUSIONS

It has been shown that significant aberrations can occur in acquired images which, unless compensated on board the spacecraft, can seriously impair throughput and timeliness for typical Earth observation missions. Conceptual compensations options were advanced to enable acquisition of images with inherent geometric and geodetic accuracy. Research needs were identified which, when implemented, will provide inherently accurate images. Agressive pursuit of these research needs is recommended.

REFERENCES

1. "Application of Solid-State Array Technology to an Operational Land-Observing System," JPL Internal Report No. 715-82, Jet Propulsion Laboratory, Pasadena, CA, 31 October 1980.

2. Driver, J.M., "A Flexible Approach to an Operational Land Observing System," AIAA Paper 81-0315, 19th Aerospace Sciences Meeting, St. Louis, MO, January 12-15, 1981.

3. Driver, J.M., "Stereosat: A New Astrodynamics Challenge," AIAA Paper 80-0237, 18th Aerospace Sciences Meeting, Pasadena CA, Jan. 15-16, 1980.

4. Driver, J.M., and Tang, C.C.H., "Earth Application Orbit Analysis for a Shuttle-Mounted Multispectral Mapper," AAS Paper 81-182, AAS/AIAA Astrodynamics Specialist Conference, Lake Tahoe, NE, Aug. 3-5, 1981.

5. Tang, C.C.H., "Imaging Spectrometer Development Program: Preliminary Orbit Characteristics Document," JPL Internal Report No. 715-145, Jet Propulsion Laboratory, Pasadena, CA, October, 1981 (in publication).

6. "Imaging Spectrometer Progress Report," JPL Internal Report No. 715-143, Jet Propulsion Laboratory, Pasadena, CA, October, 1981 (in publication).

7. Van Riper, R., "High Stability Shuttle Pointing System," Reprint from Proc. Soc. Photo-Optical Instrumentation Engineers, Vol. 265 (Shuttle Pointing of Electro-Optical Experiments), Los Angeles, CA, Feb. 9-13, 1981.

8. Iwens, R. P., et al., "Design Study for Landsat-D Attitude Control System," TRW Defense and Space Systems Group, Contract NAS5-21188, Prepared for Goddard Space Flight Center, Greenbelt, MD, Dec. 15, 1976.

9. Martin, T.V., et al., "GEODYN System Description," EG&G/Washington Analytical Services Center, Inc., Contract No. NAS 5-22849, Riverdale, MD, 1976.

Table 1. Perceived Operational Mission Needs

- DATA CONTINUITY
  - CONTINUOUS DATA ACQUISITION
  - NON-DISRUPTIVE DATA TYPE CHANGES
- DATA PROCESSING EFFICIENCY
  - QUALITY (PIXEL-LEVEL PRECISION)
  - TIMELINESS (QUICK-LOOK, THROUGHPUT)
  - PRODUCTION FACILITY (INFORMATION EXTRACTION, DISPLAY)
  - ECONOMY (PURCHASE, PROCESSING)
- OPTIMAL COVERAGE STRATEGY
  - MULTIPLE ASPECT VIEWING
    - ORTHOGRAPHIC } NEAR-GLOBAL,
    - STEREOSCOPIC } CONTINUOUS
    - OBLIQUE (MESOSCALE, INTERMITTENT)
  - CLOUD FREE SYNOPTIC GLOBAL
  - RAPID, SEASONAL, AND ANNUAL REPEAT COVERAGE
  - OPTIMAL LIGHTING
  - CONTIGUOUS SEQUENTIAL SWATHS
- TASKING CAPABILITY
  - MISSED SCENE RECOVERY
  - SELECTED AREA IMAGING
  - SELECTABLE IMAGING OPTIONS (IFOV, SWATH, BANDS, BANDWIDTHS)
  - OPTIONAL THEME SELECTION
- IMPROVED IMAGING PARAMETERS
  - SPATIAL RESOLUTION (10 TO 30 m IFOV)
  - SPECTRAL RESOLUTION ($\Delta\lambda \approx 20$ nm)
  - RADIOMETRIC SENSITIVITY ($NE\Delta\rho \approx 0.5\%$)
  - ADDITIONAL SPECTRAL BANDS (15 OR MORE)
- NEW TECHNICAL CAPABILITIES
  - SHORT WAVE INFRARED (SWIR)
  - THERMAL INFRARED (TIR)
  - MICROWAVE IMAGERY

Table 2. Instrument Capabilities

	ORTHOGRAPHIC & OBLIQUE	STEREOGRAPHIC
SPECTRAL BANDS (λ C)	30 CONTIGUOUS IN VNIR 30 CONTIGUOUS IN SWIR	SINGLE BAND BETWEEN 0.8 AND 1.0 μm
SELECTABLE BANDS	ANY 6 OF 60 AVAILABLE	NONE
BANDWIDTHS ($\Delta\lambda$)	20 TO 120 nm IN VNIR 30 TO 120 nm IN SWIR	100 nm
SPECTRAL REGISTRATION	INHERENTLY PRECISE (DISPERSIVE IMAGING)	N/A
SWATH WIDTH (SW)	60 km MAX., SELECTABLE	50 TO 60 km FIXED
INSTANTANEOUS FIELD OF VIEW (IFOV)	15, 30, 45 OR 90 m	15 m
TASKABLE PARAMETERS	SW, IFOV, λC, $\Delta\lambda$ IMAGE SITE FOR OBLIQUE	B/H, IFOV mix

Table 3. Coverage Characteristics

	ORTHOGRAPHIC	STEREOGRAPHIC	OBLIQUE
INSTRUMENT ORIENTATION	NADIR ORIENTED	23° FORE AND AFT	POINTABLE ±55° (CROSSTRACK)
COVERAGE EMPHASIS	CARTOGRAPHY	TOPOGRAPHY	AGRICULTURE AND EPISODIC EVENTS
COVERAGE EXTENT	-- NEAR GLOBAL --		GLOBAL SAMPLING
COVERAGE CONTINUITY	-- CONTINUOUS OVERLAND -- DURING DAYLIGHT HOURS		INTERMITTENT
REPEAT COVERAGE FREQUENCY	-- 50 TO 60 DAYS --		NEXT DAY ANYWHERE NEXT ORBIT AT HIGH LATITUDES
ADJACENT SWATH COVERAGE	-- NEXT DAY --		ANY SITE ON ANY DAY
SPECIAL FEATURES	UNINTERRUPTED COVERAGE, LIMITED TASKING	NEAR-GLOBAL STEREO DUAL BASE-TO-HEIGHT	• RAPID REPEAT COVERAGE • UNLIMITED TASKING • FREQUENT SITE CHANGES

TABLE 4. ORTHOGRAPHIC IMAGE ABERRATIONS

Error Types	Principal Cause	Expected Magnitudes
	INTRAFRAME	
Image Scale	Variable Altitude w/fixed focal length	2.4%
Pixel Shape	Variable Altitude w/fixed exposure time	2.4%
Keystone Distortion	Nadir Orientation on Spherical Earth	1 m @ SW=61 km 19 m @ SW=185 km
Frame Skew	Earth Rotation w/fixed S/C heading	4 deg
Image Line Rotation	Frame Skew Removal by Spacecraft Yaw	21 m @ SW=61 km 187 m @ SW=185 km
Image Line Overlap	Earth Curvature	0.07% @ SW=61 km 0.6% @ SW=185 km
Random Distortion	Platform Stability	15 m @ 10^{-4} deg/s for SW=61 km 45 m @ 10^{-4} deg/s for SW=185 km
	INTERFRAME, SWATH-TO-SWATH, AND GEODETIC	
Orbit State	Tracking Capability	10 m GPS 150 m TDRSS
Image Scale	Altitude Variation	1.7%
Displacement	Attitude Control	154 m @ 0.01 deg
Rotation	Attitude Control	11 m @ 0.01 deg for SW=61 km 32 m @ 0.01 deg for SW=185 km

TABLE 5. STEREOGRAPHIC IMAGE INTERFRAME ABERRATIONS

Error Types	Principal Cause	Expected Magnitude
Image Scale	Orbit Dynamics	900 m @ SW=61 km 1700 m @ SW=185 km
	Earth Flattening	180 m @ SW=61 km 550 m @ SW=185 km
	Attitude Control	20 m @ .01 deg for SW=61 km 60 m @ .01 deg for SW=185 km
Image Displacemen	Earth Rotation	27/55 km
	Attitude Control (0.01 deg)	
	Yaw	69/138 m
	Pitch	385 km
	Roll	156 km
	Yaw Mechanization w/fixed cameras	1.7 km
Image Line Rotation	Yaw Mechanization w/fixed cameras	4.3/8.6 mrad

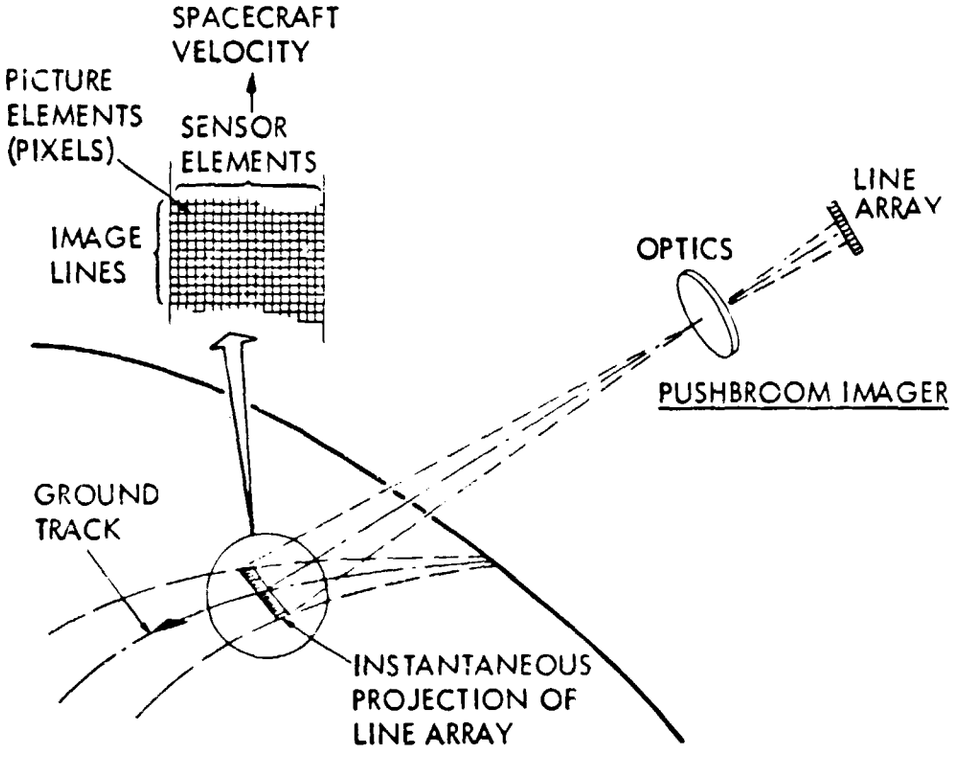

Fig. 1. Pushbroom Imaging Concept

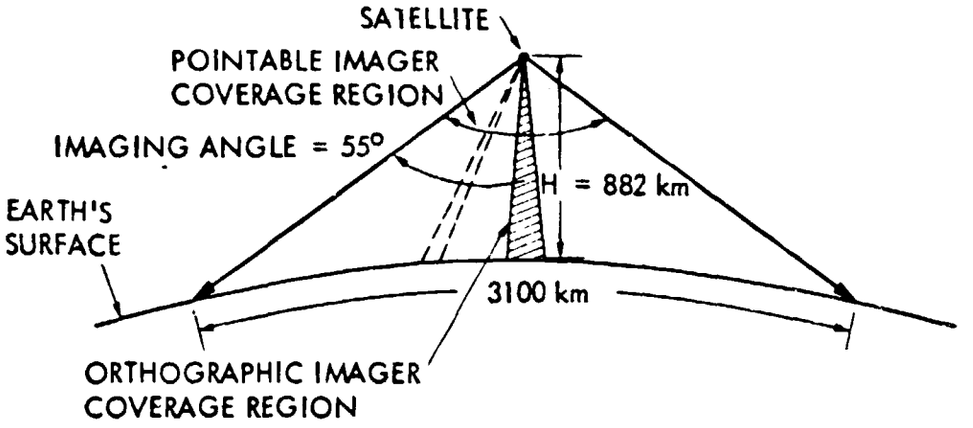

Fig. 2. Pointable Imager Coverage

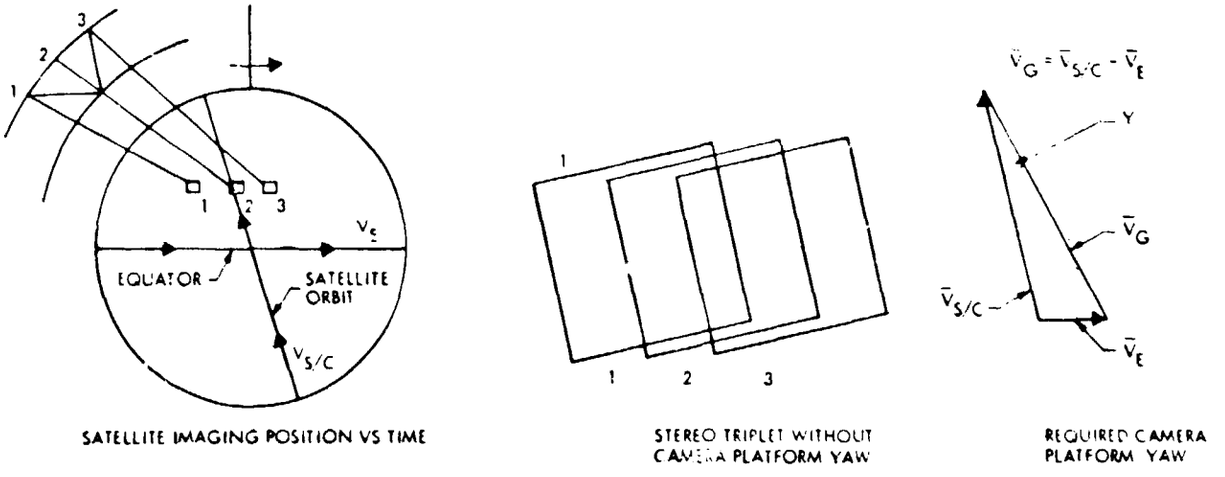

Fig. 3. Earth Motion Impact on Stereographic Imagery

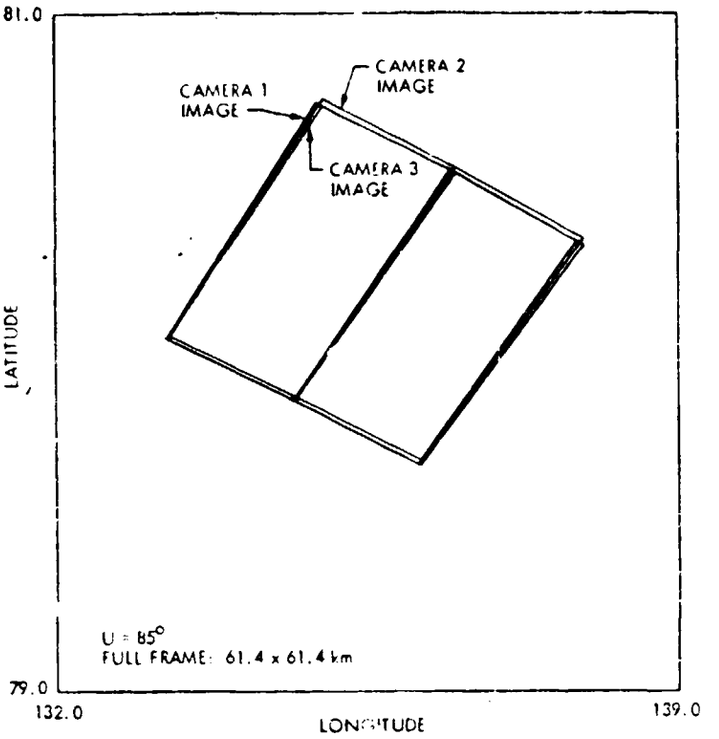

Fig. 4. Stereographic Image Compensated for Earth Motion by Platform Yaw

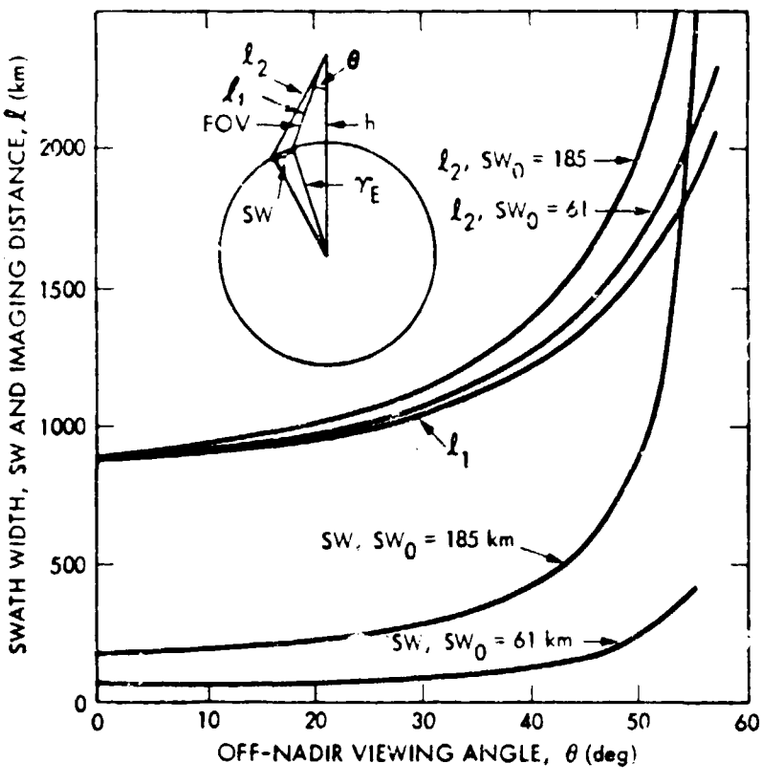

Fig. 5. Image Scale Dependence on Off-Nadir Viewing Angle With Fixed Imager Field of View

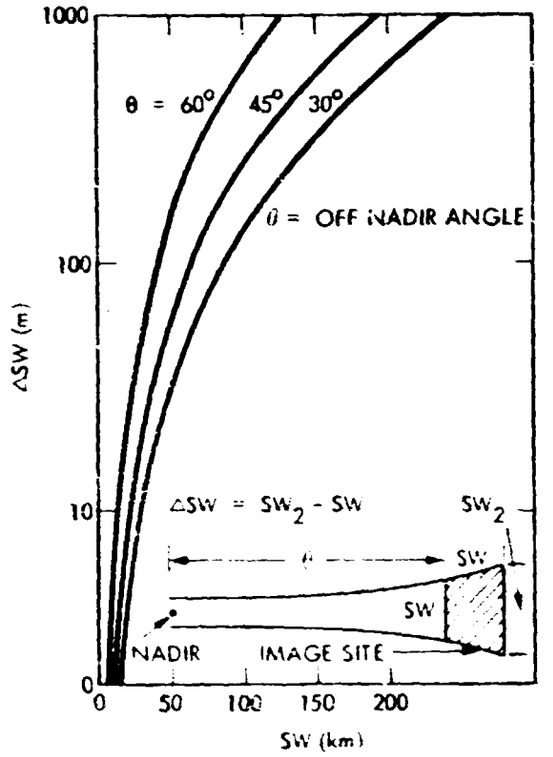

Fig. 6. Keystone Distortion Due to Off-Nadir Imaging on a Spherical Earth

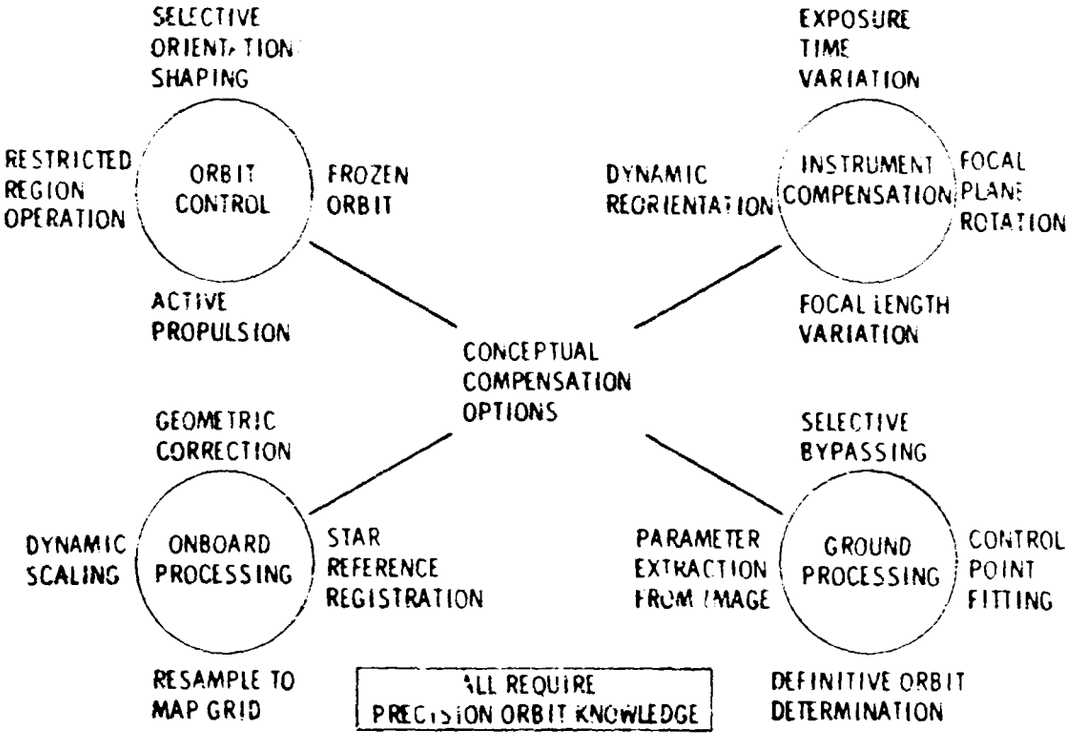

Fig. 7. Options for Compensating Orbit Dynamics Impact on Image Geometry

N82 28738

8.9 A Concept for a Future Ground Control Data Set for Image Correction

Ralph Bernstein
IBM Scientific Center
Palo Alto, CA 94304

ABSTRACT

Strips of ground control can be established with current and future satellite sensors. These can provide precise and reliable geometric references for locating and correcting satellite image data and to support temporal image registration. This paper briefly describes the concept and approach for implementing this data base called a Ground Control Strip, and recommends additional work. The advent of new solid state imaging systems, in particular the linear array detectors (pushbroom sensors), make this new concept particulary attractive and practical.

INTRODUCTION

Image data suffers from some degree of geometric error. The error sources are due to sensor characteristics and imperfections, to satellite attitude perturbations, and to orbit decay and eccentricity effects. The external geometry of a satellite can be determined from star trackers, horizon sensors and gyro-compasses, inertial platforms, and ground reference or control points. Geometric errors are currently precisely determined and corrected by the use of ground control points, which are typically 32x32 pixel subimages used to establish image geometric errors (Bernstein, 1975,1976, and Niblack, 1981).

A ground control point is a subimage which includes natural or cultural features used to establish a ground reference point to support image correction and registration. These features are selected to have the characteristics that they can be precisely located in the image and on the maps. Digital ground control points have been used for about a decade. These have replaced "film chip" ground control points commonly used in electo-optical image processing systems. Given a sufficient number of ground control points, a scene can be corrected to sub-pixel image accuracy (see Fig. 1). It is apparent from Figure 1 that many GCP's, high resolution data, and sub-pixel registration algorithms are needed to obtain high image geometry accuracy.

The problem with using conventional ground control points is that the features are initially selected and stored manually, and periodically manually updated. This operation is time-consuming, expensive, and error prone. In addition, features that are commonly selected are those preferred by the human eye, and not necessarily those that are best for machine registration.

Paper Presented at the NASA Registration and Rectification Workshop, Leesburg, VA., Nov. 17-19, 1981.

Linear array sensors have been proposed to support earth observation applications (Welch, 1971, Thompson, 1979, Tracy and Noll,1979, Wight, 1979, Colovocoresses, 1979). This note dicusses how these sensors can implement a new approach to establishing a world-wide network of ground control called a Ground Control Strip (GCS).

MOTIVATION FOR NEW APPROACH

Motivating factors for a new approach to ground control were identified at the NASA Registeration and Rectification Workshop and are summarized:

Higher Resolution Ground Control Data - Users and analysts have determined that the accuracy of establishing ground control is closely related to the resolution of the source data. Thus it is advantageous to obtain and use higher resolution data for establishing ground control.

Higher Accuracy Source Data - Due to spacecraft structure bending and vibration, even star trackers will not provide sufficiently accurate external orientation data without additional information such as angular displacement sensor data. The use of sensor coupled data has the advantage of direct and close coupling of the data used for image correction with the data to be corrected. There are no static or dynamic errors associated with using coupled image data.

More Ground Control Data - Users have indicated that more ground control data is needed, and should be made available to the user community. This approach directly constructs a large geometry control data base during mission operation.

Compatible Sensor and Ground System - The sensor and the ground system should be designed as an integrated system. With this approach, the sensor system is designed in order to improve ground processing operation efficiency and image accuracy, which may reduce mission system costs.

CONCEPT

This concept deals with the development and use of a continuous strip of ground control used to determine the sensor orientation relative to the earth. Assume a linear array sensor system with differing resolution elements such as that shown in Figure 2. The detector arrays consist of variable size detectors, with higher resolution data in the center of the image swath. While the sensor is on, the detectors "sweeps" the earth in the direction of the satellite track, providing a contiguous strip of higher resolution data (eg., 7.5 m) used for the GCS. The higher resolution data can be combined to provide normal linear array data. Over a period of time, strips of data are acquired that are wrapped around the earth and covers the earth in the vicinity of the subsatellite point. This strip of data, after editing and ground location, can than serve as the geometric reference for subsequent image location, correction, and registration. Clearly, the acquired data must be initially ground located, mosaicked, and edited.

It is apparent that satellite roll and pitch can be accurately determined with the GCS approach. To determine yaw accurately, it may be necessary to use an "out-rigger" network of ground control data. This question will involve a complete error analysis with a particular set of conditions.

SIZE OF DATA BASE

A preliminary analysis of the data base indicates that the ground control strip concept is practical from the point of view of the data storage requirements.

For the Landsat-D satellite mission, the following orbital parameters apply (NASA, 1981):

Repeat Period:	16 days
Orbits/Repeat Period:	233
Trace Spacing:	172 km

The cross-track orbital drift will be approximately 455 m RSS (1-sigma). This corresponds to about 25 Landsat-D pixels drift 90% of the time. If one assumes a ground control region four times wider or a 1820 m wide strip encircling the globe used for ground control, and a 7.5 m resolution ground control data base, and further since the oceans cover about 75% of the earth, than the total ground control strip data base would be:

$$\text{Data Base} = \frac{455\text{x}4 \text{ m} \times 233 \text{ orbits} \times 40\text{x}10^{6} \text{ m/orbit}}{7.5 \text{ m/pixel} \times 7.5 \text{ m/pixel}} \times 0.25$$

$$= 7.54 \times 10^{10} \text{ pixels}$$

Thus, the Ground Control Strip data base requirement is within the capacity of current mass memory systems, and a full earth data base could easily fit within ten high density tapes.

TIME TO ACCUMULATE DATA BASE

The orbit repeat period for the Landsat-D mission is 16 days. Due to cloud cover, and the possible need for data over differing seasons, the time to accumulate the GCS data base would become larger. Assuming that 50% of the time cloud cover can exist in a particular area, there would statistically be a minimum time of seven 16-day periods or 112 days in order to have 99% of the area covered. There are certain areas over the earth where the persistence of cloud cover may require up to several years prior to cloud free acquisition.

ADVANTAGES OF APPROACH

There are a number of advantages of this approach:

Automatic Collection of Reference Data - The strip of ground control is automatically collected and stored. This minimizes the need for manual ground control selection.

High Resolution Control Data - The use of high resolution data in the region of ground control provides the needed resolution to support precise external geometry determination and image correction.

High Density Ground Control - The contiguous data provides a dense data set for image location, correction, and registration. This dense network is an improvement over the relatively sparse network of ground control currently in existence and allows for automated alternative area selection.

Decreased Sensitivity to Cloud Cover - The continuous and extended data set available with this approach should result in a lower sensitivity to cloud cover. When cloud cover occurs and is detected, alternate nearby cloud-free ground control data can be selected and used to establish the geometic parameters. In fact, the continuous nature of the data coupled with the stability of new satellite, such as the Landsat-D (0.01 degrees and 10^{-6} degrees/sec) should allow for long segment and perhaps orbital geometric models and correction parameters to be determined.

Multi-Mission Capability - The Ground Control Strip, having high resolution characteristics, should be useable for other missions with sensors of similar spectral characteristics.

FUTURE WORK

The following needs to be done to adequately assess the value of this approach:

Error Analysis - An error analyis of the approach needs to be performed, assuming a set of satellite attitude and orbit characteritics and sensor parameters. The Landsat-D attitude control system characteristics, and a variable set of sensor resolution parameters should be used to predict the resultant image geometric characteristics. A statistical analysis of cloud cover would be necessary in order to determine the available amount of ground control.

Data Management Analysis - A detailed analysis of the data acquisition, selection, editing, storage, and retrieval of the data needs to be considered. Since this concept involves the use of a larger data set than previously considered, this analysis is particularly important.

Cost Analysis - A study to assess the cost of this approach needs to be considered. The cost savings resulting from the automation of the compilation of ground reference data may be partially offset by the increased cost associated with data storage, processsing and management.

CONCLUSIONS

A concept has been proposed that may improve the correction of remotely sensed image data from satellites. This approach may reduce the time and costs associated with building a ground control point library system, and would result in a larger and higher resolution data base to support image preprocessing. The new data, called a ground control strip is practical with todays storage and processing technologies, and could be developed for the next generation earth observation satellites. The design of the sensor system should be done in conjunction with the ground system, as the parameters are inter-related. Study efforts are necessary in order to adequately assess and evaluate this concept.

REFERENCES

Bernstein, R., "All-Digital Precision Processing of Landsat (ERTS) Images", Ralph Bernstein, NASA Contract NAS5-21716 Final Report, April 1975.

Bernstein, R., "Digital Image Processing of Earth Observation Sensor Data", IBM Journal of Research and Development, Vol. 20, No. 1, January 1976

Welch, R., "Acquisition of Remote Sensor Data with Linear Arrays", Photogrammetric Engineering and Remote Sensing, Vol. XLV, No. 1, Jan 1979.

Thompson, L.I., "Remote Sensing Using Solid-State Array Technology", Photogrammetric Engineering and Remote Sensing, Vol. XLV, No. 1, Jan 1979.

Tracy, R.A., and Noll, R.E., "User Oriented Data Processing Considerations in Linear-Array Applications", Photogrammetric Engineering and Remote Sensing, Vol. XLV, No. 1, Jan 1979.

Wight, R., "Sensor Implications of High Altitude Low Contrast Imaging", Photogrammetric Engineering and Remote Sensing, Vol. XLV, No. 1, Jan 1979.

Colvocoresses, A.P., Multispectral Linear Arrays as an Alternative to Landsat-D", Photogrammetric Engineering and Remote Sensing, Vol. XLV, No. 1, Jan 1979.

NASA, "Landsat-D Applications Notice, Landsat-D, Oct. 1981.

Niblack, W., "The Control Point Library Building System", Photogrammetric Engineering and Remote Sensing, Vol. XLVII, Dec. 1981.

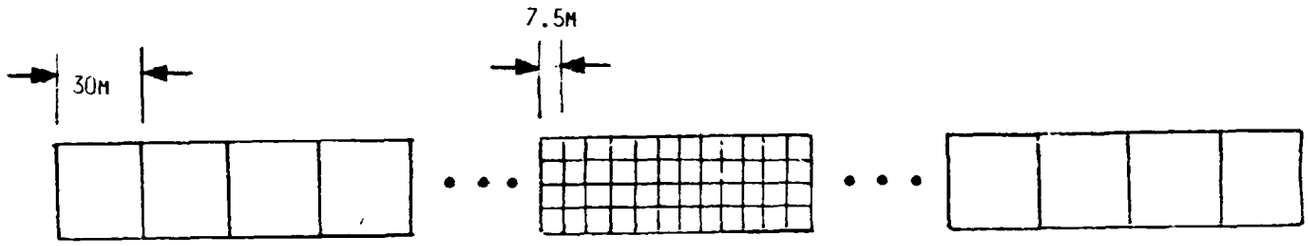

Figure 1. Imbedded Ground Control Strip Footprint

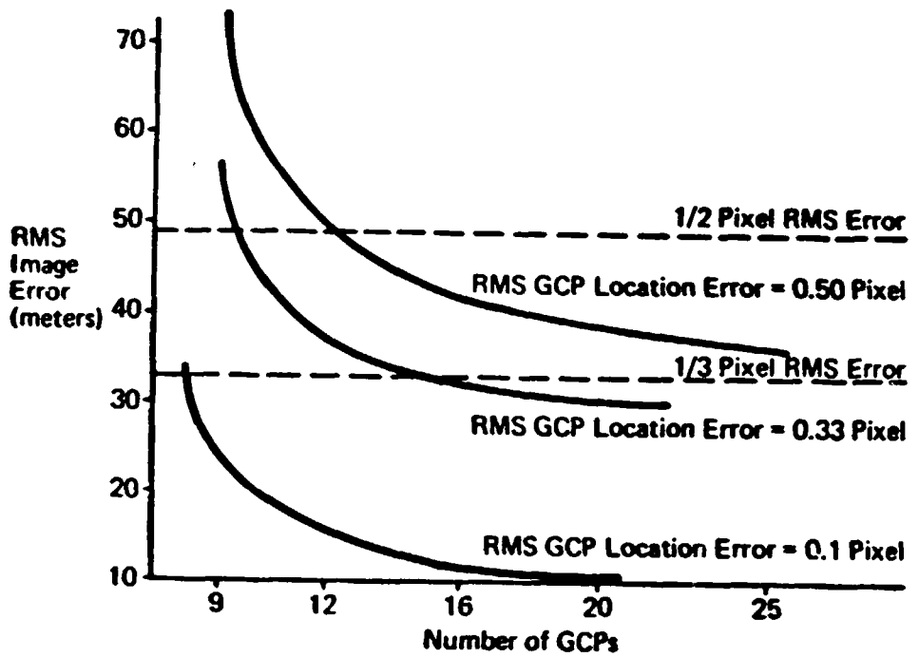

Figure 2. MSS Image Absolute Error As A Function Of The Number Of Ground Control Points

8.10 CURRENT STATUS OF METRIC REDUCTION OF (PASSIVE) SCANNER DATA*

E.M. Mikhail and J.C. McGlone, Purdue University
SCH. OF CIV. ENG.

Invited Paper, Commission III (WGIII-1)
14th Congress of the International Society for Photogrammetry
July 13-25, 1980, Hamburg, FDR

ABSTRACT:

General discussion of extraction of metric information from scanner (particularly multispectral) data is presented. Consideration is given to: data from both aircraft and spacecraft; singly scanned areas and areas with multiple coverage; various mathematical models used up to the present time; and published numerical results. Future trends are also discussed.

1. INTRODUCTION:

The emphasis in this paper is on the results from passive sensor (particularly multispectral scanner) data, because another invited paper is given in this Congress on active sensor data. It follows the excellent account by Konecny (12) on the geometric restitution of remote sensing data where mathematical models, procedures, and numerical results obtained by 1976 were given. For ease in presentation, one section briefly describes all models used. Then, a separate section is devoted to the applications with satellite and aircraft data. Another section discusses multiseries data.

2. BASIC MATHEMATICAL MODELS

In the metric reduction of digital image scanner data, a mathematical model is used to represent the platform/sensor imaging characteristics. All the published models can be classified into essentially two groups. In the first group, a parametric model based on the well known collinearity condition is used. On the other hand, the second group includes all models which are interpolative in nature. Each of these groups, with its individual modeling process, is discussed in separate section.

2.1 Parametric Models

The basis for these models is the collinearity condition that the center point of an image element or pixel, the point representing the instantaneous projection center, and the center point of the corresponding terrain resolution element, all lie on a straight line. In addition to the pixel locations (corresponding to image coordinates) and the object point coordinates, the collinearity equations usually contain six elements of exterior orientation. Theoretically, because the platform is continuously moving, there are six elements for each pixel (assuming a scanner). However, because of the relatively short time period of scanning one line of imagery, it is common to consider only one set of six elements for each line (which makes it equivalent to linear array scans). And even with this assumption, it is easily seen that there would be

---

* Basic reference paper reprinted for Workshop.

an excessive number of exterior orientation elements for any significant number of image lines. Since these elements are almost always unknown a more practical approach is used.

For each element, some function is used to mathematically model its behavior trend. Thus, for one element, the function selected represents its variation with time, or equivalently with the "line" number in the digital image. (The line number is used in a manner similar to the use of x image coordinate in a frame photograph.)

The six elements of exterior orientation are X_c, Y_c, Z_c, which are positional, and ω,ϕ,κ which are rotational. While these elements are stochastically uncorrelated in the frame photography case, there are very high correlations in scanner imagery between the ω and Y_c parameters and ϕ and Y_c parameters. In order to deal with the correlation between ω and Y_c, most scanners are roll stabilized, thus constraining ω to zero. Another possible solution for aircraft scanner imagery is the use of sidelapping data sets, in order to make ω recoverable. The ability to recover both ϕ and X_c is directly dependent on the terrain relief relative to the height of the scanner above the terrain. The greater the relief differences, the lower the correlation. Another possibility is to record the values of ω,ϕ, X_c, or Y_c in flight, then apply these values during the geometric processing. However, the most common procedure is to constrain both ω and ϕ to zero during the adjustment and make no attempt to recover their values.

2.1.1 Orbit Modeling for Images From Spacecraft

Perhaps the most direct method for functionally expressing the exterior orientation elements for spacecraft images is to model the vehicle motion by ideal orbit parameters. Bahr (1,2) recommended the use of the six parameters of the orbit: semimajor axis, a; eccentricity, e; inclination of orbital plane, i; right ascension of ascending node Ω; mean anomaly, M_T; and the argument of perigee ω_T. If these parameters are known, then the satellite position ϕ,λ, r as well as nominal heading βn can be calculated as functions of time. Ground points are then related to the image points using the collinearity equations. In these, while the rotational elements (ω,ϕ,κ) of exterior orientation appear, the positional elements are now replaced by functions of the orbital parameters. Small angle approximations are used for ω,ϕ,κ thus avoiding their trigonometric functions.

A further improvement over the orbital modeling is effected by Rifman et. al. (5,22), where a linear sequential estimator, or a Kalman filter, is developed. It is used to estimate a 13-component state vector from ground control points. Twelve of these components are the coefficients of cubic polynomials in time for the sensor attitude, and one component is for attitude bias. This sequential estimation scheme offers several advantages: (a) fewer numbers of ground control points are required to achieve a given performance level; (b) search areas for ground control points become smaller in size with each state vector update, permitting more rapid location of each successive point; (c) sequential editing of control points is possible without having to process all control points first, thus control points can be redefined or deleted as part of the editing process.

2.1.2 Vehicle/Sensor Modeling by Polynomials

Each of the six exterior orientation elements can be represented by a polynomial of a suitable order (3,9). The selected polynomial would apply to a segment of imagery with the corresponding set of coefficients. Another set of coefficients would be calculated for the second image segment, and so on. The degree of the polynomial depends, among other things, upon the length of the segments. One possibility is to take long segments with higher order polynomials; another is shorter segments with linear polynomials. The latter case seems to work better, at least for aircraft MSS data (9).

The best application of the polynomial modeling is to replace the highly nonlinear collinearity equations by their differential, and thus linear, form. Then the change in each element carried, (e.g., dY_c, $d\phi$, etc.) is written as a polynomial in the image x-coordinate (which is essentially equivalent to time). After substitution of these polynomials into the pair of differential formulas and reduction to equations are obtained, one for X and the other for Y coordinates of the object point. When several image sections are used at the same time, constraint equations are written at the section joints to guarantee uniqueness of the object coordinates.

2.1.3 Sensor Modeling Using Harmonics

An alternative to using polynomials is to use Fourier series expansion for each of the exterior orientation elements. The sine and cosine functions are usually in terms of ratios of the image coordinates and an equivalent of a constant time interval which is appropriately chosen for the frequency of the given data. The linearization of the harmonic equations requires a somewhat different procedure than that use for the case of polynomials (12).

2.1.4 Autoregressive Model For Sensor

All the models discussed so far make use of a deterministic model by writing specific functions to represent the behavior of the exterior orientation elements. Another alternative is to regard such behavior as stochastic rather than deterministic and employ an autoregressive model for the purpose. Of the many possible autoregressive processes, the Gauss-Markov, both first and second order, have been suggested (7) and applied to aircraft MSS data (8,9,10, 11,14,15).

A Gauss-Markov process is based on the Markovian assumption that the value of the process at any time depends only on the previous one or two values, depending on whether a first- or second-order process is assumed. Equations relating the the orientation parameters of each line to those of the one or two preceeding lines are used to model the sensor behavior. Control point information is included by the use of the differential collinearity equations.

2.2 Interpolative Models

In the procedures employing these models no attempt is made to model the sensor/platform behavior, as in the case of using the collinearity conditions in the parametric approach. Instead, some function or relationship is selected between the X,Y coordinates in the object space and x,y (or row, column) in the image space, and assumed to represent the mapping from one space to the

other. There are two groups of methods: one in which a general transformation is used for the entire image record (or segment thereof), and the other in which a different function is used for each point to be interpolated. Each of these will be discussed separately.

2.2.1 Interpolation Methods Using General Transformation:

The group of procedures here employ a pair of functions (one for X, and one for Y) which holds for all points in the image. This means that the numerical values of the coefficients in the equations are the same for each of the points of interest in the image. By image we mean one segment or record. Thus, if we are working with only one image segment, there will be only one set of transformation coefficients. However, if there are more image segments (in other words, if the image record is segmented into several sections), each section will have a set of coefficients with different numerical values. It is usually advisable to enforce constraints at the borders between successive segments.

The transformations used include the following: (1) Four-parameter transformation which is also called two-dimensional linear conformal, Helmert, or similarity transformation; it represents a uniform scale change, a rotation between Xy and xy axes, and two shifts. (2) Six-parameter or affine transformation, which includes two scale changes, one rotation, skewness or nonperpendicularity of the axes, and two shifts. (3) Eight-parameter projective transformation, which represents a rotation and two shifts in each of the two planes (XY and xy), and a tilt between the planes which is combined with scale to produce a continuously changing scale along lines of maximum tilt. (4) General polynomials of varying degrees; these are usually of higher than the first order (which would be the four- or six-parameter transformation.) the choice of degree depends on the length of the image segment.

2.2.2.1 Weighted Mean

For this technique, a weight function is selected which is inversely proportional to a function of the distance between the point to be interpolated and other reference points. Thus, the closer is a reference point the more is its contribution to the interpolated value, and vice versa. At any point of interest, the required vector (usually calculated in two components) is obtained as the weighted mean of all vectors at reference points surrounding the point. The choice of the weight effectively determines the limit of the region within which reference points are used to estimate at the central point of the region.

2.2.2.2 Moving Averages

This is a generalization of the weighted mean procedure which allows greater flexibility in point interpolation. The x- and y-components of the interpolated vector at a point are written as functions of the coordinates of reference points surrounding the point. Six-parameter affine equations, or second-order polynomials may be used for the purpose. Usually a sufficient number of reference points is used to yield an over determination, and the coefficients of the functions are estimated by weighted least squares. As before, the weights are evaluated from a function with the distance between the points in question and reference points as the argument. Once these coefficients are

calculated, they are substituted back into the function to compute the desired value. It is important to note that a new set of coefficients must be calculated for each point to be interpolated. This usually makes the procedure computationally time consuming. Finally, it can be seen than when the selected functions are truncated down to only the zero order terms the procedure reduces to the weighted mean.

2.2.2.3 Meshwise Linear

In this method, the reference points are connected into adjacent or contiguous meshes such as triangles or quadrilaterals. The reference points forming the mesh that includes the point to be interpolated are used for the purpose. Usually a six-parameter affine transformation is used. The method is computationally efficient within each mesh, but the formation of the meshes may be time consuming. Also unless a severe condition is placed on the reference points, the solution for points on the boundary of the image may not be accurate due to extrapolation.

2.2.2.4 Linear Least Squares Prediction

This method treats the vectors at the reference points as a random field. The covariance function associated with this field is either assumed a priori, or its shape is assumed and the numerical parameters calculated from the data (13). As applied, both stationarity and isotropy of the field are assumed. This may be true for some data (e.g., Satellite MSS) but not for other (e.g., aircraft MSS). From the covariance function, the autocovariance matrix for data at the reference points is evaluated. Also the crosscovariance matrix (or vector) between the point to be interpolated and the reference points is also needed. these, and the data vector at the reference points are used to calculate the value at the point of point data directly or filtering the data for known error proportion. The amount of filtering can also be selected.

3. APPLICATIONS TO SPACECRAFT DATA

The most widely used spacecraft data is that obtained from the LANDSAT series of satellites (see Table 1). Because of this, the majority of work on geometric properties of satellite data has been expended on LANDSAT. Interest in the Skylab conical scanner data has declined since the termination of the Skylab project.

Work on LANDSAT imagery has been mostly concerned with single scene processing, with some attempts at strip and block triangulation.

Bahr (1,2) used LANDSAT and NIMBUS imagery to compare accuracies achieved by using a conformal transformation, second-order polynomials, the collinearity condition, and linear least squares prediction.

Borgeson (4) reported on accuracy tests of bulk corrected images from the EROS data center, using 3, 4, 5, and 6 parameter transformations to check residual deformation left after bulk processing of the imagery.

Rifman et. al. (5,22) studies the use of a Kalman-filter-type estimator for registration of images from LANDSAT 1 and 2, as well as for registration of images from the same sensor.

Derouchie (6) used a strip of 11 image segments to study control densities necessary for various accuracy levels. His conclusion was that the optimum spacing of control was every 100 mirror sweeps, or 600 image lines.

Little use has been made of overlapping satellite imagery. Welch and Lo (23) report on the use of a 1-micrometer parallax bar combined with a Bausch and Lomb Zoom 70 Stereoscope to obtain elevation differences. Up to nine control points were read in each model, then a polynomial was used to correct for systematic errors. Due to the small scale and low base/height ratio of the imagery, accuracies of only 200 to 300 meters were obtained.

The Skylab S-192 scanner, with its conical scan pattern, presented special geometric problems. Murphrey, et. al. (18) published a paper explaining the geometry of the scanner and giving a method for geometric correction of the data. The suggestion was to use the orbital parameters of the satellite in collinearity equations to determine a fifth-degree polynomial to transform the image space into object space. This polynomial is used to transform a dense grid of image points, then the remaining points are determined by linear interpolation due to economic considerations. No predictions or checks were made of accuracy achieved.

Malhotra (16,17) conducted accuracy tests on the Skylab scanner imagery. The first phase of his work involved using a parametric model and obtained accuracies of 4 pixels, or about 300 meters. Another phase involved testing the accuracy of generated film images using an affine transformation to test for residual distortions. Accuracies ranged from 105 to 250 meters.

4. APPLICATIONS TO AIRCRAFT DATA

Little work is presently being done on aircraft data, due to the widespread use of LANDSAT imagery (see Table 2).

At Purdue University, the research has followed the early work of Baker and Mikhail (3). Ethridge and Mikhail (9,10,11) investigated the accuracy of various single-strip rectification methods, including the collinearity, piecewise polynomials, weighted mean, moving average, meshwise linear interpolation, and Gauss-Markov. After testing all methods on four data sets, Analysis of Variance (Anova) and Neuman-Keuls statistical testing procedures were used to conclude that there was no statistically significant difference between the results of the best five methods, with only the meshwise linear interpolation being significantly worse. When the methods were ranked in terms of their restitution results, the Gauss-Markov was best, collinearity and piecewise polynomial were second, the weighted mean was fourth, and moving averages fifth. Division of the strips into sections when using the parametric methods was shown to have a significant effect. Consideration of other factors involved, such as computational economy and control requirements, led to the conclusion that the piecewise polynomial was the optimum method.

Ethridge also investigated the use of sidelapping flight lines in a block adjustment procedure. Since no real data was available, randomly perturbed and unperturbed simulated data was used. Two algorithms were used in the tests, one a rigorous simultaneous solution while the other involved using the control points to solve for the orientation parameters, then obtaining pass point

coordinates by intersections. The resection-intersection method gave results nearly equivalent to those of the rigorous simultanous method.

McGlone, Mikhail, and Baker (14,15) reported on further tests with single-strip methods, comparing the piecewise polynomial, weighted mean, and Gauss-Markov methods. The piecewise polynomial method using multiple sections and second-order polynomials was shown to be the optimum method. Further comparison tests run on the first- and second-order Gauss-Markov methods showed in general no significant difference between the two, but the second-order tended to be slightly worse.

Ebner and Hossler (8) studies the use of second-order Gauss-Markov processes, using simulated data. It was concluded that redundant control within an image line did not improve rectification accuracy, that the control within an image line did not improve rectification accuracy, and that the control distribution could be random as long as the bridging distances were not too great. It was also concluded that the correlation time parameter of the modeling process could be chosen as infinity with no effect on the results.

5. ADJUSTMENT OF MULTISERIES DATA

Nasu and Anderson (20,21) reported on the development of a multiseries adjustment procedure. This involved the adjustment of photography of various scales along with aircraft and spacecraft scanner data in sequential and simultaneous procedures, using tie points selected on images. Digital tie point selection between the various data sets is also possible. Tests with simulated data showed a 16- to 20-percent improvement over the direct adjustment of each image separately. Tests with real data were less conclusive but did show some improvement.

Tests were also conducted on the block adjustment of sidelapping data. It was shown that planimeteric accuracy is increased by having multiple ray intersection and that elevations can be obtained, although not of sufficient accuracy in this case to use for pixel elevation assignment for geometric processing. For three strips, divided into three sections each, the RMSE in x was 15.4 meters (2.0 pixels), in Y 13.3 meters (1.74 pixels), and in Z 34.0 meters (4.46 pixels). Division of the strips into sections again increased the accuracy. Calculation of covariance information for the parameters allowed the assessment of correlations between the orientation parameters. The ω orientation angle was recoverable using multiple strips, while the ϕ was not recoverable, due to lack of relief of the terrain. The inclusion of ω increased the accuracy of the adjustment.

Nasu (19,20) studied the positioning of thermal IR scanner data using a parametric orientation model. He reported residual errors at the ground control points of 3 to 4 pixels in a test on a volcanic area with large relief differences.

Table 1

Restitution Results from Spacecraft Data

Investigator	Data	Method	Number of Control pts.	RMSE,Y Pixels	RMSE,Y Pixels
Bahr	LANDSAT	4-par	234	2.71	4.52
1976	bulk image	2 order poly	7	1.15	1.11
			9	0.68	1.15
			13	0.60	1.02
			40	0.61	0.89
			234	0.54	0.83
		L.S. filtering after 4-par.	40	0.56	0.87
		L.S. filtering after poly.	40	0.53	0.78
	NIMBUS-3	col.	67	0.68	0.80
		approx.method	67	0.89	0.73
		col.	84	0.83	0.83
		approx.method	84	0.92	0.97
		col.	81	0.79	0.86
		approx.method	81	0.74	0.87
	NIMBUS-4	col.	40	0.81	0.89
		approx.method	40	1.08	1.25
Malhotra,	Skylab	col.	—	4.0	4.3
1976		col.	—	4.0	3.7
		col.	—	3.7	3.8
				RMSE, XY Meters	
Borgeson	LANDSAT	3 par	151	159	
	System	4 par	151	130	
1979	Corrected	5 par	151	82	
		6 par	151	51	
	LANDSAT	3 par	53	165	
	Image	4 par	53	143	
		5 par	53	84	
		6 par	53	49	

Table 2
Restitution Results for Single Coverage Aircraft Data

Investigator	Data Description	Method	RMSE X pixels	RMSE Y pixels	RMSE XY pixels
Ethridge, 1977	H=1500m IFOV=.006 rad 1550 lines	col. 1 sec.	1.57	2.03	1.80
		" 2 sec.	1.51	1.68	1.59
		" 3 sec.	1.42	1.36	1.39
		p.poly 1 sec.	1.58	2.01	1.79
		2 sec.	1.51	1.69	1.60
		3 sec.	1.42	1.37	1.40
		w. mean	1.56	1.23	1.41
		m. avg.	1.32	2.04	1.72
		mesh. linear	1.35	2.26	1.86
		G. Markov, 1st	1.18	1.44	1.32
	H=1500m IFOV=.006 rad 1400 lines	Col. 1 sec.	2.70	2.19	2.45
		2 "	2.57	1.82	2.19
		3 "	2.70	1.37	2.04
		p.poly 1 sec.	2.68	2.38	2.53
		2 "	2.57	2.18	2.37
		3 "	2.71	1.36	2.03
		w.mean	3.2	1.52	2.55
		M. avg.	2.7	1.95	2.38
		mesh. linear	2.50	2.42	2.46
		G. Markow, 1st	2.05	2.33	2.20
	H=900m IFOV=.006 rad 1970 lines	Col 1 sec.	7.33	9.66	8.58
		2 "	3.69	5.17	4.49
		3 "	2.89	3.08	2.99
		p.poly 1 sec.	7.33	8.71	8.05
		2 "	3.66	4.74	4.24
		3 "	2.89	3.15	3.02
		w.mean	3.05	4.44	3.81
		m.avg.	2.62	3.91	3.33
		mesh. linear	4.35	4.82	4.59
		G. Markov, 1st	2.43	2.80	2.62
	H=900m IFOV=.006 rad 2700 lines	Col. 1 sec.	4.10	4.24	3.90
		2 "	4.23	3.76	3.34
		3 "	4.16	4.01	3.63
		p.poly 1 sec.	4.09	4.32	4.21
		2 "	4.18	3.16	3.71
		3 "	3.83	3.10	3.49
		w.mean	3.75	2.91	3.36
		m.avg.	5.33	3.58	4.54
		mesh. linear	4.23	7.65	6.18
		G. Markov 1st	3.66	3.77	3.72
Meglone, Mikhail, Baker 1980	H=3050m IFOV=0025 rad 1450 lines	p.poly 1 sec 1 order	2.76	4.76	4.14
		1 " 2 "	2.72	1.91	2.35
		2 " 1 "	2.82	2.49	2.66
		2 " 2 "	2.23	1.74	2.00
		3 " 1 "	2.22	1.98	2.10
		3 " 2 "	2.06	1.89	1.98

Table 2 (Continued)

Investigator	Data Description	Method	RMSE X pixels	RMSE Y pixels	RMSE XY pixels
		w.mean	3.34	1.90	2.72
		G. Markov 1 order	1.75	5.47	4.06
		2 "	3.80	11.20	8.36
	H=3050m	p.poly 1 sec 1 order	2.14	3.85	3.11
	IFOV=.0025 rad	1 " 2 "	2.14	3.79	3.08
	1450 lines	2 " 1 "	2.11	3.78	3.06
		2 " 2 "	1.57	3.39	2.64
		3 " 1 "	1.86	3.63	2.88
		3 " 2 "	1.69	3.50	2.75
		w. mean	3.28	3.85	3.58
		G.Markov 1 order	1.13	6.63	4.75
		2 "	1.18	7.13	5.11
	H=3050m	p.poly 1 sec 1 order	2.12	5.33	4.05
	IFOV=.0025 rad	1 " 2 "	1.31	5.38	3.92
	1450 lines	2 " 1 "	1.43	5.41	3.96
		2 " 2 "	1.28	5.26	3.83
		3 " 1 "	1.42	5.21	3.82
		3 " 2 "	1.08	7.43	5.31
		w.mean	2.80	4.17	3.55
		G.Markov 1 order	1.03	10.48	7.45
		2 "	1.67	10.11	7.25
	H=1500m	G.Markov 1 order	1.27	1.32	1.30
	IFOV=.006 rad	2 "	1.33	1.49	1.42
	H=1500m	G.Markov 1 order	3.26	2.34	2.83
	IFOV=.006 rad	2 "	3.86	2.53	3.26
	H=900m	G.Markov 1 order	0.90	2.10	1.62
	IFOV=.006 rad	2 "	1.64	2.72	2.25
	H=900m	G.Markov 1 order	1.99	1.80	1.90
	IFOV=.006 rad	2 "	2.15	5.95	4.47
	H=900m	G.Markov 1 order	3.16	2.26	2.75
	IFOV=.066 rad	2 "	3.30	2.28	2.84
	H=900m	G.Markov 1 order	6.64	3.77	5.40
	IFOV=.006 rad	2 "	14.46	4.76	10.76

References and Bibliography

1. Bahr, H.P., Analyse der Geometric auf Photodetektoren abgetasteter Aufnahmen von Erdkundungssatelliten, Hanover, 1976.

2. Bahr, H.P., "Geometrical Analysis and Rectification of LANDSAT MSS Imagery: Comparison of Different Methods", ISP Comm. III, Moscow, 1978.

3. Baker, J.R., and Mikhail, E.M., Geometric Analysis and Restitution of Digital Multispectral Scanner Data Arrays, Laboratory for Applications of Remote Sensing, Purdue University, Lafayette, Indiana. Information Note 052875, 1975.

4. Borgeson, W.T., Accuracy Test of Two 1979 LANDSAT Images made by EDIPS from NASA - System - Corrected Digital Data, GSFC, Greenbelt, MD.

5. Caron, R.H., and Simon, K.W., "Attitude Time Series Estimator for Rectification of Spaceborne Imagery", Journal of Spacecraft, Vol.12, No. 1, Jan. 1975.

6. Derouchie, W.F., "Geometric Errors in an MSS Image Strip," Proceedings of the ASP, Fall Technical Meeting, Seattle, Wash., 1976.

7. Ebner, H., "A Mathematical Model for Digital Rectification of Remote Sensing Data", ISP Comm. III, Helsinki, 1976.

8. Ebner, H., and Hossler, R., "The Use of Gauss Markov Process in Digital Rectification of Remote Sensing Data", ISP Comm. II, Moscow. 1978.

9. Ethridge, M.M., Geometric Analysis of Singly and Multiply Scanned Aircraft Digital Data Arrays, Purdue University, Lafayette, Ind., May 1977.

10. Ethridge, M.M., and Mikhail, E.M., "Geometric Rectification of Single Coverage Aircraft Multispectral Scanner Data", Proceedings of the 2nd Annual William T. Pecora Memorial Symposium, U.S.G.S. Sioux Falls, S. Dak., 1976.

11. Ethridge, M.M., and Mikhail, E.M., "Positional Information from Single and Multiple Coverage Multispectral Scanner Data", Proceedings of the ASP Fall Technical Meeting, Little Rock, Ark., 1977.

12. Kenecny, G., "Mathematical Models and Procedures for the Geometric Restitution of Remote Sensing Imagery", ISP Comm. III. Helsinki, Finland, 1976.

13. Kraus, K., and Mikhail, E.M., "Linear Least-Squares Interpolation", Photogrammetric Engineering, Vol. 38, No. 9, October, 1972.

14. McGlone, J.C., Baker, J.R., and Mikhail, E.M., "Metric Information from Aircraft Multispectral Scanner (MSS) Data", Proceedings of the ASP 45th Annual Meeting, Washington, D.C., 1979.

15. McGlone, J.C., Mikhail, E.M., and Baker, J.R., Analysis of Multispectral Scanner Digital Data for Coastal and Hydrographic Mapping, Final Technical Report, NOAA Grant No. 04-7-158-44128, Purdue University, Lafayette, Indiana, Feb. 1980.

16. Malhotra, R.C., "Geometric Evaluation of Skylab S-192 Conical Scanner Imagery," Proceedings of the ASP Fall Technical Meeting, Seattle, Wash., 1976.

17. Malhotra, R.C., "Geometric Evaluation of Skylab S-192 Conical Scanner Imagery", Photogrammetric Engineering, Vol. 43, No. 2, Feb. 1977.

18. Murphrey, S.W., Depew, R.D., and Bernstein, R., "Digital Processing of Conical Scanner Data", Photogrammetric Engineering, Vol. 43, No. 2, Feb. 1977.

19. Nasu, M., "Analytical Positioning of Thermal IR Imagery for Monitoring Volcanic Activity". Unpublished manuscript, University of California, Berkeley, CA., 1977.

20. Nasu, M., Geometric Processing for Digital Mapping with Multiseries Remote Sensing Data, University of California, Berkeley, 1976.

21. Nasu, M., and Anderson, J., "A Multiseries Digital Mapping System for Positioning MSS and Photographic Remotely Sensed Data", ISP Comm III, Helsinki, 1976.

22. Rifman, s.S., Monuki, A.T., and Shortwell, C.D., "Multisensor Landsat MSS Registration," Thirteenth Annual Symposium on Remote Sensing of Environment, ERIM, Ann Arbor, Michigan, April 1979.

23. Welch, R., and Lo, C.P., "Height Measurements from Satellite", Proceedings of the ASP 42nd Annual Meeting, Washington, D.C., 1976.

9.0 APPENDICES

9.1 ATTENDEES

Mr. William L. Alford
NASA/Goddard Space Flight Center
Code 932
Greenbelt Road
Greenbelt, MD 20771

Mr. Richard Allen
Chief, Remote Sensing Branch
SRS-SRD Room 4832 S
Department of Agriculture
Washington, DC 20250

Dr. Mohan Ananda
Aerospace Corporation
P. O. Box 92957
Los Angeles, CA 90009

Mr. Ken Ando
NASA Headquarters
Code ER
600 Independence Avenue, SW
Washington, DC 20546

Mr. Paul Anuta
LARS
1220 Potter Dr.
Purdue University
West Lafayette, IN 47907

Mr. George Austin
Lockheed
Houston, TX

Mr. G. Robinson Barker, Manager
Forest Resource Information System
St. Regis Paper Co.
Southern Timberlands Division
435 Clark Road, Suite 411
Jacksonville, FL 32218

Dr. John L. Barker
NASA/Goddard Space Flight Center
Code 923
Greenbelt, MD 20771

Dr. Lee Bender
U.S. Geological Survey
Mail Stop 522
National Headquarters
Reston, VA

Mr. Ralph Bernstein
IBM Scientific Center
1530 Page Mill Road
Palo Alto, CA 94304

Mr. Eric Beyer
General Electric Co.
Valley Forge Space Center
P. O. Box 8555
Philadelphia, PA 19101

Mr. Frederic C. Billingsley
MS 198-229
Jet Propulsion Laboratory
4800 Oak Grove Dr.
Pasadena, CA 91103

Dr. Joseph L. Bishop
NASA Headquarters
Code TS
600 Independence Avenue, SW
Washington, DC 20546

Mr. Donald Brandshaft
Santa Barbara Research Center
75 Coromar Drive Mail Stop B-11/79
Goleta, CA 93117

Dr. Nevin Bryant
Jet Propulsion Laboratory
168-514
4800 Oak Grove Drive
Pasadena, CA 91103

Mr. Michael A. Calabrese
Code ERL-2
NASA Headquarters
600 Independence Avenue SW
Washington, DC 20546

Dr. Lloyd M. Candell
Santa Barbara Research Center
75 Coromar Dr.
Bldg. 774 Mail Stop 20
Goleta, CA 93017

Mr. Jerry M. Cantril
Computer Sciences-Technicolor Associates
10210 Greenbelt Road
Suite 930
Seabrook, MD 20801

Mr. Doug Carter
USGS
EROS Office
730 National Center
Reston, VA 22090

Dr. William R. Case
NASA/Goddard Space Flight Center
Mail Code 725
Greenbelt Road
Greenbelt, MD 20771

Mr. Pat Chavez, Jr.
USGS
2255 N. Gemini Drive
Flagstaff, AZ 86001

Mr. Wm. P. Clark
Goddard Space Flight Center
Code 563
Greenbelt, MD 20771

Mr. Bob Coldonado
NASA/Goddard Space Flight Center
Greenbelt, MD 20771

Col. Alden P. Colvocoresses
U.S. Geological Survey
522 National Center
Reston, VA 22092

Mr. Victor Conocchioli
EROS Data Center
Technicolor Graphics Services
Sioux Falls, SD 57198

Mr. Scott Cox
NASA/Goddard Space Flight Center
Code 902.1
Greenbelt, MD 20771

Mr. Philip J. Cressy, Jr.
NASA/Goddard Space Flight Center
Code 902.1
Greenbelt, MD 20771

Mr. J. C. Curlander
Jet Propulsion Laboratory
4800 Oak Grove Drive
Pasadena, CA 91109

Mr. John Dalton
NASA/Goddard Space Flight Center
Code 933
Greenbelt, MD 20771

Dr. Larry Davis
Computer Science Center
University of Maryland
College Park, MD 20742

Dr. David Dow
National Space Technology Laboratories
NASA/Earth Resources Laboratory
Technique Development Group (HA20)
NSTL Station, MS 39529

Dr. Fred Doyle
U.S. Geological Survey
Mail Stop 522
National Headquarters
Reston, VA

Mr. John M. Driver
Jet Propulsion Laboratory
156-204
4800 Oak Grove Drive
Pasadena, CA 91103

Mr. Robert Dye
ERIM
P. O. Box 618
3300 Plymouth Road
Ann Arbor, MI 48107

Mr. Jack L. Engel
Santa Barbara Research Center
75 Coromar Drive Mail Stop B-11/79
Goleta, CA 93117

Mr. R. Bryan Erb
Johnson Space Center
Mail Stop SK
Earth Resources Program Management Offic
Houston, TX 77058

Mrs. Ai Fang
Code ECD-4
600 Independence Ave. SW
Washington, DC 20546

Mr. Charles J. Finley
NASA Headquarters
Code ERG-2
600 Independence Avenue, SW
Washington, DC 20546

Mr. David Fischel
NASA/Goddard Space Flight Center
Code 932
Greenbelt, MD 20771

Mr. Fred Flatow
NASA/Goddard Space Flight Center
Code 460
Greenbelt, MD 20771

Mr. Arthur J. Fuchs
NASA/Goddard Space Flight Center
Greenbelt, MD 20771

Dr. Len Gaydos
USGS National Mapping Division
Ames Research Center, Code SEA
Moffett Field, CA 94035

Dr. John Gergen
Chief, Horizontal Network Division
NOS/NGS Code C-13
Rockville, MD 20852

Mr. Carter M. Glass
Goodyear Aerospace Co.
P. O. Box 85
Litchfield Park, AZ 85340

Mr. Gerald J. Grebowsky
NASA/Goddard Space Flight Center
Code 563.2
Greenbelt, MD 20771

Mr. R. Grubic
Ground Systems Engineering
General Electric, Co.
Landsat-D Program Code 435.9
NASA/Goddard Space Flight Center
Greenbelt, MD 20771

Dr. Bert Guindon
2464 Scheffield Rd.
Ottawa, Ontario
Canada K1A OX7

Mr. Jerry Hahn
NASA/Goddard Space Flight Center
Code 435
Greenbelt, MD 20771

Dr. Robert Haralick
Department of Electrical Engineering
Virginia Polytechnic Institute
Blacksburg, VA 24060

Mr. Paul Heffner
Goddard Space Flight Center
Code 563
Greenbelt, MD 20771

Howard S. Heuberger
Goddard Space Flight Center
Code 582
Greenbelt, MD 20771

Ms. Christine A. Hlavka
NASA/Ames Research Center
Mail Stop 242-4
Moffett Field, CA 94035

Dr. Howard C. Hogg
NASA Headquarters
Code ERL-2
600 Independence Avenue, SW
Washington, DC 20546

Dr. Roger A. Holmes
Dean of Academic Affairs
General Motors Institute
Flint, MI 48502

Mr. Peter S. P. Hui
Code 725
Goddard Space Flight Center
Greenbelt, MD 20771

Mr. Peter Hyde
Computer Science Center
University of Maryland
College Park, MD 20742

Mr. Richard Juday
NASA/Johnson Space Center
Mail Code SF3
Houston, TX 77058

Ms. Maria T. Kalcic
National Space Technology Laboratories
NASA/Earth Resources Laboratory
Technique Development Group (HA20)
NSTL Station, MS 39529

Professor Laveen Kanal
Department of Computer Science
University of Maryland
College Park, MD 20742

Mr. R. Kent Lennington
Lockheed Engineering and
Management Services Company, Inc.
1830 NASA Rd. 1
Houston, TX 77058

Dr. Joseph G. Lundholm
NASA/Goddard Space Flight Center
Code 460
Greenbelt, MD 20771

Dr. Thomas Lynch
NASA/Goddard Space Flight Center
Code 930
Greenbelt, MD 20771

Mr. John Lyon
Goddard Space Flight Center
Code 932
Greenbelt, MD 20771

Dr. Robert B. MacDonald
Johnson Space Flight Center/SG
Houston, TX 77058

Mr. Harry Mannheimer
NASA Headquarters
Code ER
600 Independence Avenue, SW
Washington, DC 20546

Dr. Duane F. Marble
Geographic Information System Laboratory
SUNY Buffalo
Amherst, NY 14260

Mr. Marvin S. Maxwell
NASA/Goddard Space Flight Center
Code 940
Greenbelt, MD 20771

Mr. Paul F. Maynard
Earth Satellite Corporation
7222 47th St. (Chevy Chase)
Washington, DC 20815

Mr. Frederick W. McCaleb
NASA, Goddard Space Flight Center
Code 563
Greenbelt, MD 20771

Dr. Robert McEwen
Team Leader, DAT
519 National Center
U.S. Geological Survey
Reston, VA 22092

Dr. Edward M. Mikhail
Professor
School of Civil Engineering
Purdue University
West Lafayette, IN 47907

Dr. Allan J. Mord
Ball Aerospace System Division
P.O. Box 1062
Boulder, CO 80306

Mr. Archie H. Muse
E Systems Inc., Garland Division
1200 Jupiter Road
Garland, TX 75042

Mr. M. Naraghi
Jet Propulsion Laboratory
Pasadena, CA 91109

Mr. Dave Nichols
Jet Propulsion Laboratory
Code 168-514
4800 Oak Grove Drive
Pasadena, CA 91103

Mr. R. O'Connell
Ground Systems Engineering
General Electric, Co.
Landsat-D Program Code 435.9
NASA/Goddard Space Flight Center
Greenbelt, MD 20771

Mr. Zvi Orbach
Honeywell
Lexington, MA

Dr. Arch Park
General Electric Co.
5030 Herzel Place
Beltsville, MD 20706

Dr. Robert Pelzmann
Lockheed Missiles & Space Company, Inc.
Palo Alto Research Laboratory
3251 Hanover Street
Palo Alto, CA 94304

Mr. William L. Piotrowski
Code ER-2
NASA Headquarters
600 Independence Ave., S.W.
Washington, DC 20546

Demetrios Poros
Ground Systems Engineering
General Electric, Co.
Landsat-D Program Code 435.9
NASA/Goddard Space Flight Center
Greenbelt, MD 20771

Mr. A. Prakash
General Electric Co.
Valley Forge Space Center
P. O. Box 8555
Philadelphia, PA 19101

Ms. Donna Puequet
U.S. Geological Survey
National Headquarters
Reston, VA 22090

Mr. H. K. Ramapriyan
NASA/Goddard Space Flight Center
Code 932
Greenbelt, MD 20771

Mr. Mike Rassbach
Elogic, Inc.
4242 S.W. Freeway, Suite 304
Houston, TX 77027

Mr. Wayne Rohde
USGS
EROS Office
730 National Center
Reston, VA 22090

Mr. Marc J. Selig
Goddard Space Flight Center
Code 563
Greenbelt, MD 20771

Mr. Mark Settle
NASA Headquarters
Code ERS-2
600 Independence Avenue, SW
Washington, DC 20546

Mr. B. R. Seyfarth
National Space Technology Laboratories
NASA/Earth Resources Laboratory
Technique Development Group (HA20)
NSTL Station, MS 39529

Mr. Bill Shaffer
NASA Headquarters
Code EC-4
600 Independence Ave. SW
Washington, DC 20546

Mr. Bill M. Shelley
St. Regis Paper Company
435 Clark Road, Suite 411
Jacksonville, FL 32218

Mr. Richard Sigman
Department of Agriculture
Mathematical Statistician
SRS Room 4832 South Bldg.
14th and Independence Avenues
Washington, DC 20250

Mr. Terry Silverberg
Computer Science Center
University of Maryland
College Park, MD 20742

Dr. A. Singh
Ground Systems Engineering
General Electric, Co.
Landsat-D Program Code 435.9
NASA/Goddard Space Flight Center
Greenbelt, MD 20771

Mr. John Snyder
U.S. Geological Survey
Mail Stop 522
National Headquarters
Reston, VA

Mr. John Y. Sos
NASA/Goddard Space Flight Center
Code 560
Greenbelt, MD 20771

Mr. Bill Stevenson
Johnson Space Center
Mail Stop SK
Earth Resources Program Management Office
Houston, TX 77058

Dr. Andrew Tescher
Aerospace Corporation
P. O. Box 92957
Los Angeles, CA 90009

Mr. Pitt G. Thome
NASA Headquarters
Code ER-2
Washington, DC 20546

Ms. June Thormodsgard
EROS Data Center
Mundt Federal Building
Sioux Falls, SD 57198
Attn: Computer Services Branch

Mr. A. Tuyahov
NASA Headquarters
Code ETS-6
Washington, DC 20542

Dr. Steve Ungar
Goddard Institute for Space Studies
2880 Broadway
New York, NY 10025

Mr. Anthony Villasenor
Code ECD-4
600 Independence Ave. SW
Washington, DC 20546

Dr. Ray J. Wall
Jet Propulsion Laboratory
4800 Oak Grove Drive
Mail Stop 168-527
Pasadena, CA 91109

Mr. R. Weinstein
NASA Headquarters
Code ETS-6
Washington, DC 20542

Dr. Roy Welch
University of Georgia
Athens, GA 30602

Ms. Ruth Whitman
ORI
Space Engineering Division
Silver Spring, MD 20910

Mr. Robert Wolfe
Johnson Space Flight Center
Houston, TX 77058

Mr. Frank Wong
MacDonald Dettwiler & Associates
3751 Shell Road
Richmond, B.C.
Canada

Dr. Al Zobrist
Jet Propulsion Laboratory
Mail Stop 168-514
Pasedena, CA 91103

9.2 NAMES AND ADDRESSES OF WORKSHOP PRESENTORS AND PANEL COORDINATORS

Mr. Richard Allen — Agriculture Needs
Chief, Remote Sensing Branch
SRS-SRD Room 4832 S
Department of Agriculture
Washington, DC 20250
202-447-4896 FTS 447-4896

Dr. Mohan Ananda — NAVSTAR/GPS
Aerospace Corporation
P. O. Box 92957
Los Angeles, CA 90009
(213)647-1649

Mr. Ken Ando ER-2 — MLA Imaging Systems
NASA Headquarters
Code ER
600 Independence Avenue, SW
Washington, DC 20546
(202)755-1201 FTS 755-1201

Mr. Paul Anuta — Image Sharpness
Lab for Applications of Remote Sensing
1220 Potter Dr.
Purdue University
West Lafayette, IN 47907
(317)494-6305

Dr. John L. Barker — Error Budget Panel
NASA/Goddard Space Flight Center
Code 923
Greenbelt, MD 20771
(301)344-8978 FTS 344-8978

Dr. Ralph Bernstein — Registration Panel
IBM Scientific Center
1530 Page Mill Rd.
Palo Alto, CA 94304
(413)855-3126

Mr. Eric Beyer — Spaceborne Scanner Systems
General Electric Co.
Valley Forge Space Center
P. O. Box 8555
Philadelphia, PA 19101
(215)962-3572

Mr. Frederic C. Billingsley 198-231 Jet Propulsion Laboratory 4800 Oak Grove Dr. Pasadena, CA 91103 (213)354-2325 FTS 682-2325	Executive Committee Chairman
Dr. Nevin Bryant 168-514 Jet Propulsion Laboratory 4800 Oak Grove Drive Pasadena, CA 91103 8-792-7236 FTS 792-7236	Workshop Chairman
Mr. Pat Chavez, Jr. USGS 2255 N. Gemini Drive Flagstaff, AZ 86001 (602) 261-1558 FTS 261-1558	Geology Needs
Mr. J. C. Curlander 156-119 Jet Propulsion Laboratory 4800 Oak Grove Drive Pasadena, CA 91109 (213)354-6116 FTS 792-6116	SAR Imaging Systems
Mr. John Dalton 933 NASA/Goddard Space Flight Center Greenbelt, MD 20771 (301)344-6276 FTS 344-6276	Weather Needs
Dr. Larry Davis Computer Science Center University of Maryland College Park, MD 20742 (301)454-4526	Feature Extraction Panel
Mr. Robert Dye Environ. Res. Inst. of MI P. O. Box 618 3300 Plymouth Road Ann Arbor, MI 48107 (313)994-1200 x-277	Resampling Functions
Mr. Arthur Fuschs Goddard Space Flight Center Greenbelt, MD 20771 (301)344-6846 FTS 344-6846	Multi-Mission Spacecraft
Dr. Len Gaydos 240-8 USGS National Mapping Division Ames Research Center, Code SEA Moffett Field, CA 94035 (408)95-6368 FTS 448-6368	Land Use Needs

Dr. John Gergen Chief, Horizontal Network Division NOS/NGS Code C-13 Rockville, MD 20852 (301)443-8168 FTS 443-8168	Geodetic Control
Mr. Gerald Grebowski Code 563 Goddard Space Flight Center Greenbelt, MD 20771 (301)344-7819 FTS 344-7819	Verification Methods
Dr. Forrest Hall SF3 Earth Observations Division NASA/Johnson Space Center Houston, TX 77058 (713)483-4776 FTS 525-4505	Misregistration
Dr. Robert Haralick Department of Electrical Engineering Virginia Polytechnic Institute Blacksburg, VA 24060 (703)961-5961	Feature Extraction
Mr. Richard Juday NASA/Johnson Space Center Mail Code SF3 Houston, TX 77058 (713)483-3611 FTS 525-3611	Resampling Function Panel
Dr. Edward M. Mikhail Professor School of Civil Engineering Purdue University West Lafayette, IN 47907 (317)494-2167	Remapping Procedures
Mr. Dave Nichols Jet Propulsion Laboratory Code 168-514 4800 Oak Grove Drive Pasadena, CA 91103 (213)354-7081 FTS 354-7081	Oceanic Needs
Dr. Robert Pelzman Lockheed Missiles & Space Co. Bldg. 202 Palo Alto, CA 94304 (415)493-04411	Error Analysis Panel

Mr. A. Prakash General Electric Co. Valley Forge Space Center P. O. Box 8555 Philadelphia, PA 19101 215-962-2530	Error Budgets
Mr. H. K. Ramapriyan NASA/Goddard Space Flight Center Code 932 Greenbelt, MD 20771 (301)344-8997 FTS 344-8997	Inter-Image Matching
Mr. John Snyder U.S. Geological Survey Mail Stop 522 National Headquarters Reston, VA (703)860-6273 FTS 928-6273	Map Projections
Dr. Andrew Tescher Aerospace Corporation P. O. Box 92957 Los Angeles, CA 90009 (213)647-1649	Rectification Panel
Dr. Steve Unger Goddard Institute for Space Studies 2880 Broadway New York, NY 10025 (212)664-5603 FTS 664-5603	Airborne Scanner Systems
Mr. Anthony Villasenor Code ECD-4 Data Systems Branch NASA Headquarters 600 Independence Ave. SW Washington, DC 20546 (202)755-8573 FTS 755-8573	Workshop Sponsor
Dr. Roy Welch University of Georgia Athens, GA 30602 (404)542-2656	Map Accuracy
Dr. Robert Wolfe Johnson Space Flight Center Mail Code 56 1322 Space Park Drive Houston, TX 77058 (713)333-5060	Inter-Image Matching

Dr. Al Zobrist
Jet Propulsion Laboratory
Mail Stop 168-514
4800 Oak Grove Dr.
Pasedena, CA 91103
(213)354-3237 FTS 792-3237

Remapping Procedures

9.3 REGISTRATION AND RECTIFICATION WORKSHOP AGENDA

Tuesday, November 17, 1981

JOINT MEETING TO BE HELD IN ROOM 2464

1. Introduction (8:00-9:00) — Workshop Chairman: N. Bryant/JPL; Workshop Sponsor: A. Villasenor/NASA

2. Objectives and Format of Workshop (9:00-9:30)

a.	Format	N. Bryant/JPL
b.	Objectives	F. Billingsley/JPL

3. Presentations on Users Needs (9:30-12:00) (1:00-2:00)

a.	Agriculture/Forestry/Rangeland	R. Allen/USDA
b.	Land Use/Land Cover and Hydrology	L. Gaydos/USGS
c.	Geology	P. Chavez/USGS
d.	Severe Storms	J. Dalton/GSFC
e.	Ocean Processes	D. Nichols/JPL

4. Presentations on Space Segment Errors (2:00-4:00)

a.	Scanner Imaging Systems, Spaceborne	A. Prakash/GE
b.	Scanner Imaging Systems, Aircraft	S. Unger/GISS
c.	MLA Imaging Systems	K. Ando/NASA
d.	SAR Imaging Systems	J. Curlander/JPL
e.	Multimission Spacecraft	H. Heuberger/GSFC
f.	NAVSTAR/Global Positioning System	M. Ananda/Aerospace

5. Presentations on Ground Segment Errors (4:00-5:00)

a.	Geodetic Control Net Considerations	J. Gergen/NGS
b.	National Map Accuracy Standards	R. Welch/U OF GA
c.	Map Projections	J. Snyder/USGS

6. Systems Presentations and Discussions (7:00-9:00)

a.	Quantitative Effects of Misregistration	R. Juday/JSC
b.	Data vs. Information, A System Paradigm	F. Billingsley/JPL
c.	Panel Chairman Overview Discussions	
	- Registration Panel	R. Bernstein/IBM
	- Rectification Panel	A. Tescher/Aerospace
	- Error Analysis Panel	R. Pelzman/Lockheed

Wednesday, November 18, 1981

7. Presentations on Processing and Verification (8:00-12:00)

a.	Registration	
	- Image Sharpness	P. Anuta/Purdue
	- Feature Extraction	R. Haralick/VPI
	- Inter-Image Matching	R. Wolfe/IBM
b.	Rectification	
	- Remapping Procedures	E. Mikhail/Purdue and A. Zobrist/JPL
	- Resampling Functions	R. Dye/ERIM
c.	Error Analysis	
	- Error Characterization and Error Budgets	E. Beyer/GE
	- Methods of Verification	G. Grebowsky/GSFC

8. Panels/Subpanels Meeting (1:00-5:00)
(Identify state-of-the-art technology, recommendations, etc.)

		Chairmen
	a. Registration Subpanels	
Room 3289	- Image Sharpness	P. Anuta/Purdue
Room 3257	- Feature Extraction	L. Davis/U OF MD
Room 3263	- Inter-Image Matching	H. Ramapriyan
	b. Rectification Subpanels	
Room 3265	- Remapping Procedures	A. Tescher/Aerospace
Room 3463	- Resampling Functions	R. Juday/JSC
	c. Error Analysis	
	- Error Characterization and Error	
Room 3370	Budgets	J. Barker/GSFC
Room 3465	- Methods of Verification	R. Pelzman/Lockheed

9. Discussions by Members-at-Large (7:00-9:00)

a.	Registration Techniques Panel Chairman	R. Bernstein/IBM
b.	Rectification Techniques Panel Chairman	A. Tescher/Aerospace
c.	Error Analysis Panel Chairman	R. Pelzman/Lockheed

Thursday November 19, 1981

10. Panels/Subpanels Meetings (9:00-12:00)
(Develop program plans and recommendations)

11. Presentations to Members-at-Large (1:00-3:00)

a.	Recommendations, Registration Panel Chairman	R. Bernstein/IBM
b.	Recommendations, Rectification Panel Chairman	A. Tescher/Aerospace
c.	Recommendations, Error Analysis Chairman	R. Pelzman/Lockheed

12. Workshop Overview — F. Billingsley/JPL

9.4 PANEL DISCUSSION HANDOUTS

1. Subpanel: Image Sharpness

2. Panel: Registration

3. Chairman: Paul Anuta, Purdue University

4. Discussant: Paul Anuta, Purdue University

5. Areas of Concern: Fundamental principles in instantaneous field of view versus the point spread function in digital image enhancement. Methods for improving visual recognition of ground control point regions in images. Signal-to-noise ratio impacts associated with effective fields of view (as opposed to instantaneous fields of view).

6. Charge to Panel Working Group:

a) Develop a position statement on the state of the art for those elements in applications' techniques of concern to this subpanel for the registration/rectification of imaging sensor data. Use the paper presented as a point of departure, adding new elements neglected and deleting elements of little apparent concern to NASA and the user community.

b) Develop a position statement on anticipated requirements for those elements in applications' techniques of concern to this subpanel for the registration/rectification of imaging sensor data. Use the paper presented as a point of departure, adding new elements neglected and deleting elements of little apparent concern to NASA and the user community.

c) Outline the current status of the technology within NASA. List the centers of expertise (field center groups and university/industry support groups).

d) Propose experiments that should be conducted to test and document areas of concern to this panel in technique applications. This should include synthetic and standardized data sets.

e) Discuss the feasibility of providing tested software systems packages to implement standard procedures presently developed. Recommend candidate systems for the "registration processors" survey.

f) Identify research tasks that the subpanel feels should be pursued to enhance near- and medium-range capabilities. Recommend levels of effort (man-years, dollars) and task duration. Prioritize the research tasks.

7. General Questions to Consider:

a) Master Image Sets: In the context of image sharpness concerns, discuss whether or not there should be a set of master image sets for registration. What data should be used for this master set? Should these data be converted into a particular geometry or projection? Can a master image set serve as a reference image for future processing, eliminating or reducing the need for

establishing and maintaining a ground control point library? Should there be a national or global digital data base? If so, what registration strategy should be pursued?

b) Inaccuracies: How do inaccuracies propagate through a system?

c) Performance: What is the best achievable accuracy one could expect with the algorithms at hand for a given data type being analyzed?

d) Interpolation: What effects do the various interpolation kernels have on resolution, transient rise distances, or point spread function? For the users: are these important?

e) Which techniques are most optimal under which conditions?

f) Can we precisely define differences in radiometric and geometric errors?

g) Data: What kinds of data sets need to be registered? What are the dimensions of these data sets? What are the number and types of these data sets now and to be anticipated in the future?

h) What applications success has been achieved to date with registering data? What techniques were used? Was the data changed as a result of registration processing, and if so, what was the effect of the change?

i) Are there specific sensor subsystem parameters that can be developed or manipulated to improve image sharpness results?

j) Is it possible to define surrogate conditions for choosing optimal techniques?

1. Subpanel: Feature Extraction

2. Panel: Registration

3. Chairman: Larry Davis, University of Maryland

4. Discussant: Robert Haralick, Virginia Polytechnic Institute

5. Areas of Concern: Review processing that can be applied to images to improve the capability for discriminating features within an image to obtain improved ground control point identification. Texture processing functions to enhance image gradients and identification of subpixel texture components. Skeletonizing images for subsequent matching to a vector representation of a map area.

6. Charge to Panel Working Group:

a) Develop a position statement on the state of the art for those elements in applications' techniques of concern to this subpanel for the registration/rectification of imaging sensor data. Use the paper presented as a point of departure, adding new elements neglected and deleting elements of little apparent concern to NASA and the user community.

b) Develop a position statement on anticipated requirements for those elements in applications' techniques of concern to this subpanel for the registration/rectification of imaging sensor data. Use the paper presented as a point of departure, adding new elements neglected and deleting elements of little apparent concern to NASA and the user community.

c) Outline the current status of the technology within NASA. List the centers of expertise (field center groups and university/industry support groups).

d) Propose experiments that should be conducted to test and document areas of concern to this panel in technique applications. This should include synthetic and standardized data sets.

e) Discuss the feasibility of providing tested software systems packages to implement standard procedures presently developed. Recommend candidate systems for the "registration processors" survey.

f) Identify research tasks that the subpanel feels should be pursued to enhance near- and medium-range capabilities. Recommend levels of effort (man-years, dollars) and task duration. Prioritize the research tasks.

7. General Questions to Consider:

a) Master Image Sets: In the context of feature extraction concerns, discuss whether or not there should be a set of master image sets for registration. What data should be used for this master set? Should these data be converted into a particular geometry or projection? Can a master image set serve as a reference image for future processing, eliminating or reducing the need for

establishing and maintaining a ground control point library? Should there be a national or global digital data base? If so, what registration strategy should be pursued?

b) Performance: What is the best achievable accuracy one could expect with the algorithms at hand for a given data type being analyzed?

c) Correction Methods: What correction methods are available for system use? What correction methods are available for user use? How well can they potentially work, and how well can they be expected to work?

d) Can desirable ground control points be characterized?

e) Is it possible to correlate images to maps without manual intervention?

f) What image preprocessing is useful prior to feature extraction?

g) How should one treat relief distortion?

h) Interpolation: What effects do the various interpolation kernels have on resolution, transient rise distances, or point spread function? For the users: are these important?

i) Data: What kinds of data sets need to be registered? What are the characteristics of these data sets? What are the number and types of these data sets now and to be anticipated in the future?

j) Is the data changed when processed to achieve registration? What is the effect of this change?

k) Ground control point libraries are costly to build. What techniques/procedures are available to pattern/feature recognition to identify scene content without correlation to reference chips? Which techniques are most optimal under which conditions?

l) How do the important characters of features propagate through the system. What are these characteristics?

m) Are there specific sensor subsystem parameters that can be developed or manipulated to improve image sharpness results?

n) Is it possible to define surrogate conditions for choosing optimal techniques?

1. Subpanel: Inter-Image Matching

2. Panel: Registration

3. Chairman: H. Ramapriyan, GSFC

4. Discussant: Robert Wolfe, IBM

5. Areas of Concern: Procedures and algorithms used to determine relative positions of reference and registrant image at inter-image subimages. Including FFT, cross-correlation, and surface estimation from discrete rasters. Impacts associated with translation, rotation, scale, and keystoning of pixels on the registration process. Discuss search procedures for GCP location.

6. Charge to Panel Working Group:

a) Develop a position statement on the state of the art for those elements in applications' techniques of concern to this subpanel for the registration/rectification of imaging sensor data. Use the paper presented as a point of departure, adding new elements neglected and deleting elements of little apparent concern to NASA and the user community.

b) Develop a position statement on anticipated requirements for those elements in applications' techniques of concern to this subpanel for the registration/rectification of imaging sensor data. Use the paper presented as a point of departure, adding new elements neglected and deleting elements of little apparent concern to NASA and the user community.

c) Outline the current status of the technology within NASA. List the centers of expertise (field center groups and university/industry support groups).

d) Propose experiments that should be conducted to test and document areas of concern to this panel in technique applications. This should include synthetic and standardized data sets.

e) Discuss the feasibility of providing tested software systems packages to implement standard procedures presently developed. Recommend candidate systems for the "registration processors" survey.

f) Identify research tasks that the subpanel feels should be pursued to enhance near- and medium-range capabilities. Recommend levels of effort (man-years, dollars) and task duration. Prioritize the research tasks.

7. General Questions to Consider:

a) Master Image Sets: In the context of inter-image matching concerns, discuss whether or not there should be a set of master image sets for registration. What data should be used for this master set? Should these data be converted into a particular geometry or projection? Can a master image set serve as a reference image for future processing, eliminating or reducing the need for establishing and maintaining a ground control point library? Should there be a national or global digital data base? If so, what registration strategy should be pursued?

b) Inaccuracies: How do inaccuracies propagate through a system? How do uncertainties propagate through the system?

c) Performance: What is the best achievable accuracy one could expect with the algorithms at hand for a given data type being analyzed?

d) Correction Methods: What correction methods are available for system use? What correction methods are available for user use? How well can they potentially work, and how well can they be expected to work?

e) How does brightness response (e.g., striping) affect control point correlation?

f) What procedures should be pursued to correlate sensors having different resolutions?

g) Can desirable ground control points be characterized?

h) How can one correlate areas imaged at different seasons?

i) What preprocessing is useful?

j) How can one treat relief distortions?

k) What is the accuracy of temporal overlays using registration tiepoints vs. rectifying each image to a set of GCPs?

l) Processing: Should geographic location parameters be available to users? What accuracy should they have? Will the users be able to do precision registration with the data available within each digital frame? To what accuracy?

m) Disciplines: What is the sensitivity to data registration loss or missing temporal analysis within disciplines? What types of error description (e.g., RMS, peak, locally mapped) are needed for each discipline? Can these be provided?

n) Can a logical structure be developed to display the sequence platform modeling, platform-related sensors, NAVSTAR/GPS, ground control points, registration tiepoints, (etc.), used in the rectification process? What positional accuracy improvement might be expected at each step in the sequence?

o) Data: What kinds of data sets need to be registered? What are the dimensions of these data sets? What are the number and types of these data sets now and to be anticipated in the future?

p) Accuracy: What are the relative and absolute accuracy requirements? How is accuracy measured and evaluated?

q) What applications success has been achieved to date with registering data? What techniques were used? Was the data changed as a result of registration processing, and if so, what is the effect of the change?

r) How much human interaction is required to register data sets? Is this necessary, and, if so, to what extent can manual interaction be reduced? How much does human subjectivity affect the result?

s) How significant a role would a sensor/platform model play in registration/rectification of the data acquired from different sensors on different platforms (e.g., shuttle/SAR and Landsat/TM)?

t) Ground control point libraries are costly to build. Which techniques are most optional under which conditions?

u) Are there specific sensor subsystem parameters that can be developed or manipulated tc improve image sharpness results?

v) Is it possible to define surrogate conditions for choosing optimal techniques?

1. Subpanel: Remapping Procedures

2. Panel: Rectification

3. Chairman: Andrew Tescher, Aerospace Corp.

4. Discussants: Edward Mikhail, Purdue, and Al Zobrist, JPL

5. Areas of Concern: Procedures associated with the photogrammetric and computational aspects of remapping images from nominally orthophoto to map-projected space. Control net generation and surface remapping models; i.e., surface fitting, gridding, rubber-sheeting methods, spacecraft model incorporation, and terrain/elevation compensation.

6. Charge to Panel Working Group:

a) Develop a position statement on the state of the art for those elements in applications' techniques of concern to this subpanel for the registration/rectification of imaging sensor data. Use the paper presented as a point of departure, adding new elements neglected and deleting elements of little apparent concern to NASA and the user community.

b) Develop a position statement on anticipated requirements for those elements in applications' techniques of concern to this subpanel for the registration/rectification of imaging sensor data. Use the paper presented as a point of departure, adding new elements neglected and deleting elements of little apparent concern to NASA and the user community.

c) Outline the current status of the technology within NASA. List the centers of expertise (field center groups and university/industry support groups).

d) Propose experiments that should be conducted to test and document areas of concern to this panel in technique applications. This should include synthetic and standardized data sets.

e) Discuss the feasibility of providing tested software systems packages to implement standard procedures presently developed. Recommend candidate systems for the "registration processors" survey.

f) Identify research tasks that the subpanel feels should be pursued to enhance near- and medium-range capabilities. Recommend levels of effort (man-years, dollars) and task duration. Prioritize the research tasks.

7. General Questions to Consider:

a) Master Image Sets: In the context of remapping concerns, discuss whether or not there should be a set of master image sets for registration. What data should be used for this master set? Should these data be converted into a particular geometry or projection? Can a master image set serve as a reference image for future processing, eliminating or reducing the need for establishing and maintaining a ground control point library? Would there be a national or global digital data base? If so, what registration strategy should be pursued?

ORIGINAL PAGE IS
OF POOR QUALITY

b) Inaccuracies: How do inaccuracies propagate through a system?

c) Performance: What is the best achievable accuracy one could expect with the algorithms at hand for a given data type being analyzed?

d) Correction Methods: What correction methods are available for system use? What correction methods are available for user use? How well can they potentially work, and how well can they be expected to work?

e) With what accuracy is the platform position known with and without GCPs? How accurately can a platform be expected to repeat coverage of a given swath area? Is this the same at all earth locations? How accurately is the attitude and altitude known, and what are the accuracies (registration and rectification) possible after processing?

f) For aircraft sensors, what are the platform conditions, and are ancillary sensors necessary and/or available?

g) Can per-swath modelling really be done, and if so, how are/should the GCPs be utilized? What open loop positional accuracies are available with and without GCPs?

h) How many GCPs are needed to accurately model the distortions for given sensor systems?

i) How accurate are GCPs worldwide?

j) What preprocessing is useful?

k) How should one treat relief distortions?

l) What is the accuracy of temporal overlays using registration tiepoints vs. rectifying each image to a set of GCPs?

m) Can a world-wide map be drawn of expected geometric (including ground location) accuracy?

n) Processing: Should geographic location parameters be available to users? What accuracy should they have? Will the users be able to do precision registration with the data available with each digital frame? To what accuracy?

o) Disciplines: What is the sensitivity to data registration loss or missing temporal overlays within disciplines? What types of error description (e.g., RMS, peak, locally mapped) are needed for each discipline? Can these be provided?

p) Can a logical structure be developed to display the sequence in which platform modeling, platform-related sensors, NAVSTAR/GPS, ground control points, registration tiepoints ( ) are used in the rectification process? What accuracies might be expected at each step in the sequence?

q) Data: What kinds of data sets need to be registered? What are the dimensions of these data sets? What are the number and types of these data sets now and to be anticipated in the future?

r) Accuracy: What are the relative and absolute accuracy requirements? How is accuracy measured and evaluated?

s) What success has been achieved to date with registering data?

t) What applications success has been achieved to date with registering data? What techniques were used? Was the data changed as a result of registration processing, and if so, what is the effect of the change?

u) How much human interaction is required to register data sets? Is this necessary, and, if so, to what extent can manual interaction be reduced? How much does human subjectivity effect the result?

v) How significant a role would a sensor/platform model play in registration/rectifications of the data acquired from different sensors on different platforms (e.g., shuttle/SAR and Landsat/TM)?

w) Although the registration and rectification processes are somewhat similar, they are also somewhat different; is there a methodology that can be used for both?

x) Ground control point libraries are costly to build. Which techniques are most optimal under which conditions?

y) What is involved in remapping from one map projection or scale to another?

z) How would we relate NASA's GCP net with established geodetic control nets?
aa) Are there specific sensor subsystem parameters that can be developed or manipulated to improve remapping procedure results?

bb) Is it possible to define surrogate conditions for choosing optimal techniques?

1. Subpanel: Resampling Functions

2. Panel: Rectification

3. Chairman: Richard Juday, JSC

4. Discussant: Robert Dye, ERIM

5. Areas of Concern: The effect of resampling procedures upon signal-to-noise ratio for digital imagery. Discuss the relative impact of bilinear, nearest neighbor, cubic spline, and associated hybrid resampling algorithms upon the information content of pixels and local geometric fidelity.

6. Charge to Panel Working Group:

a) Develop a position statement on the state of the art for those elements in applications' techniques of concern to this subpanel for the registration/rectification of imaging sensor data. Use the paper presented as a point of departure, adding new elements neglected and deleting elements of little apparent concern to NASA and the user community.

b) Develop a position statement on anticipated requirements for these elements in applications' techniques of concern to this subpanel for the registration/rectification of imaging sensor data. Use the paper presented as a point of departure, adding new elements neglected and deleting elements of little apparent concern to NASA and the user community.

c) Outline the current status of the technology within NASA. List the centers of expertise (field center groups and university/industry support groups).

d) Propose experiments that should be conducted to test and document areas of concern to this panel in technique applications. This should include synthetic and standardized data sets.

e) Discuss the feasibility of providing tested software systems packages to implement standard procedures presently developed. Recommend candidate systems for the "registration processors" survey.

f) Identify research tasks that the subpanel feels should be pursued to enhance near- and medium-range capabilities. Recommend levels of effort (man-years, dollars) and task duration. Prioritize the research tasks.

7. General Questions to Consider:

a) Master Image Sets: In the context of resampling functions, discuss whether or not there should be a set of master image sets for registration. What data should be used for this master set? Should these data be converted into a particular geometry or projection? Can a master image set serve as a reference image for future processing, eliminating or reducing the need for establishing and maintaining a ground control point library? Should there be a national or global digital data base? If so, what registration strategy should be pursued?

b) Inaccuracies: How do inaccuracies propagate through a system?

c) Performance: What is the best achievable accuracy one could expect with the algorithms at hand for a given data type being analyzed?

d) Correction Methods: What correction methods are available for system use? What correction methods are available for user use? How well can they potentially work, and how well can they be expected to work?

e) Interpolation: What effects do the various interpolation kernals have on resolution, transient rise distances, or point spread function? For the users: are these important?

f) Disciplines: What is the sensitivity to data registration loss or missing temporal overlaps within disciplines? What types of error description (e.g., RMS, peak, locally mapped) are needed for each discipline? Can these be provided?

g) Is the data changed when processed to achieve registration? What is the effect of this change?

h) What applications success has been achieved to date with registering data? What techniques were used?

i) Although registration and rectification processes are somewhat similar, they are also somewhat different; is there a methodology that can be used for both?

j) Which registration/rectification techniques are most optimal under which conditions?

k) Can we precisely define differences in radiometric and geometric errors?

l) Are there different optimal sampling functions for human image interpretation analysis and machine information extraction processing?

m) Should resampling functions be the same in both the along- and across-track direction? How might interpolation functions vary according to overlap of sensor IFOV?

n) Are there specific sensor subsystem parameters that can be developed or manipulated to improve resampling procedure results?

o) Is it possible to define surrogate conditions for choosing optimal techniques?

1. Subpanel: Error Characterization and Error Budgets

2. Panel: Error Analysis

3. Chairman: John Barker, GSFC

4. Discussant: Erie, Beyer, G.E.

5. Areas of Concern: The essential components that contribute to the error associated with the projected position of pixels in spaceborne imaging systems. Distinguish between the spacecraft/sensor error ellipse budget for a given pixel location and the computational error associated with algorithm/model performance and assumptions for ground segment processing. Deal with error budgets that include and do not include ground control points.

6. Charge to Panel Working Group:

a) Develop a position statement on the state of the art for those elements in applications' techniques of concern to this subpanel for the registration/rectification of imaging sensor data. Use the paper presented as a point of departure, adding new elements neglected and deleting elements of little apparent concern to NASA and the user community.

b) Develop a position statement on anticipated requirements for those elements in applications' techniques of concern to this subpanel for the registration/rectification of imaging sensor data. Use the paper presented as a point of departure, adding new elements neglected and deleting elements of little apparent concern to NASA and the user community.

c) Outline the current status of the technology within NASA. List the centers of expertise (field center groups and university/industry support groups).

d) Propose experiments that should be conducted to test and document areas of concern to this panel in technique applications. This should include synthetic and standardized data sets.

e) Discuss the feasibility of providing tested software systems packages to implement standard procedures presently developed. Recommend candidate systems for the "registration processors" survey.

f) Identify research tasks that the subpanel feels should be pursued to enhance near- and medium-range capabilities. Recommend levels of effort (man-years, dollars) and task duration. Prioritize the research tasks.

7. General Questions to Consider:

a) Master Image Sets: In the context of error characterization and error budgets, discuss whether or not there should be a set of master image sets for registration. What data should be used for this master set? Should these data be converted into a particular geometry or projection? Can a master image set serve as a reference image for future processing, eliminating or re-

ducing the need for establishing and maintaining a ground control point library? Should there be a national or global digital data base? If so, what registration strategy should be pursued?

b) Inaccuracies: How do inaccuracies propagate through a system?

c) Performance: What is the best achievable accuracy one could expect with the algorithms at hand for a given data type being analyzed?

d) Sensor-positional errors will be of two types: those which are predictable and therefore presumably can be "calibrated out" (rectified), but with residual uncertainties in the calibration, and those which are implicitely random and for which ancillary data are required. What is the error budget for a particular sensor? What errors can be calibrated, and which must use real image data for correction? Can the sensor be adequately modeled? Is the required ancillary data available? What differences in performance are present in different types of sensors - (scanners, linear arrays, aircraft vs spacecraft, etc.)?

e) With what accuracy is the platform position known with and without GCPs? How accurately can a platform be expected to repeat coverage of a given swath area? Is this the same at all earth locations? How accurately is the attitude and altitude known, and what are the accuracies (registration and rectification) possible after processing?

f) Can a world-wide map be drawn of expected geometric (including ground location) accuracy?

g) Interpolation: What effects do the various interpolation kernels have on resolution, transient rise distances, or point spread function? For the user: are these important?

h) Processing: Should geographic location parameters be available to users? What accuracy should they have? Will the users be able to do precise registration with the data available with each digital frame? To what accuracy?

i) Disciplines: What is the sensitivity to data registration loss or missing temporal overlays within disciplines? What types of error description (e.g., RMS, peak, locally mapped) are needed for each discipline? Can these be prohvided?

j) Can a logical structure be developed to display the sequence in which platform modeling, platform-related sensors, NAVSTAR/GPS, ground control points, registration tiepoints (etc.) are used in the rectification process? What accuracies might be expected at each step in the sequence?

k) Accuracy: What are the relative and absolute accuracy requirements? How is accuracy measured and evaluated?

l) What success has been achieved to date with registering data?

m) Are there specific sensor subsystem parameters that can be developed or manipulated to improve error characterization results?

n) Is it possible to define surrogate conditions for choosing optimal techniques?

1. Subpanel: Methods of Verification

2. Panel: Error Analysis

3. Chairman: Robert Pelzmann, Lockheed

4. Discussant: Gerald Grebowsky, GSFC

5. Areas of Concern: Procedures used for verifying the positional occurance of pixel observed versus projected latitude/longitude position in spaceborne images. Procedures that include and do not include ground control points in the data projection process.

6. Charge to Panel Working Group:

a) Develop a position statement on the state of the art for those elements in applications' techniques of concern to this subpanel for the registration/rectification of imaging sensor data. Use the paper presented as a point of departure, adding new elements neglected and deleting elements of little apparent concern to NASA and the user community.

b) Develop a position statement on anticipated requirements for these elements in applications' techniques of concern to this subpanel for the registration/rectification of imaging sensor data. Use the paper presented as a point of departure, adding new elements neglected and deleting elements of little apparent concern to NASA and the user community.

c) Outline the current status of the technology within NASA. List the centers of expertise (field center groups and university/industry support groups).

d) Propose experiments that should be conducted to test and document areas of concern to this panel in technique applications. This should include synthetic and standardized data sets.

e) Discuss the feasibility of providing tested software systems packages to implement standard procedures presently developed. Recommend candidate systems for the "registration processors" survey.

f) Identify research tasks that the subpanel feels should be pursued to enhance near- and medium-range capabilities. Recommend levels of effort (man-years, dollars) and task duration. Prioritize the research tasks.

7. General Questions to Consider:

a) Master Image Sets: In the context of verification procedures, discuss whether or not there should be a set of master image sets for registration. What data should be used for this master set? Should these data be converted into a particular geometry or projection? Can a master image set serve as a reference image for future processing, eliminating or reducing the need for establishing and maintaining a ground control point library? Should there be a national or global digital data base? If so, what registration strategy should be pursued?

b) Inaccuracies: How do inaccuracies propagate through a system?

c) Performance: What is the best achievable accuracy one could expect with the algorithms at hand for a given data type being analyzed?

d) Sensor - positional errors will be of two types: those which are predictable and therefore presumably can be "calibrated out" (rectified), but with residual uncertainties in the calibration, and those which are implicitely random and for which ancillary data are required. What is the error budget for a particular sensor? What errors can be calibrated, and which much use real image data for correction? Can the sensor be adequately modeled? Is the required ancillary data available? What differences in performance are present in different types of sensors (scanners, linear arrays, aircraft vs spacecraft, etc.)?

e) Can a world-wide map be drawn of expected geometric (including ground location) accuracy?

f) Processing: Should geographic location parameters be available to users? What accuracy should they have? Will the users be able to do precision registration with the data available with each digital frame? To what accuracy?

g) How much human interaction is required to register data sets? Is this necessary, and if so to what extent can manual interaction be reduced? How much does human subjectivity effect the result?

h) Are recursive techniques of great value for modelling platform errors like attitude?

i) Is accuracy really paramount for registration/rectification?

j) Can we precisely define the distortions, errors, tolerances, reference data, and quality of processing in the rectification/registration process?

k) Is segment magnification/reduction and the overlaying of these segments for alignment a good test for accuracy?

l) What verification methods are applicable to the process? Is there a practical scheme to be implemented?

m) Can we develop standard performance parameters for reporting accuracy of a registration/rectification system?

n) What are the various verification procedures (e.g., visual, interactive, automated, analytical) and what has been the performance and limitations of each?

o) Are there specific sensor subsystem parameters that can be developed or manipulated to improve verification procedure results?

p) Is it possible to define surrogate conditions for choosing optimal techniques?

9.5 DEFINITION OF TERMS

Registration: The alignment of imaging sensor data to another image, a sub-image, or identifiable objects on a map.

Rectification: The conversion of spatially indexed sensor data to a mathematically defined coordinate system relating to latitude and longitude.

Geocoding: The process of registering spatial data in a manner that achieves retrievability by geographic referencing.

Data Integration: The process of registering discrete and spatially distributed sensor data sets and ancillary data bases in a manner which accounts for measurement incongruencies and provides spatially comparable data sets.

Systematic Error: Reproducible inaccuracy introduced by faulty equipment, calibration, or technique.

Random Error: Indefiniteness of result due to finite precision of experiment. Measure of fluctuation in result after repeated experimentation.

Probable Error: Indefiniteness of error which is estimated to have been made in determination of results.

Accuracy: Measure of how close the result of the experiment comes to the "true" value.

Precision: Measure of how exactly the result is determined without reference to any "true" value.

9.6 DATA SYSTEMS PROGRAM PLAN VIEWGRAPH PRESENTATION

A. VILLASENOR
OFFICE OF SPACE & TERRESTRIAL APPLICATIONS
COMMUNICATIONS & INFORMATION SYSTEMS BRANCH
DATA SYSTEMS BRANCH

DATA SYSTEMS PROGRAM

OVERALL GOAL:

SYSTEMATICALLY EVOLVE EFFECTIVE AND INTEGRATED DATA SYSTEMS TO:

- IMPROVE USER ACCESS AND UTILIZATION OF MULTIMISSION DATA BY DEVELOPING EFFICIENT DATA MANAGEMENT, DATA CATALOGING, DATA DISTRIBUTION, AND DATA INTEGRATION TECHNIQUES

- REDUCE COST AND RISK TO FLIGHT PROJECTS BY DEVELOPING AND DEMONSTRATING ADVANCED DATA SYSTEMS CAPABILITIES PRIOR TO IMPLEMENTATION IN OPERATIONAL ENVIRONMENTS

- ENABLE NEW DISCIPLINE AND MISSION CAPABILITIES BY DEVELOPING AND IMPROVING TOOLS AND TECHNIQUES FOR INFORMATION EXTRACTION AND DATA DISSEMINATION

DATA SYSTEMS PROGRAM

OVERALL PROGRAM PHILOSOPHY:

- o PRIMARY FOCUS IS TO UNDERSTAND AND SUPPORT THE NEEDS OF APPLICATIONS PROGRAMS AND FLIGHT PROJECTS BY ESTABLISHING PARTNERSHIPS WITH DISCIPLINE PROGRAMS
- o ENCOURAGE DEVELOPMENT OF, EVALUATE, AND APPLY ADVANCED TECHNOLOGIES TO MEET APPLICATIOS NEEDS -- FOCUS ON INNOVATVE USES OF ADVANCED TECHNOLOGIES AND STATE-OF-THE-ART EQUIPMENT
- o ACTVITIES SHOULD EMPHASIZE REQUIREMENTS COMMON TO OSTA PROGRAMS AND DEVELOPMENT OF COMPATIBLE DATA SYSTEMS
- o AVOID DISCIPLINE UDNIQUE ACTIVITIES, SUCH AS DATA INTERPRETATION TECHNIQUES
- o SUPPORT DEVELOPMENT OF IN-HOUSE NASA DATA SYSTEM EXPERTISE
- o FOSTER COOPERATIVE - NO COMPETITIVE - ACTIVITIES BETWEEN CENTERS

DATA SYSTEMS PROGRAM

OVERALL APPROACH:

IDENTIFY THE DATA SYSTEM REQUIREMENTS OF OSTA PROGRAMS, AND CONDUCT AR&D ACTIVITIES TO SUPPORT IMPLEMENTATION OF CAPABILITIES NEEDED TO MEET THESE REQUIREMENTS

- O WORK WITH DISCIPLINE PROGRAMS AND FLIGHT PROJECTS TO DEFINE REQUIREMENTS FOR AND TO PERFORM DATA SYSTEM DEMONSTRATIONS PRIOR TO IMPLEMENTATION OF FLIGHT PROJECT DATA SYSTEMS, AS IS DONE FOR SENSORS

- O SUPPORT INCORPORATION OF DEMONSTRATED CAPABILITIES INTO CURRENT AND FUTURE FLIGHT PROJECT AND DISCIPLINE SYSTEMS

- O ESTABLISH ACTIVE STEERING/WORKING GROUPS, INCLUDING APPLICATIONS SCIENTISTS, TO COORDINATE AND GUIDE COMMON R&D ACTIVITIES (E.G. REQUIREMENTS, PILOTS, DBMS, STANDARDS, ETC.)

- O DEVELOP TIME PHASED APPROACH TO MEET THE MOST URGENT NEEDS WITHIN REASONABLE BUDGET AND SCHEDULE CONSTRAINTS

- O CONDUCT PILOT R&D ACTIVITIES TO EXPLORE, DEVELOP, EVALUATE, DEMONSTRATE, AND TRANSFER SYSTEM CONCEPTS AND ADVANCED CAPABILITIES BEFORE COMMITTING TO COSTLY SYSTEM DEVELOPMENTS (I.E., WE EMPLOY A CONTROLLED EXPERIMENT APPROACH)

DATA SYSTEMS PROGRAM
ROLE IN NASA'S APPLICATIONS PROGRAM

- o DEVELOP SUPPORT TO IDENTIFY, COORDINATE, AND MEET DATA SYSTEM NEEDS COMMON TO OSTA DISCIPLINES:
  - RESPONSIBILITY TO DEVELOP, COORDINATE, AND IMPLEMENT AN OVERALL DATA SYSTEM PLAN
  - DEVELOPS COMMON DATA REGISTRATION AND INTEGRATION CAPABILITIES
  - CONTINUES COMMON DATA CATALOG AND DATA BASE MANAGEMENT ACTIVITIES
  - CONTINUES CURRENT AND FUTURE OSTA PILOT DATA SYSTEMS DEVELOPMENTS
  - SUPPORTS EFFORTS TO DEVELOP COMMON DATA CATALOG AND PROVISIONING CAPABILITIES

- o PROVIDES TECHNICAL SUPPORT TO PROGRAM OFFICES IN PLANNING FLIGHT PROJECT AND DISCIPLINE DATA SYSTEMS
  - ESTABLISHES COMPATIBLE DATA PRODUCTS, SOFTWARE, AND SYSTEMS
  - PROVIDES MANAGEMENT FOCUS FOR EVALUATING TECHNICAL CONCEPTS
  - PROVIDES ALTERNATIVE SOLUTIONS TO CURRENT PRESSING DATA SYSTEMS PROBLEMS

- o PERMITS DEVELOPMENT AND EVALUATION OF ADVANCED DATA SYSTEMS TECHNOLOGIES TO MEET ANTICIPATED NEEDS
  - ANTICIPATES DATA SYSTEM REQUIREMENTS BASED ON PAST EXPERIENCES
  - LOWERS DATA SYSTEM DEVELOPMENT RISKS FOR FLIGHT MISSIONS
  - REDUCES INCIDENTS OF COST OVERRUNS, SCHEDULE SLIPS, AND LATE DATA DELIVERY
  - ENABLES NEW MISSION AND SCIENCE ANALYSIS CAPABILITIES

DATA SYSTEM PROGRAM

ROLE, CONTINUED

- ESTABLISHES OSTA SUPPORT NEEDED TO MAINTAIN DATA SYSTEMS CAPABILITIES AND SKILLED PERSONNEL AT THE NASA CENTERS
  - BASE OF DATA SYSTEMS EXPERTISE NEEDED FOR BETTER MANAGEMENT OF FUTURE DATA SYSTEM DEVELOPMENT EFFORTS
- ESTABLISHES OSTA PROGRAMMATIC BASE NEEDED FOR DATA SYSTESM R&D IN SUPPORT OF OPERATIONAL SYSTEMS
  - AIMS TO REDUCE SYSTEM OPERATIONS COSTS
  - PERMITS AN EARLIER RETURN ON LARGE INVESTMENT IN DATA PROCESSING
- PROVIDES MANAGEMENT VISIBILITY INTO FLIGHT PROJECT AND DISCIPLINE DATA SYSTEM ACTIVITIES WITHIN OSTA
- UNIFIES OSTA DATA SYSTEM INTERFACE WITHIN NASA AND WITH OUTSIDE ORGANIZATIONS
  - ESTABLISH BASIS FOR INTERAGENCY DATA SHARING
  - VEHICLE FOR DEVELOPING STANDARDS AND GUIDELINES FOR DATA MANAGEMENT, NETWORKING, ETC.

DATA SYSTEMS PROGRAM

FY81 ACCOMPLISHMENTS - APPLICATIONS DATA SERVICE AND PILOT DATA SYSTEMS

- INITIATED DEVELOPMENT OF DISCIPLINE-ORIENTED PILOT DATA SYSTEMS
  - OCEANS/JPL: HARDWARE, CATALOG SYSTEM IN PLACE; SEASAT DATA OUTLINE; READY FOR RESEARCH APPLICATIONS
  - ATMOSPHERES/GSFC: NETWORK OPERATIONAL, ONLINE CATALOG DEVELOPED FOR CLIMATE AND WEATHER DATA; READY FOR GLOBAL WEATHER RESEARCH
  - RESOURCES/JPL: USER & DATA SYSTEM REQUIREMENTS DEVELOPED

- IMPLEMENTED NETWORK SERVICES TO EXCHANGE DATA
  - INTERCONNECTED THREE COMPUTERS IN LOCAL NETWORK
  - REMOTE SERVICES SUBSYSTEM (RSS) INSTALLED FOR EXCHANGE OF SEVERE STORMS, VAS AND CLIMATE DATA
  - ESTABLISHED REQUIREMENTS FOR HIGH-SPEED LOCAL NETWORK

- BEGAN DEFINITION OF STANDARDS GUIDELINES FOR APPLICATIONS DATA
  - SURVEYED EXISTING NATIONAL & INTERNATIONAL DATA STANDARDS FOR APPLICABILITY TO ADS
  - INTERCENTER DATA STANDARDS WORKSHOP HELD TO ASSIST IN DEVELOPING SPECIFIC APPROACHES FOR DATA FORMATS AND PROTOCOLS
  - DEVELOPED CLASSIFICATION SCHEME FOR DATA FORMATS

DATA SYSTEMS PROGRAM

FY81 ACCOMPLISHMENTS - ADVANCD PROCESSING SYSTEMS

- BEGAN DEVELOPMENT OF APPLICATIONS DEVELOPMENTAL DATA SYSTEM
  - HIGH PERFORMANCE PIPELINE ARCHITECTURE BUILT AROUND MINICOMPUTER
  - PLANNED APPLICATION TO LANDSAT-D MSS AND TM AT LAUNCH
  - GOAL IS 200 MSS/100 TM PER DAY, SIX MONTHS AFTER LAUNCH

- CONTINUED DEVELOPMENT OF INTERIM SYNTHETIC APERTURE RADAR DATA PROCESSOR
  - EMPLOYS BANK OF MULTIPLE ARRAY PROCESSORS
  - APPLICATION OF SYNTHETIC APERTURE RADAR INSTRUMENTS
  - DEMONSTRATED REDUCTION FROM 10 HOURS TO 2.5 HOURS PER SCENE
  - GOAL IS 1.5 HOURS/SCENE IN FY82

DATA SYSTEMS PROGRAM

FY81 ACCOMPLISHMENTS - DATA MANAGEMENT SYSTEMS

- EVALUATION OF COMMERCIAL DATA BASE MANAGEMENT SYSTEMS
  - COMPLETED ANALYSIS AND REPORT ON SEED, ORACLE AND RIM DATA BASE MANAGEMENT SYSTEMS
  - RIM ADAPTED BY OCEAN PILOT
  - SEED USED BY LANDSAT-D PROJECT
  - ORACLE SELECTED FOR CLIMATE DATA SYSTEM

- IMPLEMENTED CATALOGS FOR SELECTED OSTA DATA SETS
  - HARDCOPY AND ONLINE CATALOG FOR CLIMATE
  - EXPANDED VAS CATALOG FOR SEVERE STORM RESEARCH PROGRAM
  - DEVELOPED ONLINE DATA PROVISIONING SYSTEM FOR AGRISTARS
  - DEVELOPED TESTBED CENTRAL DIRECTORY FOR LOCATING DISTRIBUTED OSTA DATA SETS

DATA SYSTEMS PROGRAM

FY81 ACCOMPLISHMENTS - INFORMATION EXTRACTION

- DEVELOPED IMPROVED DATA REGISTRATION TECHNIQUES
  - MULTITEMPORAL AGRISTARS SCENES REGISTERED TO 1-PIXEL ACCURACY
  - AUTOMOSAICKING DEVELOPED FOR RENEWABLE RESOURCES
- INSTALLED INITIAL VERSIONS OF COMMON EXECUTIVE SOFTWARE
  - TRANSPORTABLE APPLICATION EXECUTIVE FOR INTERACTIVE USER CONTROL
  - REMOTE SERVICES SUBSYSTEM FOR DATA EXCHANGE BETWEEN REMOTE COMPUTERS
- DEVELOPED COMMON APPLICATIONS SOFTWARE TOOLS
  - METPAK, FOR METEOROLOGY
  - GEMPAK, FOR GEOLOGY
  - WORKING ON SEAPAK, FOR OCEANOGRAPHY
- DEMONSTRATED LOW-COST MICROPROCESSOR-BASED IMAGE ANALYSIS TERMINALS
  - TERMINALS NOW PRODUCED & DISTRIBUTED BY INDUSTRY
  - ALSO USED IN SEASAT CATALOG SYSTEM

DATA SYSTEMS PROGRAM
MAJOR PROGRAM THRUSTS - FY82, 83

1. ADVANCED PROCESSING SYSTEMS
   - APPLICATIONS DEVELOPMENTAL DATA SYSTEM
   - SYNTHETIC APERATURE RADAR DATA SYSTEM
   - VLSI TECHNOLOGY APPLICATIONS
   - DIGITAL OPTICAL APPLICATIONS

2. DISTRIBUTED DATA SYSTEMS
   - ATMOSPHERE PILOT NETWORK
   - OCEAN PILOT SYSTEM
   - RESOURCES PILOT NETWORK
   - STANDARDS

3. INFORMATION EXTRACTION
   - IMAGE REGISTRATION AND RECTIFICATION
   - DATA INTEGRATION
   - TRANSPORTABLE APPLICATIONS SOFTWARE
   - SMART USER TERMINALS

4. DATA MANAGEMENT
   - EVALUATION OF COMMERCIAL DATA BASE MANAGEMENT SYSTEMS
   - ONLINE CATALOGS
   - DATA BASE MACHINES

5. INFORMATION SCIENCE (NEW)
   - DATA COMPRESSION TECHNIQUES
   - APPROACHES FOR SELECTING, PROCESSING ONLY THE NEEDED DATA APPLICATIONS OF SOFTWARE METHODOLOGIES
   - MODELLING FOR VECTOR PROCESSOR APPLICATIONS

DATA SYSTEMS PROGRAM
IMAGE REGISTRATION AND RECTIFICATION

- RESPONSES TO FY82 DATA SYSTEMS RTOP CALL CONTAINED
  - SIMILAR INTERESTS IN ALGORITHMS AND INTERPOLATION TECHNIQUES
  - DIFFERING APPROACHES FOR RELATIVE, ABSOLUTE ACCURACIES
  - COMMON NEEDS FOR INTEGRATING MULTISENSOR DATA, AND SATELLITE DATA WITH CONVENTIONAL DATA
  - ELEMENTS INVOLVED IN FUNDAMENTAL RESEARCH PROGRAM

- PROGRAMMATIC NEEDS FOR
  - DATA COMPATIBILITY, TO PROMOTE SHARING AND EXCHANGE
  - DATA INTEGRITY, WITH KNOWN ALGORITHMS AND QUALITY STANDARDS
  - LIBRARY OF COMMON DATA PROCESSING ALGORITHMS
  - TRANSPORTABLE GEOCODED INFORMATION SYSTEMS
  - HIGH-PERFORMANCE SYSTEMS USING VLSI CHIPS AND ADVANCED ARCHITECTURES
  - ALTERNATIVES FOR FLIGHT VS. GROUND DATA PROCESSING
  - IMPROVED DATA ORDERING AND PROVISIONING
  - IDENTIFYING REQUIREMENTS FOR LOW-COST COMMERCIAL TERMINALS

- WORKSHOP ROLE
  - AMASS THE FOREMOST EXPERTS FROM GOVERNMENT, INDUSTRY AND ACADEMIA
  - IDENTIFY USER REQUIREMENTS
  - ESTABLISH BASIS TO FORMULATE AN INTEGRATED MULTIDISCIPLINARY PROGRAM PLAN
  - IDENTIFY SPECIFIC ISSUES, ACTIVITIES FOR DATA SYSTEMS PURSUIT

- WORKSHOP RESULTS
  - PROCEEDINGS TO BE DISTRIBUTED IN 1ST QUARTER 1982
  - DATA SYSTEM PROGRAM PLAN FORMULATION IN 1ST QUARTER 1982
  - FOLLOW-UP SYMPOSIUM TO BE SCHEDULED